Paleoecology and Paleoenvironments of Early Anthropoid and Hominoid Primates in Southeast Asia

Dissertation

der Mathematisch-Naturwissenschaftlichen Fakultät

der Eberhard Karls Universität Tübingen

zur Erlangung des Grades eines

Doktors der Naturwissenschaften

(Dr. rer. nat.)

vorgelegt von

Sophie Gabriele Habinger

aus Sankt Pölten/Österreich

Tübingen

2023

Gedruckt mit Genehmigung der Mathematisch-Naturwissenschaftlichen Fakultät der Eberhard Karls Universität Tübingen.

Tag der mündlichen Qualifikation:	11.07.2023
Dekan:	Prof. Dr. Thilo Stehle
1. Berichterstatter:	Prof. Dr. Hervé Bocherens
2. Berichterstatterin:	Prof. Brooke Erin Crowley PhD

- For our little bee -

This page is intentionally left blank

Table of content

List of figures I
List of tables V
Abbreviations VII
Summary VIII
Zusammenfassung IX
Résumé X
Acknowledgement XII
List of Publications XIV
Personal Contribution XIV

1. Introduction 1
1.1. Characteristics of Eocene and Miocene environments 9
1.1.1. The late Middle Eocene 12
1.1.2. The Late Miocene 13
1.2. Southeast Asia – a hotspot for primate evolution 13
1.2.1. The origin of anthropoid primates 14
1.2.2. Is there a fossil record of primates from the Oligocene in Asia? 23
1.2.3. Early apes and the evolutionary history of Ponginae 24
1.2.4. Ecology of modern *Pongo* 28
1.3. Theoretical framework 32
1.3.1. Niche theory 32
1.3.2. Principles of dental microwear texture analysis (DMTA) 33
1.3.3. Principles of stable isotope analysis (SIA) 36
1.3.4. Challenges and chances of the combination of DMTA and SIA 40
2. Objectives and research questions 40
3. Material 44
3.1. Palaeontological sites and their context 44
3.1.1. The Pondaung Fm. 44
3.1.2. The Irrawaddy Fm. 47
3.1.3. The Khorat sand pits 49
3.2. The Selenka collection of extant *Pongo* and its historical context 49
3.3. Reference data sets for DMTA 53
4. Methods 54
4.1. Dental microwear texture analysis 54

4.2. Stable isotope analysis 56
4.2.1. Data corrections 57
4.3. Statistical analysis 59
4.3.1. Bayesian niche modelling 60
5. Results and Discussion 61
5.1. Paleoecology of the primate bearing Pondaung mammal fauna 61
5.1.1. Confirmation of early monsoon onset 63
5.1.2. Microhabitat differences at the Pondaung Fm. 64
5.1.3. Ecological niche partitioning 65
5.1.4. The anthracotheres 66
5.2. Evolutionary Ecology of pongines in Southeast Asia 69
5.2.1. Paleoenvironmental reconstruction of the Yinseik habitat 70
5.2.2. Paleoecology of *Khoratpithecus ayeyarwadyensis* 74
5.2.3. Assessing ecological continuity in the Ponginae 75
5.2.4. Changes of diet from fossil to extant pongines 78
5.3. Dietary variation of a circa 1890 *Pongo* population 81
5.3.1. The mast fruiting and dietary variability in the Selenka orangutans 83
5.3.2. Are differences in dietary preferences a possible cause for patterns in dental pathologies? 85
6. Conclusion 87
7. Research perspectives 92
8. References 96
9. Appendices 125

Appendix I — Accepted Publication
Appendix II — Extended Figures and Tables

List of figures

Fig. 1 Map of Southeast Asia with a visualisation of the four main biogeographic subregions: Indochina, Sundaland, Philippines, and Wallacea modifierd from (Woodruff, 2010). The orange square shows the approximate position of the Central Basin in Myamar, the location of the fossil formations, while the blue ellipse indicates the area from which the modern orangutans were collected by Emil and Lenore Selenka. .....

Fig. 2 Visualization of modelled continental configurations of the Middle/Late Miocene (10.5 Ma) (top) (Scotese, 2014a) and the late Middle Eocene (38.8 Ma) (bottom) (Scotese, 2014b). .10

Fig. 3 Visualization of global mean temperature (°C) and atmospheric CO_2 content (ppm) in the past 100 million years, including three different modelled scenarios for future development of the earths atmosphere and glocal warming depending on CO_2 emmissions (Tierney et al., 2020). 11

Fig. 4 Map showing the modelled paleogeographic location of the Central Basin of Myanmar (or more specifically the Chindwin Basin = CB) in the Late Eocene (Westerweel et al. 2020; Huang et al. 2023). The red square marks the position of the sampled section of the Yaw Fm. from which the vegetation model calculated. Other abbreviations: BB = Bay of Bengal, BT = Burma Terrane, EAB = Eastern Andaman Basins, Fm(s). = Formation(s), GA = Gangdese Arc, GB = Greater Burma, IAT = India-Australia Transform, IBR = Indo-Burman Ranges, LT = Lhasa Terrane, MB = Minbu Basin, SB = Sibumasu, SF = Sagaing Fault, SL = Sundaland, WPA = Wuntho-Popa Arc. .....

Fig. 5 Overview of the phylogeny and visualisation of estimated divergence times based on (Williams et al., 2010; Coster et al., 2013) The circles (1, 2) mark possible phylogenetic positions of *Aseanpithecus*. The figure was originally published in a blog post by Olivier Chavasseau and Jean-Jacques Jaeger accompanying the publication of their paper (Jaeger et al., 2019) (https://go.nature.com/2GNPWqg (26.03.2023)). 16

Fig. 6 Phylogenetic analysis of early anthropoid primates. The colours of the branches correspond to geographical provenance of the taxa (red: Proteopithecidae, Parapithecoidea, Propliopithecidae, and Oligopithecidae from Afro-Arabia; green: Eosimiidae and Amphipithecidea from Asia; magenta: Platyrrhini from South America). The numbers correspond to Bremer support values and bootstrap frequencies above and below the nodes respectively. Modified from (Jaeger et al., 2020). Afrotarsiidae, which are not displayed in this phylogeny, have been found as basal anthropoids and as the sister-group of Eosimiidae by Chaimanee et al. (2012).....21

Fig. 7 Maps illustrating the changes of Ponginae distribution from the Miocene to the Holocene. Sites from which stable isotope data was used in this study: 1 Dhok Parthan, Siwaliks, Pakistan; 2 Haritalyangar, Siwaliks, India; 3 Yinseik, Irrawaddy Fm., Myanmar; 4 Longgudong, Jianshi, China; 5 Juyuandong, Liucheng Cave, Guangxi, China; 6 Sanhe Cave, Guangxi, China; 7 Nam Lot, Laos; 8 Pha Bong, Thailand; 9 Thum Wiman Nakin, Thailand; 10 Boh Dambang, Cambodia; 11 Pontianak, Indonesia; 12 Sandakan, Malaysia. Extant *Pongo* ranges were taken from the International Union for Conservation of Nature (IUCN Red List). The map was created using QGIS 3.16.....24

Fig. 8 Variation of average feeding times over the studied periods between different orangutan populations of both *P. abelii* on Sumatra and *P. pygmaeus* on Borneo from various observational studies (MacKinnon, 1974; Rodman, 1977; Galdikas, 1978; Rijksen, 1978; Galdikas, 1988; Fox et al., 2004; Morrogh-Bernard et al., 2009; Kanamori et al., 2010; Campbell-Smith et al., 2011; Vogel et al., 2017). Most study sites are from mixed dipterocarp habitats, but five represent peat swamps (bold outline) and one a mosaic agroforest habitat (dashed outline). The dietary category "Other" includes for example flowers and soil. Its compostion can vary from study to study. The numbers after "Ketambe", "Suaq Balimbing", and "Tuanan" are abbreviations for different time periods that were studied. A summary table giving more detailed information about the study areas and the exact percentages can be found in Table SI 3 in Appendix II.....29

Fig. 9 Overview of todays (2015) distribution of different primate taxa in South and Southeast Asia. Ranges decrease from Cercopithecidae to Hylobatidae (excl. *Symphalangus*) to *Symphalangus* and are smallest in Ponginae represented by the single genus *Pongo*. Smaller ranges always include the ranges of primates with a wider distribution. Extant ape ranges were taken from the International Union for Conservation of Nature (IUCN Red List). The map was created in QGIS 3.18.3. 30

Fig. 10 Schematic illustration of the mastication process from initial occlusion (preparatory stroke) over the two phases of the power stroke to subsequent opening (recovery stroke), modified from (Fiorenza et al., 2015). 34

Fig. 11 Visualisation of the different wear facets on a lower molar of *P. pygmaeus*. The colours differentiate the phases of the mastication process (blue = buccal phase I, green = lingual phase I, red = phase II). Buccal = bottom, distal = right. (Fiorenza et al. 2022). .....

Fig. 12 Schematic visualization of different microwear textures (Scott et al. 2006). A shows an anisotropic texture, B a complex one. On the bottom row, there are examples of a heterogenous (C) a homogenous (D) texture. .....

Fig. 13 Visualization of a generalized model of the canopy effect by (Krigbaum, 2003), adapted from (Jackson et al., 1993; Quade et al., 1995). 38

Fig. 14 Map showing the location of the different localities of the Pondaung Fm. and their division into the three area clusters. Coordinates for all the localities from which samples were analyzed in this study are reported in Table SI 1 of **publication 2**. The location of the detailed map is marked in the overview with a coloured rectangle. Map tiles by Stamen Design, under CC BY 3.0. Data by OpenStreetMap, under ODbL (Habinger et al., 2023). 44

Fig. 15 Map showing the general location of the Irrawaddy Fm. (left) and of the Yinseik locality (right) where the hominoid fossils have been found and from which the material used in this study comes from. Modified from (Jaeger et al. 2011). .....

Fig. 16 Emil Selenka (left) and his hunter Max Moret (right together with a Dajak) 50

Fig. 17 These two maps were originally published in Selenka's first extensive publication on the orangutan material that he obtained during his expedition 1892 – 1894 (Selenka, 1898). The position of the detailed map (right) can be estimated using the Ketungau river highlighted in grey and Smitau village on the overview (left). He marked the areas from which he collected

specimen with letters that he originally correlated with local morphotypes. We use these attributions only for estimates of areas of origin for each specimen. We displayed each area by shading in different colours, the extent of each area being based on the description of distribution of the local morphotypes in Selenka's publication and natural barriers such as mountains and major rivers. The Bogau area is not correlated with a morphotype described by Selenka and therefore was not marked in the original map. Nevertheless, it is used in the original labelling of some of the specimen. We estimated its location based on the location of the village Nanga Bogau. The Klingklang-Gebirge refers to the mountain ranges south of the border to Sarawak (Malaysian Borneo) (Habinger et al., in prep).....52

Fig. 18 Examples for the different sampling approaches. *Anthracotherium* tooth fragment (PND-30) showing bulk sampling (left), Brontotheriidae tooth fragment (PND-8) after serial sampling perpendicular to growth axis (right).....

Fig. 19 Visualization of two exemplary serially sampled Eocene specimen (*Bunobrontops* PNG-47, *Paramynodon* PNG-119) together with the modern bovid, illustrating different seasonal precipitation regimes. Plots of all the Eocene serially sampled individuals are reported in the SI of **publication 2**. The distance from the ERJ (enamel root junction) on the x-axis has been inverted. This way it represents the values in an intuitive temporal sequence from the oldest ones to the left to the youngest ones to the right. The statistical outlier (lowest $\delta^{18}O$ value) in the modern *Bos* is included in this figure, but has been excluded from the statistical analysis. Silhouettes via Phylopic under CC 3.0 license (modern *Bos* by T. Michael Keesey, *Bunobrontops* and *Paramynodon* by Zimices (Habinger et al. 2023). 63

Fig. 20 Box plots of the compiled $\delta^{13}C$ (left) and $\delta^{18}O$ (right) values per area. The Mogaung values are lower for both isotopes which is consistent with a difference in microhabitats (Habinger et al. 2023).....

Fig. 21 Ecological niche modelling of the Bahin/Pangan **(A)** and Mogaung **(B)** mammal communities based on all bulk and averaged serially sampled specimen. Ellipses represent the modelled core ecological niches. Silhouettes are from Phylopic under CC 3.0 licence by Zimices (Habinger et al., 2023). 65

Fig. 22 Modelled ecological niches of the serially sampled specimen in separate graphs per taxonomic group. Each ellipse corresponds to the modelled core ecological niche represented by SEA_C of one individual (CI = 40%) visualizing different clustering patterns especially between the Anthracotheriidae and the other three taxonomic groups. Silhouettes are from Phylopic under CC 3.0 licence by Zimices (Habinger et al., 2023).....66

Fig. 23 Ecological niche modelling of the anthracotheres from Bahin/Pangan per genus **(A)**. Ellipses represent the core ecological niches. In **(B)** the results of the shared niche area ($A_A - A_B$, and $A_B - A_A$) between each taxonomic group are visualised. Silhouettes are from Phylopic under CC 3.0 licence (*Anthracotherium* by Zimices, *Anthracokeryx* by Nobu Tamura and vectorised by T. Michael Keelsey, and *Siamotherium* is Public Domain) (Habinger et al. 2023).....

Fig. 24 Ecological niche modelling of the anthracotheres from Bahin/Pangan per species **(A)**. Ellipses represent the core ecological niches. In **(B)** the results of the shared niche area ($A_A - A_B$, and $A_B - A_A$) between each taxonomic group are visualised. Silhouettes are from Phylopic under CC 3.0 licence (*Anthracotherium* by Zimices, *Anthracokeryx* by Nobu Tamura and vectorised by T. Michael Keelsey, and *Siamotherium* is Public Domain) (Habinger et al., 2023). 68

Fig. 25 Development of the minimum $\delta^{18}O$ values from dental enamel of hipparions from the Siwaliks (Nelson 2005) over time (y = -1.1527x + 6.2827; adjusted R^2 = 0.3216; p-value = 0.01611) indicates a decrease of seasonal maximum precipitation. Minimum $\delta^{18}O$ values from the Yinseik specimens in orange do all plot below the regression line and among the lowest minima from the Siwalik hipparions. Icon obtained via PhyloPic and in public domain. (Habinger et al. 2022) .....

Fig. 26 Comparison of the intra-individual serial sampling of the Yinseik mammals with a modern bovid from the Central Basin in Myanmar. Distance from ERJ (enamel root junction) is plotted in reverse order to correctly represent the enamel mineralization from oldest (left) to youngest (right). The lowest $\delta^{18}O$ value of the modern bovid (at 36 mm from the ERJ) represents a statistical outlier (see chapter 4.3). Its removal leads to only a slight overlap of 0.3 ‰ between the highest Miocene values found in the bovid IRWD-17 (-3.6 ‰) and the lowest one of the modern bovid PND-M1 (3.9 ‰). Modified from (Habinger et al. 2022). .....

Fig. 27 Visualisation of niche partitioning using bayesian niche modelling of four fossil mammal communities. The ellipses correspond to the SEAc (standard ellipse area corrected for small sample size) or core ecological niche, which represents a 40 % CI. Summary statistics are reported in Table SI 1 of **publication 1**. A – Yinseik fauna including K. ayeyarwadyensis (~9.5 Ma), B – Chaingzauk fauna (6 ¬ 4 Ma)(Zin-Maung-Maung-Thein et al. 2011), C – Siwalik fauna including Sivapithecus (~9 Ma) (Nelson 2007), D – later Siwalik fauna (~8 Ma)(Nelson 2007). Icons from PhyloPic and in public domain or under CC 3.0 license (Rhinocerotidae, Hippopotamidae, and Tragulidae by Zimices). (Habinger et al., 2022) 73

Fig. 28 Biplot of means and dispersion (± 1 SD) of complexity and anisotropy by taxonomic group. *K. ayeyarwadyensis* and *Khoratpithecus* sp. are from the Irrawaddy Fm. in Myanmar, *K. piriyai* and *K. magnus* from the Khorat sandpits in Thailand. 75

Fig. 29 Visualisation of the shifts in ecological niches between the different fossil and extant pongine genera using bayesian niche modelling. The lines encompass the standard ellipse area or core ecological niche, corresponding to a confidence interval of 40 %(Jackson et al., 2011). Data other than *K. ayeyarwadyensis* from (Bacon et al., 2018a; Nelson, 2007; Wang et al., 2007; Pushkina et al., 2010; Jaeger et al., 2011; Thein et al., 2011; Nelson, 2014; Patnaik et al., 2014; Qu et al., 2014; Janssen et al., 2016; Bocherens et al., 2017; Ma et al., 2017; Suraprasit et al., 2018; Ma et al., 2019; Louys and Roberts, 2020; Jiang et al., 2021). Icons are public domain (*Gigantopithecus*, *Indopithecus*) or Creative Commons 3.0 license (modern & Pleistocene *Pongo* by Gareth Monder, *Khoratpithecus* by Mateus Zica (modified by T. Michael Keesey), and *Sivapithecus* by Nobu Tamura (modified by T. Michael Keesey)) via PhyloPic. (Habinger et al., 2022) 77

Fig. 30 Boxplot of Heterogeneity of Complexity (HAsfc81) per taxonomic group. HAsfc81 values for the *Khoratpithecus* sp., *K. ayeyarwadyensis* and *K. magnus* are reported in Table 7. Compared to *K. piriyai* they all fall below its median, but even if all species of *Khoratpithecus* are combined their HAsfc81 values are higher than the ones of the other pongines (see Fig. SI 1 in Appendix II).....

Fig. 31 Annual precipitation data recorded at Pontianak and originally published in the Regenwaarnemingen in the Nederlandsch-Indie by the Batavia Landsdrukkerij (Kajita, 2019). The red line indicates the ENSO index MEI.ext represented by standardized departure. Values >|2| strong ENSO events (ENSO high precipitation/La Niña = negative values, ENSO low precipitation/El Niño = positive values) (Wolter and Timlin, 2011). MEI.ext data from https://psl.noaa.gov/enso/mei.ext/ (9.3.2023) (Habinger et al., in prep).....84

Fig. 32 Boxplots of complexity (Asfc) on the shearing facet (left) and grinding facet (right) the female individuals by age groups (Habinger et al., in prep).....86

Fig. SI 1 Boxplot of Heterogeneity of Complexity (HAsfc81) per taxonomic group. *Khoratpithecus* spp. Includes *K. piriyai* and *K. magnus* from Thailand and *Khoratpithecus* sp. and *K. ayeyarwadyensis* from Myanmar. Even when looking at genus level distribution of HAsfc81 values for *Khoratpithecus* heterogeneity of complexity and thus dietary variability in regard to physical and mechanical properties of the food items are higher than in the other taxonomic groups. ..... Appendix II

List of tables

Table 1 Summary of the Pondaung primate fauna regarding their occurrences at the various localities of the Pondaung Fm., body mass (BM), and behavioural and dietary ecology. The references for each species include publication of their first description and the main references used to summarize BM and behavioural aspects. A list of all Pondaung primate specimen, the fossil locality where they have been found and reference to the publication they have been published in can be found in Table SI 1 in Appendix II. Body mass estimates from Ramdarshan et al. (2010) and Egi et al. (2004) (for *M. yarshensis*) have been used preferably. If not available in these two publications, estimates are from the literature listed under References. The basis for the summary of the diet are the studies by Kay et al. (2004) and Ramdarshan et al. (2010), with the inferred primary dietary component with the addition of secondary dietary components in brackets. 18

Table 2 Summary of the number of individuals for each age and sex group in the extant *Pongo* DMTA data set. (Habinger et al., in prep).....53

Table 3 Summary of the reference material of Pleistocene *Pongo*, *Pan*, and *Gorilla*. All individuals were adults and one crushing facet per individual was analysed. More detailed information for each individual on locality, tooth moulded, etc. is reported in Table SI 4 in Appendix II.....53

Table 4 Summary of the different SSFA and STA parameter abbreviations, their short description, and units. Adopted from (Schulz et al., 2013a).....55

Table 5 Summary of the body mass (BM) estimates and the modelled isotopic enrichment factor based on formula (5) (Tejada-Lara et al., 2018). For specimens where a taxonomic identification to species level was not possible, the mean modelled enrichment factor the highest taxonomic resolution possible was applied. In this table, whenever no body mass estimate is given, the enrichment factor corresponds to the mean value of the taxonomic groups marked by color. The specific value for the calculation of the $\delta^{13}C$ value of each specimen is reported with the calibrated data before corrections in the Table SI 2 of **publication 2** in the appendix (Habinger et al., 2023). 58

Table 6 Summary statistics for the intra-tooth serial sampling. Specimens labelled with IRWD are the fossil mammals from the Yinseik locality, whereas PND-M1 is the modern reference sample that also originates from the same geographic area, the Central Basin of Myanmar. As described in the text, the minimum $\delta^{18}O$ value of the modern bovid changes to -3.9 ‰ and the amplitude to 3.5 ‰ after the removal of the statistical outlier (PND-M1n) (Habinger et al., 2022). 72

Table 7 Summary statistics of the three main SSFA parameters per taxonomic group. Number of specimen is given as n. In cases where number of specimen and number of individuals differs the latter is reported in brackets. SD (standard deviation) was calculated with n-1. .. 79

Table 8 Results of the ANOVA on the rank transformed SSFA parameters (top) and pairwise comparisons with Tukey HSD post hoc test. Significant differences at $p < 0.05$ are highlighted in bold. 80

Table 9 List of identifiable specimens (mentioned in the text or shown in the figures with their ID) and the dental lesions recorded by Stoner (1995). Only one of them ZSM-1981-114 is part of the data set with the tooth antagonistic to the tooth with an occlusal cavity. Sex and age estimations are from Stoner (Habinger et al., in prep) 86

Table SI 1 Compiled table of published specimens of primate fossils from the late Middle Eocene Pondaung Fm. Some specimens inspected during the fieldwork in February 2020 in the National Museum of Myanmar, Nay Pyi Taw are also listed. ..... Appendix II

Table SI 2 Compiled table of *Khoratpithecus* specimens from Myanmar and Thailand with additional information on which specimens and which teeth were moulded for DMTA. ..... Appendix II

Table SI 3 Data from observational studies orangutan diets that was used for Fig. 8. ..... Appendix II

Table SI 2 Compiled SSFA and STA parameters on *Khoratpithecus* as well as *Gorilla*, *Pan*, and Pleistocene and modern *Pongo* used for the dietary reconstructions of *Khoratpithecus* from Myanmar and Thailand. ..... Appendix II

Abbreviations

General abbreviations

k	number of groups
ka	thousand years ago
Ma	million years ago
n	number of individuals
p	number of parameters

Palaeontological Sites

Fm.	fossil formation
IRWD	Irrawaddy Fm. (Lab code)
PNG	Pondaung Fm. (Lab code), synonymous with PND

Methodology

ANOVA	
CI	confidence interval
δ	notation used for to express isotopic data relative to a standard (see formula 3)
DMTA	dental microwear texture analysis
lm	linear model
H_0	null hypothesis
H_1	alternative hypothesis
HSD	Tukey's post hoc Honest Significant Difference
LSD	Fisher's post hoc Least Significant Difference
PCA	principal component analysis
σ/SD	standard deviation
SEAc	standard ellipse area corrected for small sample size ($‰^2$)
SIA	stable isotope analysis
TA	total area, corresponds to convex hull area

Dental microwear texture parameters

Sa	arithmetic mean height
Sp	maximum peak height
Sq	standard deviation of height distribution
Sv	maximum pit height
Sz	amplitude of the heights (Sv + Sp)
Sku	kurtosis of the height distribution
Ssk	skewness of the height distribution
Sal	auto-correlation length
Str	texture aspect ration
metf	mean depth of furrows
medf	mean density of furrows
Asfc	Area-Scale Fractal analysis Complexity parameter
epLsar	Exact Proportion Length-Scale Anisotropy of Relief
HAsfc	Heterogeneity of complexity

Summary

The Cenozoic fossil formations of Southeast Asia document a highly dynamic period in mammalian evolution. Many clades of modern mammals originated from this biogeographic region or experienced important radiations there including anthropoid primates and pongines. Here, I want to characterize the ecological and environmental contexts in which these developments took place, specifically regarding palaeoseasonality, vegetation structure, diet and niche partitioning. To do so, I focused on two fossil mammal assemblages from the Central Basin of Myanmar representing two key time periods in the evolutionary history of primates.

The greenhouse world of the middle Eocene Pondaung Fm. is a window to explore the ecosystem dynamics in the faunal assemblage of a habitat, which sustained a large number of different early anthropoid primates as well as a diverse fauna of herbivorous mammals. Previous studies focused on climate and vegetation of the Pondaung environment. While I also worked on aspects of paleoseasonality and vegetation structure, my focus lay on the structure of microhabitats across the different localities of the Pondaung Fm. and their use by the different taxonomic groups. Based on this work, I could infer ecological flexibility for at least some of the anthropoid primate species, based on their occurrences in different microhabitats. The second focal point of my work on the Pondaung fauna were the anthracotheres and a detailed reconstruction of their paleoecology and the competition dynamics between the five species.

With the second mammal assemblage, we want to address open questions surrounding the evolutionary ecology of Ponginae in Southeast Asia. Today, there only is one genus (*Pongo*), whose geographical distribution is highly restricted to the islands of Borneo and Sumatra. From the Miocene to the Pleistocene however, species diversity and geographic range were much more extensive. The fossil record of pongines spans the area from Turkey to southern China. The late Miocene Irrawaddy Fm. is an example for the habitat of the sister-group of extant orangutans, *Khoratpithecus*, which is represented here by the species *Khoratpithecus ayeyarwadyensis*. I characterized the habitat of this fossil pongine by reconstructing its paleoseasonality, vegetation structure and niche partitioning dynamics. Then focused my work on the question if there was ecological continuity in the pongine clade since the Miocene, with a comparison of the different taxa from South and Southeast Asia.

For my studies, I used to different analytical approaches to assess paleoecology and diet in these fossil mammal faunas. Here, I present the stable isotope analysis and subsequent niche modelling of the Eocene and Miocene fossil assemblages from Myanmar and the dental microwear texture analysis I used to get a more detailed insight into pongine evolutionary ecology with the comparison of subsistence strategies of Miocene pongines to Pleistocene and extant orangutans. With the different studies of my dissertation project I could show possibilities to push the boundaries of stable isotope niche modelling by using a different set of isotopes that are representing more general ecological characteristic of a niche rather than just trophic or dietary dimensions. I also successfully explored the application of new approaches with the modelled isotopic niches that previously were only used by stable isotope

ecologists working on modern ecosystems to geological time periods. One example is the evaluation of competition potential dynamics in the anthracothere assemblage from the Pondaung Fm. The work on the Selenka orangutans was another way in which I could bridge the gap between palaeontology and ecologists and biologists working on extant primate faunas in providing a data set that opens new research directions in both fields.

Zusammenfassung

Die fossilen Fundstellen aus dem Känozoikum Südostasiens dokumentieren eine äußerst dynamische Periode der Säugetierevolution. Viele Gruppen moderner Säugetiere entwickelten sich in dieser biogeographischen Region oder erlebten dort bedeutende Radiationen. Zu diesen zählen zum Beispiel anthropoide Primaten im Eozän und hominoide Primaten im Miozän. Hier möchte ich den ökologischen Kontext charakterisieren, in dem diese Entwicklungen stattfanden, insbesondere im Hinblick auf Paläosaisonalität, Vegetationsstruktur, Ernährung und Nischenaufteilung. Zu diesem Zweck habe ich mich auf zwei fossile Säugetierfaunen aus dem heutigen Myanmar konzentriert, die zwei Schlüsselzeiträume in der Evolutionsgeschichte der Primaten repräsentieren.

Die Treibhauswelt der Pondaung Formation (Fm.) aus dem mittleren Eozän ist ein Fenster zur Erforschung der Ökosystemdynamik der Tierwelt eines Lebensraums, der eine große Anzahl verschiedener früher anthropoider Primaten sowie eine vielfältige Fauna pflanzenfressender Säugetiere beherbergte. Frühere Studien konzentrierten sich auf das Klima und die Vegetation in der Umwelt, die die Pondaung Fm. prägte. Obwohl ich mich auch mit Aspekten der Paläosaisonalität und der Vegetationsstruktur beschäftige, liegt mein Schwerpunkt auf der Struktur der Mikrohabitate an den verschiedenen Fundstellen der Pondaung Fm. sowie ihrer Nutzung durch die verschiedenen taxonomischen Gruppen. Auf der Grundlage dieser Habitatsrekonstruktionen konnte ich für einige der anthropoiden Primatenarten aufgrund ihres Vorkommens in verschiedenen Mikrohabitaten auf ein gewisses Maß an ökologischer Flexibilität schließen. Der zweite Schwerpunkt meiner Arbeit an der Pondaung-Fauna waren die Anthracotheriidae und eine detaillierte Rekonstruktion ihrer Paläoökologie und der Konkurrenzdynamik zwischen den fünf Arten, die in der Pondaung Fm. gefunden wurden.

Mit der zweiten Säugetierfauna bearbeite ich offene Fragen zur evolutionären Ökologie der Ponginae in Südostasien, die im Miozän ihren Anfang hatte. Heute gibt es nur noch eine Gattung (*Pongo*), deren geographische Verbreitung auf die beiden Inseln Borneo und Sumatra beschränkt ist. Vom Miozän bis zum Pleistozän waren die Artenvielfalt und das geographische Verbreitungsgebiet jedoch weitaus größer. Die Fossilien von Ponginae erstrecken sich von der Türkei bis nach Südchina. Die Irrawaddy-Fm. aus dem späten Miozän ist ein Beispiel für den Lebensraum der Schwestergruppe der heutigen Orang-Utans, *Khoratpithecus*, die dort durch die Art *Khoratpithecus ayeyarwadyensis* vertreten ist. In meiner Dissertation charakterisiere ich den Lebensraum dieser fossilen Ponginae, indem ich die Paläosaisonalität, die Vegetationsstruktur und die Dynamiken zwischen den ökologischen Nischen der fossilen Fauna rekonstruiere. Anschließend konzentriert sich meine Arbeit auf die Frage, ob es eine ökologische Kontinuität in Bezug auf Ernährung, Habitatspräferenzen und –nutzung in der

Familie Ponginae seit dem Miozän gibt, wobei ich die verschiedenen Taxa aus Süd- und Südostasien vergleiche.

Für meine Studien habe ich verschiedene analytische Ansätze verwendet, um die Paläoökologie und Ernährung in diesen fossilen Säugetierfaunen zu bewerten. Hier präsentiere ich die Analyse stabiler Isotope und die anschließende Nischenmodellierung der eozänen und miozänen Fossilien aus Myanmar sowie die Analyse der Mikroläsionen an okklusalen Kaufacetten der Zähne. Die Resultate der zweiten Methode ermöglichen einen detaillierteren Einblick in die evolutionäre Ökologie der Ponginae durch den Vergleich der Subsistenzstrategien miozäner Ponginae mit pleistozänen und heutigen Orang-Utans. Mit den verschiedenen Studien meines Dissertationsprojekts konnte ich Möglichkeiten aufzeigen, wie man die Grenzen der Modellierung von Nischen mit stabilen Isotopen erweitern kann. Zum einen indem ich eine andere Gruppe von Isotopen verwendet habe, die eher allgemeine ökologische Merkmale einer Nische darstellen als nur trophische oder ernährungsbezogene Dimensionen. Zum anderen habe ich erfolgreich neue Interpretationsansätze für die modellierten Isotopennischen aus geologische Zeiträume erprobt, die bisher nur von Ökologen, die an modernen Ökosystemen arbeiten, angewendet wurden. Ein Beispiel dafür ist die Bewertung der Dynamik des Konkurrenzpotenzials in den Anthracotheriidae aus der Pondaung Fm. Die Arbeit an den Mikroläsionen (dental microwear) der Selenka-Orang-Utans war eine weitere Möglichkeit, eine Brücke zwischen der Paläontologie einerseits und Ökologie und Biologie andererseits zu schlagen. Der daraus hervorgegangene Datensatz eröffnet neue Forschungsmöglichkeiten in beiden Disziplinen, besonders im Hinblick auf den Arterhalt der Orang-Utans.

Résumé

Les formations fossiles cénozoïques de l'Asie du Sud-Est témoignent d'une période très dynamique de l'évolution des mammifères. De nombreux clades de mammifères modernes sont originaires de cette région biogéographique ou y ont connu d'importantes radiations, notamment les primates anthropoïdes de l'Éocène et les ponginés du Miocène. Le principal objectif de ma thèse est de caractériser les contextes écologiques et environnementaux dans lesquels ces évolutions ont eu lieu, en particulier en ce qui concerne la saisonnalité, la structure de la végétation, le régime alimentaire et le partage des niches dans le registre fossile. Pour ce faire, je me suis concentrée sur deux assemblages de mammifères fossiles du bassin central du Myanmar représentant deux périodes clés dans l'histoire de l'évolution des primates.

L'Éocène moyen est un example d'un monde de réchauffement global. La Formation (Fm.) de Pondaung permette d'explorer la dynamique de l'écosystème dans l'assemblage faunique d'un habitat qui a soutenu un grand nombre de primates anthropoïdes primitifs différents ainsi qu'une faune diversifiée de mammifères herbivores. Les études précédentes se sont concentrées sur le climat et la végétation de l'environnement de Pondaung. J'ai non seulement travaillé sur les aspects de la saisonnalité et de la structure de la végétation, mais également sur la structure des micro-habitats dans les différentes localités de la Fm. Pondaung et sur leur

utilisation par les différents groupes taxonomiques. Sur la base de ce travail, j'ai pu déduire une flexibilité écologique pour certaines espèces de primates anthropoïdes, sur la base de leur présence dans différents micro-habitats. Le deuxième point central de mon travail sur la faune de Pondaung a concerné une reconstitution détaillée de la paléo-écologie des anthracothères, et de la dynamique de compétition entre les cinq espèces présentes.

Le deuxième assemblage de mammifères étudié apporte de nouveaux éléments pour mieux comprendre l'écologie évolutive des Ponginae en Asie du Sud-Est. Aujourd'hui, il n'existe qu'un seul genre (*Pongo*), dont la distribution géographique est fortement restreinte aux îles de Bornéo et de Sumatra. Du Miocène au Pléistocène, la diversité des espèces et leur aire de répartition géographique étaient cependant beaucoup plus étendues. Le registre fossile des ponginés s'étend de la Turquie au sud de la Chine. La Formation d'Irrawaddy du Miocène tardif est un exemple de l'habitat du groupe frère des orangs-outans actuels, *Khoratpithecus*, qui est représenté ici par l'espèce *Khoratpithecus ayeyarwadyensis*. J'ai caractérisé l'habitat de ce ponginé fossile en reconstituant sa saisonnalité, la structure de sa végétation et la dynamique de partage des niches. J'ai ensuite concentré mon travail sur la question d'une continuité écologique dans le clade des ponginés depuis le Miocène, en comparant les différents taxons d'Asie du Sud et du Sud-Est.

Dans le cadre de cette thèse, j'ai utilisé deux approches analytiques différentes pour évaluer la paléo-écologie et le régime alimentaire de ces faunes de mammifères fossiles. Je présente ici l'analyse des isotopes stables (carbon et oxygène) et la modélisation des niches subséquentes des assemblages fossiles de l'Éocène et du Miocène du Myanmar. En outre, j'ai étudié les textures de micro-usure dentaire des ponginés pour obtenir un aperçu plus détaillé de leur écologie évolutive, en comparant les stratégies de subsistance des ponginés du Miocène à celles des orangs-outans du Pléistocène et des orangs-outans actuels.

Grâce aux différentes approches de mon projet de thèse, j'ai pu montrer qu'il était possible de repousser les limites de la modélisation des niches par isotopes stables en utilisant un ensemble différent d'isotopes qui représentent des caractéristiques écologiques plus générales d'une niche plutôt que de simples dimensions trophiques ou alimentaires. J'ai également exploré avec succès l'application de nouvelles approches aux niches isotopiques modélisées, qui n'étaient auparavant utilisées que par les écologistes spécialistes des isotopes stables travaillant sur les écosystèmes modernes et les périodes géologiques. Un exemple est l'évaluation de la dynamique du potentiel de compétition dans l'assemblage d'anthracothères de la Fm de Pondaung. Le travail sur les orangs-outans de la Sélénka a été une autre façon pour moi de combler le fossé entre la paléontologie et les écologistes et biologistes travaillant sur les faunes de primates existantes en fournissant un ensemble de données qui ouvre de nouvelles directions de recherche dans les deux domaines.

Acknowledgement

A lot of time, work, and dedication is necessary to writing a dissertation. It truly is an endeavour that cannot be brought to a successful conclusion without help. Here, I want to thank all the people that worked with me on the different projects and had my back. First I want to say how grateful I am for my supervisors Hervé Bocherens, Olivier Chavasseau, and Stéphane Ducrocq. You not only gave me the freedom and space to bring my own ideas to the table, but provided feedback and support as well. Every one of you taught me different lessons that will be with me for the rest of my life.

Cristoph Wissing is the person that encouraged me to apply for the position that led to this finished dissertation manuscript. Without him, I might not have even followed this path. The working environment and my colleagues in the AG Biogeology lab were always so supportive during the past years that definitely weren't all that easy at times. Special thanks goes to Peter without whom nothing in the AG Biogeology lab would be running.

I was very lucky to be able to join one field season at the Pondaung Fm. in Myanmar where I could meet and work with some wonderful people. After the military putch in February 2021, it was unfortunately very difficult or impossible to stay in contact with my collaborators there. I want to say that I am thinking of you often and hope you and your families are safe and unharmed.

During our apéro each evening after fieldwork, but also back in France and Germany it was always interesting to discuss my results and thoughts with Yaowalak Chaimanee and Jean-Jacques Jaeger. Our discussions often sparked new ideas.

Gildas Merceron sacrificed a lot of his time to teach me how to mould, scan, process and analyse dental microwear texture data. For that I am very grateful. I am looking forward to finally publishing those parts of my PhD project as well.

In the course of the EVEREST graduate programm at the Universität Tübingen I could meet with TAC (thesis advisory committee) members Claudio Tennie and Henri Thomassen were such a valuable support in the course of my PhD project. Their input and mentoring often put things into perspectives and opened up new ways of approaching an issue or topic. In addition to all this support that was more focused on research, I could always count on an amazing team of administrative staff at both the Universiät Tübingen and the Université de Poitiers. Gabi, Iris, Guylaine, and Laure, thank you for making my life so much easier and less stressful.

Although I had to travel between Tübingen and Poitiers quite a bit in addition to needing to stay home, due to the lockdowns I met many amazing people at both universities. Hanging out with you, chatting and having fun at the office or discussing our work and related struggles made the past years so much better. I want to mention in particular Chris, Guiseppe, Gustavo, and Tobias from Tübingen and Axelle G., Axelle W., Axelle Z., Blade, Corentin, Margot, Tomas from Poitiers. Margot, thank you in particular for proof reading the French parts of my dissertation.

I know that I can always count on my family. From the very beginning, they always encouraged me to follow my dreams and believed in my abilities. Thank you for being there for me, even when I was apart from you. Mama, Papa I can be so happy to have you by my side. Agnes, you are the best sister anyone could wish for. I also want to thank my grandparents Edith and Franz Habinger and Josefa and Josef Lechner. Since I was a baby, you have always been there for me, each of you in your own ways, and had an open ear for me. It did not matter if I talked about something you completely understood or not, you even listened to my entire master defense, even though none of you speaks any English. I am entirely grateful for every single one of you – you'll always have a place in my heart.

Last but not least, I want to thank the two beings closest to my heart. Jamie, you are the best desk buddy anybody can wish for. You accompanied me on my adventures in France and made sure I wasn't too overwhelmed with work by demanding cuddle breaks. And of course Marcel, I know it wasn't always easy, but thank you so much, for being by my side for more than seven years. You always were the voice of reason, never sugarcoating, but always on my side. Everybody needs someone like you in their lives. I love you.

I want to conclude this section with some words Emil Selenka often said to his students to encourage their curiosity.

„Nur zu!"

List of Publications

Publication 1: **Habinger, S. G.,** Chavasseau, O., Jaeger, J.-J., Chaimanee, Y., Soe, A. N., Sein, C., Bocherens, H. (2022) Evolutionary Ecology of Miocene hominoid primates in Southeast Asia. *Scientific Reports* 12, 11841; DOI: 10.1038/s41598-022-15574-z.

Publication 2: **Habinger, S. G.,** Chavasseau, O., Ducrocq, S., Chaimanee, Y., Jaeger, J.-J., Soe, A. N., Sein, C. Stern, S., Bocherens, H. (2023) Isotopic niche modelling of a mammal fauna from Southeast Asia shows microhabitat differences. Insights into early anthropoid primate habitats. *Frontiers in Ecology and Evolution* 11, 1110331 DOI 10.3389/fevo.2023.1110331.

Publication 3: **Habinger, S. G.,** Merceron, G., van Heteren, A. H., Rojas Cuyutupa, V., Bocherens, H., Chavasseau, O. (in prep.) Characterisation of a circa 1890 orangutan population's diet using dental microwear texture analysis. A reference database for intra- and interspecific variation of dental microwear of extant hominids.

Personal Contribution

Publication 1: I was the first and corresponding author, as well as the lead author of the manuscript. I worked on data analysis together with my co-authors, ran all the models and created the figures and maps.

Publication 2: I was the first and corresponding author, as well as the lead author of the manuscript. I was responsible for sampling and sample preparation. I also worked on data analysis together with my co-authors, ran all the models and created the figures and maps.

Publication 3: I was the first and corresponding author, as well as the lead author of the manuscript. I was responsible for scanning of the moulds and preparing the scans for analysis. I also worked on data analysis together with my co-authors, ran the models and created the figures and maps.

1. Introduction

Allgemeine Einleitung

Mein Dissertationsprojekt umfasst zwei geologischen Ären, zwei Fossilformationen und zwei unterschiedliche analytische Ansätze, die angewendet wurden, um die Ökologie und Umwelt der frühen eozänen anthropoiden und miozänen hominoiden Primaten Südostasiens zu rekonstruieren. Südostasien wird hier als Überbegriff für eine biogeografische Region verwendet, die zusätzlich zu Brunei, Kambodscha, Osttimor, Indonesien, Laos, Malaysien, Myanmar, den Philippinen, Singapur, Thailand und Vietnam auch andere Regionen umfasst, die im Känozoikum homogene Klima- und Umweltbedingungen aufgewiesen haben (Kreft and Jetz, 2010). Deshalb werde ich bei der Diskussion und Interpretation der Ergebnisse auch auf fossile Faunen aus Teilen Südasiens, wie Pakistan, Indien und Nepal sowie Teilen Ostasiens, vor allem Südchina, eingehen (Gibert et al., 2022).

Das eozäne Klima ist ein Beispiel für ein Treibhausklima. Obwohl auf das paläozän-eozäne klimatische Optimum eine graduelle Abkühlung im Laufe der Epoche zu beobachten war, waren die jährlichen Durchschnittstemperaturen im späten Eozän immer noch um rund 5 °C erhöht (Zachos et al., 2001; Pagani et al., 2005). Bereits im späten mittleren Eozän der Pondaung Fm. konnte ein monsunähnliches Klima (Licht et al., 2014c) sowie gesteigerte saisonale Temperaturschwankungen (Toumoulin et al., 2022) festgestellt werden. Letztere Entwicklung war allerdings vor allem in Zentralasien prävalent und spielte in den in Äquatornähe gelegenen (5 °N) eozänen Habitaten der Pondaung Fm. vermutlich nur eine geringe Rolle. Die dortige Vegetation war von Bäumen der Familie Dipterocarpaceae geprägt, die über die nordwärts driftende Indische Platte nach Asien kamen (Corlett and Primack, 2005, 2011; Corlett, 2014). Der erste fossile Nachweis dieser Pflanzen außerhalb des Indischen Subkontinents stammt von der in dieser Arbeit untersuchten Pondaung Fm. Die dort gefundenen fossilen Hölzer weisen auf einen Vegetationsgradienten von mangrovenartiger Küstenvegetation im Westen zu immergrünen Wäldern im weiter östlich gelegenen Landesinneren hin (Licht et al., 2014a; Licht et al., 2015). Am Ende des Eozäns kam es zu einem dramatischen Absinken des Meeresspiegel, der Temperaturen am Meeresgrund und an den Meeresoberflächen sowie zu einer Ausbreitung des permanenten antarktischen Inlandeises (Zachos et al., 2001; Liu et al., 2009; Westerhold et al., 2020). Damit einher ging eine massive Veränderung der Biodiversität in den terrestrischen Faunen Europas, wo dieses Ereignis als Grande Coupure (Stehlin, 1909) bekannt ist, und Asiens (Sun et al., 2014; Ni et al., 2016).

Nach einer kurzen Phase der Erwärmung am Übergang vom Oligozän zum Miozän, die im miozänen Klimaoptimum mündete, setzt sich der Trend zur graduellen Abkühlung weiter fort (Zachos et al., 2001). Weitere tektonische

Plattenverschiebungen führen zu einer Verkleinerung und teilweise vollkommenen Austrocknung der Tethys. Es entstand eine Landbrücke, die zu einem regen Austausch von Flora und Fauna zwischen Afrika und Asien, besonders Südostasien führte (Harzhauser et al., 2007). Im mittleren und späten Miozän Thailands findet sich eine große Vielfalt an unterschiedlichen Vegetationstypen, die von tropischen Wäldern zu savannenähnlichen Habitaten reichen (Badgley et al., 2008). Ein gesteigertes Maß an Saisonalität und ein zunehmend trockenes Klima führten zu einer Fragmentierung der bewaldeten Habitate, was zum Verschwinden vieler waldlebender, frugivorer Spezies führte (Badgley et al., 1988; Nelson, 2003, 2005; Badgley et al., 2008). Stattdessen hielten die an trockenes Klima angepassten C_4 Pflanzen ihren Einzug. Sie verbreiteten sich von Afrika nach Asien, wo sie zuerst in Pakistan aus Sedimenten, die auf 9,4 Ma datiert sind, belegt sind (Morgan et al., 1994). Ein erster Nachweis dieser Pflanzen aus Myanmar stammt von einer auf 6 Ma datierten Fundstelle der Irrawaddy Fm. (Thein et al., 2011).

Die beiden Primatengruppen, welche im Fokus dieser Arbeit stehen und die eben beschriebenen eozänen und miozänen Habitate Südostasiens bewohnten, sind die anthropoiden und hominoiden Primaten. Gerade was erstere taxonomische Gruppe betrifft wurde in den vergangenen Jahren viel über den Ort ihrer ursprünglichen Radiation und die Route über die sie sich von dort aus verbreitet haben diskutiert. Als mögliche Ursprungsorte standen Afrika und Asien zur Debatte. Die eozänen Primaten, die in den Fossilformationen Asiens gefunden wurden, waren dabei der zentrale Diskussionspunkt. Während einige Forscher sie als primitive anthropoide Primaten klassifizierten (Jaeger et al., 1998; Chaimanee et al., 2000; Beard, 2002; Marivaux et al., 2003; Beard, 2004; Jaeger et al., 2004; Beard et al., 2005; Beard et al., 2007; Bajpai et al., 2008; Rose et al., 2009a; Marivaux et al., 2010; Jaeger et al., 2019), sprachen sich andere dafür aus, dass es sich bei den morphologischen Merkmalen, die für die Klassifikation herangezogen wurden, um Beispiele konvergenter Evolution als Anpassung von fossilen Feuchtnasenaffen (Strepsirrhini) an Durophagie handelt (Ciochon and Holroyd, 1994; Ciochon et al., 2001; Ciochon and Gunnell, 2002b; Gunnell et al., 2002; Ciochon and Gunnell, 2004; Gunnell and Ciochon, 2008). Entdeckungen von neuen fossilen Primaten, wie zum Beispiel die Beschreibung von *Bahinia* (Jaeger et al., 1999) und die Studie zu cranialen mit assoziierten postcranialen Elementen der Gattung *Ganlea* (Jaeger et al., 2020) konnten die phylogenetische Klassifizierung als primitive Vertreter der Anthropoidea bestätigen.

Im Gegensatz zu den anthropoiden Primaten ist die Frage der Verortung der ursprünglichen Radiation der hominoiden Primaten weniger prävalent. Bemerkenswerter hingegen scheint die weit größere Artenvielfalt der Familie Ponginae vom Miozän bis zum Pleistozän. Heute ist die Gattung *Pongo* als einziger Vertreter dieser Familie noch in einem stark eingeschränkten Verbreitungsgebiet auf Sumatra und Borneo vorhanden. Im Miozän hingegen sind Funde von unterschiedlichen Gattungen und Spezies aus dem Gebiet von der Türkei bis

Südchina bekannt. *Khoratpithecus*, und besonders die in der Irrawaddy Fm. gefundene Art *Khoratpithecus ayeyarwadyensis*, ist Fokus dieser Arbeit (Jaeger et al., 2011). Drei weitere Spezies dieser Gattung sind aus dem mittleren und späten Miozän Thailands belegt (Chaimanee et al., 2003; Chaimanee et al., 2004; Chaimanee et al., 2022). Die Frage nach ökologischen Kontinua in den Habitatspräferenzen und der Ernähung der unterschiedlichen Vertreter der fossilen Ponginae und modernen Gattung *Pongo* ist essentiell für unser Verständnis der evolutionären Geschichte dieser Menschenaffen und den Erhalt und Schutz der Orangutans heute.

Ein großes Thema dieser Arbeit ist die Modellierung von Nischen der Säugetierfaunen und ihre Nutzung für die Evaluierung von Ökosystemdynamiken in den Habitaten der anthropoiden und hominoiden Primaten. Dabei wird auf das Nischenkonzept von Hutchinson zurückgegriffen (Hutchinson, 1957). Die Nische einer Art, beziehungsweise einer taxonomischen Gruppe, ist demnach ein Hypervolumen mit n Dimensionen. Jede Dimension bildet einen biotischen oder abiotischen Faktor ab. Die Summe ergibt mögliche Umweltbedingungen, die das Fortbestehen einer Art ermöglichen. In der bisherigen archäologischen und paläontologischen Forschung wurde dieses Konzept vor allem in Zusammenhang mit Nahrungsrekonstruktionen und Untersuchungen zur trophischen Ökologie angewendet. Ich werde hier jedoch stabile Kohlenstoff- und Sauerstoffisotope analysieren, wodurch die Nischendimensionen eher allgemein ökologische beziehungsweise Umweltfaktoren abbilden. Dieser Ansatz wurde erst einmal in ähnlicher Form von Nelson und Hamilton (2017) angewendet, wobei auch hier der Fokus auf Änderungen in der Nahrungsgrundlage früher Hominiden, allerdings in Zusammenhang mit ökologischen Veränderungen lag.

Eine der beiden analytischen Methoden, die ich in dieser Arbeit angewendet habe ist die Untersuchung von Mikroläsionen am Zahnschmelz, die während des Kauprozesses vor allem durch Abrasion entstehen. Abrasive Partikel, wozu Nahrung zählt, werden zwischen zwei antagonistischen Zähnen durch zyklisch sich wiederholende Kaubewegungen zerkleinert. Dadurch entstehen abgegrenzte Facetten, die unterschiedlichen Phasen dieses Kauprozesses entsprechen (Crompton and Hiiemae, 1969; Kay and Hiiemae, 1974; Ungar, 2015). Jedes Mal, wenn Nahrung konsumiert wird, entstehen neue Mikrostrukturen, die bereits bestehende nach und nach überschreiben. Diese Methode der Nahrungsrekonstruktion bildet also die Ernährung der Wochen vor dem Tod eines Individuums ab (Grine, 1986). Wie schnell das Nahrungssignal der Mikroläsionen vollständig durch neue überlagert wird, hängt von den physischen und mechanischen Eigenschaften der Nahrung ab. Harte Objekte führen zu einer schnelleren Überschreibung als weiche (Teaford and Oyen, 1989; Teaford et al., 2017; Winkler et al., 2020; Teaford et al., 2021). Traditionelle Methoden quantifizieren spezifische Strukturen anhand von zweidimensionalen Aufnahmen der Zahnoberfläche, was meist einen hohen Zeitaufwand bedeutet und vor allem zu hohem Abweichungen zwischen den Auswertungen zweier Beobachtern führt

(Grine et al., 2002; Galbany et al., 2005; Mihlbachler et al., 2012; DeSantis et al., 2013). Für meine Analysen verwende ich eine objektivere Methode, bei der die Oberfläche der Kaufacette als dreidimensionale Punktwolke erfasst wird, von der anschließend unterschiedliche Parameter extrahiert werden, die zur Unterscheidung von Nahrungsgrundlagen mit verschiedenen physikalischen und mechanischen Eigenschaften dienen (Scott et al., 2006).

Auch die zweite analytische Methode, die Analyse stabiler Kohlenstoff- und Sauerstoffisotope, konzentriert sich auf den Zahnschmelz. Durch die minimalen Massenunterschiede von Isotopen, die durch die unterschiedliche Anzahl der Neutronen im Atomkern bedingt sind, kommt es zu Fraktionierung in physischen und chemischen Prozessen. Während der Mineralisierung des Zahnschmelzes, werden Kohlenstoff- und Sauerstoffisotopen im Zahnschmelz eingelagert. Veränderungen im Vorkommen der einzelnen Isotopen im Vergleich zu ihrem natürlichen Verhältnis zueinander werden so fixiert und ermöglichen es Inferenzen zu Klima, Ernährung, Ökologie und Habitatstruktur zu ziehen. Der hohe Anteil an Hydroxylapatit ($Ca_{10}(PO_4)_6(OH)_2$) (96 – 99 %) sowie die dichte, feine kristalline Struktur des Zahnschmelzes machen dieses Gewebe resistent gegen taphonomische Veränderungen. Durch die Kohlenstoffisotope lassen sich vor allem Informationen über die Vegetation an der Basis eines Nahrungsnetzes gewinnen. Sogenannte C_3 Pflanzen haben deutlich niedrigere $\delta^{13}C$ Werte (−20 bis −37 ‰ (Kohn, 2010)), als die an trockenes Klima angepassten C_4 Pflanzen (−10 bis −20 ‰ (Bender, 1971)). Zusätzlich unterscheiden sich die $\delta^{13}C$ Werte nach dem Grad des Kronenschlusses und lassen deshalb Rückschlüsse auf die Vegetationsstruktur (offen, leicht oder dicht bewaldet) zu (Bonafini et al., 2013; Krigbaum et al., 2013; Lowry et al., 2021). Die stabilen Sauerstoffisotope des Zahnschmelzes spiegeln die Zusammensetzung des Niederschlages wider. In Kombination mit einer seriellen Beprobungsstrategie eignen sie sich gut, um saisonale Variationen in der Temperatur in gemäßigten Klimazonen, beziehungsweise in den Niederschlagsmengen in tropischen Klimazonen zu rekonstruieren (Dansgaard, 1964; Pederzani and Britton, 2019). Innerhalb einer Säugetierfauna können die Sauerstoffisotope Aussagen zur vertikalen Stratifizierung in der Habitatnutzung (Fannin and McGraw, 2020; Louys and Roberts, 2020; Lowry et al., 2021) sowie zu einem semi-aquatischen Lebensstil bestimmter Arten oder taxonomischer Gruppen ermöglichen (Bryant and Froelich, 1995; Clementz et al., 2008).

Introduction générale

Mon projet de thèse englobe deux ères géologiques, deux formations fossiles et deux approches analytiques différentes, appliquées pour reconstruire l'écologie et l'environnement des primates de l'Eocènes et hominoïdes du Miocènes d'Asie du Sud-Est. L'Asie du Sud-Est est utilisée ici comme un terme générique pour une région biogéographique qui comprend, en plus du Brunei, du Cambodge, du Timor oriental, de l'Indonésie, du Laos, de la Malaisie, du Myanmar, des Philippines, de Singapour, de la Thaïlande et du Vietnam, d'autres régions qui présentaient des

conditions climatiques et environnementales homogènes au Cénozoïque (Kreft and Jetz, 2010). C'est pourquoi, lors de la discussion et de l'interprétation des résultats, j'aborderai également les faunes fossiles de certaines parties de l'Asie du Sud, comme le Pakistan, l'Inde et le Népal, ainsi que de certaines parties de l'Asie de l'Est, en particulier le sud de la Chine (Gibert et al., 2022).

Le climat éocène est un exemple de climat réchauffé. Bien qu'un refroidissement progressif ait été observé au cours de l'époque après l'optimum climatique paléocène-éocène, les températures moyennes annuelles à la fin de l'Éocène étaient encore élevées d'environ 5 °C (Zachos et al., 2001 ; Pagani et al., 2005). Dès la fin de l'Éocène moyen de Pondaung Fm, on a pu constater un climat semblable à celui de la mousson (Licht et al., 2014c) ainsi que des variations saisonnières accrues de la température (Toumoulin et al., 2022). Cette dernière évolution était surtout présente en Asie centrale et n'a probablement joué qu'un rôle mineur dans les habitats éocènes de la Fm. de Pondaung situés à proximité de l'équateur (5 °N). La végétation y était dominée par des arbres de la famille des Dipterocarpaceae, qui sont arrivés en Asie par la plaque continentale indienne dérivant vers le nord (Corlett and Primack, 2005, 2011 ; Corlett, 2014). La première preuve fossile de ces plantes en dehors du sous-continent indien provient effectivement de la Fm. de Pondaung. Les bois fossiles qui y ont été découverts indiquent un gradient de végétation allant d'une végétation côtière de type mangrove à l'ouest à des forêts de type pervenche plus à l'est à l'intérieur des terres (Licht et al., 2014a ; Licht et al., 2015). A la fin de l'Eocène, on a assisté à une baisse spectaculaire du niveau de la mer, des températures au fond et à la surface des océans, ainsi qu'à une extension du bouclier de glace antarctique permanent (Zachos et al., 2001 ; Liu et al., 2009 ; Westerhold et al., 2020). Cela s'est accompagné d'un changement massif de la biodiversité dans les faunes terrestres d'Europe, où cet événement est connu sous le nom de Grande Coupure (Stehlin, 1909), et d'Asie (Sun et al., 2014 ; Ni et al., 2016).

Après une courte phase de réchauffement à la transition entre l'oligocène et le miocène, qui a abouti à l'optimum climatique du miocène, la tendance au refroidissement graduel se poursuit (Zachos et al., 2001). D'autres déplacements de plaques tectoniques entraînent un rétrécissement et parfois un assèchement total de la Téthys. Il en résulte la formation d'un pont terrestre qui entraîne de nombreux échanges de flore et de faune entre l'Afrique et l'Asie, notamment l'Asie du Sud-Est (Harzhauser et al., 2007). Au Miocène moyen et tardif en Thaïlande, on trouve une grande variété de types de végétation différents, allant des forêts tropicales aux habitats de type savane (Badgley et al., 2008). Un degré accru de saisonnalité et un climat de plus en plus sec ont entraîné une fragmentation des habitats forestiers, ce qui a conduit à la disparition de nombreuses espèces frugivores vivant en forêt (Badgley et al., 1988 ; Nelson, 2003, 2005 ; Badgley et al., 2008). Au lieu de cela, les plantes C_4 adaptées au climat sec ont fait leur entrée. Elles se sont répandues d'Afrique en Asie, où elles sont d'abord attestées au Pakistan dans des sédiments datés de 9,4 Ma (Morgan et al., 1994). Une première

preuve de ces plantes au Myanmar provient d'un site de l'Irrawaddy Fm daté de 6 Ma. (Thein et al., 2011).

Les deux groupes de primates, qui sont au centre de ce travail et qui ont habité les habitats éocènes et miocènes d'Asie du Sud-Est que nous venons de décrire, sont les primates anthropoïdes et hominoïdes. En ce qui concerne le premier groupe taxonomique, ces dernières années on a beaucoup discuté le lieu de leur radiation initiale et la voie par laquelle ils se sont répandus à partir de là. L'Afrique et l'Asie ont été considérées comme des lieux d'origine possibles. Les primates éocènes trouvés dans les formations fossiles d'Asie ont été au centre de ces discussions. Alors que certains chercheurs les ont classés comme primates anthropoïdes primitifs (Jaeger et al., 1998; Chaimanee et al., 2000; Beard, 2002; Marivaux et al., 2003; Beard, 2004; Jaeger et al., 2004; Beard et al., 2005; Beard et al., 2007; Bajpai et al., 2008; Rose et al., 2009a; Marivaux et al., 2010; Jaeger et al., 2019), d'autres se sont prononcés en faveur de l'idée que les caractères morphologiques utilisés pour cette classification étaient des exemples d'évolution convergente en tant qu'adaptation des singes fossiles à nez humide (Strepsirrhini) à la durophagie (Ciochon and Holroyd, 1994; Ciochon et al., 2001; Ciochon and Gunnell, 2002b; Gunnell et al., 2002; Ciochon and Gunnell, 2004; Gunnell and Ciochon, 2008). Les découvertes de nouveaux primates fossiles, comme la description de *Bahinia* (Jaeger et al., 1999) et l'étude des éléments crâniens associés avec des éléments postcrâniens du genre *Ganlea* (Jaeger et al., 2020) ont pu confirmer la classification phylogénétique comme représentants primitifs des anthropoïdes.

Contrairement aux primates anthropoïdes, la question de la localisation de la radiation originelle est moins prégnante avec les primates hominoïdes. La diversité d'espèces de la famille des Ponginae bien plus importante du Miocène au Pléistocène semble plus remarquable. Aujourd'hui, le genre *Pongo* est le seul représentant de cette famille. Il est encore présent dans une aire de répartition très restreinte à Sumatra et Bornéo. Au Miocène, en revanche, on connaît des découvertes de différents genres et espèces dans une région allant de la Turquie au sud de la Chine. *Khoratpithecus*, et en particulier l'espèce *Khoratpithecus ayeyarwadyensis* trouvée dans l'Irrawaddy Fm, est au centre de mon travail pendant mon projet thèse (Jaeger et al., 2011). Trois autres espèces de ce genre sont attestées en Thaïlande au Miocène moyen et final de la Thaïlande (Chaimanee et al. 2022 ; Chaimanee et al. 2003 ; Chaimanee et al. 2004). La question des continuums écologiques dans les préférences d'habitat et le régime alimentaire des différents représentants des Ponginae fossiles et du genre *Pongo* moderne est essentielle pour notre compréhension de l'histoire évolutive de ces grands singes et pour la conservation et la protection des orangs-outans aujourd'hui.

L'un des grands thèmes de ce travail est la modélisation des niches de la faune des mammifères et leur utilisation pour l'évaluation de la dynamique dans les écosystèmes et les habitats des primates anthropoïdes et hominoïdes. Le concept de niche de Hutchinson est utilisé pour ces analyses (Hutchinson, 1957). La niche d'une espèce ou d'un groupe taxonomique est un hypervolume à n dimensions.

Chaque dimension représente un facteur biotique ou abiotique. Chaque point dans cet hypervolume corresponde à un environnement avec des caractéristiques favorables pour la persistance d'une espèce. Jusqu'à présent ce concept a surtout été utilisé dans le cadre de reconstitutions alimentaires et d'études sur l'écologie trophique dans les recherches archéologiques et paléontologiques. Cependant, j'analyserai ici les isotopes stables du carbone et de l'oxygène, ce qui correspondent aux dimensions écologiques et plus généraux de la niche. Cette approche a été utilisée déjà une fois sous une forme similaire par Nelson et Hamilton (2017). Mais elles se sont concentrés sur les changements de la base alimentaire des hominidés anciens en relation avec les changements écologiques.

L'une des deux méthodes analytiques que j'ai utilisées dans ce travail est l'étude des micro usures de l'émail dentaire qui se produisent pendant le processus de mastication, principalement par abrasion. Les particules abrasives, dont font partie les aliments, sont broyées entre deux dents antagonistes par des mouvements de mastication cycliques et répétitifs. Il en résulte des facettes délimitées qui correspondent à différentes phases de ce processus de mastication (Crompton and Hiiemae, 1969; Kay and Hiiemae, 1974; Ungar, 2015). Chaque fois que de la nourriture est consommée, de nouvelles microstructures apparaissent et en écrasent d'autres. Cette méthode de reconstruction alimentaire reproduit donc le régime alimentaire des semaines précédant la mort d'un individu (Grine, 1986). La rapidité avec laquelle le signal alimentaire dans la micro usure dentaire est recouvert par de nouvelles microstructures dépend des propriétés physiques et mécaniques des aliments. Les objets plus durs entraînent un taux de rotation plus rapide que les objets mous (Teaford and Oyen, 1989; Teaford et al., 2017; Winkler et al., 2020; Teaford et al., 2021). Les méthodes traditionnelles quantifient les structures spécifiques à l'aide de représentations 2D de la surface dentaire, ce qui demande beaucoup de temps et entraîne des erreurs importantes entre les évaluations de deux observateurs (Grine et al., 2002; Galbany et al., 2005; Mihlbachler et al., 2012; DeSantis et al., 2013). Mes analyses utilisent une méthode plus objective qui consiste à enregistrer la surface des dents en 3D. De ces représentations on extrait ensuite différents paramètres, qui servent à distinguer les aliments ayant des propriétés physiques et mécaniques différentes (Scott et al., 2006).

La deuxième méthode analytique, l'analyse des isotopes stables du carbone et de l'oxygène, se concentre également sur l'émail dentaire. Les différences de masse des isotopes, causé par le nombre diffèrent de neutrons dans le noyau atomique, entraînent un fractionnement pendant des processus physiques et chimiques. Pendant la minéralisation de l'émail, les isotopes du carbone et de l'oxygène sont incorporées dans l'émail. Les changements dans la présence des différents isotopes par rapport à leur rapport naturel sont ainsi fixés et permettent de faire des inférences sur le climat, la nutrition, l'écologie et la structure de l'habitat. La forte teneur en hydroxyapatite ($Ca_{10}(PO_4)_6(OH)_2$) (96 - 99 %) ainsi que la structure cristalline dense et fine de l'émail dentaire rendent ce tissu résistant aux

changements taphonomiques. Les isotopes du carbone permettent surtout d'obtenir des informations sur la végétation à la base d'un réseau alimentaire. Les plantes C_3 ont des valeurs de $\delta^{13}C$ nettement plus faibles (-20 à -37 ‰ (Kohn, 2010)) que les plantes C_4 adaptées à un climat sec (-10 à -20 ‰ (Bender, 1971)). De plus, les valeurs $\delta^{13}C$ diffèrent selon le degré de fermeture de la canopée et permettent donc de tirer des conclusions sur la structure de la végétation (ouverte, légèrement ou densément boisée) (Bonafini et al., 2013; Krigbaum et al., 2013; Lowry et al., 2021). Les isotopes stables de l'oxygène de l'émail reflètent la composition des précipitations. Combinés à une stratégie d'échantillonnage en série, ils sont bien adaptés pour reconstruire les variations saisonnières de la température dans les zones tempérées et des précipitations dans les zones tropicales (Dansgaard, 1964; Pederzani and Britton, 2019). Au sein d'une faune de mammifères, les isotopes de l'oxygène peuvent fournir des informations sur la stratification verticale de l'utilisation de l'habitat (Fannin and McGraw, 2020; Louys and Roberts, 2020; Lowry et al., 2021) ainsi que sur le style de vie semi-aquatique de certaines espèces ou de certains groupes taxonomiques (Bryant and Froelich, 1995; Clementz et al., 2008).

As my dissertation project spans two different geological eras, two fossil formations, although they are from the same geographic area, and uses two distinct methodologies, most sections of the introduction will also be split into two parts. This way I can set the stage for all of the paleoecological and –dietary reconstructions that I will discuss in the Results and Discussion chapter. The main actors are the primates from each mammal community, namely the early anthropoid primates from the late Middle Eocene Pondaung Fm. and the pongine primates from the late Miocene Irrawaddy Fm. In case of the subfamily Ponginae the time frame needs to be expanded further, as questions about ecological and dietary continuity from the Miocene to the Pleistocene genera and extant Pongo, will be central discussion points in this dissertation.

The UN Statistics Division considers Brunei, Cambodia, East Timor, Indonesia, Laos, Malaysia, Myanmar, Philippines, Singapore, Thailand, and Vietnam to form the Southeast Asian region (https://unstats.un.org/unsd/methodology/m49 (18.1.2023)) (Fig. 1). However, as I am working in a paleontological context I will follow the definition of Kreft and Jetz (2010) of biogeographic regions as areas sharing similar faunas, floras, as well as homogenous climatic and environmental conditions. Therefore, I will also consider fossil mammal faunas from parts of Southern Asia, such as Pakistan, India, and Nepal, as well as Eastern Asia, mainly Southern China (Gibert et al., 2022) in my discussion and work on the paleoecology of the fossil anthropoid and hominoid primates from Southeast Asia.

Today, Southeast Asia is a biodiversity hotspot of global importance, as it is home to 20 – 25 % of plant and animal species of our planet, while only making up around 4 % of the Earth's land mass Woodruff, 2010; Corlett and Primack, 2011. Assessing paleobiodiversity of Cenozoic Southeast Asia is not that easy, given the patchy nature of the paleontological record. By its nature, the global paleontological record only provides snapshots of past biodiversity with the different fossil formations even within a biogeographic region being apart quite far on a temporal scale. It is therefore difficult to impossible to say with certainty that Southeast Asia was a global biodiversity hotspot already in the Cenozoic. However, there are some fossil formations in this biogeographic region that preserved rich fossil faunas documenting radiations and diversification in many clades. Two of them, the late Middle Eocene Pondaung Fm. and the late Miocene Irrawaddy Fm. will be the focus of my studies.

Fig. 1 Map of Southeast Asia with a visualisation of the four main biogeographic subregions: Indochina, Sundaland, Philippines, and Wallacea modifierd from (Woodruff, 2010). The orange square shows the approximate position of the Central Basin in Myamar, the location of the fossil formations, while the blue ellipse indicates the area from which the modern orangutans were collected by Emil and Lenore Selenka.

Climate and vegetation history of Cenozoic Southeast Asia

1.1. Characteristics of Eocene and Miocene environments

After the extinction of the dinosaurs a new geological era started, the Cenozoic, which is sometimes also called the Age of Mammals. In many ways the Cenozoic Earth was still a very different place to today. For example, the continents were not yet in the configuration that we know today (Fig. 2). During the Eocene the Indian tectonic plate moved northwards where it collided with the Eurasian tectonic plate in the middle Eocene. This led to the orogenesis of the Himalyas and the uplift of the Tibetan Plateau that was completed in the late Miocene (Ji et al., 2020 and references therein). New dispersal routes opened up, for example due to periodical Arabian-Eurasian continental connections in the late Early Miocene the closure of the Neotethys Seaway in the Middle Miocene (Harzhauser et al., 2007; Gibert et al., 2022).

The beginning of the Eocene was marked by a continuation of a global warming trend culminating in the Paleocene-Eocene thermal maximum (PETM) that lasted from 52 to 50 Ma. During that time global temperatures rose by ~6 °C, either dure to a rapid and massive releaseo of CO_2 or CH_4 release that was tehn rapidly oxidized to CO_2 (Kennett and Stott, 1991; Zachos et al., 2001). After this time period there there are two global climatic trends visible troughout the Eocene (Fig. 3). On the one hand there is a gradual cooling and on the other hand a decrease in CO_2 content in the atmosphere. These trends have been used to evaluate and model different climate change scenarios for the next centuries, depending on the (Tierney et al., 2020).

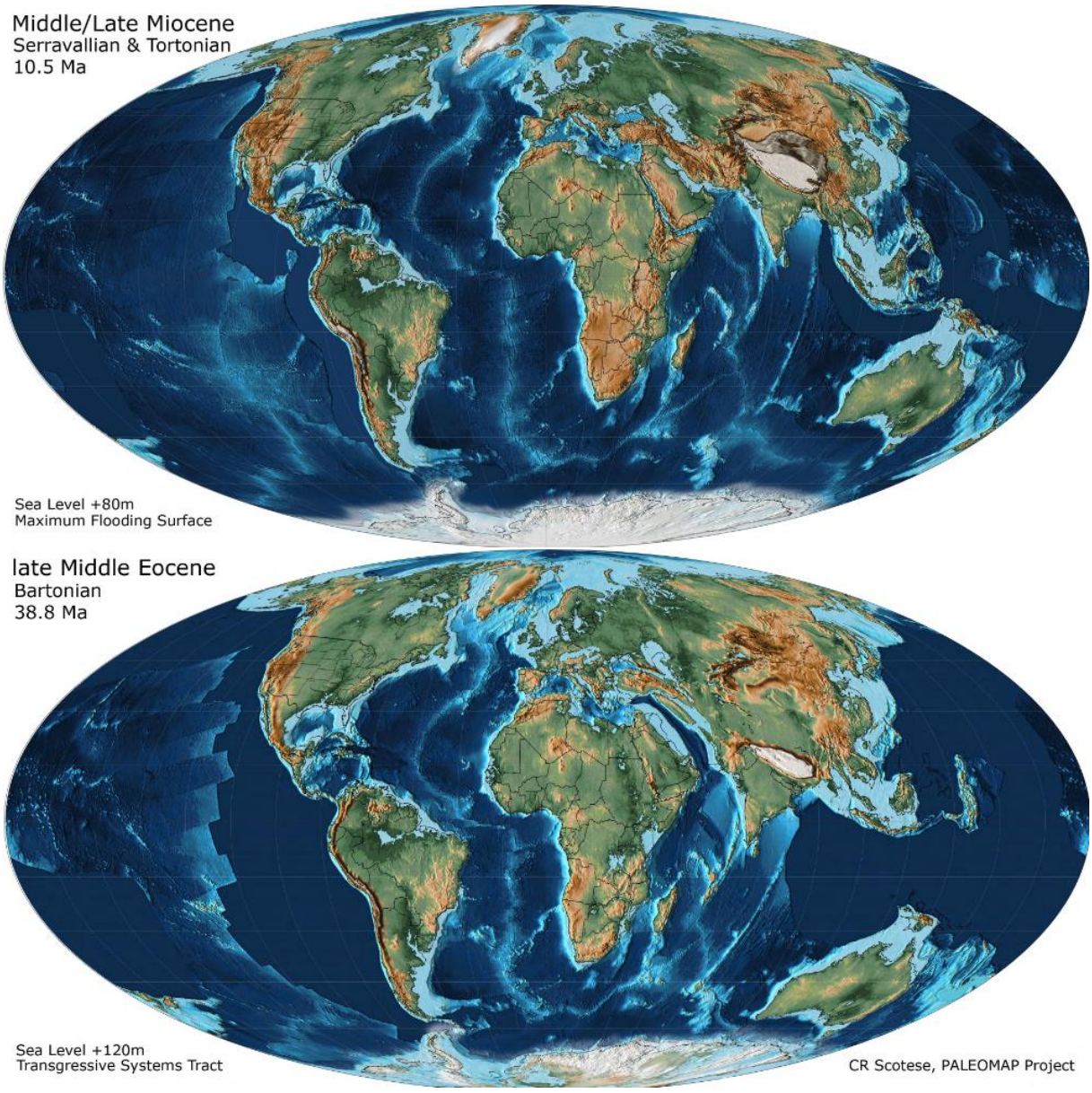

Fig. 2 Visualization of modelled continental configurations of the Middle/Late Miocene (10.5 Ma) (top) (Scotese, 2014a) and the late Middle Eocene (38.8 Ma) (bottom) (Scotese, 2014b).

The decrease in mean temperature throughout the Eocene climaxed in an event called the Eocene-Oligocene transition that was marked by a shift in oxygen isotopes in deep sea cores dating to ~33.5 Ma. This indication of a temperature drop on the ocean floor was accompanied by similar drops in sea surface temperature and sea level, which were also correlated with the formation and expansion of permanent Antarctic ice shields (Zachos et al., 2001; Liu et al., 2009; Westerhold et al., 2020). These major climatic changes coincide with faunal turnover of terrestrial communities in Europe where it is termed “La Grande Coupure” (Stehlin, 1909) and Asia (Sun et al., 2014; Ni et al., 2016). Environmental changes in terrestrial ecosystems however seemed more varied in comparison with the globally quite homogenous climatic developments (Sheldon et al., 2016; Pound and Salzmann, 2017).

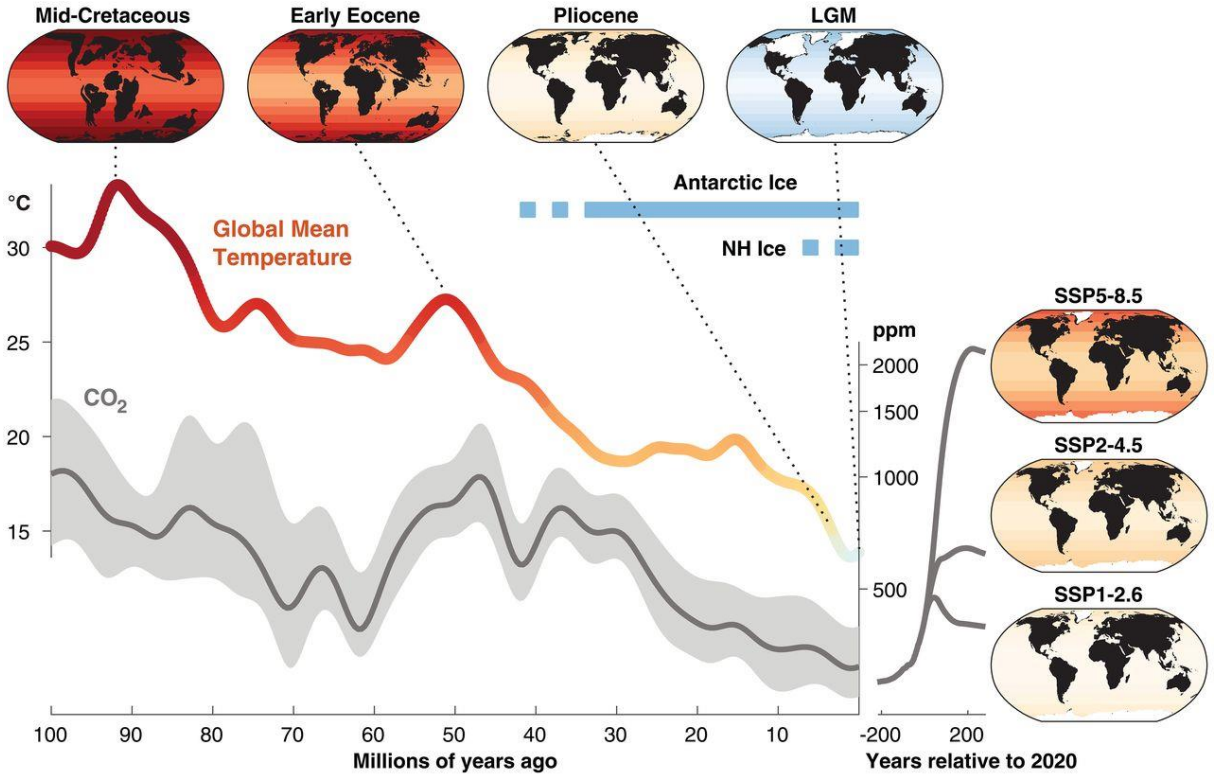

Fig. 3 Visualization of global mean temperature (°C) and atmospheric CO_2 content (ppm) in the past 100 million years, including three different modelled scenarios for future development of the earths atmosphere and glocal warming depending on CO_2 emmissions (Tierney et al., 2020).

In the course of the Miocene the Tethys Sea contracted and was eventually cut off from the Indian Ocean by the emergence of the Arabian Peninsula. Its remnants in the Mediteranean region dried up completely (Harzhauser et al., 2007). After a warming phase that reduced the Antarctic ice sheets starting in the late Oligocene and culminating in the Middle Miocene climatic optimum the gradual cooling proceeded. From the late Miocene onwards there was some glaciation in the northern hemisphere and the formation of Arctic ice shields (Zachos et al., 2001).

In the following two chapters I will discuss the broader climatic and environmental context of the two fossil formations that I studied for my dissertation, the late Middle Eocene Pondaung Fm. and the Late Miocene Irrawaddy Fm. Both are located in the Central Basin of Myanmar in more detail.

1.1.1.The late Middle Eocene

Today, the climate is changing fast and towards conditions never before experienced by humans. However, some geological time periods, such as the Eocene, might be important analogues for possible climate scenarios in the future (Fig. 3) (Burke et al., 2018; Tierney et al., 2020). Studying such time periods, their paleoenvironments, and the organization of fossil mammal communities living back then can provide valuable information to better understand various scenarios of future environments on Earth.

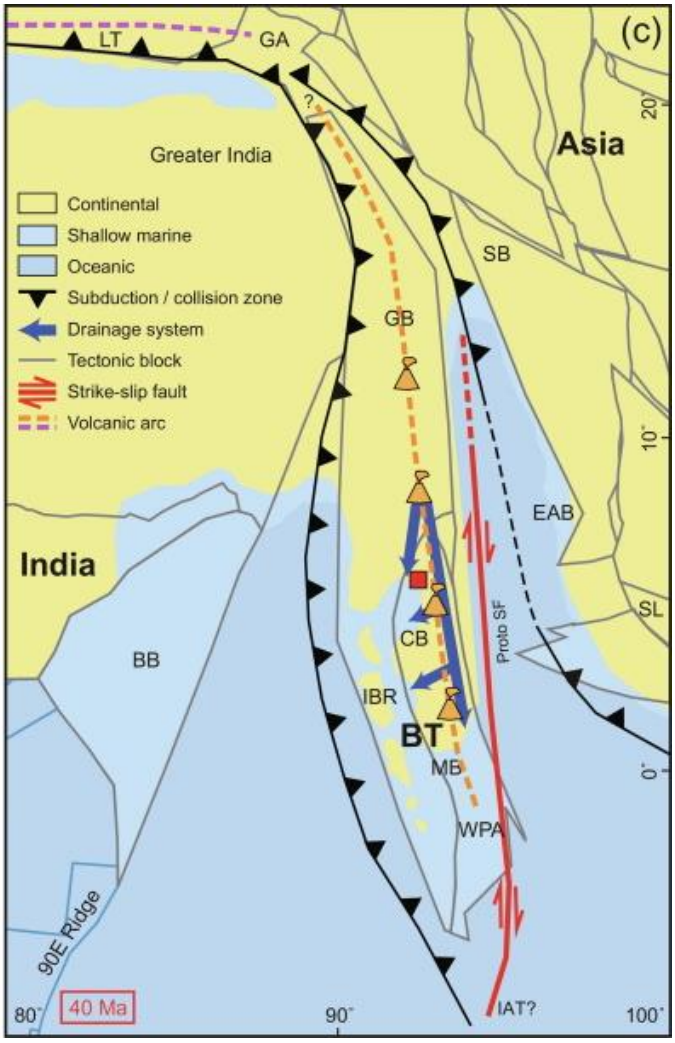

Fig. 4 Map showing the modelled paleogeographic location of the Central Basin of Myanmar (or more specifically the Chindwin Basin = CB) in the Late Eocene (Westerweel et al. 2020; Huang et al. 2023). The red square marks the position of the sampled section of the Yaw Fm. from which the vegetation model calculated. Other abbreviations: BB = Bay of Bengal, BT = Burma Terrane, EAB = Eastern Andaman Basins, Fm(s). = Formation(s), GA = Gangdese Arc, GB = Greater Burma, IAT = India-Australia Transform, IBR = Indo-Burman Ranges, LT = Lhasa Terrane, MB = Minbu Basin, SB = Sibumasu, SF = Sagaing Fault,

The Eocene was characterized climate conditions associated with a greenhouse world. Mean annual temperatures were around 5 °C higher than today in the Late Eocene (Zachos et al., 2001; Pagani et al., 2005). In spite of this increased temperature, the paleogeographic position close to the equator (~5 °N) (Fig. 4) (Westerweel et al., 2019; Westerweel et al., 2020), and the orogenesis of the Himalayas that was only in its earliest stages there already was an early or proto-monsoonal climate (Licht et al., 2014c; Huang et al., 2023). Temperature seasonality also increased from the middle to the late Eocene and across the Eocene-Oligocene transition. This trend likely was most pronounced in central Asia, where there was particularly strong cooling in winter (Toumoulin et al., 2022).

Southeast Asian dipterocarp rainforests are as the name suggests dominated by trees belonging to the family Dipterocarpaceae. They are most abundant in everwet areas such as the various islands on the Sunda Shelf, some parts of the Philippines and Sri Lanka. The first occurrence of trees belonging to this family, and therefore the first possible establishment of such habitats in Asia dates to the Middle Eocene around 45 Ma. At this time, these species have reached the Asian mainland from Africa probably via the Indian plate, which at that time got closer and closer to colliding with the Eurasian plate (Corlett and Primack, 2005, 2011; Corlett, 2014). From the Pondaung Fm. comes the first evidence of fossil dipterocarps outside the Indian subcontinent. In the distribution of the different fossil wood taxa a gradient

from coastal elements in the west over riparian to inland elements was apparent (Licht et al., 2014a; Licht et al., 2015).

1.1.2. The Late Miocene

Based on the tectonic requisites discussed in chapter 1.1 and pollen records the presence of a dispersal corridor between Africa and Southeast Asia was inferred for the Middle Miocene. The vegetation in the to some extent seasonal environment of the Ban Sa locality in northern Thailand is characterized by dominant lowland forests with interspersed tropical freshwater swamps with Syzgium a member of the Myrtaceae, which are evergreen shrubs and trees. It has been compared to extant African habitats that can for example be found at the headwaters of the White Nile (Chaimanee et al. 2003). Pollen analysis on different Middle and Late Miocene fossil localities across Thailand showed a high variability in vegetation types from tropical wood- and grasslands in the former to thermophilous forests indicating warm and relatively dry climate and grasslands in the latter (Sepulchre et al., 2010).

Other Late Miocene fossil formations in Asia document floras that are more temperate and an increased seasonality (Badgley et al., 1988; Nelson, 2003, 2005; Badgley et al., 2008). The impact on the fossil faunal communities was substantial, leading to the disappearance of many forest-dwelling taxa, especially those adapted to frugivory. Taxonomic groups that persisted throughout this climatic and environmental changes were forced to alter their dietary ecology (Badgley et al., 2008). The overarching climatic trends of decreasing temperatures, increasing aridity and seasonality were reflected in large-scale changes of vegetation structure throughout Southeast Asia. Conifer forests started to grow at the border of the Himalayas, there was an increase in the proportion of open forests interspersed with grasses, scrubs and savannah at the expense of seasonal evergreen, closed deciduous forests, and perhumid rain forests retracted from Indochina to Sundaland (Morley, 2018).

With the expansion of grasslands came the arrival of C_4 plants. They likely dispersed from Africa to Asia in the Late Miocene, where they were first recorded in Pakistan from sediments dating to 9.4 Ma (Morgan et al., 1994). Their presence has been demonstrated at the Irrawaddy Fm. from at least 6 Ma onwards (Thein et al. 2011). A link to the strengthening of the Indian monsoon at that time has been inferred for Central Asia (Wang et al., 2023).

1.2. Southeast Asia – a hotspot for primate evolution

In these Southeast Asian habitats with their tropical and humid climate with its rich and diverse vegetation, which I described in the previous chapter, many radiations of important eutherian mammal clades took place. A radiation is an elevation in speciation rates, which causes increasing taxonomic diversity (Simões et al., 2016). If this process is rapid and can be associated with the adaptation of a single lineage to its environment it is a case of adaptive radiation (Schluter, 2000). Although the next two sections will introduce only the primates, as they are the main players in this dissertation, many other clades had their origin in these time periods and geographical areas as well, which will be introduced when discussing the material on the mammal faunas associated with the primates from the Eocene and Miocene fossil formations from Myanmar.

1.2.1. The origin of anthropoid primates

There have been ongoing discussions about the place of origin of the anthropoid primates during the last century. Outside of Asia, the earliest anthropoid primates were found from the Late Eocene for example in Libya at 39 Ma (Jaeger et al., 2010), Algeria (Bonis et al., 1988), and Egypt (Seiffert et al., 2005). The debate arose over the phylogenetic attribution of the Eocene primates from Asia, for example the ones from the Pondaung Fm. While some authors were convinced that they were examples of an early radiation of stem anthropoids that later dispersed to Africa (Jaeger et al., 1998; Chaimanee et al., 2000; Beard, 2002; Marivaux et al., 2003; Beard, 2004; Jaeger et al., 2004; Beard et al., 2005; Beard et al., 2007; Bajpai et al., 2008; Rose et al., 2009a; Marivaux et al., 2010; Jaeger et al., 2019), others argued that the morphological similarities of these Eocene primates with those from the Paleogene of Africa were examples of adaptive convergence to durophagy (Ciochon and Holroyd, 1994; Ciochon et al., 2001; Ciochon and Gunnell, 2002b; Gunnell et al., 2002; Ciochon and Gunnell, 2004; Gunnell and Ciochon, 2008).

Before I summarize the most important arguments of both sides, it is necessary to clarify which morphological features are shared by all extant anthropoid primates. In the cranium these are a lacrimal bone in the highly convergent orbits with a vertical lacrimal ducts, postorbital closure, which leads to the isolation of the temporal muscles so as to not obstruct vision during chewing, no contact between the zygomatic and lacirmal bones as the lower orbital rim is formed by the maxilla, a retinal fovea instead of a tapetum lucidum, a short snout, and fusion of the metopic suture between the two halves of the frontal bone as well as at the mandibular symphysis, which is short and vertical. The last characteristic is associated with markedly less procumbent lower incisors, meaning that they are oriented more vertically on the mandible instead of outward. The teeth are bunodont and lower premolar roots are shifted. (Rose, 2006; Rossie and Smith, 2007; Fleagle, 2013). Colbert already proposed in the 1930s a relatively high mandibular corpus as another anthropoid feature (Colbert, 1937). The dental formula is 2.1.2/3.3 2.1.2/3.3, except in marmosets and tamarins, which only have two molars (Fleagle, 2013). The postcranium is characterized by a short trunk, forelimbs that are similar in length or longer than the hindlimbs, and nails instead of claws. In general, pronounced sexual size dimorphism between males and females is very typical in anthropoids (Fleagle, 2013).

Extant strepsirrhines on the other hand are most notably characterized by the presence of an orbital arch or bar instead of a full bony enclosure of the orbits, a downward oriented nose leading to a split of the maxillary bones and a medial orientation of the upper incisors, a lacrimal canal outside of the orbit, and olfactory nerves passing between the orbits. The lower incisors, sometimes also the lower canines form a tooth comb. While they also have nails instead of claws, their second digit can have a grooming claw (Rose, 2006; Fleagle, 2013).

Based on these and other morphological characteristics the phylogenetic affinities of the fossil primates from Asia were discussed. For example, Beard et al. (1994) used the deep jaw of the Eosimiidae to argue for their anthropoid affinities, which would validate the hypothesis of an Asian origin of anthropoid primates. The discovery of the eosimiid *Bahinia* in 1999 provided further compelling evidence for this hypothesis (Jaeger et al., 1999).

A critical point of debate about the affinities of the Pondaung primates were the postcranial remains. Until 2001, no postcrania of amphipithecid primates have been described. Two humeri, two ulnae, a calcanaeum, two shaft fragments and a vertebral centrum of a large-bodied primate in various states of preservation were found at the PK1 locality (NMMP 20). They were described as belonging to *Pondaungia* based on their size and the fact that this is the most abundant primate in the fossil record of the Pondaung Fm. Because of shared morphological features with North American notharctid adapiforms it was introduced as evidence for the relationship of amphipithecids with adapiformes (Ciochon et al., 2001). However, no diagnostic craniodental remains were found in association with these postcrania, making the attribution to *Pondaungia* questionable. The debate got even more heated, when Marivaux et al. (2003) described an isolated tarsal bone that exhibited derived anthropoid features and attributed it to an amphipithecid primate. After the discovery of a talus from Thandaung, both specimen have been attributed to *Pondaungia* (Marivaux et al., 2010), leading to a paradoxical situation, where one interpretation negated the other one.

One step towards solving the question of the phylogenetic attribution of amphipithecids was the discovery of the first undoubted sivaladapid primates from the Pondaung Fm. (Beard et al., 2007). This increased the paleobiodiversity of the Pondaung primate fauna and indicated that this fauna was most likely composed of both strepsirrhines and haplorrhines, a common composition found in younger Paleogene localities of the Old World. The similarities in morphology of the newly described calcanei with the one of NMMP 20 were evidence that NMMP 20 was an amphipithecid, but could represent a poorly-sampled large sivaladapid. Finally, the discovery of cranial and postcranial remains that were clearly associated with diagnostic dental remains, allowing a robust attribution to the amphipithecid *Ganlea megacanina*, provided critical information to the phylogenetic position of these primates (Jaeger et al., 2020).

There were enough cranial (e.g. lacrimal bone inside the orbit) and postcranial (e.g. long and oval shape of the trochlear notch) morphological features that unequivocally showed the anthropoid nature of this fossil primate. Thus, a recognition of Amphipithecidae as stem anthropoids is now necessary, which reinforces the hypothesis of an Asian origin of anthropoids in Asia and their diversification there (Jaeger et al., 2020).

In addition to the question about the origin of anthropoid primates and the phylogenetic attribution of the amphipithecids, the different scenarios of dispersal were also debated. It is still not completely resolved if there was only one or several dispersal events of primitive Asian anthropoid primates during the Eocene. However, the discoveries of different fossil primate specimen and other mammals that dispersed from Asia to Africa during the Eocene on both continents during the past decades is consistent with at least two dispersal events. First the eosimiiformes, which are known in Asia since the middle Eocene (~45 Ma) arrived in Africa around 39 Ma (Jaeger et al., 2010). The dispersal of other mammalian groups from Asia to Africa like hystriognathous and anomaluroid rodents (Sallam et al., 2009; Coster et al., 2015; Coster et al., 2018) was probably associated with this first dispersal wave (Jaeger et al., 2010). The anthracotheres on the other hand reached Africa not before the Latest Eocene. Their arrival could be linked with a second dispersal wave of more derived members of the diversified initial adaptive radiation of Asian anthropoid primates (Jaeger et al., 2019).

In the following two sections, I will give an overview about the morphology and ecology of the anthropoid and sivaladapid primate diversity found at the Pondaung Fm. A summary of the different taxa and some information on their size, behaviour, and diet can be found in Table 1, while a compiled table of all primate fossils found at the Pondaung Fm. with information on their taxonomic identification, locality, museum number and references can be found in in Table SI 1 in Appendix II.

Stem anthropoid primates from the Pondaung Fm.

Three different families of anthropoid primates occur in the Pondaung Fm. The Eosimiidae and the Afrotarsiidae, which together form the infraorder Eosimiiformes, are most basal groups of anthropoids, whereas the Amphipithecidae are more diverse, and more closely related to crown anthropoids (Fig. 5). A third species of anthropoids (*Aseanpithecus myanmarensis*) with unresolved phylogenetic affinities will also be described in this section. These anthropoid primate families are endemic to Asia, with the exception of *Afrotarsius*, which is found in the Eocene of Africa as well (Bonis et al., 1988; Jaeger et al., 2010).

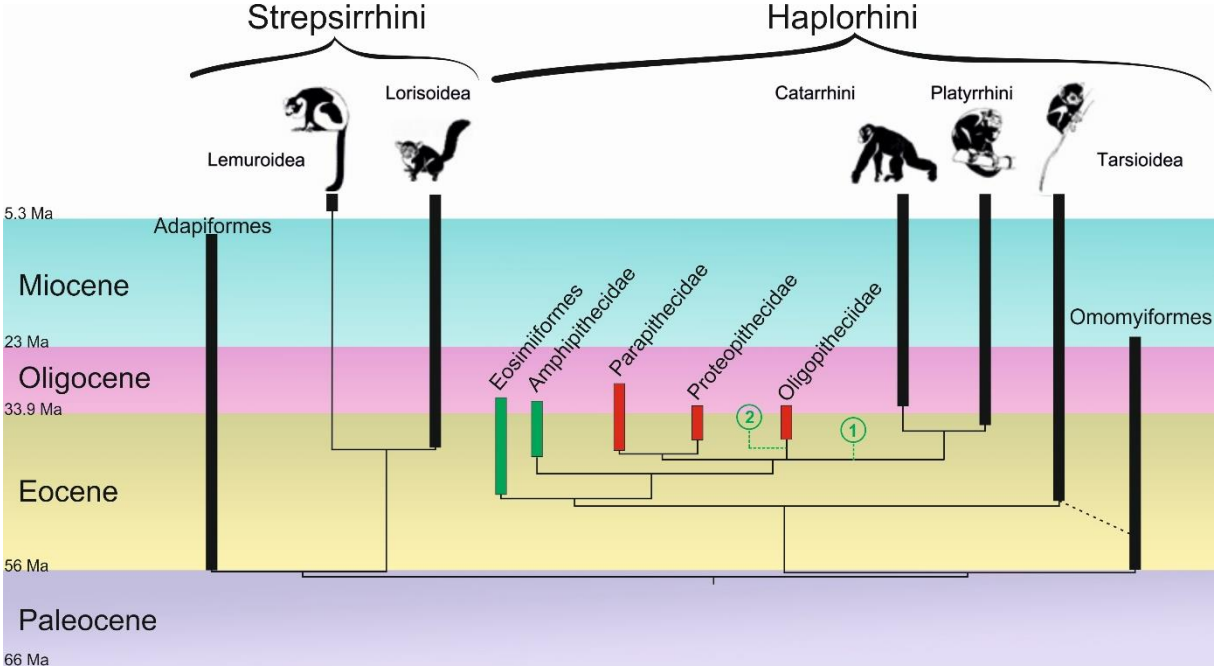

Fig. 5 Overview of the phylogeny and visualisation of estimated divergence times based on (Williams et al., 2010; Coster et al., 2013) The circles (1, 2) mark possible phylogenetic positions of Aseanpithecus. The figure was originally published in a blog post by Olivier Chavasseau and Jean-Jacques Jaeger accompanying the publication of their paper (Jaeger et al., 2019) (https://go.nature.com/2GNPWqg (26.03.2023)).

At the Yarshe Kyitchaung locality, an anthropoid primate , *Bahinia pondaungensis*, belonging to the family Eosimiidae was found (Jaeger et al., 1999). Until now, the Eosimiidae are considered the most primitive of all known anthropoid primates. It is the first occurrence of the genus *Bahinia* and this species, documented by the left and right parts of a maxilla with an associated mandibular fragment (NMMP-14, NMMP-15, and NMMP-16). Its dental formula (2.1.3.3) with three upper and lower premolars and the dorsoventrally deep symphyseal region of the mandible (Jaeger et al., 1999). These are two features that connect it with African anthropoids like *Afrotarsius libycus* with which it also shares similarities in size and age, thus establishing a tight morphological and temporal connection between Asian and African

anthropoid faunas (Jaeger et al., 2010). It is the only eosimiid known from Myanmar. *B. pondaungensis* is a small primate with an estimated body mass of around 480 g (CI 95 % = 240 – 990 g) (Ramdarshan et al., 2010). It is larger and morphologically more derived than the other described species *Eosimias sinensis* and *Eosimias centennicus* from eastern China with body masses of 67 – 137 g and 91 – 179 g respectively (Beard et al., 1994; Beard et al., 1996), and *Eosimias dawnsonae* and *Phenacopithecus xueshii* from central China (Beard and Wang, 2004). Given its tooth morphology and body mass, it likely was insectivorous. Body mass can be an indication of a primates diet as it correlates significantly with the primary dietary protein source. Kay's threshold (Kay, 1984) and the Jarman/Bell principle (Bell, 1971; Geist, 1974; Jarman, 1974), which describes this scaling relationship between body size and metabolism, predict that primates larger than 500 g cannot sustain themselves on an insectivorous diet. However, male aye-ayes for example have shown that morphological and/or behavioural adaptations can enable animals to be insectivores even though they are as heavy as 2.5 kg (Sefczek et al. 2020). An analysis of the shearing quotients of M_1 and M_2 showed that besides insects, fruit were a main component of *Bahinia*'s diet (Ramdarshan et al., 2010).

Eosimias paukkaungensis, a species based on two mandible fragments, one with an M_3 the other being edentulous (Takai et al. 2005), will be regarded here as being synonymous with *B. pondaungensis* given the similarities in size and morphology following Chaimanee et al. (2012).

Another small anthropoid primate found at the Pondaung Fm. is *Afrasia djijidae*, an eosimiiform likely phylogenetically close to Eosimiidae like *B. pondaungensis*. With its body mass between 94 and 198 g, it is smaller than *Bahinia*, from which it also differs in having less bunodont cusps in its upper molars. Its dental morphology attest to close relations to the African Eosimiiforme *Afrotarsius*. Phylogenetic analysis have shown them to be sister-groups and an attribution to the new family Afrotarsiidae has been proposed (Chaimanee et al., 2012). Until now, the fossil record of this species is very poor with only four isolated teeth. Hence, little is known about its behaviour or diet. With its small body mass, it lies well below Kay's threshold. Therefore, insects are likely to be the primary protein source (Kay, 1984). In addition, the teeth of *Afrasia* possess pointed cusps and sharp crests, which is compatible with a predominantly insectivorous diet.

Table 1 Summary of the Pondaung primate fauna regarding their occurrences at the various localities of the Pondaung Fm., body mass (BM), and behavioural and dietary ecology. The references for each species include publication of their first description and the main references used to summarize BM and behavioural aspects. A list of all Pondaung primate specimen, the fossil locality where they have been found and reference to the publication they have been published in can be found in Table SI 1 in Appendix II. Body mass estimates from Ramdarshan et al. (2010) and Egi et al. (2004) (for M. yarshensis) have been used preferably. If not available in these two publications, estimates are from the literature listed under References. The basis for the summary of the diet are the studies by Kay et al. (2004) and Ramdarshan et al. (2010), with the inferred primary dietary component with the addition of secondary dietary components in brackets.

TAXONOMY	LOCALITY	BM	BEHAVIOUR	DIET	REFERENCES
ANTHROPOIDEA					
Aseanpithecus myanmarensis (Fam.incert. sedis)	PK2	2.8 – 3.4 kg	diurnal	Leaves fruit (dental morphology)	(Jaeger et al., 2019)
Amphipithecidae					
Myanmarpithecus yarshensis	PK2, PK 12, Yarshe	1.8 kg	–	Leaves, fruit	(Takai et al., 2001; Beard et al., 2009)
Ganlea megacanina	Ganle, PK2 Than U Daw, Nyaungpinle, Thamingyauk	2.3 kg	Diurnal, arboreal quadruped	Leaves, fruit, possibly seeds	(Beard et al., 2009; Jaeger et al., 2020)
Pondaungia cotteri	Pangan 1, Pangan 2, Changan, Yarshe, Lema Kyitchaung, PK1, PK3, PK4, PK5, MGG2	5.5 – 6.4 kg	Diurnal, active arboreal quadruped	Fruits, nuts and seeds (leaves)	(Pilgrim, 1927; Shigehara et al., 2002; Marivaux et al., 2003; Marivaux et al., 2010)
Eosimiiformes					
Afrasia djijidae	PK2, Nyaungpinle, Thaminyauk	94 – 108 g	–	Insectivorous (based on Kay's threshold and dental morphology)	(Kay, 1984; Chaimanee et al., 2012)
Eosimiidae					
Bahinia pondaungensis	Yarshe, PK2, Nyaungpinle	480 g	–	Fruit (insects)	(Jaeger et al., 1999; Beard et al., 2007)
ADAPIFORMES					
Sivaladapidae					
Kytchaungia takaii	PK2, Thamingyauk	1.57 – 1.77 kg	Active arboreal quadruped, some leaping, climbing and hindlimb suspension possible	More folivorous than *P. parva*	(Beard et al., 2007; Marivaux et al., 2008b)
Paukkaungia parva	PK2, Nyaungpinle	270 g	–	Fruit (insects)	(Beard et al., 2007)
Gen et sp. indet.	PK1	5 – 6 kg	Active arboreal quadruped	–	(Ciochon et al., 2001; Beard et al., 2007; Marivaux et al., 2008a)

The most diverse primate family from the Pondaung Fm. are the Amphipithecidae, which are endemic to Southeast Asia and have now been confirmed to be stem anthropoids (Jaeger et al., 2020). We know three different genera from the Pondaung Fm., namely *Ganlea*, *Myanmarpithecus,* and *Pondaungia,* as well as *Siamopithecus eoceanus* from the late Eocene Krabi fossil locality in Thailand (Chaimanee et al., 1997) (Fig. 6).

The first primate that was discovered and described from the Pondaung Fm. was *Pondaungia cotteri*. Cotter discovered the first specimens in 1914 near the Pangan village. They were published by Pilgrim (1927). It is the largest amphipithecid primate from the Pondaung Fm. with an estimated body mass of 5.5 kg (CI 95 % = 2.2 – 13.5 kg) for *Pondaungia cotteri*. *Amphipithecus mogaungensis* is here not considered as a separate species, but as synonymous with *P. cotteri* and exhibiting sexual size dimorphism as suggested by Jaeger et al. (2004). The body mass reported of *A. mogaungensis* by Ramdarshan et al. (2010) is 6.4 kg (CI 95 % = 2.6 – 16 kg), and is thus regarded as indicative for male *Pondaungia*. Only *Siamopithecus eoceanus*, an amphipithecid from Krabi in Thailand (latest Eocene) was bigger with an estimated body mass of 10.2 kg (CI 95 % = 3.95 – 26.28 kg) (Ramdarshan et al., 2010). The diet of *Pondaungia* has been described by Kay et al. (2004) as consisting of nuts and seeds, in a later dental microwear study it was discovered that leaves were a secondary dietary component (Ramdarshan et al., 2010). Its thickly enamelled molars with poorly developed crest are consistent with the ingestion of hard objects. A small orbit size has been inferred from the inflated suborbital region of a *Pondaungia* cranium, thus indicating a diurnal activity pattern (Shigehara et al., 2002). The morphology of the two tali attributed to *Pondaungia* indicate an active arboreal quadrupedal locomotion for movement along broad, subhorizontal branches without any specializations for leaping and climbing (Marivaux et al., 2003; Marivaux et al., 2010).

Myanmarpithecus yarshensis is a medium-sized amphipithecid comparable in size to extant titi monkeys (*Callicebus*) from South America (Takai et al., 2001). Egi et al. (2004) estimate its body mass to be 1.8 kg (CI 95 % = 660 g – 3.9 kg). Its cingular hypocones on the upper molars and the lacking paraconids on M_{2-3} distinguish it from *Bahinia*. *M. yarshensis* has smaller canines than *Ganlea megacanina* (see next section). A shallower mandibular corpus, deeper molar basins, less inflated molar cusps, and a protocone in an oblique position on the upper molars further differentiates it from *Pondaungia* and *Ganlea*. (Jaeger et al., 2004; Beard et al., 2009) Kay et al. (2004) suggested a mix of fruits and leaves as the diet of *Myanmarpithecus*. In their microwear study, Ramdarshan et al. (2010) identified leaves as the primary dietary resource, which also was the main source of proteins in the fossil primates' diet. As only one maxilla and several mandibular fragments have been found no information on locomotion or other behavioural aspects are available.

Ganlea megacanina is intermediate in size between *Myanmarpithecus* and *Pondaungia* (body mass estimate = 2.3 kg, CI 95 % = 990 g – 5.2 kg) (Ramdarshan et al., 2010).The most apparent morphological feature that distinguishes *G. megacanina* from the other amphipithecids are its greatly enlarged canines relative to the M_1. With a length of 5.9 mm and a width of 4.3 mm the right canine of the holotype (NMMP 70) is even larger than canines of the much bigger *Pondaungia*. Unfortunately, the original crown height cannot be estimated, as the tooth has been worn almost down to the root. Although hypertrophied canines are common in male

anthropoid primates, which do have sexual dimorphism, this cannot be the only explanation for the size of the *Ganlea* canines. It is likely also connected to its dietary habits (Beard et al., 2009; Jaeger et al., 2020). Living anthropoid primates that have enlarged canines use them to husk hard fruits or for seed predation, for example in South American pitheciines (Kinzey, 1992; Plavcan and Ruff, 2008). Although its molar structure is consistent with a diet consisting of fruits and seeds dental microwear analysis indicates a folivorous diet with the addition of fruit (Ramdarshan et al., 2010).

Recently, the first cranial and postcranial bones that can be securely attributed to the amphipithecid *G. megacanina* have been described. The small size relative to tooth size of the preserved orbit suggests a diurnal activity pattern. Both the long and oval shape of the radial notch with a weak supinator crest distal from the joint surface and the length of the olecranon process are most similar to *Aegyptopithecus* (YPM 23940) known from the Early Oligocene Jebel Qatrani Fm. located at the Fayum Depression in Egypt. An arboreal quadrupedal locomotion pattern therefore has been inferred for *G. megacanina* (Jaeger et al., 2020).

The large to hypertrophied canines with a high degree of apical wear in all three amphipithecid genera from Myanmar suggests that they were hard objects feeders and it has been suggested that they might have been ecological equivalents to extant New World pithecine monkeys. In these, there are also sympatric species that have similar dietary ecologies in general. Competition pressure is reduced to enable the use the same habitat in this case through their use of various canopy layers and morphological adaptations that allows them to exploit resources from different microhabitats (Beard et al., 2009).

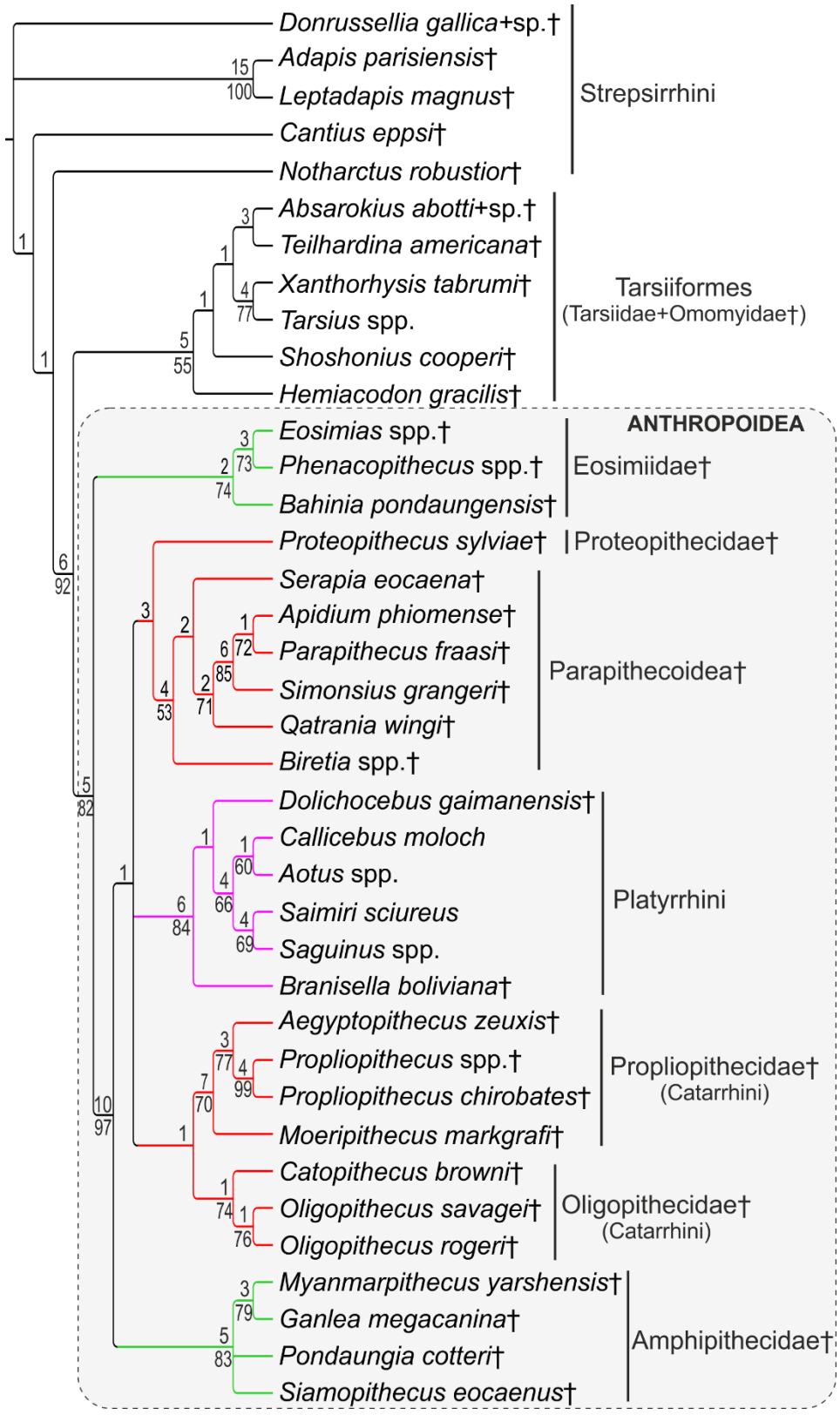

Fig. 6 Phylogenetic analysis of early anthropoid primates. The colours of the branches correspond to geographical provenance of the taxa (red: Proteopithecidae, Parapithecoidea, Propliopithecidae, and Oligopithecidae from Afro-Arabia; green: Eosimiidae and Amphipithecidea from Asia; magenta: Platyrrhini from South America). The numbers correspond to Bremer support values and bootstrap frequencies above and below the nodes respectively. Modified from (Jaeger et al., 2020). Afrotarsiidae, which are not displayed in this phylogeny, have been found as basal anthropoids and as the sister-group of Eosimiidae by Chaimanee et al. (2012).

Recent phylogenetic analysis (Fig. 6) have resolved the relationship and familiar attribution of most anthropoid primates known from the Pondaung Fm. until now. The sister group to the Eosimiidae, the Afrotarsiidae, which together form the infraorder Eosimiiformes is not shown in this figure. In the phylogenetic analysis supporting this attributions the level of bootstrap support (97 at 1000 replications) and the robust Bremer index (5) were surprising given the poor fossil record of *Afrasia* consisting of only four isolated teeth (Chaimanee et al., 2012). However, as of now there is still one genus of anthropoid primate from the Pondaung Fm. whose phylogenetic position has not been resolved.

Aseanpithecus myanmarensis is an anthropoid primate known from an upper and a lower jaw fragment as well as a lower M_3 found at the PK 2 locality (NMMP-93, NMMP-95, NMMP-96). It has been described as a medium sized primate weighing between 2.8 and 3.4 kg and similarly sized tooth as extant *Ateles*. Although the fossil record of this species is poor until now, it has been proposed to document a new family of Asian anthropoids. Their more primitive cranial morphology shares characters with the stem group of all other anthropoids, the eosiimiforms, whereas its dental morphology is more derived and different from the one of the sympatric Amphipithecidae (Jaeger et al., 2019). Their tooth morphology is similar to the ancestral upper molar morphotype of crown anthropoids proposed by Gunnell and Miller (2001) like African *Talahpithecus* (Jaeger et al., 2010)and South American *Perupithecus* (Bond et al., 2015), but more bunodont with lower cusps and absent hypocone and pericone.

Other Eocene primates from the Pondaung Fm.

In addition to the diverse Eocene anthropoid primate fauna, there is also a fossil record of two genera of sivaladapid primates. Sivaladapids are Asian adapiforms and underwent an important radiation beginning in the Eocene of Asia. The biogeographic distribution extended from China, to Thailand, and Myanmar in the Eocene. They were present in Asia throughout the Oligocene until the Late Miocene where they occurred alongside fossil hominoids. The Sivaladapidae have been defined based on Miocene genera. The close phylogenetic relationship between Eocene and Miocene genera was clarified by the discovery of a morphologically intermediate form, *Guangxilemur*, known in the late Eocene of China and the early Oligocene of Pakistan (Qi and Beard, 1998). According to recent phylogenetic analyses (e. g. Seiffert et al., 2018; Chavasseau et al., 2019), the Sivaladapidae have no close relationship to the crown strepsirrhines. Rose et al. (2009b) proposed that the Asian Early Eocene family Asiadapidae may be closely related to sivaladapids. The attribution of isolated teeth and postcranial elements from the Pondaung Fm. to the family Sivaladapidae was done by comparisons with other Paleogene representatives of the group (*Rencunius*, *Guangxilemur*, *Hoanghonius*, *Wailekia*).

The medium-sized adapoid primate from the Pondaung Fm. is *Kytchaungia takaii*, a medium sized primate from which both dental and postcranial remains have been described (Beard et al., 2007; Marivaux et al., 2008b). The holotype of *K. takaii* is an isolated lower molar, interpreted as a M_2. It differs from other sivaladapids, for example *Guangxilemur*, by its lower and less pronounced cusps of the entoconid and hypoconulid and a more buccal crista obliqua. The main difference between *K. takaii* and *P. parva* is size together and more bunodont teeth, which are consistent with a more folivorous diet of the former than the latter (Beard et al., 2007). While the holotype of *K. takaii* was found at the PK2 locality, the postcranial elements

come from another locality, Thamingyauk. The three tarsal bones and the proximal femur fragment have been ascribed to *Kyitchaungia* based on their sivaladapid characteristics and their appropriate size. The body mass inferred from the tarsal bones ranges from 685 g to 2.15 kg, while the estimates based on the femoral head dimensions are 1.57 kg (FHA = anteroposterior maximal femoral head diameter; CI 95 % = 0.68 – 3.61 kg) and 1.77 kg (FHH = femoral head height; CI 95 % = 0.97 – 3.24 kg). Functional morphological traits in the postcrania indicate active arboreal quadrupedalism with some proficiency in leaping. Branch walking and running were also important for this primate, but its hip joint morphology also allowed for relatively complex movements, making it possible that climbing and maybe some hindlimb suspension was part of the locomotor repertoire of *K. takaii* (Beard et al., 2007; Marivaux et al., 2008b).

Paukkaungia parva had a body mass of 270 g (CI 95 % = 85 – 850 g) (Ramdarshan et al., 2010). Inferred from the shearing quotients of M_1 and M_2, its diet was composed of fruits and insects, which likely were the main source of protein given its small body mass (Ramdarshan et al., 2010). It is the smallest sivaladapid that we know with only the eosimiid *Bahinia* being similar in size. Due to marked differences in dental morphology and the well documented dentition of *B. pondaungensis*, differentiating between the two is not problematic (Jaeger et al., 1999). Its lower molars are characterized by a weakly differentiated entoconid, a deep postcristid notch separating the hypoconulid from the hypoconid, and with mesiodistally less compressed trigonids than in other sivaladapids, such as *Wailekia* and *Guangxilemur*. In addition, its premolariform P_4 is markedly taller and mesiodistally longer than the P_3. All of these morphological features differentiate *P. parva* from other sivaladapids (Beard et al., 2007). As its fossil record only consists of isolated teeth, nothing can be said about its locomotion.

During the discussion of the different hypothesis about the origin of the earliest anthropoid primates and the phylogenetic affinities of Amphipithecidae, I have already introduced the postcranial remains found at PK1 (NMMP 20). They probably represent one individual belonging to a third sivaladapid primate. The large bodied primate with a body mass of 5 to 6 kg (Ciochon et al., 2001; Marivaux et al., 2008a). Its locomotion pattern was that of an active arboreal quadruped that was, although not specialized in this behaviour, capable of some leaping similar and probably above-branch running, similar to the behaviour of extant Malagasy lemurids (Marivaux et al., 2008a).

1.2.2. Is there a fossil record of primates from the Oligocene in Asia?

For the longest time, there was no primate fossil from the Oligocene of Asia. The general hypothesis was that after the Eocene-Oligocene transition 34 Ma with its climatic deterioration no suitable primate habitats were left in Asia (Beard, 2002). This explanation was given for the disappearance of fossil primates from Asia similarly to other northern continents, such as Europe, during the same time, where in spite of an otherwise rich fossil record primates are almost unknown (Köhler and Moyà-Solà, 1999). So although the Oligocene fossil record from South and Southeast Asia is scarce, the absence of primate fossils could not only be caused by taphonomy but by actual climatic changes.

In the early 2000s, a diverse primate fauna was discovered from the coastal deposits of the Early Oligocene Lower Chitarwata Fm. from Pakistan (Welcomme et al., 2001). A fossil lemur (*Bugtilemur mathesoni*), a sivaladapid adapiform (*Guanxilemur singsilai*), and three anthropoid primates (*Bugtipithecus inexpectans* and two species of the genus *Phileosimias*) have since been described from this fossil formation (Marivaux et al., 2001; Marivaux et al., 2002; Marivaux et al., 2005). They attest the presence of some South Asian refugia habitats for primates after the dramatic cooling during the Eocene-Oligocene transition.

More recently, Ni et al (2016) have described an important primate-bearing locality in China. They proposed the hypothesis that climatic and environmental changes around the Eocene-Oligocene transition were more favourable for the strepsirrhines than haplorrhines in Asia (Ni et al., 2016), while the opposite trend has been proposed for Africa (Seiffert, 2007; Vries et al., 2021).

1.2.3. Early apes and the evolutionary history of Ponginae

Although today there is only one remaining hominoid genus in the Ponginae subfamily, *Pongo* with its three extant species of orangutans *P. abelii*, *P. pygmaeus*, and *P. tapunalensis*, the fossil diversity was much greater. Similarly the modern orangutan habitats are very restricted to some forested areas on Borneo and Sumatra (Spehar et al., 2018), whereas the ranges of fossil pongines extended much farther north and westward onto mainland Southeast Asia, Southern Asia and Eastern Asia (Fig. 7).

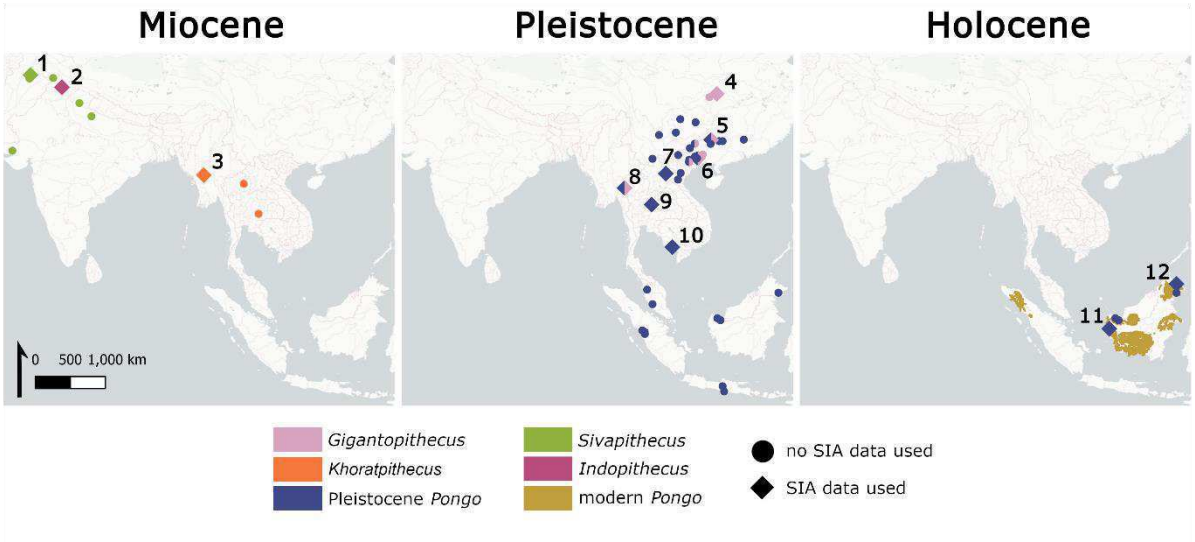

Fig. 7 Maps illustrating the changes of Ponginae distribution from the Miocene to the Holocene. Sites from which stable isotope data was used in this study: 1 Dhok Parthan, Siwaliks, Pakistan; 2 Haritalyangar, Siwaliks, India; 3 Yinseik, Irrawaddy Fm., Myanmar; 4 Longgudong, Jianshi, China; 5 Juyuandong, Liucheng Cave, Guangxi, China; 6 Sanhe Cave, Guangxi, China; 7 Nam Lot, Laos; 8 Pha Bong, Thailand; 9 Thum Wiman Nakin, Thailand; 10 Boh Dambang, Cambodia; 11 Pontianak, Indonesia; 12 Sandakan, Malaysia. Extant Pongo ranges were taken from the International Union for Conservation of Nature (IUCN Red List). The map was created using QGIS 3.16.

The oldest specimen of a fossil pongine recovered in Southeast Asia was found at the Chiang Muan Formation (Fm.) in Thailand, which has been dated to 13 – 12.6 Ma (Suganuma et al., 2006; Coster et al., 2010). In the Miocene of Asia four distinct hominoid primate genera are known, *Khoratpithecus* from Myanmar and Thailand (Chaimanee et al., 2003; Chaimanee et al., 2006; Jaeger et al., 2011), *Sivapithecus* from the Siwaliks in Pakistan, India, and Nepal (Pilbeam et al., 1977a; Pilbeam et al., 1977b; Munthe et al., 1983; Tiwari and Kumar, 1984;

Patnaik et al., 2014; Bhandari et al., 2018), and *Indopithecus* from India (Simons and Chopra, 1969; Pillans et al., 2005; Patnaik et al., 2014) and *Lufengpithecus* (Schwartz, 1990; Moyà Solà and Köhler, 1995; Begun and Kordos, 1997; Begun, 2001; Kelley and Gao, 2012; Ji et al., 2013). All but *Lufengpithecus*, which is more likely a stem hominid, are also considered to be pongines (Kelley and Gao, 2012; Ji et al., 2013; Chaimanee et al., 2019; Pugh, 2022). Recently, an indeterminate hominoid mandible fragment from the Irrawaddy Fm. has been described (Takai et al., 2021) and has been identified as *Khoratpithecus* cf. *ayeyarwadyensis* since (Chaimanee et al., 2022). The Pleistocene pongine diversity is characterized by *Gigantopithecus*, which is known from China, Thailand, and Vietnam (Chang, 1975; Ciochon et al., 1996; Nelson, 2014; Qu et al., 2014; Takai et al., 2014; Bocherens et al., 2017; Zhang and Harrison, 2017), and early *Pongo,* whose distribution extends from southern China to the islands on the Sunda Shelf including Borneo, Sumatra, and Java (Bacon et al., 2018a; Bacon et al., 2018b; Ho et al., 1995; Ciochon et al., 1996; Wei et al., 2004; Harrison et al., 2006; Westaway et al., 2007; Rink et al., 2008; Bacon et al., 2011; Wang et al., 2011; Ibrahim et al., 2013; Harrison et al., 2014; Takai et al., 2014; Bocherens et al., 2017; Louys et al., 2017).

Contrasting with the more generalist character of the overall mammal faunas of these pongine sites, the diversity and endemism of the different pongine genera and species is evidence for a dynamic evolutionary history of this taxonomic group (Chaimanee et al., 2006; Chavasseau et al., 2013; Patnaik, 2013). In the following sections, I will outline the fossil record and morphological characteristics of the two most relevant pongine genera for my dissertation project. As *Khoratpithecus ayeyarwadyensis* from Myanmar is the focus of my studies, I will discuss it in more detail, whereas I will also give brief summaries for the contemporaneous genus *Sivapithecus*.

Khoratpithecus

Currently, we have two mandibles, one maxilla and isolated teeth from representatives of the genus *Khoratpithecus* (Chaimanee et al., 2003; Chaimanee et al., 2004; Jaeger et al., 2011; Chaimanee et al., 2019). Four more mandible fragments and one maxillary fragment have been described from the Khorat sand pits in Thailand (Chaimanee et al., 2022). A compiled list of all Khoratpithecus fossils either described or studied during this dissertation project can be found in Table SI 2 in Appendix II. Due to shared derived characteristics in its dental and mandibular morphology with extant *Pongo* it has been allocated to the subfamily Ponginae. These shared derived traits are for example located in the structure of their mandibular symphyses, which show a strong inclination and a weak upper torus. One feature that only *Khoratpithecus* and *Pongo* share with one another is the lack of an insertion for the anterior digastric muscle (Chaimanee et al., 2004; Chaimanee et al., 2006). The study on the *Khoratpithecus* maxilla revealed more pongine features in its upper dentition (e.g., externally rotated canines) and subnasal anatomy (e.g., strong overlap of the premaxilla relative to the maxilla, antero-posteriorly convex nasoalveolar clivus, subhorizontal incisive foramen). Based on all this morphological evidence the two have been proposed as being sister-groups. (Chaimanee et al., 2019; Chaimanee et al., 2022). The latest phylogenetic analysis further strengthens this attribution, as it also finds *Khoratpithecus* regularly as being the sister-group to *Pongo* (Pugh, 2022). This attribution makes the investigation of the paleoecology of

Khoratpithecus crucial for our understanding of the evolutionary history and ecology of modern orangutans. Today, we know four different species of *Khoratpithecus*. *K. chiangmuanensis*, *K. piriyai*, and *K. magnus* are known from fossil localities in Thailand, whereas *K. ayeyarwadyensis* has been recovered from the Irrawaddy Fm. in Myanmar.

The oldest and most primitive (i.e. more generalized teeth and less enlarged M_3) *Khoratpithecus* species is *K. chiangmuanensis* (Chaimanee et al., 2003; Chaimanee et al., 2006). It was described from the Ban Sa coal mine, in the Ciang Muan Basin of norther Thailand and dates to the Middle Miocene. It is a large pongine, with an estimated body mass of 40 to 60 kg in males and 23 to 29 kg in females, thus displaying strong sexual size dimorphism (Chaimanee et al., 2022). In the original description the pongine was attributed to the genus *Lufengpithecus* on the basis on several similarities in their dental morphology (e.g. wrinkled enamel of similar thickness, dental wear patterns, peripheralized molar cusp, etc.) (Chaimanee et al., 2003). One reason why the enamel wrinkling is so apparent in *K. chiangmuanensis* is the early wear stage of the individuals (Chaimanee et al., 2006). However, it was already noted in the original description of the species that *K. chiangmuanensis* was more closely related to *Pongo* than *L. lufengensis*. While the isolated teeth described in 2003 were not sufficient to create a new genus (Chaimanee et al., 2003), the subsequent discovery of a hominoid jaw in Northeastern Thailand called for the establishment of the genus *Khoratpithecus* for the Thai material.

One year later, the genus *Khoratpithecus* was established together with a new Late Miocene species, *K. piriyai*. The Middle Miocene species was then also referred to this genus, which is characterized by a U-shaped dental arcade in a mandible with a thick corpus and no impression for the anterior digastric muscle, an important synapomorphy that is only shared between *Khoratpithecus* and Pleistocene and extant *Pongo* (Brown, 1997; Chaimanee et al., 2004). *K. piriyai* has an enlarged M_3 compared to *K. chiangmuanensis*. Additional differences are larger roots of the lower incisors and a buccolingually compressed canine, but they share similar molar and premolar morphology and proportions (Chaimanee et al., 2006). Its body mass is between 40 – 56 kg (Chaimanee et al., 2022). A maxilla that corresponds to the *Khoratpithecus* holotype mandible in its proportions and other metric similarities was discovered 20 km away from the type locality. Hence, it was referred to this genus, although it there were no directly associated diagnostic fossils found with it (Chaimanee et al; 2019). Pongine characters such as externally rotated canines, an oval and elongated greater palatine foramen and horizontal margin of the nasal aperture support the attribution (Ward, 1997; Begun, 2015) . One of the most interesting morphological features is the unique nasoalveolar clivus. There is substantial overlap with the palatine processes with low inclination and a very sharp tapering of the pole. Its morphology is most similar to *Sivapithecus* and *Pongo* (Chaimanee et al., 2019). A dental topographic and microwear analysis showed that the diet of *Khoratpithecus* in Thailand was primarily frugivorous without the addition of hard objects such as seeds (Merceron et al., 2006).

The newest addition to the pongine paleobiodiversity of Thailand is *K. magnus*. It has an estimated body mass of 74 kg, making it the largest of all known *Khoratpithecus* species. Its size is also apparent from the overall larger teeth, and especially the large P_4 and molars with high crowns. Consequently, the symphysis of its mandible has a thick transverse torus and a deep genioglossal fossa. The intercanine breadth however is reduced, which is reflected by the narrow anterior mandible (Chaimanee et al., 2022).

From Myanmar, one species of *Khoratpithecus* has been described until now, *K. ayeyarwadyensis*. The holotype has been found in the Irrawaddy Fm. at a locality southeast of Magway near Yinseik village dating to the Late Miocene (~9.5 Ma) (Jaeger et al., 2011). It has an estimated body mass of around 45 kg (Chaimanee et al. 2022). Although its P_3 to M_2 are almost the same size as those of *K. piriyai*, its mandibular corpus is more slender. The mandibular is also narrower anterior. Its molars differ from the ones of *K. chiangmuanensis* in that their central fovea is smaller. The distal basin of the P_3 and the talonid basin of the P_4 are also smaller in the Myanmar species. In addition to these differences, the specimen shares several important attributes with *Khoratpithecus* from Thailand, excluding at the same time affinities with other genera such as *Sivapithecus*. Most importantly, these are the absence of a muscle scar of the anterior digastric muscle and the outline and inclination of the symphysis (Jaeger et al. 2011).

Sivapithecus

Sivapithecus was the first hominoid primate that was described from Asia. Two maxillary fragments found near the village of Jabi, India were used to propose the new genus and species *Palaeopithecus* (now *Sivapithecus*) *sivalensis* (Lydekker, 1879). The taxonomy of the genus *Sivapithecus* (Pilgrim, 1910) has been debated and revised multiple times. I will not discuss all these developments and lines of argumentation here, but see for example Urcioli and Alba (2023) and Kelley (2005) for reviews of *Sivapithecus* taxonomy and systematics, as well as Hartwig (2002) for an overview focusing more on the research history and debates concerning *Sivapithecus* in general. Here, I will give a brief description of the three recognized species following Kelley (2002, 2005), their paleobiology and report some differences from *Khoratpithecus*.

Sivapithecus sivalensis (Lydekker, 1879) has been found in sediments of the Siwaliks of India and Pakistan dating to approximately 8.5 – 9.5 Ma (Hartwig, 2002). With an estimated body mass of 40 – 50 kg in proposed male individuals similar to the body mass of male chimpanzees it is bigger than *S. indicus* and significantly smaller than *S. parvada* (Kelley, 1988). The discovery of a relatively complete skull (GSP 15000) revealed the presence of orangutan like facial characteristics such as ovoid orbits with a reduced intraorbit width, a concave face, heteromorphic incisors, and more similarities in the midsagittal section, e.g. a narrow and more horizontally oriented anterior palatine foramen (Pilbeam, 1982; Chaimanee et al., 2019). *Sivapithecus indicus* (Pilgrim, 1910), the smallest of the three species, is also known from the Siwaliks of India and Pakistan, but from older sediments than *S. sivalensis* (approximately 10.5 – 12.5 Ma) (Hartwig, 2002). The most distinguishing characteristic of the third *Sivapithecus* species, *Sivapithecus parvada* (Kelley, 1988), is its size. It is significantly larger than the other species. Its fossil record is from the Siwaliks of Pakistan in sediments dated to approximately 10 Ma (Hartwig, 2002). In addition to size it also differes from the other two

Sivapithecus species in having inflated disto-lingual ridges in its P_3 and its dental dimensions. *S. parvada* has an enlarged M_3 relative to M_1 and M_2, whereas the lower molars of *S. sivalensis* and *S. indicus* are similar in size or have a smaller M_3. Its body mass was estimated to be around 68.7 kg, based on M_2 length (Kelley, 1988).

On the genus level, *Sivapithecus* differs from *Khoratpithecus* in having a smaller and unpartitioned incisive foramen, a smaller incisive canal and fossa, and less inclined symphysis with a stronger superior transverse torus (Chaimanee et al., 2022). While there are striking similarities in craniofacial characteristics of Sivapithecus with extant Pongo, the same cannot be said about its dental or postcranial features. Sivapithecus humeri for example only display general hominoid characteristics and none specific to orangutans and their typical suspensory locomotion. Instead they have a lateral curvature, which is rather associated with cercopithecoids (Pilbeam et al., 1990; Kelley, 2002).

Sivapithecus lived in a more open environment with increasing seasonality and forest fragmentation based on the composition of its associated fauna and stable isotope analysis. It is hypothesized that this development led to the extinction of this Miocene hominoid (Morgan et al., 1994; Barry et al., 2002; Nelson, 2005, 2007; Morgan et al., 2009).

1.2.4. Ecology of modern *Pongo*

Although orangutans are the most frugivorous of all extant apes, they are often described as opportunistic feeders that use a large variety of food sources (e.g. MacKinnon, 1974; Galdikas, 1978). Nevertheless, fruit consistently represents more than 50 % of their diet, as indicated by various observational studies of orangutan populations on both Sumatra and Borneo from 1969 to 2012 (Fig. 8). The only exception is Batang Serangan, which represents an agroforest habitat where anthropogenic influence and habitat destruction is very prevalent, whereas the other study sites are from either more protected areas (Morrogh-Bernard et al., 2009; Campbell-Smith et al., 2011). Most of these fruits are figs, which are multi-seeded but soft (Vogel et al., 2017). As orangutans face a large variability in fruit availability, they also consume a large variety other food items like leaves, bark, insects, and others such as flowers and occasional soil (MacKinnon, 1974; Rodman, 1977; Galdikas, 1978; Rijksen, 1978; Galdikas, 1988; Fox et al., 2004; Morrogh-Bernard et al., 2009; Kanamori et al., 2010; Campbell-Smith et al., 2011; Vogel et al., 2017). The intra- and supra-annual changes in fruit abundance is apparent in fluctuations of contribution of fruit to their diet. MacKinnon (1974), for example noted changes from a diet consisting of up to 90 % fruit in July and August to just about 20 % from February to May in his study. Kanamori et al. (2010) observed an even wider range of fruit contribution with minima of 11 % in periods of low fruit availability to up to 100 % in periods of high fruit availability.

In addition to a switch to other food groups in times of fruit-scarcity, orangutans may also apply another strategy. Built up fat reserves during times of high fruit availability could be catabolized to cover energetic needs in times of fruit scarcity (Knott, 1998). This strategy could also help explain, why captive orangutans are more prone to obesity and diabetes than other apes that are not metabolically adapted to strong fluctuations in nutrient availability (Gresl et al., 2000; Zihlman et al., 2011).

Although there are no apparent differences in average dietary ecology between the Sumatra and Borneo habitats and species across all studies based on feeding time on plant parts eaten (Fig. 8), there are other proxies that indicate the presence of such differences. The two islands differ in their intra- and supra-annual patterns of fruit availability. There is less fluctuation with less severe mast fruiting events of Sumatra, thus the effect on the dietary ecology of *P. abelii* is significantly less severe (Knott, 1998; Delgado and van Schaik, 2000; Wich et al., 2006; Marshall et al., 2009a; Kanamori et al., 2010). In addition, the robust mandibular morphology in *P. pygmaeus* has been linked to its increased exploitation of hard and tough dietary items than *P. abelii* (Vogel et al., 2014). Orangutans on Borneo also consume a much larger variety of plant species than individuals from Sumatra. This higher taxonomic breadth is also present when comparing different habitat types. More different plant species are consumed by orangutans in peat swamp forests than in mixed dipterocarp forests (Russon et al., 2009). One explanation for this pattern could be that patchier resource availability forces orangutans to exploit various dietary sources (Marshall et al., 2009b; Wich et al., 2011). General differences in floral diversity between Sumatra and Borneo or peat swamp forests and mixed dipterocarp forests could also be possible explanations.

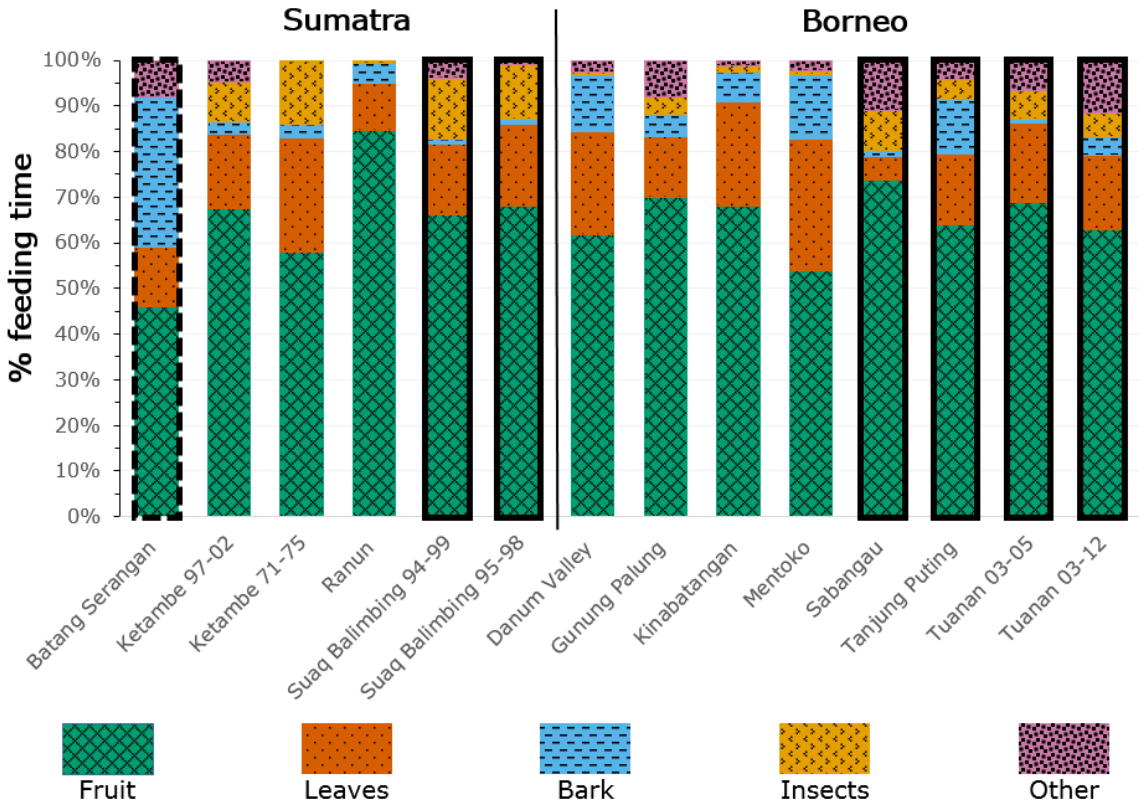

Fig. 8 Variation of average feeding times over the studied periods between different orangutan populations of both P. abelii on Sumatra and P. pygmaeus on Borneo from various observational studies (MacKinnon, 1974; Rodman, 1977; Galdikas, 1978; Rijksen, 1978; Galdikas, 1988; Fox et al., 2004; Morrogh-Bernard et al., 2009; Kanamori et al., 2010; Campbell-Smith et al., 2011; Vogel et al., 2017). Most study sites are from mixed dipterocarp habitats, but five represent peat swamps (bold outline) and one a mosaic agroforest habitat (dashed outline). The dietary category "Other" includes for example flowers and soil. Its compostion can vary from study to study. The numbers after "Ketambe", "Suaq Balimbing", and "Tuanan" are abbreviations for different time periods that were studied. A summary table giving more detailed information about the study areas and the exact percentages can be found in Table SI 3 in Appendix II.

Orangutans share their habitats with many different primate species. Hence, their ecological requirements must be different enough so no competitive-exclusion happens. The Cercopithecidae are an ecologically more diverse primate family, meaning that not all species are strictly arboreal frugivores. This ecological flexibility is also evident from the wide range of habitats that they occupy in Asia alone (Fig. 9). Here I will however only briefly discuss the relationship with of *Pongo* and the Hylobatidae. This family is represented with two genera on the islands of the Sunda Shelf, the larger siamang (*Symphalangus syndactylus*) and the gibbon of the genus *Hylobates* where we find a larger species diversity (Fig. 9). The ecological requirements seem to be too homogenous the gibbons, because there is no sympatry between them on the islands on the Sunda Shelf. They do however share the same habitats with the larger siamang and the three *Pongo* species. Body mass seems to be the predominant factor that separates the three taxonomic primate groups ecologically. Its bigger size allows the siamang to dominate the smaller gibbons in conflicts over food resources. The gibbons with lower energetic needs that allows them to travel farther during the day compensate this disadvantage and use more dispersed dietary sources. Similarly structured competition advantages and dynamics are found between *P. abelii* and *S. symphalangus*, which is expressed not in a use of different food sources or trees, but in their use (MacKinnon, 1977; Wich et al., 2002). This pattern of significant size dimorphism in closely related sympatric species is also present in the fossil primate fauna from the Pondaung Fm. (see Chapter 1.2.1).

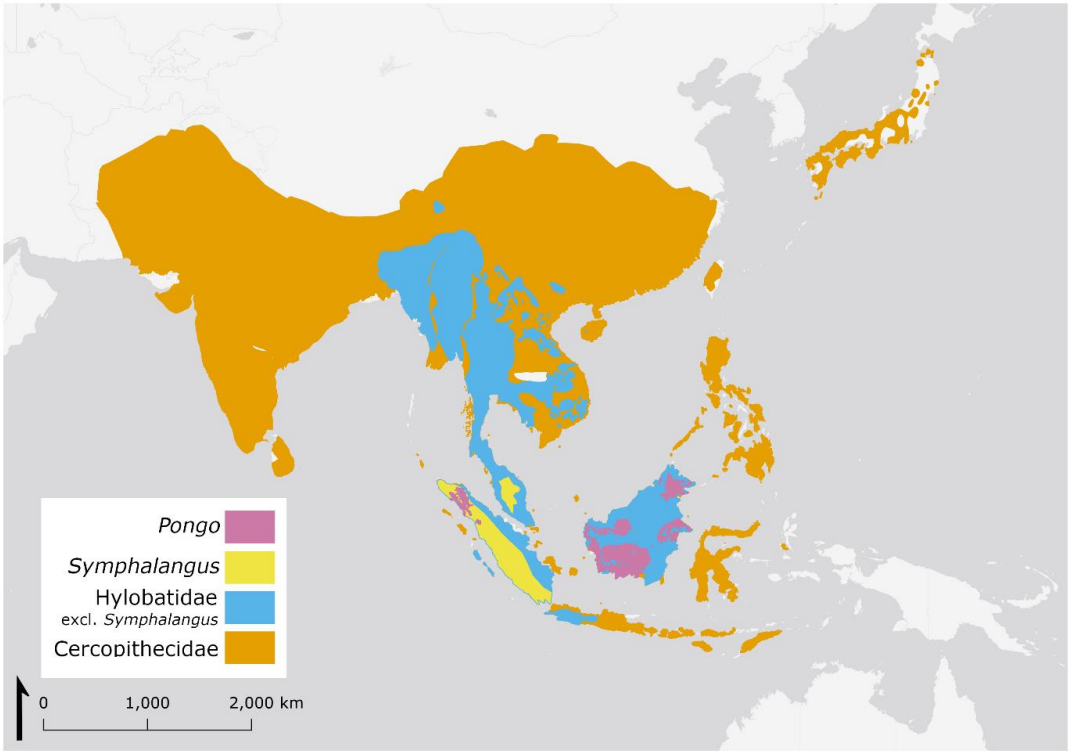

Fig. 9 Overview of todays (2015) distribution of different primate taxa in South and Southeast Asia. Ranges decrease from Cercopithecidae to Hylobatidae (excl. Symphalangus) to Symphalangus and are smallest in Ponginae represented by the single genus Pongo. Smaller ranges always include the ranges of primates with a wider distribution. Extant ape ranges were taken from the International Union for Conservation of Nature (IUCN Red List). The map was created in QGIS 3.18.3.

Two general types of primary forest are occupied by orangutans, peat swamp forest and mixed dipterocarp forest. The latter one is characterized by the various species of Dipterocarpaceae that dominate the tree flora. It occurs everywhere, where there is perhumid equatorial climate. The canopy is well stratified with emergent tree reaching 70 m and more. Species diversity and productivity is highest there compared with other forest habitats on the Sunda islands (Ashton, 2014). Most notable about their ecology are the supra-annual mast fruiting events, which are triggered by ENSO events, enabling the trees to disperse their seeds at the end of an ENSO drought (Williamson and Ickes, 2002).

Peat swamp forest is the forest growing on the peatlands of tropical regions such as Southeast Asia, where it is most extensive. These terrestrial wetland habitats receive their water almost exclusively through precipitation, meaning they are ombrogenous (Page et al., 2006; Posa et al., 2011). First records of peat land forests in Southeast Asia date back to the Early Miocene more than 20 Ma (Morley, 2000). Tree diversity is more limited than in dipterocarp forest and canopy height is reduced (15 – 25 m), due to the specific chemical (extremely acidic with pH of ≤4) and hydrological conditions (Posa et al., 2011; Ashton, 2014). As most mast-fruiting trees do not occur in peat swamp forests supra-annual variability of fruit availability is reduced (Harrison et al., 2010 and references therein).

In addition to these primary habitats, orangutans are forced by the ongoing and increasing anthropogenic influence on their habitats to use the resulting agroforest. These can be described as mosaic habitats of sizeable blocks of degraded forests interspersed with small farms, big plantations, and human settlements. The border between cultivated land and degraded forest is often not clearly discernible (Campbell-Smith et al., 2011). Recent studies demonstrated ecological resilience and the adaptations especially dietary ecology of the orangutans to these new types of habitat (Ancrenaz et al., 2010; Meijaard et al., 2010; Campbell-Smith et al., 2011; Milne et al., 2021). Ancrenaz et al. (2010) highlight the importance of light and sustainable logging practices in contrast to conventional extraction methods as a prerequisite for orangutan conservation the others focus more on dietary ecology. Bark and inner cambium of *Acacia mangium*, a popular plantation tree cultivated for pulp and paper production, could be an important fallback food, as population densities (estimated through nest counts) were surprisingly high in agroforests dominated by this plant (Meijaard et al., 2010), whereas the presence of intact strangler fig (*Ficus spp.*) trees increases ecological resilience of *P. pygmaeus* (Milne et al., 2021). In a small, isolated population of *P. abelii* crop raiding was investigated. Interestingly females take greater crop raiding risks than males. This could be because risks associated with using these dietary sources is minimized by adjusting the feeding time to time periods when farmers are absent from crops and the behaviour of the farmer in this region if an encounter occurs, who tend not to retaliate. In males on the other hand there is little intraspecific competition given the small population size, which reduces the benefit of increased crop-raiding for them (Campbell-Smith et al., 2011).

1.3. Theoretical framework

This chapter will provide the theoretic basis for this dissertation. First, I will introduce the niche concept that was applied during data analysis of both the Eocene and Miocene data sets. Then I will introduce the basic principles of the two methodologies used for the studies included in this dissertation project. Thus, it will become clear what can and what cannot be inferred from the data.

1.3.1. Niche theory

Grinnell was the first one to use the term "niche" to describe the ecological or environmental context in which a species exists (Grinnell, 1924). He uses the term to explain the mechanisms of adaptive radiations in the sense that either should a new niche space be created by changes in the environment or disappearance of the species occupying it a new species will adapt and enter this space. In that sense, his concept differs from the one of Hutchinson. He defines a niche as the set of biotic and abiotic variables that form a n-dimensional hypervolume, which outlines the range of environments in which a species can persist. Each variable is one dimension, or axes defining the model and each point within the hypervolume that is an animals niche is one state of the environment defined by these variables in which the species can persist (Hutchinson, 1957). Thus a species cannot become extinct unless the niche space is reduced or destroyed either by changes in climate and environment or niche destruction by the species itself (Holt, 2009). There is a difference between the larger fundamental niche that encompasses the entire tolerance range of a species and the realized niche that is reduced by dynamics such as competition and predation (Soberón and Arroyo-Peña, 2017). Grinnell's concept focuses more on geographic range and has been developed further by Elith et al. (2006) in their discussion of the bioclimatic niche. The Hutchinsonian niche concept with its distinction of the fundamental and realized niche on the other hand sets a bigger emphasis on the coexistence of species within a given environment and the tolerances of each species regarding both environmental conditions and competition and predation pressure. Another niche concept, the functional niche based on Elton that is centred on which role a species fulfils in a given community. This illustrates the abundance of different niche concepts that are used and discussed in ecology, without being an extensive review of all of them (but see e.g. Ackerly et al., 2006; Newsome et al., 2007; Holt, 2009.

In isotope ecology we can apply the Hutchinsonian niche concept in representing different dimensions of the realized niche (sometimes also core niche (e.g. Baumann et al., 2020)) by the isotopes we analyse. Until now, Bayesian isotopic niche modelling based on the Hutchinsonian niche concept have been mostly limited to dietary or trophic niches based on carbon and nitrogen isotopic composition of collagen (e.g. Ogloff et al., 2019; Baumann et al., 2020; Shipley and Matich, 2020; Johnson et al., 2022). With the application of carbon and oxygen isotope analysis, I proposed a modelled isotopic niche reflecting more broadly ecological characteristic of the niche of a taxonomic group that includes aspects of diet and habitat. Only Nelson and Hamilton have already adopted a similar approach focusing on the dietary transition and ecological niche of early humans (Nelson and Hamilton, 2017).

Isotopic niche modelling is a way to assess generalist versus specialist behaviour in individuals of a taxonomic group. In calculating the relative individual niche index (RINI) for an individual from which multiple data points corresponding to isotopic samples that

represent different instances in an individual's live are sampled and put into relation with the overall modelled niche of the taxonomic group (Sheppard et al., 2018). More general metrics and indices that can be applied to differentiate generalist vs. specialist behaviour in individuals have been presented by Bolnick et al. (2002). Intrapopulation niche variation can be due to sex "ecological sex dimorphism" (Shine, 1989; Shine, 1991), age "ontogenetic niche shift" (Keast, 1977; Polis, 1984), or discrete morphotype "resource polymorphism" (Wimberger, 1994; Skulason and Smith, 1995; Smith and Skulason, 1996).

In this context, it is however important to keep in mind during interpretation of the data that isotopic niches, irrespective if they model dietary/trophic or ecological/habitat niches, are only quantitative indications of the actual niche and not exact equivalents (Hette-Tronquart, 2019; Marshall et al., 2019). However, as niche space is defined as having n-dimensions, all niche models irrespective of the approaches used, are only indications or approximations of all the factors and variables that actually constitute the fundamental or realized niche of a taxonomic group.

1.3.2. Principles of dental microwear texture analysis (DMTA)

To understand the formation of dental microwear and the things we can infer from the different dental microwear textures, it is necessary to explain briefly how it forms. Through the repetition of masticatory movements, the occlusal surface of the tooth is modified through abrasion and attrition. While abrasive wear is caused by abrasive particles between the two tooth surfaces, attrition describes the wear due to tooth-on-tooth contact. Through these forces between antagonistic teeth and the influence of abrasive particles such as diet micro lesions are formed in the dental enamel (Hillson, 2005). The totality of microlesions on the occlusal surface of teeth is what is analysed in dental microwear studies. Although dental microwear is thought to mainly reflect effects of abrasion, the specific influence of attrition is poorly known (Ranjitkar et al., 2017).

The mastication process can be broken up into different phases. After taking a bite, which is usually accomplished with a vertical movement of the teeth without occlusion, the bolus is further reduced by repeated rhythmical movements of the jaw during the main mastication process (power stroke) (Fig. 10). After a preparatory stroke during which initial occlusion happens, the power stroke follows. It can be subdivided into phase I, which is dedicated to shearing as there occurs a sliding motion of the two antagonistic surfaces, and the subsequent phase II, which is about crushing and grinding the food as there is contact between the cusp tips and the opposing basins. During the recovery stroke the jaw opened again before the masticatory sequence recommences (Crompton and Hiiemae, 1969; Kay and Hiiemae, 1974; Ungar, 2015).

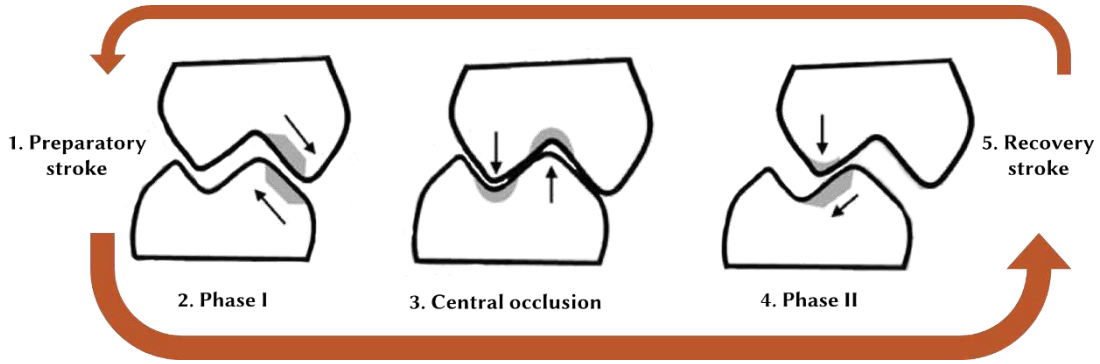

Fig. 10 Schematic illustration of the mastication process from initial occlusion (preparatory stroke) over the two phases of the power stroke to subsequent opening (recovery stroke), modified from (Fiorenza et al., 2015).

During the different phases of the power stroke, forces act on the occlusal surface of the teeth in varying intensities, directions and location on the surface (Fig. 10). It leads to the formation of polished areas, which correspond to the contact zones of two antagonistic teeth during mastication (Hillson, 2005). These areas are called facets and can be distinguished without magnification. There are different terminological systems and nomenclatures for to distinguish between the single facets. Here, I employ the system introduced by Maier and Schneck (1981). Dental microwear textures from both lingual phase I (f6) and phase II (f9) of the mastication process will be analysed.

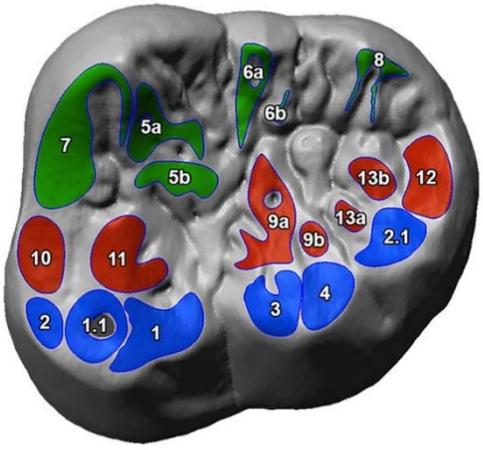

Fig. 11 Visualisation of the different wear facets on a lower molar of P. pygmaeus. The colours differentiate the phases of the mastication process (blue = buccal phase I, green = lingual phase I, red = phase II). Buccal = bottom, distal = right. (Fiorenza et al. 2022).

Every time food is consumed, there is the potential of the appearance of new dental microwear features and the disappearance of others as they are overwritten. Thus, dental microwear provides direct evidence of an animal's diet during the last days to weeks of an animal's life. This is known as the last supper effect (Grine, 1986; Teaford and Oyen, 1989; Teaford et al., 2017). How fast this turnover of dental microwear textures occurs depends on food mechanical properties. Harder/stiffer foods lead to a more rapid turnover than softer/ductile food items (Teaford and Oyen, 1989; Teaford et al., 2017; Winkler et al., 2020; Teaford et al., 2021). This effect and the resulting short time frame the dietary signal in dental microwear allows to potentially track seasonal variations in diet (Teaford and Robinson, 1989; Merceron et al., 2010; Berlioz et al., 2017; Percher et al., 2018).

Friction and compression on the dietary items between the tooth surfaces result in the formation of dental microwear on these facets like pits and scratches. In traditional 2D approaches to dental microwear these features were counted and put into relation with one another to distinguish different dietary regimes (see reviews in e.g. Grine et al., 2002; Ungar et al., 2003; Scott et al., 2009). In the early 2000s a new approach was developed to counter shortcomings like data loss during the conversion of a the actual 3D surface of a tooth into a 2D image, which subsequently is analysed, and considerable inter-observer errors rates of 9 %

on average (Grine et al., 2002). This approach was dental microwear texture analysis (Ungar et al., 2003; Scott et al., 2005; Scott et al., 2006). The method has been proven to be reduce inter- and intra-observer errors compared to former approaches based on visual counting, measurements and classifications through stereomicroscopes or computer screen (Grine et al., 2002; Galbany et al., 2005; Mihlbachler et al., 2012; DeSantis et al., 2013). DMTA is thus more objective and produces more repeatable results (Scott et al., 2006). Threedimensional surface data is collected using confocal microscopes and scale-sensitive fractal analysis (SSFA) to produce a quantitative description of the entire measured surface area using different parameters (Scott et al., 2006). In addition to the SSFA parameters, additional standardized areal surface texture variables based on the ISO 25178-2 norm have been adapted for the quantification and analysis of microwear textures and the differentiation of different dietary categories (Schulz et al., 2013a; Kaiser et al., 2016). The ones that were integrated in the DMTAs conducted for this dissertation project will be described in more detail in the Methods section. However, it has to be mentioned that it is less well understood what physical dietary properties each one of these is correlated with. In the following section, I will use three SSFA parameters (Fig. 12) to illustrate different patterns of dental microwear textures and how they relate to the physical properties of food items that were consumed.

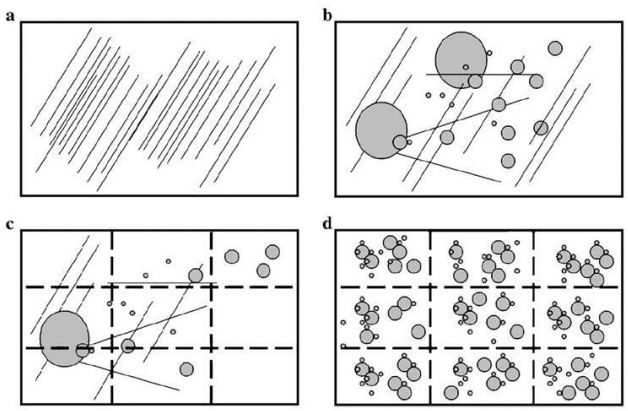

Fig. 12 Schematic visualization of different microwear textures (Scott et al. 2006). A shows an anisotropic texture, B a complex one. On the bottom row, there are examples of a heterogenous (C) a homogenous (D) texture.

The first of three SSFA parameters that I used in my dissertation project is anisotropy (epLsar = exact proportion Length-scale anisotropy of relief). This parameter describes quantifies directionality in surface roughness of a surface. At transects of differing orientation (standard measurements at 5° intervals) the relative length of the depth profile of a surface is measured at the 1.8 µm scale (Scott et al., 2006). High epLsar values correlate with the ingestion of tough food items expressed by an increase in similarly oriented dental microwear features such as parallel striations (Fig. 12 A) (Merceron et al., 2006). Complexity (Asfc = Area-scale fractal complexity) is parameter describing changes in surface roughness over different scales. High Asfc values are associated with the consumption of hard and brittle food items (Scott et al., 2006). Overlapping pits and scratches of varying sizes, depths and orientations (Fig. 12 B) characterize a complex microwear texture. The heterogeneity of the complexity (Heterogeneity of the Area scale fractal complexity, captures variation of complexity across the measured surfaces. Median absolute deviation of Asfc divided by the median Asfc is calculated across the measured area subdivided into rasters with equal numbers of rows and columns, for example 9 × 9 sub-surfaces (HAsfc81) (Fig. 12 C and D) (Scott et al., 2006).

1.3.3. Principles of stable isotope analysis (SIA)

Stable isotope analysis is based on the different abundances of non-radioactive isotopes, which are variants of chemical elements that differ in the number of neutrons from one another, resulting from differences in their behaviour during chemical and physical processes due to their differences in mass. These fractionation processes can change the relative abundances of stable isotopes in a product compared to a reactant in a chemical reaction. Understanding the different fractionation processes enables us to use the resulting isotopic signatures in organic molecules to make inferences on climate, diet, ecology, mobility, etc. depending on the isotope and tissue type. The following chapter will give a brief summary of the various relevant processes.

When we are analysing the stable isotopic composition of biogenic tissues, for example bones or teeth, then we are looking at isotopes that were taken up by the organisms via food or drink and incorporated in these tissues by physiological processes. Some tissues such as bone are remodelled during the entire lifetime of an animal. Others like dental enamel can be considered inert after their initial formation or mineralization, although they differ in their resilience against diagenetic processes. Therefore, the tissue type and its physiological and ontogenic behaviour decides which time period is represented by the isotopic data we obtain from it.

In case of enamel, the time represented by the isotopic ratios is the mineralization period of a tooth. Mineralization is a complex process that already starts prior to tooth eruption. During amelogenesis, or the formation of dental enamel, an organic matrix consisting in equal parts of mineral components, proteins and water is formed. After this first step the maturation process begins, during which the protein and water content of the enamel is continuously reduced and the size of the mineral crystallites increases. A type of cells called ameloblasts drives both steps. However, mineralization continues even when these cells have already died during and after tooth eruption (Hillson, 2005).

Given the age of the material I am working with, it was necessary to focus on the carbonate fraction of the mineral part of dental enamel. This tissue is very resistant to diagenetic alteration given its high proportion of mineral hydroxyapatite ($Ca_{10}(PO_4)_6(OH)_2$) (96 – 99 %) and its dense and fine crystalline structure (Wang and Cerling, 1994). The single apatite crystallites are long, narrow and have a hexagonal section. They are bigger than the ones in bone and dentine (Hillson, 2005). Due to these characteristics, the chance of retaining a biogenic isotopic signal from fossil dental enamel even after millions of years is high.

With the mineral fraction of skeletal tissue and in our case dental enamel we can infer many different details about climate, ecology, and habitat of an individual. When analysing carbon and oxygen, as I did for my dissertation project, trophic level information are not available. However, this information can be retrieved using isotopic pairs of other chemical elements when studying dental enamel. Calcium isotopes for example can be used to infer trophic information, which has been first shown by Skulan et al. (1997) and later further demonstrated in several paleodietary and experimental studies for example (Clementz et al., 2003; Heuser et al., 2011; Weber et al., 2021) even for *Gigantopithecus* (Hu et al., 2022). In the past years it has also been demonstrated that zinc isotopes can clearly differentiate between

herbivores, and carnivores (Jaouen et al., 2016b; Jaouen et al., 2016a; Bourgon et al., 2020; Bourgon et al., 2021; Jaouen et al., 2022).

A small part of the original protein proportion of dental enamel is preserved even after maturation. Some studies could already show that the size of these molecules as well as their amino acid composition can remain intact for thousands or even millions of years (Doberenz et al., 1969; Glimcher et al., 1990). In the past years researchers of the Max Planck Institute and the Johannes Gutenberg Universität in Mainz have developed a methodology to analyse the nitrogen in the mature enamel for its stable isotope composition and thus obtaining trophic information (Leichliter et al., 2021; Lüdecke et al., 2022; Martínez-García et al., 2022).

Carbon

Carbon atoms, which are incorporated in the carbonate fraction of the enamel, originate from the diet. In herbivores, they reflect the plants that are consumed, whereas in carnivores and omnivores they can indicate trophic level, but rather represent the plants on the basis of a foodweb. In this case they reflect the $\delta^{13}C$ values of the plants that form the basis of the food web with an approximate enrichment of up to 2 ‰ in bone collagen for each trophic level (Bocherens and Drucker, 2003). A common enrichment factor used in large ruminant mammals from diet to the carbonate fraction of the enamel is ~ 14 ‰. However, applying this universally is an oversimplification as this offset varies between species and depends on differences in digestive physiology (Cerling and Harris, 1999; Passey et al., 2005). Hence, in addition to experimental studies for example on chimpanzees (Malone et al., 2021), approaches to calculate these species specific enrichment factors have been developed. Most notably one by Tejada-Lara et al. (2018), which uses body mass as the main proxy for the estimation.

In terrestrial plants, there are three different ways in which plants can metabolize CO_2, the Calvin or C_3 cycle, the Hatch-Slack or C_4 cycle or the Crassulacean Acid Metabolism (CAM) cycle. These different photosynthetic pathways lead to distinctive isotopic ratios. The first stable photosynthetic product of the Hatch-Slack cycle is oxaloacetate, which contains four carbon atoms, whereas the metabolic equivalent in the Calvin cycle, phosphoglycerate, contains only contains three carbon atoms. Thus C_4 plants discriminate less against the heavier carbon isotope and therefore have higher $\delta^{13}C$ values (Farquhar et al., 1989). Measurements of carbon isotope ratios of modern C_3 plants yield a range of $\delta^{13}C$ values from −20 to −37 ‰ (Kohn, 2010) with an average of −27 ‰ (Cerling and Harris, 1999). C_4 plants on the other hand have higher $\delta^{13}C$ values between −10 and −20 ‰ (Bender, 1971) and an average of −13 ‰ (Cerling and Harris, 1999).

In purely C_3 environments, $\delta^{13}C$ values do also differentiate open habitats from ones with a closed canopy. This so-called canopy effect (Fig. 13) is the result of lower irradiance and recycling of CO_2 under a dense canopy. $\delta^{13}C$ values decrease with increasing forest density and are as low or lower than -30 ‰ under a closed canopy (van der Merwe and Medina, 1989, 1991; Krigbaum, 2003). The higher up in the canopy a plant tissue grows the less pronounced this effect is (Bonafini et al., 2013; Krigbaum et al., 2013; Lowry et al., 2021).

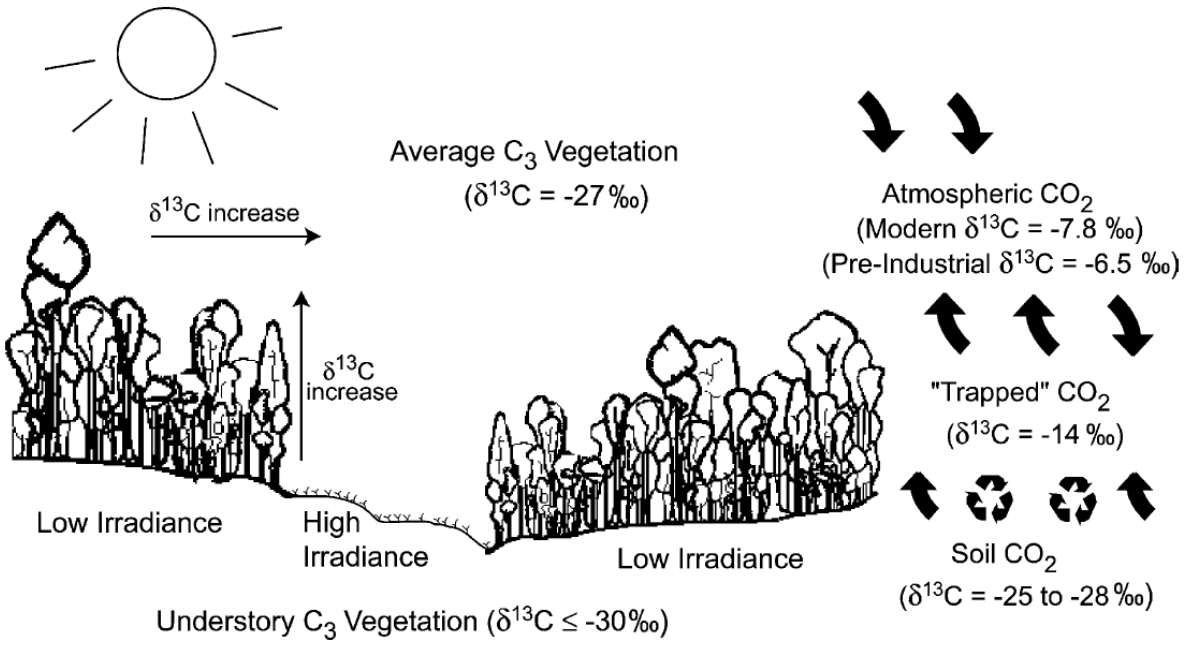

Fig. 13 Visualization of a generalized model of the canopy effect by (Krigbaum, 2003), adapted from (van der Merwe and Medina, 1991; Jackson et al., 1993; Quade et al., 1995).

Oxygen

Oxygen isotopes in skeletal tissue are obtained from the oxygen in body water or more precisely from blood biocarbonate (Ambrose and Norr, 1993; Tieszen and Fagre, 1993). The biggest influx of oxygen into an organism is by the intake of diet and drinking water. It amounts to more than 50 %. Contrary to the uptake of atmospheric oxygen gas and water vapour during inhalation, no fractionation takes place during the incorporation of oxygen into body water in this influx. Nevertheless, there is a constant offset between the $\delta^{18}O$ values of body water and phosphate (~ 18 ‰) and again between phosphate and carbonate within the bioapatite (~ 8 ‰) (Koch, 2007).

The composition of oxygen isotopes of dental enamel varies with temperature, humidity or precipitation, and various geographic variables such as altitude, latitude, and distance from the coast. Meteoric water or precipitation is the major source of terrestrial water bodies. There is fractionation occurring every time the water changes its phase, meaning during evaporation, condensation and precipitation itself. Thus, the first rainout after the evaporation of ocean water displays the highest $\delta^{18}O$ values as the heavier isotope preferentially precipitates. $\delta^{18}O$ values then decrease with increasing distance from the coast and progressive rainout from a pool increasingly depleted in the heavier ^{18}O isotope. The altitude effect has its basis on the same principle of progressive rainout, during which $\delta^{18}O$ values decrease with increasing altitude. Although all of these effects are uniform around the globe, many local modifiers such as geography and topography lead to more geospatial variation of $\delta^{18}O$ values (Dansgaard, 1964; Pederzani and Britton, 2019). Temperature affects the isotopic fractionation during condensation leading to higher $\delta^{18}O$ values when the phase change takes place at higher temperatures. This leads to seasonal and geographical variation with different climate zones. An effect that is less pronounced in tropical regions. There the amount effect is the predominant fractionation factor. More precipitation and humidity leads

to less recycling of re-evaporated moisture, and a lower $\delta^{18}O$ values. The amount effect is pronounced the most in coastal and insular areas as well as in areas with a tropical climate and mean annual temperature exceeding 20 °C (Dansgaard, 1964; Pederzani and Britton, 2019). Therefore, the lowest $\delta^{18}O$ values from sites with tropical climate correspond to seasonal precipitation maxima while they mark the coldest part of the year in other regions. In terrestrial environments $\delta^{18}O$ values can also be used to assess the overall aridity/humidity of these environments (Levin et al., 2006).

There is no fractionation taking place during the incorporation of oxygen isotopes by plants (Dawson and Ehleringer, 1991), although it does happen in hydrogen isotopes in halophytic and xerophytic plants (Ellsworth and Williams, 2007). Their oxygen isotope ratios thus depend on the composition of the meteoric water and local modifiers such as catchment areas of rivers. The variations of isotopic abundances between different water bodies have to be kept in mind when investigating drinking water. Drinking water is normally not obtained from precipitation itself, but water from streams, lakes or wells, which could be subject to evaporation leading to elevated $\delta^{18}O$ values. Nevertheless, $\delta^{18}O$ values of obligate drinking species closely mirror the $\delta^{18}O$ values of precipitation (Adams and Grierson, 2001; Barbour, 2007; Pederzani and Britton, 2019).

Leaf water has elevated $\delta^{18}O$ values compared to precipitation, although no fractionation takes place during the water uptake of plants. The cause for this enrichment with the heavier oxygen isotope is evapo-transpiration through leaf stomata (Pederzani and Britton, 2019). If a species is a non-obligate drinker that obtains the majority of their water intake from food they can also have higher $\delta^{18}O$ values due to this behaviour (Kohn, 1996). Hence it has been suggested that the degree of folivory in primates leads to a stratification of their $\delta^{18}O$ values, with the most folivorous species having the highest $\delta^{18}O$ values (Krigbaum et al., 2013; Nelson, 2013; Carter and Bradbury, 2016). However, recent studies showed that vertical stratification is likely the primary driver of variations of $\delta^{18}O$ values (Carter and Bradbury, 2016; Fannin and McGraw, 2020; Louys and Roberts, 2020; Lowry et al., 2021). The underlying process again is the canopy effect, discussed in the section on carbon isotopes.

Another way in which oxygen isotopes can inform us on an aspect of an animal's ecology is the possibility to assess semi-aquatic lifestyles in taxonomic groups. Mean $\delta^{18}O$ values in populations of semi-aquatic species that live in freshwater can be significantly lower than those of their terrestrial counterparts, and closely mirroring the water they inhabit. This is due to higher water turnover rates in their bodies (i.e., greater daily influx and efflux of water) than we find in terrestrial species (Bryant and Froelich, 1995; Bocherens et al., 1996; Clementz et al., 2008). Offsets in mean $\delta^{18}O$ values between terrestrial and freshwater semi-aquatic vary from 2 to 4 ‰ depending on climate and vegetation structure of the habitat. The effect is more pronounced the more arid and open a habitat is (Clementz et al., 2008). An additional indication of semi-aquatic behaviour in a taxonomic group is a reduced standard deviation (SD) of ≤0.5 ‰ (Yoshida and Miyazaki, 1991; Clementz and Koch, 2001).

1.3.4. Challenges and chances of the combination of DMTA and SIA

When working with a fragmented/limited data sat such as the fossil record, applying multiple different proxies is a good way to make the most of it and being able to answer many different research questions. Each proxy can be valuable in and of itself but in combination, they can strengthen certain interpretations or reveal patterns that would otherwise remain invisible. However, this combination is not a trivial effort. The different characteristics of each proxy and limitations of the methodology have to be kept in mind.

Although I also do rely on interpretations and inferences based on traditional palaeontological approaches such as morphology, I want to discuss the specific challenges and opportunities of a combination of dental microwear texture analysis and stable isotope analysis in more detail here, as these are the two methodologies applied by myself in the scope of my dissertation project.

A combination of the two methodologies allows us to get more general information on the climate, vegetation type and structure and other more general ecological characteristics on the one hand and detailed dietary information on the other hand. The dietary data from the DMTA separates animals based on the textures of their nutrition and not based on trophic level. This makes it very useful to detect dietary variation within and between different herbivorous groups. Importantly, the two methodologies represent different time periods. Whereas the stable isotopes are incorporated in the enamel matrix during ontogeny over the course of several months or even years the dental microwear represents the texture of the diet ingested during the last weeks before an animal's death. These two time periods can be very different from one another especially in animals like orangutans that have very long and slow life histories. It can therefore not be ensured that the environment and habitat reconstructed based on the stable isotopes is the one where the animal foraged in during the accumulation of the dental microwear as migration or fast paced and radical environmental or climatic changes might have occurred in the meantime.

2. Objectives and research questions

Forschungsfragen

Das übergeordnete Ziel dieser Dissertation liegt in der Rekonstruktion von Aspekten der Ökologie der frühen anthropoiden und hominoiden Primaten Südostasians am Beispiel zweier fossilen Faunen aus Myanmar. Erreicht wird dieses Ziel durch die Charakterisierung der Habitate und Ernährung der Primaten. Veränderungen und Kontinuitäten in der Primatenökologie sollen daraus extrapoliert werden. Davon lassen sich mehrere konkrete Forschungsfragen ableiten, die hier kurz vorgestellt werden sollen.

Mit den Isotopenanalysen der Säugetierfauna der Pondaung Fm. aus dem mittleren Eozän sollen zuerst Rückschlüsse über die Vegetationsstruktur und Unterschiede in den Mikrohabitaten zwischen den einzelnen Fundstellen gezogen werden sowie bestehende Hypothesen zum Bestehen eines Protomonsuns im Eozän überprüft werden. Darauf basierend wird auf die unterschiedliche Nutzung der vorhandenen Nischen durch die einzelnen Genera und Spezies und die

Konkurrenzdynamiken zwischen ihnen eingegangen. Es wird auch getestet, ob ein semi-aquatischer Lebensstil in den Anthracotheriiden nachweisbar ist.

Auch für das Miozäne Ökosystem erfolgt zuerst eine Rekonstruktion der Vegetationsstruktur und des saisonalen Klimas. Dabei liegt ein besonderes Augenmerk darauf, das potentielle Vorhandensein von C_4 Pflanzen zu überprüfen. Die Rekonstruktion der Nischenbesetzung durch die unterschiedlichen taxonomischen Gruppen der Säugetierfauna dient vor allem der Einordnung des Orangutanvorfahrens *Khoratpithecus ayeyarwadyensis* in eine der Nischen. Die Rekonstruktion wird durch einen Vergleich mit dem zur selben Zeit vorkommenden *Sivapithecus* validiert. Durch das Hinzuziehen von Daten zu anderen fossilen und modernen Ponginae wird die Hypothese überprüft, dass eine ökologische Kontinuität in dieser Familie seit dem Miozän besteht, was die Anfälligkeit der Orangutans auf die Zerstörung ihres Lebensraumes teilweise erklären würde.

Zuletzt untersuche ich eine Orangutanpopulation aus den 1890ern zu Unterschieden in der Ernährung zwischen den Geschlechtern, Altersgruppen und Fundarealen. Dies dient der Überprüfung einer Hypothese, dass derartige Unterschiede zu einem erhöhten Vorkommen von Zahnpathologien in weiblichen Individuen in dieser Population geführt hat.

Problématique

L'objectif général de cette thèse est de reconstruire certains aspects de l'écologie des premiers primates anthropoïdes et hominoïdes d'Asie du Sud-Est à partir de l'exemple de deux faunes fossiles du Myanmar. Cet objectif est atteint par la caractérisation des habitats et de l'alimentation des primates de la Fm. de Pondaung. Les changements et les continuités dans l'écologie des primates doivent être appréciés à partir de ces informations. Plusieurs questions de recherche concrètes en découlent, qui seront brièvement présentées ici.

Les analyses isotopiques de la faune de mammifères de la Fm. de Pondaung datant de l'Eocène moyen permette tout d'abord de tirer des conclusions sur la structure de la végétation et la variabilité de micro-habitats entre les différents sites, ainsi que de vérifier les hypothèses existantes sur une proto-mousson à l'Eocène. Sur cette base, je me penche sur les différences d'utilisation des niches existantes par les différents genres et espèces des mammifères fossileset sur les dynamiques de concurrence entre eux. Je teste également si un mode de vie semi-aquatique est détectable chez les anthracothères.

Pour l'écosystème miocène également, une reconstruction de la structure de la végétation et du climat saisonnier sera d'abord effectuée. Une attention particulière sera accordée à la vérification de la présence potentielle de plantes C_4. La reconstruction de l'occupation des niches par les différents groupes taxonomiques de la faune mammalienne servira avant tout à placer l'ancêtre des orangs-outans *Khoratpithecus ayeyarwadyensis* dans l'une des niches. La

reconstitution est vérifiée par une comparaison avec le *Sivapithecus* présent à la même époque. En ajoutant des données sur d'autres Ponginae fossiles et modernes, je vérifierai l'hypothèse qu'il existe une continuité écologique dans cette famille depuis le Miocène, ce qui expliquerait aussi en partie la vulnérabilité des orangs-outans à la destruction de leur habitat.

Enfin, j'étudierai une population d'orangs-outans des années 1890 afin de déterminer les différences de régime alimentaire entre les sexes, les groupes d'âge et les zones de découverte. Cela permettra de tester l'hypothèse selon laquelle de telles différences ont conduit à une augmentation des pathologies dentaires chez les individus femelles de cette population.

The overarching goal of my dissertation in the scope of the joint EVEPRIMASIA project of the Université de Poitiers and the Eberhard Karls Universität Tübingen was to characterize Southeast Asian primate habitats and diets from crucial points in their evolutionary history. The three main data sets that I analysed for this dissertation are from three different time periods, the late Middle Eocene, the late Miocene, and the end of the 19th century. From this large time frame I want to extrapolate changes and continuities in primate ecology. This general objective can be broken down into more specific research questions for each data set, which I will describe in more detail in the following chapter. Here, I will also mention some changes in the scope of the project that were necessary due to geopolitical developments.

For the oldest data set from the late Middle Eocene Pondaung Fm. the focus is on reconstructing the paleoenvironments of the mammal community to get indirect evidence for the early anthropoid primate habitats. With the isotopic data we I will build on previous sedimentological and palynological studies (Licht et al., 2015) to add another proxy to the paleoenvironmental reconstructions and to extend the isotopic data that has already been acquired by Licht et al. (2014c) from this important fossil formation. Mulitproxy approaches are especially important when attempting paleoecological reconstructions as "[…] a single fossil resembling a 'tropical' plant may or may not provide evidence for the previous occurrence of tropical vegetation. However, a combination of biological and palaeoenvironmental factors may exhibit a pattern which provides unequivocal evidence." (Morley, 2000)

With my data set, I will look a paleoseasonality, vegetation structure, and niche partitioning among the mammal fauna. Another important objective is to test, whether there is evidence for semi-aquatic lifestyle in the anthracotheres, a diverse family of ungulate mammals that are ancestral to the now semi-aquatic hippos. There are three anthracothere genera known from the Pondaung Fm. It was thus possible to look more closely on differences in their modelled ecological core niches on a generic and species level. The goal was to see, if the ecological differences inferred from their morphology were also visible in the isotopic niche modelling.

The Pondaung Fm. is very extensive with a large number of different localities. This is why, I want to test, if I can detect microhabitat differences for the various localities or locality clusters. In case there are some significant differences, I want to investigate if the isotopic data correlates with existing vegetation models or with the occurrences of the different primate taxa.

The planned incorporation of DMTA data as a dietary proxy for the anthropoid primates had to be postponed, as the sampling could not be completed in the first field season. The planned second field season had to be cancelled due to the pandemic and the political situation in Myanmar starting in February 2021. It has thus not been possible to go back there to take the necessary samples.

The basis for my studies on the late Miocene mammal fauna including *Khoratpithecus* again was a paleoenvironmental reconstruction regarding paleoseasonality, vegetation structure, and niche partitioning. I performed the same kind of analysis on published data from the contemporaneous *Sivapithecus* and its associated mammal fauna to see how similar the two environments are.

While the isotopic niche modelling and the comparison with the *Sivapithecus* localities allowed me to propose a first indication of *Khoratpithecus* paleoecology based on direct evidence, the DMTA data gave more detailed information on the dietary part of its ecology. With it I could assess how much intra-genus dietary variation there was or if the different Khoratpithecus species rather had a homogenous diet. Both the isotopic and the dental microwear data were then used in a final step to see if there is ecological continuity in the fossil pongines in regard to their environment and diet form the Miocene to the Holocene.

For the dietary reconstruction of *Khorapithecus* and testing for dietary continuity from the Miocene to extant *Pongo*, an extensive reference data set of modern orangutans was needed. I got access to the orangutans from the Selenka expedition from the 1890s in the Zoologischen Staatssammlung München. As there were some uncertainties and open questions about the Selenkas expedition, I searched for original historical documents and make the information I found available. The data set itself can be used not only for paleontological studies, but is also of importance to answer biological and conservational questions in the future. To increase the accessibility and visibility of these data for researchers from different fields, we decided to publish it as a separate study. First I tried to reconstruct the timing and duration of the Selenka expedition using primary publications on the material gathered as well as historical sources such as letters, newspapers, receipts and documents regarding the funding of the expedition. Before interpreting the dental microwear textures of the Selenka orangutans I addressed the question, if the sample represents the diet during a mast fruiting event with historical precipitation records, an index modelling ENSO cycle and the comparison with five *P. abelii* specimens that were also sampled in the scope of this study. The goal was to characterize the diet and its variation between sex, age and different localities of this geographically and temporally well restricted orangutan population. A previous pathological study on the same specimen proposed the hypothesis that dietary differences in females caused the higher incidence rates for them than in males. With my data, I want to test, if such a difference is in fact visible in the dental microwear.

3. Material

3.1. Palaeontological sites and their context

3.1.1. The Pondaung Fm.

The Eocene mammal fauna that I study for my dissertation was found at the different localities of the Pondaung Fm., which is located in the Central Basin of Myanmar (17 – 21°N, 92 – 96°E) west of the Chindwin River and northwest of the Irrawaddy River during the annual fieldwork campaigns of the French-Myanmar expedtition. The different areas can be divided into three areas – Bahin, Pangan, and Mogaung (Fig. 14). In the Middle Eocene the area of the Pondaung Fm. was a terrestrial ecosystem along several river channels as its depositional environment was characterized by fluvial sediments indicative of meandering river channels and is mostly comprised of sandstone with interspersed silt/clay bands. Fossils are mostly associated with lithofacies that are characteristic for small fluvial or crevasse channels, swale fills and point bar deposits. Some evidence of peat layers and coal seams might indicate peat swamp formation of the inter-channel areas (Soe et al., 2002). Its paleolatitude was also much farther south at around 5° N as the area was part of the Trans-Tethyan arc (Westerweel et al., 2019; Westerweel et al., 2020).

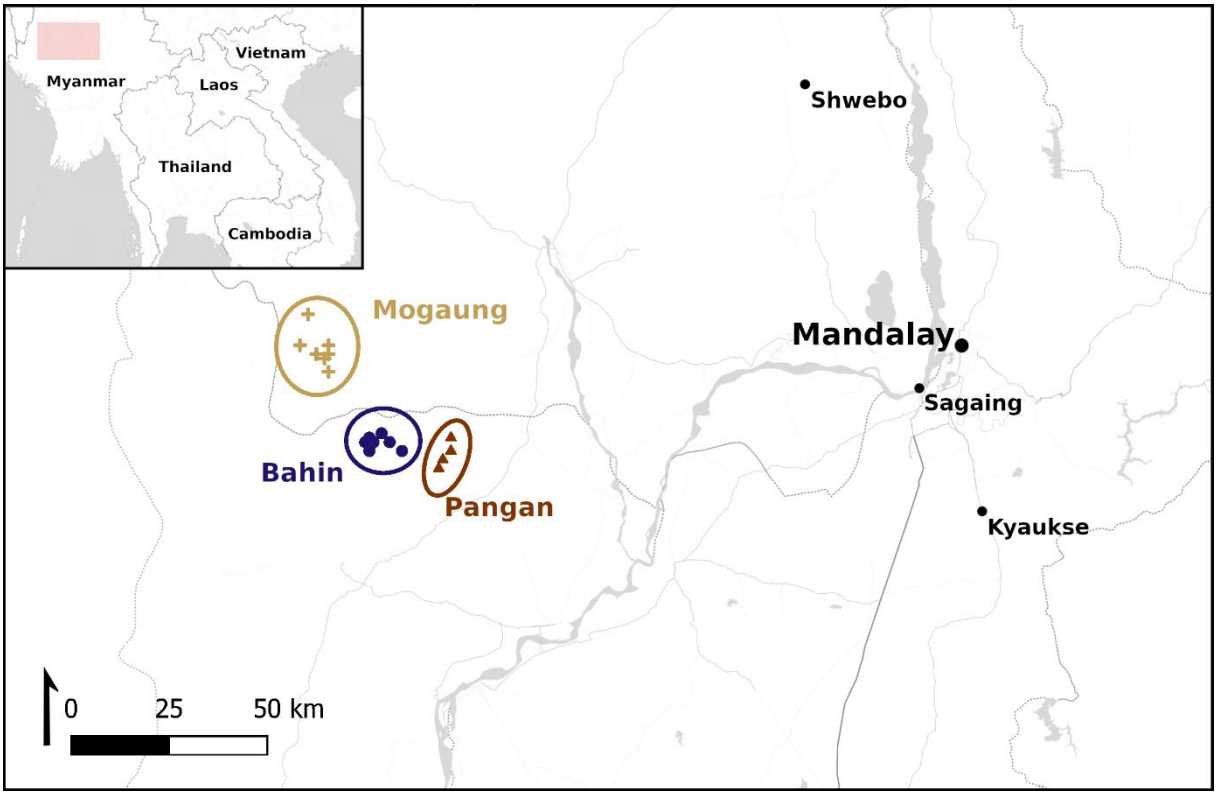

*Fig. 14 Map showing the location of the different localities of the Pondaung Fm. and their division into the three area clusters. Coordinates for all the localities from which samples were analyzed in this study are reported in Table SI 1 of **publication 2**. The location of the detailed map is marked in the overview with a coloured rectangle. Map tiles by Stamen Design, under CC BY 3.0. Data by OpenStreetMap, under ODbL (Habinger et al., 2023).*

The Middle Eocene Pondaung Fm. is framed by the underlying marine Early Eocene Tabyin and the overlying marine Late Eocene Yaw Fm. (Bender and Bannert, 1983). The sediments of the Pondaung Fm. are up to 2 km thick (Bender and Bannert, 1983) with a succession of marine to terrestrial sediments (Stamp, 1922). Only the upper part (Upper Member) yielded

significant amount of fossils representing a terrestrial mammal fauna. It is around 500 m thick (Oo et al., 2015). The stratigraphic relationship of the different fossil localities with one another has not been studied in depth as of today. More detailed information is only available for the localities from the Bahin area. The fossiliferous sediments of some localities there (PK1, PK2, PK3, PK4, PK5, and PK8) belong to the same traceable claystone named Ayoedawpon Taung Claystone, which ranges in thickness from 8 to 20 m. It is directly underlain by another widely traceable sediment, the Ayoedawpon Taung Sandstone. The stratigraphic relationship for two additional fossil localities from the Bahin area is well constrained as well. Fossil outcrops at PK9 are part of the Nyaungpinle Claystone, which is stratigraphicaly lower than the Ayoedawpon Taung Claystone, wheres the claystones at PK12 are overlain directly by the sandstones above the Ayoedawpon Taung Claystone (Maung et al., 2005; Suzuki et al., 2006).

Some direct dates are available for tuffaceous sandstones from the Bahin area (PK4 and PK8). They have been dated to 40.31 ± 0.65 Ma and 40.22 ± 0.86 Ma using LA-ICP-MS, U–Pb zircons (Zaw et al., 2014). This means that the Pondaung Fm. dates to around 40 Ma, which corresponds to the late Middle Eocene or Bartonian. An earlier magnetostratigraphic study on a 319 m thick section of the Upper Member of the Pondaung Fm. at the Yarshe locality (Bahin), Benammi et al. (2002) detected a single normal polarity. Unfortunaltely, this homogenous paleomagnetism makes correlation with a specific Bartonian chron difficult. However it indicates a high sedimentation rate of the floodplain ($>0 \cdot 3$ mm yr^{-1}) (Licht et al., 2014b) as the maximum length of the possible Bartonian polar chron is smaller than 1 Myr (Benammi et al., 2002). Further evidence that substantiates this inference comes from the results of another study on sedimentation rates in Asia (Métivier et al., 1999). Given this high sedimentation rate and the observed homogeneity of the fauna documented notably by rodents, amynodontids, anthracotheres and primates, the Pondaung fossil remains from the various localities will be treated as a contemporaneous mammal fauna assemblage (Ducrocq et al., 2019). For a more detailed evaluation of sympatry of the different taxa in the sample used for this study refer to Table SI 4 in **publication 2**.

The fossil mammal fauna preserved in the Pondaung Fm. is famous for its unique and diverse primate assemblage, which was discussed in detail in chapter 1.2.1. Given the small size of the teeth they could not be sampled for isotope analysis. The Pondaung localities also yielded some creodont (Egi and Tsubamoto, 2000; Bonis et al., 2018), fish, reptile (crocodilian, lizard, and turtle) (Hutchison et al., 2004; Tsubamoto et al., 2006a; Head et al., 2013) and bird fossils (Tsubamoto et al., 2006b). However, no extensive systematic studies on this material exist as of now and it has therefore not been included in our data set for isotopic analysis.

Large herbivorous mammals are most abundant in the fossil record of the Pondaung Fm. and can be considered as representative of the original living community, as they are not subject to sampling bias like it is the case in smaller taxa such as primates and rodents due to fieldwork being mostly conducted as surface prospecting (Tsubamoto et al., 2005). There are two taxonomic groups of Perissodactyls, the Brontotheres and the Rhinocerotoidea with the family Amynodontidae, as well as one very diverse family of Artiodactyls the Anthracotheriidae, which will be discussed in more detail in the following sections.

Brontotheriidae have been described as obligate browsers due to their brachydont teeth with bunoselenodont morphology. Therefore, a forest or woodland in warm temperate to subtropical environments si their expected preferred habitat (Mader, 1998). Some of the brontotherids in our data set have been identified as *Bunobrontops* a more primitive genus in comparison to two other known genera, *Metatelmatherium* and *Sivatitanops*, from the Pondaung Fm. (Holroyd and Ciochon, 2000). Most of the Rhinocerotoidea are probably Amynodontidae, which is the most abundant family in the Pondaung Fm. However, the fragmentary nature of the sampled fossils did not allow for an assignment to the Amynodontidae and they are therefore referred to as Rhinocerotoidea indet. Little is known about their paleoecology. Previous work on fossil Rhinocerotoidea from Late Eocene sites in Vietnam characterized them as obligate browsers and forest dwellers due to their brachydont teeth (Böhme et al., 2013). These brief descriptions of two of the main herbivorous taxonomic groups at the Pondaung Fm. reveal once more the lack of systematic studies especially on the Perissodactyl fauna.

For the stable isotope analysis published in publication 2 I sampled Brontotheriidae (n = 24), Amynodontidae (n = 16), Rhinocerotoidea indet. (n = 27), and Anthracotheriidae (n = 56). Of these tooth specimens, 38 were sampled serially (9 Brontotheriidae, 9 Amynodontidae, 8 Rhinocerotoidea indet. and 12 Anthracotheriidae), hence providing a time series across the mineralization time of the fossil enamel allowing the investigation of seasonal variations. In addition, the tapiromorph *Bahinolophus* (n = 2), Eomoropidae (n = 1), and Ruminantia (n = 2) have also been added to the data set. In four cases two teeth were sampled per individual (*Siamotherium* PNG-20 M2/M3 and PNG-141 M2/M2, *A. tenuis* PNG-22/23, *A. crassum* PNG-56/57, and Amynodontidae PNG-92/93). As a modern reference sample a bovid from the vicinity of the Pondaung Fm. has been added to the analysis as well.

The Pondaung Anthracotheriidae

As the Anthracotheriidae will be discussed in more detail regarding their paleoecology and niche partitioning in publication 2 a more detailed introcuction on the morphological differences between the species and genera and the ecological inferences based on these is necessary.

There is a diverse anthracothere fauna at the Pondaung Fm. This comes as no surprise, as they are one of the clades that had their origin and radiation in the Middle Eocene of Southeast Asia. Later on, anthracotheres spread from Asia to Europe, Africa, and North America. Anthracotheres are ancestral to extant hippopotamuses, thus semi-aquatic lifestyle and its earliest appearance in this clade has long since been a research interest. Earliest morphological adaptations to a semi-aquatic lifestyle in anthracotheres (e.g. dense petrous bone, reduced limb length, raised nasal openings and orbits) have been described in *Bothriogenys* from the Early Oligocene of Africa (O'Leary et al., 2012), which has also been demonstrated by stable isotope analysis (Clementz et al., 2008). In Asian anthracotheres, we see first semi-aquatic adaptations in ear morphology in Early Miocene *Sivameryx palaeindicus* and even more pronounced in Late Miocene *Merycopotamus nanus* (Orliac et al. 2023). No morphological adaptations to a semi-aquatic lifestyle are present in any of the Eocene anthracotheres from the Pondaung Fm.

Three different anthracothere genera are known from the Pondaung Fm. – *Anthracotherium*, *Anthracokeryx*, and *Siamotherium*. Unlike the perissodactyls from the Pondaung mammal fauna that were strictly herbivorous according to their tooth morphology, anthracotheres were more generalist and opportunistic feeders. Their diverse diets likely included leaves, fruits, roots, as well as invertebrates.

Anthracotherium (n = 20) was a medium to large sized anthracothere and the largest of the three genera found at the Pondaung Fm. (*A. pangan* = 237 kg, *A. crassum* = 131 kg) (Tsubamoto et al., 2005). Its bunodont teeth are suitable for crushing tougher food like roots or even scavenge carcasses from time to time. Hence, its cranio-dental morphology is consistent with a more generalist diet similar to the one of extant pigs (Ducrocq, 1999). With the isotopic data I will test the hypothesis that it occupied more open forests than the other two and lived closer to the river system, meaning that it was more water dependent than the other anthracothere genera known from the Pondaung Fm. Currently, there are two Anthracotherium species known, which are also represented in the sampled mammal fauna, the smaller *A. crassum* (n = 5) and the larger *A. pangan* (n = 11).

The second genus, *Anthracokeryx* (n = 13) is also represented by two species at the Pondaung Fm. the larger *A. birmanicum* (n = 4) and the smaller *A. tenuis* (n = 4). The genus represents a more typical forest dweller with bunoselenodont teeth. These characterisitcs are indicative for a more specialized herbivorous foraging ecology (Ducrocq, 1999). It has a body mass, weighing 20 to 25 kg (Lihoreau and Ducrocq, 2007). Its smaller size and its cranio-dental morphology are consistent with dwelling in denser forests and having a more specialized subsitence strategy dominated by folivory.

The newest addition to the anthracothere biodiversity at the Pondaung Fm. is *Siamotherium* (n = 4) represented by the species *S. pondaungensis*. It is the smallest and most primitive of the three genera with an estimated body mass of 7.5 kg. This small and slender animal had a short snout showing first signs of selenodonty on its molars (Ducrocq et al., 2001; Soe et al., 2017; Ducrocq et al., 2021). Its subsistence strategy has been described as more omnivorous including occasional scavenging, and it is thought to have lived in open forested areas (Soe et al., 2017). For this study, we could sample four teeth from two individuals.

3.1.2. The Irrawaddy Fm.

Here, the term Irrawaddy Fm. refers to the typical Irrawaddy series in the Magway area around the Yenangyaung “type region” of the formation (Fig. 15). Although the term fossil formation is usually defined as a body of rock that has formation status, the situation for the Irrawaddy Fm. is more complex. A Middle Miocene mammal fauna has been described from the Chaungta region north of Mandalay (Chavasseau et al., 2006) as part of the Irrawaddy Fm. although it has different sedimentological, chronological, and faunal characteristics.

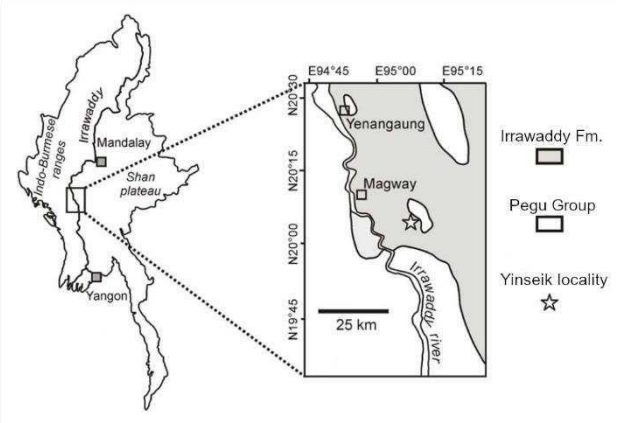

Fig. 15 Map showing the general location of the Irrawaddy Fm. (left) and of the Yinseik locality (right) where the hominoid fossils have been found and from which the material used in this study comes from. Modified from (Jaeger et al. 2011).

The sedimentary deposits of the Irrawaddy Fm. in the Magway area are of fluvial origin and around 100 m thick. They most closely resemble the sediments from the base of the Irrawaddy Fm. at Yanangyaung (Chavasseau et al., 2013). They are underlain by the marine deposits of the Obogon Fm. and its exposed Pegu group rocks. The change in depositional environment from marine to freshwater/fluvatile occurred probably before 10 Ma (Bender and Bannert, 1983; Khin and Myitta, 1999). The Irrawaddy paleoriver has been reconstructed as a through flowing river since major drainage basin reorganisation in the early Oligocene (Licht et al., 2016; Zhang et al., 2019). However the evolution of the drainage system did not reach modern levels until the late Miocene or even Pliocene (Jonell et al., 2022).

With its diverse terrestrial mammal fauna and the occurrence of hominoid primate fossils it is one of the most important fossiliferous formations in the Central Basin of Myanmar (Fig. 15). The hominoid bearing locality, called Yinseik locality, is located east of the Irrawaddy River, about 20 km southeast of Magway (Magway Region), and close to the Yinseik village. The sediments of the Irrawaddy Fm. can be characterized as poorly consolidated and coarse sandstones or hardened fine sandstones. These are alternated with clayey sandstones and claystones. There are also some frequently fossiliferous oxidized conglomeratic layers. The sedimentation rate of these deposits was likely very fast as they have a single normal magnetic polarity and the vertebrate fauna found is homogenous (Jaeger et al., 2011). Hence these deposits probably represent a short time period and it is valid to speak of a mammal community in a paleontological context. From biochronology an age bracket from 10.4 – 8.6 Ma has been inferred, which falls in the early Late Miocene. Looking at the magnetostratigraphy, two ages within this bracket, ~10 Ma and ~9 Ma, would be possible datings (Jaeger et al., 2011).

The perissodactyle fauna from this area consists of the equid *Hipparion*, a rhinocerodit and a chalicotheriine. For the proboscidean fossils attributions to *Stegolophodon* or *Tetralophodon* have been suggested. The artiodactyle fauna is more diverse with several different bovids, three genera of suids, the anthracothere *Merycopotamus medioximus*, a giraffid, and a tragulid. There also is some record of carnivore and of course the hominoid primate *K. ayeyarwadyensis*, which I already introduced and described in more detail in chapter 1.2.3. Apart from the mammal fauna there is also a rich record of trionychid turtles, crocodiles and freshwater sharks (Chavasseau et al., 2013). The mammal fauna from the Irrawaddy Fm. is very similar to those of the contemporaneous faunas associated with *K. piriyai* (Chaimanee et al., 2006) and *Sivapithecus* (Patnaik, 2013).

For the isotopic analysis, we sampled 44 teeth of various taxa, i.e. Rhinocerotidae (n = 9), Proboscidea (n = 8), Bovidae (n = 11), Suidae (n = 7), Giraffidae (n = 5), one cervid, one anthracothere, and one specimen of *K. ayeyarwadyensis* (MFI-K171). This left hemi-mandible of *K. ayeyarwadyensis* is also the holotype of this species (Jaeger et al., 2011). Sampling it for isotopic analysis was only possible, because a small enamel fragment of the m3 broke off during preparation of the fossil, which was then analysed. In addition to the fossil specimen we also used the modern bovid mentioned in 3.1.1. Data from the Yinseik Equidae (n = 6) from the Yinseik locality has already been published by Jaeger et al. (2011). For detail information on the reference data we used as well as precise taxonomic information and specimen numbers of the whole data set please refer to **publication 1** and Table SI 2 and Table SI 3 therein.

For the paleodietary reconstruction of *K. ayeyarwadyenesis* we tried to get data from the same specimen (MFI-K171) from which a broken fragment of the M_3 was sampled for SIA. Unfortunately, the occlusal surface of all the teeth that were moulded (P_3 – M_2) were either too badly preserved or still heavily covered with resin to yield any microwear signal. We could however analyse seven other *Khoratpithecus* individuals belonging to different species, six of which had well preserved facets from which dental microwear texture data could be acquired. Of these six specimen, two were from the Irrawaddy Fm. in Myanmar (*K. ayeyarwadyensis*) and four from the Khorat sandpits in Thailand (*K. piriyai*) (Chaimanee et al., 2022). One of the specimens from the Irrawaddy Fm., *Khoratpithecus sp. indet.* (MFI K-172) is extraordinarily large and might therefore even be possibly related to *K. magnus* (MFT-K178) from Thailand (Chaimanee et al., 2022). However, the discovery of more fossils would be necessary to substantiate this hypothesis.

3.1.3. The Khorat sand pits

The *Khoratpithecus* specimens from Thailand that I analysed for dental microwear textures have been recovered from the Khorat sand pits (sometimes also referred to as Tha Chang sand pits), which are located along the Mun River in Nakhon Ratchasima Province, northeastern Thailand (Saegusa et al., 2005; Chaimanee et al., 2022). Based on the composition of the large mammal fauna and its correlation with the mammal fauna from the Dhok Pathan region of the Siwaliks a Late Miocene age (9 – 6 Ma) has been proposed (Barry et al., 2002; Chaimanee et al., 2006). Like the Irrawaddy Fm. the Khorat sandpits are also characterized by fluvial sediments corresponding to a paleo river channel and its vegetation has been reconstructed as being transitional between woodland and grassland based on pollen records (Sepulchre et al., 2010). This diverse habitat was inhabited by a rich fauna with abundant crocodiles and turtles as well as many mammals such as the equid *Hipparion*, rhinocerotids, proboscideans, suids, giraffids, bovids, and the hominoid primate *K. piriyai* (Chaimanee et al., 2022 and references therein).

3.2. The Selenka collection of extant *Pongo* and its historical context

Emil Selenka (27.02.1842 – 21.01.1902) (Fig. 16, left) was a German zoologist who started his scientific career studying marine invertebrates before switching his focus to embryology. During his time as professor at the University of Erlangen, he conducted two expeditions to South and Southeast Asia. The first one in 1889 led him to Java and Borneo, where he collected material on anthropoid primates. During his second expedition he visited Sumatra and Borneo

in 1892 – 1894 where he collected around 300 orangutan skulls. Today, these are stored in the Zoologischen Staatssammlung München. As there was contradicting information in some publications mentioning his expedition and the museum documentation and the exact timing of hunting the orangutans was interesting for the interpretation of the dental microwear results I attempted to reconstruct the timeline of the expedition and some of its key events as precisely as possible using different historical documents such as letters, receipts, newspapers, and paperwork regarding funding he received for his this expedition from the Königlich preußischen Akademie der Wissenschaften (today Berlin-Brandenburgische Akademie der Wissenschaften. The shelf marks of the documents from various archives are cited and additional information for each reference is provided in a footnote.

Fig. 16 Emil Selenka (left) and his hunter Max Moret (right together with a Dajak)

In October 1892 Emil Selenka writes a research proposal to the Königlichen Preußischen Akademie der Wissenschaften in Berlin and asks for funding for his expedition to Southeast Aisa during his 18 month leave from the University of Erlangen. His request for funding is granted in December 1892 and 3500 Mark are sent to him to the German Consulate in Singapore in January 1893 (PAW(1812-1945/II-VII-113)[1]). Selenka and his wife Margarete Lenore Selenka had left Europe on board of the SS Darmstadt of the Norddeutsche Lloyd (Selenka and Selenka, 1905), which arrived in Singapore on the 18.11.1892 (The Singapore Free Press and Mercantile Advertiser, 19.11.1892). Shortly after he started an eight months long expedition to Borneo and Sumatra during which he collected orangutan, gibbon, and siamang specimen especially for his embryological studies. In this endeavour, Max Moret, a Swiss soldier in Dutch employ, joined his team as a hunter (Fig. 16, right). Unfortunately, much of the material collected was lost during a shipwreck on the Kapuas River (West Kalimantan, Borneo) during transportation from the collection sites to the port to be shipped back to Europe late in 1893 (Selenka, 1896). This news reached Selenka, when he had already travelled onward to Japan to study the primate fauna there and purchase some

[1] Documents and correspondance related to Selenkas research proposal to the Königlichen Preußischen Akademie der Wissenschaften housed in the archives of the Berlin-Brandenburgischen Akademie der Wissenschaften.

specimens (UBH NL 238 : B 2[2]). In January and February he stays in Sumatra to organize a new hunting expedition to cover the losses his collection experienced due to the shipwreck. Because he is experiencing health problems, his wife takes over most of these responsibilities. His health and the nearing end of his leave from the university are the reasons why he cannot join this second hunting trip himself. He travelled back to Europe after making a stop in India (UBH NL 238 : Aa 6,1[3]). His wife probably accompanied him to India (UBH NL 238 : Aa 1,1-2[4]), although the account of Hubrecht in Selenkas obituary suggests that she stayed longer in Borneo than her husband and had a very active, leading role during most of the second hunting trip (Hubrecht, 1902-1903). During this second hunting expedition during ten month in 1894 most of the losses of the shipwreck could be cut (Selenka, 1896). Hence, although Selenkas expedition lasted from November 1892 to 1894 most orangutan skulls in the collection of the Zoologischen Staatssammlung München were likely collected during a ten-month period in 1894. His hunters were active in the area on the right bank of the Kapuas River. Here they also traded and purchased orangutan skulls from the local Dajak and Malay. The Selenka collection then counted around 300 orangutan skulls across all age groups from northwestern Borneo (Selenka, 1896, 1898). On the map (Fig. 17) the areas where the individuals were hunted are marked.

The habitat north of the Kapuas River is a mixed dipterocarp forest. Peat swamp forests are only present in the most southwest parts of the Landak region close to the coast (Phillips, 1998). During their expedition around the same time, the Dutch team around Büttikofer and Jentink only observed the orangutan at altitudes of 700 m (Büttikofer, 1896). No similar notes are available directly from the Selenka expedition himself. The range of altitudes of the collection area in (Fig. 1) are however all very low, usually below 300 m. Exceptions are Mount Genepai ("Berg Genepai" in the map, which probably corresponds to Gunung Kenepai, 1112 m, 0° 42' 36'' N, 111° 43' 3'' E), Mount Dadap ("Berg Dadap on the map, which probably corresponds to Gunung Tutoop, 805 m, 0° 55' 00'' N, 111° 37' 53'' E), Mount Gedang ("Berg Gedang" in the map, which corresponds to an unnamed peak of 835 m, 0° 54' 87'' N, 111° 27' 13'' E), and Mount Rabor ("Berg Rabor" on the map, which probably corresponds to Gunung Kehuma, 1210 m, 0° 56' 6'' N, 111° 20' 18'' E) (mountains listed here from east to west).

[2] Receipt over 100 Yen for the purchase of monkeys and monkey embryos from Kakichi Mitsukuri, Tokio dated to 6.12.1893. The document is housed at the library of the University of Basel.
[3] Letter of Emil Selenka to his parents written on the 1.2.1894 in Medan (Sumatra) in which he discusses the problems he is facing with his health, the shipwreck and his travel plans for the next weeks. It is housed at the library of the University of Basel.
[4] Two letters from Punchanun Bhuttacharjee to Margarete L. Selenka mentioning the time they spent together in Calcutta dating to 27.3.1894 and 26.12.1894. Housed at the library of the University of Basel.

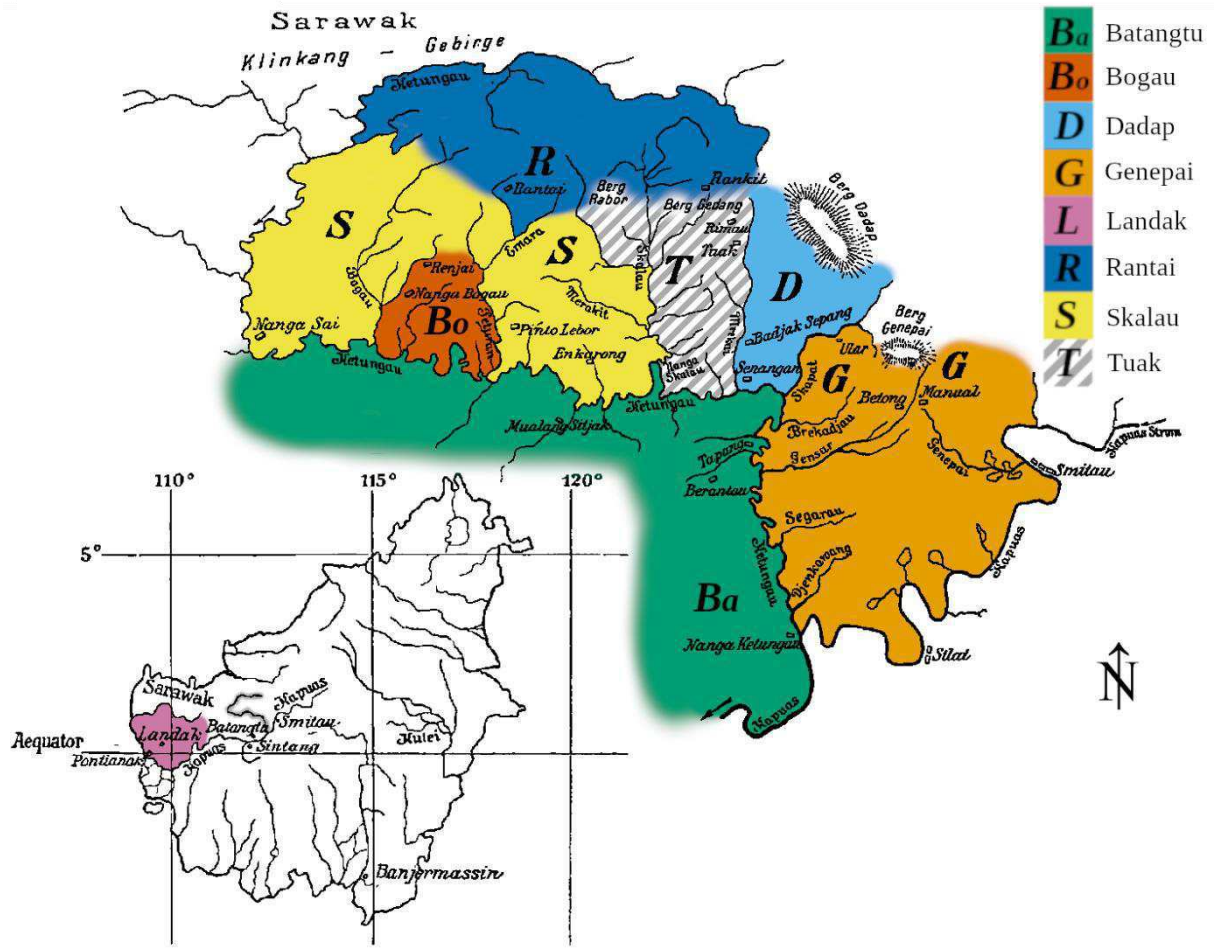

Fig. 17 These two maps were originally published in Selenka's first extensive publication on the orangutan material that he obtained during his expedition 1892 – 1894 (Selenka, 1898). The position of the detailed map (right) can be estimated using the Ketungau river highlighted in grey and Smitau village on the overview (left). He marked the areas from which he collected specimen with letters that he originally correlated with local morphotypes. We use these attributions only for estimates of areas of origin for each specimen. We displayed each area by shading in different colours, the extent of each area being based on the description of distribution of the local morphotypes in Selenka's publication and natural barriers such as mountains and major rivers. The Bogau area is not correlated with a morphotype described by Selenka and therefore was not marked in the original map. Nevertheless, it is used in the original labelling of some of the specimen. We estimated its location based on the location of the village Nanga Bogau. The Klingklang-Gebirge refers to the mountain ranges south of the border to Sarawak (Malaysian Borneo) (Habinger et al., in prep).

I studied dental microwear texture of 89 wild *Pongo pygmaeus* individuals from the Selenka collection. All of the locations in Fig. 17 except for Tuak are represented in this data set. Five adult *Pongo abelii* individuals collected by Schmidt, Schmidt and Adam in 1913 (Table 2) complemented the sample. All specimens are housed in the Zoologische Staatssammlung München, Germany (ZSM). Both sexes are represented equally in the *P. abelii* sample. In the Selenka sample however, females are far more numerous than males. The representation of different age groups is also more differentiated in the Selenka *Pongo* than in the Sumatran orangutans. Sample sizes for age groups other than adults are however very low. Aging and sexing information was obtained from the databases of the ZSM. Unfortunately, the methodology used for the classification has not been recorded.

Table 2 Summary of the number of individuals for each age and sex group in the extant Pongo DMTA data set. (Habinger et al., in prep)

	female				male			indet
	juvenile	subadult	adult	senil	juvenile	subadult	adult	adult
Pongo abelii	-	-	2	-	-	-	2	1
Pongo pygmaeus	5	4	45	1	1	6	27	-

3.3. Reference data sets for DMTA

Although *Pongo* was still widely distributed in mainland Asia in the Early and Middle Pleistocene, where they were sometimes occurring sympatrically with another pongine, *Gigantopithecus*, (Fig. 7) (Tshen, 2016) all of the data comes from sites in Sumatra. Orangutans earliest occurrence on the Sunda Islands dates to the Middle Pleistocene of Java (Trinil) (Hooijer, 1948). The Pleistocene have also been demonstrated to have a higher body mass in the Early Pleisotcene and decrease in size throughout the Pleistocene to the Holocene (Tshen, 2016). For the dietary reconstruction of *Khoratpithecus*, I was kindly provided with the scan data on Pleistocene *Pongo* (n = 29) from Sumatra sites by Larisa de Santis (Louys et al., 2021). The Pleistocene *Pongo* specimens, which will be referred to as Pongo sp. have been collected from a sinkhole in Lida Ajer cave (62 – 72 ka) (Westaway et al., 2017), Ngalau Gupin (~130 ka) (Smith et al., 2021), and Ngalau Sampit (~90 ka) (Louys et al., 2017) (Table 3). The study by Louys et al. (2021) on their dental microwear and the differences to extant *Pongo* showed that Pleistocene *Pongo* sp ate less tough food than *P. pygmaeus*. They interpreted this result as evidence that differences in vegetation and fruit availability between Borneo and Sumatra, which have been discussed in chapter 1.2.4, were already present in the Pleistocene.

For the reconstruction of the *Khoratpithecus* paleodiet using DMTA I did not only use the modern and Pleistocene orangutan samples described in the previous sections. Instead I also integrated smaller data sets of both wild shot chimpanzees (*Pan troglodytes*) (n = 34) and gorillas (*Gorilla gorilla*) (n = 30) from collections at the Musée Royal de l'Afrique Centrale (MRAC, Belgium), Staatliches Museum für Naturkunde Stuttgart (SMNS, Germany), and the Zoologische Staatssammlung München (ZSM, Germany) in the analysis.

Table 3 Summary of the reference material of Pleistocene Pongo, Pan, and Gorilla. All individuals were adults and one crushing facet per individual was analysed. More detailed information for each individual on locality, tooth moulded, etc. is reported in Table SI 4 in Appendix II.

Taxon	n	Location	Reference
Gorilla gorilla	30	Central Africa	-
Pan troglodytes	34	Central Africa	-
Pongo sp.	6	Lida Ajer	Louys et al. 2021
Pongo sp.	22	Ngalau Gupin	Louys et al. 2021
Pongo sp.	1	Ngalau Sampit	Louys et al. 2021

4. Methods

4.1. Dental microwear texture analysis

Before moulding the teeth any any dirt or coatings used for preservation need to be removed. Therefore the occlusal surfaces of the teeth were cleaned with ethanol or acetone using cotton swabs. Whenever possible, we took silicone moulds (President Regular Body, ref. 6015 – ISO 4823, medium consistency, polyvinylsiloxane addition-type, Coltène-Whaledent) of the second lower molars. Usually the second molars are not too worn, to still have intact wear facets, but enough to already display dental microwear and have well defined facets. There seems to be no statistically significant difference between the microwear texture of upper and lower second molars (Teaford and Walker, 1984; Merceron et al., 2006). I however decided to sample the lower second molar whenever possible to maximize sample homogeneity. The specific tooth moulded for each individual is reported in Table SI 1 of **publication 3** for the Selenka *Pongo* and Table SI 4 in Appendix II for the *Khoratpithecus*, *Pongo* sp., *Pan*, and *Gorilla* data set.

As the entire tooth was moulded per individual the moulds were cut to represent a single wear facets, oriented as horizontally as possible and then scanned with "TRIDENT", a Leica DCM 8 white-light scanning confocal microscope (Leica Microsystems) with a 100x objective (Numerical aperture = 0.90, Working distance = 0.9 mm) located in the facilities of the PALEVOPRIM laboratory, CNRS and Université de Poitiers, France. We chose facets that represented both phase I shearing facets (f6) and phase II grinding facets (f9) (Maier and Schneck, 1981). Each scan generates a point cloud of 350 x 264 µm. The surfaces were imported in the LeicaMap v. 8.0 software (Mountain technology, Leica microsystems), and treated following the workflow described in Merceron et al. (2016), which will be summarized briefly in the following section. As the scans were obtained from moulds instead of casts, the surfaces were mirrored along the z-axis. Then non-measured points (not exceeding 2 % of the total number of pixels) were filled with a shape calculated from adjacent points (Laplacian filter). Furthermore, aberrant peaks were removed following an automated workflow including a morphological filter described by Merceron et al. (2006). Following this step, the exact 200 x 200 µm grid (1550 × 1550 pixels) that was later used to calculate the textural parameters, was automatically generated in the centre of the levelled surface. In cases where there were dirt particles, resin residue from preservation efforts, or other disturbances visible, I shifted the grid to remove these artefacts from the analysed frame. In cases where this was not possible, these areas were smoothened (Laplacian filter) along a manually set border. For the use of Laplacian filter and possible alternatives, see Francisco et al. (2020). Photosimulations and false colour maps of all scans used in this study are reported in the Supplementary Information of **publication 3** (Selenka *Pongo*) or Appendix II (*Khoratpithecus*, *Pongo* sp., *Pan*, *Gorilla*).

After the surfaces are saved as .sur files, I applied a second workflow on each surface, which is reported in a generalized form as a template in the appendix. During this process a second-order least square polynomial surface (PS2) is substracted to remove convexity of the dental facets, and thus allowing for a better visualisation of the relief formed by dental microwear (Francisco et al., 2018a; Francisco et al., 2018b). Afterwards, a spatial filter was run (denoising

median 5 × 5 filter size and Gaussian 3 × 3 filter size) and the surfaces were levelled (least square plane by subtraction).

From these surfaces, the Scale Sensitive Fractal Analysis (SSFA) parameters (Scott et al., 2006) were computed. This analysis is based on a principle from fractal geometry that states that a surface that appears to be smooth on a large scale, can have a rougher more textured profile on a sufficiently fine scale (Scott et al., 2005). In addition, we also calculated Surface Texture Analysis (STA) parameters following well-established procedures (Schulz et al., 2013a; Kaiser et al., 2016). The combination of both SSFA and ISO 25178-2 textural parameters allows for a more comprehensive representation of the surface textural information (Calandra et al., 2012).

During the analysis, I used three different SFFA parameters, complexity (Asfc), anisotropy (epLsar), and heterogeneity of the complexity (HAsfc 81), which is calculated on each surface divided into a raster of 9 x 9 subsurfaces. For a more detailed description of these parameters, refer to chapter 1.3.2. For STA we focused on height (Sq, Ssk, Sku, Sp, Sv, Sz, Sa), surface/spatial (Sal2_0.5, Str2_0.5), and volume (metf, medf) parameters. All parameters are presented in Table 4. A detailed description of STA parameters is available in Calandra et al. (2012; but see also Schulz et al., 2013b; Schulz et al., 2013a; Kaiser et al., 2016).

Table 4 Summary of the different SSFA and STA parameter abbreviations, their short description, and units. Adopted from (Schulz et al., 2013a).

Abbreviation	Parameter type	Description	Unit
Asfc	SSFA	Complexity, area-scale fractal complexity	-
epLSar	SSFA	Anisotropy, exact proportion Length-scale anisotropy of relief	-
HAsfc9	SSFA	Heterogeneity of complexity, surface subdivided into 9 x 9 sub-surfaces	-
HAsfc81	SSFA	Heterogeneity of complexity, surface subdivided into 3 x 3 sub-surfaces	-
Sq	STA	Standard deviation of the height distribution, or root mean square values (RMS) surface roughness	µm
Ssk	STA	Skewness of the height distribution	-
Sku	STA	Kurtosis of the height distribution	-
Sp	STA	Maximum peak height, height between the highest peak and the mean plane	µm
Sv	STA	Maximum pit height, height between the mean plane and the deepest valley	µm
Sz	STA	Maximum height, height between the highest peak and the deepest valley	µm
Sa	STA	Arithmetic mean height or mean surface roughness	µm
Sal2_0.5	STA	Auto-correlation length (s=0.5)	µm
Str2_0.5	STA	Texture aspect ration (s=0.5)	-
metf	STA	Mean depth of furrows	µm
medf	STA	Mean density of furrows	cm/cm^2

4.2. Stable isotope analysis

The enamel was sampled using a micromotor rotating device to retrieve 6 – 10 mg of powdered sample. I took bulk samples of most of the teeth (Fig. 18, left). In these cases, the drilling was done in a band along the whole growth axis of the tooth. These values represent the average isotopic composition over the whole mineralization time of the tooth crown during ontogeny. In cases of well-preserved high-crowned teeth, it was possible to conduct intra-individual serial sampling (Fig. 18, right). This means that multiple samples were drilled as bands that are oriented perpendicular to the growth axis of the tooth, thus providing a continuous record of isotopic variation during the mineralization time of this tooth.

Fig. 18 Examples for the different sampling approaches. Anthracotherium tooth fragment (PND-30) showing bulk sampling (left), Brontotheriidae tooth fragment (PND-8) after serial sampling perpendicular to growth axis (right).

In addition to the enamel, I also took some dentine and sediment samples. These are used to assess the extent of diagenetic alteration of the isotopic composition. If the biogenic signal has been altered, it can be detected by shifts in the $\delta^{13}C$ and $\delta^{18}O$ values correlated to the $CaCO_3$ content.

All of the powdered samples were pretreated and the carbonate fraction of the dental enamel was analysed in the laboratory of the Department of Geosciences (Biogeology working group) at the University of Tübingen (Germany). Fossil enamel, dentine and sediment samples were let to react with 1.35 ml of a NaOCl solution at a concentration of 2.5 % for 24 h to remove all the organic matter. After rinsing them with Milli-Q H_2O the fossil enamel and dentine samples were then also let to react with 1.35 ml of 1M acetic acid buffered solution (CH_3COOH) for 24 h to remove exogenous carbonates and were rinsed again with Milli-Q H_2O before being dried at 40 °C. This method for the pretreatment follows procedures described in (Bocherens et al., 1994; Koch et al., 1997; Wright and Schwarcz, 1999). Two internal enamel standards (Elephant SRM, Hippo SRM) (SRM = secondary reference material) were added to each set of samples and pretreated accordingly. Additionally, two international (IAEA-603, NBS-18) and one internal (LM = Laaser Marmor SRM) pure carbonate standards were added to the sets prior to analysis in the IRMS (isotope ratio mass spectrometer). No pretreatment was done for them. After every 15 samples in the IRMS, all of the standards were measured routinely.

2.5 – 3 mg or 0.1 mg of sample for enamel and pure carbonates respectively was used for the analysis with the IRMS. The vials are put into the multiflow device and heated to 70 °C for 4 hours prior to analysis. The vials were then flushed with helium (He) to replace the air in them. Around 5 drops of 99 % phosphoric acid (H_3PO_4) were inserted into each vial to react with the carbonate (1).

$$CaCO_3 + H_3PO_4 \leftrightarrow CaHPO_4 + CO_2 + H_2O \quad (1)$$

The gaseous products of this reaction are separated on a gas chromatography (GC) column. One of the products of this reaction, the CO_2 gas, was then analysed with the Elementar IsoPrime 100 IRMS 4 times over a 15-minute time span. Repeating the measurements enabled

us to monitor measurement precision by calculating the mean and the standard deviation for each sample (Szpak et al., 2017). These metrics are reported together with the isotopic data in the appendices. Calibration of the measured isotopic ratios was done relative to VPDB (Vienna Pee Dee Belemnite) using the two internal enamel standards. The results are reported using the δ-notation (in per mill) calculated following formula (2) where ^{j}X is the heavier and ^{i}X the lighter isotope.

$$\delta^{j/i}X = \frac{(^{j}X/^{i}X)_{sample}}{(^{j}X/^{i}X)_{standard}} - 1 \quad (2)$$

With the internal enamel standards the isotopic ratios were calibrated relative to VPDB (Vienna Pee Dee Belemnite). Oxygen isotopic ratios have been subsequently converted to δ18OVSMOW values (Vienna Standard Mean Ocean Water) using formula (3) by (Coplen, 1988)

$$\delta^{18}O_{VSMOW} = (1.03091 \text{ x } \delta^{18}O_{VPDB} + 30.91) \quad (3)$$

As the $CaCO_3$ content of each sample is an important metric to assess diagenetic alteration, I report this metric for each specimen in the tables in the appendices as well. For its estimation, we calculated an estimated elemental composition based on sample weight, peak area and the internal LM SRM using the Ion Vantage software. The $CaCO_3$ values are then scaled up, until one of the international pure carbonate standards (IAEA-603, NBS-18) reaches 100 %.

4.2.1. Data corrections

As I am comparing different species, sites, and time periods to answer my research question, it was necessary to apply various data corrections especially to the $\delta^{13}C$ values. All the $\delta^{13}C_{apatite}$ values were transformed to $\delta^{13}C_{diet}$ values. To do so enrichment factors (ε, in per mill) specific for the various taxonomic groups were used. Formula (4) shows how ε is defined (Craig, 1954; Coplen, 2011). In this formula a stands for diet and b for apatite.

$$\varepsilon^{13}C_{a-b} = \alpha^{13}C_{a-b} - 1 = \frac{\delta^{13}C_{a/standard}+1}{\delta^{13}C_{b/standard}+1} - 1 \quad (4)$$

The isotopic fractionation factor (α), which is derived from the δ-values as defined in (1) forms the basis for the calculation of ε. Isotopic fractionation from diet to apatite is not explainable by a single kinetic or equilibrium process (Coplen, 2011). To account for this complexity I will use terms apparent isotopic fractionation factor (α^*) and apparent enrichment factor (ε^*) in the rest of this thesis.

For the Miocene data set, we applied ε^* based on results from published studies of controlled feeding experiments. These were -14 ‰ for large-bodied herbivores (Cerling and Harris, 1999; Passey et al., 2005), and -11 ‰ for omnivores including suids (Howland et al., 2003; Passey et al., 2005) and primates, specifically orangutan and its fossil relatives (Crowley et al., 2010). As the data set from the Pondaung mammal fauna includes more extinct clades, I decided to apply the formula (5) proposed by Tejada-Lara et al. (2018) to calculate ε^* for the different taxonomic groups. Although many different factors including digestive physiology influence the isotopic enrichment between diet and apatite (Passey et al., 2005), body mass seems to be the driving factor (Tejada-Lara et al., 2018).

$$\varepsilon^* = e^{[2.4 + 0.034\ (BM)]} \quad (5)$$

Here, BM stands for the log transformed (ln) body mass in kg (6). Table 5 reports the body mass estimations used for the calculation of $\delta^{13}C_{diet}$ values in the Pondaung data set.

$$\delta^{13}C_{diet} = \delta^{13}C_{apatite} + \varepsilon^* \quad (6)$$

*Table 5 Summary of the body mass (BM) estimates and the modelled isotopic enrichment factor based on formula (5) (Tejada-Lara et al., 2018). For specimens where a taxonomic identification to species level was not possible, the mean modelled enrichment factor the highest taxonomic resolution possible was applied. In this table, whenever no body mass estimate is given, the enrichment factor corresponds to the mean value of the taxonomic groups marked by color. The specific value for the calculation of the $\delta^{13}C$ value of each specimen is reported with the calibrated data before corrections in the Table SI 2 of **publication 2** in the appendix (Habinger et al., 2023).*

Taxonomy	BM (kg)	ε^* (‰)	Reference for BM estimation
Anthracotheriidae		-12.5	
Anthracotherium		-13.1	
Anthracotherium pangan	237	-13.3	Tsubamoto et al., 2005
Anthracotherium crassum	131	-13.0	Tsubamoto et al. 2005
Anthracokeryx		-12.3	
Anthracokeryx birmanicum	59.4	-12.7	Tsubamoto et al. 2005
Anthracokeryx tenuis	16.1	-12.1	Tsubamoto et al. 2005
Anthracokeryx (lower limit)	20	-12.2	Lihoreau and Ducrocq, 2007
Anthracokeryx (upper limit)	25	-12.3	Lihoreau and Ducrocq, 2007
Siamotherium pondaungensis	7.5	-11.8	(Ducrocq et al., 2021)
Rhinocerotoidea		-13.6	
Amynodontidae indet.	154	-13.1	Tsubamoto et al. 2005
Paramynodon		-13.8	
Paramynodon cotteri	1010	-13.9	Tsubamoto et al. 2005
Paramynodon birmanicus	441	-13.6	Tsubamoto et al. 2005
Brontotheriidae		-14.1	
Sivatitanops birmanicus	5110	-14.7	Tsubamoto et al. 2005
Sivatitanops cotteri	2080	-14.3	Tsubamoto et al. 2005
Bunobrontops sp.	512	-13.6	Tsubamoto et al. 2005
Bunobrontops savagei	987	-13.9	Tsubamoto et al. 2005
Ruminantia		-12.2	
Artiodactyla indet	9.47	-11.9	Tsubamoto et al. 2005
Indolophus guptai	20.7	-12.2	Tsubamoto et al. 2005
Bahinolophus birmanicus	51.6	-12.6	Tsubamoto et al. 2005
Eomoropidae indet.	18.4	-12.2	Tsubamoto et al. 2005
Eomorops pawnyunti	15.2	-12.1	Tsubamoto et al. 2005

When delta values of animals from different time periods are compared like in chapter 5.2 it is necessary to correct the $\delta^{13}C$ values for changes of the $\delta^{13}C_{CO2}$ values in the atmosphere and the Suess effect (Keeling, 1979). All values discussed in this chapter have been corrected to pre-industrial values from 1850 of -6.5 ‰ (Marino et al., 1992). $\delta^{13}C_{CO2}$ values of Miocene sites older than 6 Ma were assumed to be -6.1 ‰ and therefore a correction of 0.4 ‰ was applied to them (Tipple et al., 2010). Modern atmospheric $\delta^{13}C_{CO2}$ values are -8 ‰ as published by Cerling et al. (2010) based on Zachos et al. (2001) and derived from the global mean $\delta^{13}C$ values from 1998 measured at ten stations covering an area from the Arctic to the South Pole (Keeling et al., 2001, 2005). Hence, all post-1930 samples were corrected by 1.5 ‰. Pre 1930 to 6 Ma old values are treated as equivalent to the pre-industrial ones (Friedli et al., 1986), and hence no correction was applied to them.

As no such comparisons were done using the Eocene isotopic data from the Pondaung Fm. no correction due to changing $\delta^{13}C_{CO2}$ values have been applied to this data set, but they have been factored in the threshold values for forest cover or C4 plant consumption. We discuss these modifications briefly in chapter 5.1.

All the ε^* as well as the atmosphere correction used for each specimen are reported together with the calibrated data and corrected δ-values used in the analysis in the SI tables of **publication 1 and 2** in the appendices.

4.3. Statistical analysis

In the following section, the different statistical methods that were applied for this thesis will be described. Given the small sample sizes in our data set as well as the presence of outliers and not normally distributed data we decided to use the non-parametric Wilcox rank sum test when testing for differences of the medians between two groups throughout this study. The tests were run in R using `wilcox.test()` (package stats version 4.1.2, one of the base packages in R).

In cases of suspected statistical outliers I conducted a Grubb's test with `grubbs.test()` (package outliers version 0.15). In cases of statistical tests or models, such as the Grubb's test that assume normal distribution of the data, I tested if this was the case with a Shapiro-Wilk test of normality using `shapiro.test()` (package stats version 4.1.2, one of the base packages in R). The results for the $\delta^{18}O$ value of PND-M1 showed that the p-value is higher than 0.05 (W = 0.94899, p-value = 0.4094), indicating that we do not reject the null hypothesis that the data follow a normal distribution. The Grubbs' test for outliers was run in R using `grubbs.test(data, opposite = T)` (package outliers version0.15, (Komsta, 2006)) to test if the minimum value of the data set was an outlier. The results show that this is in fact the case (G = 2.5669, U = 0.6136, p-value = 0.0427). We therefore excluded this data point from all our models and analysis.

We re-ran the linear regression on minimum $\delta^{18}O$ values over time (Ma = *Mega annum* = million years ago) published by Nelson(Nelson, 2005) using `lm()` (package stats version 4.1.2, one of the base packages in R). We then added the data from the Yinseik equids to the figure in order to compare them to the regression line.

The analysis of the dental microwear involves a lot of different variables and is ran on two types of dental facets per individual in the case of the study of dietary variation in the Selenka orangutans (**publication 3**). I therefore performed principal component analysis (PCA) to reduce dimensionality and identify the most discriminant parameters. To maximize variation along a lower number of variables I ran a first PCA round on all variables of all individuals, followed by a second PCA round which only included variables contributing significantly to PC1 and PC2 of the first round. PCAs and visualisations were run in R with the factoMineR (version 1.34) and factoextra (version 1.0.7) packages (Lê et al., 2008).

To test for significant differences in dental microwear between groups, I conducted ANOVAs after a rank transformation of the data using `rank()`. To run the ANOVA, I created a linear model with `lm()` of the data and ran `aov()` on the linear model. In cases, where there were significant differences between some of the groups the pairings that differed significantly from one another were identified with a post hoc test. I ran Tukey's HSD with `TukeyHSD()` on the output of `aov()` with confidence level set at 0.95.

Statistical tests and modelling (linear models and Bayesian niche modelling) were conducted usin R version 4.1.2 (2021-11-01) "Bird Hippie". Figures were generated using Excel (2016) or with different plot functions in R (packages ggplot2 version 3.3.5 (Wickham, 2016), and SIBER version 2.1.6 (Jackson et al., 2011)), except for the maps for which we used QGIS (version 3.16). All figures were further modified using GIMP (version 2.10.18).

4.3.1. Bayesian niche modelling

Bayesian niche modelling enables us to quantify and thus better compare niche width and niche partitioning of different mammal communities. Although niches can be modelled with n dimensions (see chapter 1.3.1), for the case studies of my dissertation project I focused only on the isotopic data, the $\delta^{13}C$ and $\delta^{18}O$ values. I used the R package SIBER (version 2.1.6) (Jackson et al., 2011) for the modelling of the ecological core niches. For my interpretations, I used standard ellipse area corrected for small sample sizes (SEAc) that corresponds to a confidence interval (CI) of 40 % (Jackson et al., 2011). Its calculations are based on a maximum likelihood estimation in a Bayesian framework. This framework counteracts the effects small sample sizes have on statistical power. Nevertheless, increasing sample sizes would still lead to more robust results. With the SEA_Cs I calculated three different metrics to quantify niche overlap in the different mammal communities defined as follows, where A_O is the overlap area of two SEA_Cs obtained with `maxLikOverlap()` included in the SIBER package:

- The percentage of niche area of taxon A (A_A) that overlaps the niche space of taxon B (A_O/A_A)
- The percentage of niche area of taxon B (A_B) that overlaps the niche space of taxon A (A_O/A_B)
- The percentage of the total niche space of the two taxa that is shared between them, which is calculated with formula (7) (Ogloff et al., 2019).

$$\% \text{ overlap } = \frac{A_O}{A_A + A_B - A_O} \times 100 \quad (7)$$

As more specimens were suitable for intra-individual sampling from the Pondaung data set I also calculated the relative individual niche (RINI) (Sheppard et al., 2018) for these individuals based on their modelled ecological niches. This metric relates the individual niche area to the population niche area. Here, it expresses the proportion of one SEA_C (CI = 40 %), which represents one individual, that is shared with the union of all the SEA_Cs of the serially sampled individuals from a taxonomic group. For this I used `siberKapow()` that is part of the SIBER package. Code examples can be found in the explanatory vignettes at the SIBER Github repository (https://github.com/AndrewLJackson/SIBER).

5. Results and Discussion

In the following sections, I would like to discuss the interpretations of my results and answer the research questions outlined in chapter 2. To do so, I will mainly refer to the results of my three publications (attached as **publications 1 – 3**) and some preliminary results on the dietary reconstruction of *K. ayeyarwadyensis*. The methods used are described in chapter 4 in general terms. The specifics for each study can be found in the methods sections of the respective publications.

5.1. Paleoecology of the primate bearing Pondaung mammal fauna

In the following chapter, I summarize the isotopic niche modelling and paleoecological reconstruction of the late Middle Eocene Pondaung mammal fauna that has been published as **publication 2**.

Zusammenfassung

Die Sedimente der Pondaung Fm., eine fossile Fundstelle des mittleren Eozäns (~40 Ma), sind ein Fenster, das uns einen Blick auf die Umweltbedingungen und Dynamiken eines vergangenen Ökosystems erlaubt. Dieses Ökosystem ist eine gute Analogie zu unserer heutigen Welt, genauer gesagt eines Szenarios in die sie sich unter Einfluss des Klimawandels und Treibhauseffekts entwickeln kann. Aus evolutionsökologischer Sicht ist das Eozän Südostasiens besonders spannend, da viele der modernen Säugetierlinien dort ihren Ursprung haben und auch eine starke Diversifizierung dieser stattfand. Eine davon sind die anthropoiden Primaten. In der bisherigen Forschung lag der Fokus auf einer allgemeinen Charakterisierung des Klimas und der Vegetation des Ökosystems, in dem die Pondaung-Fauna lebte. Erste Belege für ein frühes Einsetzen eines monsunähnlichen Klimas schon bevor der Orogenese des Himalayas wurden erbracht. Hier werde ich einerseits das frühe monsunartige Klima genauer charakterisieren und detaillierter auf die Nutzung des Habitats durch die einzelnen Säugetiergattungen eingehen sowie die Nischen und Mikrohabitate, die sie jeweils besetzt haben.

Die Auswertung der Sauerstoffisotopen zeigte ein saisonales Niederschlagsmuster, das einem Klima mit höheren maximalen Niederschlagsmengen als im heutigen Myanmar entsprechen könnte. Das ist durchaus überraschend, vor allem da die Sedimente der Pondaung Fm. nahe des Äquators (5° N) lagen. Mittels Nischenmodellierung unter Verwendung der Kohlenstoff- und Sauerstoffisotope konnte ich Aspekte der ökologischen Nischen der unterschiedlichen Säugetiere gewinnen. Besonders für die Anthracotheriidae, einer heute ausgestorbenen Säugetiergattung von denen die modernen Flusspferde (Hippopotamidae) abstammen, erlaubte es die feinkörnige Bestimmung der fossilen Überreste, Informationen zum Konkurrenzpotenzial zu gewinnen. Weiter konnte ich auch signifikante Unterschiede in den Mikrohabitaten zwischen den Regionen mit den verschiedenen Fundstellen der Pondaung Fm. feststellen, die gut mit den Vegetationsmodellen früherer Studien korrelieren. Die Auswertung der Verbreitung der anthropoiden Primatenspezies über die Fundstellen mit unterschiedlichen Mikroklimata und Vegetation lieferte Hinweise auf ökologische Flexibilität, da einige beide Habitate nutzten.

Résumé

Les sédiments de la Fm. de Pondaung, un site fossile de l'Éocène moyen (~40 Ma), sont une fenêtre qui nous permet d'observer les conditions environnementales et la dynamique d'un écosystème passé. Cet écosystème est une bonne analogie de notre monde actuel, plus précisément d'un scénario vers lequel il peut évoluer sous l'influence du changement climatique et de l'effet de serre. Du point de vue de l'écologie évolutive, l'éocène d'Asie du Sud-Est est particulièrement intéressant, car de nombreuses lignées de mammifères modernes y ont vu le jour et se sont fortement diversifiées. Les primates anthropoïdes en font partie. Jusqu'à présent, les recherches se sont concentrées sur une caractérisation générale du climat et de la végétation de l'écosystème dans lequel vivait la faune de Pondaung. Les premières preuves d'un début précoce d'un climat de type mousson, avant même l'orogenèse de l'Himalaya, ont été apportées. Ici, je vais d'une part caractériser plus précisément le climat de type mousson précoce et aborder en détail l'utilisation de l'habitat par les différents genres de mammifères et les niches et micro-habitats qu'ils ont respectivement occupés.

L'évaluation des isotopes de l'oxygène a révélé un modèle saisonnier de précipitations qui pourrait correspondre à un climat avec des précipitations maximales plus élevées que celles du Myanmar actuel. C'est tout à fait surprenant, d'autant plus que les sédiments de la Fm. de Pondaung se trouvaient près de l'équateur (5° N). Grâce à une modélisation de niche utilisant les isotopes du carbone et de l'oxygène, j'ai pu obtenir des aspects des niches écologiques des différents mammifères. En particulier pour les Anthracotheriidae, un genre de mammifères éteint, qui sont les ancêtres des hippopotames modernes (Hippopotamidae), la détermination précise des restes fossiles a permis d'obtenir des informations sur le potentiel de compétition entre les espèces. J'ai également pu constater des différences significatives dans les micro-habitats entre les

différents sites de la Fm. de Pondaung, qui sont en accord avec les modèles de végétation des études précédentes. L'évaluation de la distribution des espèces de primates anthropoïdes à travers les sites avec des microclimats et structures de la végétation différents, a fourni des indices de flexibilité écologique, car certains utilisaient les deux habitats.

5.1.1. Confirmation of early monsoon onset

When we compare the $\delta^{18}O$ values of the modern bovid from the Central Basin of Myanmar and the fossil mammals from the Pondaung Fm. the latter are significantly lower (W = 0, p-value = 7.349e-12). Sinusoidal patterns that indicate seasonal climate were present in both the modern and the fossil specimen (Fig. 19). Even though the temperatures today nowadays are around 5 °C lower than in the Middle Eocene the lowest $\delta^{18}O$ value of the modern bovid is higher than all the Eocene ones. Minimum $\delta^{18}O$ values represent the seasonal precipitation maxima in tropical environments (Dansgaard, 1964; Sun et al., 2021). These consistently lower minimum $\delta^{18}O$ values indicate a more humid climate in the Eocene than in modern Myanmar and are even consistent with an increased monsoon intensity with higher seasonal precipitation maxima in the Eocene. However a reduced distance of the fossil localities to the Eocene coast than we see in the Central Basin of Myanmar today, could also decrease the $\delta^{18}O$ values (Westerweel et al., 2019; Westerweel et al., 2020).

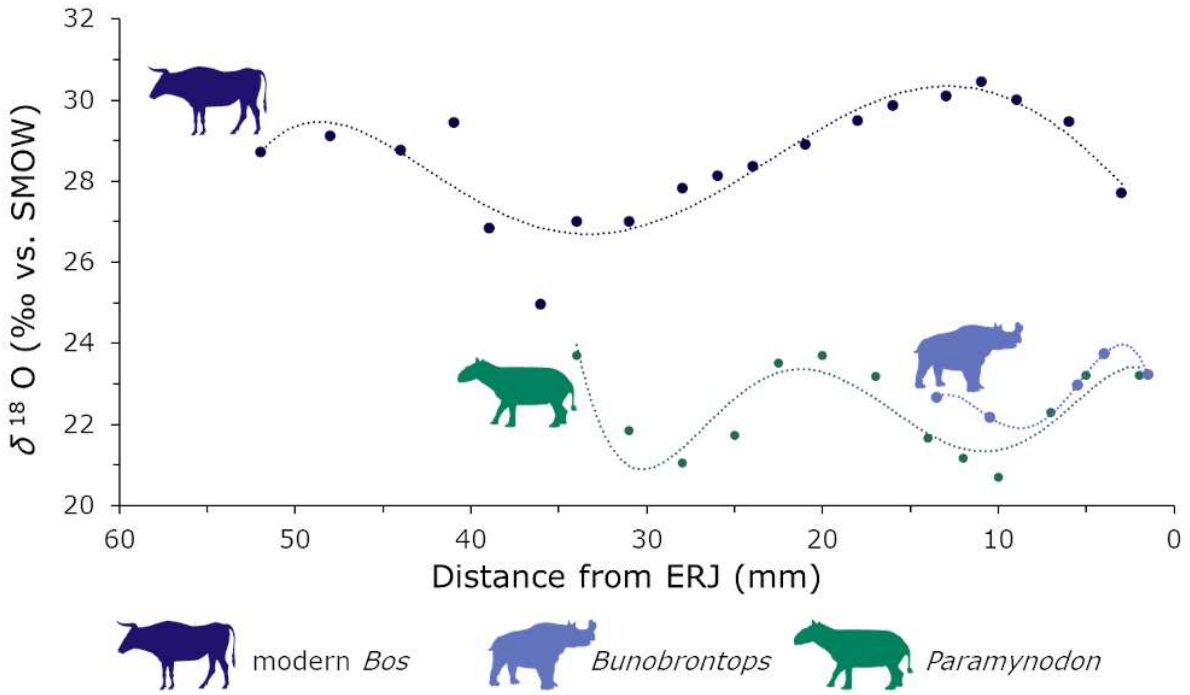

*Fig. 19 Visualization of two exemplary serially sampled Eocene specimen (Bunobrontops PNG-47, Paramynodon PNG-119) together with the modern bovid, illustrating different seasonal precipitation regimes. Plots of all the Eocene serially sampled individuals are reported in the SI of **publication 2**. The distance from the ERJ (enamel root junction) on the x-axis has been inverted. This way it represents the values in an intuitive temporal sequence from the oldest ones to the left to the youngest ones to the right. The statistical outlier (lowest $\delta^{18}O$ value) in the modern Bos is included in this figure, but has been excluded from the statistical analysis. Silhouettes via Phylopic under CC 3.0 license (modern Bos by T. Michael Keesey, Bunobrontops and Paramynodon by Zimices (Habinger et al. 2023).*

Another way to assess paleoseasonality is to check for a correlation of the $\delta^{18}O$ with the $\delta^{13}C$ values. Although no overall pattern was found in the Eocene specimens, significant correlations of these values in some of the taxonomic groups would also indicate a pronounced seasonality that influenced diet and habitat of the Anthracotheriidae, Amynodontidae, and Rhinocerotoidea, but not of the Brontotheriidae. For a more detailed discussion, refer to **publication 2**.

5.1.2. Microhabitat differences at the Pondaung Fm.

The localities from which the Pondaung mammal specimens were recovered into three areas, Bahin, Pangan, and Mogaung. I therefore wanted to test for microhabitat differences between them with the isotopic data. Both $\delta^{13}C$ and $\delta^{18}O$ values are lower in specimens from Mogaung than at Bahin and Pangan (Fig. 20). A Wilcox rank sum test confirmed that this difference is statistically significant (Mogaung/Bahin C: p = 0.001, O: p = 0.001; Mogaung – Pangan C: p = 0.003, O: p = 0.110). This indicates a denser vegetation and a more humid climate and/or the prevalence of shaded water sources with lower $\delta^{18}O$ values due to lower evaporation rates in the Mogaung area compared to the Bahin and Pangan area. The latter two did not differ significantly from one another.

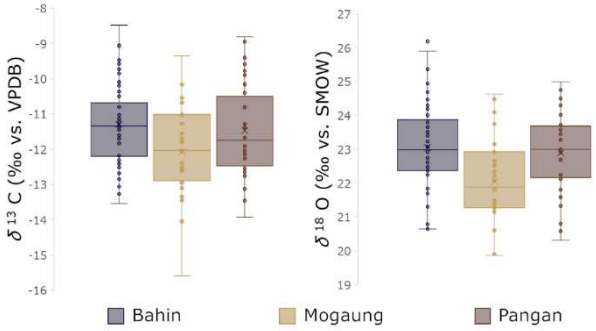

Fig. 20 Box plots of the compiled $\delta^{13}C$ (left) and $\delta^{18}O$ (right) values per area. The Mogaung values are lower for both isotopes which is consistent with a difference in microhabitats

Although these microhabitat differences are consistent with vegetation models the absence of a demonstrated stratigraphic relationship between the different localities and direct dating being only available from Bahin localities necessitates a discussion, if these patterns are caused be spatial or temporal differences between the areas. The current lack of knowledge does not allow excluding the possibility that diachronic differences and changes in habitats over time cause the different habitat reconstructions. However, the similarity between the geographically closer Bahin and Pangan areas is expected, if a spatial difference in vegetation and microclimates was in fact present.

In general, the Pondaung Fm. was a habitat consisting only of C_3 vegetation, as all the $\delta^{13}C_{diet}$ values are below –17.5 ‰ (Fig. 21), which marks the upper limit of the range of $\delta^{13}C$ values we expect from Eocene C_3 plants. The threshold was calculated according to the methodology explained in chapter 4.2.1 based on modern thresholds from Kohn (2010). C_4 plants evolved adaptations in their photosynthetic pathway to dry and hot climatic conditions and spread to Asia in the Late Miocene (Cerling et al., 1993; Cerling et al., 1997). Thus, I did not expect any values high enough to indicate their presence in the Pondaung data set. For a brief discussion of the first arrival of C_4 plants to Cenozoic Myanmar see chapter 5.2.1 or **publication 1**.

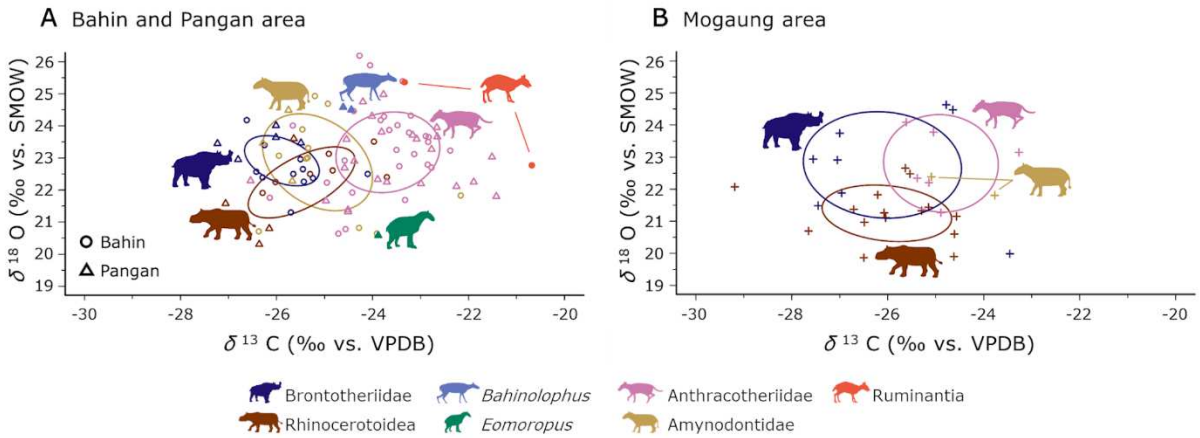

*Fig. 21 Ecological niche modelling of the Bahin/Pangan **(A)** and Mogaung **(B)** mammal communities based on all bulk and averaged serially sampled specimen. Ellipses represent the modelled core ecological niches. Silhouettes are from Phylopic under CC 3.0 licence by Zimices (Habinger et al., 2023).*

The ranges of $\delta^{13}C_{diet}$ values from both the Bahin/Pangan (−20.7 to −27.2 ‰) and the Mogaung specimens (−21.2 to −29.2 ‰) are indicative of open-forested woodlands, thus corresponding nicely to reconstructions of the vegetation in the upper deltaic plain by Licht et al. (2015). The woodlands were denser in the Mogaung area, and as the lowest $\delta^{13}C_{diet}$ values from there are just below the threshold for closed canopy vegetation at least proximity to if not presence of the more closed dipterocarp forests in the upstream areas from the same vegetation model (Licht et al., 2015) can be inferred.

Considering the occurrences of fossil primates (see detailed discussion of the Pondaung primates in chapter 1.2.1 and Table SI 4 from **publication 2**) at both habitat types, we see some evidence for ecological flexibility at least in *Aseanpithecus* and *Pondaungia*, which have been found at all three areas.

5.1.3. Ecological niche partitioning

I compared both the amount of overlap of the modelled isotopic niche space as well as the amount of overlap on taxonomic family level. % overlap showed no significant differences between the Bahin/Pangan and Mogaung areas (W = 9, p-value = 0.786), while the medians of the sizes of the modelled isotopic niches (SEA_C) are almost identical. Furthermore, the relative positions of the taxonomic groups to one another do not differ as well (Fig. 21). Summary statistics isotopic data as well as results from the niche overlap calculations are reported in Table 2 and Table 3 of **publication 2** respectively. Apparently, the differences in microhabitat are not reflected in differences in the organization of the niche space of the mammal fauna. Anthracotheriidae always occupied the more open patches of the habitat. This pattern seems to be more pronounced in the Bahin/Pangan area, likely due to the presence of more open areas than at Mogaung. The modelled anthracothere niche with its high $\delta^{13}C$ values could also be influenced by their more omnivorous subsistence strategy compared to the purely herbivorous one of the rest of the Pondaung mammal fauna analyzed for this study. Brontotheriidae, Rhinocerotoidea, and in the Bahin/Pangan area also Amynodontidae shared similar modelled isotopic niche spaces in the paleolandscape. There only is a bit of separation of the Brontotheriidae and Rhinocerotoidea niche in the $\delta^{18}O$ values. This could be due to the exploitation of isotopically different water sources.

As intra-individual serial sampling could be done in a decent number of specimens I decided to also model individual isotopic niche spaces. From this model, I calculated the relative isotopic niche index (RINI) that can give an indication about generalist versus specialist individuals or species. This approach revealed different patterns of the distribution of modelled ecological niches in the Anthracotheriidae (Fig. 22) than in the other taxonomic groups. While all the Anthracotheriidae appear to share the modelled aspects of their ecological niches, there is more separation between some of the individual modelled niches in the Brontotheriidae, Amynodontidae, and Rhinocerotoidea. However, there were no statistically significant differences in either SEA_C or RINI between Anthracotheriidae and the other taxonomic groups. Given the low taxonomic resolution in most of our data set, except for in the Anthracotheriidae, a reason for the intragroup niche differentiation cannot be inferred. I discuss the issue of RINI in specimens with low taxonomic resolution more detailed in **publication 2**.

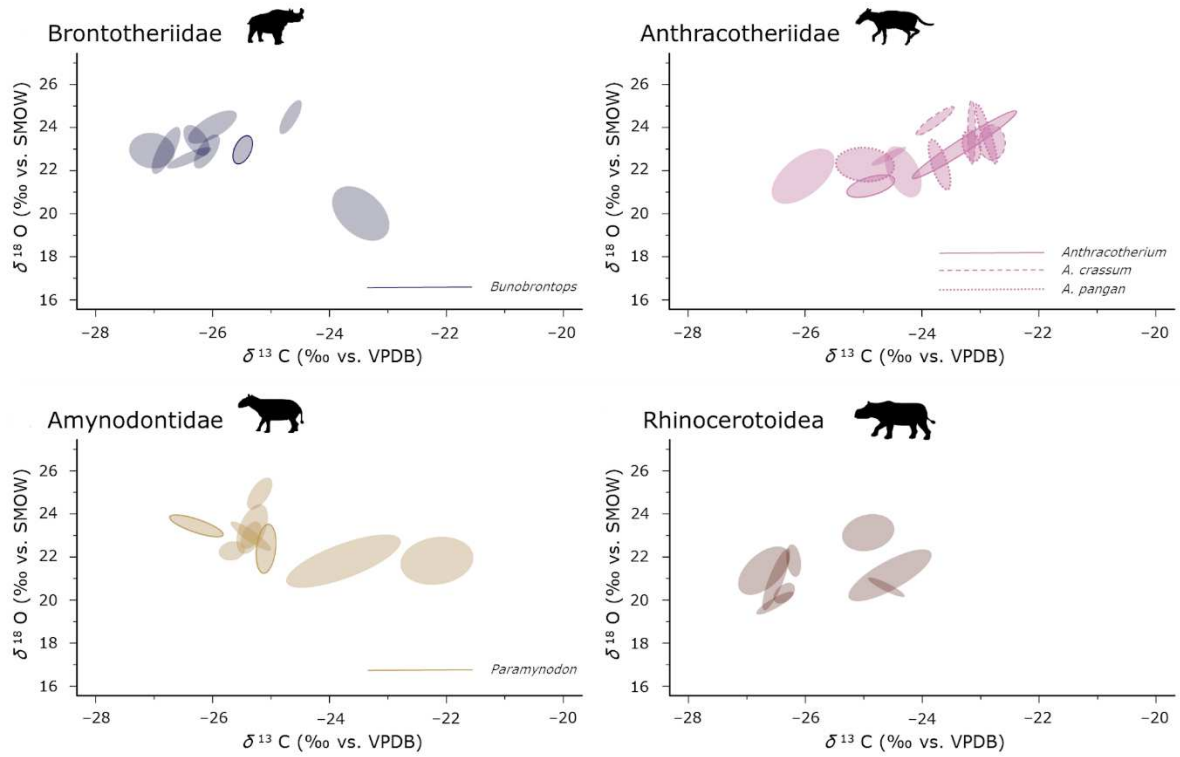

Fig. 22 Modelled ecological niches of the serially sampled specimen in separate graphs per taxonomic group. Each ellipse corresponds to the modelled core ecological niche represented by SEA_C of one individual (CI = 40%) visualizing different clustering patterns especially between the Anthracotheriidae and the other three taxonomic groups. Silhouettes are from Phylopic under CC 3.0 licence by Zimices (Habinger et al., 2023).

5.1.4. The anthracotheres

The first research question that I wanted to answer with my data was if there already is evidence for a semi-aquatic lifestyle in the anthracotheres although no morphological adaptations in the cranium or postcranium are present yet. The evaluation of the $\delta^{18}O$ values however show, that although the localities are located along a paleo river system, the anthroctheres and none of the other taxonomic groups has values low enough to support semi-aquatic behavior. Depending on the overall humidity an offset of 2 – 4 ‰ between freshwater living semi-aquatic species and terrestrial ones would be expected

(Clementz et al., 2008). With the exception of taxonomic groups with very low sample sizes (MNI = minimum number of individuals = 2) standard deviations of 0.5 ‰ or lower that would also be indications for a semi-aquatic lifestyle (Yoshida and Miyazaki, 1991; Clementz and Koch, 2001) are also absent from the data set.

Taking a closer look at the Anthracotheriidae and their niche partitioning per genus, revealed that there was a lot of niche overlap (Fig. 23). This trend was already visible in the niche modelling of the anthracotheres from which serial samples could be taken (Fig. 22) even though only *Anthracotherium* was represented in these individuals. This high degree of overlap is consistent with the sharing of habitats with similar ecological characteristics. The Pondaung habitat must have provided sufficient areas that fulfil the ecological requirements of the anthracotheres to sustain all of the anthracothere genera and species sampled in this study. It also means that the differences in habitat preferences and feeding ecologies that were inferred from tooth and bone morphology (Ducrocq, 1999) discussed in chapter 3.1.1. There I described the hypothetical ecology of *Anthracotherium* as being both more water dependent and more reliant on open spaces in the habitat for their subsistence. However, this is not reflected with significantly higher $\delta^{13}C$ values or lower $\delta^{18}O$ values in Anthracotherium compared to the other genera. The isotopic data therefore are not consistent with this hypothesis.

What can this niche modelling tell us about the competition potential in the Anthracotheriidae? *Anthracotherium* shares almost all of its modelled ecological core niche space with *Anthracokeryx* (Fig. 23), while Anthracokerys only shares a bit more than half of its niche space with Anthracotherium. This pattern is consistent with Anthracotherium facing a heightened competition pressure (Ogloff et al., 2019). The larger body mass of *Anthracotherium* counteracts this effect, as it could indicate that *Anthracotherium* used its advantage of being larger to push into the *Anthracokeryx* niche space (Schoener, 1983; Persson, 1985; Law et al., 1997). This pattern is repeated in the comparison of *Anthracokeryx* and *Siamotherium*, pointing towards similar interpretations. *Siamotherium* is only represented by four samples from two individuals that differ vastly in $\delta^{13}C$ values. Further interpretations will therefore depend on a larger sample size for *Siamotherium*.

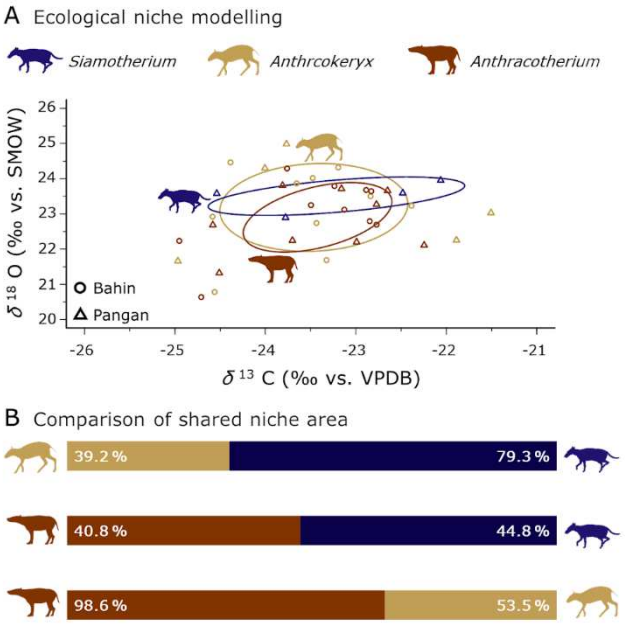

*Fig. 23 Ecological niche modelling of the anthracotheres from Bahin/Pangan per genus **(A)**. Ellipses represent the core ecological niches. In **(B)** the results of the shared niche area ($A_A - A_B$, and $A_B - A_A$) between each taxonomic group are visualised. Silhouettes are from Phylopic under CC 3.0 licence (Anthracotherium by Zimices, Anthracokeryx by Nobu Tamura and vectorised by T. Michael Keelsey, and Siamotherium is Public Domain) (Habinger et al. 2023).*

When switching to an even finer grained taxonomic resolution the limitation of sample size of course is even more prevalent. While acknowledging this limitation, I still want to discuss briefly niche partitioning between the anthracothere species (Fig. 24), especially between the *Anthracokeryx* and *Anthracotherium* species. Like in the anthracothere genera there is also a lot of niche overlap between the anthracothere species as well. Generalizing the results formed based on the comparison of *Anthracotherium* and *Anthracokeryx* in the previous section a hypothesis can be deduced: Species with higher body mass have a competition advantage; hence, we expect them to have a higher percentage of shared niche space with the smaller species.

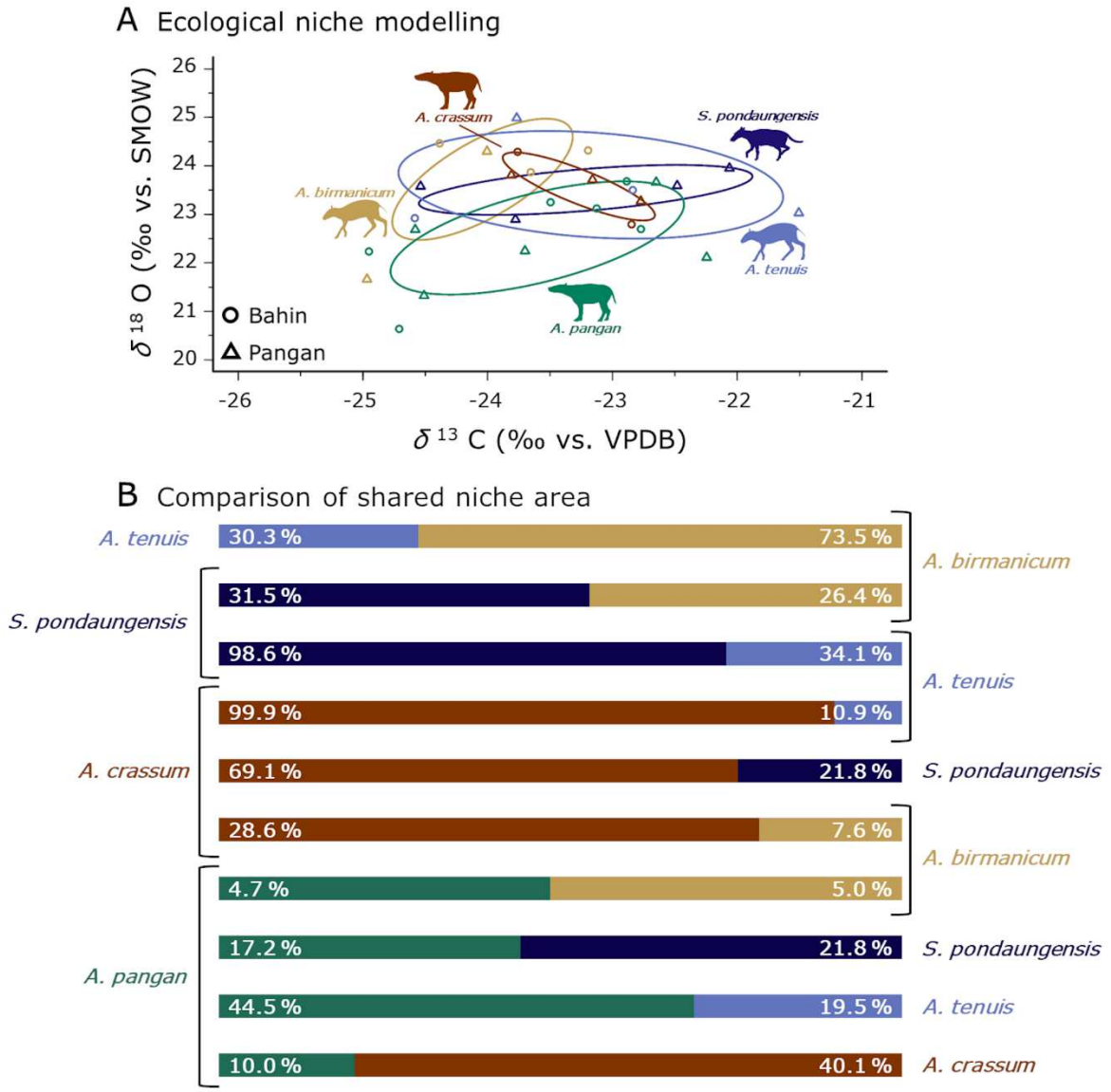

*Fig. 24 Ecological niche modelling of the anthracotheres from Bahin/Pangan per species **(A)**. Ellipses represent the core ecological niches. In **(B)** the results of the shared niche area ($A_A - A_B$, and $A_B - A_A$) between each taxonomic group are visualised. Silhouettes are from Phylopic under CC 3.0 licence (Anthracotherium by Zimices, Anthracokeryx by Nobu Tamura and vectorised by T. Michael Keelsey, and Siamotherium is Public Domain) (Habinger et al., 2023).*

The smallest of these anthracotheres, *Anthracokeryx tenuis*, follows this prediction in every instance and always shares a smaller percentage of its niche area than the bigger species with which it is compared. However, this the other species do not follow the predictions as consistently. *Anthracotherium pangan* is the largest anthracothere from Pondaung. Still, the smaller *A. crassum* shares more of its core niche with it than vice versa. One possible explanation would be that *A. crassum* also has a much narrower core ecological niche than *A. pangan*. It would be consistent with the interpretation of A. pangan being more generalist in its ecological requirements. *Anthracokeryx birmanicum* mostly fulfils the expectations based on our hypothesis with the exception that the % overlap between it and *A. pangan* is very balanced in spite of the significant body mass differences. However, the overlap is very small indicating more distinct ecological requirements. These lead to a reduction in competition potential.

5.2. Evolutionary Ecology of pongines in Southeast Asia

In this chapter, I summarize the reconstruction of paleoecology and paleodiet of *Khoratpithecus ayeyarwadyensis* and its comparison with contemporaneous *Sivapithecus* from the Siwaliks of India, Nepal, and Pakistan. It is then put into context with other Ponginae from Southeast Asia and discusses implications for the evolutionary ecology of *Pongo*. For the paleoecological reconstructions based on stable carbon and oxygen isotopes, I will mainly refer to **publication 1**, whereas the dietary reconstructions using DMTA are preliminary results from my ongoing research.

Zusammenfassung

Trotz des im Vergleich zu anderen Menschenaffen reichen bekannten fossilen Materials bleiben bis heute viele Aspekte der Evolutionsgeschichte und Paläoökologie des Orangutans ungeklärt. Der geographisch stark eingeschränkte Lebensraum des einzigen heute noch existenten Genus *Pongo* weist auf spezifische ökologische Bedürfnisse hin. Es ist jedoch unklar, ob diese von den vielfältigen fossilen Vertretern der Unterfamilie Ponginae, die vom Miozän bis zum Pleistozän verbreitet waren, geteilt wurden. In diesem Kapitel zeige ich, wie die Modellierung ökologischer Nischen unter Verwendung der stabilen Kohlenstoff- und Sauerstoffisotope im Karbonatanteil von Zahnschmelz dazu genutzt werden kann, um die Paläoökologie von fossilen Vertretern der Ponginae zu rekonstruieren und mit der moderner Orangutans zu vergleichen. Der Fokus liegt hierbei auf *K. ayeyarwadyensis*, der zur Schwestergruppe der Gattung *Pongo* zählt, und der mit ihm assoziierten spätmiozänen Säugetierfauna aus dem heutigen Myanmar.

Die Ergebnisse stimmen mit einer vertikalen Positionierung von *K. ayeyarwadyensis* oben in der Baumschicht beziehungsweise den Baumkronen in einem bewaldeten Habitat durchgehend bestehend aus C_3 Vegetation überein. Die Bewaldung ist lichter als in heutigen tropischen Regenwäldern, das heißt es ist von einem unvollständigen Kronenschluss mit gelegentlichen Lichtungen auszugehen. Diese Interpretation stimmt mit der rekonstruierten Paläoökologie des ungefähr zur gleichen Zeit vorkommenden *Sivapithecus* überein, obwohl dessen Habitat vermutlich eine noch geringere Walddichte aufweist.

Diese modellierte ökologische Kernnische und die Nahrungsgrundlage der beiden miozänen Ponginae stimmt oberflächlich betrachtet mit der moderner Orangutans überein. Ein konkreter Vergleich der modellierten Isotopennischen zeigt allerdings Unterschiede in der Habitatstruktur und der Nutzung des Habitats. Auch die primär frugivore Ernährungweise zeigt erhebliche Variation, auch innerhalb der Miozänen Ponginae.

Résumé

Malgré l'abondance des matériaux fossiles connus par rapport à d'autres grands singes, de nombreux aspects de l'histoire évolutive et de la paléo-écologie des orang-outan restent flous. L'habitat géographiquement très restreint du seul genre *Pongo*, qui existe encore aujourd'hui, indique des besoins écologiques spécifiques. Cependant, on ne sait pas si ces spécialisations sont partagées par les divers représentants fossiles de la sous-famille des Ponginae, présents du Miocène au Pléistocène. Dans ce chapitre, je montre comment la modélisation des niches écologiques à l'aide des isotopes stables du carbone et de l'oxygène dans la partie carbonatée de l'émail dentaire peut être utilisée pour reconstruire la paléo-écologie des Ponginae fossiles, et comment la relier à celle des orangs-outans modernes. L'accent est mis ici sur *K. ayeyarwadyensis*, qui appartient au groupe frère du genre *Pongo*, et la faune mammifère qui est associée avec lui. Les fossiles ont été découverts dans la formation Irrawaddy au Myanmar, datant de la fin du Miocène moyen.

Les résultats sont cohérents avec un positionnement vertical de *K. ayeyarwadyensis* au sommet de la canopée dans un habitat forestier composé en totalité de végétation à photosynthèse en C_3. Le couvert forestier est moins dense que dans les forêts tropicales humides d'aujourd'hui, ce qui suggère une fermeture incomplète de la canopée avec d'éventuelles clairières. Cette interprétation est cohérente avec la paléo-écologie reconstituée pour le Ponginae contemporain *Sivapithecus*, bien que son habitat soit considéré comme encore moins densément boisé.

Cette niche écologique de base modélisée et le base alimentaire des deux Ponginae du Miocène sont superficiellement cohérentes avec celles des orangs-outans modernes. Cependant, une comparaison concrète des niches isotopiques modélisées montre des différences dans la structure et l'utilisation de l'habitat. Le mode d'alimentation frugivore primaire présente également des variations considérables, même au sein des Ponginae miocènes.

5.2.1. Paleoenvironmental reconstruction of the Yinseik habitat

Before focusing on *Khoratpithecus ayeyarwadyensis* itself the overall climatic and environmental characteristics of its habitat should be established. While the general climatic conditions of late Miocene Southeast Asia have already been discussed in chapter 1.1.2, the focus in this section will be on a more local geographical scale and will discuss the paleoseasonality and forest structure of the Yinseik locality. For this reconstruction I used data on intra-individual variation of $\delta^{18}O$ values of several (n = 5) high crowned mammal

specimen from this locality. Then the vegetation and forest density of the Yinseik habitat will be discussed using the $\delta^{13}C_{diet}$ values of the complete mammal fauna. Building on this the niche partitioning this mammal community will be interpreted. Only then the focus will shift on *K. ayeyarwadyensis* and how the relationship of the data from the one M_3 that was available for sampling as well as the comparison with contemporaneous *Sivapithecus* from the Siwaliks in Pakistan can inform us on its paleoecology.

A commonly used proxy for paleoseasonality is the intra-individual variation of $\delta^{18}O$ values in fossil enamel. The temperature effect on these values is overwritten by the amount effect in regions with monsoonal climate (Dansgaard, 1964). Hence, the wet season is characterized by lower $\delta^{18}O$ values than the dry season in such regions.

Lower $\delta^{18}O$ values in fossils in comparison to modern reference data, have been interpreted as an indication of a wetter climate during the Late Miocene than today (Sun et al., 2021). We see the same pattern in the hipparions from the Siwaliks of Pakistan (Nelson, 2005). The minimum $\delta^{18}O$ values measured from the serially sampled hypsodont teeth rise over time. A trend that is consistent with a decreasing amount of seasonal precipitation (Fig. 25). These data are consistent with a seasonal precipitation regime with a dry season of five to six months similar to the monsoonal forests in southern China today, for the Late Miocene Siwaliks (Nelson, 2005).

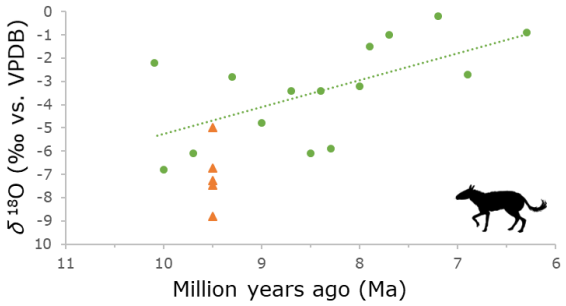

Fig. 25 Development of the minimum $\delta^{18}O$ values from dental enamel of hipparions from the Siwaliks (Nelson 2005) over time ($y = -1.1527x + 6.2827$; adjusted $R^2 = 0.3216$; p-value = 0.01611) indicates a decrease of seasonal maximum precipitation. Minimum $\delta^{18}O$ values from the Yinseik specimens in orange do all plot below the regression line and among the lowest minima from the Siwalik hipparions. Icon obtained via PhyloPic and in public domain. (Habinger et al. 2022)

The lowest $\delta^{18}O$ value (-5.7 ‰) measured in the serially sampled modern bovid specimen (PND-M1) looked like an anomaly during visual inspection. I therefore tested it with a Grubb's test that confirmed this suspicion as the p-value is higher than O.O5 (G = 2.5669, U = 0.88801,

p = 1). Hence, it is excluded from all further model, but it is still shown in Fig. 26. Testing the difference between the $\delta^{18}O$ values of the modern bovid from Myanmar and the Miocene bovid, whose values were closest to the modern reference sample from all the Yinseik herbivores (Fig. 26), showed a significant difference (W = 6, p-value = 0.0001248). This together with the comparison with the contemporaneous equids (Fig. 25) is a clear indication of a wetter climate in Miocene Myanmar than today and in the contemporaneous Siwaliks. Another Wilcoxon rank sum test showed that $\delta^{18}O$ values of bulk samples from the *Khoratpithecus* fauna (maximum = −3.3 ‰, mean = −6.5 ‰) (Fig. 27 A) are significantly lower in comparison with the *Sivapithecus* fauna (maximum = 0.7 ‰, mean = −4.5 ‰) (Fig. 27 C) (W = 4056, p-value = 1.245e-06) (Fig. 27 C). This is also consistent with the interpretations of the $\delta^{18}O$ values as being an indicator of a more humid climate for the Yinseik than for the Siwalik localities. The comparison of the amplitude, defined as the difference between maximum and minimum values of one tooth, of Yinseik and the modern values, however shows an increase from the Miocene to today (Table 6). The amplitude for is 3.5 ‰, which is still higher than the maximum amplitude found in the Miocene specimen, the Giraffid (IRWD-42) with 2.8 ‰. Such a pattern is consistent with a less pronounced difference in seasonal precipitation and hence an overall more humid climate in the Miocene, as compared to the present day monsoonal climate in Myanmar. The covariance of the $\delta^{13}C$ and the $\delta^{18}O$ values is another factor consistent with this interpretation. It is discussed in more detail in **publication 1**.

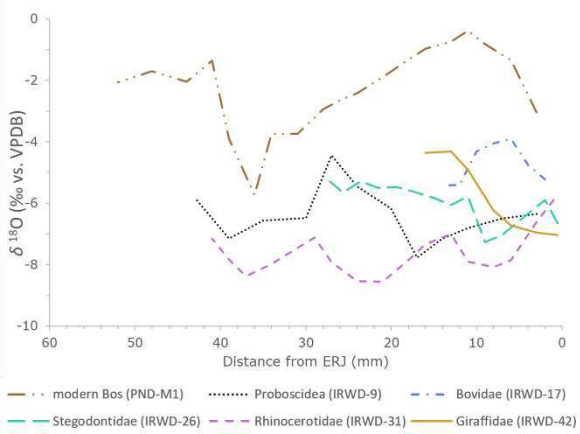

Fig. 26 Comparison of the intra-individual serial sampling of the Yinseik mammals with a modern bovid from the Central Basin in Myanmar. Distance from ERJ (enamel root junction) is plotted in reverse order to correctly represent the enamel mineralization from oldest (left) to youngest (right). The lowest $\delta^{18}O$ value of the modern bovid (at 36 mm from the ERJ) represents a statistical outlier (see chapter 4.3). Its removal leads to only a slight overlap of 0.3 ‰ between the highest Miocene values found in the bovid IRWD-17 (-3.6 ‰) and the lowest one of the modern bovid PND-M1 (3.9 ‰). Modified from (Habinger et al. 2022).

Table 6 Summary statistics for the intra-tooth serial sampling. Specimens labelled with IRWD are the fossil mammals from the Yinseik locality, whereas PND-M1 is the modern reference sample that also originates from the same geographic area, the Central Basin of Myanmar. As described in the text, the minimum $\delta^{18}O$ value of the modern bovid changes to -3.9 ‰ and the amplitude to 3.5 ‰ after the removal of the statistical outlier (PND-M1n) (Habinger et al., 2022).

Specimen n°	N° of samples	Taxonomy	$\delta^{18}O_{VPDB}$			$\delta^{13}C_{diet}$			C & O covariance
			min	max	amplitude	min	max	amplitude	
IRWD-9	12	Proboscidea	-7.3	-4.1	3.2	-27.2	-26.2	1.1	0.2
IRWD-17	8	Bovidae	-5.0	-3.6	1.4	-25.4	-24.6	1.4	-0.1
IRWD-26	14	Stegolophodon	-6.8	-5.5	1.2	-27.2	-25.4	1.8	0.1
IRWD-31	17	Rhinocerotidae	-8.8	-6.1	2.7	-27.9	-27.5	0.4	0.0
IRWD-42	7	Giraffidae	-7.5	-4.6	2.8	-27.6	-27.1	0.5	0.0
PND-M1	19	Bos	-5.7	-0.4	5.3	-15.4	-13.7	1.7	-0.3

The $\delta^{13}C_{diet}$ values of the *Khoratpithecus* fauna from the Yinseik locality represent almost the entire range of modern C_3 plants (−33 to −22 ‰) (Bender, 1971). Giraffidae and Rhinocerotidae have the lowest and Suidae having the highest values (Fig. 27 A). The latter can be related to the omnivorous subsistence strategy of suids which leads to an enrichment of the dental tissue with the heavier carbon isotope and not only to the canopy effect. Interestingly the equids from the Yinseik locality did not use the more open parts of the habitat according to their $\delta^{13}C$ values. This together with the lower $\delta^{13}C$ values of the Yinseik mammals in general indicates a more densely forested habitat there than in the Siwaliks.

After correcting the $\delta^{13}C$ values of C_3 plants from the modern values reported by Bender(Bender, 1971) to preindustrial ones, which we use to compare isotopic values from different geological eras to one another, the cut-off point for C_3 vegetation lies at −20.5 ‰. Values higher than that would indicate the presence of C_4 plants in an individual's diet. Such high values are only visible in the post-Sivapithecus (Fig. 27 D) and the even younger Chaingzauk locality from Myanmar (Fig. 27 B). The broad range of $\delta^{13}C$ values in both the Yinseik data set (−30.3 to −21.3 ‰) and the contemporaneous *Sivapithecus* fauna from the Dhok Pathan and Khaur regions of the Siwaliks (−29.0 to − 20.8 ‰) indicates that, both *K. ayeyarwadyensis* and *Sivapithecus* lived in a mosaic landscape solely comprised of C_3 plants.

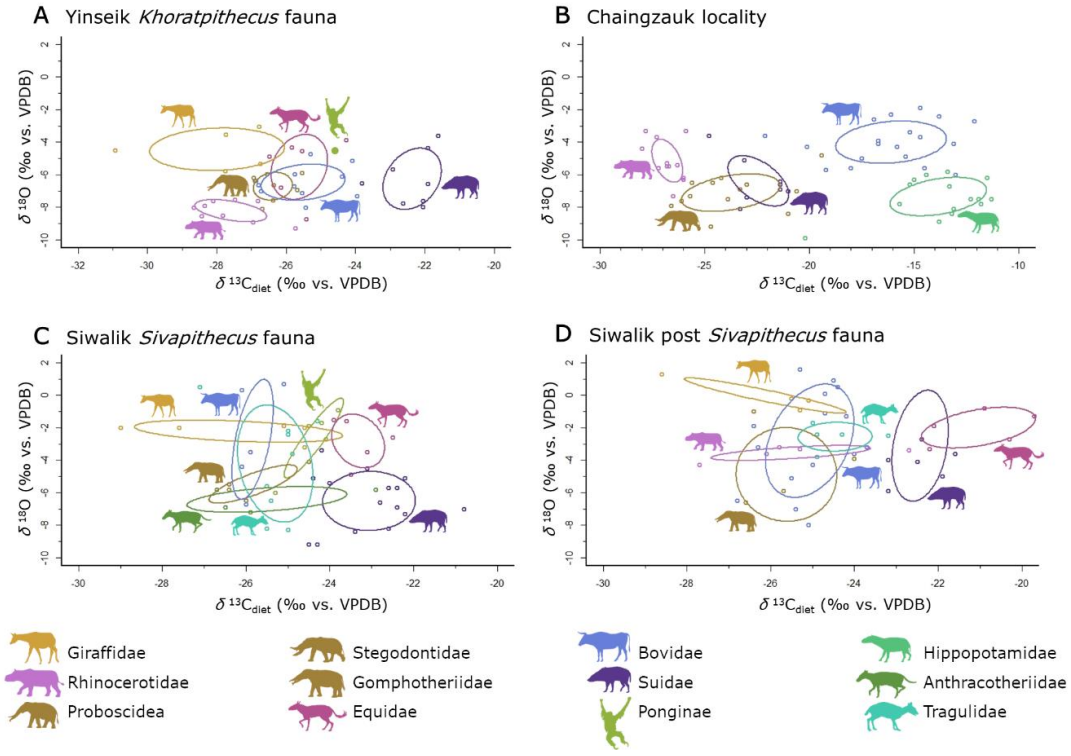

Fig. 27 Visualisation of niche partitioning using bayesian niche modelling of four fossil mammal communities. The ellipses correspond to the SEAc (standard ellipse area corrected for small sample size) or core ecological niche, which represents a 40 % CI. Summary statistics are reported in Table SI 1 of ***publication 1****. A – Yinseik fauna including K. ayeyarwadyensis (~9.5 Ma), B – Chaingzauk fauna (6 ¬ 4 Ma)(Zin-Maung-Maung-Thein et al. 2011), C – Siwalik fauna including Sivapithecus (~9 Ma) (Nelson 2007), D – later Siwalik fauna (~8 Ma)(Nelson 2007). Icons from PhyloPic and in public domain or under CC 3.0 license (Rhinocerotidae, Hippopotamidae, and Tragulidae by Zimices). (Habinger et al., 2022)*

The two younger data sets from the Chaingzauk (6 – 4 Ma) locality in Myanmar (Fig. 27 B) and the post-*Sivapithecus* (~8 Ma) layers from the Siwaliks (Fig. 27 D) both show similar trends. There is a visible shift towards more positive $\delta^{13}C$ values in the Siwaliks at ~8 Ma (−28.6 to −19.7 ‰) and a drastic increase of range for $\delta^{13}C$ values in the Chaingzauk data (−28.0 to −11.3 ‰). This shows a continuous opening of the landscape and forest fractionation as well as it illustrates the appearance of C_4 plants in these habitats throughout the Late Miocene in South and Southeast Asia. Some groups of mammals adapt their ecological niches to these changes, such as the suids and equids in the Siwaliks and the bovids and rhinos in the Chaingzauk mammal communities, which start to incorporate C_4 plants into their diet. Although for the omnivorous suids it is more likely that the high $\delta^{13}C$ values reflect the incorporation of animal protein in their diet and that might also have utilized the more open habitat patches.

5.2.2. Paleoecology of *Khoratpithecus ayeyarwadyensis*

Which part of this mosaic woodland forest habitat was inhabited by *K. ayeyarwadyensis*? Its $\delta^{13}C$ value is consistent with the more open parts of the forest or high up in the canopy where the canopy effect is less pronounced, and its $\delta^{18}O$ value is most similar to those of giraffids and equids. While a diet consisting of leaves or fruit with higher $\delta^{18}O$ values due to evapotranspiration is a probable explanation for the pongine, drinking from evaporated water sources like ponds seem more likely for the other two. As expected, the $\delta^{18}O$ values of browsers foraging on leaves closer to the forest floor like the rhinos are lower than the ones from more arboreal browsers like giraffids. Thus, the $\delta^{18}O$ value of *K. ayeyarwadyensis* is also consistent with foraging high up in the canopy.

Previous dental topography and dental microwear studies applying traditional 2D approaches have suggested a predominantly frugivorous diet, without any evidence for the consumption of hard objects for *K. piriyai* and *K. chiangmuanensis*, the two closest allies of the Myanmar species (Merceron et al., 2006). Newly analysed dental microwear texture data on *K. piriyai* confirm this dietary pattern, which is also consistent with the isotopic data. In this new study on the paleodiet of *Khoratpithcus* I also included two specimens from Myanmar, one of which could be identified as *K. ayeyarwadyensis*. The second one is much larger, and in the size range of *K. magnus* from Thailand. However, attribution to this species solely based on an isolated tooth is not possible, thus I refer to it as *Khoratpithecus* sp. *K. ayeyarwadyensis*, displays much higher complexity in their dental microwear textures than *K. piriyai*, whereas *Khoratpithecus* sp. has lower Asfc values, similar to those of extant *Pongo* and *Gorilla* (Fig. 28). While seed predation and the consumption of hard foods in general has already been ruled out for Pleistocene *Pongo* (Louys et al., 2021), the heightened Asfc values of the one specimen of *K. ayeyarwadyensis* would be consistent with such a dietary regime (Fig. 28). This is consistent with the diet inferred for *Sivapithecus*, which also included some hard objects like seeds and nuts into its diet (Kay, 1981; Nelson, 2003). An interpretation as a first indication of diversity in dietary regimes in the genus *Khoratpithecus* is consistent with these results, though severely limited by the low sample sizes in species other than *K. piriyai*. I will discuss the results of this new dental microwear texture data regarding changes in dietary ecology in the pongines in more detail in chapter 5.2.4.

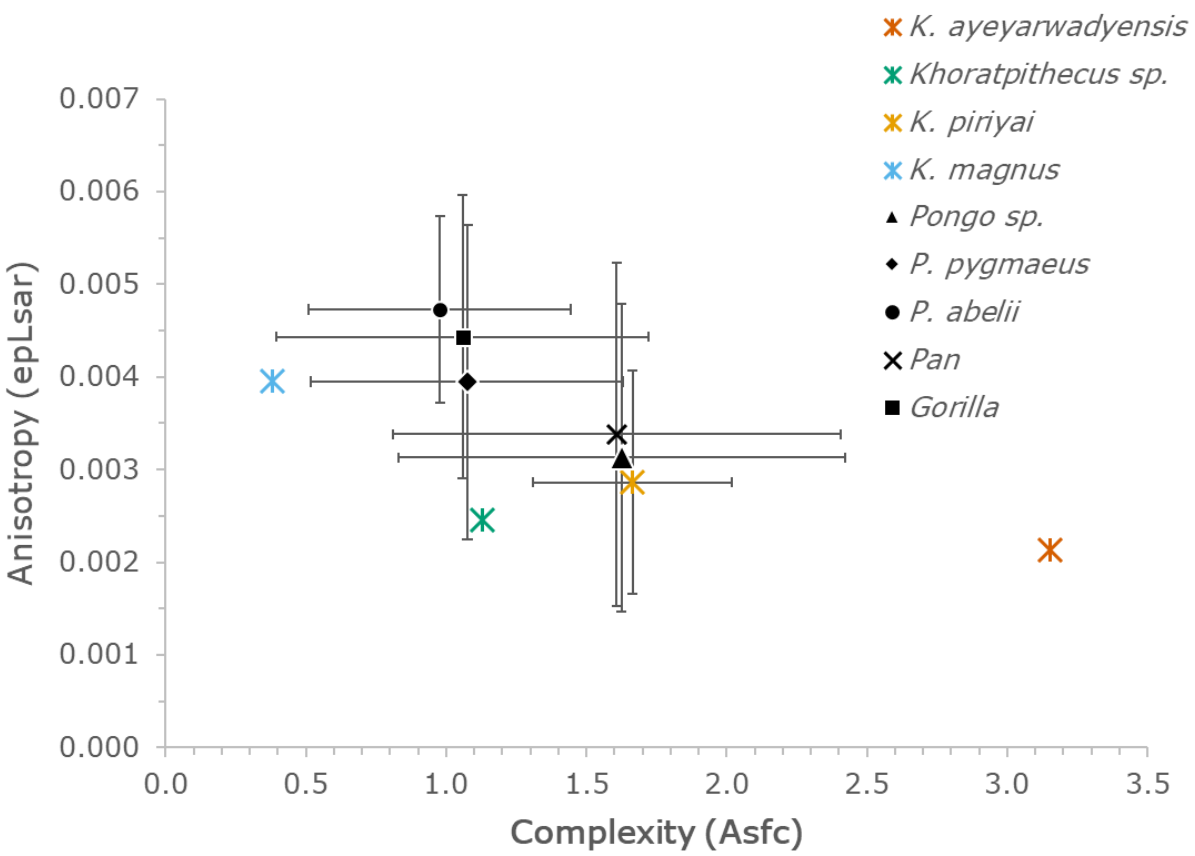

Fig. 28 Biplot of means and dispersion (± 1 SD) of complexity and anisotropy by taxonomic group. K. ayeyarwadyensis and Khoratpithecus sp. are from the Irrawaddy Fm. in Myanmar, K. piriyai and K. magnus from the Khorat sandpits in Thailand.

To test if the difference in dietary ecology between *Khoratpithecus* sp. and *Sivapithecus* could be related to differences in competition potential I used % overlap of the SEACs between all the taxonomic groups of the two mammal faunas (Fig. 27 A and C). The Wilcox rank sum test only shows a significant difference (W = 48, p-value = 0.01008), when pairings between two taxonomic groups where the % overlap is 0 % are excluded. Otherwise the p-value is bigger than 0.05 (W = 273.5, p-value = 0.06895). Hence, the isotopic niche modelling does not clearly indicate a significantly heightened pressure due to competition in one of the two mammal communities. The different number of taxonomic groups present in the two datasets probably has an impact on these results as well.

5.2.3. Assessing ecological continuity in the Ponginae

Here, I want to focus on the discussion of *Khoratpithecus*, *Sivapithecus*, and *Pongo*. For the detailed interpretations of the *Gigantopithecus* and *Indopithecus* data in this context please refer to **publication 1**. When we compare the ecological niches of *Sivapithecus* and *K. ayeyarwadyensis* inferred from the modelled isotopic niches and the comparison with associated mammal fauna to one another and to modern orangutans there are some shared characteristics. All could be described as predominantly frugivorous, arboreal forest dwellers. However, in a direct comparison of ecological niches of the various fossil and extant pongines, there are apparent differences in their ecology and habitat use (Fig. 29). Of course the facts that only one sample of *Khoratpithecus* was available and that there is a high variation in both the $\delta^{13}C$ and $\delta^{18}O$ values of the other pongine genera do limit the interpretations we can make

in regard to this specific pongine. Nevertheless, I can give a first approximation of its ecology and show that it is consistent with the trends visible through the contemporaneous *Sivapithecus*, for which the sample size (n = 5) was large enough to model an isotopic niche with reasonable confidence given the Bayesian modelling approach I am using (Jackson et al., 2011).

The higher $\delta^{13}C$ in the Miocene pongines indicate that although they also lived in a forested habitat, it seemed to either be fragmented forest or higher up in the canopy (Fig. 29), whereas the ecological niches of both modern and Pleistocene *Pongo* are consistent with a more closed canopy or foraging lower down in the canopy or even on the ground. Various other paleoenvironmental proxies, such as palynological data, paleosol isotopic data, and climate and vegetation models(Quade et al., 1989; Hoorn et al., 2000; Zachos et al., 2001; Sepulchre et al., 2010; Morley, 2012, 2018) also indicate similar changes in forest structure from the Miocene to the Pleistocene. These changes could be connected with the marked and extensive climate changes during the end of the Neogene (Zachos et al., 2001).

I wanted to test, if these indicated differences in vegetation structure of the modelled niches of *Sivapithecus* and Pleistocene *Pongo*, are statistically significant. Therefore, I conducted a Wilcoxon Rank Sum test that showed that this is in fact the case (W = 4.5, p-value = 0.01422). This means that although the ecological niche of *Sivapithecus* and *K. ayeyarwadyensis* within their respective mammal communities resemble that of modern *Pongo*, a direct comparison of these ecological variables with the other pongines on a broader scope reveals that the microhabitats they occupied or their habitat use differed significantly.

The difference in modelled isotopic niches between Miocene and the Pleistocene pongines as well as modern *Pongo* is not only related to the vegetation structure of the habitats, but also the different ways in which they were used by these primates becomes even more apparent when the $\delta^{18}O$ values are incorporated in the interpretation. These also point towards a canopy habitat for Miocene pongines *K. ayeyarwadyensis* and *Sivapithecus*. There is a trend of decreasing $\delta^{13}C_{diet}$ and $\delta^{18}O$ values that coincides with increasing body mass from *Khoratpithecus* and *Sivapithecus*, to *Pongo*, and to *Gigantopithecus*. The exception to this trend is *Indopithecus* who has both a high body mass (150 kg) and high $\delta^{13}C_{diet}$ and $\delta^{18}O$ values (Fleagle et al., 1999). For this hominoid a more open habitat has been suggested previously and its isotopic data might have an analytical bias and therefore be less comparable to the rest of the data set as it was analysed using laser ablation (Pilbeam, 1970; Patnaik et al., 2014). A higher body mass makes foraging high up in the canopy and close to terminal branches increasingly difficult. However, brachiation in conjunction with high hip flexibility in *Pongo* counters the negative impact of higher body mass during climbing to a certain extent, as the weight can be distributed over many smaller branches this way(Thorpe and Crompton, 2006; Zihlman et al., 2011; Hunt, 2016).

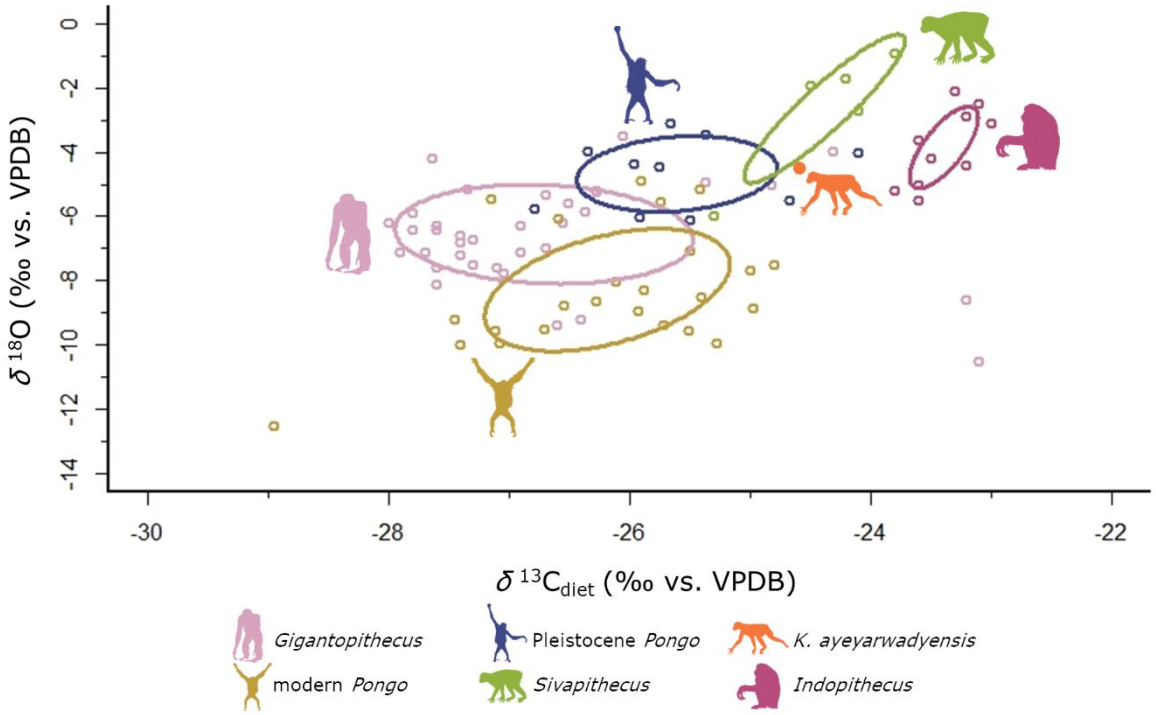

Fig. 29 Visualisation of the shifts in ecological niches between the different fossil and extant pongine genera using bayesian niche modelling. The lines encompass the standard ellipse area or core ecological niche, corresponding to a confidence interval of 40 %(Jackson et al., 2011). Data other than K. ayeyarwadyensis from (Bacon et al., 2018a; Nelson, 2007; Wang et al., 2007; Pushkina et al., 2010; Jaeger et al., 2011; Thein et al., 2011; Nelson, 2014; Patnaik et al., 2014; Qu et al., 2014; Janssen et al., 2016; Bocherens et al., 2017; Ma et al., 2017; Suraprasit et al., 2018; Ma et al., 2019; Louys and Roberts, 2020; Jiang et al., 2021). Icons are public domain (Gigantopithecus, Indopithecus) or Creative Commons 3.0 license (modern & Pleistocene Pongo by Gareth Monder, Khoratpithecus by Mateus Zica (modified by T. Michael Keesey), and Sivapithecus by Nobu Tamura (modified by T. Michael Keesey)) via PhyloPic. (Habinger et al., 2022)

Although it sound promising to relate the decreasing $\delta^{18}O$ values from the Miocene to the Pleistocene genera (Fig. 29) to the increasing competition with cercopithecoid monkeys, which became increasingly abundant in Southeast Asia from the Late Miocene and especially the Plio-Pleistocene onward (Barry, 1987; Jablonski et al., 2000; Takai et al., 2006), this hypothesis has several problems. The higher body mass of pongines in comparison with the contemporaneous monkeys gives them a competitional advantage such as dominating in physical encounters regarding access to food resources. Therefore, it is unlikely that the pongines were pressured by cercopithecines to resort to lower canopy layers for foraging (Schoener, 1983; Persson, 1985; Law et al., 1997; Houle et al., 2010). Even more so, as it has been suggested that the feeding behaviour of monkeys, which are capable of eating unripe fruits, creates a pattern of fruit availability that forces pongines to use terminal branches for their subsistence (Hunt, 2016). This could have rather been an incentive to develop brachiation to still be able to access ripe fruit up in the canopy while also having a relatively high body mass.

As this comparison covers a wide geographic and temporal range it was necessary to assess to what extent the $\delta^{18}O$ values still reflect ecological differences of the pongines. For this I used a data set of the pongine values in combination with suids and bovids from the same sites. The detailed discussion on how I made these estimations can be found in the SI of

publication 1. Here it suffices to say that apart from the difference in $\delta^{18}O$ values between modern and Pleistocene Pongo, which is likely predominantly caused by differences in climate and a more intense monsoon on the Sunda Shelf than in mainland Southeast Asia (Vuille et al., 2005), the rest of the variation probably mainly reflects differences in habitat use by the pongines.

As a last point, I want to mention some implications for conservational biology. The different distributions of $\delta^{13}C$ values between Pleistocene and modern *Pongo* do not indicate changes in vegetation density as shown by a Wilcoxon Rank Sum test (W = 86.5, p-value = 0.2123). This means, that at least until a century ago, the time period represented in our modern *Pongo* sample, modern orangutans have not yet been pushed into denser forest habitats or to the forest margins and more open spaces due to deforestation. My results also show that even when their habitats became more fragmented, pongines remained dependent on closed habitats and were unable to adapt and move into more open forested woodlands. The ongoing opening of the landscape in the Siwaliks from 9 to 8 Ma and the disappearance of *Sivapithecus* during this time indicates, that if a certain threshold deforestation or forest fragmentation occurs this could lead to the extinction of a pongine.

5.2.4. Changes of diet from fossil to extant pongines

In this chapter, I will present the results of my dental microwear texture analysis on the fossil pongines of Southeast Asia. The focus will be on the comparison of *Khoratpithecus* with Pleistocene (*Pongo* sp.) from Sumatra and extant *Pongo* (*P. abelii*, *P. pygmaeus*). These results will be put into context with data sets on dental microwear textures from extant *Pan troglodytes* and *Gorilla gorilla*.

Looking back at Fig. 28, the different taxonomic groups seem to form two clusters. The two species of extant *Pongo* plot together with *Gorilla*. They display intermediate complexity paired with high anisotropy. High epLsar values were expected for *Gorilla*, as it is the most folivorous of the apes, however this is especially true for mountain gorillas (*G. beringei*) (e. g. Watts, 1984), whereas lowland gorillas (*G. gorilla*) have a much more varied diet (e.g. Rogers et al., 2004). They preferentially consume soft fruit, but fall back on tough foods (leaves, pith, etc.) when those are not abundant enough (e.g. Doran-Sheehy et al., 2009).Given the dietary regime of *Pongo* observed in orangutan populations from the 1960s onwards, dental microwear textures more similar to those of *Pan* would be expected. However, the percentage of specimens with anisotropic microwear textures (epLsar > 0.005) in *G. gorilla* (20 %, n = 15) and *P. pygmaeus* (26.7 %, n = 15) was very similar in the comparative study on anthropoid diets by Scott et al. (2012). It is nevertheless surprising that *P. abelii* has the highest mean epLsar values, as it presumably has a more abundant and reliable supply of fruits and therefore has to rely less on tougher fallback foods, such as mature leaves, lianas, or bark than *P. pygmaeus* (Delgado and van Schaik, 2000; Russon et al., 2009; Wich et al., 2011). Although the small sample size in *P. abelii* has to be considered when interpreting the results, they still can provide valuable insights for the paleodiet of pongines (Table 7).

Table 7 Summary statistics of the three main SSFA parameters per taxonomic group. Number of specimen is given as n. In cases where number of specimen and number of individuals differs the latter is reported in brackets. SD (standard deviation) was calculated with n-1.

Taxon	n	SSFA parameter	min	max	range	median	mean	SD (n-1)
Khoratpithecus sp. (Myanmar)	1	Asfc	-	-	0	1.131	-	0
		epLsar	-	-	0	0.003	-	0
		HAsfc81	-	-	0	0.646	-	0
K. ayeyarwadyensis (Myanmar)	1	Asfc	-	-	0	3.153	-	0
		epLsar	-	-	0	0.002	-	0
		HAsfc81	-	-	0	0.825	-	0
K. magnus (Thailand)	1	Asfc	-	-	0	0.380	-	0
		epLsar	-	-	0	0.004	-	0
		HAsfc81	-	-	0	0.489	-	0
K. piriyai (Thailand)	4 (3)	Asfc	1.158	1.915	0.757	1.792	1.664	0.355
		epLsar	0.002	0.004	0.002	0.003	0.003	0.001
		HAsfc81	0.514	1.044	0.530	0.932	0.856	0.242
Pongo sp. Pleistocene	29	Asfc	0.512	4.142	3.630	1.447	1.625	0.796
		epLsar	0.001	0.007	0.006	0.003	0.003	0.002
		HAsfc81	0.223	0.986	0.763	0.365	0.414	0.168
Pongo pygmaeus	89	Asfc	0.127	3.706	3.579	1.001	1.075	0.557
		epLsar	0.000	0.008	0.007	0.004	0.004	0.002
		HAsfc81	0.236	7.553	7.317	0.622	0.819	0.849
Pongo abelii	7	Asfc	0.519	3.573	3.054	0.769	1.293	1.085
		epLsar	0.003	0.006	0.003	0.004	0.005	0.001
		HAsfc81	0.385	1.759	1.374	0.635	0.957	0.584
Gorilla gorilla	30	Asfc	0.221	3.467	3.245	0.995	1.064	0.706
		epLsar	0.002	0.008	0.006	0.005	0.004	0.002
		HAsfc81	0.301	1.624	1.322	0.624	0.766	0.412
Pan troglodytes	34	Asfc	0.285	3.469	3.183	1.513	1.608	0.799
		epLsar	0.000	0.008	0.008	0.003	0.003	0.002
		HAsfc81	0.273	1.535	1.262	0.622	0.698	0.325

Miocene *K. piriyai*, Pleistocene *Pongo* sp., and *Pan* are even more closely together. In comparison to the first cluster, anisotropy is reduced and complexity is elevated. Differences in complexity after rank transformation are statistically significant in the comparisons of *Pongo* sp. and *Pan* with both *P. pygmaeus* and *G. gorilla* (Table 8). This indicates less tough and maybe the incorporation of some harder food items. Still significant seed predation was excluded for *Pongo* sp. in the study of Louys et al. (2021) and is also not supposed for the dietary regime of *P. paniscus*.

These results uphold the interpretation of Louys et al. that *Pongo* sp. had a less tough diet than extant *P. pygmaeus*. The interpretation that this is due to similar environmental differences between Sumatra and Borneo, and thus differences in dietary habits between *P. abelii* and *P. pygmaeus* are not reflected in my data, as *P. abelii* is much closer in microwear texture to *P. pygmaeus* than to *Pongo* sp. The results indicate a shift in dietary ecology from the Pleistocene to the Holocene in *Pongo*. Possible causes could be changes in vegetation, fruit abundance, resource competition, or anthropogenic impact.

Table 8 Results of the ANOVA on the rank transformed SSFA parameters (top) and pairwise comparisons with Tukey HSD post hoc test. Significant differences at p < 0.05 are highlighted in bold.

SSFA parameter		F	df	p
Asfc		4.736	5, 189	< 0.0001
epLsar		2.456	5, 189	0.0149
HAsfc81		4.684	5, 189	< 0.0001
Taxonomic pairs		**p-values**		
		Asfc	**epLsar**	**HAsfc81**
K. piriyai	Gorilla	0.278	0.635	0.990
K. piriyai	P. abelii	0.503	0.607	0.960
K. piriyai	P. pygmaeus	0.301	0.907	0.962
K. piriyai	Pan	0.996	1.000	0.955
K. piriyai	Pongo sp.	0.998	1.000	**0.031**
Pongo sp.	G. gorilla	**0.019**	0.053	**0.000**
Pongo sp.	P. abelii	0.533	0.390	0.549
Pongo sp.	P. pygmaeus	**0.006**	0.326	**0.000**
Pongo sp.	Pan	1.000	1.000	**0.001**
P. pygmaeus	Gorilla	1.000	0.886	1.000
P. pygmaeus	P. abelii	1.000	0.940	1.000
P. pygmaeus	Pan	**0.005**	0.542	1.000
P. abelii	Gorilla	1.000	1.000	1.000
P. abelii	Pan	0.565	0.506	1.000
Pan	Gorilla	**0.018**	0.107	1.000

There could to be some evidence for variation within the genus *Khoratpithecus*, although sample sizes of only one specimen in taxonomic groups other than *K. piriyai* limit the robustness of this interpretation. *K. ayeyarwadyensis* has a much higher Asfc value than the other specimens in this genus, indicating the integration of hard food items such as seeds and nuts into its diet. However maximum Asfc values in the Pleistocene and Holocene pongines and apes are even higher. *K. magnus* on the other hand has a much lower Asfc value than the other Miocene pongine specimens, but again minimum Asfc values in some of the extant apes (*P. pygmaeus*, *G.gorilla*, and *P. troglodytes*) are lower (Table 7).

The two *Khoratpithecus* specimen with higher body mass, *K. magnus* from Thailand and *Khoratpithecus* sp. from Myanmar, have lower complexity in their dental microwear textures and in the case of *K. magnus* higher anisotropy similar to mean values of extant *Pongo* and *G. gorilla* (Table 7). Thus body mass could be a factor separating different species in their dietary ecology similar to dynamics in extant sympatric primate communities in the Sunda Islands, discussed in more detail in chapter 1.2.4 (MacKinnon, 1977; Wich et al., 2002).

Looking at the distribution of HAsfc81 values (Fig. 30), which represent heterogeneity of complexity, among the different taxonomic groups there is a pattern visible with higher heterogeneity in the Miocene pongines, intermediate ones in all modern apes, and lower ones in the Pleistocene *Pongo*. The difference between the *K. piriyai* and *Pongo* sp. is also statistically significant (Table 8). HAsfc is an indicator for diversity of physical and mechanical properties in the ingested dietary items, with increasing values with increasing variability of textures.

The evidence for ecological continuity in habitat preferences that we discussed in chapter 5.2.3 are not reflected in the same degree in the dietary reconstruction based on microwear textures. It seems that while habitat preferences and limited tolerances to forest fragmentation remained rather stable in the Ponginae, there were shifts in dietary ecology from the Miocene to the Pleistocene and again to the Holocene in both physical and mechanical properties of the food as well as variability in dietary textures. The dental microwear textures on the different species of *Khoratpithecus* are also consistent with a higher diversity of subsistence strategies in Miocene pongines, although increased sample sizes are needed to substantiate this interpretation.

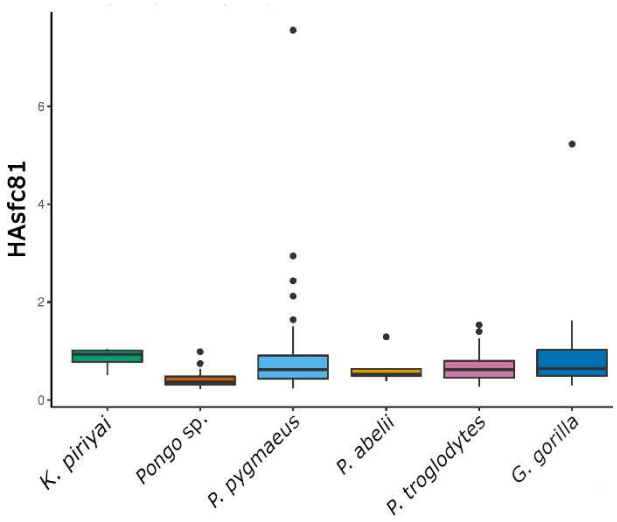

Fig. 30 Boxplot of Heterogeneity of Complexity (HAsfc81) per taxonomic group. HAsfc81 values for the Khoratpithecus sp., K. ayeyarwadyensis and K. magnus are reported in Table 7. Compared to K. piriyai they all fall below its median, but even if all species of Khoratpithecus are combined their HAsfc81 values are higher than the ones of the other pongines (see Fig. SI 1 in Appendix II).

5.3. Dietary variation of a circa 1890 *Pongo* population

This chapter focuses on the dental microwear analysis of the Selenka orangutans from **publication 3**. After an assessment of mast fruiting in the years of specimen collection, I looked at intra-population dietary variation between sexes, sex-age groups and localities. I also discuss a hypothesis that different dietary ecologies in male and female orangutans from the Selenka collection caused higher incidence rates in the female individuals.

Zusammenfassung

Da Orangutans die fossilen Menschenaffen mit der am besten durch Fossilien dokumentieren evolutionären Geschichte sind, macht es die Ponginae zu einer wichtigen Familie für unser Verständnis der Hominidenevolution. Weiter bieten sie uns eine Möglichkeit Umwelt- und Klimaentwicklungen sowie deren Einfluss auf die Ökologie insbesondere der Primaten in Südostasien vom Miozän bis heute besser zu nachvollziehen zu können. Aus diesem Grund wurden in den letzten Jahrzehnten mehrere Studien zu Umwelt- und Nahrungsrekonstruktion der Orangutans und ihrer Vorfahren durchgeführt. Die dafür eingesetzten Methoden waren unter anderem Isotopenanalysen, und Untersuchungen zur Zahntopographie und Mikroläsionen des Zahnschmelzes. Allerdings stand vor allem für Letzteres kein großes Set an Vergleichsmaterial zur Verfügung. An diesem Punkt werde ich hier ansetzen und die Nahrung einer zeitlich (1892 – 1894) und räumlich (nördlich des Kapuas Flusses auf Borneo) gut begrenzten Orangutanpopulation anhand der Mikroläsionen am Zahnschmelz beschreiben. Die untersuchten Orangutanzähne wurden während der Expedition von Emil Selenka gesammelt und sind in der Zoologischen Staatssammlung

München zugänglich. Die Ergebnisse meiner Forschung sind nicht nur für die Paläoökologie von Bedeutung, sondern auch für Biologen, Ökologen und alle Wissenschaftler, die sich mit dem Schutz der Orangutans und deren Lebensraum befassen.

Mit einer Analyse der mikroskopischen Zahntexturen und Mikroläsionen basierend auf dreidimensionalen Daten (dental microwear texture analysis = DMTA) können die physischen Eigenschaften der Nahrungsgrundlage von Individuen rekonstruiert werden. Zuerst wurde untersucht, ob es sich bei keinem der Jahre, in denen die Orangutans erlegt wurden, um ein Mastjahr handelt. In solchen Jahren kommt es durch synchrone zyklische Fruktifikation der Dipterocarpacae und anderer fruchttragender Bäume zu einer extrem gesteigerten Verfügbarkeit von Früchten. Dies war für die Jahre 1892 – 1894 nicht der Fall. Danach wurden die Daten auf Unterschieden in der Nahrungsgrundlage zwischen den Geschlechtern, Altersklassen und den unterschiedlichen Fundstellen untersucht. Keine der angewendeten Klassifizierungen erbrachte signifikante Unterschiede, was für eine homogene Nahrungsgrundlage spricht. Dieses Ergebnis widerlegt die Hypothese zu Unterschieden im Vorkommen von Zahnpahtologien in derselben Orangutanpopulation. Stoner (1995) hat die These aufgestellt, dass Unterschiede in der Ernährung zwischen männlichen und weiblichen Orangutans zu dem gesteigerten Vorkommen von Zahnerkrankungen beziehungsweise Entzündungen des umliegenden Gewebes bei Weibchen geführt haben. Meine Analyse deutet hingegen auf eine Begründung abseits der Ernährung, wie zum Beispiel Schwangerschaften und das damit einhergehende erhöhte Risiko von Infektionen des periodontanlen Gewebes, hin.

Résumé

Les orangs-outans étant les grands singes fossiles dont l'histoire évolutive est la mieux documentée par des fossiles, cela fait d'eux une famille importante pour notre compréhension de l'évolution des hominidés. Ils nous offrent également la possibilité de mieux comprendre les évolutions environnementales et climatiques ainsi que leur influence sur l'écologie, en particulier chez les primates d'Asie du Sud-Est, du Miocène à nos jours. C'est pourquoi plusieurs études de reconstitution de l'environnement et de l'alimentation des orangs-outans et de leurs ancêtres ont été menées au cours des dernières décennies. Les méthodes utilisées à cet effet étaient notamment des analyses isotopiques, et des études sur la topographie des dents et les micro-usures de l'émail dentaire. Cependant, surtout pour cette dernière, il n'y avait pas un grand ensemble de matériel de comparaison à disposition. C'est sur ce point que je vais m'appuyer ici pour décrire le régime alimentaire d'une population d'orangs-outans bien délimitée dans le temps (1892 - 1894) et dans l'espace (au nord du fleuve Kapuas à Bornéo) à travers leurs micro-usures dentaires. Les échantillons d'orangs-outans étudiés ont été collectés lors de l'expédition d'Emil Selenka et sont accessibles à la collection zoologique nationale de Munich. Les résultats de mes recherches sont importants non seulement pour la paléo-écologie, mais aussi pour les biologistes, les écologistes

et tous les scientifiques qui s'intéressent à la protection des orangs-outans et de leur habitat.

Une analyse des textures dentaires microscopiques, la microusure dentaire, sur des données tridimensionnelles (dental microwear texture analysis = DMTA) permet de reconstituer les caractéristiques physiques de l'alimentation des individus. Tout d'abord, il a été vérifié qu'aucune des années de collecte des orangs-outans n'était une année d'engraissement. Dans de telles années, la fructification cyclique synchrone des diptérocarpacées et d'autres arbres fruitiers entraîne une disponibilité extrêmement accrue de fruits. Cela n'a pas été le cas pour les années 1892 - 1894. Ensuite, les données ont été effectuées en fonction des différences de ressources alimentaires entre les sexes, les classes d'âge et les différentes stations. Aucune des classifications appliquées n'a révélé de différences significatives, ce qui plaide en faveur d'un regime alimentaire homogène. Cela m'a également permis de tester une hypothèse basée sur l'étude paléopathologique de la même population d'orangs-outans. Stoner (1995) a émis l'hypothèse que les différences de régime alimentaire entre les orangs-outans mâles et femelles ont entraîné une augmentation des maladies dentaires ou des inflammations des tissus environnants. Mon analyse indique en revanche une explication autre que l'alimentation, comme par exemple les grossesses et le risque accru d'infection des tissus parodontaux qui en découle.

5.3.1. The mast fruiting and dietary variability in the Selenka orangutans

Mast fruiting events, are synchronized, supra-annually fruiting events leading to a spike in fruit availability, and thus have an enormous impact on orangutan diets. Their effect is more pronounced in Borneo than in Sumatra and also effects mixed dipterocarp forests such as the study area north of the Kapuas River more than peat swamp forests (Delgado and van Schaik, 2000; Russon et al., 2009; Harrison, 2010; Wich et al., 2011). In the masting years, observational studies have shown that the percentage of fruit in these apes' diet may reach 100 % (Kanamori et al., 2010). However, even in periods of fruit scarcity fruit still accounts for at least 12-20 % of the orangutan diet (MacKinnon, 1974; Kanamori et al., 2010). For the interpretation of the dental microwear texture data of the Selenka orangutans and its use in future studies, it is important to assess the probability that some of the specimens were collected in a mast fruiting year. This could drastically impact their dental microwear textures and the overall degree of dietary variability we observe in the data set.

Unfortunately, no field notes are available from the Selenka expedition where direct information on mast fruting in the regions, from which the specimens were collected, could be found. No mast fruiting events were mentioned in reports from other zoological expeditions to the area around the same time (Büttikofer, 1896, 1897; Jentink, 1897). Recently published data on precipitation from 1879 to 1900 recorded at a meteorological station at Pontianak (Fig. 31) (Kajita, 2019). Pontianak is located northeast of the Kapuas River delta (Fig. 17). Mast fruiting events have been shown linked to the ENSO (El Niño Southern Oxcillation) cycle. The fruiting occurs right at the end of an ENSO low (precipitation) El Niño event (Ashton et al., 1988; Yasuda et al., 1999; Williamson and Ickes, 2002). The drastic drop in annual amount of precipitation in 1891 therefore is a good indication for a mast fruiting

event. No such drop in precipitation is visible for any of the years of the Selenka expedition (1892 – 1894), on the contrary precipitation levels are relatively high for this time period. Another available indicator for a reconstruction of ENSO events in the 1890s is the extended MEI (Multivariate ENSO index) established by Wolter and Timlin (2011) based on reconstructed SST (sea surface temperature) (Kaplan et al., 1998; Rayner, 2003; Smith and Reynolds, 2003) and SLP (sea level pressure) (Allan and Ansell, 2006) grids. From 1888 to 1898 this index documents three El Niño events, two strong ones in 1888/1889 and 1896/1897, and a weak one corresponding to the drop in precipitation in 1891 visible in the precipitation records (Fig. 31) (Wolter and Timlin, 2011). Again, the time period of the Selenka expedition is not affected by El Niño events according to extended MEI. Furthermore, a comparison of dental microwear texture of the Bornean Selenka orangutans with five specimens from Sumatra, where masting events have a significantly less severe effect on orangutan diet (Knott, 1998; Delgado and van Schaik, 2000; Wich et al., 2006), in our data set showed no significant differences. All of this evidence indicates that no mast fruiting occurred during the time entire time period of Selenka's expedition.

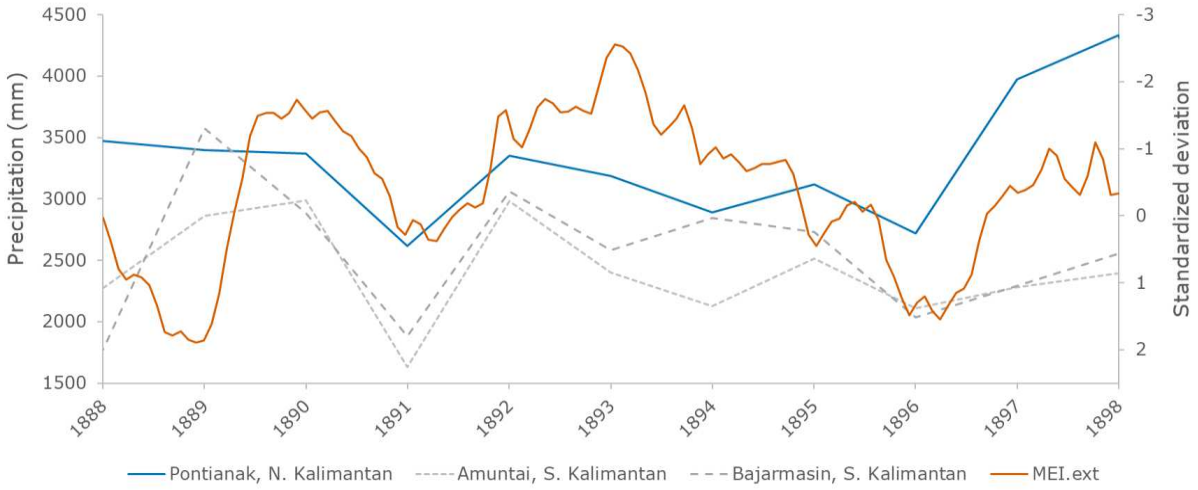

Fig. 31 Annual precipitation data recorded at Pontianak and originally published in the Regenwaarnemingen in the Nederlandsch-Indie by the Batavia Landsdrukkerij (Kajita, 2019). The red line indicates the ENSO index MEI.ext represented by standardized departure. Values >|2| strong ENSO events (ENSO high precipitation/La Niña = negative values, ENSO low precipitation/El Niño = positive values) (Wolter and Timlin, 2011). MEI.ext data from https://psl.noaa.gov/enso/mei.ext/ (9.3.2023) (Habinger et al., in prep).

No statistically significant differences have been found between any of the groups, regardless if we use sex, sex-age or locality as grouping factors. This holds true for a simple analysis of three commonly used SSFA parameters (Asfc, epLsar, and HAsfc81) as well as when we test for differences in the groups after running the PCA workflow described in chapter 4.3 on all SSFA and STA parameters combined.

Unlike Percher et al. (2018), who found variation of Asfc, epLsar, and HAsfc reflecting seasonal differences in mandrill diets as well as separation of the sexes in Asfc, no significant differences could be detected in the Selenka orangutans. This absence of significant differences between sexes and age groups indicates a homogenous diet of the whole population, at least regarding the physical properties of the food items consumed. The homogenous dental microwear textures are visible, when we group the individuals by the localities, at which they were found. Most localities of the localities are from a relatively

confined area north of the Kapuas River along both sides of the Ketungau River, except for Landak (n = 1) which is farther to the west and much closer to the coast (Fig. 17). Bornean orangutans in particular consume a wide variety of plant taxa, a fact that might be causing this pattern (Russon et al., 2009). Switches to other resources or deviations from a specific resource pool should be more visible in a species, which focuses their diet on a limited amount of taxa, thus representing a limited amount of physical properties. In the case of P. pygameus, which incorporates many different food items with different physical and mechanical properties in its diet, such changes could be obscured by the already highly variable dietary baseline signal.

5.3.2. Are differences in dietary preferences a possible cause for patterns in dental pathologies?

A study on dental pathologies in the Selenka orangutans showed that old adult females have more dental pathologies than males of the same age category. This difference is statistically significant for local infections and horizontal bone loss. However, the sample she used was not well balanced with 62 old adult females but only 32 old adult males. This however is also true for the sample used in this study. Based on her results, Stoner formulated the hypothesis that different dietary choices and strategies between the sexes are the cause for the different dental pathology patterns, as diet is an important cause for these types of diseases (Stoner, 1995).

In her study, she unfortunately only published summary statistics and not the pathologies per individual. Table 9 is a summary of all the individuals that could be identified with their specimen ID from figures and tables in her publication. Except for one young female orangutan, none of these individuals are in my data set. However, as the large caries cavity is on the antagonist tooth that I sampled for the DMT analysis, an impact on the microwear texture of this individual is possible.

Table 9 List of identifiable specimens (mentioned in the text or shown in the figures with their ID) and the dental lesions recorded by Stoner (1995). Only one of them ZSM-1981-114 is part of the data set with the tooth antagonistic to the tooth with an occlusal cavity. Sex and age estimations are from Stoner (Habinger et al., in prep).

Museum ID	tooth for DMTA	Sex	Age	pathologies (teeth affected)	
				pathology 1	pathology 2
ZSM-1981-84	-	f	old ad.	bone resorption due to premortem loss of buccal roots (left M^1)	interproximal cavity left P^4
ZSM-1981-92	-	f	old ad.	premortem tooth loss (right I^1, P^3-M^2, left P^4-M^3)	-
ZSM-1981-101	-	f	old ad.	interproximal cavity (right and left I^1)	interproximal cavity (left P^2)
ZSM-1981-114	right M_2	f	young ad.	large occlusal cavity, right (M^2)	-
ZSM-1981-176	-	f	old ad.	occlusal cavity (left M^1)	
ZSM-1981-181	-	f	old ad.	infa-alveolar osseous defect (right M_1-M_2)	horizontal bone loss on the entire mandible
ZSM-1981-185	-	f	old ad.	lingual periapical osseous defect (left M^1)	-
ZSM-1981-201	-	f	old ad.	horizontal bone loss on entire mandible and maxilla	-
ZSM-1981-223	-	f	old ad.	premortem tooth loss (left lower C)	-
ZSM-1981-238	-	m	old ad.	periapical osseous defects (left upper C, P^3, M^1)	horizontal bone loss on the left maxilla
ZSM-1981-242	-	m	old ad.	interproximal cavity (right and left I^1)	-
ZSM-1981-243	-	f	old ad.	cemental root caries (right P^3-P^4)	cemental root caries (right M_1-M_2)
ZSM-1981-251	-	f	young ad.	periapical abcess (left P^3)	horizontal bone loss on left maxilla and periapical osseous defects (P^4, M^2)
ZSM-1981-999	-	f	old ad.	cavity (right M^2) that continues in lingual roots (right M^1-M^2)	-

If we only look at the SSFA parameters (complexity, anisotropy, and heterogeneity) there seems to be some tendencies in DMTA signal between juveniles, subadults, and adults. They are more consistently visible and more pronounced in females across the different wear facets (Fig. 32). The only exception to this pattern is the shearing facet f6, where the trends are more pronounced in the males in some instances (see Fig. SI 8 of **publication 3**). Although such patterns could correspond to differences in dietary ecology across ontology, they are not statistically significant.

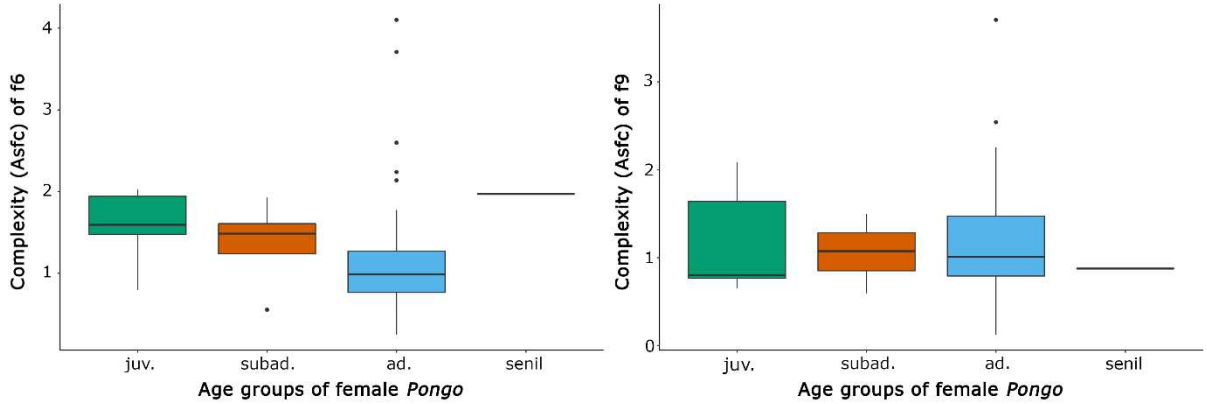

Fig. 32 Boxplots of complexity (Asfc) on the shearing facet (left) and grinding facet (right) the female individuals by age groups (Habinger et al., in prep).

In addition to that, these patterns also do not correspond to the expectations based on the hypothesis proposed by Stoner (1995), which suggests that the higher percentage of sugar-rich, soft fruits in female orangutans lead to the higher incidence rates of dental pathologies in them. Differences in dietary ecology, that would corroborate this hypothesis have been

proposed by Galdikas (1978, 1988) and Rodman (1977, 1988). Based on their observations and Stoner's hypothesis, we would expect more complex wear facets in males as they spend more time foraging on resources closer to the ground. Females on the other hand would have facets with higher anisotropy as they incorporate more young leaves and bark into their diet. Additionally, there should be higher dispersion in the Asfc values and an increase in the HAsfc values in males, as they tend to incorporate a bigger variety of food sources into their diet, given the larger distances they travel. No such differences in either the adults or the younger individuals could be detected, thus I cannot substantiate the hypothesis that diet caused differences in pathology patterns between sexes with the dental microwear texture data.

One possible non-dietary explanation for the prevalence of dental pathologies in females are pregnancies and the heightened risk for infectious diseases of periodontal females they pose. The reason behind this heightened risk are immunological and physiological changes in the mother that are necessary to prevent a rejection of the foetus (Armitage, 2013). Local infections and horizontal bone loss, the two lesion types in which differences between sexes were significant (Stoner, 1995), with higher incidence rates in females than in males are both associated with inflammations of periodontal tissue (Lovell, 1991).

If there is a survivorship bias in the sample, meaning that female orangutans are more likely to survive with dental pathologies than males, for example due to lower energetic needs, this could also explain the prevalence of females with dental pathologies in the sample. Lower energetic needs in females are mostly inferred from differences in body mass between the sexes. However these difference are less pronounced between adult females and unflanged males and the former might have even higher caloric requirements when the additional costs of reproduction are considered (Harrison et al., 2010).

Another possible explanation would be trauma to the teeth as a result of aggressive behaviour and conflicts. Cracked and broken teeth are more susceptible to the development of carious lesions, which could then lead to infectious diseases in the periodontal tissue (Lovell, 1991). There are several reasons why this is unlikely. Aggression and aggressive conflict as root cause of dental pathologies in females does not fit the pattern of posterior teeth being affected at slightly higher rates in females, whereas in males anterior and posterior teeth are equally affected (Stoner, 1995). Additionally, there are general trends in female apes towards less aggressive conflicts. The mostly solitary ranging behaviour in orangutans further reduces the change of encounters (Knott et al., 2008), thus making trauma from aggressive conflict an even unlikelier explanation.

6. Conclusion

Zusammenfassung

Meine Dissertation liefert neue Erkenntnisse über die Lebensräume der frühen anthropoiden und hominoiden Primaten in Südostasien. Der große Datensatz an seriell beprobten Säugetierzähnen der Pondaung Fm. aus dem mittleren Eozän konnte die Existenz eines Protomonsus bereits vor der Orogenese der Himalayas weiter bestätigen. Ich konnte auch das Vorhandensein unterschiedlicher

Mikrohabitate zwischen den verschiedenen Fundorten der Pondaung Fm. Nachweisen. Diese stimmen mit dem Gradienten in der Vegetationsstruktur überein, der bereits in früheren Vegetationsmodellen vorgeschlagen wurde. Da die beprobten pflanzenfressenden Säugetiere sowie zwei anthropoide Primatenarten in beiden modellierten Mikrohabitaten vorkommen, kann von einem gewissen Grad an ökologischer Flexibilität für diese taxonomischen Gruppen ausgegangen werden. Interessanterweise gibt es bei keinem der beprobten Arten Hinweise auf eine semi-aquatische Anpassung, obwohl der mit dem Pondaung Fm. verbundene Paläofluss genügend geeignete Habitate für diese Lebensweise geboten hätte. Dieses Ergebnis deutet auch darauf hin, dass die Anthracotheriidae, die Vorfahren der Flusspferde, zu einer Zeit, als die angestammten Wale bereits zu einer aquatischen Lebensweise zurückkehrten, noch vollständig an Land lebten. Die Pondaung Fm. repräsentiert verschiedene unterschiedlichen Mikrohabitate, die von einer dynamisch organisierten Säugetierfauna genutzt wurden. Diese Umwelt erwies sich als günstig für die Diversifizierung und Radiation vieler taxonomischer Gruppen wie Primaten, Anthracotheriidae und Nagetiere.

Die spätmiozäne Umwelt des Irrawaddy Fm. ist durch ein relativ dichtes Mosaik an bewaldeten und offeneren Flächen und ein Monsunklima gekennzeichnet, wahrscheinlich mit weniger ausgeprägten saisonalen Niederschlagsmaxima als im heutigen Myanmar. *K. ayeyarwadyensis* bewohnte eine Nische im Kronendach, wo er sich von Früchten ernährte. Im Gegensatz zu den *Khoratpithecus* Arten aus Thailand könnte er harte Nahrung wie Samen und Nüsse in seinen Speiseplan aufgenommen haben, wie der zeitgenössische *Sivapithecus* der Siwaliks aus Indien, Pakistan und Nepal. Insgesamt scheinen die Lebensräume der beiden miozänen Hominoiden denen des modernen Orang-Utans ähnlich zu sein, da alle drei baumbewohnende Primaten mit einer überwiegend frugivoren Ernährung waren. Die spezifische Nutzung des Lebensraums und einige Aspekte ihrer ökologischen Nischen scheinen sich jedoch zwischen den miozänen Ponginae und dem heutigen Orangutans zu unterscheiden. Im Fall von *K. ayeyarwadyensis* und *Pongo* könnten sie ähnliche Ressourcen nutzen, jedoch auf unterschiedlichen Ebenen des Kronendachs. Die Wälder des Miozäns unterscheiden sich auch von den heutigen Lebensräumen der Orang-Utans, da sie stärker fragmentiert waren, möglicherweise einen höheren Antail an laubabwerfender Vegetation aufwiesen und ein trockeneres Klima hatten.

Während es bei den fossilen Ponginae Kontinuität in den Habitatspräferenzen gibt, die auf den durch stabile Isotope modellierten ökologischen Merkmalen beruhen, scheint es zwischen dem Miozän und dem Pleistozän größere Veränderungen in der Nahrungsökologie und den existierenden Ponginae zu geben. *K. piriyai* und *K. magnus* aus Thailand sowie *Khoratpithecus* sp. Aus Myanmar waren sehr frugivor und konzentrierten sich vor allem auf weichere und duktile Nahrung, wohingegen *Sivapithecus* und möglicherweise auch *K. ayeyarwadyensis* auch auf harte Nahrungmittel wie Samen und Nüsse

zurückgriffen. *Pongo* sp. aus dem Pleistozän von Sumatra nahmen, ähnlich wie *K. piriyai* ebenfalls Elemente mit unterschiedlichen physikalischen Eigenschaften in ihre Hauptnahrung auf und weisen ähnliche Texturen der Zahnmikrobearbeitung auf wie die heutigen *Pan troglodytes*. Im Gegensatz dazu scheinen sich die rezenten Orangutans (*P. pygmaeus* und *P. abelii*) aufgrund ihrer anisotroperen Zahntexturen eher von widerstandsfähigen und faserigen Nahrungsmitteln wie reifen Blättern und Rinden zu ernähren, ähnlich wie *G. gorilla*.

Eine genauere Untersuchung Mikroläsionen an den Orangutans aus der Sammlung Selenka ergab eine homogene Nahrungsökologie. Es konnten keine signifikanten Unterschiede in der Ernährung zwischen den Geschlechtern, Altersgruppen und verschiedenen Fundorten nördlich des Kapuas-Flusses auf der Insel Borneo festgestellt werden. Durch die Verwendung historischer Niederschlagsdaten, eines ENSO-Indexes und der Probe von P. abelii aus Sumatra konnte ich bestätigen, dass die homogenen Texturen der okklusalen Mikroläsionen nicht durch ein stark erhöhtes Fruchtvorkommen im Zuge eines Mastjahres beeinflusst werden konnent. Mit den Ergebnissen meiner Studie konnte ich auch Belegen gegen die Hypothese, dass die höheren Inzidenzraten von Zahnerkrankungen bei Orang-Utan-Weibchen im Vergleich zu Männchen auf Unterschiede in der Nahrungsökologie zurückzuführen sind. Ich schlage vor, dass nicht-ernährungsbedingte Gründe wie zum Beispiel das höhere Risiko von des periodontalen Gewebes während der Schwangerschaft eine wahrscheinlichere Erklärung sind. Meine Studien über fossile und heutige Ponginas haben nicht nur zu einem besseren Verständnis ihrer evolutionären Ökologie beigetragen, sondern auch wertvolle Informationen und Ressourcen für den Schutz der Orang-Utans geliefert.

Résumé

Mon travail de thèse apporte de nouvelles connaissances sur les habitats des premiers primates anthropoïdes et hominoïdes d'Asie du Sud-Est. L'ensemble de données étendu provenant de la Fm. de Pondaung de l'Éocène moyen a permis de prouver l'existence d'un climat proto-montagnard déjà avant l'orogenèse de l'Himalaya. J'ai également pu démontrer la présence de différents microhabitats entre les différentes localités de la Fm. de Pondaung, ce qui a révélé un gradient dans la structure de la végétation et l'humidité globale, en accord avec les modèles de végétation précédents. Comme les mammifères herbivores échantillonnés ainsi que deux espèces de primates anthropoïdes sont présents dans les deux micro-habitats modélisés, on peut supposer un certain degré de flexibilité écologique pour ces groupes taxonomiques. Il est intéressant de noter qu'il n'y a aucune preuve d'adaptation semi-aquatique dans aucun des taxons échantillonnés, bien que le paléo-chenal fluvial associé à la Fm. de Pondaung aurait offert suffisamment d'habitats appropriés pour ce mode de vie. Ce résultat indique également que les anthracothères, qui sont les ancêtres des hippopotames, étaient encore entièrement terrestres à l'époque où les baleines ancestrales retournaient déjà à la

vie aquatique. La Fm. de Pondaung représente divers environnements avec différents microhabiats qui ont été utilisés par une faune de mammifères organisée de manière dynamique. Cet environnement s'est avéré propice à la diversification et à la radiation de nombreux groupes taxonomiques tels que les primates, les anthracothères et les rongeurs.

L'environnement du Miocène tardif de la Fm. de l'Irrawaddy est caractérisé par une forêt boisée et un climat de mousson, probablement avec des maxima de précipitations saisonnières moins prononcés qu'au Myanmar aujourd'hui. *K. ayeyarwadyensis* occupait une niche dans la canopée où il se nourrissait de fruits. Contrairement aux espèces de *Khoratpithecus* de Thaïlande, il est possible qu'il ait incorporé des aliments durs comme des graines et des noix dans son régime alimentaire, comme les *Sivapithecus* contemporains des Siwaliks de l'Inde, du Pakistan et du Népal. Dans l'ensemble, les habitats des deux hominoïdes du Miocène semblent être similaires à ceux du *Pongo* moderne, tous les trois étant des primates arboricoles au régime alimentaire principalement frugivore. Cependant, l'utilisation spécifique de l'habitat et certains aspects de leurs niches écologiques semblent être différents entre les ponginés du Miocène et le *Pongo*. Dans le cas de *K. ayeyarwadyensis* et de *Pongo*, ils pourraient utiliser des ressources similaires, mais à des niveaux différents de la canopée. La forêt du Miocène diffère également des habitats actuels des orangs-outans car elle était plus fragmentée, avec une végétation plus caduque et un climat plus aride.

Alors qu'il y a plus de continuité dans les exigences d'habitat basées sur les caractéristiques écologiques modélisées par les isotopes stables chez les pongines fossiles, il semble y avoir des changements plus importants dans l'écologie alimentaire entre le Miocène et le Pléistocène et les pongines existantes. *K. piriyai* et *K. magnus* de Thaïlande et *Khoratpithecus* sp. de Myanmar étaient très frugivores et se concentraient principalement sur des aliments plus mous et ductiles, alors que *Sivapithecus* et peut-être aussi *K. ayeyarwadyensis* utilisaient aussi des aliments durs comme des graines et des noix. Les *Pongo* sp. du Pléistocène de Sumatra, tout comme *K. piriyai*, incorporaient également des éléments aux propriétés physiques différentes dans leur régime alimentaire principal et présentent des textures de micro-usure dentaire similaires à celles des *Pan troglodytes* actuels. En revanche, les orangs-outans récents (*P. pygmaeus* et *P. abelii*), en raison de leurs textures dentaires plus anisotropes, semblent se nourrir davantage d'aliments résistants et fibreux tels que des feuilles et des écorces mûres, à l'instar de *G. gorilla*.

Un examen plus approfondi de l'ensemble des données de référence de *P. pygmaeus* de la collection Selenka a révélé une écologie alimentaire plutôt homogène entre les sexes, les groupes d'âge et les différentes localités situées au nord de la rivière Kapuas sur l'île de Bornéo. Grâce à l'utilisation de données historiques sur les précipitations, d'un indice ENSO et de l'échantillon de *P. abelii* de Sumatra, j'ai pu confirmer que les textures homogènes de micro-usure dentaire de cet échantillon n'ont pas été influencées par un événement de fructification

> abondantes (le masting our mast-seeding). Les résultats de cette thèse conduisent au rejet de l'hypothèse selon laquelle les taux d'incidence plus élevés de pathologies dentaires chez les femelles orangs-outans par rapport aux mâles sont dus à des différences dans l'écologie alimentaire. Je propose que des raisons non-alimentaires telles que le risque plus élevé d'infections parodontales pendant les grossesses soit une explication plus probable. Mes études sur les ponginés fossiles et actuels ont non seulement contribué à améliorer notre compréhension de leur écologie évolutive, mais ont également fourni des informations et des ressources précieuses pour la conservation des orangs-outans.

With my thesis I provide new insights into the habitats of early anthropoid and hominoid primates from Southeast Asia. Here, I want to summarize the most important findings for each data set.

The extended data set from the middle Eocene Pondaung Fm. further proved the existence of a proto-monsoonal climate already before the orogenesis of the Himalaya. I could also demonstrate the presence of different microhabitats between the different localities of the Pondaung Fm., which revealed a gradient in vegetation structure and overall humidity consistent with previous vegetation models. As the sampled herbivorous mammals as well as two species of anthropoid primates occur at both modelled microhabitats, some degree of ecological flexibility can be presumed for theses taxonomic groups. Interestingly, there is no evidence for semi-aquatic adaptations in any of the sampled taxa, although the paleo river channel associated with the Pondaung Fm. would have offered enough suitable habitats for this lifestyle. This result also indicates that anthracotheres, which are ancestral to hippos, still were fully terrestrial at the same time when ancestral whales were already returning to aquatic life. The Pondaung Fm. represents diverse environments with different microhabitats that were used by a dynamically organized mammal fauna. This environment proved to be conducive for the diversification and radiation of many taxonomic groups such as primates, anthracotheres and rodents.

The late Miocene environment of the Irrawaddy Fm. is characterized by woodland forest and a monsoon like climate, likely with less pronounced seasonal precipitation maxima than in Myanmar today. *K. ayeyarwadyensis* occupied the niche up in the canopy where it foraged for fruits. Unlike the species of *Khoratpithecus* from Thailand there is the possibility of an incorporation of hard food items like seeds and nuts into its diet, similar to contemporaneous *Sivapithecus* from the Siwaliks of India, Pakistan, and Nepal. Overall, the habitats of the two Miocene hominoids seem to be similar to that of the modern *Pongo*. All three of them are arboreal primates with a predominantly frugivorous diet. However, the specific habitat use and some aspects of their ecological niches seem to be different between the Miocene pongines and *Pongo*. In the case of *K. ayeyarwadyensis* and *Pongo* they might use similar resources, but at different levels in the canopy. The Miocene forests also differed from extant orangutan habitats as they were more fragmented with more deciduous vegetation and a more arid climate.

While there is more continuity in habitat requirements based on ecological characteristics modelled by stable isotopes in fossil pongines, there seem to be bigger shifts in dietary ecology from Miocene to Pleistocene and extant pongines. While *K. piriyai* from Thailand was highly frugivorous and solely focusing on soft, ductile food items, *Sivapithecus* and potentially *K. ayeyarwadyensis* also incorporated hard items like seeds and nuts into their diet. Pleistocene *Pongo* from Sumatra also incorporated items with differing physical properties into their diet and have similar dental microwear textures as extant *Pan troglodytes*, whereas extant Pongo seem to rely more heavily on tough, fibrous food items like mature leaves and bark given their more anisotrophic dental microwear textures.

Taking a closer look at the reference data set of extant *P. pygmaeus* from the Selenka collection revealed a rather homogenous dietary ecology across sexes, sex-age groups and the different localities located north of the Kapuas River on Borneo. With the use of historical precipitation data, an ENSO index and the outgroup sample of *P. abelii* from Sumatra I could confirm that the homogenous dental microwear textures of this sample was not influenced by a mast fruiting event. The results of this thesis lead to the rejection of the hypothesis that higher incidence rates of dental pathologies in female orangutan when compared with males are due to differences in dietary ecology. I propose that non-dietary reasons such as the higher risk of periodontal infections during pregnancies are a likelier explanation. My studies on fossil and extant pongines not only contributed to improving our understanding of their evolutionary ecology but also provided valuable insights and resources for orangutan conservation.

7. Research perspectives

Zusammenfassung

Basierend auf den Ergebnissen der einzelnen in dieser Dissertation vorgestellten Studien ergeben sich mehrere Möglichkeiten zur Vertiefung und Fortführung der Forschung sowie einige Forschungsdesiderata.

Eine Ausweitung der Datierung und gezielte Studie zu den stratigraphischen Zusammenhängen der unterschiedlichen Fundstellen der Pondaung Fm. sollte hierbei hohe Priorität haben. Unser Verständnis der Struktur des Eozänen Ökosystems hat sich wesentlich durch die Isotopenanalysen und Nischenmodellierungen der Pondaung Säugetierfauna wesentlich erweitert. Es stellt sich jedoch die Frage, in welcher Hinsicht sich das Modell verändert, wenn Vertreter aller Gattungen, die die Artenvielfalt prägten mit einbezogen werden würden. Durch Analysen von Fischen und Krokodilen (Crocodylia) wäre eine feinere Unterscheidung von aquatischen, semi-aquatischen und terrestrischen ökologischen Nischen möglich. Zusätzlich wären dadurch auch mögliche Predatoren, wozu natürlich auch die terrestrisch lebenden Creodonta zu zählen sind, vertreten. Um dann die trophischen Beziehungen zwischen den einzelnen Arten nachvollziehen zu können, müssten allerdings auch neue Isotopen in die Analyse integriert werden. Sowohl Calcium, als auch Zink und der in der Matrix des Zahnschmelzes enthaltene Stickstoff bieten die potentielle Möglichkeiten,

diese Informationen potentiell auch aus derart altem fossilen Material zu extrahieren.

Eine weitere Möglichkeit ist eine ökosystemübergreifende Analyse der Mikroläsionen, um die Nischenorganisation in Hinsicht der Ernährung näher zu beleuchten. Bei dieser Herangehensweise ist es auch möglich, die Primatenfauna mit einzubeziehen, was aufgrund der geringen Größe der Zähne bei den Isotopenanalysen nicht beziehungsweise nur sehr schwer möglich wäre. Erster Schritte in diese Richtung wurden bereits unternommen. Die Analyse der im Rahmen dieser Dissertation erstellten Zahnabrücke wurde allerdings ausgesetzt, da eine Vervollständigung des Datensatzes durch den Ausfall der Feldsaisonen der letzten Jahre unmöglich war.

Ähnliche Forschungsmöglichkeiten bestehen auch bei dem Miozänen Datensatz durch eine Ausweitung der Beprobung anderer *Khoratpithecus* Individuen und den möglichen Einsatz anderer Isotope zur Beleuchtung der trophischen Verflechtungen, insbesondere wenn auch Predatoren in den Datensatz mit aufgenommen werden. Weitere Fragen, die zu beantworten wären betreffen die evolutionäre Geschichte und Ökologie der Hylobatidae und Cercopithecidae. Hypothesen zur Veränderung der durch die Ponginae besetzten Nischen durch die Ausbreitung der Cercopithecidae wurde noch nicht empirisch untersucht.

Relevanz für den Artenschutz hat vor allem eine Untersuchung der Veränderung der Nahrung der Orangutans im letzten Jahrhundert unter stetig steigendem menschlichen Einfluss auf ihren Lebensraum. Die Untersuchung der Selenka Orangutans bildet hierfür die Grundlage. Die Charakterisierung der Nahrung kann durch Proben an Individuen, die jüngere Zeitstufen repräsentieren erweitert werden, um die Möglichkeit einer kontinuierlichen Veränderung der Nahrungsgrundlage der Orangutans zu testen.

Résumé

Sur la base des résultats des différentes études présentées dans cette thèse, plusieurs possibilités d'approfondissement et de poursuite de la recherche se présentent. L'extension de la datation et l'étude ciblée des relations stratigraphiques entre les différents sites de la Fm. de Pondaung devraient être une priorité.

Bien que les analyses isotopiques et la modélisation des niches de la faune mammalienne de Pondaung aient considérablement amélioré la compréhension de la structure de l'écosystème éocène, la question se pose de savoir dans quelle mesure le modèle serait modifié si l'on incluait des représentants de tous les genres qui ont façonné la biodiversité. L'analyse des poissons et des crocodiles (Crocodylia) permettrait de distinguer plus finement les niches écologiques aquatiques, semi-aquatiques et terrestres. De plus, les éventuels prédateurs, parmi lesquels il faut bien sûr compter les Creodonta terrestres, seraient ainsi représentés. Pour pouvoir comprendre les relations trophiques entre les

différentes espèces, il faudrait toutefois intégrer de nouveaux isotopes dans l'analyse. Le calcium, le zinc et l'azote contenu dans la matrice de l'émail offrent des possibilités d'obtenir potentiellement ces informations sur un matériel fossile aussi ancien.

Une autre possibilité est d'analyser les micro-usures dentaires à l'échelle de l'écosystème afin d'éclairer l'organisation de la niche en termes de propriétés physiques et mécaniques de l'alimentation. Dans cette approche, il est également possible d'inclure la faune des primates, ce qui ne serait pas possible ou très difficile à réaliser en raison de la petite taille des dents lors des analyses isotopiques. Les premiers pas dans cette direction ont déjà été faits, mais les analyses de cet indicateur ont toutefois été impactées par la crise sanitaire et l'absence de missions de terrain au cours de ce travail de thèse.

Des possibilités de recherche similaires existent également pour le jeu de données du Miocène, par l'extension de l'échantillonnage d'autres individus de *Khoratpithecus* et l'utilisation possible d'autres isotopes pour éclairer les liens trophiques, en particulier si les prédateurs sont également inclus dans le jeu de données. D'autres questions auxquelles il faudrait répondre concernent l'histoire évolutive et l'écologie des Hylobatidae et des Cercopithecidae. Des hypothèses sur la modification des niches occupées par les Ponginae par l'expansion des Cercopithecidae n'ont pas encore fait l'objet d'une étude empirique.

L'étude de la modification de l'alimentation des orangs-outans au cours du siècle dernier, sous l'influence croissante de l'homme sur leur habitat, est particulièrement pertinente pour la protection des espèces. L'étude des orangs-outans de Selenka constitue la base de ce travail. La caractérisation du régime alimentaire peut être étendue par des échantillons prélevés sur des individus représentant des périodes plus récentes, afin de tester la possibilité d'un changement continu du régime alimentaire des orangs-outans.

The results of the studies that I conducted in the scope of my dissertation project answered many research questions and enhanced our understanding of ecological dynamics in the environments of two fossil mammal faunas from Myanmar. However, based on these results there are many possible research directions that could be followed in the next years. One of the most pressing matters definitely is an extension of directly dated sediment units and stratigraphic relationships between the different localities from the Pondaung Fm. to test the hypothesis of relative synchronicity, which is what researchers are currently investigating.

While the Pondaung mammal fauna and the relationships of their modelled isotopic niches are now well understood, it would be interesting to see how predators such as creodonts or truly aquatic and semi-aquatic species such as the fish and crocodilians from the same context influence the niche partitioning model. It would also establish a true aquatic baseline against which the $\delta^{18}O$ values of the mammal fauna studied here can be evaluated. Especially in the context of an integration of some creodont specimen, although their fossil record from the Pondaung is relatively scarce, an expansion of the methodological approach needs to be considered, as carbon and oxygen isotopes do not reflect trophic relationships. Calcium or

new approaches such as zinc or nitrogen isotopes from dental enamel, although the latter one has not yet been used on data sets this old, would be valid possibilities to explore to reconstruct the food web of the Pondaung fauna.

Another interesting possibility to access the dietary aspects of the ecology of the Pondaung fauna would be dental microwear texture analysis on the taxa we analysed for isotopes, including the primate fauna. Although I already started work on this topic during the last years, given the delays and inaccessibility of the samples in Myanmar as of 2021 this aspect of the project, especially regarding the primate fauna, which needs more extensive sampling, has been put on hold for now.

Regarding the Miocene data set, similar ideas, such as integration of predator and non-mammalian fauna in the niche modelling and expansion of the analytical approach to use more isotope proxies, would be interesting research topics for future projects. Sampling additional *Khoratpithecus* specimen would be essential to test the inferences based on the holotype specimen and *Sivapithecus* discussed in chapter 5.2. In this chapter, I also discuss the possible influence on the pongine ecology and distribution by the expansion of cercopithecid primates into the pongine ranges. Studying their paleoecology and evolutionary history would be an important addition to the discussion of hominoid primate evolutionary ecology in Southeast Asia. Comparing the niche partitioning of extant and fossil *Pongo* with their respective sympatric primate fauna to test whether the relationship changed over the millennia, maybe in correlation with climatic changes or human impact on habitats, or if there is a continuum. Including fossil hylobatids into such a study would be very interesting as well, however the very scarce fossil record probably makes it not feasible at the moment (Ortiz et al., 2015; Ji et al., 2022, and references therein).

The reference data set on the DMTA of the Selenka orangutans from the 1890s opens interesting possibilities to answer questions relevant for orangutan conservation and to assess changes in their diet in the past century. However, a comparison of the dental microwear texture data with observational data is difficult, because dental microwear is not directly correlated with particular food sources, but only indicates different dietary regimes based on the physical properties of different food groups. Observational data on orang-utan diet is mostly quantified using foraging time spent on different food categories or species (see Table 3 in Appendix II). However, this does not translate well to the actual amount of a food item of a specific type that was ingested. A lot of time might be spent on foraging for nutritious but fiddly items. Therefore, it would be necessary, to obtain moulds from living wild orangutans today for such a study. Alternatively, or in addition to that, more data from wild shot specimen from the past century could be obtained. This would be a possibility to assess in detail the impact of progressive anthropogenic habitat destruction on orangutan dietary ecology through the past century.

8. References

Ackerly, D. D., Schwilk, D. W., and Webb, C. O. (2006). Niche evolution and adaptive radiation: Testing the order of trait divergence. *Ecology* 87, S50–S61. doi: 10.1890/0012-9658(2006)87[50:NEAART]2.0.CO;2

Adams, M. A., and Grierson, P. F. (2001). Stable Isotopes at Natural Abundance in Terrestrial Plant Ecology and Ecophysiology: An Update. *Plant Biology* 3, 299–310. doi: 10.1055/s-2001-16454

Allan, R., and Ansell, T. (2006). A New Globally Complete Monthly Historical Gridded Mean Sea Level Pressure Dataset (HadSLP2): 1850–2004. *Journal of Climate* 19, 5816–5842. doi: 10.1175/JCLI3937.1

Ambrose, S. H., and Norr, L. (1993). "Experimental evidence for the relationship of the carbon stable isotope ratios of whole diet and dietary proteins to those of bone collagen and carbonate," in *Prehistoric Human Bone: Archaeology at the molecular level*, eds. J. B. Lambert, and G. Grupe (Berlin, Heidelberg, New York: Springer), 1–38.

Ancrenaz, M., Ambu, L., Sunjoto, I., Ahmad, E., Manokaran, K., Meijaard, E., et al. (2010). Recent surveys in the forests of Ulu Segama Malua, Sabah, Malaysia, show that orang-utans (*P. p. morio*) can be maintained in slightly logged forests. *Plos ONE* 5, e11510. doi: 10.1371/journal.pone.0011510

Armitage, G. C. (2013). Bi-directional relationship between pregnancy and periodontal disease. *Periodontology 2000* 61, 160–176. doi: 10.1111/j.1600-0757.2011.00396.x

Ashton, P. S. (2014). *On the Forests of Tropical Asia: Lest the Memory Fade*. Kew: Kew Royal Botanics Garden.

Ashton, P. S., Givnish, T. J., and Appanah, S. (1988). Staggered Flowering in the Dipterocarpaceae: New Insights Into Floral Induction and the Evolution of Mast Fruiting in the Aseasonal Tropics. *Am Nat* 132, 44–66. doi: 10.1086/284837

Bacon, A.-M., Bourgon, N., Dufour, E., Zanolli, C., Duringer, P., Ponche, J.-L., et al. (2018a). Nam Lot (MIS 5) and Duoi U'Oi (MIS 4) Southeast Asian sites revisited: Zooarchaeological and isotopic evidences. *Palaeogeography, Palaeoclimatology, Palaeoecology* 512, 132–144. doi: 10.1016/j.palaeo.2018.03.034

Bacon, A.-M., Duringer, P., Antoine, P.-O., Demeter, F., Shackelford, L., Sayavongkhamdy, T., et al. (2011). The Middle Pleistocene mammalian fauna from Tam Hang karstic deposit, northern Laos: New data and evolutionary hypothesis. *Quaternary International* 245, 315–332. doi: 10.1016/j.quaint.2010.11.024

Bacon, A.-M., Duringer, P., Westaway, K. E., Joannes-Boyau, R., Zhao, J., Bourgon, N., et al. (2018b). Testing the savannah corridor hypothesis during MIS2: The Boh Dambang hyena site in southern Cambodia. *Quaternary International* 464, 417–439. doi: 10.1016/j.quaint.2017.10.047

Badgley, C., Barry, J. C., Morgan, M. E., Nelson, S. V., Behrensmeyer, A. K., Cerling, T. E., et al. (2008). Ecological changes in Miocene mammalian record show impact of prolonged climatic forcing. *Proc Natl Acad Sci U S A* 105, 12145–12149. doi: 10.1073/pnas.0805592105

Badgley, C., Guoqin, Q., Wanyong, C., and Defen, H. (1988). Paleoecology of a Miocene, tropical, upland fauna: Lufeng. *China. Nation. Geogr. Res.* 4, 178–195.

Bajpai, S., Kay, R. F., Williams, B. A., Das, D. P., Kapur, V. V., and Tiwari, B. N. (2008). The oldest Asian record of Anthropoidea. *Proc Natl Acad Sci U S A* 105, 11093–11098. doi: 10.1073/pnas.0804159105

Barbour, M. M. (2007). Stable oxygen isotope composition of plant tissue: a review. *Functional plant biology* 34, 83–94. doi: 10.1071/FP06228

Barry, J. C. (1987). The History and Chronology of Siwalik Cercopithecids. *Journal of Human Evolution* 2, 47–58. doi: 10.1007/BF02436530

Barry, J. C., Morgan, M. E., Flynn, L. J., Pilbeam, D. R., Behrensmeyer, A. K., Raza, S. M., et al. (2002). Faunal and Environmental Change in the Late Miocene Siwaliks of Northern Pakistan. *Paleobiology* 28, 1–71. doi: 10.1666/0094-8373(2002)28[1:FAECIT]2.0.CO;2

Baumann, C., Bocherens, H., Drucker, D. G., and Conard, N. J. (2020). Fox dietary ecology as a tracer of human impact on Pleistocene ecosystems. *Plos ONE* 15, e0235692. doi: 10.1371/journal.pone.0235692

Beard, K. C. (2002). "Basal anthropoids," in *The Primate Fossil Record*, ed. W. C. Hartwig (Cambridge: Cambridge University Press), 133–150.

Beard, K. C. (2004). *The Hunt for the Dawn Monkey: Unearthing the Origins of Monkeys, Apes, and Humans*. Berkeley: University of California Press.

Beard, K. C., Jaeger, J.-J., Chaimanee, Y., Rossie, J. B., Soe, A. N., Tun, S. T., et al. (2005). Taxonomic status of purported primate frontal bones from the Eocene Pondaung Formation of Myanmar. *Journal of Human Evolution* 49, 468–481. doi: 10.1016/j.jhevol.2005.05.008

Beard, K. C., Marivaux, L., Chaimanee, Y., Jaeger, J.-J., Marandat, B., Tafforeau, P., et al. (2009). A new primate from the Eocene Pondaung Formation of Myanmar and the monophyly of Burmese amphipithecids. *Proc Biol Sci* 276, 3285–3294. doi: 10.1098/rspb.2009.0836

Beard, K. C., Marivaux, L., Tun, S. T., Soe, A. N., Chaimanee, Y., Htoon, W., et al. (2007). New Sivaladapid Primates from the Eocene Pondaung Formation of Myanmar and the Anthropoid Status of Amphipithecidae. *Bulletin of Carnegie Museum of Natural History* 39, 67–76. doi: 10.2992/0145-9058(2007)39[67:NSPFTE]2.0.CO;2

Beard, K. C., Qi, T., Dawson, M. R., Wang, B., and Li, C. (1994). A diverse new primate fauna from middle Eocene fissure-fillings in southeastern China. *Nature* 368, 604–609. doi: 10.1038/368604a0

Beard, K. C., Tong, Y., Dawson, M. R., Wang, J., and Huang, X. (1996). Earliest Complete Dentition of an Anthropoid Primate from the Late Middle Eocene of Shanxi Province, China. *Science* 272, 82–85. doi: 10.1126/science.272.5258.82

Beard, K. C., and Wang, J. (2004). The eosimiid primates (Anthropoidea) of the Heti Formation, Yuanqu Basin, Shanxi and Henan Provinces, People's Republic of China. *Journal of Human Evolution* 46, 401–432. doi: 10.1016/j.jhevol.2004.01.002

Begun, D. R. (2001). "African and Eurasian Miocene hominoids and the origins of Hominidae," in *Hominoid Evolution and Climate Change in Europe. Human Evolution and Climate Change in Europe, Volume 2: Phylogeny of the Neogene Hominoid Primates of Eurasia*, eds. L. de Bonis, G. D. Koufos, and P. J. Andrews (Cambridge: Cambridge University Press), 231–243.

Begun, D. R. (2015). "Fossil record of Miocene hominoids," in *Handbook of Palaeoanthropology, Vol 2: Primate Evolution and Human Origins*, eds. W. Henke, and I. E. Tattersall (Berlin: Springer), 1261–1332.

Begun, D. R., and Kordos, L. (1997). "Phyletic Affinities and Functional Convergence in *Dryopithecus* and Other Miocene and Living Hominids," in *Function, Phylogeny, and Fossils: Miocene Hominoid Evolution and Adaptations*, eds. D. R. Begun, C. V. Ward, and M. D. Rose (New York: Plenum), 291–316.

Bell, R. H. V. (1971). A Grazing Ecosystem in the Serengeti. *Scientific American* 225, 86–93.

Benammi, M., Soe, A. N., Tun, T., Bo, B., Chaimanee, Y., Ducrocq, S., et al. (2002). First Magnetostratigraphic Study of the Pondaung Formation: Implications for the Age of the Middle Eocene Anthropoids of Myanmar. *The Journal of Geology* 110, 748–756. doi: 10.1086/342868

Bender, F., and Bannert, D. N. (1983). *Geology of Burma.* Berlin: Gebr. Borntraeger.

Bender, M. M. (1971). Variations in the $^{13}C/^{12}C$ ratios of plants in relation to the pathway of photosynthetic carbon dioxide fixation. *Phytochemistry* 10, 1239–1244. doi: 10.1016/S0031-9422(00)84324-1

Berlioz, E., Azorit, C., Blondel, C., Tellado Ruiz, M. S., and Merceron, G. (2017). Deer in an arid habitat: dental microwear textures track feeding adaptability. *Hystrix, the Italian Journal of Mammalogy* 28, 222–230. doi: 10.4404/hystrix-28.2-12048

Bhandari, A., Kay, R. F., Williams, B. A., Tiwari, B. N., Bajpai, S., and Hieronymus, T. (2018). First record of the Miocene hominoid *Sivapithecus* from Kutch, Gujarat state, western India. *Plos ONE* 13, e0206314. doi: 10.1371/journal.pone.0206314

Bocherens, H., and Drucker, D. (2003). Trophic level isotopic enrichment of carbon and nitrogen in bone collagen: case studies from recent and ancient terrestrial ecosystems. *International Journal of Osteoarchaeology* 13, 46–53. doi: 10.1002/oa.662

Bocherens, H., Fizet, M., and Mariotti, A. (1994). Diet, physiology and ecology of fossil mammals as inferred from stable carbon and nitrogen biogeochemistry: Implications for Pleistocene bears. *Palaeogeography, Palaeoclimatology, Palaeoecology* 107, 213–225. doi: 10.1016/0031-0182(94)90095-7

Bocherens, H., Koch, P. L., Mariotti, A., Geraads, D., and Jaeger, J.-J. (1996). Isotopic Biogeochemistry (^{13}C, ^{18}O) of Mammalian Enamel from African Pleistocene Hominid Sites. *Palaios* 11, 306–318. doi: 10.2307/3515241

Bocherens, H., Schrenk, F., Chaimanee, Y., Kullmer, O., Mörike, D., Pushkina, D., et al. (2017). Flexibility of diet and habitat in Pleistocene South Asian mammals: Implications for the fate of the giant fossil ape *Gigantopithecus*. *Quaternary International* 434, 148–155. doi: 10.1016/j.quaint.2015.11.059

Böhme, M., Aiglstorfer, M., Antoine, P.-O., Appel, E., Havlik, P., Métais, G., et al. (2013). Na Duong (northern Vietnam) - an exceptional window into Eocene ecosystems from Southeast Asia. *Zitteliana* A 53, 121–167. doi: 10.5282/UBM/EPUB.19019

Bolnick, D. I., Yang, L. H., Fordyce, J. A., Davis, J. M., and Svanbäck, R. (2002). Measuring individual-level resource specialization. *Ecology* 83, 2936–2941. doi: 10.1890/0012-9658(2002)083[2936:MILRS]2.0.CO;2

Bonafini, M., Pellegrini, M., Ditchfield, P., and Pollard, A. M. (2013). Investigation of the 'canopy effect' in the isotope ecology of temperate woodlands. *Journal of Archaeological Science* 40, 3926–3935. doi: 10.1016/j.jas.2013.03.028

Bond, M., Tejedor, M. F., Campbell, K. E., Chornogubsky, L., Novo, N., and Goin, F. (2015). Eocene primates of South America and the African origins of New World monkeys. *Nature* 520, 538–541. doi: 10.1038/nature14120

Bonis, L. de, Jaeger, J.-J., and Coiffait, B., Coiffait, P. E. (1988). Découverte du plus ancien primate catarrhinien connu dans l'Eocène supérieur d'Afrique du Nord. *Comptes Rendus de l'Académie des Sciences, Série 2* 306, 929–934.

Bonis, L. de, Solé, F., Chaimanee, Y., Naing Soe, A., Sein, C., Lazzari, V., et al. (2018). New hyaenodonta (Mammalia) from the middle Eocene of Myanmar. *Comptes Rendus Palevol* 17, 357–365. doi: 10.1016/j.crpv.2017.12.003

Bourgon, N., Jaouen, K., Bacon, A.-M., Dufour, E., McCormack, J., Tran, N.-H., et al. (2021). Trophic ecology of a Late Pleistocene early modern human from tropical Southeast Asia inferred from zinc isotopes. *Journal of Human Evolution* 161, 103075. doi: 10.1016/j.jhevol.2021.103075

Bourgon, N., Jaouen, K., Bacon, A.-M., Jochum, K. P., Dufour, E., Duringer, P., et al. (2020). Zinc isotopes in Late Pleistocene fossil teeth from a Southeast Asian cave setting preserve paleodietary information. *Proc Natl Acad Sci U S A* 117, 4675–4681. doi: 10.1073/pnas.1911744117

Brown, B. (1997). "Miocene Hominoid Mandibles," in *Function, Phylogeny, and Fossils: Miocene Hominoid Evolution and Adaptations*, eds. D. R. Begun, C. V. Ward, and M. D. Rose (New York: Plenum), 153–171.

Bryant, D. J., and Froelich, P. N. (1995). A model of oxygen isotope fractionation in body water of large mammals. *Geochimica et Cosmochimica Acta* 59, 4523–4537. doi: 10.1016/0016-7037(95)00250-4

Burke, K. D., Williams, J. W., Chandler, M. A., Haywood, A. M., Lunt, D. J., and Otto-Bliesner, B. L. (2018). Pliocene and Eocene provide best analogs for near-future climates. *Proc Natl Acad Sci U S A* 115, 13288–13293. doi: 10.1073/pnas.1809600115

Büttikofer, M. J. (1896). "Zoologische Skizzen aus der niederländischen Expedition nach Central-Borneo," in *Compte-rendu des séances du Troisième congrès international de zoologie: Leyden - 16-21 Septembre - 1895*, ed. P. P. C. Hoek (Leyden: E.J. Brill), 212–227.

Büttikofer, M. J. (1897). Zoological results of the Dutch scientific expedition to Central Borneo: Introduction. *Notes from the Leyden Museum* 19, 1–25.

Calandra, I., Schulz, E., Pinnow, M., Krohn, S., and Kaiser, T. M. (2012). Teasing apart the contributions of hard dietary items on 3D dental microtextures in primates. *Journal of Human Evolution* 63, 85–98. doi: 10.1016/j.jhevol.2012.05.001

Campbell-Smith, G., Campbell-Smith, M., Singleton, I., and Linkie, M. (2011). Raiders of the lost bark: orangutan foraging strategies in a degraded landscape. *Plos ONE* 6, e20962. doi: 10.1371/journal.pone.0020962

Carter, M. L., and Bradbury, M. W. (2016). Oxygen isotope ratios in primate bone carbonate reflect amount of leaves and vertical stratification in the diet. *Am J Primatol* 78, 1086–1097. doi: 10.1002/ajp.22432

Cerling, T. E., and Harris, J. M. (1999). Carbon isotope fractionation between diet and bioapatite in ungulate mammals and implications for ecological anc paleoecological studies. *Oecologia* 120, 347–363. doi: 10.1007/s004420050868

Cerling, T. E., Harris, J. M., Leakey, M. G., Passey, B. H., and Levin, N. E. (2010). "Stable Carbon and Oxygen Isotopes in East African Mammals: Modern and Fossil," in *Cenozoic Mammals of Africa*, ed. L. Werdelin (Berkeley, Los Angeles: University of California Press), 941–952.

Cerling, T. E., Harris, J. M., MacFadden, B. J., Leakey, M. G., Quade, J., Eisenmann, V., et al. (1997). Global vegetation change through the Miocene/Pliocene boundary. *Nature* 389, 153–158. doi: 10.1038/38229

Cerling, T. E., Wang, Y., and Quade, J. (1993). Expansion of C_4 ecosystems as an indicator of global ecological change in the late Miocene. *Nature* 361, 344–345. doi: 10.1038/361344a0

Chaimanee, Y., Chavasseau, O., Beard, K. C., Kyaw, A. A., Soe, A. N., Sein, C., et al. (2012). Late Middle Eocene primate from Myanmar and the initial anthropoid colonization of Africa. *Proc Natl Acad Sci U S A* 109, 10293–10297. doi: 10.1073/pnas.1200644109

Chaimanee, Y., Jolly, D., Benammi, M., Tafforeau, P., Duzer, D., Moussa, I., et al. (2003). A Middle Miocene hominoid from Thailand and orangutan origins. *Nature* 422, 61–65. doi: 10.1038/nature01449

Chaimanee, Y., Lazzari, V., Chaivanich, K., and Jaeger, J.-J. (2019). First maxilla of a late Miocene hominid from Thailand and the evolution of pongine derived characters. *Journal of Human Evolution* 134, 102636. doi: 10.1016/j.jhevol.2019.06.007

Chaimanee, Y., Lazzari, V., Yamee, C., Suraprasit, K., Rugbumrung, M., Chaivanich, K., et al. (2022). New materials of *Khoratpithecus*, a late Miocene hominoid from Nakhon Ratchasima Province, Northeaster Thailand, confirm its pongine affinities. *Palaeontographica Abteilung A* 323, 147–186. doi: 10.1127/pala/2022/0129

Chaimanee, Y., Suteethorn, V., Jaeger, J. J., and Ducrocq, S. (1997). A new Late Eocene anthropoid primate from Thailand. *Nature* 385, 429–431. doi: 10.1038/385429a0

Chaimanee, Y., Suteethorn, V., Jintasakul, P., Vidthawanon, C., Marandat, B., and Jaeger, J.-J. (2004). A new orang-utan relative from the Late Miocene of Thailand. *Nature* 427, 439–441. doi: 10.1038/nature02245

Chaimanee, Y., Thein, T., Ducrocq, S., Aung, N. S., Benammi, M., Than Tun, et al. (2000). A lower jaw of *Pondaungia cotteri* from the Late Middle Eocene Pondaung Formation (Myanmar) confirms its anthropoid status. *Proceedings of the National Academy of Science* 97, 4102–4105. doi: 10.1073/pnas.97.8.4102

Chaimanee, Y., Yamee, C., Tian, P., Khaowiset, K., Marandat, B., Tafforeau, P., et al. (2006). *Khoratpithecus piriyai*, a Late Miocene Hominoid of Thailand. *Am J Phys Anthropol* 131, 311–323. doi: 10.1002/ajpa.20437

Chang, Y. (1975). Discovery of a *Gigantopithecus* tooth from Bama District in Kwangsi. *Vertebrata PalAsiatica* 13, 148–153.

Chavasseau, O., Chaimanee, Y., Ducrocq, S., Lazzari, V., Pha, P. d., Rugbumrung, M., et al. (2019). A new primate from the late Eocene of Vietnam illuminates unexpected strepsirrhine diversity and evolution in Southeast Asia. *Scientific Reports* 9, 19983. doi: 10.1038/s41598-019-56255-8

Chavasseau, O., Chaimanee, Y., Tun, S. T., Soe, A. N., Barry, J. C., Marandat, B., et al. (2006). Chaungtha, a new Middle Miocene mammal locality from the Irrawaddy Formation, Myanmar. *Journal of Asian Earth Sciences* 28, 354–362. doi: 10.1016/j.jseaes.2005.10.012

Chavasseau, O., Khyaw, A. A., Chaimanee, Y., Coster, P., Emonet, E.-G., Soe, A. N., et al. (2013). "Advances in the biochronology and biostratigraphy of the continental Neogene of

Myanmar," in *Fossil mammals of Asia: Neogene biostratigraphy and chronology*, eds. X. Wang, L. J. Flynn, and M. Fortelius (New York: Columbia University Press), 461–474.

Ciochon, R. L., Gingerich, P. D., Gunnell, G. F., and Simons, E. L. (2001). Primate postcrania from the late middle Eocene of Myanmar. *Proc Natl Acad Sci U S A* 98, 7672–7677. doi: 10.1073/pnas.051003298

Ciochon, R. L., and Gunnell, G. F. (2002a). Chronology of primate discoveries in Myanmar: Influences on the anthropoid origins debate. *Am J Phys Anthropol* 119, 2–35. doi: 10.1002/AJPA.10175

Ciochon, R. L., and Gunnell, G. F. (2002b). Eocene primates from Myanmar: Historical perspectives on the origin of Anthropoidea. *Evolutionary Anthropology: Issues, News, and Reviews* 11, 156–168. doi: 10.1002/evan.10032

Ciochon, R. L., and Gunnell, G. F. (2004). "Eocene large-bodied primates of Myanmar and Thailand: morphological considerations and phylogenetic affinities," in *Anthropoid Origins: New Visions*, eds. C. F. Ross, and R. F. Kay (New York: Springer), 249–282.

Ciochon, R. L., and Holroyd, P. A. (1994). "The Asian origin of Anthropoidea revisited," in *Anthropoid Origins*, eds. J. G. Fleagle, and R. F. Kay (Springer, Boston, MA), 143–162.

Ciochon, R. L., Long, V. T., Larick, R., González, L., Grün, R., Vos, J. de, et al. (1996). Dated co-occurrence of *Homo erectus* and *Gigantopithecus* from Tham Khuyen Cave, Vietnam. *Proc Natl Acad Sci U S A* 93, 3016–3020. doi: 10.1073/pnas.93.7.3016

Ciochon, R. L., Savage, D. E., Tint, T., and Maw, B. (1985). Anthropoid origins in Asia? New discovery of *Amphipithecus* from the eocene of Burma. *Science* 229, 756–759. doi: 10.1126/science.229.4715.756

Clementz, M. T., Holden, P., and Koch, P. L. (2003). Are calcium isotopes a reliable monitor of trophic level in marine settings? *International Journal of Osteoarchaeology* 13, 29–36. doi: 10.1002/oa.657

Clementz, M. T., Holroyd, P. A., and Koch, P. L. (2008). Identifying Aquatic Habits Of Herbivorous Mammals Through Stable Isotope Analysis. *Palaios* 23, 574–585. doi: 10.2110/palo.2007.p07-054r

Clementz, M. T., and Koch, P. L. (2001). Differentiating aquatic mammal habitat and foraging ecology with stable isotopes in tooth enamel. *Oecologia* 129, 461–472. doi: 10.1007/s004420100745

Colbert, E. H. (1937). A new primate from the Upper Eocene Pondaung Formation of Burma. *American Museum Novitates* 951, 1–18.

Coplen, T. B. (1988). Normalization of oxygen and hydrogen isotope data. *Chemical Geology (Isotope Geoscience Section)* 72, 293–297. doi: 10.1016/0168-9622(88)90042-5

Coplen, T. B. (2011). Guidelines and recommended terms for expression of stable-isotope-ratio and gas-ratio measurment results. *Rapid Communications in Mass Spectrometry* 25, 2538–2560. doi: 10.1002/rcm.5129

Corlett, R. (2014). *The ecology of tropical East Asia*. Oxford: Oxford University Press.

Corlett, R., and Primack, R. B. (2005). Dipterocarps: Trees That Dominate the Asian Rain Forest. *Arnoldia* 63, 3–7.

Corlett, R., and Primack, R. B. (2011). *Tropical rain forests: An ecological and biogeographical comparison*. Oxford: Wiley-Blackwell.

Coster, P., Beard, K. C., Soe, A. N., Sein, C., Chaimanee, Y., Lazzari, V., et al. (2013). Uniquely derived upper molar morphology of Eocene Amphipithecidae (Primates: Anthropoidea): homology and phylogeny. *Journal of Human Evolution* 65, 143–155. doi: 10.1016/j.jhevol.2013.04.009

Coster, P., Benammi, M., Chaimanee, Y., Yamee, C., Chavasseau, O., Emonet, E.-G., et al. (2010). A complete magnetic-polarity stratigraphy of the Miocene continental deposits of Mae Moh Basin, northern Thailand, and a reassessment of the age of hominoid-bearing localities in northern Thailand. *Geological Society of America Bulletin* 122, 1180–1191. doi: 10.1130/B26568.1

Coster, P. M., Soe, A. N., Beard, K. C., Chaimanee, Y., Sein, C., Lazzari, V., et al. (2018). Astragalus of *Pondaungimys* (Rodentia, Anomaluroidea) from the late middle Eocene Pondaung Formation, central Myanmar. *Journal of Vertebrate Paleontology* 38, e1552156. doi: 10.1080/02724634.2018.1552156

Coster, P. M. C., Beard, K. C., Salem, M. J., Chaimanee, Y., and Jaeger, J.-J. (2015). New fossils from the Paleogene of central Libya illuminate the evolutionary history of endemic African anomaluroid rodents. *Front. Earth Sci.* 3, 56. doi: 10.3389/feart.2015.00056

Craig, H. (1954). Carbon 13 in Plants and the Relationships between Carbon 13 and Carbon 14 Variations in Nature. *The Journal of Geology* 62, 115–149. doi: 10.1086/626141

Crompton, A. W., and Hiiemae, K. M. (1969). How mammalian molar teeth work. *Discovery* 5, 23–34.

Crowley, B. E., Carter, M. L., Karpanty, S. M., Zihlman, A. L., Koch, P. L., and Dominy, N. J. (2010). Stable carbon and nitrogen isotope enrichment in primate tissues. *Oecologia* 164, 611–626. doi: 10.1007/s00442-010-1701-6

Dansgaard, W. (1964). Stable isotopes in precipitation. *Tellus* 16, 436–468. doi: 10.3402/tellusa.v16i4.8993

Dawson, T. E., and Ehleringer, J. R. (1991). Streamside trees that do not use stream water. *Nature* 350, 335–337. doi: 10.1038/350335a0

Delgado, R. A., and van Schaik, C. P. (2000). The behavioral ecology and conservation of the orangutan (*Pongo pygmaeus*): A tale of two islands. *Evolutionary Anthropology: Issues, News, and Reviews* 9, 201–218. doi: 10.1002/1520-6505(2000)9:5<201:AID-EVAN2>3.0.CO;2-Y

DeSantis, L. R. G., Scott, J. R., Schubert, B. W., Donohue, S. L., McCray, B. M., van Stolk, C. A., et al. (2013). Direct comparisons of 2D and 3D dental microwear proxies in extant herbivorous and carnivorous mammals. *Plos ONE* 8, e71428. doi: 10.1371/journal.pone.0071428

Doberenz, A. R., Miller, M. F., and Wyckoff, R. W. (1969). An analysis of fossil enamel protein. *Calcified Tissue Research* 3, 93–95. doi: 10.1007/BF02058649

Doran-Sheehy, D., Mongo, P., Lodwick, J., and Conklin-Brittain, N. L. (2009). Male and female western gorilla diet: preferred foods, use of fallback resources, and implications for ape versus old world monkey foraging strategies. *Am J Phys Anthropol* 140, 727–738. doi: 10.1002/ajpa.21118

Ducrocq, S. (1999). The Late Eocene Anthracotheriidae (Mammalia, Artiodactyla) from Thailand. *Palaeontographica Abteilung A* 252, 93–140. doi: 10.1127/pala/252/1999/93

Ducrocq, S., Chaimanee, Y., Aung, N. S., Sein, C., Jaeger, J.-J., and Chavasseau, O. (2021). First report of the lower dentition of *Siamotherium pondaungensis* (Cetartiodactyla,

Hippopotamoidea) from the late middle Eocene of the Pondaung Formation Myanmar. *Neues Jahrbuch für Geologie und Paläontologie Abhandlungen* 301, 217–228.

Ducrocq, S., Soe, A. N., Aung, A. K., Benammi, M., Bo, B., Chaimanee, Y., et al. (2001). A new anthracotheriid artiodactyl from Myanmar, and the relative ages of the Eocene anthropoid primate-bearing localities of Thailand (Krabi) and Myanmar (Pondaung). *Journal of Vertebrate Paleontology* 20, 755–760. doi: 10.1671/0272-4634(2000)020[0755:ANAAFM]2.0.CO;2

Ducrocq, S., Soe, A. N., Chavasseau, O., Sein, C., Chaimanee, Y., Lazzari, V., et al. (2019). New basal ruminants from the Eocene of the Pondaung Formation, Myanmar. *Journal of Vertebrate Paleontology* 39, e1722682. doi: 10.1080/02724634.2019.1722682

Egi, N., Takai, M., Shigehara, N., and Tsubamoto, T. (2004). Body Mass Estimates for Eocene Eosimiid and Amphipithecid Primates Using Prosimian and Anthropoid Scaling Models. *International Journal of Primatology* 25, 211–236. doi: 10.1023/B:IJOP.0000014651.82525.54

Egi, N., and Tsubamoto, T. (2000). A preliminary report on carnivorous mammals from Pondaung fauna. *Asian Paleoprimatology* 1, 103–114.

Elith, J., Graham, C. H., Anderson, R. P., Dudík, M., Ferrier, S., Guisan, A., et al. (2006). Novel methods improve prediction of species' distributions from occurrence data. *Ecography* 29, 129–151. doi: 10.1111/j.2006.0906-7590.04596.x

Ellsworth, P. Z., and Williams, D. G. (2007). Hydrogen isotope fractionation during water uptake by woody xerophytes. *Plant and Soil* 291, 93–107. doi: 10.1007/s11104-006-9177-1

Fannin, L. D., and McGraw, W. S. (2020). Does Oxygen Stable Isotope Composition in Primates Vary as a Function of Vertical Stratification or Folivorous Behaviour? *Folia Primatol* 91, 219–227. doi: 10.1159/000502417

Farquhar, G. D., Ehleringer, J. R., and Hubick, K. T. (1989). Carbon isotope discrimination and photosynthesis. *Annual Review of Plant Physiology and Plant Molecular Biology* 40, 503–537.

Fiorenza, L., Nguyen, H. N., and Benazzi, S. (2015). Stress Distribution and Molar Macrowear in *Pongo pygmaeus*: A New Approach through Finite Element and Occlusal Fingerprint Analyses. *Human Evolution* 30, 215–226. doi: 10.14673/HE2015341009

Fleagle, J. G. (2013). *Primate Adaptation and Evolution*. Amsterdam, et al. Elsevier.

Fleagle, J. G., Janson, C. H., and Reed, K. E. (1999). *Primate communities*. Cambridge, New York: Cambridge University Press.

Fox, E. A., van Schaik, C. P., Sitompul, A., and Wright, D. N. (2004). Intra-and interpopulational differences in orangutan (*Pongo pygmaeus*) activity and diet: implications for the invention of tool use. *Am J Phys Anthropol* 125, 162–174. doi: 10.1002/ajpa.10386

Francisco, A., Blondel, C., Brunetière, N., Ramdarshan, A., and Merceron, G. (2018a). Enamel surface topography analysis for diet discrimination. A methodology to enhance and select discriminative parameters. *Surface Topography: Metrology and Properties* 6, 15002. doi: 10.1088/2051-672X/aa9dd3

Francisco, A., Brunetière, N., and Merceron, G. (2018b). Gathering and Analyzing Surface Parameters for Diet Identification Purposes. *Technologies* 6, 75. doi: 10.3390/technologies6030075

Francisco, A., Brunetière, N., and Merceron, G. (2020). Damaged digital surfaces also deserve realistic healing. *Surface Topography: Metrology and Properties* 8, 35008. doi: 10.1088/2051-672X/aba7a3

Friedli, H., Lötscher, H., Oeschger, H., Siegenthaler, U., and Stauffer, B. (1986). Ice core record of the $^{13}C/^{12}C$ ratio of atmospheric CO_2 in the past two centuries. *Nature* 324, 237–238. doi: 10.1038/324237a0

Galbany, J., Martínez, L. M., López-Amor, H. M., Espurz, V., Hiraldo, O., Romero, A., et al. (2005). Error rates in buccal-dental microwear quantification using scanning electron microscopy. *Scanning* 27, 23–29. doi: 10.1002/sca.4950270105

Galdikas, B. M. F. (1978). *Orangutan Adaptation at Tanjung Puting Reserve, Central Borneo*. PhD thesis. Los Angeles: University of California.

Galdikas, B. M. F. (1988). Orangutan diet, range, and activity at Tanjung Puting, Central Borneo. *International Journal of Primatology* 9, 1–35. doi: 10.1007/BF02740195

Gebo, D. L., Gunnell, G. F., Ciochon, R. L., Takai, M., Tsubamoto, T., and Egi, N. (2002). New eosimiid primate from Myanmar. *Journal of Human Evolution* 43, 549–553. doi: 10.1006/jhev.2002.0571

Geist, V. (1974). On the Relationship of Social Evolution and Ecology in Ungulates. *American Zoologist* 14, 205–220. doi: 10.1093/icb/14.1.205

Gibert, C., Zacaï, A., Fluteau, F., Ramstein, G., Chavasseau, O., Thiery, G., et al. (2022). A coherent biogeographical framework for Old World Neogene and Pleistocene mammals. *Palaeontology* 65. doi: 10.1111/pala.12594

Glimcher, M. J., Cohen-Solal, L., Kossiva, D., and Ricqles, A. de (1990). Biochemical analyses of fossil enamel and dentin. *Paleobiology* 16, 219–232. doi: 10.1017/S0094837300009891

Gresl, T. A., Baum, S. T., and Kemnitz, J. W. (2000). Glucose regulation in captive *Pongo pygmaeus abeli*, *P. p. pygmaeus*,and *P. p. abeli* x *P. p. pygmaeus* orangutans. *Zoo Biology* 19, 193–208. doi: 10.1002/1098-2361(2000)19:3<193:AID-ZOO3>3.0.CO;2-M

Grine, F. E. (1986). Dental evidence for dietary differences in *Australopithecus* and *Paranthropus*: a quantitative analysis of permanent molar microwear. *Journal of Human Evolution* 15, 783–822. doi: 10.1016/S0047-2484(86)80010-0

Grine, F. E., Ungar, P. S., and Teaford, M. F. (2002). Error rates in dental microwear quantification using scanning electron microscopy. *Scanning* 24, 144–153. doi: 10.1002/sca.4950240307

Grinnell, J. (1924). Geography and Evolution. *Ecology* 5, 225–229. doi: 10.2307/1929447

Gunnell, G. F., and Ciochon, R. L. (2008). "Revisiting Primate Postcrania from the Pondaung Formation of Myanmar," in *Elwyn Simons: A Search for Origins*, eds. J. G. Fleagle, and C. C. Gilbert (New York: Springer), 211–228.

Gunnell, G. F., Ciochon, R. L., Gingerich, P. D., and Holroyd, P. A. (2002). New assessment of *Pondaungia* and *Amphipithecus* (Primates) from the late Middle Eocene of Myanmar, with a comment on "Amphipithecidae". *Contributions from the Museum of Paleontology the University of Michigan* 30, 337–372.

Gunnell, G. F., and Miller, E. R. (2001). Origin of anthropoidea: Dental evidence and recognition of early anthropoids in the fossil record, with comments on the Asian anthropoid radiation. *Am J Phys Anthropol* 114, 177–191. doi: 10.1002/1096-8644(200103)114:3<177:AID-AJPA1019>3.0.CO;2-O

Habinger, S. G., Chavasseau, O., Ducrocq, S., Chaimanee, Y., Jaeger, J. J., Sein, C., et al. (2023). Isotopic niche modelling of the Pondaung mammal fauna (middle Eocene, Myanmar) shows

microhabitat differences. Insights into paleoecology and early anthropoid primate habitats. *Frontiers in Ecology and Evolution* 11, 1110331. doi: 10.3389/fevo.2023.1110331

Habinger, S. G., Chavasseau, O., Jaeger, J.-J., Chaimanee, Y., Soe, A. N., Sein, C., et al. (2022). Evolutionary ecology of Miocene hominoid primates in Southeast Asia. *Scientific Reports* 12, 11841. doi: 10.1038/s41598-022-15574-z

Habinger, S. G., Merceron, G., van Heteren, A. H., Rojas Cuyutupa, V., Bocherens, H., and Chavasseau, O. (in prep). Characterisation of a circa 1890 orangutan population's diet using dental microwear texture analysis: A reference data set for intra- and interspecific variation of dental microwear of extant hominids.

Harrison, M. E., Morrogh-Bernard, H. C., and Chivers, D. J. (2010). Orangutan Energetics and the Influence of Fruit Availability in the Nonmasting Peat-swamp Forest of Sabangau, Indonesian Borneo. *International Journal of Primatology* 31, 585–607. doi: 10.1007/s10764-010-9415-5

Harrison, T. (2010). Apes among the tangled branches of human origins. *Science* 327, 532–534. doi: 10.1126/science.1184703

Harrison, T., Jin, C., Zhang, Y., Wang, Y., and Zhu, M. (2014). Fossil *Pongo* from the Early Pleistocene *Gigantopithecus* fauna of Chongzuo, Guangxi, southern China. *Quaternary International* 354, 59–67. doi: 10.1016/j.quaint.2014.01.013

Harrison, T., Krigbaum, J., and Manser, J. (2006). "Primate Biogeography and Ecology on the Sunda Shelf Islands: A Paleontological and Zooarchaeological Perspective," in *Primate biogeography: Progress and prospects*, eds. S. M. Lehman, and J. G. Fleagle (Toronto: Springer), 331–372.

Hartwig, W. C., ed (2002). *The Primate Fossil Record*. Cambridge: Cambridge University Press.

Harzhauser, M., Kroh, A., Mandic, O., Piller, W. E., Göhlich, U., Reuter, M., et al. (2007). Biogeographic responses to geodynamics: A key study all around the Oligo–Miocene Tethyan Seaway. *Zoologischer Anzeiger - A Journal of Comparative Zoology* 246, 241–256. doi: 10.1016/j.jcz.2007.05.001

Head, J. J., Gunnell, G. F., Holroyd, P. A., Hutchison, J. H., and Ciochon, R. L. (2013). Giant lizards occupied herbivorous mammalian ecospace during the Paleogene greenhouse in Southeast Asia. *Proc Biol Sci* 280, 20130665. doi: 10.1098/rspb.2013.0665

Hette-Tronquart, N. (2019). Isotopic niche is not equal to trophic niche. *Ecol Lett* 22, 1987–1989. doi: 10.1111/ele.13218

Heuser, A., Tütken, T., Gussone, N., and Galer, S. J. (2011). Calcium isotopes in fossil bones and teeth — Diagenetic versus biogenic origin. *Geochimica et Cosmochimica Acta* 75, 3419–3433. doi: 10.1016/j.gca.2011.03.032

Hillson, S. (2005). *Teeth*. Cambridge: Cambridge University Press.

Ho, C. K., Zhou, G. X., and Swindler, D. R. (1995). Dental evolution of the orang-utan in China. *Human Evolution* 10, 249–264. doi: 10.1007/BF02438962

Holroyd, P. A., and Ciochon, R. L. (2000). *Bunobrontops savagei* a new genus and species of brontotheriid perissodactyl from the Eocene Pondaung fauna of Myanmar. *Journal of Vertebrate Paleontology* 20, 408–410. doi: 10.1671/0272-4634(2000)020[0408:BSANGA]2.0.CO;2

Holt, R. D. (2009). Bringing the Hutchinsonian niche into the 21st century: ecological and evolutionary perspectives. *Proc Natl Acad Sci U S A* 106 Suppl 2, 19659–19665. doi: 10.1073/pnas.0905137106

Hooijer, D. A. (1948). Prehistoric teeth of man and of the orang-utan from central Sumatra, with notes on the fossil orang-utan from Java and southern China. *Zoologische Mededeelingen* 29, 175–301.

Hoorn, C., Ohja, T., and Quade, J. (2000). Palynological evidence for vegetation development and climatic change in the Sub-Himalayan Zone (Neogene, Central Nepal). *Palaeogeography, Palaeoclimatology, Palaeoecology* 163, 133–161. doi: 10.1016/S0031-0182(00)00149-8

Houle, A., Chapman, C. A., and Vickery, W. L. (2010). Intratree vertical variation of fruit density and the nature of contest competition in frugivores. *Behav Ecol Sociobiol* 64, 429–441. doi: 10.1007/s00265-009-0859-6

Howland, M. R., Corr, L. T., Young, S. M. M., Jones, V., Jim, S., van der Merwe, N. J., et al. (2003). Expression of the dietary isotope signal in the compound-specific $\delta^{13}C$ values of pig bone lipids and amino acids. *International Journal of Osteoarchaeology* 13, 54–65. doi: 10.1002/oa.658

Hu, Y., Jiang, Q., Liu, F., Guo, L., Zhang, Z., and Zhao, L. (2022). Calcium isotope ecology of early *Gigantopithecus blacki* (~2 Ma) in South China. *Earth and Planetary Science Letters* 584, 117522. doi: 10.1016/j.epsl.2022.117522

Huang, H., Morley, R. J., Licht, A., Dupont-Nivet, G., Pérez-Pinedo, D., Westerweel, J., et al. (2023). A proto-monsoonal climate in the late Eocene of Southeast Asia: Evidence from a sedimentary record in central Myanmar. *Geoscience Frontiers* 14, 101457. doi: 10.1016/j.gsf.2022.101457

Hubrecht, A. A. W. (1902-1903). "Emil Selenka," in *Menschenaffen (Anthropomorphae): Studien über Entwicklung und Schädelbau*, ed. E. Selenka (Wiesbaden: C.W. Kreidel), 1–14.

Hunt, K. D. (2016). Why are there apes? Evidence for the co-evolution of ape and monkey ecomorphology. *J Anat* 228, 630–685. doi: 10.1111/joa.12454

Hutchinson, G. E. (1957). Concluding Remarks. *Cold spring harbor symposium on quantitative biology* 22, 415.

Hutchison, J. H., Holroyd, P. A., and Ciochon, R. L. (2004). Preliminary report on Southeast Asia's Oldest Cenozoic Turtle Fauna from the late Middle Eocene Pongaung Formation, Myanmar. *Asiatic Herpetological Research* 10, 38–52.

Ibrahim, Y. K., Tshen, L. T., Westaway, K. E., Cranbrook, E. o., Humphrey, L., Muhammad, R. F., et al. (2013). First discovery of Pleistocene orangutan (*Pongo* sp.) fossils in Peninsular Malaysia: Biogeographic and paleoenvironmental implications. *Journal of Human Evolution* 65, 770–797. doi: 10.1016/j.jhevol.2013.09.005

Jablonski, N. G., Whitfort, M. J., Roberts-Smith, N., and Qinqi, X. (2000). The influence of life history and diet on the distribution of catarrhine primates during the Pleistocene in eastern Asia. *Journal of Human Evolution* 39, 131–157. doi: 10.1006/jhev.2000.0405

Jackson, A. L., Inger, R., Parnell, A. C., and Bearhop, S. (2011). Comparing isotopic niche widths among and within communities: SIBER - Stable Isotope Bayesian Ellipses in R. *The Journal of Animal Ecology* 80, 595–602. doi: 10.1111/j.1365-2656.2011.01806.x

Jackson, P. C., Meinzer, F. C., Goldstein, G., Holbrook, N. M., Cavelier, J., and Rada, F. (1993). "Environmental and Physiological Influences on Carbon Isotope Composition of Gap and Understory Plants in a Lowland Tropical Forest," in *Stable isotopes and plant carbon-water relations*, eds. J. R. Ehleringer, A. E. Hall, and G. D. Farquhar (San Diego: Academic Press), 131–140.

Jaeger, J., Thein, T., Benammi, M., Chaimanee, Y., Soe, A. N., Lwin, T., et al. (1999). A new primate from the Middle Eocene of Myanmar and the Asian early origin of anthropoids. *Science* 286, 528–530. doi: 10.1126/science.286.5439.528

Jaeger, J.-J., Aung, N. S., Chavasseau, O., Coster, P., Emonet, E.-G., Guy, F., et al. (2011). First Hominoid from the Late Miocene of the Irrawaddy Formation (Myanmar). *Plos ONE* 6, 1–14. doi: 10.1371/journal.pone.0017065

Jaeger, J.-J., Beard, K. C., Chaimanee, Y., Salem, M., Benammi, M., Hlal, O., et al. (2010). Late middle Eocene epoch of Libya yields earliest known radiation of African anthropoids. *Nature* 467, 1095–1098. doi: 10.1038/nature09425

Jaeger, J.-J., Chaimanee, Y., Tafforeau, P., Ducrocq, S., Soe, A. N., Marivaux, L., et al. (2004). Systematics and paleobiology of the anthropoid primate *Pondaungia* from the late Middle Eocene of Myanmar. *Comptes Rendus Palevol* 3, 243–255. doi: 10.1016/j.crpv.2004.05.003

Jaeger, J.-J., Chavasseau, O., Lazzari, V., Naing Soe, A., Sein, C., Le Maître, A., et al. (2019). New Eocene primate from Myanmar shares dental characters with African Eocene crown anthropoids. *Nature Communications* 10, 3531. doi: 10.1038/s41467-019-11295-6

Jaeger, J.-J., Chit Sein, Gebo, D. L., Chaimanee, Y., M. T. Nyein, Oo, T. Z., et al. (2020). Amphipithecine primates are stem anthropoids: cranial and postcranial evidence. *Proceedings of the Royal Society B* 287, 20202129. doi: 10.1098/rspb.2020.2129

Jaeger, J.-J., Soe, U. A. N., Aung, A. K., Benammi, M., Chaimanee, Y., Ducrocq, R.-M., et al. (1998). New Myanmar middle Eocene anthropoids. An Asian origin for catarrhines? *Comptes Rendus de l'Académie des Sciences - Series III - Sciences de la Vie* 321, 953–959. doi: 10.1016/S0764-4469(99)80010-9

Janssen, R., Joordens, J. C., Koutamanis, D. S., Puspaningrum, M. R., Vos, J. de, van der Lubbe, Jeroen H.J.L., et al. (2016). Tooth enamel stable isotopes of Holocene and Pleistocene fossil fauna reveal glacial and interglacial paleoenvironments of hominins in Indonesia. *Quaternary Science Reviews* 144, 145–154. doi: 10.1016/j.quascirev.2016.02.028

Jaouen, K., Beasley, M., Schoeninger, M., Hublin, J.-J., and Richards, M. P. (2016a). Zinc isotope ratios of bones and teeth as new dietary indicators: results from a modern food web (Koobi Fora, Kenya). *Scientific Reports* 6, 26281. doi: 10.1038/srep26281

Jaouen, K., Szpak, P., and Richards, M. P. (2016b). Zinc Isotope Ratios as Indicators of Diet and Trophic Level in Arctic Marine Mammals. *Plos ONE* 11, e0152299. doi: 10.1371/journal.pone.0152299

Jaouen, K., Villalba-Mouco, V., Smith, G. M., Trost, M., Leichliter, J., Lüdecke, T., et al. (2022). A Neandertal dietary conundrum: Insights provided by tooth enamel Zn isotopes from Gabasa, Spain. *Proc Natl Acad Sci U S A* 119, e2109315119. doi: 10.1073/pnas.2109315119

Jarman, P. J. (1974). The Social Organisation of Antelope in Relation To Their Ecology. *Behaviour* 48, 215–267. doi: 10.1163/156853974X00345

Jentink, F. A. (1897). Zoological results of the Dutch scientific expedition to Central Borneo: The mammals. *Notes from the Leyden Museum* 19, 26–66.

Ji, W.-Q., Wu, F.-Y., Wang, J.-M., Liu, X.-C., Liu, Z.-C., Zhang, Z., et al. (2020). Early Evolution of Himalayan Orogenic Belt and Generation of Middle Eocene Magmatism: Constraint From Haweng Granodiorite Porphyry in the Tethyan Himalaya. *Front. Earth Sci.* 8, 236. doi: 10.3389/feart.2020.00236

Ji, X., Harrison, T., Zhang, Y., Wu, Y., Zhang, C., Hu, J., et al. (2022). The earliest hylobatid from the Late Miocene of China. *Journal of Human Evolution* 171, 103251. doi: 10.1016/j.jhevol.2022.103251

Ji, X., Jablonski, N. G., Su, D. F., Deng, C., Flynn, L. J., You, Y., et al. (2013). Juvenile hominoid cranium from the terminal Miocene of Yunnan, China. *Chinese Science Bulletin* 58, 3771–3779. doi: 10.1007/s11434-013-6021-x

Jiang, Q.-Y., Zhao, L., Guo, L., and Hu, Y. (2021). First direct evidence of conservative foraging ecology of early *Gigantopithecus blacki* (~2 Ma) in Guangxi, southern China. *Am J Phys Anthropol.* doi: 10.1002/ajpa.24300

Johnson, D. L., Henderson, M. T., Anderson, D. L., Booms, T. L., and Williams, C. T. (2022). Isotopic niche partitioning and individual specialization in an Arctic raptor guild. *Oecologia* 198, 1073–1084. doi: 10.1007/s00442-022-05154-3

Jonell, T. N., Giosan, L., Clift, P. D., Carter, A., Bretschneider, L., Hathorne, E. C., et al. (2022). No modern Irrawaddy River until the late Miocene-Pliocene. *Earth and Planetary Science Letters* 584, 117516. doi: 10.1016/j.epsl.2022.117516

Kaiser, T. M., Clauss, M., and Schulz-Kornas, E. (2016). A set of hypotheses on tribology of mammalian herbivore teeth. *Surface Topography: Metrology and Properties* 4, 14003. doi: 10.1088/2051-672X/4/1/014003

Kajita, R. (2019). Historical precipitation data in Sumatra and Kalimantan from 1879 to 1900, by using Dutch colonial materials. *IOP Conference Series: Earth and Environmental Science* 361, 12003. doi: 10.1088/1755-1315/361/1/012003

Kanamori, T., Kuze, N., Bernard, H., Malim, T. P., and Kohshima, S. (2010). Feeding ecology of Bornean orangutans (*Pongo pygmaeus morio*) in Danum Valley, Sabah, Malaysia: a 3-year record including two mast fruitings. *Am J Primatol* 72, 820–840. doi: 10.1002/ajp.20848

Kaplan, A., Cane, M. A., Kushnir, Y., Clement, A. C., Blumenthal, M. B., and Rajagopalan, B. (1998). Analyses of global sea surface temperature 1856-1991. *Journal of Geophysical Research: Oceans* 103, 18567–18589. doi: 10.1029/97JC01736

Kay, R. F. (1981). The Nut-Crackers - A New Theory of the Adaptations of the Ramapithecinae. *Am J Phys Anthropol* 55, 141–151. doi: 10.1002/ajpa.1330550202

Kay, R. F. (1984). "On the Use of Anatomical Features To Infer Foraging Behavior in Extinct Primates," in *Adaptations for Foraging in Nonhuman Primates: Contributions to an Organismal Biology of Prosimians, Monkeys, and Apes*, eds. P. S. Rodman, and J. G. H. Cant (New York: Columbia University Press), 21–53.

Kay, R. F., and Hiiemae, K. M. (1974). Jaw movement and tooth use in recent and fossil primates. *Am J Phys Anthropol* 40, 227–256. doi: 10.1002/ajpa.1330400210

Kay, R. F., Schmitt, D., Vinyard, C. J., Perry, J. M. G., Shigehara, N., Takai, M., et al. (2004). The paleobiology of Amphipithecidae, South Asian late Eocene primates. *Journal of Human Evolution* 46, 3–24. doi: 10.1016/j.jhevol.2003.09.009

Keast, A. (1977). "Mechanisms expanding niche width and minimizing intraspecific competition in two centrarchid fishes," in *Evolutionary biology*, eds. M. K. Hecht, W. C. Steere, and B. Wallace (New York: Plenum Press), 333–395.

Keeling, C. D. (1979). The Suess effect: ^{13}Carbon-^{14}Carbon interrelations. *Environment International* 2, 229–300. doi: 10.1016/0160-4120(79)90005-9

Keeling, C. D., Piper, S. C., Bacastow, R. B., Wahlen, M., Whorf, T. P., Heimann, M., et al. (2001). *Exchanges of atmospheric CO_2 and $^{13}CO_2$ with the terrestrial biosphere and oceans from 1978 to 2000: I. Global aspects*. San Diego: Scripps Institution of Oceanography.

Keeling, C. D., Piper, S. C., Bacastow, R. B., Wahlen, M., Whorf, T. P., Heimann, M., et al. (2005). "Atmospheric CO_2 and $^{13}CO_2$ Exchange with the Terrestrial Biosphere and Oceans from 1978 to 2000: Observations and Carbon Cycle Implications," in *A history of atmospheric CO_2 and its effects on plants, animals, and ecosystems*, eds. J. R. Ehleringer, T. E. Cerling, and M. D. Dearing (New York, Great Britain: Springer), 83–113.

Kelley, J. (1988). A new large species of *Sivapithecus* from the Siwaliks of Pakistan. *Journal of Human Evolution* 17, 305–324. doi: 10.1016/0047-2484(88)90073-5

Kelley, J. (2002). "The hominoid radiation in Asia," in *The Primate Fossil Record*, ed. W. C. Hartwig (Cambridge: Cambridge University Press), 369–384.

Kelley, J. (2005). "Twenty-five Years Contemplating *Sivapithecus* Taxonomy," in *Interpreting the Past: Essays on Human, Primate, and Mammal Evolution*, eds. J. Kelley, D. Lieberman, and R. W. Smith (Leiden, Boston: Brill), 123–143.

Kelley, J., and Gao, F. (2012). Juvenile hominoid cranium from the late Miocene of southern China and hominoid diversity in Asia. *Proc Natl Acad Sci U S A* 109, 6882–6885. doi: 10.1073/pnas.1201330109

Kennett, J. P., and Stott, L. D. (1991). Abrupt deep-sea warming, palaeoceanographic changes and benthic extinctions at the end of the Palaeocene. *Nature* 353, 225–229. doi: 10.1038/353225a0

Khin, K., and Myitta (1999). Marine transgression and regression in Miocene sequences of northern Pegu (Bago) Yoma, Central Myanmar. *Journal of Asian Earth Sciences* 17, 369–393. doi: 10.1016/S0743-9547(98)00065-8

Kinzey, W. G. (1992). Dietary and dental adaptations in the Pitheciinae. *Am J Phys Anthropol* 88, 499–514. doi: 10.1002/ajpa.1330880406

Knott, C. D. (1998). Changes in Orangutan Caloric Intake, Energy Balance, and Ketones in Response to Fluctuating Fruit Availability. *International Journal of Primatology* 19, 1061–1079. doi: 10.1023/A:1020330404983

Knott, C. D., Beaudrot, L., Snaith, T., White, S., Tschauner, H., and Planansky, G. (2008). Female-Female Competition in Bornean Orangutans. *International Journal of Primatology* 29, 975–997. doi: 10.1007/s10764-008-9278-1

Koch, P. L. (2007). "Isotopic study of the biology of modern and fossil vertebrates," in *Stable isotopes in ecology and environmental science*, eds. R. Michener, and K. Lajtha (Oxford: Blackwell Publishing), 99–154.

Koch, P. L., Tuross, N., and Fogel, M. L. (1997). The Effects of Sample Treatment and Diagenesis on the Isotopic Integrity of Carbonate in Biogenic Hydroxylapatite. *Journal of Archaeological Science* 24, 417–429. doi: 10.1006/jasc.1996.0126

Köhler, M., and Moyà-Solà, S. (1999). A finding of Oligocene primates on the European continent. *Proc Natl Acad Sci U S A* 96, 14664–14667. doi: 10.1073/pnas.96.25.14664

Kohn, M. J. (1996). Predicting animal $\delta^{18}O$: Accounting for diet and physiological adaptation. *Geochimica et Cosmochimica Acta* 60, 4811–4829. doi: 10.1016/S0016-7037(96)00240-2

Kohn, M. J. (2010). Carbon isotope compositions of terrestrial C_3 plants as indicators of (paleo)ecology and (paleo)climate. *Proceedings of the National Academy of Science* 107, 19691–19695. doi: 10.1073/pnas.1004933107

Komsta, L. (2006). Processing data for outliers. *R News* 6, 10–13.

Kreft, H., and Jetz, W. (2010). A framework for delineating biogeographical regions based on species distributions. *Journal of Biogeography* 37, 2029–2053. doi: 10.1111/j.1365-2699.2010.02375.x

Krigbaum, J. (2003). Neolithic subsistence patterns in northern Borneo reconstructed with stable carbon isotopes of enamel. *Journal of Anthropological Archaeology* 22, 292–304. doi: 10.1016/S0278-4165(03)00041-2

Krigbaum, J., Berger, M. H., Daegling, D. J., and McGraw, W. S. (2013). Stable isotope canopy effects for sympatric monkeys at Tai Forest, Cote d'Ivoire. *Biol Lett* 9, 20130466. doi: 10.1098/rsbl.2013.0466

Law, R., Marrow, P., and Dieckmann, U. (1997). On evolution under asymmetric competition. *Evolutionary Ecology* 11, 485–501. doi: 10.1023/A:1018441108982

Lê, S., Josse, J., and Husson, F. (2008). FactoMineR: An R Package for Multivariate Analysis. *Journal of Statistical Software* 25, 1–18.

Leichliter, J. N., Lüdecke, T., Foreman, A. D., Duprey, N. N., Winkler, D. E., Kast, E. R., et al. (2021). Nitrogen isotopes in tooth enamel record diet and trophic level enrichment: Results from a controlled feeding experiment. *Chemical Geology* 563, 120047. doi: 10.1016/j.chemgeo.2020.120047

Levin, N. E., Cerling, T. E., Passey, B. H., Harris, J. M., and Ehleringer, J. R. (2006). A stable isotope aridity index for terrestrial environments. *Proc Natl Acad Sci U S A* 103, 11201–11205. doi: 10.1073/pnas.0604719103

Licht, A., Boura, A., Franceschi, D. de, Ducrocq, S., Soe, A. N., and Jaeger, J.-J. (2014a). Fossil woods from the late middle Eocene Pondaung Formation, Myanmar. *Review of Palaeobotany and Palynology* 202, 29–46. doi: 10.1016/j.revpalbo.2013.12.002

Licht, A., Boura, A., Franceschi, D. de, Utescher, T., Sein, C., and Jaeger, J.-J. (2015). Late middle Eocene fossil wood of Myanmar: Implications for the landscape and the climate of the Eocene Bengal Bay. *Review of Palaeobotany and Palynology* 216, 44–54. doi: 10.1016/j.revpalbo.2015.01.010

Licht, A., Cojan, I., Caner, L., Soe, A. N., Jaeger, J.-J., and France-Lanord, C. (2014b). Role of permeability barriers in alluvial hydromorphic palaeosols: The Eocene Pondaung Formation, Myanmar. *Sedimentology* 61, 362–382. doi: 10.1111/sed.12059

Licht, A., Reisberg, L., France-Lanord, C., Naing Soe, A., and Jaeger, J.-J. (2016). Cenozoic evolution of the central Myanmar drainage system: insights from sediment provenance in the Minbu Sub-Basin. *Basin Research* 28, 237–251. doi: 10.1111/bre.12108

Licht, A., van Cappelle, M., Abels, H. A., Ladant, J.-B., Tracucho-Alexandre, J., France-Lanord, C., et al. (2014c). Asian monsoons in a late Eocene greenhouse world. *Nature* 513, 501–506. doi: 10.1038/nature13704

Lihoreau, F., and Ducrocq, S. (2007). "Family Anthracotheriidae," in *The Evolution of Atiodactyls*, eds. D. R. Prothero, and S. E. Foss (Baltimore: The Johns Hopkin University Press), 89–105.

Liu, Z., Pagani, M., Zinniker, D., Deconto, R., Huber, M., Brinkhuis, H., et al. (2009). Global cooling during the Eocene-Oligocene climate transition. *Science* 323, 1187–1190. doi: 10.1126/science.1166368

Louys, J., Kealy, S., O'Connor, S., Price, G. J., Hawkins, S., Aplin, K., et al. (2017). Differential preservation of vertebrates in Southeast Asian caves. *International Journal of Speleology* 46, 379–408. doi: 10.5038/1827-806X.46.3.2131

Louys, J., and Roberts, P. (2020). Environmental drivers of megafauna and hominin extinction in Southeast Asia. *Nature* 586, 402–406. doi: 10.1038/s41586-020-2810-y

Louys, J., Zaim, Y., Rizal, Y., Aswan, Puspaningrum, M. R., Trihascaryo, A., et al. (2021). Sumatran orangutan diets in the Late Pleistocene as inferred from dental microwear texture analysis. *Quaternary International* 603, 74–81. doi: 10.1016/j.quaint.2020.08.040

Lovell, N. C. (1991). An evolutionary framework for assessing illness and injury in nonhuman primates. *Am J Phys Anthropol* 34, 117–155. doi: 10.1002/ajpa.1330340608

Lowry, B. E., Wittig, R. M., Pittermann, J., and Oelze, V. M. (2021). Stratigraphy of stable isotope ratios and leaf structure within an African rainforest canopy with implications for primate isotope ecology. *Scientific Reports* 11, 14222. doi: 10.1038/s41598-021-93589-8

Lüdecke, T., Leichliter, J. N., Aldeias, V., Bamford, M. K., Biro, D., Braun, D. R., et al. (2022). Carbon, nitrogen, and oxygen stable isotopes in modern tooth enamel: A case study from Gorongosa National Park, central Mozambique. *Front. Ecol. Evol.* 10. doi: 10.3389/fevo.2022.958032

Lydekker, R. (1879). Further notices of Siwalik mammalia. *Records of the Geological Survey of India* 12, 33–52.

Ma, J., Wang, Y., Jin, C., Hu, Y., and Bocherens, H. (2019). Ecological flexibility and differential survival of Pleistocene Stegodon orientalis and Elephas maximus in mainland southeast Asia revealed by stable isotope (C, O) analysis. *Quaternary Science Reviews* 212, 33–44. doi: 10.1016/j.quascirev.2019.03.021

Ma, J., Wang, Y., Jin, C., Yan, Y., Qu, Y., and Hu, Y. (2017). Isotopic evidence of foraging ecology of Asian elephant (Elephas maximus) in South China during the Late Pleistocene. *Quaternary International* 443, 160–167. doi: 10.1016/j.quaint.2016.09.043

MacKinnon, J. (1974). The behaviour and ecology of wild orang-utans (*Pongo pygmaeus*). *Animal Behaviour* 22, 3–12.

MacKinnon, J. (1977). A comparative ecology of Asian apes. *Primates* 18, 747–772. doi: 10.1007/BF02382929

Mader, B. J. (1998). "Bronthotheriidae," in *Evolution of tertiary mammals of North America: Volume 1, terrestrial carnivores, ungulates, and ungulate like mammals*, eds. C. M. Janis, K. M. Scott, and L. L. Jacobs (Cambridge: Cambridge University Press), 525–536.

Maier, W., and Schneck, G. (1981). Konstruktionsmorphologische Untersuchungen am Gebiß der hominoiden Primaten. *Zeitschrift für Morphologie und Anthropologie* 72, 127–169.

Malone, M. A., MacLatchy, L. M., Mitani, J. C., Kityo, R., and Kingston, J. D. (2021). A chimpanzee enamel-diet $\delta^{13}C$ enrichment factor and a refined enamel sampling strategy:

Implications for dietary reconstructions. *Journal of Human Evolution* 159, 103062. doi: 10.1016/j.jhevol.2021.103062

Marino, B. D., McElroy, M. B., Salawitch, R. J., and Spaulding, W. G. (1992). Glacial-to-interglacial variations in the carbon isotopic composition of atmospheric CO_2. *Nature* 357, 461–466. doi: 10.1038/357461a0

Marivaux, L., Antoine, P.-O., Baqri, S. R. H., Benammi, M., Chaimanee, Y., Crochet, J.-Y., et al. (2005). Anthropoid primates from the Oligocene of Pakistan (Bugti Hills): data on early anthropoid evolution and biogeography. *Proceedings of the National Academy of Sciences* 102, 8436–8441. doi: 10.1073/pnas.0503469102

Marivaux, L., Beard, K. C., Chaimanee, Y., Dagosto, M., Gebo, D. L., Guy, F., et al. (2010). Talar morphology, phylogenetic affinities, and locomotor adaptation of a large-bodied amphipithecid primate from the late middle Eocene of Myanmar. *Am J Phys Anthropol* 143, 208–222. doi: 10.1002/ajpa.21307

Marivaux, L., Beard, K. C., Chaimanee, Y., Jaeger, J.-J., Marandat, B., Soe, A. N., et al. (2008a). Anatomy of the bony pelvis of a relatively large-bodied strepsirrhine primate from the late middle Eocene Pondaung Formation (central Myanmar). *Journal of Human Evolution* 54, 391–404. doi: 10.1016/j.jhevol.2007.09.007

Marivaux, L., Beard, K. C., Chaimanee, Y., Jaeger, J.-J., Marandat, B., Soe, A. N., et al. (2008b). Proximal femoral anatomy of a sivaladapid primate from the late middle Eocene Pondaung formation (central Myanmar). *Am J Phys Anthropol* 137, 263–273. doi: 10.1002/ajpa.20866

Marivaux, L., Chaimanee, Y., Ducrocq, S., Marandat, B., Sudre, J., Soe, A. N., et al. (2003). The anthropoid status of a primate from the late middle Eocene Pondaung Formation (Central Myanmar): tarsal evidence. *Proceedings of the National Academy of Sciences* 100, 13173–13178. doi: 10.1073/pnas.2332542100

Marivaux, L., Welcomme, J.-L., Antoine, P.-O., Métais, G., Baloch, I. M., Benammi, M., et al. (2001). A fossil lemur from the Oligocene of Pakistan. *Science* 294, 587–591. doi: 10.1126/science.1065257

Marivaux, L., Welcomme, J.-L., Ducrocq, S., and Jaeger, J.-J. (2002). Oligocene sivaladapid primate from the Bugti Hills (Balochistan, Pakistan) bridges the gap between Eocene and Miocene adapiform communities in Southern Asia. *Journal of Human Evolution* 42, 379–388. doi: 10.1006/jhev.2001.0529

Marshall, A. J., Ancrenaz, M., Brearley, F. Q., Frederiksson, G., Ghaffar, N., Heydon, M., et al. (2009a). "Are Sumatran forests better orangutan habitat than Bornean forests?" in *Orangutans: Geographic variation in behavioral ecology and conservation*, eds. S. A. Wich, S. S. Utami-Atmoko, T. Mitra Setia, and C. P. van Schaik (Oxford University Press), 97–117.

Marshall, A. J., Boyko, C. M., Feilen, K. L., Boyko, R. H., and Leighton, M. (2009b). Defining fallback foods and assessing their importance in primate ecology and evolution. *Am J Phys Anthropol* 140, 603–614. doi: 10.1002/ajpa.21082

Marshall, H. H., Inger, R., Jackson, A. L., McDonald, R. A., Thompson, F. J., and Cant, M. A. (2019). Stable isotopes are quantitative indicators of trophic niche. *Ecol Lett* 22, 1990–1992. doi: 10.1111/ele.13374

Martínez-García, A., Jung, J., Ai, X. E., Sigman, D. M., Auderset, A., Duprey, N. N., et al. (2022). Laboratory Assessment of the Impact of Chemical Oxidation, Mineral Dissolution, and

Heating on the Nitrogen Isotopic Composition of Fossil-Bound Organic Matter. *Geochemistry, Geophysics, Geosystems* 23, e2022GC010396. doi: 10.1029/2022GC010396

Maung, M., Htike, T., Tsubamoto, T., Suzuki, H., Sein, C., Egi, N., et al. (2005). Stratigraphy of the primate-bearing beds of the Eocene Pondaung Formation at Paukkaung area, Myanmar. *Anthropological Science* 113, 11–15. doi: 10.1537/ase.04S002

Meijaard, E., Albar, G., Nardiyono, Rayadin, Y., Ancrenaz, M., and Spehar, S. (2010). Unexpected ecological resilience in Bornean orangutans and implications for pulp and paper plantation management. *Plos ONE* 5, e12813. doi: 10.1371/journal.pone.0012813

Merceron, G., Escarguel, G., Angibault, J.-M., and Verheyden-Tixier, H. (2010). Can dental microwear textures record inter-individual dietary variations? *Plos ONE* 5, e9542. doi: 10.1371/journal.pone.0009542

Merceron, G., Novello, A., and Scott, R. S. (2016). Paleoenvironments inferred from phytoliths and Dental Microwear Texture Analyses of meso-herbivores. *Geobios* 49, 135–146. doi: 10.1016/j.geobios.2016.01.004

Merceron, G., Taylor, S., Scott, R., Chaimanee, Y., and Jaeger, J.-J. (2006). Dietary characterization of the hominoid *Khoratpithecus* (Miocene of Thailand): evidence from dental topographic and microwear texture analyses. *Naturwissenschaften* 93, 329–333. doi: 10.1007/s00114-006-0107-0

Métivier, F., Gaudemer, Y., Tapponnier, P., and Klein, M. (1999). Mass accumulation rates in Asia during the Cenozoic. *Geophysical Journal International* 137, 280–318. doi: 10.1046/j.1365-246X.1999.00802.x

Mihlbachler, M. C., Beatty, B. L., Caldera-Siu, A., Chan, D., and Lee, R. (2012). Error rates and observer bias in dental microwear analysis using light microscopy. *Palaeontologia Electronica* 15, 1–22. doi: 10.26879/298

Milne, S., Martin, J. G. A., Reynolds, G., Vairappan, C. S., Slade, E. M., Brodie, J. F., et al. (2021). Drivers of Bornean Orangutan Distribution across a Multiple-Use Tropical Landscape. *Remote Sensing* 13, 458. doi: 10.3390/rs13030458

Morgan, M. E., Behrensmeyer, A. K., Badgley, C., Barry, J. C., Nelson, S., and Pilbeam, D. R. (2009). Lateral trends in carbon isotope ratios reveal a Miocene vegetation gradient in the Siwaliks of Pakistan. *Geology* 37, 103–106. doi: 10.1130/G25359A.1

Morgan, M. E., Kingston, J. D., and Marino, B. D. (1994). Carbon isotopic evidence for the emergence of C_4 plants in the Neogene from Pakistan and Kenya. *Nature* 367, 162–165. doi: 10.1038/367162a0

Morley, R. J. (2000). *Origin and Evolution of Tropical Rain Forests*. Chichester, New York, Weinheim, Brisbane, Singapore, Toronto: Wiley-Blackwell.

Morley, R. J. (2012). "A review of the Cenozoic palaeoclimate history of Southeast Asia," in *Biotic Evolution and Environmental Change in Southeast Asia*, eds. D. Gower, K. Johnson, J. Richardson, B. Rosen, L. Ruber, and S. Williams (Cambridge: Cambridge University Press), 79–114.

Morley, R. J. (2018). Assembly and division of the South and South-East Asian flora in relation to tectonics and climate change. *Journal of Tropical Ecology* 34, 209–234. doi: 10.1017/S0266467418000202

Morrogh-Bernard, H. C., Husson, S. J., Knott, C. D., Wich, S. A., van Schaik, C. P., van Noordwijk, M. A., et al. (2009). "Orangutan activity budgets and diet: A comparison between

species, populations and habitats," in *Orangutans: Geographic variation in behavioral ecology and conservation*, eds. S. A. Wich, S. S. Utami-Atmoko, T. Mitra Setia, and C. P. van Schaik (Oxford University Press), 119–134.

Moyà Solà, S., and Köhler, M. (1995). New partial cranium of *Dryopithecus lartet*, 1863 (Hominoidea, Primates) from the upper Miocene of Can Llobateres, Barcelona, Spain. *Journal of Human Evolution* 29, 101–139. doi: 10.1006/jhev.1995.1049

Munthe, J., Dongol, B., Hutchison, J. H., Kean, W. F., Munthe, K., and West, R. M. (1983). New fossil discoveries from the Miocene of Nepal include a hominoid. *Nature* 303, 331–333. doi: 10.1038/303331a0

Nelson, S. (2003). *The Extinction of Sivapithecus: Faunal and Environmental Changes Surrounding the Disappearance of a Miocene Hominoid in the Siwaliks of Pakistan*. Boston: Brill Academic Publishers.

Nelson, S. (2005). Paleoseasonality inferred from equid teeth and intra-tooth isotopic variability. *Palaeogeography, Palaeoclimatology, Palaeoecology* 222, 122–144. doi: 10.1163/9789004494251_010

Nelson, S. (2007). Isotopic reconstruction of habitat change surrounding the extinction of *Sivapithecus*, a Miocene hominoid, in the Siwalik Group of Pakistan. *Palaeogeography, Palaeoclimatology, Palaeoecology* 243, 204–222. doi: 10.1016/j.palaeo.2006.07.017

Nelson, S. (2013). Chimpanzee fauna isotopes provide new interpretations of fossil ape and hominin ecologies. *Proceedings of the Royal Society B: Biological Sciences* 280, 20132324. doi: 10.1098/rspb.2013.2324

Nelson, S. (2014). The paleoecology of early Pleistocene *Gigantopithecus blacki* inferred from isotopic analyses. *Am J Phys Anthropol* 155, 571–578. doi: 10.1002/ajpa.22609

Nelson, S., and Hamilton, M. I. (2017). "Evolution of the Human Dietary Niche: Initial Transitions," in *Chimpanzees and Human Evolution*, eds. M. N. Muller, R. W. Wrangham, and D. R. Pilbeam (Cambridge: Harvard University Press), 286–310.

Newsome, S. D., Martinez del Rio, C., Bearhop, S., and Phillips, D. L. (2007). A niche for isotopic ecology. *Frontiers in Ecology and the Environment* 5, 429–436. doi: 10.1890/060150.1

Ni, X., Li, Q., Li, L., and Beard, K. C. (2016). Oligocene primates from China reveal divergence between African and Asian primate evolution. *Science* 352, 673–677. doi: 10.1126/science.aaf2107

Ogloff, W. R., Yurkowski, D. J., Davoren, G. K., and Ferguson, S. H. (2019). Diet and isotopic niche overlap elucidate competition potential between seasonally sympatric phocids in the Canadian Arctic. *Marine Biology* 166, 1–12. doi: 10.1007/s00227-019-3549-6

O'Leary, M. A., Patel, B. A., and Coleman, M. N. (2012). Endocranial petrosal anatomy of *Bothriogenys* (Mammalia, Artiodactyla, Anthracotheriidae), and petrosal volume and density comparisons among aquatic and terrestrial artiodactyls and outgroups. *Journal of Paleontology* 86, 44–50. doi: 10.1666/10-091.1

Oo, K. L., Zaw, K., Meffre, S., Myitta, Aung, D. W., and Lai, C.-K. (2015). Provenance of the Eocene sandstones in the southern Chindwin Basin, Myanmar: Implications for the unroofing history of the Cretaceous–Eocene magmatic arc. *Journal of Asian Earth Sciences* 107, 172–194. doi: 10.1016/j.jseaes.2015.04.029

Ortiz, A., Pilbrow, V., Villamil, C. I., Korsgaard, J. G., Bailey, S. E., and Harrison, T. (2015). The Taxonomic and Phylogenetic Affinities of *Bunopithecus sericus*, a Fossil Hylobatid from the Pleistocene of China. *Plos ONE* 10, e0131206. doi: 10.1371/journal.pone.0131206

Pagani, M., Zachos, J., Freeman, K., Tipple, B., and Bohaty, S. (2005). Marked decline in atmospheric carbon dioxide concentrations during the Paleogene. *Science* 309, 600–603. doi: 10.1126/science.1110063

Page, S. E., Rieley, J. O., and Wüst, R. (2006). "Chapter 7 Lowland tropical peatlands of Southeast Asia," in *Developments in Earth Surface Processes : Peatlands*, eds. I. P. Martini, A. Martínez Cortizas, and W. Chesworth (Elsevier), 145–172.

Passey, B. H., Robinson, T. F., Ayliffe, L. K., Cerling, T. E., Sponheimer, M., Dearing, M. D., et al. (2005). Carbon isotope fractionation between diet, breath CO_2, and bioapatite in different mammals. *Journal of Archaeological Science* 32, 1459–1470. doi: 10.1016/j.jas.2005.03.015

Patnaik, R. (2013). "Indian Neogene Siwalik Mammalian Biostratigraphy: An Overview," in *Fossil mammals of Asia: Neogene biostratigraphy and chronology*, eds. X. Wang, L. J. Flynn, and M. Fortelius (New York: Columbia University Press), 423–444.

Patnaik, R., Cerling, T. E., Uno, K. T., and Fleagle, J. G. (2014). Diet and Habitat of Siwalik Primates *Indopithecus*, *Sivaladapis* and *Theropithecus*. *Annales Zoologici Fennici* 51, 123–142. doi: 10.5735/086.051.0214

Pederzani, S., and Britton, K. (2019). Oxygen isotopes in bioarchaeology: Principles and applications, challenges and opportunities. *Earth-Science Reviews* 188, 77–107. doi: 10.1016/j.earscirev.2018.11.005

Percher, A. M., Merceron, G., Nsi Akoue, G., Galbany, J., Romero, A., and Charpentier, M. J. (2018). Dental microwear textural analysis as an analytical tool to depict individual traits and reconstruct the diet of a primate. *Am J Phys Anthropol* 165, 123–138. doi: 10.1002/ajpa.23337

Persson, L. (1985). Asymmetrical Competition: Are Larger Animals Competitively Superior? *Am Nat* 126, 261–266. doi: 10.1086/284413

Phillips, V. D. (1998). Peatswamp ecology and sustainable development in Borneo. *Biodivers Conserv* 7, 651–671. doi: 10.1023/A:1008808519096

Pilbeam, D. R. (1970). *Gigantopithecus* and the Origins of Hominidae. *Nature* 225, 516–519. doi: 10.1038/225516a0

Pilbeam, D. R. (1982). New hominoid skull material from the Miocene of Pakistan. *Nature* 295, 232–234. doi: 10.1038/295232a0

Pilbeam, D. R., Barry, J. C., Meyer, G. E., Shah, S. M. I., Pickford, M. H. L., Bishop, W. W., et al. (1977a). Geology and palaeontology of Neogene strata of Pakistan. *Nature* 270, 684–689. doi: 10.1038/270684a0

Pilbeam, D. R., Meyer, G. E., Badgley, C., Rose, M. D., Pickford, M. H. L., Behrensmeyer, A. K., et al. (1977b). New hominoid primates from the Siwaliks of Pakistan and their bearing on hominoid evolution. *Nature* 270, 689–695. doi: 10.1038/270689a0

Pilbeam, D. R., Rose, M. D., Barry, J. C., and Shah, S. M. I. (1990). New *Sivapithecus* humeri from Pakistan and the relationship of *Sivapithecus* and *Pongo*. *Nature* 348, 237–239. doi: 10.1038/348237a0

Pilgrim, G. E. (1910). Notices of new mammalian genera and species from the Tertiaries of India. *Records of the Geological Survey of India* 40, 1–74.

Pilgrim, G. E. (1927). A *Sivapithecus* plate and other primate fossils from India. *Palaeontologia Indica* 14, 1–26.

Pillans, B., Williams, M., Cameron, D. W., Patnaik, R., Hogarth, J., Sahni, A., et al. (2005). Revised correlation of the Haritalyangar magnetostratigraphy, Indian Siwaliks: implications for the age of the Miocenen hominids *Indopithecus* and *Sivapithecus*, with a note on a new hominid tooth. *Journal of Human Evolution* 48, 507–515.

Plavcan, J. M., and Ruff, C. B. (2008). Canine size, shape, and bending strength in primates and carnivores. *Am J Phys Anthropol* 136, 65–84. doi: 10.1002/ajpa.20779

Polis, G. A. (1984). Age Structure Component of Niche Width and Intraspecific Resource Partitioning: Can Age Groups Function as Ecological Species? *Am Nat* 123, 541–564. doi: 10.1086/284221

Posa, M. R. C., Wijedasa, L. S., and Corlett, R. T. (2011). Biodiversity and Conservation of Tropical Peat Swamp Forests. *BioScience* 61, 49–57. doi: 10.1525/bio.2011.61.1.10

Pound, M. J., and Salzmann, U. (2017). Heterogeneity in global vegetation and terrestrial climate change during the late Eocene to early Oligocene transition. *Scientific Reports* 7, 43386. doi: 10.1038/srep43386

Pugh, K. D. (2022). Phylogenetic analysis of Middle-Late Miocene apes. *Journal of Human Evolution* 165, 1–33.

Pushkina, D., Bocherens, H., Chaimanee, Y., and Jaeger, J.-J. (2010). Stable carbon isotope reconstructions of diet and paleoenvironment from the late Middle Pleistocene Snake Cave in Northeastern Thailand. *Naturwissenschaften* 97, 299–309. doi: 10.1007/s00114-009-0642-6

Qi, T., and Beard, K. C. (1998). Late eocene sivaladapid primate from Guangxi Zhuang Autonomous Region, People's Republic of China. *Journal of Human Evolution* 35, 211–220. doi: 10.1006/jhev.1998.0240

Qu, Y., Jin, C., Zhang, Y., Hu, Y., Shang, X., and Wang, C. (2014). Preservation assessments and carbon and oxygen isotopes analysis of tooth enamel of *Gigantopithecus blacki* and contemporary animals from Sanhe Cave, Chongzuo, South China during the Early Pleistocene. *Quaternary International* 354, 52–58. doi: 10.1016/j.quaint.2013.10.053

Quade, J., Cerling, T. E., Andrews, P. J., and Alpagut, B. (1995). Paleodietary reconstruction of Miocene faunas from Paşalar, Turkey using stable carbon and oxygen isotopes of fossil tooth enamel. *Journal of Human Evolution* 28, 373–384. doi: 10.1006/jhev.1995.1029

Quade, J., Cerling, T. E., and Bowman, J. R. (1989). Development of Asian monsoon revealed by marked ecological shift during the latest Miocene in northern Pakistan. *Nature* 342, 163–166. doi: 10.1038/342163a0

Ramdarshan, A., Merceron, G., Tafforeau, P., and Marivaux, L. (2010). Dietary reconstruction of the Amphipithecidae (Primates, Anthropoidea) from the Paleogene of South Asia and paleoecological implications. *Journal of Human Evolution* 59, 96–108. doi: 10.1016/j.jhevol.2010.04.007

Ranjitkar, S., Turan, A., Mann, C., Gully, G. A., Marsman, M., Edwards, S., et al. (2017). Surface-Sensitive Microwear Texture Analysis of Attrition and Erosion. *Journal of Dental Research* 96, 300–307. doi: 10.1177/0022034516680585

Rayner, N. A. (2003). Global analyses of sea surface temperature, sea ice, and night marine air temperature since the late nineteenth century. *Journal of Geophysical Research: Oceans* 108. doi: 10.1029/2002JD002670

Rijksen, H. D. (1978). *A field study on Sumatran orang utans (Pongo pygmaeus abelii Lesson 1827) : ecology, behaviour and conservation.* Wageningen: Veenman.

Rink, W. J., Wei, W., Bekken, D., and Jones, H. L. (2008). Geochronology of *Ailuropoda–Stegodon* fauna and *Gigantopithecus* in Guangxi Province, southern China. *Quaternary Research* 69, 377–387. doi: 10.1016/j.yqres.2008.02.008

Rodman, P. S. (1977). "Feeding behavior of orang-utans of the Kutai Nature Reserve, East Kalimantan," in *Primate Ecology: Studies of feeding and ranging behaviour in lemurs, monkeys and apes*, ed. T. H. Clutton-Brock (London: Academic Press), 383–413.

Rodman, P. S. (1988). "Diversity and Consistency in Ecology and Behavior," in *Orang-Utan biology*, ed. J. H. Schwartz (Oxford: Oxford University Press), 31–51.

Rogers, M. E., Abernethy, K., Bermejo, M., Cipolletta, C., Doran, D., McFarland, K., et al. (2004). Western gorilla diet: a synthesis from six sites. *Am J Primatol* 64, 173–192. doi: 10.1002/ajp.20071

Rose, K. D., Rana, R. S., Sahni, A., Kumar, K., Missiaen, P., Singh, L., et al. (2009a). Early Eocene primates from Gujarat, India. *Journal of Human Evolution* 56, 366–404. doi: 10.1016/j.jhevol.2009.01.008

Rose, K. D., Rana, R. S., Sahni, A., Kumar, K., Missiaen, P., Singh, L., et al. (2009b). Early Eocene primates from Gujarat, India. *Journal of Human Evolution* 56, 366–404. doi: 10.1016/j.jhevol.2009.01.008

Rose, K. R. (2006). *The Beginning of the Age of Mammals.* Baltimore: The Johns Hopkin University Press.

Rossie, J. B., and Smith, T. D. (2007). Ontogeny of the nasolacrimal duct in primates: functional and phylogenetic implications. *J Anat* 210, 195–208. doi: 10.1111/j.1469-7580.2006.00682.x

Russon, A. E., Wich, S. A., Ancrenaz, M., Kanamori, T., Knott, C. D., Kuze, N., et al. (2009). "Geographic variation in orangutan diets," in *Orangutans: Geographic variation in behavioral ecology and conservation*, eds. S. A. Wich, S. S. Utami-Atmoko, T. Mitra Setia, and C. P. van Schaik (Oxford University Press), 135–156.

Saegusa, H., Thasod, Y., and Ratanasthien, B. (2005). Notes on Asian stegodontids. *Quaternary International* 126-128, 31–48. doi: 10.1016/j.quaint.2004.04.013

Sallam, H. M., Seiffert, E. R., Steiper, M. E., and Simons, E. L. (2009). Fossil and molecular evidence constrain scenarios for the early evolutionary and biogeographic history of hystricognathous rodents. *Proc Natl Acad Sci U S A* 106, 16722–16727. doi: 10.1073/pnas.0908702106

Schluter, D. (2000). *The Ecology of Adaptive Radiation.* Oxford: Oxford University Press.

Schoener, T. W. (1983). Field experiments on interspecific competition. *Am Nat* 122, 240–285. doi: 10.1086/284133

Schulz, E., Calandra, I., and Kaiser, T. M. (2013a). Feeding ecology and chewing mechanics in hoofed mammals: 3D tribology of enamel wear. *Wear* 300, 169–179. doi: 10.1016/j.wear.2013.01.115

Schulz, E., Piotrowski, V., Clauss, M., Mau, M., Merceron, G., and Kaiser, T. M. (2013b). Dietary abrasiveness is associated with variability of microwear and dental surface texture in rabbits. *Plos ONE* 8, e56167. doi: 10.1371/journal.pone.0056167

Schwartz, J. H. (1990). *Lufengpithecus* and its potential relationship to an orang-utan clade. *Journal of Human Evolution* 19, 591–605. doi: 10.1016/0047-2484(90)90001-R

Scotese, C. R. (2014a). *Atlas of Neogene Paleogeographic Maps (Mollweide Projection), Maps 1-7, Volume 1, The Cenozoic, PALEOMAP Atlas for ArcGIS, PALEOMAP Project, Evanston, IL*. PALEOMAP Project, Evanston, IL.

Scotese, C. R. (2014b). *Atlas of Paleogene Paleogeographic Maps (Mollweide Projection), Maps 8-15, Volume 1, The Cenozoic, PALEOMAP Atlas for ArcGIS, PALEOMAP Project, Evanston, IL*. PALEOMAP Project, Evanston, IL.

Scott, J. R., Godfrey, L. R., Jungers, W. L., Scott, R. S., Simons, E. L., Teaford, M. F., et al. (2009). Dental microwear texture analysis of two families of subfossil lemurs from Madagascar. *Journal of Human Evolution* 56, 405–416. doi: 10.1016/j.jhevol.2008.11.003

Scott, R. S., Ungar, P. S., Bergstrom, T. S., Brown, C. A., Childs, B. E., Teaford, M. F., et al. (2006). Dental microwear texture analysis: technical considerations. *Journal of Human Evolution* 51, 339–349. doi: 10.1016/j.jhevol.2006.04.006

Scott, R. S., Ungar, P. S., Bergstrom, T. S., Brown, C. A., Grine, F. E., Teaford, M. F., et al. (2005). Dental microwear texture analysis shows within-species diet variability in fossil hominins. *Nature* 436, 693–695. doi: 10.1038/nature03822

Seiffert, E. R. (2007). Evolution and extinction of Afro-Arabian primates near the Eocene-Oligocene boundary. *Folia Primatol* 78, 314–327. doi: 10.1159/000105147

Seiffert, E. R., Boyer, D. M., Fleagle, J. G., Gunnell, G. F., Heesy, C. P., Perry, J. M. G., et al. (2018). New adapiform primate fossils from the late Eocene of Egypt. *Historical Biology* 30, 204–226. doi: 10.1080/08912963.2017.1306522

Seiffert, E. R., Simons, E. L., Clyde, W. C., Rossie, J. B., Attia, Y., Bown, T. M., et al. (2005). Basal anthropoids from Egypt and the antiquity of Africa's higher primate radiation. *Science* 310, 300–304. doi: 10.1126/science.1116569

Selenka, E. (1896). Die Rassen und der Zahnwechsel des Orang-Utan: vorgelegt von Hrn. Schulze am 5. März. *Sitzungsberichte der königlich preussischen Akademie der Wissenschaften zu Berlin*, 381–392.

Selenka, E. (1898). *Menschenaffen (Anthropomorphae) : Studien über Entwickelung und Schädelbau: Erste Lieferung: Rassen, Schädel und Bezahnung des Orangutan*. Wiesbaden: C.W. Kreidel.

Selenka, E., and Selenka, L. (1905). *Sonnige Welten: Ostasiatische Reiseskizzen*. Wiesbaden: C.W. Kreidel.

Sepulchre, P., Jolly, D., Ducrocq, S., Chaimanee, Y., Jaeger, J.-J., and Raillard, A. (2010). Mid-Tertiary paleoenvironments in Thailand: pollen evidence. *Climates of the Past* 6, 461–473. doi: 10.5194/cp-6-461-2010

Sheldon, N. D., Grimes, S. T., Hooker, J. J., Collinson, M. E., Bugler, M. J., Hren, M. T., et al. (2016). Coupling of marine and continental oxygen isotope records during the Eocene-Oligocene transition. *GSA Bulletin* 128, 502–510. doi: 10.1130/B31315.1

Sheppard, C. E., Inger, R., McDonald, R. A., Barker, S., Jackson, A. L., Thompson, F. J., et al. (2018). Intragroup competition predicts individual foraging specialisation in a group-living mammal. *Ecol Lett* 21, 665–673. doi: 10.1111/ele.12933

Shigehara, N., Takai, M., Kay, R. F., Aung, A. K., Soe, A. N., Tun, S. T., et al. (2002). The upper dentition and face of *Pondaungia cotteri* from central Myanmar. *Journal of Human Evolution* 43, 143–166. doi: 10.1006/jhev.2002.0567

Shine, R. (1989). Ecological causes for the evolution of sexual dimorphism: a review of the evidence. *Q Rev Biol* 64, 419–461. doi: 10.1086/416458

Shine, R. (1991). Intersexual Dietary Divergence and the Evolution of Sexual Dimorphism in Snakes. *Am Nat* 138, 103–122. doi: 10.1086/285207

Shipley, O. N., and Matich, P. (2020). Studying animal niches using bulk stable isotope ratios: an updated synthesis. *Oecologia* 193, 27–51. doi: 10.1007/s00442-020-04654-4

Simões, M., Breitkreuz, L., Alvarado, M., Baca, S., Cooper, J. C., Heins, L., et al. (2016). The Evolving Theory of Evolutionary Radiations. *Trends Ecol Evol (Amst)* 31, 27–34. doi: 10.1016/j.tree.2015.10.007

Simons, E. L., and Chopra, S. R. K. (1969). *Gigantopithecus* (Pongidae, Hominoidea): A new spedies from north India. *Postilla* 138, 1–18.

Skulan, J., DePaolo, D. J., and Owens, T. L. (1997). Biological control of calcium isotopic abundances in the global calcium cycle. *Geochimica et Cosmochimica Acta* 61, 2505–2510. doi: 10.1016/S0016-7037(97)00047-1

Skulason, S., and Smith, T. B. (1995). Resource polymorphisms in vertebrates. *Trends Ecol Evol (Amst)* 10, 366–370. doi: 10.1016/S0169-5347(00)89135-1

Smith, H. E., Price, G. J., Duval, M., Westaway, K. E., Zaim, J., Rizal, Y., et al. (2021). Taxonomy, taphonomy and chronology of the Pleistocene faunal assemblage at Ngalau Gupin cave, Sumatra. *Quaternary International* 603, 40–63. doi: 10.1016/j.quaint.2021.05.005

Smith, T. B., and Skulason, S. (1996). Evolutionary Significance of Resource Polymorphisms in Fishes, Amphibians, and Birds. *Annual Review of Ecology and Systematics* 27, 111–133. doi: 10.1146/annurev.ecolsys.27.1.111

Smith, T. M., and Reynolds, R. W. (2003). Extended Reconstruction of Global Sea Surface Temperatures Based on COADS Data (1854-1997). *Journal of Climate* 16, 1495–1510. doi: 10.1175/1520-0442(2003)016<1495:EROGSS>2.0.CO;2

Soberón, J., and Arroyo-Peña, B. (2017). Are fundamental niches larger than the realized? Testing a 50-year-old prediction by Hutchinson. *Plos ONE* 12, e0175138. doi: 10.1371/journal.pone.0175138

Soe, A. N., Chavasseau, O., Chaimanee, Y., Sein, C., Jaeger, J.-J., Valentin, X., et al. (2017). New remains of *Siamotherium pondaungensis* (Cetartiodactyla, Hippopotamoidea) from the Eocene of Pondaung, Myanmar: Paleoecologic and phylogenetic implications. *Journal of Vertebrate Paleontology* 37, e1270290. doi: 10.1080/02724634.2017.1270290

Soe, A. N., Myitta, Tun, S. T., Aung, A. K., Thein, T., Marandat, B., et al. (2002). Sedimentary facies of the late Middle Eocene Pondaung Formation (central Myanmar) and the palaeoenvironments of its Anthropoid Primates. *Comptes Rendus Palevol* 1, 153–160. doi: 10.1016/S1631-0683(02)00020-9

Spehar, S. N., Sheil, D., Harrison, T., Louys, J., Ancrenaz, M., Marshall, A. J., et al. (2018). Orangutans venture out of the rainforest and into the Anthropocene. *Sci Adv* 4, e1701422. doi: 10.1126/sciadv.1701422

Stamp, L. D. (1922). An Outline of the Tertiary Geology of Burma. *Geological Magazine* 59, 481–501. doi: 10.1017/S001675680010915X

Stehlin, H. G. (1909). Remarques sur les faunules de mammifère des couches éocènes et Oligocènes du Bassin de Paris. *Bulletin de la Société Géologique de France* 19, 488–520.

Stoner, K. E. (1995). Dental pathology in *Pongo satyrus borneensis*. *Am J Phys Anthropol* 98, 307–321. doi: 10.1002/ajpa.1330980305

Suganuma, Y., Hamada, T., Tanaka, S., Okada, M., Nakaya, H., Kunimatsu, Y., et al. (2006). Magnetostratigraphy of the Miocene Chiang Muan Formation, northern Thailand: Implications for revised chronology of the earliest Miocene hominoid in Southeast Asia. *Palaeogeography, Palaeoclimatology, Palaeoecology* 239, 75–86. doi: 10.1016/j.palaeo.2006.01.010

Sun, F., Wang, Y., Jablonski, N. G., Hou, S., Ji, X., Wolff, B., et al. (2021). Paleoenvironment of the late Miocene Shuitangba hominoids from Yunnan, Southwest China: Insights from stable isotopes. *Chemical Geology* 569, 120123. doi: 10.1016/j.chemgeo.2021.120123

Sun, J., Ni, X., Bi, S., Wu, W., Ye, J., Meng, J., et al. (2014). Synchronous turnover of flora, fauna, and climate at the Eocene-Oligocene Boundary in Asia. *Scientific Reports* 4, 7463. doi: 10.1038/srep07463

Suraprasit, K., Bocherens, H., Chaimanee, Y., Panha, S., and Jaeger, J.-J. (2018). Late Middle Pleistocene ecology and climate in Northeastern Thailand inferred from the stable isotope analysis of Khok Sung herbivore tooth enamel and the land mammal cenogram. *Quaternary Science Reviews* 193, 24–42. doi: 10.1016/j.quascirev.2018.06.004

Suzuki, H., Maung, M., Win, Z., Tsubamoto, T., Zin Maung Maung Thein, Egi, N., et al. (2006). Stratigraphic positions of the Eocene vertebrate localities in the Paukkaung area (Pondaung Formation, central Myanmar). *Asian Paleoprimatology* 4, 67–74.

Szpak, P., Metcalfe, J. Z., and Macdonald, R. A. (2017). Best practices for calibrating and reporting stable isotope measurments in archaeology. *Journal of Archaeological Science: Reports* 13, 609–616. doi: 10.1016/j.jasrep.2017.05.007

Takai, M., Nyo, K., Kono, R. T., Htike, T., Kusuhashi, N., and Thein, Z. M. M. (2021). New hominoid mandible from the early Late Miocene Irrawaddy Formation in Tebingan area, central Myanmar. *Anthropological Science*. doi: 10.1537/ase.2012131

Takai, M., Saegusa, H., Thaung-Htike, and Thein, Z. M. M. (2006). Neogene mammalian fauna in Myanmar. *Asian Paleoprimatology* 4, 143–172.

Takai, M., Sein, C., Tsubamoto, T., Egi, N., Maung, M., and Shigehara, N. (2005). A new eosimiid from the latest middle Eocene in Pondaung, central Myanmar. *Anthropological Science* 113, 17–25. doi: 10.1537/ase.04S003

Takai, M., Shigehara, N., Aung, A. K., Tun, S. T., Soe, A. N., Tsubamoto, T., et al. (2001). A new anthropoid from the latest middle Eocene of Pondaung, central Myanmar. *Journal of Human Evolution* 40, 393–409. doi: 10.1006/jhev.2001.0463

Takai, M., Zhang, Y., Kono, R. T., and Jin, C. (2014). Changes in the composition of the Pleistocene primate fauna in southern China. *Quaternary International* 354, 75–85. doi: 10.1016/j.quaint.2014.02.021

Teaford, M. F., and Oyen, O. J. (1989). In vivo and in vitro turnover in dental microwear. *Am J Phys Anthropol* 80, 447–460. doi: 10.1002/ajpa.1330800405

Teaford, M. F., and Robinson, J. G. (1989). Seasonal or ecological differences in diet and molar microwear in *Cebus nigrivittatus*. *Am J Phys Anthropol* 80, 391–401. doi: 10.1002/ajpa.1330800312

Teaford, M. F., Ross, C. F., Ungar, P. S., Vinyard, C. J., and Laird, M. F. (2021). Grit your teeth and chew your food: Implications of food material properties and abrasives for rates of dental microwear formation in laboratory *Sapajus apella* (Primates). *Palaeogeography, Palaeoclimatology, Palaeoecology* 583. doi: 10.1016/j.palaeo.2021.110644

Teaford, M. F., Ungar, P. S., Taylor, A. B., Ross, C. F., and Vinyard, C. J. (2017). In vivo rates of dental microwear formation in laboratory primates fed different food items. *Biosurface and Biotribology* 3, 166–173. doi: 10.1016/j.bsbt.2017.11.005

Teaford, M. F., and Walker, A. (1984). Quantitative differences in dental microwear between primate species with different diets and a comment on the presumed diet of *Sivapithecus*. *Am J Phys Anthropol* 64, 191–200. doi: 10.1002/ajpa.1330640213

Tejada-Lara, J. V., MacFadden, B. J., Bermudez, L., Rojas, G., Salas-Gismondi, R., and Flynn, J. J. (2018). Body mass predicts isotope enrichment in herbivorous mammals. *Proc Biol Sci* 285. doi: 10.1098/rspb.2018.1020

Thein, Z. M. M., Takai, M., Uno, H., Wynn, J. G., Egi, N., Tsubamoto, T., et al. (2011). Stable isotope analysis of the tooth enamel of Chaingzauk mammalian fauna (late Neogene, Myanmar) and its implication to paleoenvironment and paleogeography. *Palaeogeography, Palaeoclimatology, Palaeoecology* 300, 11–22. doi: 10.1016/j.palaeo.2010.11.016

Thorpe, S. K., and Crompton, R. H. (2006). Orangutan positional behavior and the nature of arboreal locomotion in Hominoidea. *Am J Phys Anthropol* 131, 384–401. doi: 10.1002/ajpa.20422

Tierney, J. E., Poulsen, C. J., Montañez, I. P., Bhattacharya, T., Feng, R., Ford, H. L., et al. (2020). Past climates inform our future. *Science* 370, eaay3701. doi: 10.1126/science.aay3701

Tieszen, L., and Fagre, T. (1993). "Effect of diet quality and composition on the isotopic composition of respiratory CO_2, bone collagen, bioapatite, and soft tissues," in *Prehistoric Human Bone: Archaeology at the molecular level*, eds. J. B. Lambert, and G. Grupe (Berlin, Heidelberg, New York: Springer), 121–155.

Tipple, B. J., Meyers, S. R., and Pagani, M. (2010). Carbon isotope ratio of Cenozoic CO_2: A comparative evaluation of available geochemical proxies. *Paleoceanography* 25, PA3202. doi: 10.1029/2009PA001851

Tiwari, B. N., and Kumar, K. (1984). A new Locality for *Ramapithecus* (Hominoidea): Lower Siwaliks of the Dhara Reserve Forest, Uttar Pradesh. *Man and Environment* 8, 8–12.

Toumoulin, A., Tardif, D., Donnadieu, Y., Licht, A., Ladant, J.-B., Kunzmann, L., et al. (2022). Evolution of continental temperature seasonality from the Eocene greenhouse to the Oligocene icehouse –a model–data comparison. *Climate of the Past* 18, 341–362. doi: 10.5194/cp-18-341-2022

Tshen, L. T. (2016). Biogeographic distribution and metric dental variation of fossil and living orangutans (Pongo spp.). *Primates* 57, 39–50. doi: 10.1007/s10329-015-0493-z

Tsubamoto, T., Egi, N., and Takai, M. (2006a). Notes on fish, reptilian, and several fragmentary mammalian dental fossils from the Pondaung Formation. *Asian Paleoprimatology* 4, 98–110.

Tsubamoto, T., Egi, N., Takai, M., Sein, C., and Maung, M. (2005). Middle Eocene ungulate mammals from Myanmar: A review with description of new specimens. *Acta Palaeontologica Polonia* 50, 117–138.

Tsubamoto, T., Egi, N., Takai, M., Shigehara, N., Suzuki, H., Nishimura, T., et al. (2006b). A summary of the Pondaung fossil expeditions. *Asian Paleontology* 4, 1–66.

Ungar, P. S. (2015). Mammalian dental function and wear: A review. *Biosurface and Biotribology* 1, 25–41. doi: 10.1016/j.bsbt.2014.12.001

Ungar, P. S., Brown, C. A., Bergstrom, T. S., and Walkers, A. (2003). Quantification of dental microwear by tandem scanning confocal microscopy and scale-sensitive fractal analyses. *Scanning* 25, 185–193. doi: 10.1002/sca.4950250405

Urciuoli, A., and Alba, D. M. (2023). Systematics of Miocene apes: State of the art of a neverending controversy. *Journal of Human Evolution* 175, 103309. doi: 10.1016/j.jhevol.2022.103309

van der Merwe, N. J., and Medina, E. (1989). Photosynthesis and ratios in Amazonian rain forests. *Geochimica et Cosmochimica Acta* 53, 1091–1094. doi: 10.1016/0016-7037(89)90213-5

van der Merwe, N. J., and Medina, E. (1991). The canopy effect, carbon isotope ratios and foodwebs in amazonia. *Journal of Archaeological Science* 18, 249–259. doi: 10.1016/0305-4403(91)90064-V

Vogel, E. R., Alavi, S. E., Utami-Atmoko, S. S., van Noordwijk, M. A., Bransford, T. D., Erb, W. M., et al. (2017). Nutritional ecology of wild Bornean orangutans (*Pongo pygmaeus wurmbii*) in a peat swamp habitat: Effects of age, sex, and season. *Am J Primatol* 79, 1–20. doi: 10.1002/ajp.22618

Vogel, E. R., Zulfa, A., Hardus, M., Wich, S. A., Dominy, N. J., and Taylor, A. B. (2014). Food mechanical properties, feeding ecology, and the mandibular morphology of wild orangutans. *Journal of Human Evolution* 75, 110–124. doi: 10.1016/j.jhevol.2014.05.007

Vries, D. de, Heritage, S., Borths, M. R., Sallam, H. M., and Seiffert, E. R. (2021). Widespread loss of mammalian lineage and dietary diversity in the early Oligocene of Afro-Arabia. *Communications Biology* 4, 1172. doi: 10.1038/s42003-021-02707-9

Vuille, M., Werner, M., Bradley, R. S., and Keimig, F. (2005). Stable isotopes in precipitation in the Asian monsoon region. *Journal of Geophysical Research* 110, D23108.

Wang, J., Zhou, X., Wang, S., Xu, H., Behling, H., Ye, J., et al. (2023). C_4 expansion of Central Asia in the middle Miocene linked to the strengthening Indian monsoon. *Global and Planetary Change*. doi: 10.1016/j.gloplacha.2023.104096

Wang, W., Huang, C. L., Xie, S. W., and Yan, C. L. (2011). Late Pleistocene hominin teeth from the Jimuyan Cave, Pingle County, Guangxi, south China. *Quaternary Sciences* 31, 699–704.

Wang, W., Potts, R., Baoyin, Y., Huang, W., Cheng, H., Edwards, R. L., et al. (2007). Sequence of mammalian fossils, including hominoid teeth, from the Bubing Basin caves, South China. *Journal of Human Evolution* 52, 370–379. doi: 10.1016/j.jhevol.2006.10.003

Wang, Y., and Cerling, T. E. (1994). A model of fossil tooth and bone diagenesis: implications for paleodiet reconstructions from stable isotopes. *Palaeogeography, Palaeoclimatology, Palaeoecology* 107, 281–289.

Ward, S. (1997). "The Taxonomy and Phylogenetic Relationship of *Sivapithecus* Revisited," in *Function, Phylogeny, and Fossils: Miocene Hominoid Evolution and Adaptations*, eds. D. R. Begun, C. V. Ward, and M. D. Rose (New York: Plenum), 269–290.

Watts, D. P. (1984). Composition and variability of mountain gorilla diets in the Central Virungas. *Am J Primatol* 7, 323–356. doi: 10.1002/ajp.1350070403

Weber, K., Weber, M., Menneken, M., Kral, A. G., Mertz-Kraus, R., Geisler, T., et al. (2021). Diagenetic stability of non-traditional stable isotope systems (Ca, Sr, Mg, Zn) in teeth – An in-vitro alteration experiment of biogenic apatite in isotopically enriched tracer solution. *Chemical Geology* 572, 120196. doi: 10.1016/j.chemgeo.2021.120196

Wei, W., Liu, J., Hou, Y., Si, X., Huang, W., Schepartz, L. A., et al. (2004). Panxian Dadong, South China: Establishing a Record of Middle Pleistocene Climatic Changes. *Asian Perspectives* 43, 302–313. doi: 10.1353/asi.2004.0030

Welcomme, J.-L., Benammi, M., Crochet, J.-Y., Marivaux, L., Métais, G., Antoine, P.-O., et al. (2001). Himalayan Forelands: palaeontological evidence for Oligocene detrital deposits in the Bugti Hills (Balochistan, Pakistan). *Geological Magazine* 138, 397–405.

Westaway, K. E., Louys, J., Awe, R. D., Morwood, M. J., Price, G. J., Zhao, J.-X., et al. (2017). An early modern human presence in Sumatra 73,000-63,000 years ago. *Nature* 548, 322–325. doi: 10.1038/nature23452

Westaway, K. E., Morwood, M. J., Roberts, R. G., Rokus, A. D., Zhao, J., Storm, P., et al. (2007). Age and biostratigraphic significance of the Punung Rainforest Fauna, East Java, Indonesia, and implications for *Pongo* and *Homo*. *Journal of Human Evolution* 53, 709–717. doi: 10.1016/j.jhevol.2007.06.002

Westerhold, T., Marwan, N., Drury, A. J., Liebrand, D., Agnini, C., Anagnostou, E., et al. (2020). An astronomically dated record of Earth's climate and its predictability over the last 66 million years. *Science* 369, 1383–1387. doi: 10.1126/science.aba6853

Westerweel, J., Licht, A., Cogné, N., Roperch, P., Dupont-Nivet, G., Kay Thi, M., et al. (2020). Burma Terrane Collision and Northward Indentation in the Eastern Himalayas Recorded in the Eocene-Miocene Chindwin Basin (Myanmar). *Tectonics* 39, e2020TC006413. doi: 10.1029/2020TC006413

Westerweel, J., Roperch, P., Licht, A., Dupont-Nivet, G., Win, Z., Poblete, F., et al. (2019). Burma Terrane part of the Trans-Tethyan Arc during collision with India according to palaeomagnetic data. *Nature Geoscience* 12, 863–868. doi: 10.1038/s41561-019-0443-2

Wich, S. A., Frederiksson, G., and Sterck, E. H. M. (2002). Measuring Fruit Patch Size for Three Sympatric Indonesian Primate Species. *Primates* 43, 19–27.

Wich, S. A., Utami-Atmoko, S. S., Mitra Setia, T., Djoyosudharmo, S., and Geurts, M. L. (2006). Dietary and Energetic Responses of *Pongo abelii* to Fruit Availability Fluctuations. *International Journal of Primatology* 27, 1535–1550. doi: 10.1007/s10764-006-9093-5

Wich, S. A., Vogel, E. R., Larsen, M. D., Fredriksson, G., Leighton, M., Yeager, C. P., et al. (2011). Forest fruit production is higher on Sumatra than on Borneo. *Plos ONE* 6, e21278. doi: 10.1371/journal.pone.0021278

Wickham, H. (2016). *ggplot2: Elegant Graphics for Data Analysis*. New York: Springer.

Williams, B. A., Kay, R. F., and Kirk, E. C. (2010). New perspectives on anthropoid origins. *Proc Natl Acad Sci U S A* 107, 4797–4804. doi: 10.1073/pnas.0908320107

Williamson, G. B., and Ickes, K. (2002). Mast fruiting and ENSO cycles - does the cue betray a cause? *Oikos* 97, 459–461. doi: 10.1034/j.1600-0706.2002.970317.x

Wimberger, P. H. (1994). "Trophic polymorphisms, plasticity, and speciation in vertebrates," in *Advances in fish foraging theory and ecology*, eds. D. J. Stouder, and K. Fresh (Columbia, S. C. Belle Baruch Press), 19–43.

Winkler, D. E., Schulz-Kornas, E., Kaiser, T. M., Codron, D., Leichliter, J., Hummel, J., et al. (2020). The turnover of dental microwear texture: Testing the" last supper" effect in small mammals in a controlled feeding experiment. *Palaeogeography, Palaeoclimatology, Palaeoecology* 557, 109930. doi: 10.1016/j.palaeo.2020.109930

Wolter, K., and Timlin, M. S. (2011). El Niño/Southern Oscillation behaviour since 1871 as diagnosed in an extended multivariate ENSO index (MEI.ext). *International Journal of Climatology* 31, 1074–1087. doi: 10.1002/joc.2336

Woodruff, D. S. (2010). Biogeography and conservation in Southeast Asia: how 2.7 million years of repeated environmental fluctuations affect today's patterns and the future of the remaining refugial-phase biodiversity. *Biodivers Conserv* 19, 919–941. doi: 10.1007/s10531-010-9783-3

Wright, L. E., and Schwarcz, H. P. (1999). Correspondence Between Stable Carbon, Oxygen and Nitrogen Isotopes in Human Tooth Enamel and Dentine: Infant Diets at Kaminaljuyú. *Journal of Archaeological Science* 26, 1159–1170.

Yasuda, M., Matsumoto, J., Osada, N., Ichikawa, S., Kachi, N., Tani, M., et al. (1999). The mechanism of general flowering in Dipterocarpaceae in the Malay Peninsula. *Journal of Tropical Ecology* 15, 437–449. doi: 10.1017/S0266467499000930

Yoshida, N., and Miyazaki, N. (1991). Oxygen isotope correlation of cetacean bone phosphate with environmental water. *Journal of Geophysical Research: Oceans* 96, 815–820. doi: 10.1029/90JC01580

Zachos, J., Pagani, M., Sloan, L., Thomas, E., and Billups, K. (2001). Trends, Rhythms, and Aberrations in Global Climate 65 Ma to Present. *Science* 292, 686–693.

Zaw, K., Meffre, S., Takai, M., Suzuki, H., Burrett, C., Thaung-Htike, et al. (2014). The oldest anthropoid primates in SE Asia: Evidence from LA-ICP-MS U-Pb zircon age in the Late Middle Eocene Pondaung Formatio, Myanmar. *Gondwana Research* 26, 122–131. doi: 10.1016/j.gr.2013.04.007

Zhang, P., Najman, Y., Mei, L., Millar, I., Sobel, E. R., Carter, A., et al. (2019). Palaeodrainage evolution of the large rivers of East Asia, and Himalayan-Tibet tectonics. *Earth-Science Reviews* 192, 601–630. doi: 10.1016/j.earscirev.2019.02.003

Zhang, Y., and Harrison, T. (2017). *Gigantopithecus blacki*: a giant ape from the Pleistocene of Asia revisited. *Am J Phys Anthropol* 162 Suppl 63, 153–177. doi: 10.1002/ajpa.23150

Zihlman, A. L., Mcfarland, R. K., and Underwood, C. E. (2011). Functional Anatomy and Adaptation of Male Gorillas (*Gorilla gorilla gorilla*) With Comparison to Male Orangutans (*Pongo pygmaeus*). *The Anatomical Record: Advances in Integrative Anatomy and Evolutionary Biology* 294, 1842–1855. doi: 10.1002/ar.21449

9. Appendices

Appendix I

The accepted publications and the submitted manuscript that are the basis of the thesis chapters in the order as in the **List of Publications**.

Publication 1

Evolutionary ecology of Miocene hominoid primates in Southeast Asia

Authors: Sophie G. Habinger, Olivier Chavasseau, Jean-Jacques Jaeger, Yaowalak Chaimanee, Aung Naing Soe, Chit Sein, Hervé Bocherens

Journal: Scientific Reports (Sci Rep)

Initial submission: 3.05.2022

Accepted: 27.06.2022

DOI: 10.1038/s41598-022-15574-z

Publication date: 12.07.2022

Journal volume: 12

Article number: 11841

scientific reports

Check for updates

OPEN

Evolutionary ecology of Miocene hominoid primates in Southeast Asia

S. G. Habinger[1,2]✉, O. Chavasseau[2], J.-J. Jaeger[2], Y. Chaimanee[2], A. N. Soe[3], C. Sein[4] & H. Bocherens[1,5]

The evolutionary history and palaeoecology of orangutans remains poorly understood until today. The restricted geographic distribution of extant *Pongo* indicates specific ecological needs. However, it is not clear whether these needs were shared by the great diversity of fossil pongines known from the Miocene to the Pleistocene. Here we show how niche modelling of stable carbon and oxygen isotope data of the carbonate fraction of dental enamel can be used to reconstruct the paleoecology of fossil and modern pongines and associated mammal communities. We focus on *Khoratpithecus ayeyarwadyensis*, a Late Miocene pongine from Myanmar and the sister clade to extant orangutans, and compare it to its associated mammal fauna and other fossil and extant pongines. The results are consistent with a vertical position high up in the canopy of a forested habitat with purely C_3 vegetation for *K. ayeyarwadyensis* as well as the contemporaneous *Sivapithecus*. Although their positions in the modelled isotopic niche space look similar to the ecological niche occupied by modern *Pongo*, a comparison of the modelled niches within the pongine clade revealed possible differences in the use of microhabitats by the Miocene apes.

Today, the only remaining genus of the Ponginae subfamily is the genus *Pongo*, including the three extant species of orangutans, whose distribution is highly restricted to forested areas of Borneo and Sumatra[1] (Fig. 1). In contrast, paleontological data document a much greater diversity of pongine genera, with the earliest fossils recovered in Southeast Asia from the Chiang Muan Formation (Fm.) in Thailand and dating to 13–12.6 Ma[2,3]. Several different fossil pongine genera such as *Khoratpithecus* (Myanmar, Thailand), *Sivapithecus* (Pakistan, India, and Nepal), and *Indopithecus* (India) are known from the Miocene, as well as *Gigantopithecus* (China, Thailand, Vietnam) and early *Pongo* from the Pleistocene[4,5]. This high degree of diversification and endemism of the hominoid primates contrasts with the much more generalist character of the associated mammal fauna across different Southeast Asian sites[6–8]. The question now arises if this high pongine diversity also coincides with a diversity of subsistence strategies in this clade.

Khoratpithecus is known from isolated teeth, two mandibles and a maxilla[9–12]. This genus has been first allocated to the pongines based on shared derived dental and mandibular characters with *Pongo*[6,10]. It has been hypothesized that *Khoratpithecus* may represent the sister-group of *Pongo* based on the lack of an insertion for the anterior digastric muscle, a feature exclusively shared between these genera, and structural similarities of their mandibular symphyses[6,10] (e.g., strong symphyseal inclination and weak upper transverse torus). More recently, the analysis of a maxilla of *Khoratpithecus* has revealed several additional pongine features for this genus in its upper dentition (e.g., externally rotated canines) and subnasal anatomy (e.g., strong overlap of the premaxilla relative to the maxilla, antero-posteriorly convex nasoalveolar clivus, subhorizontal incisive foramen)[11]. Phylogenetic analyses[5,13] strengthen the hypothesis of a pongine clade including *Pongo* and large Asian Neogene hominoids (*Sivapithecus*, *Indopithecus*, *Gigantopithecus*, *Khoratpithecus*, *Ankarapithecus*, and irregularly *Lufengpithecus*). In the most recent phylogenetic analysis[5], *Khoratpithecus ayeyarwadyensis* is regularly found as the sister-group of *Pongo*. Among the fossil genera of Asian hominoids, only the pongine status of *Lufengpithecus* is highly controversial according to investigations of its skull anatomy (in particular the orbital region)[14] and further comparisons of its craniofacial features with other Asian Miocene hominoids[11]. This hominoid probably represents a stem hominid.

[1]Department of Geosciences, University of Tübingen, Tübingen, Germany. [2]Laboratoire PALEVOPRIM, Université de Poitiers, Poitiers, France. [3]Mandalay University of Distance Education, Mandalay, Myanmar. [4]Department of Higher Education, Ministry of Higher Education, Nay Pyi Taw, Myanmar. [5]Senckenberg Centre for Human Evolution and Palaeoenvironment at the University of Tübingen, Tübingen, Germany. ✉email: sophie-gabriele.habinger@uni-tuebingen.de

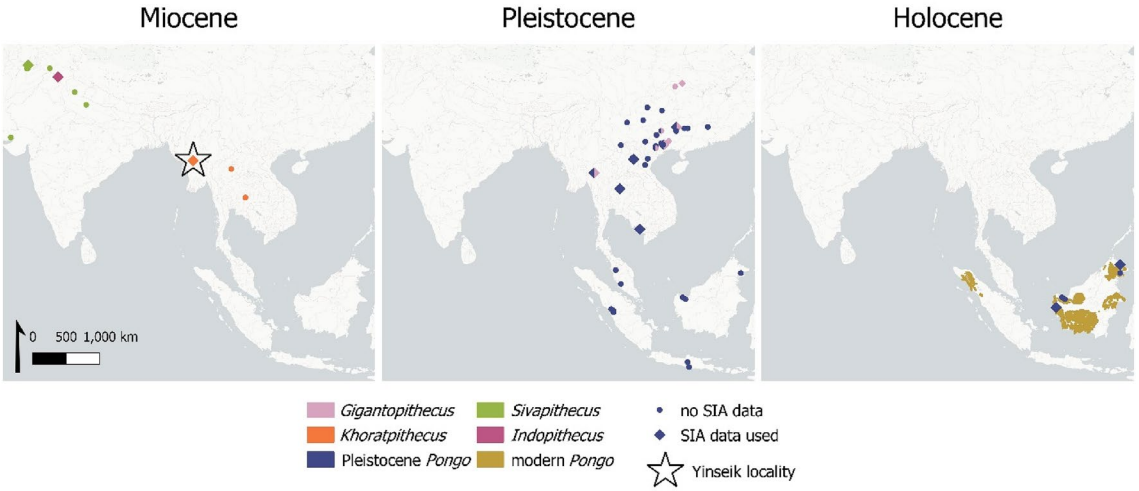

Figure 1. Location of fossil pongine localities from the Miocene to the Holocene in Southern Asia, Southeast Asia and Southern China including the present distribution of extant orangutans. The stable isotope data used in the study originates from the localities marked with a diamond (SIA = stable isotope analysis) and the Yinseik locality where *K. ayeyarwadyensis* was found is labelled with a star. A map version with labels for all the sites from which we used stable isotope data can be found in the Supplementary Information (Fig. SI 4). The map was created using QGIS 3.16.

As the genus *Khoratpithecus* is hypothesized to be the sister-clade to *Pongo*[6], investigating its paleoecology is crucial to understand the evolutionary history of modern orangutans. There are currently three different known species of *Khoratpithecus*. The Middle Miocene *K. chiangmuanensis*[9] and the Late Miocene *K. piriyai*[6] have been found in Thailand, but teeth from these two species were not available for sampling. However, one specimen of the Myanmar species *K. ayeyarwadyensis* could be sampled for stable isotope analysis. It is, together with its associated mammal fauna, the focus of our study. The fossil remains have been found in the Irrawaddy Fm. at a locality southeast of Magway near Yinseik village dating to the Late Miocene (~ 9.5 Ma)[12]. Hence, it will be referred to as Yinseik locality hereafter.

The important phylogenetic role of the genus *Khoratpithecus* as a sister clade of modern *Pongo* made us particularly interested in its palaeoecology and habitat. We wanted to characterize this habitat concerning its palaeoseasonality, vegetation structure, and the niche partitioning of the mammal fauna associated with *K. ayeyarwadyensis*. In a second step, we used the available stable isotopic data of fossil and extant pongines (Fig. 1) to assess if there is evidence for ecological continuity within the pongine clade, an important question to enhance our understanding of the evolutionary ecology of the Ponginae. The response of fossil pongines to climatic changes and forest fragmentation additionally can provide information for conservation efforts of orangutan populations today, which are continuously put under stress due to anthropogenic disturbances and habitat loss[15,16]. Similar conditions of continuing forest fragementation have been hypothesised to be the cause of the extinction of *Sivapithecus* during the Late Miocene[17].

To answer these questions, we performed stable isotopic analysis (SIA), and used these data to reconstruct the niche partitioning in this habitat, as well as palaeoseasonality and to get a first direct indication of the ecology of this fossil pongine. Carbon and oxygen isotopes from the carbonate fraction of dental enamel that we analysed are commonly used as proxies for vegetation type[18,19], and canopy density[20,21]; temperature, humidity[22], as well as vertical stratification[23,24] in primates, respectively. In this study, we will discuss $\delta^{13}C$ values corrected for isotopic enrichment from diet to bioapatite and for changes in the isotopic composition of CO_2. These corrections are discussed in detail in the Methods section. With these data, we modelled the core ecological niches of the different taxonomic groups and could characterize the niche partitioning in the Yinseik mammal fauna, quantify niche width and niche packing.

The modelled ecological niches form the basis for our comparison of the *Khoratpithecus* fauna with a younger locality from the Irrawaddy Fm, which did not yield any *Khoratpithecus* fossils[25]. This is a similar approach as the comparison of the *Sivapithecus* and the post-*Sivapithecus* fauna performed by Nelson[17]. This comparison will enhance our understanding of the paleoecology of *K. ayeyarwadyensis* and the changes happening in its habitat especially regarding the introduction of C_4 plants and the general opening of the landscape. Ecological core niches were also modelled for other fossil and extant pongines. These niches were compared to one another to see, if they are consistent with the hypothesis of ecological continuity in the Ponginae.

Material and methods

The fluvial deposits of the Irrawaddy Fm. represent one of the most important fossiliferous formations located in the Central Basin of Myanmar (Fig. 1). The hominoid-bearing locality of Yinseik from which the *K. ayeyarwadyensis* specimen and the associated mammal fauna analysed in this study originate is located close to the village Yinseik, east of the Irrawaddy River and about 20 km southeast of Magway (Magway Region). The section in the Yinseik area, which represents the base of the Irrawaddy Fm., is composed of about 100 m of fluviatile

sediments with low dipping mostly constituted of poorly consolidated and coarse sandstones and hardened fine sandstones alternated with clayey sandstones and claystones. Oxidized conglomeratic layers also occur and are frequently fossiliferous. These deposits most probably represent a small lapse of time because they have yielded a homogeneous vertebrate fauna and have recorded a single normal magnetic polarity[12]. A 10.4–8.6 Ma age bracket (early Late Miocene) has been as inferred from biochronology. Two ages within this bracket, ~ 10 Ma and ~ 9 Ma, are compatible with the magnetostratigraphy[12]. There are great similarities in the composition of the associated mammal fauna of *K. ayeyarwadyensis*[7] and of the contemporaneous faunas associated with *K. piriyai*[6] and *Sivapithecus*[8].

For this study, we sampled 44 teeth of various taxa, i.e. Rhinocerotidae (n = 9), Proboscidea (n = 8), Bovidae (n = 11), Suidae (n = 7), Giraffidae (n = 5), and one specimen of *K. ayeyarwadyensis* (MFI-K171) as well as one cervid and one anthracothere. The pongine specimen is a left hemi-mandible of K. ayeyarwadyensis, which is also the holotype of this species[12]. Sampling it for isotopic analysis was possible, as during preparation of the fossil a small enamel fragment of the m3 broke of, which was then analysed. We also included one modern bovid from the same area in our data set. Data from the Yinseik Equidae (n = 6) from the Yinseik locality has already been published by Jaeger et al.[12].

Data from published studies with a similar scope and objective were used as reference (Table SI 3)[12,17,25–37]. These studies also analysed the carbonate fraction of dental enamel. However, the *Indopithecus* specimen was sampled using laser ablation instead of micro drilling. We use the normalized $\delta^{13}C$ and $\delta^{18}O$ values proposed by the authors[26] to compare them to the other conventional $CaCO_3$ data. However, especially the $\delta^{18}O$ values might still be biased, due to the different methodologies. We complemented our data by the addition of Louys and Roberts[24] data set on modern orangutans. Precise taxonomic information and specimen numbers of the whole data set used in this study are reported in Table SI 2.

Sample preparation. The enamel was sampled using a micro dremel tool to retrieve 6–10 mg of powdered sample during fieldwork in Myanmar conducted in 2017. We took bulk samples of most of the teeth, where the drilling was done in a band along the whole growth axis of the tooth. Values represent the average isotopic composition over the mineralization time of the tooth during ontogeny. For some high-crowned teeth, it was possible to conduct intra-individual serial sampling (IRWD-9, IRWD-17, IRWD-24, IRWD-31, IRWD-42, and PND-M1). In these cases, multiple samples were drilled from bands perpendicular to the growth axis of the tooth providing a continuous record of isotopic variation during the mineralization time of this tooth.

The powdered samples were pretreated and the carbonate fraction of the dental enamel was analysed in the laboratory of the Department of Geosciences (Biogeology working group) at the University of Tübingen (Germany). They were let to react with 1.35 ml of a NaOCl solution at a concentration of 2.5% for 24 h to remove all the organic matter. After rinsing them with Milli-Q H_2O the samples reacted with 1.35 ml of 1 M acetic acid buffered solution (CH_3COOH) for 24 h to remove all exogenous carbonates. The method for the pretreatment of the samples followed the methodology described in[38–40]. When the reaction was completed, the samples were dried at 40 °C. With each set of samples, two internal modern enamel standards (Elephant SRM (SRM = secondary reference material), Hippo SRM) were processed following the same pretreatment protocol. The internal standards were complemented by two international (IAEA-603, NBS-18) and one internal (LM = Laaser Marmor SRM) pure carbonate standards. Pure carbonate standards were not subjected to any pretreatment. All of the standards were measured after every 15 samples in the IRMS (isotope ratio mass spectrometer).

2.5–3 mg or 0.1 mg of sample for enamel and pure carbonates respectively was then reacted with phosphoric acid (H_3PO_4) at a concentration of ~ 99%. The CO_2 gas that resulted from this reaction was then analysed with the Elementar IsoPrime 100 IRMS 5 times over a 15-min time span. These repeated measurements were then used to monitor measurement precision by calculating the mean and the standard deviation for each sample[41]. Measurement uncertainty, as assessed using the standards and is reported for each sample in Table SI 2. The measured isotopic ratios were then calibrated relative to VPDB (Vienna Pee Dee Belemnite) using the two internal enamel standards. They are reported using the δ-notation (in per mill) whose calculation is based on the following formula[42,43] where ^{j}X is the heavier and ^{i}X the lighter isotope.

$$\delta^{j/i}X = \frac{(^{j}X/^{i}X)_{sample}}{(^{j}X/^{i}X)_{standard}} - 1 \quad (1)$$

We also report an estimation of the $CaCO_3$ content of each sample (Table SI 2). With the Ion Vantage software, we calculated an estimated elemental composition based on sample weight, peak area and the internal LM SRM. The obtained $CaCO_3$ values are then scaled up, until one of the international pure carbonate standards (IAEA-603, NBS-18) reaches 100%.

Data correction. To enable the comparison of specimens from different species, sites, and time periods it was necessary to apply different corrections of the data, especially the $\delta^{13}C$ values. All the $\delta^{13}C$apatite values were transformed to $\delta^{13}C$diet values. This was done using different enrichment factors (ε, in per mill) for different groups of animals. It is calculated using this formula[42,44], where a stands for diet and b for apatite:

$$\varepsilon^{13}C_{a-b} = \alpha^{13}C_{a-b} - 1 = \frac{\delta^{13}C_{a/standard} + 1}{\delta^{13}C_{b/standard} + 1} - 1 \quad (2)$$

ε is based on the isotopic fractionation factor (α), which is derived from the δ-values as defined in (1). Isotopic fractionation from diet to apatite is not explainable by a single kinetic or equilibrium process[42]. We account for

this complexity by the use of the terms apparent isotopic fractionation factor (α^*) and apparent enrichment factor (ε^*) in the rest of this paper. Using Δ ($\delta^{13}C_{diet} - \delta^{13}C_{apatite}$) decreases in accuracy when the isotopic differences among tissues are ≥ 10‰[45], which is the reason why we decided to use ε instead.

We applied apparent enrichment factors based on the results of published studies of controlled feeding experiments of − 14‰ for large-bodied, ruminant herbivores[45,46], − 11‰ for omnivores including suids[46,47] and primates[48].

For the comparison of animals from different time periods it is necessary to correct the $\delta^{13}C$ values for changes of the $\delta^{13}C_{CO2}$ values in the atmosphere caused by the Suess effect[49]. All values have been corrected to the pre-industrial values from 1850 of − 6.5‰[50]. The $\delta^{13}C_{CO2}$ values of Miocene data points from sites that are older than 6 Ma were assumed to be − 6.1‰ and therefore a correction of 0.4‰ was applied to them[51]. Modern atmospheric $\delta^{13}C_{CO2}$ values are − 8‰[52,53], so all post 1930 samples were corrected by 1.5‰. Pre 1930 to 6 Ma old values are treated as equivalent to the pre-industrial ones[54], and hence are not corrected. As the maximum age of the Chaingzauk fauna, from the other Miocene locality of the Irrawaddy Fm., is constrained to 6 Ma by its biostratigraphy[25] no corrections were applied to the $\delta^{13}C$ values from this site. The ε as well as the atmosphere correction used for each specimen are reported in Table SI 2 and Table SI 3 together with the calibrated data and corrected δ-values used in the analysis.

Statistical analysis. For this study, we applied different statistical methods, which we want to describe in the following section. Given the small sample sizes in our data set as well as the presence of outliers and not normally distributed data we decided to use the non-parametric Wilcox rank sum test when testing for differences of the medians between two groups throughout this study. The tests were run in R using the wilcox.test() function (package stats version 4.1.2, one of the base packages in R).

We re-ran the linear regression on minimum $\delta^{18}O$ values over time (Ma = million years ago) published by Nelson[55] using the lm() function (package stats version 4.1.2, one of the base packages in R) and added that data from the Yinseik equids to the figure in order to compare them to the regression line.

The lowest $\delta^{18}O$ value (− 5.7‰) measured in the serially sampled modern bovid specimen (PND-M1) looked like an anomaly during visual inspection. We therefore wanted to test if it was a statistical outlier. Before that, it was necessary to test if the assumption of the Grubbs' test that the data are normally distributed was fulfilled. Therefore we conducted a Shapiro–Wilk test of normality using the shapiro.test() function (package stats version 4.1.2, one of the base packages in R). The results of this test for the $\delta^{18}O$ value of PND-M1 show that the p-value is bigger than 0.05 (W = 0.94899, p-value = 0.4094), indicating that we do not reject the null hypothesis that the data follow a normal distribution. The Grubbs' test for outliers was run in R using the grubbs.test(data, opposite = T) function (package outliers[56] version 0.15) to test, if the minimum value of the data set was an outlier.

To be able to quantify and better compare the niche width and niche partitioning of the different mammal communities we applied isotopic niche modelling. Until now, isotopic niches based on the niche concept of Hutchinson[57,58] have been mostly limited to dietary or trophic niches based on carbon and nitrogen isotopic composition of collagen[59]. As we analysed the carbonate fraction of the fossil dental enamel and therefore have data on two proxies reflecting more general ecological characteristics of an individuals' habitat, we will model more general ecological niches for the pongines and the associated mammal fauna using the R package SIBER (version 2.1.6)[60]. Nelson and Hamilton already adopted a similar approach focusing on the dietary transition and ecological niche of early humans[61]. In this study we use standard ellipse area corrected for small sample sizes (SEAc) that corresponds to a confidence interval (CI) of 40%[60]. These calculations are based on a maximum likelihood estimation in a Bayesian framework. This framework is well suited for small sample sizes in general as it counteracts their effects on the statistical power of the analysis to a certain extent. However, it should be noted that increasing the sample size especially for the Miocene hominoids would lead to more robust results.

Statistical tests and modelling (linear models and Bayesian niche modelling) were conducted using R version 4.1.2 (2021-11-01) "Bird Hippie". Most figures were generated using Excel (2016) except for the maps for which we used QGIS (version 3.16) and the visualisation of the models, which were created using the plot functions in R (packages ggplot2 version 3.3.5, and SIBER version 2.1.6). All figures were further modified using GIMP (version 2.10.18).

Results and discussion

Paleoseasonality estimations for Late Miocene of Myanmar. Intra-individual variation of $\delta^{18}O$ values is routinely used to infer paleoseasonality. In regions with monsoonal climate, the temperature effect on these values is overwritten with the amount effect[22]. Therefore, the wet season is characterized in these regions by lower $\delta^{18}O$ values and the dry season by higher ones.

Sun and collaborators interpreted the lower $\delta^{18}O$ values from the Shuitangba locality (~ 6.2 Ma) from the Yunnan province in southwest China, in comparison to modern reference data, as an indication of a wetter climate during the Late Miocene than today[62]. The same pattern is also present in the hipparions from the Siwaliks of Pakistan[55]. The minimum $\delta^{18}O$ values of the carbonate fraction of their dental enamel measured through the serial sampling of hypsodont teeth rise over time, which is consistent with a decreasing amount of seasonal precipitation (Fig. 2). For the Late Miocene, seasonal precipitation regime with a dry season of five to six months (similar to the monsoonal forests in southern China today) was inferred from intra-individual serial sampling of equid dental enamel[55].

For our data set, we used a modern bovid from Myanmar as reference for the seasonal variation of the $\delta^{18}O$ values in the study area today. The $\delta^{18}O$ values of the modern bovid from Myanmar are significantly higher than the Miocene values from the Yinseik locality (Table 1). We tested this with a Wilcoxon rank sum test comparing the modern with the Miocene bovid, which was the individual whose $\delta^{18}O$ values were closest to the modern

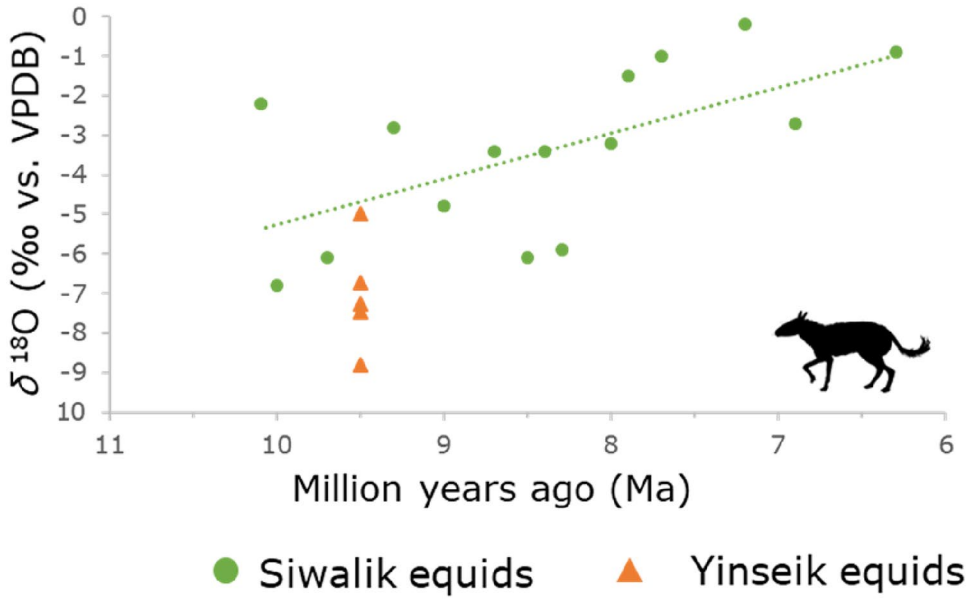

Figure 2. Development of the minimum $\delta^{18}O$ values from dental enamel of hipparions from the Siwaliks[21] over time. The linear regression line. ($y = -1.1527x + 6.2827$; adjusted $R^2 = 0.3216$; p-value = 0.01611) based on these values shows a trend towards more positive $\delta^{18}O$ values towards the end of the Miocene corresponding to lower seasonal maxima of precipitation. Minimum $\delta^{18}O$ values from the Yinseik specimens were added in orange. All of them plot below the regression line among the lowest minima from the Siwalik hipparions. Icon obtained via PhyloPic and in public domain.

Specimen no.	No. of samples	Taxonomy	$\delta^{18}O_{VPDB}$			$\delta^{13}C_{diet}$			C&O covariance
			Min	Max	Amplitude	Min	Max	Amplitude	
IRWD-9	12	Proboscidea	−7.3	−4.1	3.2	−27.2	−26.2	1.1	0.2
IRWD-17	8	Bovidae	−5.0	−3.6	1.4	−25.4	−24.6	1.4	−0.1
IRWD-26	14	Stegolophodon	−6.8	−5.5	1.2	−27.2	−25.4	1.8	0.1
IRWD-31	17	Rhinocerotidae	−8.8	−6.1	2.7	−27.9	−27.5	0.4	0.0
IRWD-42	7	Giraffidae	−7.5	−4.6	2.8	−27.6	−27.1	0.5	0.0
PND-M1	19	Bos	−5.7	−0.4	5.3	−15.4	−13.7	1.7	−0.3

Table 1. Summary statistics for the intra-tooth serial sampling. IRWD specimens are from the Miocene locality, whereas PND-M1 is a modern reference sample also originating from the Central Basin of Myanmar.

specimen ($W = 6$, p-value = 0.0001248). This indicates a wetter climate in Miocene Myanmar than today and is clearly visible when plotting the $\delta^{18}O$ values against the distance from the ERJ (enamel root junction) (Fig. 3). A comparison of the minimum $\delta^{18}O$ values from the Siwaliks and the Yinseik locality also shows that the climate in Miocene Myanmar was likely even wetter than in the contemporaneous Siwaliks (Fig. 2). Only the bovid from the Yinseik locality plots among the equids from the Siwaliks and are near the regression line. The specimen did not have a high tooth crown preserved, due to tooth wear, and therefore our data might not cover the time period of maximum seasonal precipitation, which would explain the higher minimum $\delta^{18}O$ value in comparison to the other mammals from the same locality. An alternative explanation would be differences in metabolism. High $\delta^{18}O$ values are expected in water independent species, because they obtain their water mostly from their food and not meteoric water, which reduces the loss of body water since it is recycled. However, modern bovids are not considered to be such a water independent species.

A Wilcoxon rank sum test showed that $\delta^{18}O$ values of bulk samples from the *Khoratpithecus* fauna (Fig. 4a) are significantly lower in comparison with the *Sivapithecus* fauna ($W = 4056$, p-value = 1.245e−06) (Fig. 4c). This is also consistent with this interpretation. However, the amplitude of the $\delta^{18}O$ values, defined as the difference between maximum and minimum values of one tooth, is smaller for the Miocene specimen than for the modern reference sample (Table 1). If we remove the outlier (PND-M1n) (tested with the Grubbs' test for outliers ($G = 2.5669$, $U = 0.6136$, p-value = 0.0427)) of the modern bovid the amplitude drops from 5.3 to 3.5‰, which is still higher than the maximum amplitude from a Miocene specimen, the Giraffid (IRWD-42) with 2.8‰. This is consistent with a less pronounced difference in seasonal precipitation in the Miocene, as compared to the climate in modern day Myanmar.

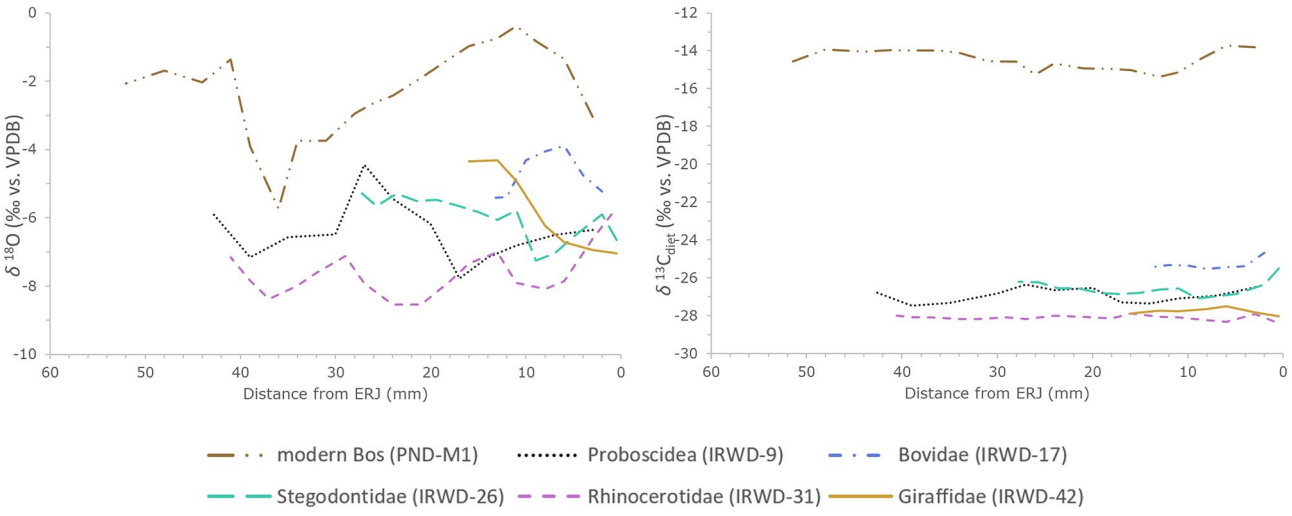

Figure 3. Comparison of the intra-individual serial sampling of a Miocene rhino from the Irrawaddy Fm. with a modern bovid from the Central Basin in Myanmar. Distance from ERJ (enamel root junction) is plotted in reverse order to correctly represent the enamel mineralization from oldest (left) to youngest (right).

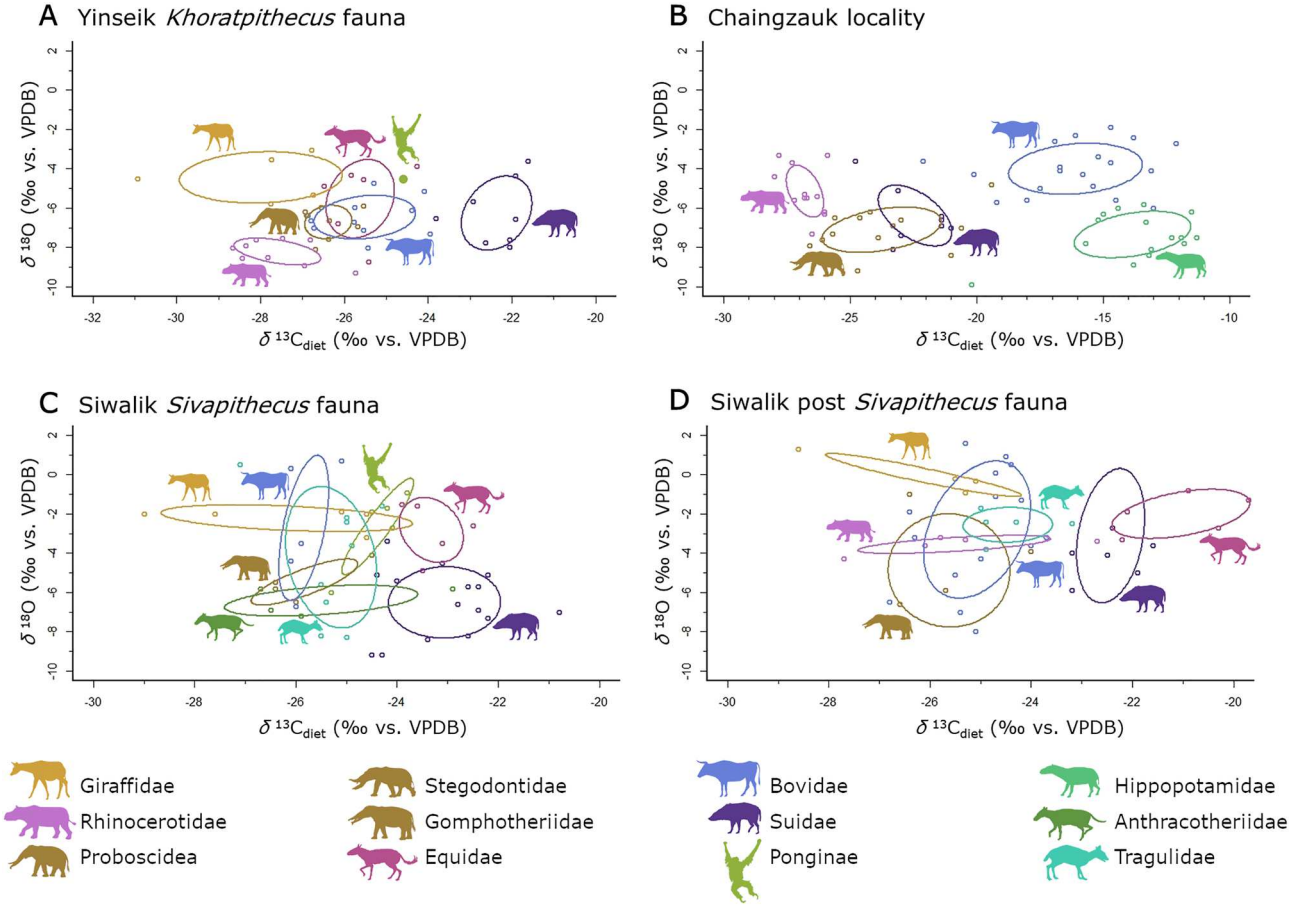

Figure 4. Bayesian niche modelling of four mammal communities. The ellipses mark the SEA (standard ellipse area) or core ecological niche, which corresponds to a 40% CI. Summary statistics are reported in Table SI 1. (**A**) Yinseik fauna including *K. ayeyarwadyensis* (~9.5 Ma), (**B**) Chaingzauk fauna (6 4 Ma)[25], (**C**) Siwalik fauna including *Sivapithecus* (~9 Ma)[17], (**D**) later Siwalik fauna (~8 Ma)[17]. Icons from PhyloPic and in public domain or under CC 3.0 license (Rhinocerotidae, Hippopotamidae, and Tragulidae by Zimices).

In addition, we do not see the same pattern of covariation between the $\delta^{13}C$ and the $\delta^{18}O$ values. In the Miocene specimens, we see marginal positive correlations, whereas $\delta^{13}C$ and $\delta^{18}O$ values of the modern bovid are slightly negatively correlated. The stronger a positive or negative correlation is, the more seasonality effects an individuals diet, e.g. its quality or source. Hence, the results suggest a different influence of the seasonal extremes on the food resources in the Miocene than today. What the difference between a positive or negative covariation of $\delta^{13}C$ and $\delta^{18}O$ values reflects still needs to be characterised by further studies. The $\delta^{13}C_{diet}$ values have been corrected for variations of isotopic composition of the CO_2 in the atmosphere as well as isotopic enrichment factors from diet to enamel. A detailed discussion can be found in the Methods section.

Paleoecology and niche partitioning of the Khoratpithecus mammal community. The $\delta^{13}C_{diet}$ values of the *Khoratpithecus* fauna from the Irrawaddy Fm. at the Yinseik locality span almost the entire range of modern C_3 plants (− 33 to − 22‰)[18], with Giraffidae and Rhinocerotidae having the lowest and Suidae having the highest values (Fig. 4a). When we correct the $\delta^{13}C$ values of C_3 plants from the modern values reported by Bender[18] to preindustrial ones (used in this paper to compare data sets from different eras to one another) the cut-off point for C_3 vegetation lies at − 20.5‰. Higher values would indicate the presence of C_4 plants in an individual's diet.

A comparison of the range of $\delta^{13}C$ values of the Yinseik data set (− 30.3 to − 21.3‰) to the contemporaneous *Sivapithecus* fauna from the Dhok Pathan and Khaur regions of the Siwaliks (− 29.0 to − 20.8‰) shows that, both *K. ayeyarwadyensis* and *Sivapithecus* lived in a mosaic landscape. The isotopic data from the two areas are consistent with a woodland forest with open patches that were mostly occupied by suids. In the Siwalik fauna the equids also have $\delta^{13}C$ values indicating more open habitats. In contrast, the equids from the Yinseik locality lived in more closed parts of the habitat according to their $\delta^{13}C$ values. Therefore, it seems that the Yinseik habitat was a bit more densely forested than the Siwalik one. None of the mammals from the Yinseik locality have $\delta^{13}C$ values above the cut-off point of − 20.5‰ including the equids, indicating a pure C_3 vegetation. Considerably higher $\delta^{18}O$ values of the *Sivapithecus* fauna (maximum = 0.7‰, mean = − 4.5‰) in comparison to the *Khoratpithecus* fauna (maximum = − 3.3‰, mean = − 6.5‰) are consistent with a slightly cooler and more humid climate at the Yinseik locality than in the Siwaliks. This pattern was also present in the comparison of minimum $\delta^{18}O$ values discussed in the previous section (Fig. 2).

The $\delta^{13}C$ value of *K. ayeyarwadyensis* place its habitat in the more open parts of the forest. It does plot among the data points with the highest $\delta^{18}O$ values similar to those of giraffids and equids. For the former, consumption of leaves or fruit with higher $\delta^{18}O$ values due to evapotranspiration is the most probable reason for these values whereas drinking from evaporated water sources like ponds seem more likely for the latter. As expected, the $\delta^{18}O$ values of browsers foraging on leaves closer to the forest floor like the rhinos are lower than the ones from more arboreal browsers like giraffids.

In primates folivory/frugivory as well as vertical stratification in habitat use have been discussed as drivers of oxygen isotope fractionation[21,63]. Recent studies however showed that vertical stratification probably is the primary driver of variations of $\delta^{18}O$ values[23,24]. Hence, the $\delta^{18}O$ value of *K. ayeyarwadyensis* is consistent with foraging high up in the canopy. The corresponding $\delta^{13}C$ value is also consistent with this interpretation, because the canopy effect is less pronounced high up in the canopy leading to higher $\delta^{13}C$ values of animals foraging there. A predominantly frugivorous diet, without any evidence for the consumption of hard objects has been reconstructed using dental microwear texture analysis and dental topography of *K. piriyai* and *K. chiangmuanensis*, the two closest allies of the Myanmar species[64], a subsistence strategy consistent with our data. *K. piriyai* is known from fossil localities in Thailand contemporaneous to the Yinseik locality with *K. ayeyarwadyensis* discussed in this paper where it is associated with a similar mammal fauna[6,7].

The two younger data sets from the Chaingzauk (6–4 Ma) locality in Myanmar (Fig. 4b) and the post-*Sivapithecus* (~ 8 Ma) layers from the Siwaliks (Fig. 4d) show similar trends. A slight shift towards more positive $\delta^{13}C$ values in the Siwaliks (− 28.6 to − 19.7‰) and a drastic shift plus an increasing range for $\delta^{13}C$ values in the Chaingzauk data (− 28.0 to − 11.3‰) both illustrate an ongoing opening of the landscape. As the Chaingzauk locality is 2–4 Ma younger than the post-*Sivapithecus* Siwalik data set, it becomes apparent, that the opening of the landscape was an ongoing process in South and Southeast Asia throughout the Late Miocene. The introduction of C_4 plants results in the adaptation of the ecological niches of some groups of mammals, especially the suids and equids in the Siwalik and bovids and rhinos in the Chaingzauk community.

Assessing the ecological niches of fossil pongines. The ecological niches of *Sivapithecus* and *K. ayeyarwadyensis* inferred from the modelled isotopic niches and the comparison with associated mammal fauna look very similar to each other and to modern orangutans in some general characteristics. The ecological niches of the fossil pongines are consistent with predominantely frugivorous, arboreal forest dwellers, characteristics that can also be applied to orang-utans today. The direct comparison of the ecological niches of the various fossil and extant pongines however, indicates differences in their ecology and habitat use (Fig. 5). The facts that only one sample of *Khoratpithecus* was available and we do see a high variation in both the $\delta^{13}C$ and $\delta^{18}O$ values of the other pongine genera do limit the interpretations we can make in regard to this specific pongine. We can however give a first approximation of its ecology and show that it is consistent with the trends visible through the contemporaneous *Sivapithecus*, for which the sample size (n = 5) was large enough to model an isotopic niche with reasonable confidence[60].

Modern species of *Pongo* are the most frugivorous of all extant apes. Although the diets of the two Miocene pongines were reconstructed as predominantly frugivorous, the addition of some hard objects like seeds and nuts for *Sivapithecus* but not for *Khoratpithecus*[64–66], highlights a difference in the dietary ecologies between the

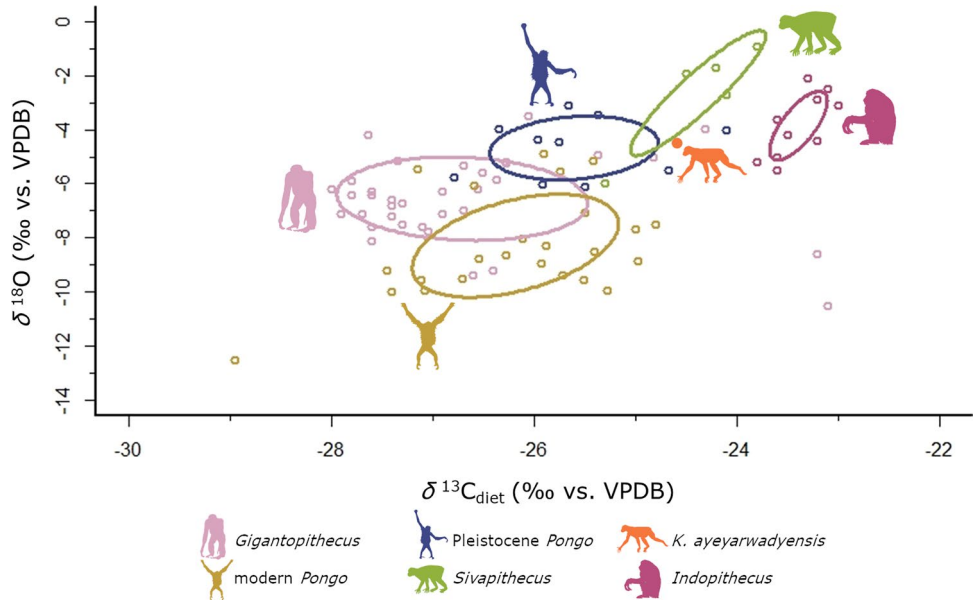

Figure 5. Bayesian niche modelling of fossil and extant pongines. The lines encompass the standard ellipse area or core ecological niche, corresponding to a confidence interval of 40%[60]. Icons are public domain (*Gigantopithecus*, *Indopithecus*) or Creative Commons 3.0 license [modern and Pleistocene *Pongo* by Gareth Monder, *Khoratpithecus* by Mateus Zica (modified by T. Michael Keesey), and *Sivapithecus* by Nobu Tamura (modified by T. Michael Keesey)] via PhyloPic.

genera. Modern orangutans rely on a number of fallback foods (e.g. inner bark, pith, young leaves, and flowers)[67,68] in times of fruit scarcity, which are tough, but not hard, and have therefore different microwear patterns[69].

To test the similarity of habitat between *Sivapithecus* and Pleistocene *Pongo*, we conducted a Wilcoxon Rank Sum test to see if there is a difference in $\delta^{13}C_{diet}$ values between both pongines. The result shows a significant difference ($W = 4.5$, p-value = 0.01422). Therefore, although the ecological niche of *Sivapithecus* and *K. ayeyarwadyensis* within their respective mammal communities resemble that of modern *Pongo*, a comparison of these ecological variables with the other pongines on a broader scope (Fig. 5) reveals that the microhabitats they occupied or their habitat use differed significantly.

Although all groups of pongines lived in a forested habitat, *K. ayeyarwadyensis*, *Sivapithecus* and *Indopithecus* seem to be located in a more fragmented forest or higher up in the canopy where the canopy effect is less pronounced. The ecological niches of both modern and Pleistocene *Pongo* as well as *Gigantopithecus* are indicating a more closed canopy or foraging lower down in the canopy or even on the ground where the canopy effect is more pronounced. A difference in forest structure between the Miocene and Pleistocene is also suggested by palynological data, paleosol isotopic data, and climate and vegetation models[52,70–75]. The change in vegetation and landscape structure could be explained by the marked climate change during the end of the Neogene[52].

The difference in isotopic niches between Miocene and the Pleistocene pongines as well as modern *Pongo* is likely not only related to the general structure of the habitats, but also to the nature of habitat use. The data on the Miocene pongines *K. ayeyarwadyensis* and *Sivapithecus* are consistent with using areas higher up in the canopy, as they have both higher $\delta^{18}O$ and $\delta^{13}C_{diet}$ values. This correlates nicely with a lower body mass in comparison with the Pleistocene pongines. However, the estimated body mass of around 150 kg or more of *Indopithecus*, comparable with extant *Gorilla*[76], is more similar to *Gigantopithecus*[77] and makes an arboreal habitat less probable. Nevertheless, its isotopic niche is more similar to the Miocene pongines from Myanmar and Pakistan than to *Gigantopithecus* or *Pongo*. As the similar sized gorillas exploit arboreal resources and climb trees, a similar behaviour of *Indopithecus* would be possible. Alternatively, its isotopic niche would be also consistent with a more open habitat, which has already been suggested for *Indopithecus*[78]. In addition, the interpretation of the *Indopithecus* ecological core niche based on the data available for this study should be regarded as preliminary, especially for the $\delta^{18}O$ values, given the fact that all the data come from one individual from which intra-individual serial samples were taken using laser ablation. Although we used the $\delta^{18}O$ values corrected by an offset of 5.1‰ ("CO_3 equivalent")[26] for our study, we cannot exclude that they are not biased due to the different sampling methodology.

Gigantopithecus seems to have occupied the most densely-forested habitats, given the low $\delta^{18}O$ and $\delta^{13}C_{diet}$ values. Within this genus, there are two outliers with high $\delta^{13}C$ values, which are two of the samples from the Early Pleistocene Longgudong Cave in Southern China[28]. These values are consistent with a more open habitat for these two individuals, although their $\delta^{18}O$ values do not correspond to plants subjected to evaporative stress as food sources. However, Jiang and collaborators re-analysed one of these two samples and reported a value 1.6‰ lower[79]. It cannot be ruled out that the variation is partly caused by the different pretreatment method applied by Nelson[28].

Wilcoxon Rank Sum test confirmed that Pleistocene and modern *Pongo* did not differ significantly in their $\delta^{13}C$ values ($W = 86.5$, p-value $= 0.2123$). Hence, modern orangutans have not yet been pushed by human pressure into denser forest habitats or to the forest margins and more open spaces due to deforestation around a century ago, which is the time period our sample dates to. All the dates are reported in Table SI 2 and Table SI 3. These results also show that although their habitats became increasingly fragmented, pongines remained dependent on closed habitats and were unable to adapt and move into more open forested woodlands.

The data are consistent with shifts in $\delta^{18}O$ consistent with differences in vertical stratification[23,24]. Decreasing $\delta^{13}C_{diet}$ values from the Miocene pongines (except in *Indopithecus*), to Pleistocene and modern *Pongo*, to *Gigantopithecus* are also consistent with this interpretation, as the canopy effect is more pronounced lower down in the canopy. This seems plausible for *K. ayeyarwadyensis*, *Sivapithecus*, Pleistocene *Pongo* and *Gigantopithecus* as this coincides nicely with increasing body mass in these three genera. The higher body mass of *Pongo* in comparison to both *K. ayeyarwadyensis* and *Sivapithecus* would make foraging high up in the canopy and close to terminal branches increasingly difficult. However, brachiation in conjunction with high hip flexibility in *Pongo* counters the negative impact of higher body mass during climbing to a certain extent, due to weight distribution over many smaller branches[80–82].

At first it sound promising to relate the decreasing $\delta^{18}O$ values from the Miocene to the Pleistocene genera (see in Fig. 5) to the increasing competition with cercopithecoid monkeys, which became increasingly abundant in Southeast Asia from the Late Miocene and especially the Plio-Pleistocene onward[83–85],. Nevertheless, the higher body mass of pongines in comparison with the contemporaneous monkeys makes it very unlikely that the former had to resort to lower canopy layers for foraging due to increased competition[86]. On the contrary, it has been suggested that monkeys that are capable of eating unripe fruit create a pattern of ripe fruit availability that is more restricted to terminal branches and therefore forcing apes to adapt to exploit these resources[80].

As discussed earlier on, it was necessary to assess to what extent changes in $\delta^{18}O$ values might reflect climatic changes over time and geographical distance. Although climatic changes were responsible for part of the $\delta^{18}O$ variation that we see between the different pongine genera (Fig. 5), we are confident that an ecological signal is also visible. Especially between the Miocene and Pleistocene taxa, the relative position of $\delta^{18}O$ values of bovids, pongines and suids across time and space (see more detailed discussion in the Supplementary Information) and the overall consistency of our interpretations with body mass differences between the genera. The data are therefore consistent with the possiblity that there is a difference in the usage of the canopy between the two Miocene pongines *Sivapithecus* and *K. ayeyarwadyensis*, which could forage even higher up, and *Pongo*. Relative position of $\delta^{18}O$ values of bovids, pongines and suids suggest that the difference between Pleistocene and extant *Pongo* however is probably predominantly caused by differences in climate between the islands of the Sunda Shelf and mainland Southeast Asia. This is consistent with the $\delta^{18}O$ values of modern *Pongo* being well correlated well with $\delta^{18}O$ values of precipitation from Sumatra and Borneo. These values are lower on the islands in the Sunda Shelf as compared to mainland Southeast Asia, predominantly caused by a more intense monsoon[87]. These preliminary interpretations should be further investigated with bigger data sets for a more robust assessment of the variations of $\delta^{18}O$ values as they span a large spatio-temporal range and variation in these values can be caused by many different factors[22].

Conclusions

Khoratpithecus ayeyarwadyensis, a Late Miocene pongine from Myanmar, lived in a woodland forest. The $\delta^{13}C$ value is consistent with a microhabitat where the canopy effect is not strongly pronounced; so either in the lighter forest or higher up in the canopy, but not in the dense understory forest. Its high $\delta^{18}O$ value is similar to those of sympatric giraffids and equids. Hence, the data are consistent with *K. ayeyarwadyensis* foraging higher up in the canopy where evapotranspiration leads to a depletion of ^{18}O in food and water sources. Given that we could only sample one specimen of this genus, this only gives a first indication of the palaeoecology of *K. ayeyarwadyensis*, and should more specimen of this important pongine genus become available for stable isotope analysis, it would further improve our understanding of its palaeoecology and make our interpretations more robust. The precipitation regime in the habitat of *K. ayeyarwadyensis* was similar to the monsoon regime in present-day Myanmar, although seasonality was probably less pronounced. The high $\delta^{18}O$ value is consistent with a diet consisting of plant tissues enriched in the heavier ^{18}O isotope due to evapotranspiration like fruit or leaves. However, the results from dental microwear texture analysis of *K. piriyai* from Thailand suggest a predominantly frugivorous diet without the use of tough objects, so *K. ayeyarwadyensis* was likely also a frugivore and not a folivore. Overall, the habitats of these two Miocene hominoids seem to be similar to that of the modern *Pongo*, however the exploitation of these habitats and the ecological niches occupied by each species seem to be distinct. In the case of *K. ayeyarwadyensis* and *Pongo* they might use similar resources, but at different levels in the canopy.

The comparison of all Asian Miocene apes showed that the reconstructed ecological niches of *Sivapithecus* and *K. ayeyarwadyensis* seem to be superficially similar to the modern *Pongo*. They are all three predominantly frugivorous primates foraging high up in the canopy of forests with a seasonal monsoon-like precipitation regime. However, the density of the Miocene forest in the Siwalik and Irrawaddy region seems to be more fragmented with more deciduous vegetation. The overall climate was also drier than in modern Indonesia. Palynological and isotopic data on paleosols and benthic foraminifera as well as climate models suggest a similar development in vegetation structure and climate[52,70–75]. *Gigantopithecus* was adapted to foraging in denser forests, and given its immense body mass this was likely the the understory or forest floors. On the other hand, the data from modern and Pleistocene *Pongo* are consistent with using resources in the lower areas of the forest canopy.

As we compare pongine genera from different time periods with one another it was necessary to correct the $\delta^{13}C$ values for changes in the isotopic composition of the atmospheric CO_2. Such a correction is not possible for the $\delta^{18}O$ values, as their variation is impacted by many different factors. We therefore assessed if some of the

variation can be attributed to changes in ecology. We do however acknowledge, that the interpretations of variations and shifts in $\delta^{18}O$ values are less robust, than the ones based on the $\delta^{13}C$ values. Large scale investigations of $\delta^{18}O$ variation over the spatio-temporal range of this study would improve the robustness of the interpretations.

As mentioned in the introduction, the present study contributes to improving our understanding of the evolutionary ecology of the fossil pongines that can provide valuable insight for current orangutan conservation. It seems that at least at the time from which the samples of modern *Pongo* originate, around a century ago, there was still enough suitable habitat available for the orangutans not to be pressured to leave their ancestral niche. However, the shifts in the environment we see in the isotopic niche modelling of the *Sivapithecus* and the associated *K. ayeyarwadyensis* fauna to later time periods after the decline and extinction of these Miocene ponginesillustrate the fate, which awaits the Southeast Asian apes if the habitats become more and more fragmented that of extinction.

Data availability

All data generated or analysed during this study are included in this published article (and its supplementary information files).

Received: 3 May 2022; Accepted: 27 June 2022
Published online: 12 July 2022

References

1. Spehar, S. N. *et al.* Orangutans venture out of the rainforest and into the anthropocene. *Sci. Adv.* **4**, e1701422. https://doi.org/10.1126/sciadv.1701422 (2018).
2. Suganuma, Y. *et al.* Magnetostratigraphy of the Miocene Chiang Muan Formation, northern Thailand. Implications for revised chronology of the earliest Miocene hominoid in Southeast Asia. *Palaeogeogr. Palaeoclimatol. Plaeoecol.* **239**, 75–86 (2006).
3. Coster, P. *et al.* A complete magnetic-polarity stratigraphy of the Miocene continental deposits of Mae Moh Basin, northern Thailand, and a reassessment of the age of hominoid-bearing localities in northern Thailand. *Geol. Soc. Am. Bull.* **122**, 1180–1191 (2010).
4. Begun, D. R. The Miocene hominoid radiations. In *A Companion to Paleoanthropology* (ed. Begun, D. R.) 398–416 (Blackwell Publishing, 2013).
5. Pugh, K. D. Phylogenetic analysis of Middle-Late Miocene apes. *J. Hum. Evol.* **165**, 1–33 (2022).
6. Chaimanee, Y. *et al. Khoratpithecus piriyai*, a Late Miocene Hominoid of Thailand. *Am. J. Phys. Anthropol.* **131**, 311–323 (2006).
7. Chavasseau, O. *et al.* Advances in the biochronology and biostratigraphy of the continental Neogene of Myanmar. In *Fossil Mammals in Asia. Neogene Biostratigraphy and Chronology* (eds Wang, X. *et al.*) 461–474 (Columbia University Press, 2013).
8. Patnaik, R. Indian Neogene Siwalik Mammalian biostratigraphy. An overview. In *Fossil Mammals in Asia Neogene Biostratigraphy and Chronology* (eds Wang, X. *et al.*) 423–444 (Columbia University Press, 2013).
9. Chaimanee, Y. *et al.* A middle Miocene hominoid from Thailand and orangutan origins. *Nature* **422**, 61–65 (2003).
10. Chaimanee, Y. *et al.* A new orang-utan relative from the Late Miocene of Thailand. *Nature* **427**, 439–441 (2004).
11. Chaimanee, Y., Lazzari, V., Chaivanich, K. & Jaeger, J.-J. First maxilla of a late Miocene hominid from Thailand and the evolution of pongine derived characters. *J. Hum. Evol.* **134**, 102636. https://doi.org/10.1016/j.jhevol.2019.06.007 (2019).
12. Jaeger, J.-J. *et al.* First Hominoid from the Late Miocene of the Irrawaddy formation (Myanmar). *PLoS ONE* **6**, 1–14 (2011).
13. Begun, D. R. European hominoids. In *The Primate Fossil Record* (ed. Hartwig, W. C.) 339–368 (Cambridge University Press, 2002).
14. Kelley, J. & Gao, F. Juvenile hominoid cranium from the late Miocene of southern China and hominoid diversity in Asia. *Proc. Natl. Acad. Sci. U.S.A.* **109**, 6882–6885 (2012).
15. Kettle, C. J., Maycock, C. R. & Burslem, D. New directions in dipterocarp biology and conservation: A synthesis. *Biotropica* **44**, 658–660. https://doi.org/10.1111/j.1744-7429.2012.00912.x (2012).
16. Cannon, C. H., Morley, R. J. & Bush, A. B. G. The current refugial rainforests of Sundaland are unrepresentative of their biogeographic past and highly vulnerable to disturbance. *Proc. Natl. Acad. Sci. U.S.A.* **106**, 11188–11193. https://doi.org/10.1073/pnas.0809865106 (2009).
17. Nelson, S. V. Isotopic reconstruction of habitat change surrounding the extinction of *Sivapithecus*, a Miocene hominoid, in the Siwalik Group of Pakistan. *Palaeogeogr. Palaeoclimatol. Palaeoecol.* **243**, 204–222 (2007).
18. Bender, M. M. Variations in the $^{13}C/^{12}C$ ratios of plants in relation to the pathway of photosynthetic carbon dioxide fixation. *Phytochemistry* **10**, 1239–1244 (1971).
19. Kohn, M. J. Carbon isotope compositions of terrestrial C3 plants as indicators of (paleo)ecology and (paleo)climate. *Proc. Natl. Acad. Sci.* **107**, 19691–19695 (2010).
20. Bonafini, M., Pellegrini, M., Ditchfield, P. & Pollard, A. M. Investigation of the 'canopy effect' in the isotope ecology of temperate woodlands. *J. Archaeol. Sci.* **40**, 3926–3935. https://doi.org/10.1016/j.jas.2013.03.028 (2013).
21. Krigbaum, J., Berger, M. H., Daegling, D. J. & McGraw, W. S. Stable isotope canopy effects for sympatric monkeys at Tai Forest, Cote d'Ivoire. *Biol. Lett.* **9**, 20130466. https://doi.org/10.1098/rsbl.2013.0466 (2013).
22. Dansgaard, W. Stable isotopes in precipitation. *Tellus* **16**, 436–468 (1964).
23. Fannin, L. D. & McGraw, W. S. Does oxygen stable isotope composition in primates vary as a function of vertical stratification or folivorous behaviour?. *Folia Primatol. Int. J. Primatol.* **91**, 219–227. https://doi.org/10.1159/000502417 (2020).
24. Louys, J. & Roberts, P. Environmental drivers of megafauna and hominin extinction in Southeast Asia. *Nature* **586**, 402–406. https://doi.org/10.1038/s41586-020-2810-y (2020).
25. Zin-Maung-Maung-Thein, *et al.* Stable isotope analysis of the tooth enamel of Chaingzauk mammalian fauna (late Neogene, Myanmar) and its implication to paleoenvironment and paleogeography. *Palaeogeogr. Palaeoclimatol. Palaeoecol.* **300**, 11–22. https://doi.org/10.1016/j.palaeo.2010.11.016 (2011).
26. Patnaik, R., Cerling, T. E., Uno, K. T. & Fleagle, J. G. Diet and habitat of Siwalik primates *Indopithecus*, *Sivaladapis* and *Theropithecus*. *Ann. Zool. Fenn.* **51**, 123–142. https://doi.org/10.5735/086.051.0214 (2014).
27. Pushkina, D., Bocherens, H., Chaimanee, Y. & Jaeger, J.-J. Stable carbon isotope reconstructions of diet and paleoenvironment from the late Middle Pleistocene Snake Cave in Northeastern Thailand. *Naturwissenschaften* **97**, 299–309 (2010).
28. Nelson, S. V. The paleoecology of early Pleistocene *Gigantopithecus blacki* inferred from isotopic analyses. *Am. J. Phys. Anthropol.* **155**, 571–578. https://doi.org/10.1002/ajpa.22609 (2014).
29. Qu, Y. *et al.* Preservation assessments and carbon and oxygen isotopes analysis of tooth enamel of *Gigantopithecus blacki* and contemporary animals from Sanhe Cave, Chongzuo, South China during the Early Pleistocene. *Quat. Int.* **354**, 52–58. https://doi.org/10.1016/j.quaint.2013.10.053 (2014).
30. Bocherens, H. *et al.* Flexibility of diet and habitat in Pleistocene South Asian mammals. Implications for the fate of the giant fossil ape *Gigantopithecus*. *Quat. Int.* **434**, 148–155 (2017).

31. Bacon, A.-M. *et al.* Nam Lot (MIS 5) and Duoi U'Oi (MIS 4) Southeast Asian sites revisited. Zooarchaeological and isotopic evidences. *Palaeogeogr. Palaeoclimatol. Palaeoecol.* **512**, 132–144. https://doi.org/10.1016/j.palaeo.2018.03.034 (2018).
32. Jiang, Q.-Y., Zhao, L., Guo, L. & Hu, Y.-W. First direct evidence of conservative foraging ecology of early *Gigantopithecus blacki* (~2 Ma) in Guangxi, southern China. *Am. J. Phys. Anthropol.* https://doi.org/10.1002/ajpa.24300 (2021).
33. Ma, J. *et al.* Isotopic evidence of foraging ecology of Asian elephant (*Elephas maximus*) in South China during the Late Pleistocene. *Quat. Int.* **443**, 160–167. https://doi.org/10.1016/j.quaint.2016.09.043 (2017).
34. Ma, J., Wang, Y., Jin, C., Hu, Y. & Bocherens, H. Ecological flexibility and differential survival of Pleistocene *Stegodon orientalis* and *Elephas maximus* in mainland southeast Asia revealed by stable isotope (C, O) analysis. *Quat. Sci. Rev.* **212**, 33–44. https://doi.org/10.1016/j.quascirev.2019.03.021 (2019).
35. Janssen, R. *et al.* Tooth enamel stable isotopes of Holocene and Pleistocene fossil fauna reveal glacial and interglacial paleoenvironments of hominins in Indonesia. *Quat. Sci. Rev.* **144**, 145–154. https://doi.org/10.1016/j.quascirev.2016.02.028 (2016).
36. Wang, W. *et al.* Sequence of mammalian fossils, including hominoid teeth, from the Bubing Basin caves, South China. *J. Hum. Evol.* **52**, 370–379. https://doi.org/10.1016/j.jhevol.2006.10.003 (2007).
37. Suraprasit, K., Bocherens, H., Chaimanee, Y., Panha, S. & Jaeger, J.-J. Late Middle Pleistocene ecology and climate in Northeastern Thailand inferred from the stable isotope analysis of Khok Sung herbivore tooth enamel and the land mammal cenogram. *Quat. Sci. Rev.* **193**, 24–42. https://doi.org/10.1016/j.quascirev.2018.06.004 (2018).
38. Bocherens, H., Fizet, M. & Mariotti, A. Diet, physiology and ecology of fossil mammals as inferred from stable carbon and nitrogen biogeochemistry. Implications for Pleistocene bears. *Palaeogeogr. Palaeoclimatol. Palaeoecol.* **107**, 213–225 (1994).
39. Koch, P. L., Tuross, N. & Fogel, M. L. The effects of sample treatment and diagenesis on the isotopic integrity of carbonate in biogenic hydroxylapatite. *J. Archaeol. Sci.* **24**, 417–429 (1997).
40. Wright, L. E. & Schwarcz, H. P. Correspondence between stable carbon, oxygen and nitrogen isotopes in human tooth enamel and dentine. Infant diets at Kaminaljuyú. *J. Archaeol. Sci.* **26**, 1159–1170 (1999).
41. Szpak, P., Metcalfe, J. Z. & Macdonald, R. A. Best practices for calibrating and reporting stable isotope measurments in archaeology. *J. Archaeol. Sci. Rep.* **13**, 609–616 (2017).
42. Coplen, T. B. Guidelines and recommended terms for expression of stable-isotope-ratio and gas-ratio measurement results. *Rapid Commun. Mass Spectrom.* **25**, 2538–2560 (2011).
43. Bond, A. L. & Hobson, K. A. Reporting stable-isotope ratios in ecology. Recommended terminology, guidelines and best practices. *Waterbirds* **35**, 324–331 (2012).
44. Craig, H. Carbon 13 in plants and the relationships between carbon 13 and carbon 14 variations in nature. *J. Geol.* **62**, 115–149. https://doi.org/10.1086/626141 (1954).
45. Cerling, T. E. & Harris, J. M. Carbon isotope fractionation between diet and bioapatite in ungulate mammals and implications for ecological and paleoecological studies. *Oecologia* **120**, 347–363 (1999).
46. Passey, B. H. *et al.* Carbon isotope fractionation between diet, breath CO2, and bioapatite in different mammals. *J. Archaeol. Sci.* **32**, 1459–1470. https://doi.org/10.1016/j.jas.2005.03.015 (2005).
47. Howland, M. R. *et al.* Expression of the dietary isotope signal in the compound-specific $\delta^{13}C$ values of pig bone lipids and amino acids. *Int. J. Osteoarchaeol.* **13**, 54–65. https://doi.org/10.1002/oa.658 (2003).
48. Crowley, B. E. *et al.* Stable carbon and nitrogen isotope enrichment in primate tissues. *Oecologia* **164**, 611–626. https://doi.org/10.1007/s00442-010-1701-6 (2010).
49. Keeling, C. D. The Suess effect: 13Carbon–14Carbon interrelations. *Environ. Int.* **2**, 229–300. https://doi.org/10.1016/0160-4120(79)90005-9 (1979).
50. Marino, B. D., McElroy, M. B., Salawitch, R. J. & Spaulding, W. G. Glacial-to-interglacial variations in the carbon isotopic composition of atmospheric CO_2. *Nature* **357**, 461–466. https://doi.org/10.1038/357461a0 (1992).
51. Tipple, B. J., Meyers, S. R. & Pagani, M. Carbon isotope ratio of Cenozoic CO2 A comparative evaluation of available geochemical proxies. *Paleoceanography* https://doi.org/10.1029/2009PA001851 (2010).
52. Zachos, J., Pagani, M., Sloan, L., Thomas, E. & Billups, K. Trends, rhythms, and aberrations in global climate 65 Ma to present. *Science* **292**, 686–693 (2001).
53. Cerling, T. E., Harris, J. M., Leakey, M. G., Passey, B. H. & Levin, N. E. Stable carbon and oxygen isotopes in East African Mammals. Modern and fossil. In *Cenozoic Mammals of Africa* (ed. Werdelin, L.) 941–952 (University of California Press, 2010).
54. Friedli, H., Lötscher, H., Oeschger, H., Siegenthaler, U. & Stauffer, B. Ice core record of the $^{13}C/^{12}C$ ratio of atmospheric CO_2 in the past two centuries. *Nature* **324**, 237–238. https://doi.org/10.1038/324237a0 (1986).
55. Nelson, S. V. Paleoseasonality inferred from equid teeth and intra-tooth isotopic variability. *Palaeogeogr. Palaeoclimatol. Palaeoecol.* **222**, 122–144 (2005).
56. Komsta, L. Processing data for outliers. *R News* **6**, 10–13 (2006).
57. Hutchinson, G. E. Concluding remarks. In *Cold spring Harbor Symposium on Quantitative Biology,* edited by Q. Biology (1957).
58. Hutchinson, G. E. *An Introduction to Population Ecology* (Yale University Press, 1978).
59. Baumann, C., Bocherens, H., Drucker, D. G. & Conard, N. J. Fox dietary ecology as a tracer of human impact on Pleistocene ecosystems. *PLoS ONE* **15**, e0235692. https://doi.org/10.1371/journal.pone.0235692 (2020).
60. Jackson, A. L., Inger, R., Parnell, A. C. & Bearhop, S. Comparing isotopic niche widths among and within communities: SIBER—Stable Isotope Bayesian Ellipses in R. *J. Anim. Ecol.* **80**, 595–602. https://doi.org/10.1111/j.1365-2656.2011.01806.x (2011).
61. Nelson, S. V. & Hamilton, M. I. Evolution of the human dietary niche. Initial transitions. In *Chimpanzees and Human Evolution* (eds Muller, M. N. *et al.*) 286–310 (Harvard University Press, 2017).
62. Sun, F. *et al.* Paleoenvironment of the late Miocene Shuitangba hominoids from Yunnan, Southwest China: Insights from stable isotopes. *Chem. Geol.* **569**, 120123. https://doi.org/10.1016/j.chemgeo.2021.120123 (2021).
63. Nelson, S. V. Chimpanzee fauna isotopes provide new interpretations of fossil ape and hominin ecologies. *Proc. R. Soc. B: Biol. Sci.* **280**, 20132324. https://doi.org/10.1098/rspb.2013.2324 (2013).
64. Merceron, G., Taylor, S., Scott, R., Chaimanee, Y. & Jaeger, J.-J. Dietary characterization of the hominoid Khoratpithecus (Miocene of Thailand). Evidence from dental topographic and microwear texture analyses. *Naturwissenschaften* **93**, 329–333. https://doi.org/10.1007/s00114-006-0107-0 (2006).
65. Kay, R. F. The nut-crackers—A new theory of the adaptations of the ramapithecinae. *Am. J. Phys. Anthropol.* **55**, 141–151 (1981).
66. Nelson, S. V. *The Extinction of Sivapithecus. Faunal and Environmental Changes Surrounding the Disappearance of a Miocene Hominoid in the Siwaliks of Pakistan* (Brill Academic Publishers, 2003).
67. Kanamori, T., Kuze, N., Bernard, H., Malim, T. P. & Kohshima, S. Feeding ecology of Bornean orangutans (*Pongo pygmaeus morio*) in Danum Valley, Sabah, Malaysia: A 3-year record including two mast fruitings. *Am. J. Primatol.* **72**, 820–840. https://doi.org/10.1002/ajp.20848 (2010).
68. Vogel, E. R. *et al.* Nutritional ecology of wild Bornean orangutans (*Pongo pygmaeus wurmbii*) in a peat swamp habitat. Effects of age, sex, and season. *Am. J. Primatol.* **79**, 1–20. https://doi.org/10.1002/ajp.22618 (2017).
69. Louys, J. *et al.* Sumatran orangutan diets in the Late Pleistocene as inferred from dental microwear texture analysis. *Quat. Int.* **603**, 74–81. https://doi.org/10.1016/j.quaint.2020.08.040 (2021).
70. Quade, J., Cerling, T. E. & Bowman, J. R. Development of Asian monsoon revealed by marked ecological shift during the latest Miocene in northern Pakistan. *Nature* **342**, 163–166 (1989).

71. Hoorn, C., Ohja, T. & Quade, J. Palynological evidence for vegetation development and climatic change in the sub-Himalayan Zone (Neogene, Central Nepal). *Palaeogeogr. Palaeoclimatol. Palaeoecol.* **163**, 133–161 (2000).
72. Morley, R. J. A review of the Cenozoic palaeoclimate history of Southeast Asia. In *Biotic Evolution and Environmental Change in Southeast Asia* (eds Gower, D. *et al.*) 79–114 (Cambridge University Press, 2012).
73. Morley, R. J. Assembly and division of the South and South-East Asian flora in relation to tectonics and climate change. *J. Trop. Ecol.* **34**, 209–234. https://doi.org/10.1017/S0266467418000202 (2018).
74. Sepulchre, P. *et al.* Mid-tertiary paleoenvironments in Thailand. Pollen evidence. *Clim. Past* **6**, 461–473 (2010).
75. Sepulchre, P., Jolly, D., Ducrocq, S., Chaimanee, Y. & Jaeger, J.-J. Mid-tertiary palaeoenvironments in Thailand. Pollen evidence. *Clim. Past Discuss.* **5**, 709–734 (2009).
76. Fleagle, J. G., Janson, C. H. & Reed, K. E. *Primate Communities* (Cambridge University Press, 1999).
77. Fleagle, J. G. *Primate Adaptation and Evolution* 3rd edn. (Elsevier, 2013).
78. Pilbeam, D. *Gigantopithecus* and the origins of Hominidae. *Nature* **225**, 516–519. https://doi.org/10.1038/225516a0 (1970).
79. Jiang, Q.-Y., Zhao, L.-X. & Hu, Y.-W. Isotopic (C, O) variations of fossil enamel bioapatite caused by different preparation and measurement protocols: A case study of *Gigantopithecus* fauna. *Vertebr. PalAsiat.* **58**, 159–168 (2020).
80. Hunt, K. D. Why are there apes? Evidence for the co-evolution of ape and monkey ecomorphology. *J. Anat.* **228**, 630–685. https://doi.org/10.1111/joa.12454 (2016).
81. Zihlman, A. L., Mcfarland, R. K. & Underwood, C. E. Functional anatomy and adaptation of male gorillas (*Gorilla gorilla gorilla*) with comparison to male orangutans (*Pongo pygmaeus*). *Anat. Rec. Adv. Integr. Anat. Evol. Biol.* **294**, 1842–1855. https://doi.org/10.1002/ar.21449 (2011).
82. Thorpe, S. K. & Crompton, R. H. Orangutan positional behavior and the nature of arboreal locomotion in Hominoidea. *Am. J. Phys. Anthropol.* **131**, 384–401. https://doi.org/10.1002/ajpa.20422 (2006).
83. Barry, J. C. The history and chronology of Siwalik cercopithecids. *J. Hum. Evol.* **2**, 47–58 (1987).
84. Jablonski, N. G., Whitfort, M. J., Roberts-Smith, N. & Qinqi, X. The influence of life history and diet on the distribution of catarrhine primates during the Pleistocene in eastern Asia. *J. Hum. Evol.* **39**, 131–157 (2000).
85. Takai, M., Saegusa, H., Thaung-Htike, & Zin-Maung-Maung-Thein,. Neogene mammalian fauna in Myanmar. *Asian Paleoprimatol.* **4**, 143–172 (2006).
86. Houle, A., Chapman, C. A. & Vickery, W. L. Intratree vertical variation of fruit density and the nature of contest competition in frugivores. *Behav. Ecol. Sociobiol.* **64**, 429–441. https://doi.org/10.1007/s00265-009-0859-6 (2010).
87. Vuille, M., Werner, M., Bradley, R. S. & Keimig, F. Stable isotopes in precipitation in the Asian monsoon region. *J. Geophys. Res.* **110**, D23108 (2005).

Acknowledgements

This research was funded by the ANR (EVEPRIMASIA) and DFG (Grant BO 3478/7-)1, the Fondation Fyssen (Grant to O.C.) and the laboratory PALEVOPRIM. Sample preparation and analysis took place at the Eberhard-Karls Universität Tübingen in the laboratories of the AG Biogeologie. Thanks are due to P. Tung for conducting the isotopic analyses and to Catalina Labra Odde for proof reading the manuscript. We would also like to thank our reviewers for their time and effort they took with their feedback. It greatly increased the quality of our manuscript.

Author contributions

S.G.H., O.C., and H.B. wrote the main manuscript text. S.G.H. prepared the figures and performed data analysis. O.C., J.-J.J., Y.C., A.N.S., and C.S. performed field work and sample collection. All authors reviewed the manuscript.

Competing interests

The authors declare no competing interests.

Additional information

Supplementary Information The online version contains supplementary material available at https://doi.org/10.1038/s41598-022-15574-z.

Correspondence and requests for materials should be addressed to S.G.H.

Reprints and permissions information is available at www.nature.com/reprints.

Publisher's note Springer Nature remains neutral with regard to jurisdictional claims in published maps and institutional affiliations.

Supplementary Information

Pairwise comparison of $\delta^{18}O$ values of pongines, suids and bovids

To facilitate a more accurate interpretation of the differences in $\delta^{18}O$ values we systematically compared the pongine values with those of bovids and suids. With this method we tried to estimate how much of the variation was a result of climate and temperature variations over time and what can be actually attributed to changes in the ecology of the fossil and modern pongines. Bovids and suids were chosen, because we have data from these taxonomic groups associated with all the pongines. The data used for this comparison are reported in Table SI 3.

At first, we explored how the $\delta^{18}O$ values vary within the taxonomic groups over the different geological eras (Fig. SI 1). Bovids and pongines show a very similar pattern of $\delta^{18}O$ variation with the exception of the Holocene where pongines show lower values. However, especially in the Early Pleistocene, from where most of the *Pongo* and *Gigantopithecus* samples are, there is much more variability in the pongines, as they continuously cover the whole range of $\delta^{18}O$ values. This is a first slight indication that there is the potential of interpreting the $\delta^{18}O$ in terms of differences in the ecological niches of fossil pongines. The suids do not show any variation in $\delta^{18}O$ except for lower values in the Holocene.

In both the pongines and the suids the Holocene values are lower than in the other eras. This can be attributed to the fact that all of the samples come from islands on the Sunda Shelf, whereas the data set for the Holocene bovids encompasses sites from the Southeast Asian mainland. Lower $\delta^{18}O$ values for the Sunda Shelf region were expected given the higher monsoon intensity there in comparison to mainland Southeast Asia. This is also confirmed by climate and vegetation models[35,36,47].

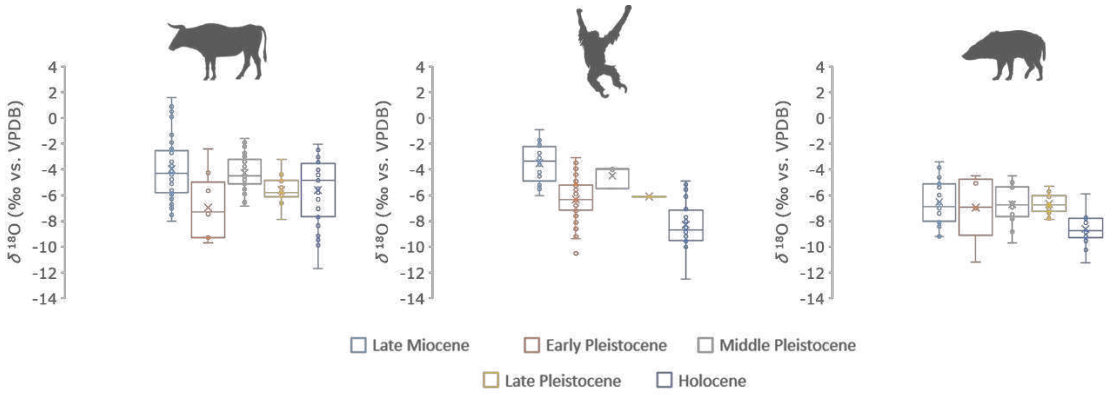

Fig. SI 1 Box plot of the $\delta^{18}O$ values of the three taxonomic groups (bovids – left, pongines – middle, suids – right) per geological era. Icons obtained via PhyloPic and in Public Domain.

In a second step, we plotted each fossil pongine next to the associated bovids and suids (Fig. SI 2). Although the relative positions of the pongines to the other two groups varies from genus to genus, bovids always have higher $\delta^{18}O$ values than suids. This is an indication that the differences in $\delta^{18}O$ values in fossil pongines has some significance for the specific ecological niches of the different genera and does not only reflect climatic changes over time.

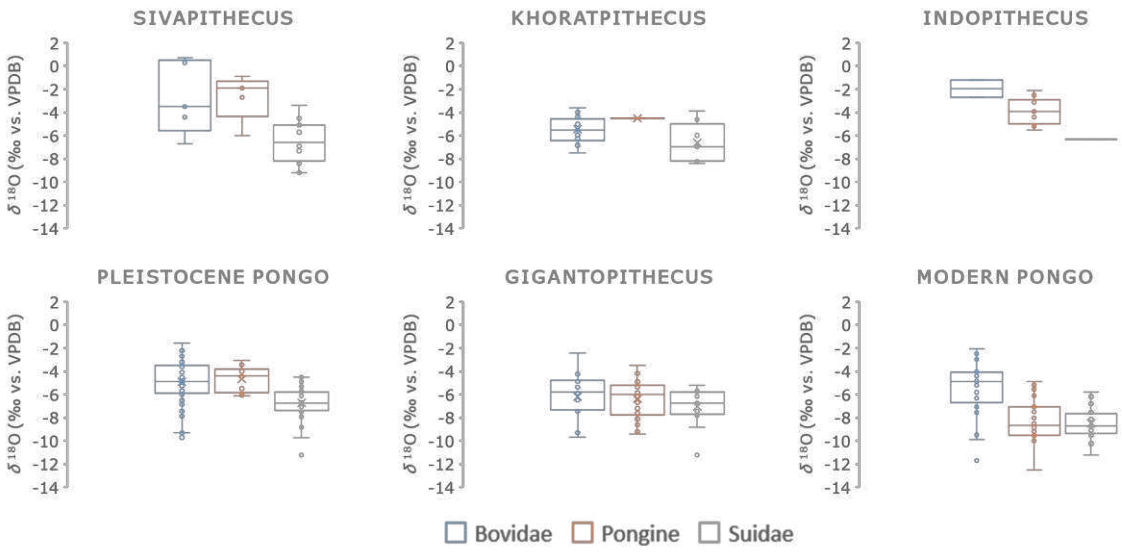

Fig. SI 2 Box plot of the $\delta^{18}O$ values of fossil and modern pongines with the associated bovids and suids.

Calculation of niche overlaps

Based on the isotopic niche modelling in SIBER we quantified the niche overlap based on the SEA_C, the standard ellipse area corrected for small sample sizes that is visualized in the plots in Fig. 4 and 5 using R. It is possible to calculate three different percentages for each overlapping instance, where A_O is the overlap area of the two SEA_Cs:

- The percentage of niche area of taxon A (A_A) that overlaps the niche space of taxon B (A_O/A_A)
- The percentage of niche area of taxon B (A_B) that overlaps the niche space of taxon A (A_O/A_B)
- The percentage of the total niche space of the two taxa that is shared between them, which is calculated with the following formula:

$$\%\ \text{overlap} = \frac{A_O}{A_A + A_B - A_O} \times 100 \quad \text{(SI 1)}$$

[71]

For the comparison of niche overlap between the different taxonomic groups and pongine genera we focused on the percentage of the total niche space, that is shared between the compared groups.

Niche overlap for the *Khoratpithecus* and *Sivapithecus* mammal faunas

To compare the structure of niche partitioning between the *Sivapithecus* and *Khoratpithecus* mammal fauna we calculated the % overlap between all the groups.

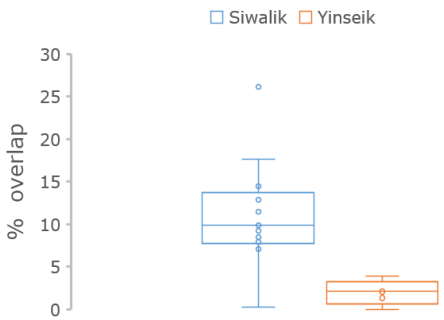

Fig. SI 3 Box plot of the *Sivapithecus* (Siwalik, left) and *Khoratpithecus* (Yinseik, right) mammal faunas comparing the niche overlap of the taxonomic groups (% overlap). Groups with an overlap of 0 % were not included in this plot.

A Wilcox rank sum test revealed, that the distributions are not significantly different (W = 273.5, p-value = 0.06895), when all the possible pairings between two taxonomic groups where the % overlap is 0 % are included. Hence, the isotopic niche modelling does not indicate a significantly heightened pressure due to competition in one of the two mammal communities. This would be consistent with an interpretation of the difference in dietary preference between the two fossil pongine genera based on dental microwear as being related to ecology and not to competition pressure.

If we do exclude all instances where the % overlap is zero (Fig. SI 3) the difference is significant (W = 48, p-value = 0.01008). According to this result, here is a difference in competition potential between the mammal community of *Sivapithecus* and *Khoratpithecus.* That could be an explanation of the incorporation of harder objects in the *Sivapithecus* diet. However, difference in the number of taxonomic groups present between the two datasets definitely has an impact on the statistical tests applied.

Including all the possible pairings between two taxonomic groups where the % overlap is 0 % resulting in mean values of 5.1 % for the *Sivapithecus* fauna and 2.4 % for the *Khoratpithecus* fauna. When excluded the mean % overlap shifts to 5.1 % for *Sivapithecus* and 0.8 % for the *Khoratpithecus* fauna. For the visualisation of the distribution of % overlap between the two communities we excluded these groups. A_O values and % overlap for each pairing is reported in Table SI 4.

Niche overlap between fossil and extant pongines

Gigantopithecus (G) and modern *Pongo* (mP) ($A_{O\ G\ mP}$ = 1.6) had the biggest niche overlap between the fossil and extant pongines (16.46 %), which is already clearly visible in Fig. 4, followed by *Sivapithecus* (S) and Pleistocene *Pongo* (PP) ($A_{O\ S\ PP}$ = 0.18) (3.91 %) and *Gigantopithecus* and Pleistocene *Pongo* ($A_{O\ G\ PP}$ = 0.2) (2.3 %). The most likely reason for the niche overlap between *Gigantopithecus* and modern *Pongo* not being bigger, is due to the bias introduced by the impact of climate differences between the Holocene Sunda Shelf and Pleistocene mainland Southeast Asia. This has been discussed in the chapter on the pairwise comparison of $\delta^{18}O$ values of pongine, bovid, and suid isotopic data. Given that we could only sample one specimen of *K. ayeyarwadyensis*, no Bayesian standard ellipse could be modelled for this taxon.

Supplementary Material

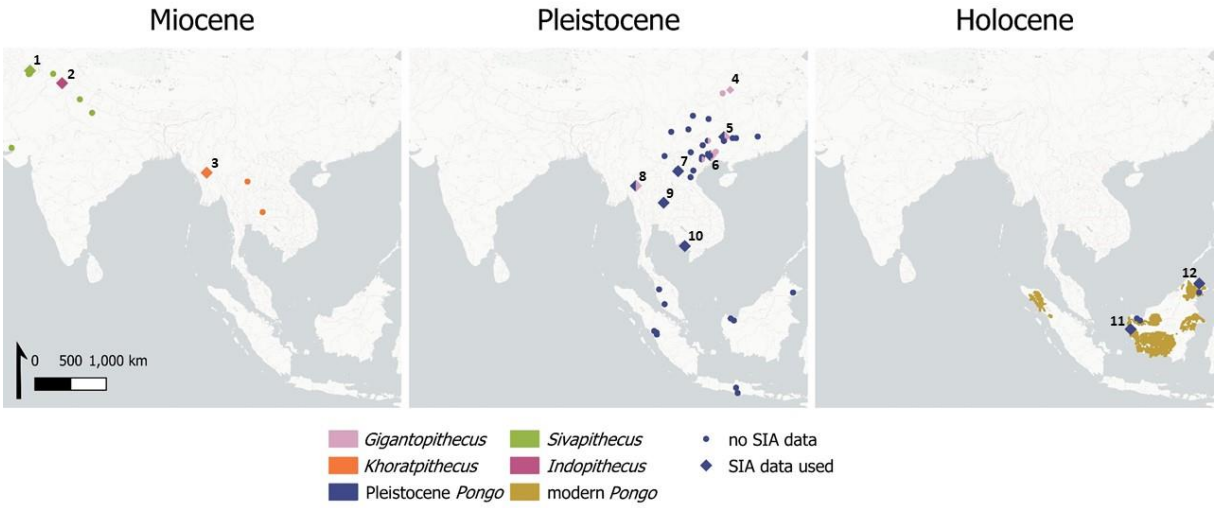

Fig. SI 4 Maps of fossil pongine localities from the Miocene to the Holocene including the current distribution. Sites from which stable isotope data was used in this study: 1 Dhok Parthan, Siwaliks, Pakistan; 2 Haritalyangar, Siwaliks, India; 3 Yinseik, Irrawaddy Fm., Myanmar; 4 Longgudong, Jianshi, China; 5 Juyuandong, Liucheng Cave, Guangxi, China; 6 Sanhe Cave, Guangxi, China; 7 Nam Lot, Laos; 8 Pha Bong, Thailand; 9 Thum Wiman Nakin, Thailand; 10 Boh Dambang, Cambodia; 11 Pontianak, Indonesia; 12 Sandakan, Malaysia. The map was created using QGIS 3.16.

Table SI 1 Summary statistics of the four late Miocene mammal communities we compared to get information on the palaeoecology of K. ayeyarwadyensis as well as the fossil to extant pongines used in the assessment of ecological continuity. TA refers to the convex hull area and SEA_C for the area of the modelled standard ellipses corrected for small sample sizes[17].

Taxonomic groups	n° specimen	$\delta^{13}C_{diet}$ (‰ vs. VPDB) mean	SD	$\delta^{18}O$ (‰ vs. VPDB) mean	SD	TA	SEA_C
Yinseik locality							
Giraffidae	11	-28.0	1.7	-4.4	1.2	6.2	8.3
Rhinocerotoidae	25	-27.6	1.0	-8.2	0.6	2.7	1.9
Proboscidea	32	-26.4	0.5	-6.7	0.8	1.9	1.5
Equidae*	7	-25.6	0.8	-5.5	1.9	5.5	5.5
Bovidae	17	-25.5	1.0	-6.5	1.0	6.5	3.4
Suidae	8	-22.4	0.7	-6.3	1.6	4.4	4.1
Chaingzauk locality							
Rhinocerotoidae	12	-26.8	0.7	-5.2	1.2	5.6	2.7
Proboscidea	13	-23.7	2.2	-7.1	1.1	17.1	7.7
Bovidae	19	-16.1	2.5	-4.0	1.3	27.3	10.4
Suidae	8	-22.4	1.3	-6.4	1.4	6.5	5.8
Hippopotamidae	16	-13.8	2.2	-7.4	1.1	16.2	7.8
Sivapithecus horizon							
Giraffidae	5	-26.2	2.0	-2.2	0.5	2.9	4.2
Gomphotheridae	4	-25.8	0.9	-5.5	1.0	1.3	2.5
Equidae	5	-23.3	0.5	-2.8	1.4	2.3	3.1
Bovidae	5	-25.8	0.4	-2.7	3.2	3.8	4.7
Suidae	15	-23.1	1.1	-6.5	1.7	11.8	6.2
Sivapithecus	5	-24.4	0.6	-2.6	2.0	1.6	1.9
Anthracotheriidae	4	-25.5	1.8	-6.4	0.7	3.0	5.5
Tragulidae	9	-25.3	0.8	-4.2	3.1	12.2	8.3
post-*Sivapithecus* horizon							
Giraffidae	4	-26.1	1.7	0.0	0.9	1.2	2.4
Rhinocerotoidae	5	-25.5	1.8	-3.6	0.4	1.9	2.6
Gomphotheridae	5	-25.6	1.0	-4.9	2.5	9.2	10.7
Equidae	5	-21.0	1.1	-2.0	1.0	3.8	4.2
Bovidae	15	-25.1	0.9	-2.8	3.0	18.4	8.6
Suidae	7	-22.4	0.6	-3.1	3.1	8.1	6.8
Tragulidae	5	-24.5	0.8	-2.6	0.8	1.9	2.4
other fossil and extant pongines							
Gigantopithecus	36	-26.7	1.2	-6.5	1.5	24.2	5.9
Pleistocene *Pongo*	10	-25.61	0.77	-4.67	1.10	5.1	3.0
modern *Pongo*	24	-26.18	0.98	-8.29	1.85	16.6	5.4
Indopithecus	1	-23.39	0.26	-3.85	1.19	1.3	0.8

Table SI 2 This table reports all the raw SIA data including metadata from the Miocene mammal faunas (including Khoratpithecus and Sivapithecus) from the Yinseik and Chaingzauk localities in Myanmar, the Sivapithecus and post-Sivapithecus horizons form the Siwaliks of Pakistan, as well as the modern bovid from Myanmar. We included both the raw data ($\delta^{13}C_{VPDB}$) as well as the corrections applied to each data point and the corrected values ($\delta^{13}C_{diet}$) used for our analysis. $\delta^{18}O_{SMOW}$ values were calculated using the formula proposed by Coplen [72].

Lab-Code	Locality	Age (Ma)	Taxon	Tooth	$\delta^{13}C_{VPDB}$	SD C	corrections		$\delta^{13}C_{diet}$	$\delta^{18}O_{VPDB}$	SD O	Dist. ERJ (mm)	$CaCO_3$ (%)	Ref.	Field/ museum ID
							ε^*	CO_2 atm.							
IRWD 1E	Yinseik	9.5	*Hipparion*	P3 or P4	-9.9	-	-14.0	-0.4	-24.3	-3.9	-	-	4.0	11	IF-19-12-07-9
IRWD 2E	Yinseik	9.5	*Hipparion*	left m3	-11.4	-	-14.0	-0.4	-25.8	-4.3	-	-	4.0	11	IF-28-12-07-5
IRWD 3E	Yinseik	9.5	*Hipparion*	left P2	-12.1	-	-14.0	-0.4	-26.5	-4.9	-	-	4.9	11	IF-26-12-07-1
IRWD 4E	Yinseik	9.5	*Hipparion*	premolar	-11.7	-	-14.0	-0.4	-26.1	-6.8	-	-	4.4	11	IF-26-12-07-2
IRWD 5E	Yinseik	9.5	*Hipparion*	left P3	-11.0	-	-14.0	-0.4	-25.4	-8.8	-	-	5.2	11	IF-26-12-07-16
IRWD 6E	Yinseik	9.5	*Hipparion*	-	-11.1	-	-14.0	-0.4	-25.5	-4.5	-	-	3.6	11	IF-26-12-07-11
IRWD 7E	Yinseik	9.5	*K. ayeyarwadyensis*	m3	-13.2	0.10	-11.0	-0.4	-24.6	-4.5	0.20	-	4.9	new	MFI-K-171
IRWD-8a	Yinseik	9.5	-	-	-14.0	0.03	-14.0	-0.4	-28.4	-8.0	-8.56	-	4.5	new	23/02/2017
IRWD-9a	Yinseik	9.5	-	molar	-12.1	0.10	-14.0	-0.4	-26.3	-6.0	-6.36	3	2.6	new	19 & 20/02/17
IRWD-9b	Yinseik	9.5	-	molar	-12.5	0.10	-14.0	-0.4	-26.8	-6.1	-6.50	7	2.7	new	19 & 20/02/17
IRWD-9c	Yinseik	9.5	-	molar	-12.7	0.08	-14.0	-0.4	-26.9	-6.4	-6.81	11	2.7	new	19 & 20/02/17
IRWD-9d	Yinseik	9.5	-	molar	-12.9	0.06	-14.0	-0.4	-27.2	-6.7	-7.15	14	2.9	new	19 & 20/02/17
IRWD-9e	Yinseik	9.5	-	molar	-12.9	0.12	-14.0	-0.4	-27.1	-7.3	-7.77	17	2.7	new	19 & 20/02/17
IRWD-9f	Yinseik	9.5	-	molar	-12.1	0.14	-14.0	-0.4	-26.4	-5.8	-6.17	20	2.7	new	19 & 20/02/17
IRWD-9g	Yinseik	9.5	-	molar	-12.2	0.06	-14.0	-0.4	-26.5	-5.0	-5.45	24	2.6	new	19 & 20/02/17
IRWD-9h	Yinseik	9.5	-	molar	-11.9	0.05	-14.0	-0.4	-26.2	-4.1	-4.44	27	2.9	new	19 & 20/02/17
IRWD-9i	Yinseik	9.5	-	molar	-12.4	0.03	-14.0	-0.4	-26.7	-6.1	-6.48	30	2.5	new	19 & 20/02/17
IRWD-9j	Yinseik	9.5	-	molar	-12.9	0.04	-14.0	-0.4	-27.1	-6.1	-6.56	35	3.0	new	19 & 20/02/17
IRWD-9k	Yinseik	9.5	-	molar	-13.1	0.05	-14.0	-0.4	-27.2	-6.7	-7.15	39	3.1	new	19 & 20/02/17
IRWD-9l	Yinseik	9.5	-	molar	-12.3	0.10	-14.0	-0.4	-26.5	-5.5	-5.82	43	3.7	new	19 & 20/02/17
IRWD-10	Yinseik	9.5	*Merycopotamus*	-	-12.1	0.14	-14.0	-0.4	-26.4	-9.9	-10.56	-	1.8	new	19/02/2017
IRWD-11	Yinseik	9.5	-	molar	-12.3	0.07	-14.0	-0.4	-26.7	-7.6	-8.11	-	4.1	new	21/02/2017
IRWD-12	Yinseik	9.5	-	molar	-12.0	0.05	-14.0	-0.4	-26.4	-6.2	-6.65	-	4.3	new	Fev 2017
IRWD-13	Yinseik	9.5	-	m3	-9.7	0.12	-14.0	-0.4	-24.1	-4.8	-5.15	-	3.3	new	IF-09-01-11-11
IRWD-14	Yinseik	9.5	-	m1	-11.4	0.05	-14.0	-0.4	-25.8	-6.3	-6.71	-	3.2	new	IF-28-12-07-3
IRWD-15	Yinseik	9.5	-	P3	-11.3	0.07	-14.0	-0.4	-25.7	-5.5	-5.95	-	3.0	new	IRRAW.09.4
IRWD-16	Yinseik	9.5	-	P4	-12.5	0.04	-14.0	-0.4	-26.9	-5.9	-6.38	-	3.2	new	IF-10-1-11-15
IRWD-17a	Yinseik	9.5	-	M	-10.3	0.06	-14.0	-0.4	-24.6	-4.8	-5.23	2	3.7	new	IF-14-01-11-4
IRWD-17b	Yinseik	9.5	-	M	-11.0	0.01	-14.0	-0.4	-25.2	-4.4	-4.75	4	3.4	new	IF-14-01-11-4
IRWD-17c	Yinseik	9.5	-	M	-11.0	0.09	-14.0	-0.4	-25.3	-3.6	-3.89	6	3.2	new	IF-14-01-11-4
IRWD-17d	Yinseik	9.5	-	M	-11.1	0.08	-14.0	-0.4	-25.4	-3.7	-4.05	8	3.6	new	IF-14-01-11-4
IRWD-17e	Yinseik	9.5	-	M	-10.9	0.06	-14.0	-0.4	-25.2	-4.0	-4.32	10	3.2	new	IF-14-01-11-4
IRWD-17f	Yinseik	9.5	-	M	-10.9	0.07	-14.0	-0.4	-25.2	-5.0	-5.39	12	3.4	new	IF-14-01-11-4
IRWD-17g	Yinseik	9.5	-	M	-11.0	0.07	-14.0	-0.4	-25.3	-5.0	-5.42	14	3.7	new	IF-14-01-11-4
IRWD-18	Yinseik	9.5	-	M	-11.1	0.07	-14.0	-0.4	-25.5	-6.6	-7.12	-	3.1	new	IR-19-12-07-13
IRWD-19E	Yinseik	9.5	-	m3	-9.6	0.10	-14.0	-0.4	-24.0	-6.8	-7.31	-	2.8	new	IF-28-12-07-1
IRWD-20E	Yinseik	9.5	-	m2	-12.3	0.04	-14.0	-0.4	-26.7	-6.6	-7.02	-	3.5	new	IF-26-12-07-03
IRWD-21	Yinseik	9.5	-	M	-12.4	0.06	-14.0	-0.4	-26.8	-6.2	-6.64	-	2.8	new	IF-10-1-11-8
IRWD-22	Yinseik	9.5	-	M3	-11.0	0.06	-14.0	-0.4	-25.4	-7.5	-8.01	-	3.0	new	IF-28-12-07-4
IRWD-23	Yinseik	9.5	-	m3	-10.0	0.04	-14.0	-0.4	-24.4	-5.7	-6.14	-	2.3	new	IF-14-1-11-2
IRWD-24E	Yinseik	9.5	-	right M	-10.9	0.08	-14.0	-0.4	-25.3	-5.6	-5.98	-	1.3	new	19/2/17 morning
IRWD-25E	Yinseik	9.5	*Stegolophodon*	m	-12.0	0.06	-14.0	-0.4	-26.4	-7.1	-7.59	-	2.8	new	IF-11-1-11-1
IRWD-26a	Yinseik	9.5	*Stegolophodon*	molar	-11.1	0.02	-14.0	-0.4	-25.4	-6.2	-6.64	0.5	4.8	new	IF-11-1-11-09
IRWD-26b	Yinseik	9.5	*Stegolophodon*	molar	-11.9	0.04	-14.0	-0.4	-26.2	-5.5	-5.89	2	3.1	new	IF-11-01-11-9
IRWD-26c	Yinseik	9.5	*Stegolophodon*	molar	-12.4	0.05	-14.0	-0.4	-26.6	-6.1	-6.55	5	3.2	new	IF-11-01-11-9
IRWD-26d	Yinseik	9.5	*Stegolophodon*	molar	-12.6	0.06	-14.0	-0.4	-26.8	-6.5	-7.03	7	2.4	new	IF-11-01-11-9
IRWD-26e	Yinseik	9.5	*Stegolophodon*	molar	-12.7	0.11	-14.0	-0.4	-26.9	-6.8	-7.26	9	2.1	new	IF-11-01-11-9
IRWD-26f	Yinseik	9.5	*Stegolophodon*	molar	-12.1	0.29	-14.0	-0.4	-26.3	-6.1	-5.78	11	2.4	new	IF-11-01-11-9
IRWD-26g	Yinseik	9.5	*Stegolophodon*	molar	-12.2	0.09	-14.0	-0.4	-26.3	-6.4	-6.06	13	2.4	new	IF-11-01-11-9
IRWD-26h	Yinseik	9.5	*Stegolophodon*	molar	-12.4	0.04	-14.0	-0.4	-26.5	-6.1	-5.83	15	2.5	new	IF-11-01-11-9
IRWD-26i	Yinseik	9.5	*Stegolophodon*	molar	-12.5	0.15	-14.0	-0.4	-26.8	-6.5	-5.63	17.3	1.7	new	IF-11-01-11-9
IRWD-26j	Yinseik	9.5	*Stegolophodon*	molar	-12.4	0.08	-14.0	-0.4	-26.8	-6.5	-5.47	19.4	1.4	new	IF-11-01-11-9
IRWD-26k	Yinseik	9.5	*Stegolophodon*	molar	-12.1	0.15	-14.0	-0.4	-26.9	-6.6	-5.50	21.5	1.2	new	IF-11-01-11-9
IRWD-26l	Yinseik	9.5	*Stegolophodon*	molar	-12.1	0.09	-14.0	-0.4	-27.0	-6.6	-5.29	23.6	0.9	new	IF-11-01-11-9
IRWD-26m	Yinseik	9.5	*Stegolophodon*	molar	-11.8	0.06	-14.0	-0.4	-27.1	-6.7	-5.65	25.7	0.6	new	IF-11-01-11-9
IRWD-26n	Yinseik	9.5	*Stegolophodon*	molar	-11.8	0.06	-14.0	-0.4	-27.2	-6.7	-5.15	27.8	0.4	new	IF-11-01-11-9
IRWD-27	Yinseik	9.5	-	molar	-12.5	0.03	-14.0	-0.4	-26.9	-6.5	-6.18	-	3.4	new	IF-19-12-07-8
IRWD-28	Yinseik	9.5	-	molar	-11.1	0.05	-14.0	-0.4	-25.5	-6.2	-5.90	-	6.5	new	IF-19-12-07-10
IRWD-29	Yinseik	9.5	-	molar	-11.3	0.04	-14.0	-0.4	-25.7	-7.3	-6.93	-	5.7	new	IF-26-12-07-12
IRWD-31a	Yinseik	9.5	-	M3	-13.9	0.06	-14.0	-0.4	-27.9	-6.1	-5.89	1	4.5	new	IF-09-01-11-2
IRWD-31b	Yinseik	9.5	-	M3	-13.5	0.03	-14.0	-0.4	-27.5	-6.9	-6.61	3	3.6	new	IF-09-01-11-2
IRWD-31c	Yinseik	9.5	-	M3	-13.9	0.06	-14.0	-0.4	-27.9	-8.1	-7.85	6	3.1	new	IF-09-01-11-2
IRWD-31d	Yinseik	9.5	-	M3	-13.8	0.03	-14.0	-0.4	-27.8	-8.3	-8.07	8	2.9	new	IF-09-01-11-2
IRWD-31e	Yinseik	9.5	-	M3	-13.7	0.15	-14.0	-0.4	-27.7	-8.1	-7.90	11	2.0	new	IF-09-01-11-2
IRWD-31f	Yinseik	9.5	-	M3	-13.7	0.08	-14.0	-0.4	-27.6	-7.3	-7.00	13	2.7	new	IF-09-01-11-2
IRWD-31g	Yinseik	9.5	-	M3	-13.5	0.09	-14.0	-0.4	-27.5	-7.6	-7.33	16	2.0	new	IF-09-01-11-2
IRWD-31h	Yinseik	9.5	-	M3	-13.7	0.11	-14.0	-0.4	-27.7	-8.1	-7.84	18	2.1	new	IF-09-01-11-2
IRWD-31i	Yinseik	9.5	-	M3	-13.7	0.06	-14.0	-0.4	-27.6	-8.8	-8.54	21	2.5	new	IF-09-01-11-2
IRWD-31j	Yinseik	9.5	-	M3	-13.6	0.05	-14.0	-0.4	-27.5	-8.8	-8.54	24	2.8	new	IF-09-01-11-2
IRWD-31k	Yinseik	9.5	-	M3	-13.8	0.12	-14.0	-0.4	-27.7	-8.1	-7.91	27	2.4	new	IF-09-01-11-2
IRWD-31l	Yinseik	9.5	-	M3	-13.7	0.11	-14.0	-0.4	-27.6	-7.4	-7.12	29	2.1	new	IF-09-01-11-2
IRWD-31m	Yinseik	9.5	-	M3	-13.8	0.07	-14.0	-0.4	-27.7	-7.8	-7.62	32	2.6	new	IF-09-01-11-2
IRWD-31n	Yinseik	9.5	-	M3	-13.8	0.10	-14.0	-0.4	-27.8	-8.3	-7.99	34	2.5	new	IF-09-01-11-2
IRWD-31o	Yinseik	9.5	-	M3	-13.7	0.03	-14.0	-0.4	-27.6	-8.6	-8.37	37	3.0	new	IF-09-01-11-2
IRWD-31p	Yinseik	9.5	-	M3	-13.7	0.07	-14.0	-0.4	-27.7	-8.1	-7.83	39	3.1	new	IF-09-01-11-2
IRWD-31q	Yinseik	9.5	-	M3	-13.6	0.06	-14.0	-0.4	-27.6	-7.4	-7.14	41	3.9	new	IF-09-01-11-2
IRWD-32	Yinseik	9.5	-	m	-13.1	0.14	-14.0	-0.4	-27.5	-7.8	-7.55	-	2.7	new	MFI-67
IRWD-33	Yinseik	9.5	-	m	-14.3	0.07	-14.0	-0.4	-28.7	-8.3	-8.01	-	3.3	new	IF-07-01-11-4
IRWD-34	Yinseik	9.5	-	P	-11.3	0.65	-14.0	-0.4	-25.7	-9.3	-9.30	-	2.9	new	IF-10-01-11-10
IRWD-35E	Yinseik	9.5	-	m	-12.6	0.04	-14.0	-0.4	-27.0	-9.1	-8.91	-	1.5	new	IF-26-12-07-8
IRWD-36E	Yinseik	9.5	-	M	-14.0	0.06	-14.0	-0.4	-28.4	-8.1	-7.90	-	3.1	new	IF-19-12-07-11
IRWD-37	Yinseik	9.5	-	-	-12.4	0.09	-14.0	-0.4	-26.8	-7.8	-7.63	-	2.4	new	IF-11-1-11-3
IRWD-38E	Yinseik	9.5	-	p4	-13.4	0.12	-14.0	-0.4	-27.8	-8.7	-8.51	-	2.8	new	IF-09-01-11-1
IRWD-39E	Yinseik	9.5	-	left m1	-16.5	0.06	-14.0	-0.4	-30.9	-4.8	-4.52	-	3.9	new	IF-26-02-13-1

IRWD-40	Yinseik	9.5	-	M	-13.3	0.08	-14.0	-0.4	-27.7	-3.8	-3.55	-	4.1	new	IF-27-02-13-1
IRWD-41	Yinseik	9.5	-	M	-12.4	0.05	-14.0	-0.4	-26.8	-5.8	-5.32	-	3.6	new	MFI-52
IRWD-42a	Yinseik	9.5	-	left p4	-13.6	0.04	-14.0	-0.4	-27.6	-7.5	-7.03	0.5	4.1	new	IF-09-01-11-5
IRWD-42b	Yinseik	9.5	-	left p4	-13.4	0.10	-14.0	-0.4	-27.5	-7.4	-6.94	3	2.7	new	IF-09-01-11-5
IRWD-42c	Yinseik	9.5	-	left p4	-13.1	0.07	-14.0	-0.4	-27.1	-7.2	-6.72	6	3.4	new	IF-09-01-11-5
IRWD-42d	Yinseik	9.5	-	left p4	-13.2	0.02	-14.0	-0.4	-27.3	-6.7	-6.23	8	3.6	new	IF-09-01-11-5
IRWD-42e	Yinseik	9.5	-	left p4	-13.3	0.09	-14.0	-0.4	-27.4	-5.2	-4.91	11	3.6	new	IF-09-01-11-5
IRWD-42f	Yinseik	9.5	-	left p4	-13.3	0.07	-14.0	-0.4	-27.4	-4.6	-4.31	13	3.7	new	IF-09-01-11-5
IRWD-42g	Yinseik	9.5	-	left p4	-13.5	0.08	-14.0	-0.4	-27.5	-4.7	-4.35	16	3.6	new	IF-09-01-11-5
IRWD-43E	Yinseik	9.5	-	M	-12.4	0.05	-14.0	-0.4	-26.8	-3.3	-3.04	-	3.3	new	IF-28-12-07-2
IRWD-44	Yinseik	9.5	*Propotamo-choerus*	left M3	-11.2	0.11	-11.0	-0.4	-22.6	-8.3	-7.75	-	2.8	new	IF-07-01-11-1
IRWD-45	Yinseik	9.5	*Tetraconodon Minor*	P4	-11.5	0.12	-11.0	-0.4	-22.9	-6.0	-5.67	-	2.9	new	IF-2X-02-12-1
IRWD-46	Yinseik	9.5	*Propotamo-choerus*	m2	-12.4	0.06	-11.0	-0.4	-23.8	-6.9	-6.54	-	3.4	new	IF-07-01-11-6
IRWD-47	Yinseik	9.5	*Propotamo-choerus*	m3	-10.7	0.14	-11.0	-0.4	-22.1	-8.0	-7.63	-	2.6	new	MFI-59
IRWD-48	Yinseik	9.5	*Hippopotamodon*	m3	-10.5	0.12	-11.0	-0.4	-21.9	-6.9	-6.56	-	2.8	new	MFI-51
IRWD-49	Yinseik	9.5	*Tetraconodon Minor*	m3	-10.6	0.11	-11.0	-0.4	-22.0	-8.4	-7.98	-	2.5	new	IF-26-12-07-5
IRWD-50	Yinseik	9.5	*Propotamo-choerus*	M3	-10.2	0.13	-11.0	-0.4	-21.6	-3.8	-3.60	-	3.0	new	IF-09-01-11-6
IRWD-50BIS	Yinseik	9.5	*Propotamo-choerus*	M1	-10.5	0.05	-11.0	-0.4	-21.9	-4.6	-4.35	-	3.6	new	-
PND-M1a	Central Basin Myanmar	modern	*Bos*	M1	-1.3	0.07	-14.0	1.5	-13.8	-3.0	0.12	3	4.9	new	-
PND-M1b	Central Basin Myanmar	modern	*Bos*	M1	-1.2	0.07	-14.0	1.5	-13.7	-1.3	0.16	6	4.0	new	-
PND-M1c	Central Basin Myanmar	modern	*Bos*	M1	-2.0	0.08	-14.0	1.5	-14.5	-0.8	0.14	9	4.5	new	-
PND-M1d	Central Basin Myanmar	modern	*Bos*	M1	-2.6	0.11	-14.0	1.5	-15.1	-0.4	0.10	11	3.4	new	-
PND-M1e	Central Basin Myanmar	modern	*Bos*	M1	-2.9	0.07	-14.0	1.5	-15.4	-0.7	0.14	13	3.7	new	-
PND-M1f	Central Basin Myanmar	modern	*Bos*	M1	-2.5	0.05	-14.0	1.5	-15.0	-1.0	0.05	16	4.3	new	-
PND-M1g	Central Basin Myanmar	modern	*Bos*	M1	-2.5	0.09	-14.0	1.5	-15.0	-1.3	0.12	18	3.8	new	-
PND-M1h	Central Basin Myanmar	modern	*Bos*	M1	-2.4	0.05	-14.0	1.5	-14.9	-1.9	0.12	21	3.5	new	-
PND-M1i	Central Basin Myanmar	modern	*Bos*	M1	-2.2	0.06	-14.0	1.5	-14.7	-2.4	0.15	24	3.4	new	-
PND-M1j	Central Basin Myanmar	modern	*Bos*	M1	-2.7	0.05	-14.0	1.5	-15.2	-2.6	0.17	26	4.1	new	-
PND-M1k	Central Basin Myanmar	modern	*Bos*	M1	-2.1	0.02	-14.0	1.5	-14.6	-2.9	0.09	28	3.2	new	-
PND-M1l	Central Basin Myanmar	modern	*Bos*	M1	-2.1	0.06	-14.0	1.5	-14.6	-3.7	0.08	31	3.7	new	-
PND-M1m	Central Basin Myanmar	modern	*Bos*	M1	-1.6	0.10	-14.0	1.5	-14.1	-3.7	0.04	34	3.4	new	-
PND-M1n	Central Basin Myanmar	modern	*Bos*	M1	-1.5	0.08	-14.0	1.5	-14.0	-5.7	0.13	36	3.0	new	-
PND-M1o	Central Basin Myanmar	modern	*Bos*	M1	-1.5	0.05	-14.0	1.5	-14.0	-3.9	0.12	39	3.4	new	-
PND-M1p	Central Basin Myanmar	modern	*Bos*	M1	-1.5	0.05	-14.0	1.5	-14.0	-1.4	0.08	41	3.0	new	-
PND-Mq	Central Basin Myanmar	modern	*Bos*	M1	-1.5	0.06	-14.0	1.5	-14.0	-2.0	0.08	44	3.3	new	-
PND-M1r	Central Basin Myanmar	modern	*Bos*	M1	-1.4	0.05	-14.0	1.5	-13.9	-1.7	0.03	48	3.8	new	-
PND-M1s	Central Basin Myanmar	modern	*Bos*	M1	-2.2	0.06	-14.0	1.5	-14.7	-2.1	0.06	52	3.0	new	-
IR1306	Chaingzauk	6	*Merycopotamus*	P4	-1.1	-	-14.0	0.0	-15.1	-6.4	-	-	-	25	-
IR0819	Chaingzauk	6	*Cf. Tragopartax*	m3	-2.7	-	-14.0	0.0	-16.7	-4.1	-	-	-	25	-
IR1104	Chaingzauk	6	*Cf. Tragopartax*	m3	-6.1	-	-14.0	0.0	-20.1	-4.3	-	-	-	25	-
IR0809	Chaingzauk	6	*cf. S. vexillaris*	m3	-2.7	-	-14.0	0.0	-16.7	-3.9	-	-	-	25	-
IR0811	Chaingzauk	6	*cf. S. vexillaris*	m3	-0.7	-	-14.0	0.0	-14.7	-1.9	-	-	-	25	-
IR0823	Chaingzauk	6	*cf. S. vexillaris*	m3	1.9	-	-14.0	0.0	-12.1	-2.7	-	-	-	25	-
IR0824	Chaingzauk	6	*cf. S. vexillaris*	m3	0.9	-	-14.0	0.0	-13.1	-4.1	-	-	-	25	-

IR0827	Chaingzauk	6	*cf. S. vexillaris*	m2	-1.8	-	-14.0	0.0	-15.8	-4.3	-	-	-	25	-
IR1094	Chaingzauk	6	*cf. S. vexillaris*	m3	1.0	-	-14.0	0.0	-13.0	-6.0	-	-	-	25	-
IR1170	Chaingzauk	6	*cf. S. vexillaris*	m1	-0.7	-	-14.0	0.0	-14.7	-3.7	-	-	-	25	-
IR0808	Chaingzauk	6	*cf. S. lydekkeri*	m2	0.2	-	-14.0	0.0	-13.8	-2.4	-	-	-	25	-
IR0817	Chaingzauk	6	*cf. S. lydekkeri*	m3	-2.9	-	-14.0	0.0	-16.9	-2.6	-	-	-	25	-
IR0818	Chaingzauk	6	*cf. S. lydekkeri*	m3	-2.1	-	-14.0	0.0	-16.1	-2.3	-	-	-	25	-
IR0828	Chaingzauk	6	*cf. S. lydekkeri*	m3	-3.5	-	-14.0	0.0	-17.5	-5.0	-	-	-	25	-
IR0826	Chaingzauk	6	*cf. S. lydekkeri*	m3	-4.0	-	-14.0	0.0	-18.0	-5.6	-	-	-	25	-
IR0825	Chaingzauk	6	*cf. S. lydekkeri*	p4	-1.4	-	-14.0	0.0	-15.4	-4.9	-	-	-	25	-
IR1194	Chaingzauk	6	*cf. S. lydekkeri*	m3	-8.1	-	-14.0	0.0	-22.1	-3.6	-	-	-	25	-
IR1105	Chaingzauk	6	*cf. S. lydekkeri*	m1	-5.2	-	-14.0	0.0	-19.2	-5.7	-	-	-	25	-
IR1204	Chaingzauk	6	*cf. S. lydekkeri*	m3	-1.2	-	-14.0	0.0	-15.2	-3.4	-	-	-	25	-
IR1092	Chaingzauk	6	*cf. S. lydekkeri*	m3	-0.5	-	-14.0	0.0	-14.5	-5.6	-	-	-	25	-
IR0544	Chaingzauk	6	*Sinomastodon*	m3	-10.9	-	-14.0	0.0	-24.9	-6.8	-	-	-	25	-
IR0797	Chaingzauk	6	*Hexaprotodon iravaticus*	m2	-1.7	-	-14.0	0.0	-15.7	-7.8	-	-	-	25	-
IR0802	Chaingzauk	6	*Hexaprotodon sivalensis*	M3	-0.4	-	-14.0	0.0	-14.4	-6.0	-	-	-	25	-
IR0803	Chaingzauk	6	*Hexaprotodon sivalensis*	canine	-1.2	-	-14.0	0.0	-15.2	-6.6	-	-	-	25	-
IR0806	Chaingzauk	6	*Hexaprotodon sivalensis*	M3	-1.2	-	-14.0	0.0	-15.2	-6.6	-	-	-	25	-
IR0807	Chaingzauk	6	*Hexaprotodon sivalensis*	P4	-1.0	-	-14.0	0.0	-15.0	-6.3	-	-	-	25	-
IR0815	Chaingzauk	6	*Hexaprotodon*	canine	0.7	-	-14.0	0.0	-13.3	-6.7	-	-	-	25	-
IR1332	Chaingzauk	6	*Hexaprotodon*	m3	2.5	-	-14.0	0.0	-11.5	-6.2	-	-	-	25	-
IR1124	Chaingzauk	6	*Hexaprotodon*	canine	2.7	-	-14.0	0.0	-11.3	-7.5	-	-	-	25	-
IR1125	Chaingzauk	6	*Hexaprotodon*	m3	0.8	-	-14.0	0.0	-13.2	-8.4	-	-	-	25	-
IR1126	Chaingzauk	6	*Hexaprotodon*	M2	-6.2	-	-14.0	0.0	-20.2	-9.9	-	-	-	25	-
IR1128	Chaingzauk	6	*Hexaprotodon iravaticus*	m3	0.2	-	-14.0	0.0	-13.8	-8.9	-	-	-	25	-
IR1129	Chaingzauk	6	*Hexaprotodon*	m3	0.9	-	-14.0	0.0	-13.1	-8.1	-	-	-	25	-
IR1268	Chaingzauk	6	*Hexaprotodon*	p4	0.6	-	-14.0	0.0	-13.4	-5.8	-	-	-	25	-
IR1273	Chaingzauk	6	*Hexaprotodon*	canine	2.2	-	-14.0	0.0	-11.8	-7.8	-	-	-	25	-
IR1310	Chaingzauk	6	*Hexaprotodon sivalensis*	m3	2.1	-	-14.0	0.0	-11.9	-7.5	-	-	-	25	-
IR1333	Chaingzauk	6	*Hexaprotodon*	m3	1.7	-	-14.0	0.0	-12.3	-7.5	-	-	-	25	-
IR0294	Chaingzauk	6	*Rhinoceros*	molar	-11.9	-	-14.0	0.0	-25.9	-3.3	-	-	-	25	-
IR0820	Chaingzauk	6	*Rhinoceros*	m3	-12.8	-	-14.0	0.0	-26.8	-5.5	-	-	-	25	-
IR0991	Chaingzauk	6	*Rhinoceros*	molar	-12.3	-	-14.0	0.0	-26.3	-5.4	-	-	-	25	-
IR1133	Chaingzauk	6	*Rhinoceros*	m1	-13.8	-	-14.0	0.0	-27.8	-3.3	-	-	-	25	-
IR1134	Chaingzauk	6	*Rhinoceros*	P3	-14.0	-	-14.0	0.0	-28.0	-4.4	-	-	-	25	-
IR1135	Chaingzauk	6	*Rhinoceros*	M3	-12.0	-	-14.0	0.0	-26.0	-6.2	-	-	-	25	-
IR1136	Chaingzauk	6	*Rhinoceros*	P2	-12.7	-	-14.0	0.0	-26.7	-5.5	-	-	-	25	-
IR 1138	Chaingzauk	6	*Rhinoceros*	m1	-13.3	-	-14.0	0.0	-27.3	-3.7	-	-	-	25	-
IR1139	Chaingzauk	6	*Rhinoceros*	p3	-12.8	-	-14.0	0.0	-26.8	-5.3	-	-	-	25	-
IR1140	Chaingzauk	6	*Rhinoceros*	P2	-13.2	-	-14.0	0.0	-27.2	-5.6	-	-	-	25	-
IR1260	Chaingzauk	6	*Rhinoceros*	P3	-12.5	-	-14.0	0.0	-26.5	-7.3	-	-	-	25	-
IR1335	Chaingzauk	6	*Rhinoceros*	molar	-12.0	-	-14.0	0.0	-26.0	-6.3	-	-	-	25	-
IR0800	Chaingzauk	6	*Stegodon*	molar	-11.7	-	-14.0	0.0	-25.7	-7.3	-	-	-	25	-
IR0821	Chaingzauk	6	*Stegodon*	molar	-9.9	-	-14.0	0.0	-23.9	-7.5	-	-	-	25	-
IR1143	Chaingzauk	6	*Stegodon*	molar	-10.6	-	-14.0	0.0	-24.6	-6.5	-	-	-	25	-
IR1144	Chaingzauk	6	*Stegodon*	molar	-12.6	-	-14.0	0.0	-26.6	-7.9	-	-	-	25	-
IR1150	Chaingzauk	6	*Stegodon*	molar	-12.1	-	-14.0	0.0	-26.1	-7.6	-	-	-	25	-
IR1152	Chaingzauk	6	*Stegodon*	molar	-6.6	-	-14.0	0.0	-20.6	-7.0	-	-	-	25	-

IR1159	Chaingzauk	6	*Stegodon*	molar	-11.6	-	-14.0	0.0	-25.6	-6.5	-	-	-	25	-
IR1151	Chaingzauk	6	*Stegodon*	molar	-5.4	-	-14.0	0.0	-19.4	-4.8	-	-	-	25	-
IR1153	Chaingzauk	6	*Stegodon*	molar	-10.7	-	-14.0	0.0	-24.7	-9.2	-	-	-	25	-
IR1157	Chaingzauk	6	*Stegodon*	molar	-9.0	-	-14.0	0.0	-23.0	-6.6	-	-	-	25	-
IR1158	Chaingzauk	6	*Stegodon*	molar	-9.3	-	-14.0	0.0	-23.3	-6.9	-	-	-	25	-
IR1161	Chaingzauk	6	*Stegodon*	molar	-7.0	-	-14.0	0.0	-21.0	-8.4	-	-	-	25	-
IR1162	Chaingzauk	6	*Stegodon*	molar	-10.2	-	-14.0	0.0	-24.2	-6.2	-	-	-	25	-
IR0805	Chaingzauk	6	*Sivachoerus*	m3	-10.4	-	-11.0	0.0	-21.4	-6.9	-	-	-	25	-
IR0553	Chaingzauk	6	*Sivachoerus*	M3	-12.1	-	-11.0	0.0	-23.1	-5.1	-	-	-	25	-
IR0812	Chaingzauk	6	*Sivachoerus*	m2	-13.8	-	-11.0	0.0	-24.8	-3.6	-	-	-	25	-
IR0813	Chaingzauk	6	*Sivachoerus*	m3	-10.4	-	-11.0	0.0	-21.4	-6.6	-	-	-	25	-
IR0814	Chaingzauk	6	*Sivachoerus*	m3	-12.3	-	-11.0	0.0	-23.3	-8.1	-	-	-	25	-
IR0804	Chaingzauk	6	*Propotamochoerus*	m2	-12.0	-	-11.0	0.0	-23.0	-7.4	-	-	-	25	-
IR0816	Chaingzauk	6	*Propotamochoerus*	m2	-10.0	-	-11.0	0.0	-21.0	-7.0	-	-	-	25	-
IR1458	Chaingzauk	6	*Propotamochoerus*	m3	-10.4	-	-11.0	0.0	-21.4	-6.4	-	-	-	25	-
IR1308	Chaingzauk	6	*Dorcabune*	m2	-9.7	-	-14.0	0.0	-23.7	-6.3	-	-	-	25	-
IR0542	Chaingzauk	6	*Agriotherium*	m3	-3.6	-	-9.0	0.0	-12.6	-8.2	-	-	-	25	-
Y47024	Y317	9.3–9.2	*Sivapithecus*	-	-12.4	-	-11	-0.4	-23.8	-0.9	-	-	-	17	-
Y13933	Y260	9.3–9.2	*Sivapithecus*	-	-13.1	-	-11	-0.4	-24.5	-1.9	-	-	-	17	-
Y47023	Y182	9.3–9.2	*Sivapithecus*	-	-12.8	-	-11	-0.4	-24.2	-1.7	-	-	-	17	-
Y47021	Y182	9.3–9.2	*Sivapithecus*	-	-13.9	-	-11	-0.4	-25.3	-6	-	-	-	17	-
Y13811	Y224	9.3–9.2	*Sivapithecus*	-	-12.7	-	-11	-0.4	-24.1	-2.7	-	-	-	17	-
SN2	Y260	9.3–9.2	*Gomphothere*	-	-12	-	-14	-0.4	-26.4	-5.5	-	-	-	17	-
Y5290	Y211	9.3–9.2	*Gomphothere*	-	-12	-	-14	-0.4	-26.4	-5.8	-	-	-	17	-
Y11022	Y313	9.3–9.2	*Gomphothere*	-	-11.6	-	-14	-0.4	-26	-6.5	-	-	-	17	-
SN1	KL01	9.3–9.2	*Gomphothere*	-	-10.1	-	-14	-0.4	-24.5	-4.1	-	-	-	17	-
Y3548	Y163	9.3–9.2	*Bramatherium megacephalum*	-	-14.6	-	-14	-0.4	-29	-2	-	-	-	17	-
Y16759	KL03	9.3–9.2	*Bramatherium megacephalum*	-	-13.2	-	-14	-0.4	-27.6	-2	-	-	-	17	-
Y10296	Y309	9.3–9.2	*Bramatherium megacephalum*	-	-10.7	-	-14	-0.4	-25.1	-1.9	-	-	-	17	-
Y40145	Y403	9.3–9.2	*Bramatherium megacephalum*	-	-10.2	-	-14	-0.4	-24.6	-2	-	-	-	17	-
Y11678	Y317	9.3–9.2	*Bramatherium megacephalum*	-	-10.2	-	-14	-0.4	-24.6	-3.2	-	-	-	17	-
Y14502	Y269	9.3–9.2	*Propotamocherus hysudricus*	-	-11	-	-11	-0.4	-22.4	-6.9	-	-	-	17	-
Y41368	Y269	9.3–9.2	*Propotamocherus hysudricus*	-	-12.9	-	-11	-0.4	-24.3	-9.2	-	-	-	17	-
Y4554	Y182	9.3–9.2	*Propotamocherus hysudricus*	-	-12.6	-	-11	-0.4	-24	-5.4	-	-	-	17	-
Y6753	Y227	9.3–9.2	*Propotamocherus hysudricus*	-	-11	-	-11	-0.4	-22.4	-5.7	-	-	-	17	-
Y10224	Y309	9.3–9.2	*Propotamocherus hysudricus*	-	-12	-	-11	-0.4	-23.4	-8.4	-	-	-	17	-
Y11007	Y314	9.3–9.2	*Propotamocherus hysudricus*	-	-11.2	-	-11	-0.4	-22.6	-8.2	-	-	-	17	-
Y13524	Y239	9.3–9.2	*Hippopotamodon sivalense*	-	-10.8	-	-11	-0.4	-22.2	-7.3	-	-	-	17	-
Y47176	Y159	9.3–9.2	*Hippopotamodon sivalense*	-	-11.4	-	-11	-0.4	-22.8	-6.6	-	-	-	17	-
Y12708	Y260	9.3–9.2	*Hippopotamodon sivalense*	-	-11.7	-	-11	-0.4	-23.1	-4.5	-	-	-	17	-
Y5276	Y211	9.3–9.2	*Hippopotamodon sivalense*	-	-9.4	-	-11	-0.4	-20.8	-7	-	-	-	17	-
Y4226	Y182	9.3–9.2	*Hippopotamodon sivalense*	-	-10.8	-	-11	-0.4	-22.2	-5.1	-	-	-	17	-
Y27915	Y260	9.3–9.2	*Hippopotamodon sivalense*	-	-11.2	-	-11	-0.4	-22.6	-5.7	-	-	-	17	-
Y17069	Y315	9.3–9.2	*Tetraconocon magnus*	-	-12.8	-	-11	-0.4	-24.2	-3.4	-	-	-	17	-
Y4630	Y182	9.3–9.2	*Schizocheros gandakasensis*	-	-13	-	-11	-0.4	-24.4	-5.1	-	-	-	17	-
Y14499	Y269	9.3–9.2	*Schizocheros gandakasensis*	-	-13.1	-	-11	-0.4	-24.5	-9.2	-	-	-	17	-
Y5124	Y211	9.3–9.2	*Microbunodon punjabiense*	-	-11.5	-	-14	-0.4	-25.9	-7.2	-	-	-	17	-
Y9799	Y269	9.3–9.2	*Microbunodon punjabiense*	-	-12.3	-	-14	-0.4	-26.7	-5.8	-	-	-	17	-
Y11797	Y317	9.3–9.2	*Microbunodon punjabiense*	-	-12.1	-	-14	-0.4	-26.5	-6.9	-	-	-	17	-
Y47066	Y317	9.3–9.2	*Merycopotamus*	-	-8.5	-	-14	-0.4	-22.9	-5.8	-	-	-	17	-
Y27044	Y224	9.3–9.2	*Dorcabune nagrii*	-	-11	-	-14	-0.4	-25.4	-6.5	-	-	-	17	-
Y6857	Y227	9.3–9.2	*Dorcabune nagrii*	-	-10.6	-	-14	-0.4	-25	-2.4	-	-	-	17	-
Y11155	Y310	9.3–9.2	*Dorcabune nagrii*	-	-9.9	-	-14	-0.4	-24.3	-1.6	-	-	-	17	-
Y10220	Y309	9.3–9.2	*Dorcabune nagrii*	-	-11.1	-	-14	-0.4	-25.5	-8.2	-	-	-	17	-
Y10886	Y312	9.3–9.2	*Dorcatherium majus*	-	-10.6	-	-14	-0.4	-25	-2.2	-	-	-	17	-

Y10965	Y314	9.3–9.2	*Dorcatherium majus*	-	-10.5	-	-14	-0.4	-24.9	-3.6	-	-	-	17	-
Y7310	Y227	9.3–9.2	*Dorcatherium majus*	-	-12.7	-	-14	-0.4	-27.1	0.5	-	-	-	17	-
Y50921	Y227	9.3–9.2	*Dorcatherium majus*	-	-10.6	-	-14	-0.4	-25	-8.3	-	-	-	17	-
Y5567	Y310	9.3–9.2	*Dorcatherium majus*	-	-11.1	-	-14	-0.4	-25.5	-5.6	-	-	-	17	-
Y19770	Y240	9.3–9.2	*Chalicothere*	-	-11	-	-14	-0.4	-25.4	-3.3	-	-	-	17	-
Y19802	Y182	9.3–9.2	*Chalicothere*	-	-11.1	-	-14	-0.4	-25.5	-3.8	-	-	-	17	-
Y5127-M2	Y211	9.3–9.2	*Tragoceridus*	-	-11.6	-	-14	-0.4	-26	-6.7	-	-	-	17	-
Y5127-M3	Y211	9.3–9.2	*Tragoceridus*	-	-11.5	-	-14	-0.4	-25.9	-3.5	-	-	-	17	-
Y15118-M3	Y227	9.3–9.2	*Tragoceridus*	-	-11.7	-	-14	-0.4	-26.1	0.3	-	-	-	17	-
Y11593-M2	Y227	9.3–9.2	*Tragoceridus*	-	-11.7	-	-14	-0.4	-26.1	-4.4	-	-	-	17	-
Y11593-M3	Y312	9.3–9.2	*Tragoceridus*	-	-10.7	-	-14	-0.4	-25.1	0.7	-	-	-	17	-
Y19813	Y312	9.3–9.2	*Hipparion*	-	-9.5	-	-14	-0.4	-23.9	-1.5	-	-	-	17	-
Y47080	Y312	9.3–9.2	*Hipparion*	-	-8.1	-	-14	-0.4	-22.5	-2.6	-	-	-	17	-
Y19810a	Y312	9.3–9.2	*Hipparion*	-	-9.2	-	-14	-0.4	-23.6	-1.6	-	-	-	17	-
Y19810	Y312	9.3–9.2	*Hipparion*	-	-8.7	-	-14	-0.4	-23.1	-3.5	-	-	-	17	-
Y46248	Y418	9.3–9.2	*Hipparion*	-	-9.1	-	-14	-0.4	-23.5	-4.9	-	-	-	17	-
Y51694	Y545	8.1–8.0	*Rhinoceros*	-	-10.9	-	-14	-0.4	-25.3	-3.3	-	-	-	17	-
Y51551	Y542	8.1–8.0	*Rhinoceros*	-	-11.7	-	-14	-0.4	-26.1	-3.6	-	-	-	17	-
Y51734	Y889	8.1–8.0	*Rhinoceros*	-	-13.3	-	-14	-0.4	-27.7	-4.3	-	-	-	17	-
Y51572	KL11A	8.1–8.0	*Rhinoceros*	-	-11.4	-	-14	-0.4	-25.8	-3.2	-	-	-	17	-
Y51776	Y1000	8.1–8.0	*Rhinoceros*	-	-8.3	-	-14	-0.4	-22.7	-3.4	-	-	-	17	-
Y51576	Y539	8.1–8.0	*Gomphothere*	-	-11.3	-	-14	-0.4	-25.7	-5.9	-	-	-	17	-
Y51774	Y1000	8.1–8.0	*Gomphothere*	-	-12	-	-14	-0.4	-26.4	-1	-	-	-	17	-
Y51559	KL11A	8.1–8.0	*Gomphothere*	-	-11	-	-14	-0.4	-25.4	-7	-	-	-	17	-
Y51782	Y547	8.1–8.0	*Gomphothere*	-	-12.2	-	-14	-0.4	-26.6	-6.6	-	-	-	17	-
Y51704	Y545	8.1–8.0	*Gomphothere*	-	-9.6	-	-14	-0.4	-24	-3.9	-	-	-	17	-
Y16986	Y545	8.1–8.0	*Deinotherium*	-	-11.7	-	-14	-0.4	-26.1	0	-	-	-	17	-
Y5694	Y017	8.1–8.0	*Bramatherium megacephalum*	-	-14.2	-	-14	-0.4	-28.6	1.3	-	-	-	17	-
Y18385	Y605	8.1–8.0	*Bramatherium megacephalum*	-	-10.7	-	-14	-0.4	-25.1	-0.3	-	-	-	17	-
Y2798	Y019	8.1–8.0	*Bramatherium megacephalum*	-	-11.1	-	-14	-0.4	-25.5	-0.2	-	-	-	17	-
Y18412	Y605	8.1–8.0	*Bramatherium megacephalum*	-	-10.9	-	-14	-0.4	-25.3	-0.9	-	-	-	17	-
Y351	Y024	8.1–8.0	*Propotamocherus hysudricus*	-	-10.5	-	-11	-0.4	-21.9	-5	-	-	-	17	-
Y51554	Y542	8.1–8.0	*Propotamocherus hysudricus*	-	-11.8	-	-11	-0.4	-23.2	-4	-	-	-	17	-
Y51700	Y545	8.1–8.0	*Propotamocherus hysudricus*	-	-11.8	-	-11	-0.4	-23.2	-5.9	-	-	-	17	-
Y49515	Y599	8.1–8.0	*Propotamocherus hysudricus*	-	-10.2	-	-11	-0.4	-21.6	-3.6	-	-	-	17	-
Y31474	Y545	8.1–8.0	*Propotamocherus hysudricus*	-	-11	-	-11	-0.4	-22.4	-2.7	-	-	-	17	-
Y51745	Y599	8.1–8.0	*Hippopotamodon sivalense*	-	-10.8	-	-11	-0.4	-22.2	3.5	-	-	-	17	-
Y330	Y017	8.1–8.0	*Hippopotamodon sivalense*	-	-11.1	-	-11	-0.4	-22.5	-4.1	-	-	-	17	-
Y499	Y024	8.1–8.0	*Dorcatherium majus*	-	-10.5	-	-14	-0.4	-24.9	-3.8	-	-	-	17	-
Y16270	Y539	8.1–8.0	*Dorcatherium majus*	-	-8.8	-	-14	-0.4	-23.2	-2.5	-	-	-	17	-
Y16236	Y540	8.1–8.0	*Dorcatherium majus*	-	-10.6	-	-14	-0.4	-25	-1.7	-	-	-	17	-
Y49530	Y888	8.1–8.0	*Dorcatherium majus*	-	-9.9	-	-14	-0.4	-24.3	-2.4	-	-	-	17	-
Y679	Y033	8.1–8.0	*Dorcatherium majus*	-	-10.5	-	-14	-0.4	-24.9	-2.4	-	-	-	17	-
Y9203-M2	Y017	8.1–8.0	*Tragoceridus*	-	-11	-	-14	-0.4	-25.4	-7	-	-	-	17	-
Y9203-M3	Y017	8.1–8.0	*Tragoceridus*	-	-10	-	-14	-0.4	-24.4	0.5	-	-	-	17	-
Y717011	Y545	8.1–8.0	*Tragoceridus*	-	-12.4	-	-14	-0.4	-26.8	-6.5	-	-	-	17	-
Y9208	Y017	8.1–8.0	*Tragoceridus*	-	-10.3	-	-14	-0.4	-24.7	0.1	-	-	-	17	-
Y51687	Y545	8.1–8.0	*Tragoceridus*	-	-10.1	-	-14	-0.4	-24.5	0.9	-	-	-	17	-
Y263-M2	Y017	8.1–8.0	*Tragoceridus*	-	-11.1	-	-14	-0.4	-25.5	-5.1	-	-	-	17	-
Y263-M3	Y017	8.1–8.0	*Tragoceridus*	-	-9.8	-	-14	-0.4	-24.2	-1.3	-	-	-	17	-
Y17007	Y545	8.1–8.0	*Tragoceridus*	-	-12	-	-14	-0.4	-26.4	-1.9	-	-	-	17	-
Y2817-M2	Y017	8.1–8.0	*Docadoxa porrecticornis*	-	-10.9	-	-14	-0.4	-25.3	1.6	-	-	-	17	-
Y2817-M3	Y017	8.1–8.0	*Docadoxa porrecticornis*	-	-9.6	-	-14	-0.4	-24	-3.6	-	-	-	17	-
Y461-M2	Y024	8.1–8.0	*Docadoxa porrecticornis*	-	-11.9	-	-14	-0.4	-26.3	-3.2	-	-	-	17	-
Y461-M3	Y024	8.1–8.0	*Docadoxa porrecticornis*	-	-10.7	-	-14	-0.4	-25.1	-8	-	-	-	17	-
Y9207-M2	Y017	8.1–8.0	*Docadoxa porrecticornis*	-	-10.3	-	-14	-0.4	-24.7	-1.1	-	-	-	17	-
Y9207-M3	Y017	8.1–8.0	*Docadoxa porrecticornis*	-	-10.6	-	-14	-0.4	-25	-4.3	-	-	-	17	-
Y49550	Y606	8.1–8.0	*Docadoxa porrecticornis*	-	-9.3	-	-14	-0.4	-23.7	-3.2	-	-	-	17	-
Y49674	Y542	8.1–8.0	*Hipparion*	-	-5.3	-	-14	-0.4	-19.7	-1.3	-	-	-	17	-
Y18418	Y606	8.1–8.0	*Hipparion*	-	-7.7	-	-14	-0.4	-22.1	-1.9	-	-	-	17	-
Y17859	Y599	8.1–8.0	*Hipparion*	-	-5.9	-	-14	-0.4	-20.3	-2.7	-	-	-	17	-
Y49548a	Y890	8.1–8.0	*Hipparion*	-	-6.5	-	-14	-0.4	-20.9	-0.8	-	-	-	17	-
Y49548	Y890	8.1–8.0	*Hipparion*	-	-7.8	-	-14	-0.4	-22.2	-3.3	-	-	-	17	-

Table SI 3 This table reports all the raw SIA data used in this study, including metadata from fossil and modern pongines as well as data from bovids and suids used for the pairwise comparison with the pongines ranging from the Miocene to the Holocene. We included both the raw data ($\delta^{13}C_{VPDB}$) as well as the corrections applied to each data point and the corrected values ($\delta^{13}C_{diet}$) used for our analysis. $\delta^{18}O_{SMOW}$ values were calculated using the formula proposed by Coplen[72].

Lab-Code	Site/Locality	Country	Age	Period	Species	Tooth	$\delta^{13}C_{VPDB}$	SD C	corrections ε^*	corrections $CO_{2\ atm.}$	$\delta^{13}C_{diet}$	$\delta^{18}O_{VPDB}$	*SD O*	Ref.
PB-11-Q	Pha Bong	Thailand	0.3-1 Ma	Middle Pleistocene	*G. blacki*	-	-13.3	-	-11.0	0.0	-24.3	-4.0	-	30
CA-735-E	China?	China	-	Pleistocene	*G. blacki*	-	-16.0	-	-11.0	0.0	-27.0	-7.8	-	30
CA-764-E	China?	China	-	Pleistocene	*G. blacki*	-	-15.6	-	-11.0	0.0	-26.6	-6.2	-	30
CA-568-E	China?	China	-	Pleistocene	*G. blacki*	-	-13.8	-	-11.0	0.0	-24.8	-5.0	-	30
20	Juyuandong	China	>0.9-1.2 Ma	Early Pleistocene	*G. blacki*	-	-16.4	-	-11.0	0.0	-27.4	-7.2	-	28
21	Juyuandong	China	>0.9-1.2 Ma	Early Pleistocene	*G. blacki*	-	-16.4	-	-11.0	0.0	-27.4	-6.6	-	28
19	Juyuandong	China	>0.9-1.2 Ma	Early Pleistocene	*G. blacki*	-	-16.3	-	-11.0	0.0	-27.3	-6.7	-	28
22	Juyuandong	China	>0.9-1.2 Ma	Early Pleistocene	*G. blacki*	-	-16.1	-	-11.0	0.0	-27.1	-7.6	-	28
25	Longgudong	China	1.8-2.0 Ma	Early Pleistocene	*G. blacki*	-	-16.6	-	-11.0	0.0	-27.6	-8.1	-	28
23	Longgudong	China	1.8-2.0 Ma	Early Pleistocene	*G. blacki*	-	-15.6	-	-11.0	0.0	-26.6	-9.4	-	28
24	Longgudong	China	1.8-2.0 Ma	Early Pleistocene	*G. blacki*	-	-15.4	-	-11.0	0.0	-26.4	-9.2	-	28
36	Longgudong	China	1.8-2.0 Ma	Early Pleistocene	*G. blacki*	-	-12.2	-	-11.0	0.0	-23.2	-8.6	-	28
26	Longgudong	China	1.8-2.0 Ma	Early Pleistocene	*G. blacki*	-	-12.1	-	-11.0	0.0	-23.1	-10.5	-	28
34	Longgudong	China	1.8-2.0 Ma	Early Pleistocene	*G. blacki*	-	-16.6	-	-11.0	0.0	-27.6	-7.6	-	28
35	Longgudong	China	1.8-2.0 Ma	Early Pleistocene	*G. blacki*	-	-15.7	-	-11.0	0.0	-26.7	-7.0	-	28
E8	Sanhe cave	China	1.2-1.6 Ma	Early Pleistocene	*G. blacki*	-	-16.6	-	-11.0	0.0	-27.6	-4.2	-	29
E5	Sanhe cave	China	1.2-1.6 Ma	Early Pleistocene	*G. blacki*	-	-16.4	-	-11.0	0.0	-27.4	-5.2	-	29
E4	Sanhe cave	China	1.2-1.6 Ma	Early Pleistocene	*G. blacki*	-	-15.7	-	-11.0	0.0	-26.7	-5.3	-	29
E7	Sanhe cave	China	1.2-1.6 Ma	Early Pleistocene	*G. blacki*	-	-15.5	-	-11.0	0.0	-26.5	-5.6	-	29
E3	Sanhe cave	China	1.2-1.6 Ma	Early Pleistocene	*G. blacki*	-	-15.4	-	-11.0	0.0	-26.4	-5.8	-	29
E1	Sanhe cave	China	1.2-1.6 Ma	Early Pleistocene	*G. blacki*	-	-15.3	-	-11.0	0.0	-26.3	-5.2	-	29
E2	Sanhe cave	China	1.2-1.6 Ma	Early Pleistocene	*G. blacki*	-	-15.3	-	-11.0	0.0	-26.3	-5.2	-	29
E6	Sanhe cave	China	1.2-1.6 Ma	Early Pleistocene	*G. blacki*	-	-15.1	-	-11.0	0.0	-26.1	-3.5	-	29
E9	Sanhe cave	China	1.2-1.6 Ma	Early Pleistocene	*G. blacki*	-	-14.4	-	-11.0	0.0	-25.4	-4.9	-	29
201811	Sumatra east coast	Indonesia	-	Holocene	*P. abelii*	-	-14.7	0.17	-11.0	0.0	-25.7	-5.5	0.12	24
200898	Borneo	Borneo	1928	Holocene	*P. pygmaeus*	-	-18.0	0.11	-11.0	0.0	-29.0	-12.5	0.08	24
28253	Borneo	Borneo	1907	Holocene	*P. pygmaeus*	-	-15.6	0.15	-11.0	0.0	-26.6	-6.1	0.09	24
18010	Borneo	Borneo	1902	Holocene	*P. pygmaeus*	-	-14.9	0.22	-11.0	0.0	-25.9	-8.3	0.10	24
28252	Borneo	Borneo	1907	Holocene	*P. pygmaeus*	-	-14.5	0.19	-11.0	0.0	-25.5	-7.1	0.11	24
200900	Borneo	Borneo	1928	Holocene	*P. pygmaeus*	-	-14.4	0.17	-11.0	0.0	-25.4	-5.2	0.12	24
140426	Borneo, Sabah, Sandakan S. West	Borneo	-	Holocene	*P. pygmaeus*	-	-16.2	0.14	-11.0	0.0	-27.2	-5.4	0.11	24
SEA-10	Borneo	Borneo	pre1930	Holocene	*P. pygmaeus*	-	-16.4	-	-11.0	0.0	-27.4	-10.0	-	30
SEA-8	Borneo	Borneo	pre1930	Holocene	*P. pygmaeus*	-	-16.1	-	-11.0	0.0	-27.1	-9.5	-	30
SEA-16	Borneo	Borneo	pre1930	Holocene	*P. pygmaeus*	-	-16.1	-	-11.0	0.0	-27.1	-9.9	-	30
SEA-14	Borneo	Borneo	pre1930	Holocene	*P. pygmaeus*	-	-15.7	-	-11.0	0.0	-26.7	-9.5	-	30
SEA-9	Borneo	Borneo	pre1930	Holocene	*P. pygmaeus*	-	-15.3	-	-11.0	0.0	-26.3	-8.6	-	30
SEA-15	Borneo	Borneo	pre1930	Holocene	*P. pygmaeus*	-	-15.1	-	-11.0	0.0	-26.1	-8.0	-	30
SEA-11	Borneo	Borneo	pre1930	Holocene	*P. pygmaeus*	-	-14.5	-	-11.0	0.0	-25.5	-9.5	-	30
SEA-12	Borneo	Borneo	pre1930	Holocene	*P. pygmaeus*	-	-14.3	-	-11.0	0.0	-25.3	-10.0	-	30
SEA-13	Borneo	Borneo	pre1930	Holocene	*P. pygmaeus*	-	-14.0	-	-11.0	0.0	-25.0	-8.9	-	30
ZRC4.754	Borneo	Borneo	1925	Holocene	*P. pygmaeus*	right M2	-15.5	0.22	-11.0	0.0	-26.5	-8.8	0.12	24
ZRC4.755	Borneo	Borneo	1925	Holocene	*P. pygmaeus*	right M2	-14.4	0.10	-11.0	0.0	-25.4	-8.5	0.10	24
ZRC4.750	Pontianak	Borneo	1926	Holocene	*P. pygmaeus*	right M2	-16.5	0.10	-11.0	0.0	-27.5	-9.2	0.10	24
ZRC4.746	Pontianak	Borneo	1925	Holocene	*P. pygmaeus*	right M2	-14.9	0.20	-11.0	0.0	-25.9	-8.9	0.10	24
MNHM ZM-MO-CG-1893-594/A10683	Borneo	Borneo	1893	Holocene	*P. pygmaeus*	left m2	-14.9	0.20	-11.0	0.0	-25.9	-4.9	0.30	24
MNHM ZM-MO-CG-1894-1419	Borneo	Borneo	1894	Holocene	*P. pygmaeus*	left M3	-14.0	0.20	-11.0	0.0	-25.0	-7.7	0.30	24
MNHM ZM-MO-CG-1892-546	Semiasalyres, Borneo	Borneo	1892	Holocene	*P. pygmaeus*	left M3	-13.8	0.30	-11.0	0.0	-24.8	-7.5	0.30	24
SEA-5	Singapore	Singapore	post 2000	Holocene	*P. pygmaeus*	-	-16.2	-	-11.0	1.5	-25.7	-9.4	-	27, new
TWN-7-1	Tham Wiman Nakin	Thailand	~170 ka	Middle Pleistocene	*P. pygmaeus*	-	-13.1	-	-11.0	0.0	-24.1	-4.0	-	27, 30
NL-302	Nam Lot	Laos	86–72 ka	Late Pleistocene	*P. pygmaeus*	-	-14.5	-	-11.0	0.0	-25.5	-6.1	-	31
CA-148-E	China?	China	-	Pleistocene	*Pongo sp.*	-	-15.8	-	-11.0	0.0	-26.8	-5.8	-	30
CA-161-E	China?	China	-	Pleistocene	*Pongo sp.*	-	-14.9	-	-11.0	0.0	-25.9	-6.0	-	30
CA-212-E	China?	China	-	Pleistocene	*Pongo sp.*	-	-14.8	-	-11.0	0.0	-25.8	-4.4	-	30
PB-10-1	Pha Bong	Thailand	1-0.3 Ma	Middle Pleistocene	*Pongo sp.*	-	-13.7	-	-11.0	0.0	-24.7	-5.5	-	30
E13	Sanhe cave	China	1.2-1.6 Ma	Early Pleistocene	*Pongo sp.*	-	-15.3	-	-11.0	0.0	-26.3	-4.0	-	29
E11	Sanhe cave	China	1.2-1.6 Ma	Early Pleistocene	*Pongo sp.*	-	-15.0	-	-11.0	0.0	-26.0	-4.4	-	29
E12	Sanhe cave	China	1.2-1.6 Ma	Early Pleistocene	*Pongo sp.*	-	-14.7	-	-11.0	0.0	-25.7	-3.1	-	29
E10	Sanhe cave	China	1.2-1.6 Ma	Early Pleistocene	*Pongo sp.*	-	-14.4	-	-11.0	0.0	-25.4	-3.4	-	29
IRWD 7E	Yinseik	Myanmar	8.8-10.4 Ma	Late Miocene	*K. ayeyarwadyensis*	m3	-13.2	0.10	-11.0	-0.4	-24.6	-4.5	0.20	new
Y47024	Y317	Pakistan	9.2-9.3 Ma	Late Miocene	*Sivapithecus sp.*	-	-12.4	-	-11.0	-0.4	-23.8	-0.9	-	17
Y13933	Y260	Pakistan	9.2-9.3 Ma	Late Miocene	*Sivapithecus sp.*	-	-13.1	-	-11.0	-0.4	-24.5	-1.9	-	17
Y47023	Y182	Pakistan	9.2-9.3 Ma	Late Miocene	*Sivapithecus sp.*	-	-12.8	-	-11.0	-0.4	-24.2	-1.7	-	17
Y47021	Y182	Pakistan	9.2-9.3 Ma	Late Miocene	*Sivapithecus sp.*	-	-13.9	-	-11.0	-0.4	-25.3	-6.0	-	17
Y13811	Y224	Pakistan	9.2-9.3 Ma	Late Miocene	*Sivapithecus sp.*	-	-12.7	-	-11.0	-0.4	-24.1	-2.7	-	17
HD1-A	Haritalyangar	India	8.85 Ma	Late Miocene	*Indopithecus*	right M2	-12.2	-	-11.0	-0.4	-23.6	-5.5	-	26
HD1-B	Haritalyangar	India	8.85 Ma	Late Miocene	*Indopithecus*	right M2	-11.8	-	-11.0	-0.4	-23.2	-4.4	-	26
HD1-C	Haritalyangar	India	8.85 Ma	Late Miocene	*Indopithecus*	right M2	-11.7	-	-11.0	-0.4	-23.1	-2.5	-	26
HD1-D	Haritalyangar	India	8.85 Ma	Late Miocene	*Indopithecus*	right M2	-11.9	-	-11.0	-0.4	-23.3	-2.1	-	26
HD1-E	Haritalyangar	India	8.85 Ma	Late Miocene	*Indopithecus*	right M2	-11.8	-	-11.0	-0.4	-23.2	-2.9	-	26
HD1-F	Haritalyangar	India	8.85 Ma	Late Miocene	*Indopithecus*	right M2	-11.6	-	-11.0	-0.4	-23.0	-3.1	-	26
HD1-G	Haritalyangar	India	8.85 Ma	Late Miocene	*Indopithecus*	right M2	-12.4	-	-11.0	-0.4	-23.8	-5.2	-	26
HD1-H	Haritalyangar	India	8.85 Ma	Late Miocene	*Indopithecus*	right M2	-12.1	-	-11.0	-0.4	-23.5	-4.2	-	26
HD1-I	Haritalyangar	India	8.85 Ma	Late Miocene	*Indopithecus*	right M2	-12.2	-	-11.0	-0.4	-23.6	-5.0	-	26
HD1-J	Haritalyangar	India	8.85 Ma	Late Miocene	*Indopithecus*	right M2	-12.2	-	-11.0	-0.4	-23.6	-3.6	-	26
LC47	5704.C	China	~2 Ma	Early Pleistocene	*G. blacki*	m	-16.8	-	-11.0	0.0	-27.8	-6.4	-	32
LC48	5704.C	China	~2 Ma	Early Pleistocene	*G. blacki*	M	-16.6	-	-11.0	0.0	-27.6	-6.3	-	32
LC49	5704.C	China	~2 Ma	Early Pleistocene	*G. blacki*	M	-16.8	-	-11.0	0.0	-27.8	-5.9	-	32
LC50	5704.C	China	~2 Ma	Early Pleistocene	*G. blacki*	m	-15.9	-	-11.0	0.0	-26.9	-6.3	-	32
LC51	5704.C	China	~2 Ma	Early Pleistocene	*G. blacki*	m	-16.6	-	-11.0	0.0	-27.6	-6.4	-	32

LC52	5704.C	China	~2 Ma	Early Pleistocene	*G. blacki*	left p4	-15.9	-	-11.0	0.0	-26.9	-7.1	-	32
LC53	5704.63	China	~2 Ma	Early Pleistocene	*G. blacki*	P4	-16.3	-	-11.0	0.0	-27.3	-7.5	-	32
LC54	5704(E)	China	~2 Ma	Early Pleistocene	*G. blacki*	P4	-15.9	-	-11.0	0.0	-26.9	-6.3	-	32
LC55	5704.C	China	~2 Ma	Early Pleistocene	*G. blacki*	m	-16.9	-	-11.0	0.0	-27.9	-7.1	-	32
LC56	5704.B	China	~2 Ma	Early Pleistocene	*G. blacki*	m	-16.7	-	-11.0	0.0	-27.7	-7.1	-	32
LC57	5704.C	China	~2 Ma	Early Pleistocene	*G. blacki*	M	-17.0	-	-11.0	0.0	-28.0	-6.2	-	32
LC58	5704.C	China	~2 Ma	Early Pleistocene	*G. blacki*	m	-16.4	-	-11.0	0.0	-27.4	-6.8	-	32
E14	Sanhe Cave	China	1.6-1.2 Ma	Early Pleistocene	Bovidae	-	-15.1	-	n.a.	n.a.	n.a.	-7.3	-	29
E15	Sanhe Cave	China	1.6-1.2 Ma	Early Pleistocene	Bovidae	-	-15.8	-	n.a.	n.a.	n.a.	-5.7	-	29
E16	Sanhe Cave	China	1.6-1.2 Ma	Early Pleistocene	Bovidae	-	-17.1	-	n.a.	n.a.	n.a.	-7.5	-	29
E17	Sanhe Cave	China	1.6-1.2 Ma	Early Pleistocene	Bovidae	-	-15.9	-	n.a.	n.a.	n.a.	-2.4	-	29
E18	Sanhe Cave	China	1.6-1.2 Ma	Early Pleistocene	Bovidae	-	-15.6	-	n.a.	n.a.	n.a.	-4.3	-	29
1	Longgudong Cave	China	1.8-2.0 Ma	Early Pleistocene	Bovidae	-	-14.4	-	n.a.	n.a.	n.a.	-9.7	-	28
2	Longgudong Cave	China	1.8-2.0 Ma	Early Pleistocene	Bovidae	-	-14.5	-	n.a.	n.a.	n.a.	-9.3	-	28
3	Longgudong Cave	China	1.8-2.0 Ma	Early Pleistocene	Bovidae	-	-15.8	-	n.a.	n.a.	n.a.	-9.3	-	28
4	Longgudong Cave	China	1.8-2.0 Ma	Early Pleistocene	Bovidae	-	-14.3	-	n.a.	n.a.	n.a.	-7.2	-	28
LC27	5704(W?)	China	~2 Ma	Early Pleistocene	Bovidae	M	-14.8	-	n.a.	n.a.	n.a.	-9.1	-	32
LC28	5704(E)	China	~2 Ma	Early Pleistocene	Bovidae	M	-12.9	-	n.a.	n.a.	n.a.	-6.5	-	32
LC29	5704(E)	China	~2 Ma	Early Pleistocene	Bovidae	M	-16.4	-	n.a.	n.a.	n.a.	-6.9	-	32
LC30	5704.C	China	~2 Ma	Early Pleistocene	Bovidae	m	-15.2	-	n.a.	n.a.	n.a.	-5.5	-	32
LC31	5704.C	China	~2 Ma	Early Pleistocene	Bovidae	m	-16.4	-	n.a.	n.a.	n.a.	-5.3	-	32
631045-2	Sangiran	Indonesia	<1.51-0.8 Ma	Early Pleistocene	Suidae	-	-0.2	-	n.a.	n.a.	n.a.	-4.5	-	35
631045-4	Sangiran	Indonesia	<1.51-0.8 Ma	Early Pleistocene	Suidae	-	-12.1	-	n.a.	n.a.	n.a.	-7.0	-	35
631045-6	Sangiran	Indonesia	<1.51-0.8 Ma	Early Pleistocene	Suidae	-	1.9	-	n.a.	n.a.	n.a.	-5.1	-	35
631045-9	Sangiran	Indonesia	<1.51-0.8 Ma	Early Pleistocene	Suidae	-	-1.6	-	n.a.	n.a.	n.a.	-7.0	-	35
31	Longgudong Cave	China	1.8-2.0 Ma	Early Pleistocene	Suidae	-	-3.4	-	n.a.	n.a.	n.a.	-11.2	-	28
LC12	5704.C	China	~2 Ma	Early Pleistocene	Suidae	right M3	-14.7	-	n.a.	n.a.	n.a.	-5.4	-	32
LC13	5704.C	China	~2 Ma	Early Pleistocene	Suidae	right M3	-13.0	-	n.a.	n.a.	n.a.	-8.9	-	32
LC14	5704.IIIa	China	~2 Ma	Early Pleistocene	Suidae	left M3	-13.3	-	n.a.	n.a.	n.a.	-7.3	-	32
LC15	5704.C	China	~2 Ma	Early Pleistocene	Suidae	left M3	-13.6	-	n.a.	n.a.	n.a.	-6.8	-	32
LC16	5704	China	~2 Ma	Early Pleistocene	Suidae	M2	-18.0	-	n.a.	n.a.	n.a.	-6.5	-	32
17651	Hoekgrot	Indonesia	~2.6, 3.3 ka	Holocene	Bovidae	-	-9.7	-	n.a.	n.a.	n.a.	-2.9	-	35
102400	-	Thailand	modern	Holocene	Bovidae	-	-5.9	-	n.a.	n.a.	n.a.	-7.7	-	27, 30
102900	-	Laos	modern	Holocene	Bovidae	-	-15.9	-	n.a.	n.a.	n.a.	-8.4	-	27, 30
SEA-24	Sumatra	Indonesia	>100	Holocene	Bovidae	-	-10.2	-	n.a.	n.a.	n.a.	-8.1	-	30
MNHM ZM-MO-1894-408	-	China	1884	Holocene	Bovidae	left m2	-11.2	0.18	n.a.	n.a.	n.a.	-11.7	0.33	24
MNHM ZM-MO-1993-4629	-	China	1993	Holocene	Bovidae	right m2	-14.8	0.25	n.a.	n.a.	n.a.	-9.9	0.08	24
MNHM ZM-MO-1877-651	-	-	1877	Holocene	Bovidae	left P1	-2.5	0.17	n.a.	n.a.	n.a.	-5.5	0.06	24
MNHM ZM-MO-1895-343	Java	Indonesia	-	Holocene	Bovidae	right m3	-3.1	0.19	n.a.	n.a.	n.a.	-4.9	0.13	24
MNHM ZM-MO-A6707	-	Indochina	-	Holocene	Bovidae	left m3	-2.2	0.17	n.a.	n.a.	n.a.	-7.0	0.14	24
MNHM ZM-MO-1902-411	-	Indochina	1902	Holocene	Bovidae	right m3	-10.7	0.19	n.a.	n.a.	n.a.	-9.5	0.06	24
MNHM ZM-MO-1908-12	Tching-king	China	1908	Holocene	Bovidae	left M3	-12.9	0.21	n.a.	n.a.	n.a.	-7.5	0.14	24
MNHM ZM-MO-1993-4240	Sumatra	Indonesia	1933	Holocene	Bovidae	left M3	-15.2	0.23	n.a.	n.a.	n.a.	-4.1	0.14	24
54582	-	Indochina	-	Holocene	Bovidae	-	1.3	0.17	n.a.	n.a.	n.a.	-4.4	0.07	24
54584	-	-	-	Holocene	Bovidae	-	-0.4	0.23	n.a.	n.a.	n.a.	-4.8	0.14	24
87621	-	-	-	Holocene	Bovidae	-	-6.5	0.11	n.a.	n.a.	n.a.	-5.8	0.08	24
113755	Annan, Dong Me		1936	Holocene	Bovidae	-	-7.5	0.11	n.a.	n.a.	n.a.	-2.0	0.09	24
113756	Annan, Dong Me		1936	Holocene	Bovidae	-	1.1	0.12	n.a.	n.a.	n.a.	-4.0	0.09	24
113758	Cochin China, Lagua River	China	1936	Holocene	Bovidae	-	-3.1	0.15	n.a.	n.a.	n.a.	-4.6	0.12	24
54583	-	Indochina	-	Holocene	Bovidae	-	-3.1	0.18	n.a.	n.a.	n.a.	-4.7	0.12	24
119696	-	-	-	Holocene	Bovidae	-	-0.1	0.11	n.a.	n.a.	n.a.	-6.3	0.08	24
54469	Mysore	India	-	Holocene	Bovidae	-	-1.5	0.18	n.a.	n.a.	n.a.	-3.0	0.10	24
54470	Mysore	India	1923	Holocene	Bovidae	-	-3.5	0.20	n.a.	n.a.	n.a.	-3.4	0.09	24
112979	-	India	-	Holocene	Bovidae	-	-3.4	0.10	n.a.	n.a.	n.a.	-3.8	0.06	24
113747	Madras	India	-	Holocene	Bovidae	-	0.1	0.12	n.a.	n.a.	n.a.	-2.3	0.07	24
ZRC4.1685	Muang Prae (Meh Lem)	Thailand	1916	Holocene	Bovidae	right M2	-13.4	0.12	n.a.	n.a.	n.a.	-3.0	0.08	24
ZRC4.1686	Bencoolen, Sumatra	Indonesia	1917	Holocene	Bovidae	left M2	-19.7	0.07	n.a.	n.a.	n.a.	-9.1	0.10	24
ZRC4.1688	Koh Lok	Thailand	1905	Holocene	Bovidae	left M2	-11.3	0.12	n.a.	n.a.	n.a.	-2.5	0.11	24
ZRC4.1691	Bangkok	Thailand	-	Holocene	Bovidae	right M2	-12.2	0.09	n.a.	n.a.	n.a.	-5.2	0.09	24
17674	Hoekgrot	Indonesia	~2.6, 3.3 ka	Holocene	Suidae	-	-13.4	-	n.a.	n.a.	n.a.	-5.9	-	35
102185	Sumatra	Indonesia	1933	Holocene	Suidae	-	-14.9	0.13	n.a.	n.a.	n.a.	-8.7	0.12	24
107184	Borneo	Indonesia	1937	Holocene	Suidae	-	-14.1	0.17	n.a.	n.a.	n.a.	-10.2	0.09	24
103983	Borneo	-	1935	Holocene	Suidae	-	-14.4	0.13	n.a.	n.a.	n.a.	-11.2	0.05	24
29760	-	-	-	Holocene	Suidae	-	-13.8	0.17	n.a.	n.a.	n.a.	-7.9	0.11	24
24999	-	-	1904	Holocene	Suidae	-	-13.7	0.18	n.a.	n.a.	n.a.	-7.8	0.13	24
24979	-	-	-	Holocene	Suidae	-	-13.9	0.17	n.a.	n.a.	n.a.	-7.7	0.08	24
24976	-	-	1904	Holocene	Suidae	-	-13.4	0.19	n.a.	n.a.	n.a.	-9.3	0.12	24
24980	-	-	1904	Holocene	Suidae	-	-13.5	0.19	n.a.	n.a.	n.a.	-7.5	0.11	24
ZRC4.1829	Sumatra	Indonesia	1937	Holocene	Suidae	right M2	-15.2	0.07	n.a.	n.a.	n.a.	-9.5	0.13	24
ZRC4.1831	Java	Indonesia	1926	Holocene	Suidae	right M3	-10.4	0.18	n.a.	n.a.	n.a.	-7.9	0.12	24
ZRC4.1835	Klebang, Perak	Malaysia	6	Holocene	Suidae	right M2	-13.9	0.06	n.a.	n.a.	n.a.	-8.1	0.08	24
ZRC4.1850	Borneo	-	1928	Holocene	Suidae	right M2	-13.0	0.13	n.a.	n.a.	n.a.	-8.9	0.15	24
ZRC4.1853	Sumatra	Indonesia	1936	Holocene	Suidae	right m2	-12.1	0.16	n.a.	n.a.	n.a.	-7.5	0.10	24
ZRC4.1856	Sumatra	Indonesia	1937	Holocene	Suidae	right M2	-13.9	0.19	n.a.	n.a.	n.a.	-9.4	0.13	24
ZRC4.1858	Sumatra	Indonesia	1939	Holocene	Suidae	right M2	-14.5	0.13	n.a.	n.a.	n.a.	-8.9	0.07	24
ZRC4.1928	Sumatra	Indonesia	-	Holocene	Suidae	right M2	-15.3	0.11	n.a.	n.a.	n.a.	-9.2	0.08	24
ZRC4.1934	Borneo	-	1920	Holocene	Suidae	right M2	-14.1	0.08	n.a.	n.a.	n.a.	-9.1	0.04	24
ZRC4.1936	Sumatra	Indonesia	1914	Holocene	Suidae	right M2	-16.7	0.11	n.a.	n.a.	n.a.	-8.7	0.07	24
IRWD-13	Yinseik	Myanmar	8.8-10.4 Ma	Late Miocene	Bovidae	m3	-9.6	0.12	n.a.	n.a.	n.a.	-4.8	0.19	new
IRWD-14	Yinseik	Myanmar	8.8-10.4 Ma	Late Miocene	Bovidae	m1	-11.2	0.05	n.a.	n.a.	n.a.	-6.3	0.14	new
IRWD-15	Yinseik	Myanmar	8.8-10.4 Ma	Late Miocene	Bovidae	P3	-11.2	0.07	n.a.	n.a.	n.a.	-5.5	0.11	new

IRWD-16	Yinseik	Myanmar	8.8-10.4 Ma	Late Miocene	Bovidae	P4	-12.3	0.04	n.a.	n.a.	n.a.	-5.9	0.11	new
IRWD-17	Yinseik	Myanmar	8.8-10.4 Ma	Late Miocene	Bovidae	M	-10.8	0.06	n.a.	n.a.	n.a.	-4.4	0.10	new
IRWD-18	Yinseik	Myanmar	8.8-10.4 Ma	Late Miocene	Bovidae	M	-11.0	0.07	n.a.	n.a.	n.a.	-6.6	0.14	new
IRWD-19E	Yinseik	Myanmar	8.8-10.4 Ma	Late Miocene	Bovidae	m3	-9.5	0.10	n.a.	n.a.	n.a.	-6.8	0.17	new
IRWD-20E	Yinseik	Myanmar	8.8-10.4 Ma	Late Miocene	Bovidae	m2	-12.2	0.04	n.a.	n.a.	n.a.	-6.6	0.11	new
IRWD-21	Yinseik	Myanmar	8.8-10.4 Ma	Late Miocene	Bovidae	M	-12.2	0.06	n.a.	n.a.	n.a.	-6.2	0.14	new
IRWD-22	Yinseik	Myanmar	8.8-10.4 Ma	Late Miocene	Bovidae	M3	-10.9	0.06	n.a.	n.a.	n.a.	-7.5	0.14	new
IRWD-23	Yinseik	Myanmar	8.8-10.4 Ma	Late Miocene	Bovidae	m3	-9.9	0.04	n.a.	n.a.	n.a.	-5.7	0.17	new
IR0819	Chingzauk	Myanmar	6 Ma	Late Miocene	Bovidae	m3	-2.7	-	n.a.	n.a.	n.a.	-4.1	-	25
IR1104	Chingzauk	Myanmar	6 Ma	Late Miocene	Bovidae	m3	-6.1	-	n.a.	n.a.	n.a.	-4.3	-	25
IR0809	Chingzauk	Myanmar	6 Ma	Late Miocene	Bovidae	m3	-2.7	-	n.a.	n.a.	n.a.	-3.9	-	25
IR0811	Chingzauk	Myanmar	6 Ma	Late Miocene	Bovidae	m3	-0.7	-	n.a.	n.a.	n.a.	-1.9	-	25
IR0823	Chingzauk	Myanmar	6 Ma	Late Miocene	Bovidae	m3	1.9	-	n.a.	n.a.	n.a.	-2.7	-	25
IR0824	Chingzauk	Myanmar	6 Ma	Late Miocene	Bovidae	m3	0.9	-	n.a.	n.a.	n.a.	-4.1	-	25
IR0827	Chingzauk	Myanmar	6 Ma	Late Miocene	Bovidae	m2	-1.8	-	n.a.	n.a.	n.a.	-4.3	-	25
IR1094	Chingzauk	Myanmar	6 Ma	Late Miocene	Bovidae	m3	1.0	-	n.a.	n.a.	n.a.	-6.0	-	25
IR1170	Chingzauk	Myanmar	6 Ma	Late Miocene	Bovidae	m1	-0.7	-	n.a.	n.a.	n.a.	-3.7	-	25
IR0808	Chingzauk	Myanmar	6 Ma	Late Miocene	Bovidae	m2	0.2	-	n.a.	n.a.	n.a.	-2.4	-	25
IR0817	Chingzauk	Myanmar	6 Ma	Late Miocene	Bovidae	m3	-2.9	-	n.a.	n.a.	n.a.	-2.6	-	25
IR0818	Chingzauk	Myanmar	6 Ma	Late Miocene	Bovidae	m3	-2.1	-	n.a.	n.a.	n.a.	-2.3	-	25
IR0828	Chingzauk	Myanmar	6 Ma	Late Miocene	Bovidae	m3	-3.5	-	n.a.	n.a.	n.a.	-5.0	-	25
IR0826	Chingzauk	Myanmar	6 Ma	Late Miocene	Bovidae	m3	-4.0	-	n.a.	n.a.	n.a.	-5.6	-	25
IR0825	Chingzauk	Myanmar	6 Ma	Late Miocene	Bovidae	p4	-1.4	-	n.a.	n.a.	n.a.	-4.9	-	25
IR1194	Chingzauk	Myanmar	6 Ma	Late Miocene	Bovidae	m3	-8.1	-	n.a.	n.a.	n.a.	-3.6	-	25
IR1105	Chingzauk	Myanmar	6 Ma	Late Miocene	Bovidae	m1	-5.2	-	n.a.	n.a.	n.a.	-5.7	-	25
IR1204	Chingzauk	Myanmar	6 Ma	Late Miocene	Bovidae	m3	-1.2	-	n.a.	n.a.	n.a.	-3.4	-	25
IR1092	Chingzauk	Myanmar	6 Ma	Late Miocene	Bovidae	m3	-0.5	-	n.a.	n.a.	n.a.	-5.6	-	25
Y5127-M2	Dokh Pathan	Pakistan	9.3-9.4 Ma	Late Miocene	Bovidae	M2	-11.6	-	n.a.	n.a.	n.a.	-6.7	-	17
Y5127-M3	Dokh Pathan	Pakistan	9.3-9.4 Ma	Late Miocene	Bovidae	M3	-11.5	-	n.a.	n.a.	n.a.	-3.5	-	17
Y15118-M3	Dokh Pathan	Pakistan	9.3-9.4 Ma	Late Miocene	Bovidae	M3	-11.7	-	n.a.	n.a.	n.a.	0.3	-	17
Y11593-M2	Dokh Pathan	Pakistan	9.3-9.4 Ma	Late Miocene	Bovidae	M2	-11.7	-	n.a.	n.a.	n.a.	-4.4	-	17
Y11593-M3	Dokh Pathan	Pakistan	9.3-9.4 Ma	Late Miocene	Bovidae	M3	-10.7	-	n.a.	n.a.	n.a.	0.7	-	17
Y9203-M2	Dokh Pathan	Pakistan	8.1-8.0 Ma	Late Miocene	Bovidae	M2	-11.0	-	n.a.	n.a.	n.a.	-7.0	-	17
Y9203-M3	Dokh Pathan	Pakistan	8.1-8.0 Ma	Late Miocene	Bovidae	M3	-10.0	-	n.a.	n.a.	n.a.	0.5	-	17
Y717011	Dokh Pathan	Pakistan	8.1-8.0 Ma	Late Miocene	Bovidae	-	-12.4	-	n.a.	n.a.	n.a.	-6.5	-	17
Y9208	Dokh Pathan	Pakistan	8.1-8.0 Ma	Late Miocene	Bovidae	-	-10.3	-	n.a.	n.a.	n.a.	0.1	-	17
Y51687	Dokh Pathan	Pakistan	8.1-8.0 Ma	Late Miocene	Bovidae	-	-10.1	-	n.a.	n.a.	n.a.	0.9	-	17
Y263-M2	Dokh Pathan	Pakistan	8.1-8.0 Ma	Late Miocene	Bovidae	M2	-11.1	-	n.a.	n.a.	n.a.	-5.1	-	17
Y263-M3	Dokh Pathan	Pakistan	8.1-8.0 Ma	Late Miocene	Bovidae	M3	-9.8	-	n.a.	n.a.	n.a.	-1.3	-	17
Y17007	Dokh Pathan	Pakistan	8.1-8.0 Ma	Late Miocene	Bovidae	-	-12.0	-	n.a.	n.a.	n.a.	-1.9	-	17
Y2817-M2	Dokh Pathan	Pakistan	8.1-8.0 Ma	Late Miocene	Bovidae	M2	-10.9	-	n.a.	n.a.	n.a.	1.6	-	17
Y2817-M3	Dokh Pathan	Pakistan	8.1-8.0 Ma	Late Miocene	Bovidae	M3	-9.6	-	n.a.	n.a.	n.a.	-3.6	-	17
Y461-M2	Dokh Pathan	Pakistan	8.1-8.0 Ma	Late Miocene	Bovidae	M2	-11.9	-	n.a.	n.a.	n.a.	-3.2	-	17
Y461-M3	Dokh Pathan	Pakistan	8.1-8.0 Ma	Late Miocene	Bovidae	M3	-10.7	-	n.a.	n.a.	n.a.	-8.0	-	17
Y9207-M2	Dokh Pathan	Pakistan	8.1-8.0 Ma	Late Miocene	Bovidae	M2	-10.3	-	n.a.	n.a.	n.a.	-1.1	-	17
Y9207-M3	Dokh Pathan	Pakistan	8.1-8.0 Ma	Late Miocene	Bovidae	M3	-10.6	-	n.a.	n.a.	n.a.	-4.3	-	17
Y49550	Dokh Pathan	Pakistan	8.1-8.0 Ma	Late Miocene	Bovidae	-	-9.3	-	n.a.	n.a.	n.a.	-3.2	-	17
HD1-C	Dokh Pathan	Pakistan	8.9 Ma	Late Miocene	Bovidae	-	-11.6	-	n.a.	n.a.	n.a.	-2.7	-	26
D1-1	Dokh Pathan	Pakistan	10.1 Ma	Late Miocene	Bovidae	-	-10.7	-	n.a.	n.a.	n.a.	-1.2	-	26
IRWD-44	Yinseik	Myanmar	8.8-10.4 Ma	Late Miocene	Suidae	left M3	-11.0	0.11	n.a.	n.a.	n.a.	-8.3	0.20	new
IRWD-45	Yinseik	Myanmar	8.8-10.4 Ma	Late Miocene	Suidae	P4	-11.2	0.12	n.a.	n.a.	n.a.	-6.0	0.07	new
IRWD-46	Yinseik	Myanmar	8.8-10.4 Ma	Late Miocene	Suidae	m2	-12.1	0.06	n.a.	n.a.	n.a.	-6.9	0.13	new
IRWD-47	Yinseik	Myanmar	8.8-10.4 Ma	Late Miocene	Suidae	m3	-10.4	0.14	n.a.	n.a.	n.a.	-8.0	0.21	new
IRWD-48	Yinseik	Myanmar	8.8-10.4 Ma	Late Miocene	Suidae	m3	-10.2	0.12	n.a.	n.a.	n.a.	-6.9	0.21	new
IRWD-49	Yinseik	Myanmar	8.8-10.4 Ma	Late Miocene	Suidae	m3	-10.4	0.11	n.a.	n.a.	n.a.	-8.4	0.16	new
IRWD-50	Yinseik	Myanmar	8.8-10.4 Ma	Late Miocene	Suidae	M3	-10.0	0.13	n.a.	n.a.	n.a.	-3.8	0.16	new
IRWD-50BIS	Yinseik	Myanmar	8.8-10.4 Ma	Late Miocene	Suidae	M1	-10.3	0.05	n.a.	n.a.	n.a.	-4.6	0.14	new
IR0805	Chingzauk	Myanmar	6 Ma	Late Miocene	Suidae	m3	-10.4	-	n.a.	n.a.	n.a.	-6.9	-	25
IR0553	Chingzauk	Myanmar	6 Ma	Late Miocene	Suidae	M3	-12.1	-	n.a.	n.a.	n.a.	-5.1	-	25
IR0812	Chingzauk	Myanmar	6 Ma	Late Miocene	Suidae	m2	-13.8	-	n.a.	n.a.	n.a.	-3.6	-	25
IR0813	Chingzauk	Myanmar	6 Ma	Late Miocene	Suidae	m3	-10.4	-	n.a.	n.a.	n.a.	-6.6	-	25
IR0814	Chingzauk	Myanmar	6 Ma	Late Miocene	Suidae	m3	-12.3	-	n.a.	n.a.	n.a.	-8.1	-	25
IR0804	Chingzauk	Myanmar	6 Ma	Late Miocene	Suidae	m2	-12.0	-	n.a.	n.a.	n.a.	-7.4	-	25
IR0816	Chingzauk	Myanmar	6 Ma	Late Miocene	Suidae	m2	-10.0	-	n.a.	n.a.	n.a.	-7.0	-	25
IR1458	Chingzauk	Myanmar	6 Ma	Late Miocene	Suidae	m3	-10.4	-	n.a.	n.a.	n.a.	-6.4	-	25
Y14502	Dokh Pathan	Pakistan	9.3-9.4 Ma	Late Miocene	Suidae	-	-11.0	-	n.a.	n.a.	n.a.	-6.9	-	17
Y41368	Dokh Pathan	Pakistan	9.3-9.4 Ma	Late Miocene	Suidae	-	-12.9	-	n.a.	n.a.	n.a.	-9.2	-	17
Y4554	Dokh Pathan	Pakistan	9.3-9.4 Ma	Late Miocene	Suidae	-	-12.6	-	n.a.	n.a.	n.a.	-5.4	-	17
Y6753	Dokh Pathan	Pakistan	9.3-9.4 Ma	Late Miocene	Suidae	-	-11.0	-	n.a.	n.a.	n.a.	-5.7	-	17
Y10224	Dokh Pathan	Pakistan	9.3-9.4 Ma	Late Miocene	Suidae	-	-12.0	-	n.a.	n.a.	n.a.	-8.4	-	17
Y11007	Dokh Pathan	Pakistan	9.3-9.4 Ma	Late Miocene	Suidae	-	-11.2	-	n.a.	n.a.	n.a.	-8.2	-	17
Y13524	Dokh Pathan	Pakistan	9.3-9.4 Ma	Late Miocene	Suidae	-	-10.8	-	n.a.	n.a.	n.a.	-7.3	-	17
Y47176	Dokh Pathan	Pakistan	9.3-9.4 Ma	Late Miocene	Suidae	-	-11.4	-	n.a.	n.a.	n.a.	-6.6	-	17
Y12708	Dokh Pathan	Pakistan	9.3-9.4 Ma	Late Miocene	Suidae	-	-11.7	-	n.a.	n.a.	n.a.	-4.5	-	17
Y5276	Dokh Pathan	Pakistan	9.3-9.4 Ma	Late Miocene	Suidae	-	-9.4	-	n.a.	n.a.	n.a.	-7.0	-	17
Y4226	Dokh Pathan	Pakistan	9.3-9.4 Ma	Late Miocene	Suidae	-	-10.8	-	n.a.	n.a.	n.a.	-5.1	-	17
Y27915	Dokh Pathan	Pakistan	9.3-9.4 Ma	Late Miocene	Suidae	-	-11.2	-	n.a.	n.a.	n.a.	-5.7	-	17
Y17069	Dokh Pathan	Pakistan	9.3-9.4 Ma	Late Miocene	Suidae	-	-12.8	-	n.a.	n.a.	n.a.	-3.4	-	17
Y4630	Dokh Pathan	Pakistan	9.3-9.4 Ma	Late Miocene	Suidae	-	-13.0	-	n.a.	n.a.	n.a.	-5.1	-	17
Y14499	Dokh Pathan	Pakistan	9.3-9.4 Ma	Late Miocene	Suidae	-	-13.1	-	n.a.	n.a.	n.a.	-9.2	-	17
Y351	Dokh Pathan	Pakistan	8.1-8.0 Ma	Late Miocene	Suidae	-	-10.5	-	n.a.	n.a.	n.a.	-5.0	-	17
Y51554	Dokh Pathan	Pakistan	8.1-8.0 Ma	Late Miocene	Suidae	-	-11.8	-	n.a.	n.a.	n.a.	-4.0	-	17
Y51700	Dokh Pathan	Pakistan	8.1-8.0 Ma	Late Miocene	Suidae	-	-11.8	-	n.a.	n.a.	n.a.	-5.9	-	17
Y49515	Dokh Pathan	Pakistan	8.1-8.0 Ma	Late Miocene	Suidae	-	-10.2	-	n.a.	n.a.	n.a.	-3.6	-	17
Y31474	Dokh Pathan	Pakistan	8.1-8.0 Ma	Late Miocene	Suidae	-	-11.0	-	n.a.	n.a.	n.a.	-2.7	-	17
Y51745	Dokh Pathan	Pakistan	8.1-8.0 Ma	Late Miocene	Suidae	-	-10.8	-	n.a.	n.a.	n.a.	3.5	-	17
Y330	Dokh Pathan	Pakistan	8.1-8.0 Ma	Late Miocene	Suidae	-	-11.1	-	n.a.	n.a.	n.a.	-4.1	-	17
f	Dokh Pathan	Pakistan	8.8	Late Miocene	Suidae	-	-11.0	-	n.a.	n.a.	n.a.	-6.3	-	26
1014-z-1	Padang	Indonesia	158-115 ka	Late Pleistocene	Bovidae	-	-11.7	-	n.a.	n.a.	n.a.	-5.7	-	35
1014-z-2-A	Padang	Indonesia	158-115 ka	Late Pleistocene	Bovidae	-	-12.8	-	n.a.	n.a.	n.a.	-5.5	-	35
1014-z-4-A	Padang	Indonesia	158-115 ka	Late Pleistocene	Bovidae	-	-1.4	-	n.a.	n.a.	n.a.	-6.0	-	35
1014-z-5	Padang	Indonesia	158-115 ka	Late Pleistocene	Bovidae	-	-17.1	-	n.a.	n.a.	n.a.	-7.9	-	35
1457-177	Wajak	Indonesia	~6.5, 10.6 ka	Late Pleistocene	Bovidae	-	-0.8	-	n.a.	n.a.	n.a.	-3.2	-	35
80108	Punung	Indonesia	143-115 ka	Late Pleistocene	Bovidae	-	-13.5	-	n.a.	n.a.	n.a.	-5.8	-	35

NL-139	Nam Lot	Laos	86-72 ka	Late Pleistocene	Bovidae	-	-4.7	-	n.a.	n.a.	n.a.	-6.5	-	31
NL-143	Nam Lot	Laos	86-72 ka	Late Pleistocene	Bovidae	-	-9.5	-	n.a.	n.a.	n.a.	-4.4	-	31
NL-116	Nam Lot	Laos	86-72 ka	Late Pleistocene	Bovidae	-	-9.8	-	n.a.	n.a.	n.a.	-5.9	-	31
NL-117	Nam Lot	Laos	86-72 ka	Late Pleistocene	Bovidae	-	0.3	-	n.a.	n.a.	n.a.	-4.9	-	31
NL-125	Nam Lot	Laos	86-72 ka	Late Pleistocene	Bovidae	-	-13.5	-	n.a.	n.a.	n.a.	-4.7	-	31
28	Baxian	China	0.1 Ma	Late Pleistocene	Bovidae	-	-14.7	-	n.a.	n.a.	n.a.	-6.6	-	33
-	Quzai	China	100–60ka	Late Pleistocene	Bovidae	-	-19.9	-	n.a.	n.a.	n.a.	-5.4	-	34
-	Quzai	China	100–60ka	Late Pleistocene	Bovidae	-	-16.6	-	n.a.	n.a.	n.a.	-5.9	-	34
836ab-5	Sibrambang	Indonesia	158-115 ka	Late Pleistocene	Suidae	-	-12.6	-	n.a.	n.a.	n.a.	-6.6	-	35
836ab-7	Sibrambang	Indonesia	158-115 ka	Late Pleistocene	Suidae	-	-11.9	-	n.a.	n.a.	n.a.	-7.1	-	35
GD39	Punung	Indonesia	143-115 ka	Late Pleistocene	Suidae	-	-9.5	-	n.a.	n.a.	n.a.	-7.4	-	35
NL-162	Nam Lot	Laos	86-72 ka	Late Pleistocene	Suidae	-	-13.7	-	n.a.	n.a.	n.a.	-5.7	-	31
NL-208	Nam Lot	Laos	86-72 ka	Late Pleistocene	Suidae	-	-12.4	-	n.a.	n.a.	n.a.	-6.0	-	31
NL-216	Nam Lot	Laos	86-72 ka	Late Pleistocene	Suidae	-	-12.8	-	n.a.	n.a.	n.a.	-5.3	-	31
NL-218	Nam Lot	Laos	86-72 ka	Late Pleistocene	Suidae	-	-14.1	-	n.a.	n.a.	n.a.	-6.8	-	31
NL-SS-1	Nam Lot	Laos	86-72 ka	Late Pleistocene	Suidae	-	-13.1	-	n.a.	n.a.	n.a.	-6.0	-	31
17	Baxian	China	0.1 Ma	Late Pleistocene	Suidae	-	-15.7	-	n.a.	n.a.	n.a.	-7.8	-	33
18	Baxian	China	0.1 Ma	Late Pleistocene	Suidae	-	-14.6	-	n.a.	n.a.	n.a.	-6.9	-	33
19	Baxian	China	0.1 Ma	Late Pleistocene	Suidae	-	-12.9	-	n.a.	n.a.	n.a.	-6.7	-	33
-	Quzai	China	100–60ka	Late Pleistocene	Suidae	-	-14.0	-	n.a.	n.a.	n.a.	-7.9	-	34
-	Quzai	China	100–60ka	Late Pleistocene	Suidae	-	-13.3	-	n.a.	n.a.	n.a.	-6.1	-	34
-	Quzai	China	100–60ka	Late Pleistocene	Suidae	-	-11.1	-	n.a.	n.a.	n.a.	-7.2	-	34
Trinilbox-01	Trinil	Indonesia	0.64-0.38 Ma	Middle Pleistocene	Bovidae	-	2.9	-	n.a.	n.a.	n.a.	-2.2	-	35
Trinilbox-03	Trinil	Indonesia	0.64-0.38 Ma	Middle Pleistocene	Bovidae	-	3.6	-	n.a.	n.a.	n.a.	-3.8	-	35
Trinilbox-07	Trinil	Indonesia	0.64-0.38 Ma	Middle Pleistocene	Bovidae	-	3.1	-	n.a.	n.a.	n.a.	-5.8	-	35
Trinilbox-11	Trinil	Indonesia	0.64-0.38 Ma	Middle Pleistocene	Bovidae	-	-0.2	-	n.a.	n.a.	n.a.	-5.0	-	35
DUB13254	Trinil	Indonesia	0.64-0.38 Ma	Middle Pleistocene	Bovidae	-	-6.5	-	n.a.	n.a.	n.a.	-6.5	-	35
DUB13304	Trinil	Indonesia	0.64-0.38 Ma	Middle Pleistocene	Bovidae	-	-4.4	-	n.a.	n.a.	n.a.	-6.8	-	35
DUB13267	Trinil	Indonesia	0.64-0.38 Ma	Middle Pleistocene	Bovidae	-	-4.5	-	n.a.	n.a.	n.a.	-6.5	-	35
TWN-4-1	Thum Wiman Nakin	Thailand	~170 ka	Middle Pleistocene	Bovidae	-	-2.4	-	n.a.	n.a.	n.a.	-3.2	-	27, 30
TWN-4-2	Thum Wiman Nakin	Thailand	~170 ka	Middle Pleistocene	Bovidae	-	-2.9	-	n.a.	n.a.	n.a.	-5.9	-	27, 30
TWN-4-3	Thum Wiman Nakin	Thailand	~170 ka	Middle Pleistocene	Bovidae	-	0.9	-	n.a.	n.a.	n.a.	-3.6	-	27, 30
TWN-4-4	Thum Wiman Nakin	Thailand	~170 ka	Middle Pleistocene	Bovidae	-	-0.6	-	n.a.	n.a.	n.a.	-5.5	-	27, 30
TWN-4-5	Thum Wiman Nakin	Thailand	~170 ka	Middle Pleistocene	Bovidae	-	2.8	-	n.a.	n.a.	n.a.	-4.7	-	27, 30
PB-4-1	Pha Bong	Thailand	1-0.3 Ma	Middle Pleistocene	Bovidae	-	-0.1	-	n.a.	n.a.	n.a.	-4.7	-	30
PB-4-2	Pha Bong	Thailand	1-0.3 Ma	Middle Pleistocene	Bovidae	-	1.6	-	n.a.	n.a.	n.a.	-2.9	-	30
PB-4-3	Pha Bong	Thailand	1-0.3 Ma	Middle Pleistocene	Bovidae	-	-0.1	-	n.a.	n.a.	n.a.	-4.4	-	30
PB-4-4	Pha Bong	Thailand	1-0.3 Ma	Middle Pleistocene	Bovidae	-	-1.3	-	n.a.	n.a.	n.a.	-4.2	-	30
PB-4-5	Pha Bong	Thailand	1-0.3 Ma	Middle Pleistocene	Bovidae	-	-0.9	-	n.a.	n.a.	n.a.	-2.2	-	30
PB-7-1 (E)	Pha Bong	Thailand	1-0.3 Ma	Middle Pleistocene	Bovidae	-	-0.8	-	n.a.	n.a.	n.a.	-3.5	-	30
PB-7-2	Pha Bong	Thailand	1-0.3 Ma	Middle Pleistocene	Bovidae	-	-1.2	-	n.a.	n.a.	n.a.	-1.6	-	30
PB-7-3	Pha Bong	Thailand	1-0.3 Ma	Middle Pleistocene	Bovidae	-	-1.6	-	n.a.	n.a.	n.a.	-3.9	-	30
PB-7-4	Pha Bong	Thailand	1-0.3 Ma	Middle Pleistocene	Bovidae	-	-1.0	-	n.a.	n.a.	n.a.	-3.0	-	30
PB-7-5	Pha Bong	Thailand	1-0.3 Ma	Middle Pleistocene	Bovidae	-	-1.5	-	n.a.	n.a.	n.a.	-3.5	-	30
PBM-3	Pha Bong	Thailand	1-0.3 Ma	Middle Pleistocene	Bovidae	-	0.2	-	n.a.	n.a.	n.a.	-3.3	-	30
PBM-4	Pha Bong	Thailand	1-0.3 Ma	Middle Pleistocene	Bovidae	-	1.0	-	n.a.	n.a.	n.a.	-2.0	-	30
PBM-5	Pha Bong	Thailand	1-0.3 Ma	Middle Pleistocene	Bovidae	-	-0.3	-	n.a.	n.a.	n.a.	-5.3	-	30
PBM-6	Pha Bong	Thailand	1-0.3 Ma	Middle Pleistocene	Bovidae	-	-1.5	-	n.a.	n.a.	n.a.	-1.9	-	30
PBM-7	Pha Bong	Thailand	1-0.3 Ma	Middle Pleistocene	Bovidae	-	-2.5	-	n.a.	n.a.	n.a.	-4.1	-	30
PBM-8	Pha Bong	Thailand	1-0.3 Ma	Middle Pleistocene	Bovidae	-	0.0	-	n.a.	n.a.	n.a.	-1.9	-	30
PBM-12	Pha Bong	Thailand	1-0.3 Ma	Middle Pleistocene	Bovidae	-	1.7	-	n.a.	n.a.	n.a.	-3.2	-	30
PBM-9	Pha Bong	Thailand	1-0.3 Ma	Middle Pleistocene	Bovidae	-	-8.7	-	n.a.	n.a.	n.a.	-3.9	-	30
PBM-10	Pha Bong	Thailand	1-0.3 Ma	Middle Pleistocene	Bovidae	-	-10.3	-	n.a.	n.a.	n.a.	-5.0	-	30
MH 556	Mohui Cave	China	-	Middle Pleistocene	Bovidae	-	-14.4	-	n.a.	n.a.	n.a.	-6.5	-	36
DMR-KS-05-04-01-7	Khok Sung	Thailand	213-188 ka	Middle Pleistocene	Bovidae	P3	-3.4	-	n.a.	n.a.	n.a.	-4.9	-	37
DMR-KS-05-04-05-2	Khok Sung	Thailand	213-188 ka	Middle Pleistocene	Bovidae	molar	-0.8	-	n.a.	n.a.	n.a.	-5.1	-	37
DMR-KS-05-03-22-16	Khok Sung	Thailand	213-188 ka	Middle Pleistocene	Bovidae	molar	1.0	-	n.a.	n.a.	n.a.	-5.1	-	37
DMR-KS-05-03-18-21 (1)	Khok Sung	Thailand	213-188 ka	Middle Pleistocene	Bovidae	molar	1.7	-	n.a.	n.a.	n.a.	-3.4	-	37
DMR-KS-05-03-28-13	Khok Sung	Thailand	213-188 ka	Middle Pleistocene	Bovidae	m3	-6.7	-	n.a.	n.a.	n.a.	-4.8	-	37
DMR-KS-05-03-15-9	Khok Sung	Thailand	213-188 ka	Middle Pleistocene	Bovidae	molar	-1.6	-	n.a.	n.a.	n.a.	-5.0	-	37
DMR-KS-05-04-8-7	Khok Sung	Thailand	213-188 ka	Middle Pleistocene	Bovidae	molar	-0.6	-	n.a.	n.a.	n.a.	-5.9	-	37
DMR-KS-05-03-23-2	Khok Sung	Thailand	213-188 ka	Middle Pleistocene	Bovidae	M2	1.1	-	n.a.	n.a.	n.a.	-4.5	-	37
DMR-KS-05-03-15-9	Khok Sung	Thailand	213-188 ka	Middle Pleistocene	Bovidae	molar	1.6	-	n.a.	n.a.	n.a.	-4.5	-	37
DMR-KS-05-03-14-6	Khok Sung	Thailand	213-188 ka	Middle Pleistocene	Bovidae	molar	1.9	-	n.a.	n.a.	n.a.	-4.5	-	37
DMR-KS-05-03-19-5	Khok Sung	Thailand	213-188 ka	Middle Pleistocene	Bovidae	incisor	2.0	-	n.a.	n.a.	n.a.	-2.7	-	37
DMR-KS-05-03-28-10	Khok Sung	Thailand	213-188 ka	Middle Pleistocene	Bovidae	m3	-14.3	-	n.a.	n.a.	n.a.	-6.4	-	37
TWN-1-1	Thum Wiman Nakin	Thailand	~170 ka	Middle Pleistocene	Suidae	-	-13.0	-	n.a.	n.a.	n.a.	-6.6	-	27, 30
TWN-1-2	Thum Wiman Nakin	Thailand	~170 ka	Middle Pleistocene	Suidae	-	-8.6	-	n.a.	n.a.	n.a.	-4.5	-	27, 30
TWN-1-3	Thum Wiman Nakin	Thailand	~170 ka	Middle Pleistocene	Suidae	-	-7.9	-	n.a.	n.a.	n.a.	-7.4	-	27, 30
TWN-1-4	Thum Wiman Nakin	Thailand	~170 ka	Middle Pleistocene	Suidae	-	-13.1	-	n.a.	n.a.	n.a.	-9.7	-	27, 30
TWN-1-5	Thum Wiman Nakin	Thailand	~170 ka	Middle Pleistocene	Suidae	-	-13.8	-	n.a.	n.a.	n.a.	-8.8	-	27, 30
PB-1-1	Pha Bong	Thailand	1-0.3 Ma	Middle Pleistocene	Suidae	-	-13.6	-	n.a.	n.a.	n.a.	-6.4	-	30
PB-1-2	Pha Bong	Thailand	1-0.3 Ma	Middle Pleistocene	Suidae	-	-9.4	-	n.a.	n.a.	n.a.	-6.8	-	30
PB-1-3	Pha Bong	Thailand	1-0.3 Ma	Middle Pleistocene	Suidae	-	-9.3	-	n.a.	n.a.	n.a.	-6.8	-	30
PB-1-4	Pha Bong	Thailand	1-0.3 Ma	Middle Pleistocene	Suidae	-	-6.4	-	n.a.	n.a.	n.a.	-4.9	-	30
PB-1-5	Pha Bong	Thailand	1-0.3 Ma	Middle Pleistocene	Suidae	-	-7.0	-	n.a.	n.a.	n.a.	-5.0	-	30
PBM-17	Pha Bong	Thailand	1-0.3 Ma	Middle Pleistocene	Suidae	-	-10.8	-	n.a.	n.a.	n.a.	-6.4	-	30
PBM-18	Pha Bong	Thailand	1-0.3 Ma	Middle Pleistocene	Suidae	-	-8.2	-	n.a.	n.a.	n.a.	-7.8	-	30
MH 417	Mohui Cave	China	-	Middle Pleistocene	Suidae	-	-14.8	-	n.a.	n.a.	n.a.	-7.5	-	36
MH 478	Mohui Cave	China	-	Middle Pleistocene	Suidae	-	-12.5	-	n.a.	n.a.	n.a.	-7.8	-	36

DMR-KS-05-04-19-4	Khok Sung	Thailand	213-188 ka	Middle Pleistocene	Suidae	M3	-12.0	-	n.a.	n.a.	n.a.	-6.9	-	37
DMR-KS-05-04-19-3	Khok Sung	Thailand	213-188 ka	Middle Pleistocene	Suidae	m3	-10.0	-	n.a.	n.a.	n.a.	-5.3	-	37
DMR-KS-05-03-18-23	Khok Sung	Thailand	213-188 ka	Middle Pleistocene	Suidae	M2	-7.7	-	n.a.	n.a.	n.a.	-5.4	-	37

Table SI 4 Summary of A0 and the % overlap per taxonomic group for the mammal faunas from the Yinseik locality (Khoratpithecus fauna) and the Siwaliks (Sivapithecus fauna) used in the comparison of niche overlaps.

ID taxonomic group	***Sivapithecus* fauna**	SEA_C
1	Giraffidae	4.2
3.2	Gomphotheridae	2.5
4	Equidae	3.1
5	Bovidae	4.7
6	Suidae	6.2
7.2	*Sivapithecus*	1.9
9	Anthracotheriidae	5.5
10	Tragulidae	8.3

pair	**1_4**	**1_5**	**1_7.2**	**1_10**	**3.2_5**	**3.2_7.2**	**3.2_9**	**3.2_10**	**5_9**	**5_10**	**6_9**	**7.2_10**	**9_10**
A_O	0.0	0.9	0.3	1.4	0.7	0.2	0.9	1.4	0.2	2.5	0.7	0.6	1.8
% overlap	0.2	11.4	17.6	7.9	14.5	26.1	12.9	9.2	9.9	7.6	8.5	9.9	7.1
mean Sivapithecus % overlap	**11.0**												
mean incl. not overlapping groups	**5.1**												

ID taxonomic group	***Khoratpithecus* fauna**	SEA_C
1	Giraffidae	8.3
2	Rhinocerotoidae	1.9
3	Proboscidea	1.5
4	Equidae*	5.5
5	Bovidae	3.4
6	Suidae	4.1

pair	**1_4**	**3_4**	**3_5**	**4_5**	**4_5**
A_O	0.2	0.7	0.9	2.5	2.5
% overlap	1.3	2.7	3.9	2.1	2.1
mean Yinseik % overlap	2.4				
mean incl. not overlapping groups	0.8				

Publication 2

Isotopic niche modelling of the Pondaung mammal fauna (middle Eocene, Myanmar) shows microhabitat differences. Insights into paleoecology and early anthropoid primate habitats

Authors: Sophie G. Habinger, Olivier Chavasseau, Stéphane Ducrocq, Yaowalak Chaimanee, Jean-Jacques Jaeger, Chit Sein, Aung Naing Soe, Samuel Stern, Hervé Bocherens

Journal: Frontiers in Ecology and Evolution

Initial submission: 28.11.2022

Accepted: 17.03.2023

DOI: 10.3389/fevo.2023.1110331

Publication date: 17.04.2023

Journal volume: 11

Article number: 1110331

frontiers | Frontiers in Ecology and Evolution

TYPE Original Research
PUBLISHED 17 April 2023
DOI 10.3389/fevo.2023.1110331

OPEN ACCESS

EDITED BY
Daniel J. Peppe,
Baylor University, United States

REVIEWED BY
Manuel Hernández Fernández,
Complutense University of Madrid, Spain
David L. Fox,
University of Minnesota Twin Cities,
United States

*CORRESPONDENCE
Sophie G. Habinger
✉ sophie-gabriele.habinger@uni-tuebingen.de

SPECIALTY SECTION
This article was submitted to Paleoecology, a section of the journal Frontiers in Ecology and Evolution

RECEIVED 28 November 2022
ACCEPTED 17 March 2023
PUBLISHED 17 April 2023

CITATION
Habinger SG, Chavasseau O, Ducrocq S, Chaimanee Y, Jaeger J-J, Sein C, Soe AN, Stern S and Bocherens H (2023) Isotopic niche modelling of the Pondaung mammal fauna (middle Eocene, Myanmar) shows microhabitat differences. Insights into paleoecology and early anthropoid primate habitats. *Front. Ecol. Evol.* 11:1110331. doi: 10.3389/fevo.2023.1110331

Isotopic niche modelling of the Pondaung mammal fauna (middle Eocene, Myanmar) shows microhabitat differences. Insights into paleoecology and early anthropoid primate habitats

Sophie G. Habinger[1,2]*, Olivier Chavasseau[1], Stéphane Ducrocq[1], Yaowalak Chaimanee[1], Jean-Jacques Jaeger[1], Chit Sein[3], Aung Naing Soe[4], Samuel Stern[2] and Hervé Bocherens[2,5]

[1]Laboratoire PALEVOPRIM, Université de Poitiers, Poitiers, France, [2]Department of Geosciences, Eberhard Karls Universität Tübingen, Tübingen, Germany, [3]Yangon University of Distance Education, Yangon, Myanmar, [4]Mandalay University of Distance Education, Mandalay, Myanmar, [5]Senckenberg Centre for Human Evolution and Palaeoenvironment at the University of Tübingen, Tübingen, Germany

The late Middle Eocene Pondaung Fm. is a window to understand the environment and ecosystem dynamics of a past greenhouse world and the paleoenvironments where modern mammal clades such as anthropoid primates originated. Previous studies focused on the overall climate and vegetation of this Eocene habitat and provided first evidence for an early monsoon onset before the orogenesis of the Himalayan-Tibetan range. Here, we wanted to investigate how the mammal fauna used this habitat and which different ecological niches and microhabitats they occupied. We analyzed the carbonate fraction of dental enamel of a fossil mammal assemblage from various localities of the Pondaung Fm. in Myanmar. Bayesian niche modelling of the $\delta^{13}C$ and $\delta^{18}O$ values allowed us to quantify aspects of the ecological core niches occupied by these taxa, to calculate niche overlap and to use these data to infer directional competition potential in this mammal assemblage. Furthermore, comparison of different areas of the Pondaung Fm. revealed two different microhabitats whose distribution is consistent with existing vegetation models. Most primate taxa were found in both described environments, which gives a first indication about their ecological flexibility.

KEYWORDS

isotopic niche, Pondaung Formation, Anthracotheriidae, anthropoid primates, competition potential, Eocene, paleoecology

1. Introduction

The climate today is changing fast and towards conditions never before experienced by humans. Some geological time periods might however be important analogues for possible climate scenarios in the future. One of these epochs is the Eocene that spans from 56 to 34 Ma (million years ago). The Eocene Earth was a greenhouse world with mean annual temperatures around 5°C higher than today in the Late Eocene (Zachos et al., 2001; Pagani et al., 2005). It was a world not unlike the possible man-made greenhouse world in our future (Burke et al., 2018;

Tierney et al., 2020). Studying this time period, the paleoenvironments, and the organization of fossil mammal communities can therefore provide valuable information to better understand various scenarios of future environments on Earth. In addition, it was also the period when modern mammals started their ecological radiation (e.g., Coster et al., 2018; Ducrocq et al., 2019; Jaeger et al., 2020). Here we want to focus on one mammal community, characterize its habitat and niche partitioning and explore if and to what extent approaches from ecology such as directional competition potential and individual specialization can be applied to paleoecology.

The mammal assemblage we focus on is from the late Middle Eocene Pondaung Formation (Fm.) located in modern day Myanmar. Southeast Asia is a hotspot for understanding mammal evolution during that time, as many radiations of important clades such as early anthropoid primates (Jaeger et al., 2020) and anthracotheres that are believed to be ancestral to the extant hippopotamids (Lihoreau et al., 2015), but also ruminants, pigs and hystricognath and anomalurid rodents took place there (Marivaux et al., 2005; Beard, 2016; Coster et al., 2018). The Pondaung Fm. is one of the fossil formations that document the rich biodiversity in this important biogeographic region. In this study we report the first substantial sample of isotopic data from herbivorous mammals and we correlate it to previously studied paleoenvironmental proxies. Our research questions can be structured around three topics: paleoseasonality, microhabitat differences, and niche partitioning from which we try to infer competition potential of the Pondaung mammal fauna with a focus on the Anthracotheriidae.

It has been thought that the Tibetan-Himalayan orogenesis was a prerequisite for a strong monsoonal climate in Southeast Asia, which could therefore not have originated earlier than 25 to 22 Ma. Studies on different climatic proxies including stable isotope analysis of gastropod shells and mammal teeth from the Pondaung Fm. revealed however that a monsoon-like climate was already present in the Eocene (Licht et al., 2014c; Toumoulin et al., 2022; Huang et al., 2023). With our larger data set, covering some of the localities represented in the previous study by Licht et al. (2014c) and more, we will try to test whether the same pattern is present. Furthermore, we investigated possibilities to compare monsoon intensity. For this we are comparing the Eocene data to a specimen of modern *Bos* from the Central Myanmar Basin (Habinger et al., 2022). $\delta^{18}O$ values of the Eocene mammals as low or lower than in the modern specimen together with a sinusoidal variation pattern would be evidence for a seasonal precipitation regime similar or even more pronounced as in Myanmar today. Our goal is not only to substantiate the hypothesis of an early onset Eocene monsoon-like precipitation regime, but also to characterize the environmental conditions linked to this kind of climate in more detail.

The localities of the Pondaung Fm. represent a terrestrial paleoecosystem with several river channels. They are situated in the Central Myanmar Basin (17–21°N, 92–96°E) west of the Chindwin River and northwest of the Irrawaddy River. However, in the late Middle Eocene the Pondaung Fm. was part of the Trans-Tethyan arc and therefore located farther south close to the equator (Westerweel et al., 2019, 2020). According to paleoenvironmental reconstructions, the ancient Eocene coastline with its mangrove forests lay farther to the west of the fossil localities. The vertebrate fossil bearing area was located further inland in a deltaic plain with reconstructed environments ranging from littoral to riparian forests and open-forested seasonal wetlands to dry dipterocarp and Schima forests in the upstream areas (Licht et al., 2013, 2014a, 2015; Gentis et al., 2021). Morphological adaptations to leaping in the primate taxa suggest that the Eocene forest density was high enough to allow for such a locomotive repertoire for example in the medium sized sivaladapid *Kytchaungia takaii* (body mass 1.6–1.8 kg; Kay et al., 2004; Beard et al., 2007; Marivaux et al., 2008a,b). The elevated temperatures during the Eocene led to a northward expansion of tropical and subtropical climatic zones, where rainforests could grow (Morley, 2018). We will test if microhabitat differences between the three geographic clusters of localities—the Bahin, Pangan, and Mogaung areas (Figure 1)—can be detected. Based on their geographic distribution and the vegetation model published by Licht et al. (2015) we have formulated two hypotheses. First, as the Mogaung area is further upstream the paleoriver system we are expecting the habitat there to be more densely forested and humid, as suggested by the different modelled vegetation regimes described above. Thus, both the $\delta^{13}C$ and $\delta^{18}O$ values of the mammals from this areas should be lower than at the other two areas. Second, should we detect microhabitat differences the probability that these differences are in fact correlated with spatial factors and not differences in exact dating of the localities of the different areas rise, if the Bahin and Pangan areas are more similar to one another than to the Mogaung area, and if they exhibit higher $\delta^{13}C$ and $\delta^{18}O$ values than the mammals from Mogaung.

As described above, the paleoenvironment of the Pondaung Fm. has already been characterized using different approaches, from ecomorphology to vegetation modelling based on fossil plant remains (Licht et al., 2015). However, to our knowledge no studies on niche partitioning and habitat use of this mammal fauna have been conducted yet. Increasing our knowledge on the organization of this fossil mammals has also implications on our knowledge about the palaeoecology of the earliest anthropoid primates, which makes studying it so important. Though these primates are not directly part of the data set used in this study, they were part of this same fossil mammal assemblage occurring sympatric with them in all three areas with fossil localities (see Supplementary Table SI 4). Reconstructing the paleoecology and niche partitioning among other members of this mammal fauna forms the basis on which we can discuss the paleoecology of the anthropoid primates in more detail. With our approach we can model aspects of the ecological niche of a taxonomic group reflecting the habitat and its use as well as dietary ecology. Should we detect microhabitat differences, but have some of the fossil primates occur in more than one this indicates a certain degree of ecological flexibility in these taxonomic groups.

Many open questions remain also regarding the anthracotheres, a group widely considered to be ancestral to hippos (Lihoreau et al., 2015), which are of special interest given their abundance and diversity in the Pondaung mammal fauna and the possibility to detect an ecological transition from a fully terrestrial to a semi-aquatic lifestyle around that time. As of today, three genera are known in this fossil assemblage. The taxonomy of this clade has been discussed and revised several times (Tsubamoto et al., 2002; Lihoreau and Ducrocq, 2007; Soe, 2008). With our isotopic data, we want to characterize aspects of their ecological niches at the genus and species level to see if there are any notable differences. In addition, we will calculate the niche overlap and explore the possibility to infer directional competition potential from these calculations. To our knowledge, this approach used by ecologists (Ogloff et al., 2019) has not yet been applied to fossil mammal communities. We expect that anthracothere taxa with higher body mass

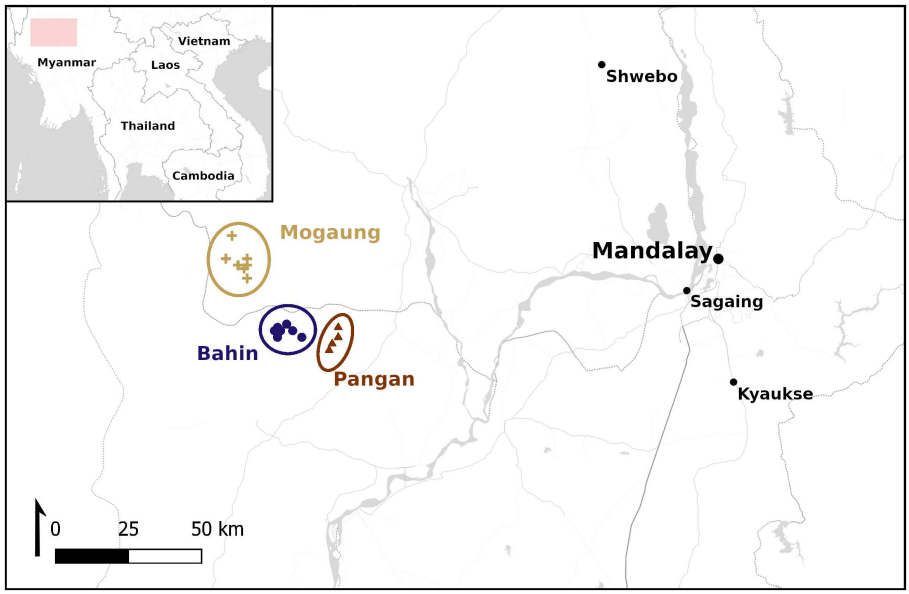

FIGURE 1
Map showing the location of the different localities of the Pondaung Fm. and their division into the three area clusters. Coordinates for all the localities from which samples were analyzed in this study are reported in Supplementary Table SI 1. The location of the detailed map is marked in the overview with a colored rectangle. Map tiles by Stamen Design, under CC BY 3.0. Data by OpenStreetMap, under ODbL.

share more of their niche space with other anthracotheres, as they can balance the higher degree of competition potential this implies with their size. For several medium to large sized anthracotheres from periods younger than the Eocene, such as *Arretotherium*, *Merycopotamus*, and *Libycosaurus* with body masses ranging from 150 to 1,000 kg, semi-aquatic lifestyle similar to extant hippos has been inferred (Orliac et al., 2013). They also displayed morphological adaptation to such a lifestyle that have often been referred to as hippo-ecomorph (Clementz et al., 2008), such as elevated orbits, external nares at the top of the snout, and massive limbs with high bone density (Lihoreau and Ducrocq, 2007). None of these morphological adaptations is present in the anthracotheres from the Pondaung Fm. We nevertheless wanted to test if their oxygen isotopic abundances already indicate semi-aquatic behavior before morphological adaptations to this lifestyle are visible. To do so we will test, if their $\delta^{18}O$ values are lower than the ones of the other taxonomic groups and if the variation in these values is reduced. Similar studies have been conducted on Eocene early whales (Thewissen et al., 2007; Cooper et al., 2016).

To answer all of these questions, we conducted stable isotope analysis on the carbonate fraction of fossil tooth enamel on the terrestrial mammal fauna from the Pondaung Fm. Due to its high content of inorganic hydroxyapatite and the fine and dense crystalline structure, enamel is very resistant to diagenetic changes. In addition, the Pondaung sediments that we analyzed are low in carbonate content, thus reducing the probability of diagenetic alteration of the original biological isotopic signal in the fossil teeth (for details see Methods section).

2. Materials and methods

2.1. The geological context

The mammal fauna that we analyzed for this study originates from the Pondaung Fm. in the Central Basin of Myanmar. During annual fieldwork campaigns of the French-Myanmar expedition, the fossils were collected from different localities that can be attributed to one of three areas—Bahin, Pangan, and Mogaung (Figure 1).

The Middle Eocene Pondaung Fm. is framed by the underlying Early Eocene Tabyin and the overlying Late Eocene Yaw Fm., both of which are marine deposits (Bender and Bannert, 1983). The Pondaung Fm. itself is up to 2 km thick (Bender and Bannert, 1983) with a succession of marine to terrestrial sediments (Stamp, 1922), but only the upper part (Upper Member) with a thickness of around 500 m (Oo et al., 2015) yielded significant amount of fossils representing a terrestrial mammal fauna. The stratigraphic positions of the different fossil localities to one another has not been studied in depth as of today. Nevertheless, the fossiliferous sediments of some localities from the Bahin area (PK1, PK2, PK3, PK4, PK5, and PK8) belong to the same traceable claystone named Ayoedawpon Taung Claystone ranging in thickness from 8 to 20 m. It is underlain directly by another widely traceable sediment, the Ayoedawpon Taung Sandstone. For two other fossil localities from the same region, the stratigraphic relationship is well constrained. The fossil outcrops at PK9 are part of the Nyaungpinle Claystone, which is stratigraphically lower than the Ayoedawpon Taung Claystone. The claystones at the PK12 locality on the other hand overlay directly the sandstones above the Ayoedawpon Taung Claystone (Maung et al., 2005; Suzuki et al., 2006). It has been dated to 40.31 ± 0.65 Ma and 40.22 ± 0.86 Ma using LA-ICP-MS, U–Pb zircons on tuffaceous sandstones from the Bahin area (PK4 and PK8; Zaw et al., 2014). This means that the Pondaung Fm. dates to around 40 Ma, which corresponds to the late Middle Eocene or Bartonian.

Its depositional environment was characterized by fluvial sediments of meandering river channels and is mostly comprised of sandstone with interspersed silt/clay bands. Fossils are mostly associated with lithofacies indicative of small fluvial or crevasse channels, swale fills and point bar deposits. Some evidence of peat layers and coal seams might indicate peat swamp formation of the inter-channel areas (Soe et al., 2002).

In their magnetostratigraphic study on a 319 m thick section of the Upper Member of the Pondaung Fm., Benammi et al. (2002) detected a single normal polarity. Although this homogenous paleomagnetism makes correlation with a specific Bartonian chron difficult, it indicates a high sedimentation rate of the floodplain (>0.3 mm $yr.^{-1}$; Licht et al., 2014b) as the maximum length of the possible Bartonian polar chron is smaller than 1 Myr (Benammi et al., 2002). This inference can be further substantiated by the results of another study on sedimentation rates in Asia (Métivier et al., 1999). Given this high sedimentation rate and the observed homogeneity of the fauna documented notably by rodents, amynodontids, anthracotheres and primates, we will consider that the Pondaung fossil remains correspond to a contemporaneous mammal fauna assemblage (Ducrocq et al., 2019). We give a detailed evaluation of sympatry of the different taxa in our sample per locality and area in Table SI 1.

2.2. The Pondaung mammal fauna

The fossil mammal fauna preserved in the Pondaung Fm. is famous for its unique and diverse primate assemblage. Two Sivaladapid adapiformes (*Kyitchaungia takaii*, and *Paukkaungia parva*), one Eosimiiforme (*Afrasia djijidae*), one Eosimiidae (*Bahinia pondaungensis*), a yet undescribed tarsid and most notably three different Amphipithecidae (*Ganlea megacanina*, *Pondaungia cotteri*, and *Myanmarpithecus yarshensis*) were found there (Marivaux et al., 2008b; Chaimanee et al., 2012; Fleagle, 2013; Jaeger et al., 2020). The phylogenetic position of the amphipithecids has been highly debated in the past century, but these primates are now firmly established as stem anthropoids by cranial, postcranial, and phylogenetic evidence (Jaeger et al., 2020). The high diversity in species underlines the importance of the Pondaung Fm. and Southeast Asia as the biogeographic region of early diversification and origin of this clade. This fact, together with the co-occurrence of three different stem anthropoid species together with eosimiids, which are basal anthropoids, and other primate taxa raises the interest in the paleoenvironment in which they all existed.

The diet of the Pondaung primates has been inferred from both dental morphology as well as dental microwear analysis. *Pondaungia* was likely predominantly frugivorous and also included some hard items in its diet. *Myanmarpithecus* subsisted on a mix of fruit and leaves (Kay et al., 2004; Ramdarshan et al., 2010). Although the unique tooth morphology of *Ganlea* complicates the dietary interpretations, this amphipithecid likely also ingested a mixture of leaves and fruit, but also engaged in seed predation (Beard et al., 2009; Jaeger et al., 2020). For the smaller primates *Bahinia* and *Paukkaungia* an insectivorous diet has been suggested (Kay et al., 2004; Ramdarshan et al., 2010). Only few primate postcranial remains have been found from the Pondaung Fm. Both *Pondaungia* and *Ganlea* have been described as active arboreal quadrupeds (Marivaux et al., 2003, 2010; Jaeger et al., 2020). For the Sivaladapidae a generalized locomotor profile as an arboreal quadruped has been suggested as well (Kay et al., 2004; Beard et al., 2007), with some evidence for leaping capabilities due to hip and pelvis morphology in *K. takaii* (Beard et al., 2007; Marivaux et al., 2008a,b). Given the small size of the teeth and their importance and rarity it was not possible to sample any of the Eocene anthropoid primates for stable isotope analysis.

Four large herbivore groups make up the majority of our sample of the Pondaung mammal fauna. The numbers in brackets correspond to the number of specimens sampled. There are three groups of perissodactyls, Brontotheriidae ($n = 24$), Amynodontidae ($n = 16$), Rhinocerotoidea indet. ($n = 27$), and the artiodactyl Anthracotheriidae ($n = 56$). Of these tooth specimens, 38 were sampled serially (9 Brontotheriidae, 9 Amynodontidae, 8 Rhinocerotoidea indet., and 12 Anthracotheriidae), hence providing a time series across the mineralization time of the fossil enamel allowing the investigation of seasonal variations. Brontotheriidae are described as being obligate browsers due to their brachydont teeth with bunoselenodont morphology and therefore preferring forest to woodland habitats in warm temperate to subtropical environments (Mader, 1998). Some of the brontotherids in our data set have been identified as *Bunobrontops* a more primitive genus in comparison to two other known genera, *Metatelmatherium* and *Sivatitanops*, from the Pondaung Fm. (Holroyd and Ciochon, 2000). Most of the Rhinocerotoidea are probably Amynodontidae, the most abundant family in the Pondaung Fm., but the fragmentary nature of the sampled fossils did not allow for an assignment of this taxonomic label with enough certainty. Previous work on fossil Rhinocerotoidea from Late Eocene sites in Vietnam characterized them as forest dwellers with their brachydont teeth and as being obligate browsers as well (Böhme et al., 2013). These brief descriptions of two of the main herbivorous taxonomic groups at the Pondaung Fm. reveal once more the lack of systematic studies especially on the Perissodactyl fauna. In addition, the tapiromorph *Bahinolophus* ($n = 2$), Eomoropidae ($n = 1$), and Ruminantia ($n = 2$) are also part of our data set. In four cases two teeth were sampled per individual (*Siamotherium* PNG-20 M2/M3 and PNG-141 M2/M2, *Anthracokeryx tenuis* PNG-22/23, *Anthracotherium crassum* PNG-56/57, and Amynodontidae PNG-92/93). In general, the ungulate fauna in the Pondaung mammal fauna is considered to be representative of the original living community, while a sampling bias is likely in the case of rodents and other small mammals including primates. This is due to the fieldwork method applied by the different teams of researchers, which mainly conduct surface prospecting in the area (Tsubamoto et al., 2005).

The Pondaung Fm. has also yielded some creodont (Egi and Tsubamoto, 2000; de Bonis et al., 2018), fish, reptile (crocodilian, lizard, and turtle; Hutchison et al., 2004; Tsubamoto et al., 2006a; Head et al., 2013) and bird fossils (Tsubamoto et al., 2006b). However, no extensive systematic studies on this material exist as of now and it has therefore not been included in our data set for isotopic analysis.

2.3. The anthracotheres

In the Pondaung Fm., we find a high diversity of anthracothere taxa. This comes as no surprise, as this taxonomic group likely originated in Southeast Asia and experienced a radiation there in the late Middle Eocene. Later on, anthracotheres spread from Asia to Europe, Africa, and North America. Three different anthracothere genera are known from the Pondaung Fm.—*Anthracotherium*, *Anthracokeryx*, and *Siamotherium*. In contrast to the perissodactyls from the Pondaung mammal fauna that were strictly herbivorous according to their tooth morphology, anthracotheres were more opportunistic feeders. They likely had a much more diversified diet that included leaves, fruits, roots, and invertebrates.

Anthracotherium ($n = 20$) was a medium to large sized anthracothere and the largest of the three genera found at the Pondaung Fm. It has bunodont teeth suitable for crushing tougher food like roots or even scavenge carcasses from time to time. Hence, its cranio-dental morphology indicates a more generalist diet not unlike the one of extant pigs (Ducrocq, 1999). Therefore, we hypothesize that it occupied more open forests than the other two and probably lived closer to the river system, meaning that it was more water dependent than the other anthracothere genera known from the Pondaung Fm. Two species could be identified in our sample, the smaller *A. crassum* ($n = 5$) and the larger *A. pangan* ($n = 11$).

The second genus, *Anthracokeryx* ($n = 13$) with the two species, the larger *Anthracokeryx birmanicum* ($n = 4$) and the smaller *A. tenuis* ($n = 4$), represents a more typical forest dweller with bunoselenodont teeth. These are typical for a more specialized herbivorous foraging ecology (Ducrocq, 1999). It has a body mass, of about 20–25 kg (Lihoreau and Ducrocq, 2007). This and its cranio-dental morphology are consistent with dwelling in denser forests and having a more specialized folivorous diet.

Siamotherium ($n = 4$) is the smallest and most primitive of the three genera with an estimated body mass of 7.5 kg for *S. pondaungensis*. It was a small, slender animal with a short snout showing first signs of selenodonty on its molars (Ducrocq et al., 2001; Soe et al., 2017; Ducrocq et al., 2021). Its subsistence strategy has been described as more omnivorous including occasional scavenging, and it is thought to have lived in open forested areas (Soe et al., 2017). For this study, we could sample four teeth from two individuals.

2.4. Sample preparation and analysis

We sampled the specimens during a museum visit to the National Museum in Nay Pyi Taw in February 2020 and the fieldwork campaign in the following weeks. The specimens were cleaned from dust and sediment using ethanol and the outermost layer of fossil enamel was removed on the sampling site as these would be most susceptible to diagenetic alteration. During sampling 6–12 mg of fossil enamel powder were drilled using a portable diamond coated micro drill station. Dentine samples from these specimens were also sampled using the same sampling methodology. Sediment attached to the specimens was also collected in some instances, depending on availability. Both of these tissue types were used to assess diagenesis (see SI). They are reported in Supplementary Table SI 3.

The pretreatment and analysis in the IRMS (isotopic ratio mass spectrometer) was conducted in the laboratories of the Biogeology working group (Department of Geosciences) at the University of Tübingen using a modified Koch method (Bocherens et al., 1994; Koch et al., 1997; Wright and Schwarcz, 1999). We added 1.35 ml of NaOCl at a concentration of 2.5% to each of the powdered samples and left it react for 24 h to remove organic matter that might be present in the sample. Then the liquid was removed and after rinsing the samples three times with distilled water, 1.35 ml of 1 M acetic acid buffer solution (CH_3COOH) was added to the enamel and dentine samples and let to react with the samples for 24 h. Given difference in crystalline structure between enamel and other exogenous sources of carbonates, the latter ones were removed by this step. The samples were once again rinsed three times with distilled water and then dried at 35°C for 72 h. With each set of samples two internal standards of elephant and hippo enamel were treated following the same protocol. Prior to analysis one internal (LM = Laaser Marmor) and two international (IAEA-603, NBS-18) pure carbonate standards were added to the data set after every 15 samples. These were not subjected to any pretreatment prior to analysis.

For the analysis with the Elementar IsoPrime 100 IRMS 2.5–3 mg of enamel or 0.1 mg of pure carbonate were reacted with 99% phosphoric acid (H_3PO_4) at 70°C for 4 h. The isotopic ratios of the resulting CO_2 gas were measured four times for each sample over a time span of 15 min. This allowed us to monitor measurement precision by calculating the mean and standard deviation of these repeated measurements for each sample (Szpak et al., 2017). In addition, measurement uncertainty was assessed using the standards. It is reported for each sample in Supplementary Table SI 2. Isotopic ratios are reported using the δ-notation (in per mill). The calculation is based on formula (1) (Coplen, 2011; Bond and Hobson, 2012) where j marks the heavier and i the lighter isotope.

$$\delta^{j/i}X = \frac{\left({}^{j}X/{}^{i}X\right)_{sample}}{\left({}^{j}X/{}^{i}X\right)_{standard}} - 1 \qquad (1)$$

With the internal enamel standards the isotopic ratios were calibrated relative to VPDB (Vienna Pee Dee Belemnite). Oxygen isotopic ratios have been subsequently converted to $\delta^{18}O_{VSMOW}$ values (Vienna Mean Ocean Water) using the formula (2) by (Coplen, 1988).

$$\delta^{18}O_{VSMOW} = \left(1.03091 \times \delta^{18}O_{VPDB} + 30.91\right) \qquad (2)$$

In Supplementary Tables SI 2, SI 3 we also report the $CaCO_3$ content of each sample. It was calculated with the Ion Vantage software based on an estimated elemental composition with sample weight, peak area and the internal LM standard as variables. The resulting $CaCO_3$ values are subsequently scaled up until one of the international pure carbonate standards reaches 100%. $CaCO_3$ content of sediment samples from various Pondaung localities was too low when we used the regular amount of 0.1 mg of powdered sediment sample in the IRMS. Even when we raised the sample size to 2.5–3 mg of powdered sample, $CaCO_3$ content remained very low for the Pondaung sediments (Supplementary Table SI 3). We discuss the results of the sediment and dentine samples in the Supplementary Information to evaluate the risk of diagenetic alteration of the original biogenic isotopic signal in our data set.

2.5. Data correction and statistical analysis

Prior to data analysis and isotopic niche modelling two types of data corrections were applied to account for differences in enrichment of $\delta^{13}C$ values between diet and bioapatite as well as changing $\delta^{13}C$ baselines, due to shifts of the isotopic composition of CO_2 in the atmosphere. All the data before and after the corrections were applied as well as the specific enrichment factor used to calculate $\delta^{13}C_{diet}$ values are reported in Table 1.

In the past one uniform enrichment factor of 14‰ for the carbon isotope ratio from diet to apatite in dental enamel has been used for all medium to large bodied herbivores (Cerling and Harris, 1999). Recent studies however showed, that many different factors such as body mass and digestive physiology influence this enrichment factor (Passey et al., 2005; Tejada-Lara et al., 2018). Conducting an experimental study to establish a specific ε^* for a species is only possible for extant animals. For our study we therefore apply the regression formula (3) proposed by Tejada-Lara et al. (2018) to account for differences of ε^* due to variations in body mass. This is the conservative formula, which is not specific to foregut or hindgut fermenters.

$$\varepsilon^* = e^{\left[2.4+0.034(\mathrm{BM})\right]}. \quad (3)$$

Here, BM stands for the log transformed (ln) body mass in kg. The resulting enrichment factor is in per mill (‰), which can then be applied to the data prior to isotopic modelling (Table 1) to calculate $\delta^{13}C_{diet}$ values (4).

$$\delta^{13}C_{diet} = \delta^{13}C_{apatite} + \varepsilon^*. \quad (4)$$

Instead of correcting the individual $\delta^{13}C$ values for changes in $\delta^{13}C_{CO2}$ of the atmosphere, which is the pool from which plants extract the carbon in their tissue during photosynthesis, we chose to apply the corrections to the thresholds used for the interpretation of vegetation type and density. Post-1,930 the $\delta^{13}C_{CO2}$ values were −8‰ (Zachos et al., 2001; Cerling et al., 2010 but see Keeling et al., 2005 for fluctuations within this time period). Tipple et al. (2010) reconstructed Cenozoic $\delta^{13}C_{CO2}$ values based on stable isotope analysis of benthic foraminifera. For the middle Eocene at 40 Ma their model suggest higher $\delta^{13}C_{CO2}$ values than today with an estimate of −5.5‰ (ranging from −6‰ to −5.2‰ at a confidence interval of 90%). Thus, we corrected the modern thresholds by +2.5‰ before interpreting the Eocene data.

Following the Hutchinsonian niche concept (Hutchinson, 1957, 1978), we calculated core ecological niches for each taxonomic group using the R package SIBER (version 2.1.6; Jackson et al., 2011). For this study, we quantify niches using standard ellipse area corrected for small sample sizes (SEA_C). They correspond to a confidence interval (CI) of 40%. As this modelling approach is based on a maximum likelihood estimation in a Bayesian framework, the limiting effect of small sample sizes on statistical power of our analysis is counteracted to a certain extent. Should the sample size of a taxonomic group be below five individuals we mention it explicitly during the interpretation of the results.

For the evaluation of niche packing and directional competition potential, we calculated three metrics to quantify niche overlap between two taxonomic groups. These are the percentage of the total niche space of the two taxa that is shared between them (% overlap), which is calculated with formula (5; Ogloff et al., 2019), the percentage of niche area of taxon A (A_A) that overlaps the niche space of taxon B (A_B), and vice versa. The latter two are reported as A_A–A_B and A_B–A_A, respectively. A_O which is the area shared between taxon A and taxon B was acquired by using the maxLikOverlap() function of the SIBER package. A_A and A_B are calculated using A_O and the unitary method.

TABLE 1 Summary of the body mass (BM) estimates and the modelled isotopic enrichment factor based on formula (3).

Taxonomy	BM (kg)	ε^* (‰) Tejada-Lara et al. (2018)	Reference for BM estimation
Anthracotheriidae		−12.5	
Anthracotherium		−13.1	
Anthracotherium pangan	237	−13.3	Tsubamoto et al. (2005)
Anthracotherium crassum	131	−13.0	Tsubamoto et al. (2005)
Anthracokeryx		−12.3	
Anthracokeryx birmanicum	59.4	−12.7	Tsubamoto et al. (2005)
Anthracokeryx tenuis	16.1	−12.1	Tsubamoto et al. (2005)
Anthracokeryx (lower limit)	20	−12.2	Lihoreau and Ducrocq (2007)
Anthracokeryx (upper limit)	25	−12.3	Lihoreau and Ducrocq (2007)
Siamotherium pondaungensis	7.5	−11.8	Ducrocq et al. (2021)
Rhinocerotoidea		−13.6	
Amynodontidae indet.	154	−13.1	Tsubamoto et al. (2005)
Paramynodon		−13.8	
Paramynodon cotteri	1,010	−13.9	Tsubamoto et al. (2005)
Paramynodon birmanicus	441	−13.6	Tsubamoto et al. (2005)
Brontotheriidae		−14.1	
Sivatitanops birmanicus	5,110	−14.7	Tsubamoto et al. (2005)
Sivatitanops cotteri	2,080	−14.3	Tsubamoto et al. (2005)
Bunobrontops sp.	512	−13.6	Tsubamoto et al. (2005)
Bunobrontops savagei	987	−13.9	Tsubamoto et al. (2005)
Ruminantia		−12.2	
Artiodactyla indet	9.47	−11.9	Tsubamoto et al. (2005)
Indolophus guptai	20.7	−12.2	Tsubamoto et al. (2005)
Bahinolophus birmanicus	51.6	−12.6	Tsubamoto et al. (2005)
Eomoropidae indet.	18.4	−12.2	Tsubamoto et al. (2005)
Eomoropus pawnyunti	15.2	−12.1	Tsubamoto et al. (2005)

For specimen where a taxonomic identification to species level was not possible, the mean modelled enrichment factor the highest taxonomic resolution possible was applied. In this table, whenever no body mass estimate is given, the enrichment factor corresponds to the mean value of the taxonomic groups marked by color. The specific value for the calculation of the $\delta^{13}C$ value of each specimen is reported with the calibrated data before corrections in Supplementary Table SI 2.

$$\%\mathrm{overlap} = \frac{A_O}{A_A + A_B - A_O} \times 100 \quad (5)$$

Based on the modelled ecological niches we also calculated the relative individual niche (RINI; Sheppard et al., 2018) for the individuals from which serial samples were taken. RINI is a metric that relates the individual niche area to the population niche area. Here, it expresses the proportion the SEA_Cs (CI = 40%) of an individual that is shared with the union of all the SEA_Cs of the serially sampled individuals from a taxonomic group. For this we used the

siberKapow() function that is part of the SIBER package. Code examples can be found in the explanatory vignettes at the SIBER Github repository.

Given the small sample sizes we are working with and the fact that normal distribution of our data cannot be attested in all cases non-parametric Wilcox rank sum tests are used to test for statistically significant differences in this study. To screen for relationships between $\delta^{13}C$ and $\delta^{18}O$ values in the specimen where intra-individual serial samples were taken, we performed Spearman correlation analyses. Habinger et al. (2022) identified one statistical outlier in the modern *Bos* data we also use in our study. This outlier was not included in the statistical analysis, but is shown in the plots. Statistical significance is ascribed to test results where $p = <0.05$. In cases where several statistical tests were run on the same data set, value of ps have been adjusted with the Bonferroni correction, a conservative method to correct for multiple comparisons (Bonferroni, 1936). All statistical tests and models were run in R version 4.1.2.

3. Results

A comparison of the $\delta^{18}O$ values of the modern bovid from the Central Basin of Myanmar and the fossil mammals from the Pondaung Fm. showed a significant difference ($W = 0$, value of $p < 0.001$), with the Eocene $\delta^{18}O$ values being lower. Sinusoidal patterns were present in both the modern and the fossil specimen. Two of the 38 specimens that were sampled serially are plotted together with the modern *Bos* in Figure 2. Figures of all the serially sampled individuals are provided in the Supplementary Information. We also tested if there was a correlation between the $\delta^{13}C$ and $\delta^{18}O$ values, which would indicate a consistent influence of seasonal precipitation on the plants consumed. We found no constant relationship of these values across all the mammal data (rho = 0.10, $S = 2{,}366{,}301$, $p = 0.106$). However, when we sorted the specimen based on taxonomy (family level), we found significant positive correlation in Anthracotheriidae (rho = 0.56, $S = 9{,}147.2$, $p = 2.28e\text{-}05$) and Amynodontidae (rho = −0.37, $S = 125{,}705$, $p = <0.001$) as well as significant negative correlation in Rhinocerotoidea (rho = 0.33, $S = 18{,}683$, $p = 0.015$). Only in the Brontotheriidae no statistically significant correlation was present (rho = 0.1923064, S = 35,280, $p = 0.128$). The negative correlation in the modern *Bos* also was not statistically significant (rho = −0.34, $S = 1{,}299$, $p = 0.170$).

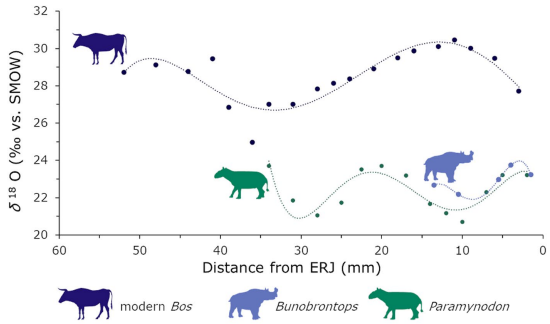

FIGURE 2
Visualization of some exemplary serially sampled specimen, the modern bovid and two of the Eocene specimen from the Pondaung Fm. (*Bunobrontops* PNG-47, *Paramynodon* PNG-119), illustrating different seasonal precipitation regimes. The distance from the ERJ (enamel root junction) on the x-axis has been inverted. This way it represents the values in an intuitive temporal sequence from the oldest ones to the left to the youngest ones to the right. The statistical outlier (lowest $\delta^{18}O$ value) in the modern *Bos* is included in this figure, but has been excluded from the statistical analysis. Silhouettes *via* Phylopic under CC 3.0 license (modern *Bos* by T. Michael Keesey, *Bunobrontops* and *Paramynodon* by Zimices).

The different localities where the fossil specimens analyzed in this study have been found can be separated into three areas. Therefore, we wanted to test if the isotopic ratios indicate a difference in environment between them. Visual inspection of the $\delta^{13}C$ and $\delta^{18}O$ values per area (Figure 3) showed some inter-area differences. The comparison of $\delta^{13}C$ and $\delta^{18}O$ values from the Bahin and Pangan localities using Wilcox rank sum tests showed no significant difference ($p = 1$ in both cases). Hence, these two areas will be grouped together for the ecological niche modelling. We then conducted a Wilcox rank sum test, to see if the $\delta^{13}C$ and $\delta^{18}O$ values were significantly different in the Mogaung area than in the Bahin and Pangan ones. All of these test results showed significant differences (Mogaung—Bahin C: $p = 0.001$, O: $p = 0.001$; Mogaung—Pangan C: $p = 0.003$, O: $p = 0.110$). Hence, we modelled the ecological niches separately for the mammals from the Mogaung localities.

The Bahin and Pangan areas ($\delta^{13}C$: −27.2 to −20.7‰; $\delta^{18}O$: 26.2 to 19.8‰) do not only have significantly higher $\delta^{13}C$ and $\delta^{18}O$ values, the variation of these data is also smaller than in the Mogaung area ($\delta^{13}C$: −29.2 to −21.2‰; $\delta^{18}O$: 25.9 to 18.1‰). Bulk and averaged serial sampling are visualized in Figure 4. Summary statistics for the mammal communities from the Bahin/Pangan and Mogaung area are reported in Table 2 and results of the niche overlap calculations in Table 3. The median % overlap of the Bahin/Pangan area is higher (17.8%) than in the Mogaung area (16.3%). This difference is not statistically significant ($W = 9$, value of $p = 0.786$). The median SEA_C is almost identical in both areas with 3.6 in Bahin/Pangan and 3.5 in Mogaung.

Additionally, we calculated the RINI for the individuals that were sampled serially. A first visual inspection of the patterns between taxonomic groups shows that in Brontotheriidae, as well as the Amynodontidae and Rhinocerotoidea most individuals cluster closely together except for only two or three (Figure 5). In the Anthracotheriidae the individual niches plot more continuously without an apparent split in discrete clusters. It also looks as if the modelled ecological niches of the Anthracotheriidae are slightly bigger than the ones of the other taxonomic groups. This is confirmed when we look at the different median SEA_Cs (Table 4). There we also see that they also have the highest median RINI of all the taxonomic groups. However, these differences are not significant (SEA_C: $W = 162$, value of $p = 0.863$; RINI: $W = 155$, value of $p = 0.280$).

4. Discussion

4.1. Paleoseasonality

The $\delta^{18}O$ values including the minimum values, which represent the seasonal precipitation maxima in tropical environments (Dansgaard, 1964; Sun et al., 2021), of the modern bovid are higher than the Eocene (Figure 2) ones even though the temperatures nowadays are around 5°C lower than they were back then. The temperature effect leads to higher $\delta^{18}O$ values under warmer

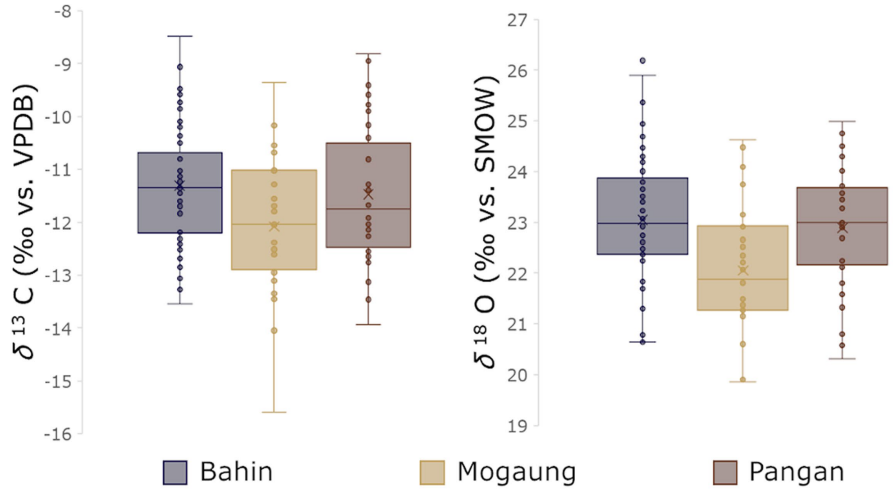

FIGURE 3
Box plots of the compiled $\delta^{13}C$ (left) and $\delta^{18}O$ (right) values per area. The Mogaung values are lower for both isotopes which is consistent with a difference in microhabitats.

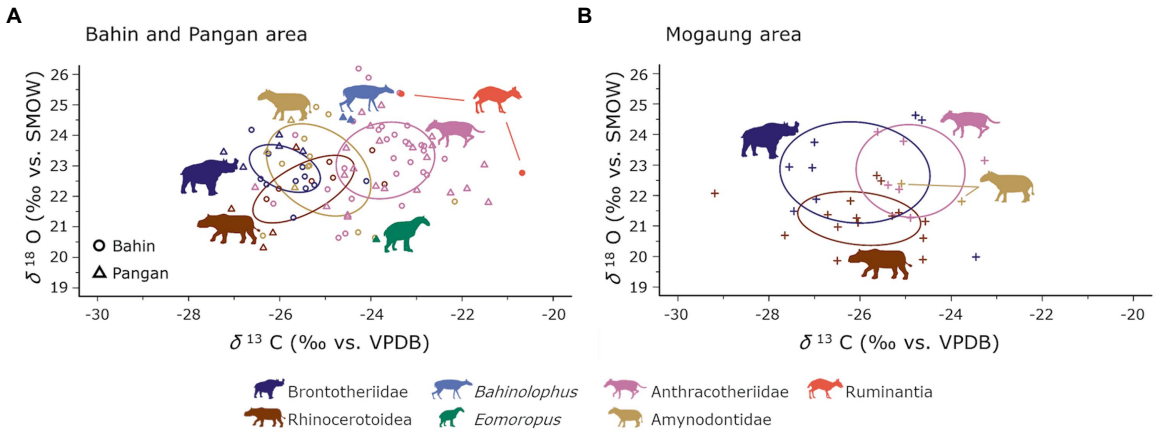

FIGURE 4
Ecological niche modelling of the Bahin/Pangan **(A)** and Mogaung **(B)** mammal communities based on all bulk and averaged serially sampled specimen. Ellipses represent the modelled core ecological niches. Silhouettes are from Phylopic under CC BY 3.0 license by Zimices.

conditions (Dansgaard, 1964). However, the pattern in the comparison of the modern bovid with the Eocene mammals is reversed. This would be consistent with a generally wetter, more humid climate in the Eocene than in Myanmar today. Consistently lower minimum $\delta^{18}O$ might even indicate an increased monsoon intensity in the Eocene, although they could have also been influenced by the possible closer paleogeographic proximity of the fossil localities to the coast at 40 Ma (Westerweel et al., 2019, 2020).

We screened for a correlation between the $\delta^{13}C$ and $\delta^{18}O$ values of the serially sampled specimen; as such a relationship would be consistent with an influence of seasonality on variation in the diet (e.g., the type of plant or plant part ingested) or habitat. We do see that there is a statistically significant correlation between seasonal precipitation and diet/habitat in the Anthracotheriidae, Amynodontidae, and Rhinocerotoidea as opposed to the Brontotheriidae. This relation however is not uniform across the taxonomic groups. This pattern is consistent with an interpretation of different strategies of the taxonomic groups to react to seasonal habitat changes such as for example adapting their subsistence strategy or migration. As there is no correlation of the $\delta^{13}C$ or $\delta^{18}O$ values diagenesis is likely not the cause for these correlations (see discussion in the Supplementary Information). The correlation in Anthracotheriidae and Amynodontidae is positive, whereas it is negative in Rhinocerotoidea. This difference between Amynodontidae and Rhinocerotoidea is surprising, since as stated earlier, most specimens which are classified as Rhinocerotoidea are likely amynodonts as no other genus from this superfamily has been described yet. Of course, this difference could be introduced by a sampling bias. If not, it could indicate that either there are two groups of amynodonts that have different ecological strategies to cope with seasonality or that these different ecological strategies also coincide with a taxonomic distinction on a generic level that has not been described as of yet. As there are no experimental studies that focus on this relationship, we cannot precisely characterize the difference

10.3389/fevo.2023.1110331

TABLE 2 Summary statistics from the isotope data used for ecological niche modelling (bulk and averaged intra individual serial samples).

Taxonomy	n°	$\delta^{13}C_{diet}$ (‰ VPDB)		$\delta^{18}O$ (‰ VSMOW)		TA (‰^{2})	SEA_C (‰^{2})
		Mean	SD	Mean	SD		
Bahin/Pangan							
Brontotheriidae	16	−25.9	0.7	22.9	0.7	4.4	1.7
Anthracotheriidae	50 (46)	−23.7	1.1	23.2	1.2	16.6	4.2
Anthracotherium	19 (18)	−23.4	0.8	22.9	0.9	5.7	2.2
A. crassum	5 (4)	−23.3	0.5	23.6	0.6	0.6	0.6
A. pangan	11	−23.6	1.0	22.5	0.9	4.6	2.5
Anthracokeryx	15 (14)	−23.5	1.0	23.2	1.2	8.2	4.0
A. birmanicum	5	−24.0	0.7	23.7	1.2	1.7	2.4
A. tenuis	4 (3)	−23.2	1.3	23.6	1.0	3.1	5.8
Amynodontidae	14 (13)	−25.1	1.1	22.9	1.4	11.4	5.1
Rhinocerotoidea	11	−25.5	1.0	22.2	1.0	6.1	3.0
Siamotherium pondaungensis	4 (2)	−23.2	1.1	23.5	0.4	1.1	2.0
Bahinolophus	2	−24.5	0.1	24.5	0.1	-	-
Eomoropidae	1	−23.9	-	20.6	-	-	-
Ruminantia	2	−22.0	1.9	24.1	1.8	-	-
Mogaung							
Brontotheriidae	8	−26.1	1.6	22.8	1.6	11.3	9.1
Anthracotheriidae	6	−24.9	0.8	22.8	1.1	3.3	3.5
Anthracotherium	5	−24.9	0.9	22.6	1.1	-	-
A. crassum	1	−25.4	-	22.3	-	-	-
Anthracokeryx birmanicum	1	−25.0	-	23.8	-	-	-
Amynodontidae	2	−24.4	0.9	22.1	0.4	-	-
Rhinocerotoidea	15	−26.0	1.2	21.2	0.8	8.2	3.3

The numbers under n° correspond to number of specimen, which were used to calculate the summary statistics. In cases where multiple teeth from the same individual have been sampled the number of individuals is given in brackets. All specimens from levels of higher taxonomic resolution (anthracothere genus and species level) are included in the calculation and modelled groups at a lower taxonomic level (anthracothere genus and family level) for summary statistics, niche modelling and niche overlap calculations. Total area (TA; Layman et al., 2007) corresponds to the convex hull area of a taxonomic group whereas SEA_C is the modelled core ecological niche area corrected for small sample sizes (CI = 40%).

between a positive versus a negative correlation of $\delta^{13}C$ and $\delta^{18}O$ values in plants or herbivorous animals.

Nevertheless, the occurrence of significant correlation of $\delta^{13}C$ and $\delta^{18}O$ values can be interpreted as an increased influence, e.g., due to the reconstructed monsoon intensity in the Eocene, of seasonality on the diet/habitat on some of the mammal groups from the Pondaung Fm when compared with the modern cow. Two important limitations of this interpretation are the small sample size for modern *Bos*, which is only represented by one individual and the fact that we are comparing wild Eocene mammals with a modern domestic *Bos*, whose precise diet is unknown. But even the statistically significant correlations of $\delta^{13}C$ and $\delta^{18}O$ values in the Eocene alone are another indication of an intense Eocene monsoon.

4.2. Paleoenvironmental differences between the Bahin, Pangan, and Mogaung areas

The Pondaung Fm. was a habitat with only C_3 plants present. When we consider the changes in $\delta^{13}C_{CO2}$ values of the atmosphere discussed in the Methods section, modern C_3 plants would lead to $\delta^{13}C_{diet}$ values of −17.5 to −34.5‰ (modern thresholds from Kohn, 2010). Hence, $\delta^{13}C_{diet}$ values higher than −17.5‰ would be evidence for the presence of C_4 plants in the Eocene. The $\delta^{13}C$ values of all the mammals in the data set used in this study range from −20.7 to −29.2‰, and thus falling within the range of Eocene C_3 plants. As C_4 plants with their photosynthetic pathway adapted to dry and hot climatic conditions did not evolve and spread to Asia until the Late Miocene (Cerling et al., 1993, 1997) we did not expect to find any values that high in our data set. In Myanmar, the first evidence of the presence of C_4 plants based on isotopic data is from 6 Ma (Thein et al., 2011; Habinger et al., 2022).

The variation of $\delta^{13}C_{diet}$ values that we observed within and between the two study areas is caused by differences in vegetation structure. Due to the canopy effect, including factors such as low irradiance and carbon recycling, $\delta^{13}C$ values decrease with an increased canopy density (van der Merwe and Medina, 1989; Jackson et al., 1993; Bonal et al., 2000; Leffler and Enquist, 2002; Bonafini et al., 2013). This effect is less pronounced high up in the canopy and more open patches of a habitat. In these microhabitats C_3 plants yield delta-values of −18.5 to −24.5‰, whereas $\delta^{13}C_{diet}$ values of −29‰ and

10.3389/fevo.2023.1110331

TABLE 3 Summary of the results of the niche overlap in the Bahin/Pangan and Mogaung mammal communities.

Species order (A_A–A_B)	A_O	% Overlap	A_A–A_B	A_B–A_A
Bahin/Pangan				
Amynodontidae—Rhinocerotoidea	2.0	32.9%	39.2%	67.0%
Amynodontidae—Brontotheriidae	1.3	23.5%	25.4%	76.3%
Amynodontidae—Anthracotheriidae	0.9	10.4%	17.1%	20.9%
Rhinocerotoidea—Brontotheriidae	0.7	17.8%	23.7%	41.7%
Rhinocerotoidea—Anthracotheriidae	0.3	3.8%	8.7%	6.2%
A. pangan—A. crassum	0.3	8.7%	10.0%	40.1%
A. pangan—A. tenuis	1.1	15.7%	44.5%	19.5%
A. pangan—S. pondaungensis	0.4	10.6%	17.2%	21.8%
A. pangan—A. birmanicum	0.1	2.5%	4.7%	5.0%
A. crassum—A. birmanicum	0.2	6.4%	28.6%	7.6%
A. crassum—S. pondaungensis	0.4	19.8%	69.1%	21.8%
A. crassum—A. tenuis	0.6	10.9%	99.9%	10.9%
S. pondaungensis—A. tenuis	2.0	34.0%	98.6%	34.1%
S. pondaungensis—A. birmanicum	0.6	16.8%	31.5%	26.4%
A. tenuis—A. birmanicum	1.7	27.3%	30.3%	73.5%
Anthracotherium—Anthracokeryx	2.2	53.1%	98.6%	53.5%
Anthracotherium—Siamotherium	0.9	27.2%	40.8%	44.8%
Anthracokeryx—Siamotherium	1.6	35.5%	39.2%	79.3%
Mogaung				
Rhinocerotoidea—Brontotheriidae	1.7	16.3%	52.5%	19.1%
Rhinocerotoidea—Anthracotheriidae	0.0	0.4%	0.9%	0.8%
Brontotheriidae—Anthracotheriidae	2.5	24.8%	27.5%	71.6%

A_0 is the area of the niche space shared between two taxonomic groups (‰^{2}). % overlap is the percentage of the total niche space of the two taxa that is shared between them. A_A—A_B is the percentage of niche area of taxonomic group A that is shared with taxonomic group B. A_B—A_A is the same metric, but it gives the percentage of shared niche area of taxonomic group B. The three overlap metrics were calculated for each pair of taxonomic groups whose core ecological niches overlap. All specimens from levels of higher taxonomic resolution (anthracothere genus and species level) are included in the calculation and modelled groups at a lower taxonomic level (anthracothere genus and family level) for summary statistics, niche modelling and niche overlap calculations.

below are indicative for the understory of a closed canopy forest (modern thresholds from Kohn, 2010). $\delta^{13}C$ values from both the Bahin/Pangan (−20.7 to −27.2‰) and the Mogaung area (−21.2 to −29.2‰) are consistent with open-forested seasonal woodlands, like the ones reconstructed for the upper deltaic plain by Licht et al. (2015). These woodlands were denser in the Mogaung area, given the significantly lower $\delta^{13}C$ values (Figure 3), and with specimen with the lowest $\delta^{13}C_{diet}$ values falling just below the threshold for closed canopy vegetation. This possibly indicates proximity to the more closed dipterocarp forests in the upstream areas from the same vegetation model (Licht et al., 2015). An interpretation of the microhabitat differences as being caused by such spatial factors is also consistent with the paleoenvironmental similarities of the geographically close Bahin and Pangan areas with one another. However, given the currently available dates and correlations of the stratigraphic sequences of the different fossil localities of the Pondaung Fm. we cannot rule out the possibility of the two microhabitats representing a changing environment at two different late Middle Eocene time intervals completely.

The significant difference in the $\delta^{18}O$ values between the Bahin/Pangan and the Mogaung area is consistent with a more humid climate in the latter. As the Mogaung area was probably more densely forested as well, the data are also consistent with a consumption of drinking water from water sources that are more protected from direct sunlight. Water sources that are subjected to evaporation would have higher $\delta^{18}O$ values as the lighter oxygen isotope would evaporate more readily. However, there is no significant difference in the ranges of $\delta^{18}O$ values of the intra-individually sampled individuals between the Bahin/Pangan and the Mogaung area ($W = 104$, value of $p = 0.07336$). Range here is defined as the minimum $\delta^{18}O$ value subtracted from the maximum one. This indicates that there is no difference in the intensity of the seasonality.

Considering the occurrences of fossil primates (Supplementary Table SI4) in relation with these two different habitat types, we see that so far for only two of the four genera of the anthropoid Amphipithecidae have been found at all three localities, *Aseanpithecus* and *Pondaungia*. So at least for these two amphipithecid genera we can propose a certain degree of ecological flexibility. A more detailed discussion of the fossil primate occurrences and how they relate to the localities and the other mammal taxa in our data set can be found in the Supplementary Information.

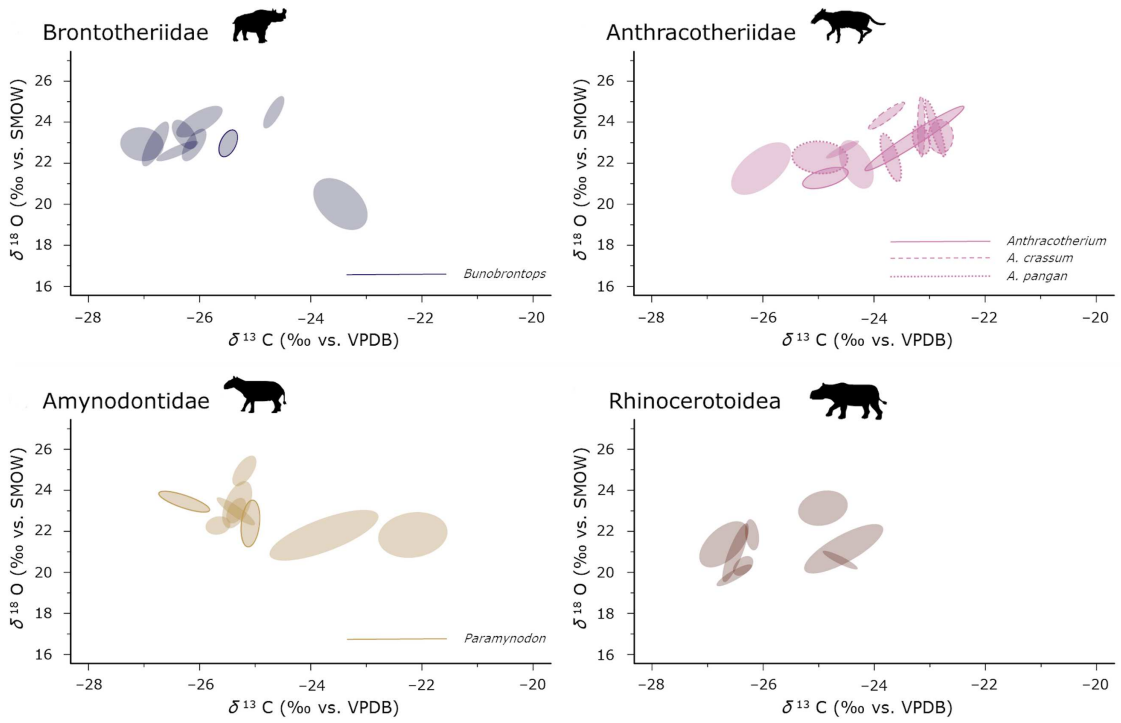

FIGURE 5
Modelled ecological niches of the serially sampled specimen in separate graphs per taxonomic group. Each ellipse corresponds to the modelled core ecological niche represented by SEA_C of one individual (CI=40%) visualizing different clustering patterns especially between the Anthracotheriidae and the other three taxonomic groups. Silhouettes are from Phylopic under CC BY 3.0 license by Zimices.

4.3. Niche partitioning and directional competition potential

An evaluation of differences in size of combined ecological niches on taxonomic family level, which potentially consist of multiple species, and their % overlap showed no significant differences between the two areas. In addition to these similarities the relative positions of the taxonomic groups to one another are very similar as well (Figure 4). Anthracotheriidae were occupying the more open patches of the habitat, which is most apparent in the Bahin/Pangan area. However, the high $\delta^{13}C$ values that would indicate a more open vegetation in the anthracothere habitat can also be partly influenced by their more omnivorous subsistence strategy. As the Anthracotheriidae are more omnivorous than the other taxonomic group they had an ecological advantage there. They were able to reduce competition potential as evidenced by the indication of their use of more open habitats in the Bahin/Pangan area than in the more closed Mogaung habitat. Brontotheriidae, Rhinocerotoidea, and in the Bahin/Pangan area also Amynodontidae shared their aspects of their ecological niches as modelled by the carbon and oxygen isotopes in parts of the paleolandscape. The differentiation between the Brontotheriidae and Rhinocerotoidea niche space is mostly due to the $\delta^{18}O$, which would be consistent with the former drinking from more evaporated water sources than the latter. Given all these similarities in the relative positioning of the different taxonomic groups to one another, the differences that we saw between the paleoenvironments between the Bahin/Pangan and the Mogaung area, apparently did not translate to a different organization of the habitat use of the mammal communities there.

We took our analysis of the niche modelling of the Pondaung mammal fauna one step further and looked at the serially sampled individuals (Figure 5) separately. This revealed different patterns of the distribution of modelled ecological niches especially in the Anthracotheriidae. While the Anthracotheriidae appear to share the modelled aspects of their ecological niches, there is more diversity in the Brontotheriidae, Amynodontidae, and Rhinocerotoidea. This makes sense as the taxonomic resolution in the Anthracotheriidae is better (Figure 5), where all but two individuals could be identified as to at least belonging to the genus *Anthracotherium*, whereas potentially multiple genera or species with different ecologies could be included in the sample for the other taxonomic groups. Several individuals of the Brontotheriidae, Amynodontidae, and Rhinocerotoidea seem to have occupied different microhabitat niches than the other specimen of these groups. Given that this approach requires multiple samples per individual, it becomes apparent why the species diversity in Anthracotheriidae is not reflected here in its entirety as this sampling technique could only be applied to larger teeth, such as the two *Anthracotherium* species and some undetermined Anthracotheriidae.

Based on the ecological niche modelling on the individual level for the four main taxonomic groups we calculated a metric used in ecology to differentiate generalist from specialist individuals. Large modelled niche areas for a taxon or a taxonomic group are consistent with an overall generalist behavior. It can however, be caused by two different reasons. It can result either from many specialist individuals with different ecologies that would have a low RINI, or from generalist individuals that all more or less use the entire niche space of their taxonomic group and thus having a high RINI. As the total modelled

TABLE 4 Summary of the calculation of RINI for the specimen from which intra-individual serial samples were taken.

Specimen ID	*n*°Samples	SEA_C	RINI	Speciemen ID	*n*°Samples	SEA_C	RINI
Brontotheriidae				**Amynodontidae**			
Bahin/Pangan				*Bahin/Pangan*			
A6	3	0.54	-	A1	9	0.31	0.06
PND-8	13	0.71	0.19	A10	7	0.46	0.09
PNG-109	8	0.32	0.08	A2	17	2.15	0.44
PNG-47	5	0.30	0.08	PNG-35	7	0.82	0.17
PNG-76	9	0.41	0.11	PNG-50	8	0.31	0.06
PNG-78	5	0.42	0.11	PNG-61	5	0.32	0.06
Mean		*0.45*	*0.11*	PNG-75	5	0.39	0.08
SD		*0.16*	*0.04*	*Mean*		*0.68*	*0.14*
Mogaung				SD		*0.67*	*0.14*
A9	10	0.31	0.08	*Mogaung*			
PND-18	6	1.74	0.45	A5	11	2.56	0.52
PNG-106	5	1.00	0.26	PNG-119	13	0.56	0.12
Mean		1.01	0.26	*mean*		1.56	0.32
SD		0.71	0.19	SD		1.41	0.29
Anthracotheriidae				**Rhinocerotoidea**			
Bahin/Pangan				*Bahin/Pangan*			
A4	3	1.76	-	A7	4	1.16	0.30
PNG-21	4	1.20	0.37	PND-22	8	0.24	0.06
PNG-31	3	0.18	-	PND-34	13	1.27	0.33
PNG-34	5	1.02	0.31	*Mean*		*0.89*	*0.23*
PNG-36	4	0.33	0.10	SD		*0.56*	*0.15*
PNG-42	6	0.50	0.15	*Mogaung*			
PNG-45	5	0.36	0.11	A3	4	1.64	0.43
PNG-51	4	0.27	0.08	PND-19	5	0.27	0.07
PNG-56	4	0.33	0.10	PND-1	8	0.56	0.15
PNG-57	4	0.56	0.17	PND-31	7	0.29	0.08
Mean		*0.65*	*0.18*	PND-33	6	0.19	0.05
SD		*0.51*	*0.11*	*Mean*		0.59	0.15
Mogaung				SD		0.60	0.16
A8	4	1.00	0.31				
PNG-115	4	0.55	0.17				
Mean		0.77	0.24				
SD		0.32	0.10				

For each individual we report the number of samples taken, the SEA_C (‰^{2}) corresponding to a CI of 40% and the RINI as well as the median and standard deviation for these two metrics.

niche area of the taxonomic groups is based on higher level taxa (families) there is the possibility of an overestimation of the isotopically modelled niche aspect, if there are big differences in habitat preferences and use in the lower level taxa. Hence, the RINIs could be lower in these cases. Both SEA_C and RINI were not significantly different between Anthracotheriidae and the rest of the taxonomic groups. The fact the same pattern is present in both metrics is an indication that no particular generalist or specialist individuals were present, and that the bias towards an underestimation of the RINIs has no significant effect on this comparison. The clustering pattern in Anthracotheriidae seems to be different than in the other three taxonomic groups. The lack of individuals plotting apart from the main cluster of modelled ecological core niches without overlapping them is consistent with a more continuous variation of ecological requirements in this group whereas the pattern in Brontotheriidae, Amynodontidae, and Rhinocerotoidea indicates more discrete ecological niches reflecting aspects of habitat use and dietary ecology.

4.4. Paleoecology of the Pondaung Anthracotheriidae

Although the localities are located along a paleo river system, none of the taxonomic groups has $\delta^{18}O$ values low enough to suggest semi-aquatic behavior. Previous studies showed that depending on the humidity of the terrestrial habitat, this offset can be 2–4‰ lower in freshwater living semi-aquatic species than in terrestrial ones (Clementz et al., 2008). An additional indication of semi-aquatic behavior in a taxonomic group is a reduced standard deviation (SD) of ≤0.5‰ (Yoshida and Miyazaki, 1991; Clementz and Koch, 2001). In our dataset such low SDs are only present in *S. pondaungensis*, *Bahinolophus*, and Amynodontidae from Mogaung (Table 2). These are all taxonomic groups with very low sample sizes (MNI = minimum number of individuals = 2). Therefore, we do not consider the low SD as an indication for semi-aquatic behavior in any of these cases. Differences in $\delta^{18}O$ values can however result from the use of different water sources. The lower $\delta^{18}O$ values in Rhinocerotoidea in comparison to Brontotheriidae would be consistent with them drinking from less evaporated water sources. This could mean shaded water or flowing and not stagnant water.

Between the three different anthracothere genera found in the Pondaung Fm. there is a lot of niche overlap (Figure 6), which was already suggested by the niche modelling of the serially sampled anthracotheres (Figure 5), although none of the smaller genera (*Anthracokeryx* and *Siamotherium*) were in this sample group. Apparently, the three genera did share habitats with similar ecological characteristics. Hence, the different feeding ecologies and habitat preferences in regard to forest density inferred from tooth and bone morphology (Ducrocq, 1999) do not translate to different habitats occupied by them based on the modelled core ecological niches. No clear patterns are visible that would differentiate the anthracothere genera based on canopy closure or isotopically different water sources. We described the hypothetical ecology of *Anthracotherium* as being both more water dependent and more reliant on open spaces in the habitat for their subsistence. *Anthracotherium* however does not have significantly higher $\delta^{13}C$ values or lower $\delta^{18}O$ values than the other genera, thus the isotopic data are not consistent with this hypothesis.

Anthracotherium shares almost all of its modelled ecological core niche space with *Anthracokeryx* (Figure 6B). This can indicate that *Anthracotherium* experienced a higher competition potential for its ecological niche than *Anthracokeryx* (Ogloff et al., 2019). However, the larger body mass of *Anthracotherium* counteracts this effect. The

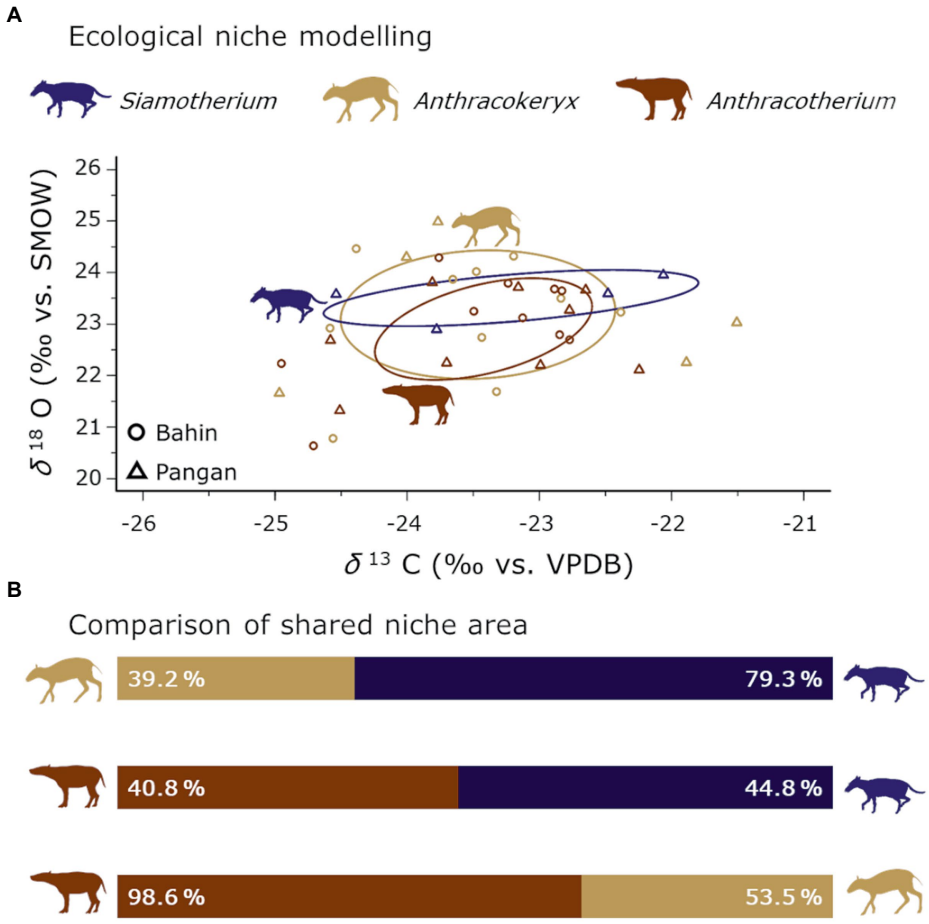

FIGURE 6
Ecological niche modelling of the anthracotheres from Bahin/Pangan per genus **(A)**. Ellipses represent the core ecological niches. In **(B)** the results of the shared niche area ($A_A—A_B$, and $A_B—A_A$) between each taxonomic group are visualized. Silhouettes are from Phylopic under CC BY 3.0 license (*Anthracotherium* by Zimices, *Anthracokeryx* by Nobu Tamura and vectorised by T. Michael Keelsey, and *Siamotherium* is Public Domain).

higher %overlap of the *Anthracotherium* with the *Anthracokeryx* niche could also mean that the advantage of being larger and more generalist in its diet enabled *Anthracotherium* to use more of the *Anthracokeryx* niche space (Schoener, 1983; Persson, 1985; Law et al., 1997). A similar pattern is also visible in the comparison of *Anthracokeryx* and *Siamotherium*, which would be consistent with similar interpretations. However, it is important to keep in mind that the *Siamotherium* niche is based on only two individuals, with two sampled teeth each, which differ vastly in $\delta^{13}C$ values, and further interpretations will depend on a larger sample size for *Siamotherium*.

The limitation of sample size of course is even more prevalent when we are looking at niche partitioning between the anthracothere species (Figure 7A). Nevertheless, we wanted to investigate possible interesting patterns of niche partitioning and directional competition potential detectable to open new directions for future research. Given the severe problems with sample size in *S. pondaungensis* discussed in the previous section, we cannot discuss its niche overlap in comparison with the other species. It is apparent that there is a lot of niche overlap between the anthracothere species, leading to more diffuse competition than niche partitioning in this context (Figure 7). The Pondaung habitat must have provided sufficient area to fulfil the ecological requirements of the anthracotheres and sustain all of the species sampled in this study.

When we generalize the results formed based on the comparison *Anthracotherium* and *Anthracokeryx* in the previous section we propose the following hypothesis: Species with higher body mass have a competition advantage; hence, we expect them to have a higher percentage of shared niche space with the smaller species (Figure 7B). *Anthracokeryx tenuis*, the smallest of these anthracotheres, follows this prediction in every instance and always shares a smaller percentage of its niche area than the bigger species with which it is compared. For the other species this relationship is not as simple. *Anthracotherium pangan* is the largest anthracothere from Pondaung. However, the second largest *A. crassum* shares more of its core niche with it than vice versa. This might be because *A. crassum* also has a much narrower core ecological niche than *A. pangan*. This fact would be consistent with the latter having more generalist ecological requirements than the former. *Anthracokeryx birmanicum* mostly fulfils the expectations based on our hypothesis. The shared niche space between it and *A. pangan* however, are the same. They only share around 5% of their ecological core niches with one another. Given this small overlap area, distinct ecological requirements of these two anthracothere species probably led to a reduced competition potential where the body mass advantage of *A. pangan* was irrelevant.

To sum up, we could further prove the existence of a proto-monsoon already in the Eocene even at the low paleolatitude of 5°N

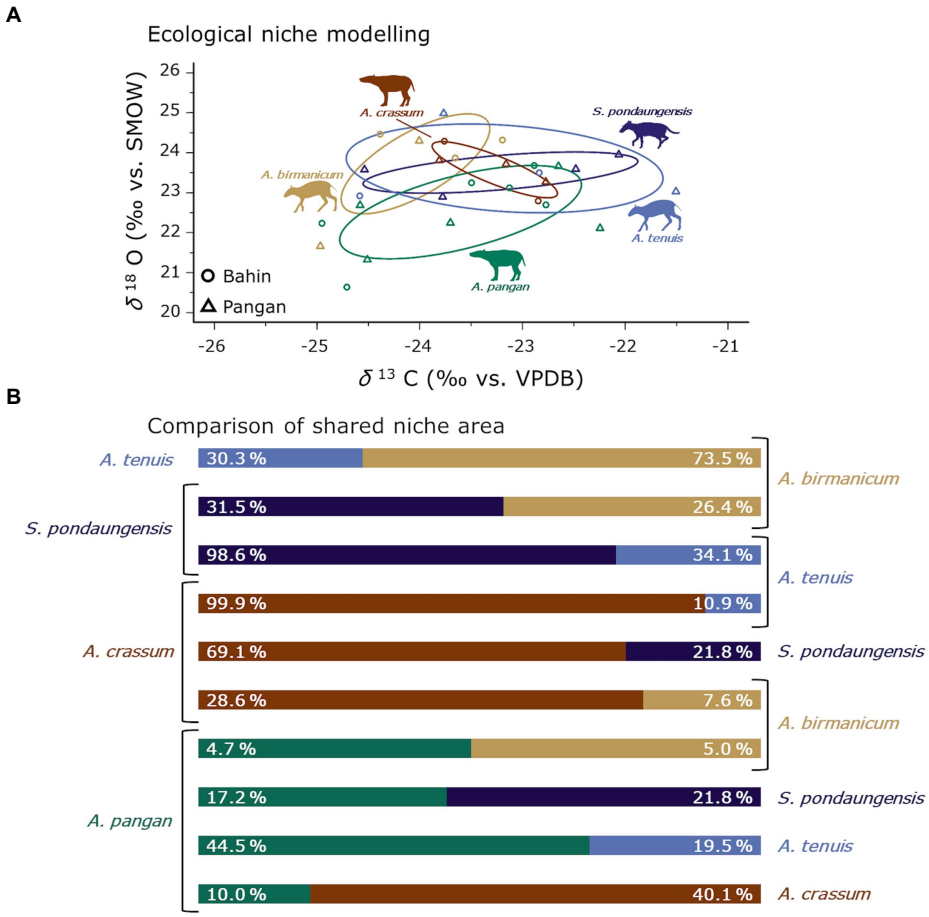

FIGURE 7
Ecological niche modelling of the anthracotheres from Bahin/Pangan per species **(A)**. Ellipses represent the core ecological niches. In **(B)** the results of the shared niche area (A_A—A_B, and A_B—A_A) between each taxonomic group are visualized. Silhouettes are from Phylopic under CC BY 3.0 license (*Anthracotherium* by Zimices, *Anthracokeryx* by Nobu Tamura and vectorised by T. Michael Keelsey, and *Siamotherium* is Public Domain).

of the equator. The $\delta^{13}C$ and $\delta^{18}O$ values also showed significant differences in both overall humidity and vegetation structure between the Bahin/Pangan and Mogaung areas. Although our results are consistent with the hypothesis that favor a spatial pattern of the vegetation structure, temporal differences cannot be ruled out and require more detailed investigation of the dating and stratigraphic relationship of the different fossil localities of the Pondaung Fm. Although the Mogaung area was more humid and more densely forested than the other two, the organization of the mammal fauna was not different, which is consistent with ecological flexibility of this Middle Eocene greenhouse mammal fauna. A high degree of niche overlap was observed on genus and species level resolution for the anthracotheres. Interestingly, there is no evidence for semi-aquatic adaptations in any of the taxonomic groups, when we test for significant offsets in $\delta^{18}O$ values and a reduction of their variability. This means that at the same time when ancestral whales were already returning to aquatic life, anthracotheres that are ancestral to hippos still were fully terrestrial even though the paleo river channel associated with the Pondaung Fm. would have offered enough suitable habitats for this lifestyle. That the primate fossil record from the Pondaung Fm. also does not show any significant differences in the occurrences of the different taxa is also consistent with this and also indicates ecological flexibility in this taxonomic group. Therefore, the Pondaung Fm. represents diverse microhabitats that were used by a dynamically organized mammal fauna. This environment proved to be conducive for the diversification and radiation of many taxonomic groups such as primates, anthracotheres and rodents.

Data availability statement

The original contributions presented in the study are included in the article/Supplementary material, further inquiries can be directed to the corresponding author.

Author contributions

SH, OC, and HB contributed to conception and design of the study and worked together with SD on data analysis. SH and SS performed the sampling, sample preparation and SH did the statistical analysis and wrote the first draft of the manuscript. OC, YC, JJ, CS, and AS were essential for fieldwork during which the fossil specimens were collected. All authors contributed to the article and approved the submitted version.

Funding

This research was funded by the ANR (ANR-18-CE92-0029) and DFG (BO 3478/7-1). Sample preparation and analysis took place at the Eberhard Karls Universität Tübingen in the laboratories of the AG Biogeology (Department of Geosciences).

Acknowledgments

We want to thank our collaborators from Myanmar that supported us during the fieldwork and sampling campaign in 2020, M. Rugbumrung for fossil preparation, and P. Tung for conducting the isotopic analysis and proofreading the manuscript. We also want to thank our reviewers for their constructive criticism and ideas that helped us to further improve this article.

Conflict of interest

The authors declare that the research was conducted in the absence of any commercial or financial relationships that could be construed as a potential conflict of interest.

Publisher's note

Supplementary material

The Supplementary material for this article can be found online at: https://www.frontiersin.org/articles/10.3389/fevo.2023.1110331/full#supplementary-material

References

Beard, K. C. (2016). Out of Asia: anthropoid origins and the colonization of Africa. *Annu. Rev. Anthropol.* 45, 199–213. doi: 10.1146/annurev-anthro-102215-100019

Beard, K. C., Marivaux, L., Chaimanee, Y., Jaeger, J.-J., Marandat, B., Tafforeau, P., et al. (2009). A new primate from the Eocene Pondaung formation of Myanmar and the monophyly of Burmese amphipithecids. *Proc. Biol. Sci.* 276, 3285–3294. doi: 10.1098/rspb.2009.0836

Beard, K. C., Marivaux, L., Tun, S. T., Soe, A. N., Chaimanee, Y., Htoon, W., et al. (2007). New Sivaladapid primates from the Eocene Pondaung formation of Myanmar and the anthropoid status of Amphipithecidae. *Bull. Carnegie Museum Nat. Hist.* 39, 67–76. doi: 10.2992/0145-9058(2007)39[67:NSPFTE]2.0.CO;2

Benammi, M., Soe, A. N., Tun, T., Bo, B., Chaimanee, Y., Ducrocq, S., et al. (2002). First magnetostratigraphic study of the Pondaung formation: implications for the age of the middle Eocene anthropoids of Myanmar. *J. Geol.* 110, 748–756. doi: 10.1086/342868

Bender, F., and Bannert, D. N. (1983). *Geology of Burma*. Berlin: Gebr. Borntraeger.

Bocherens, H., Fizet, M., and Mariotti, A. (1994). Diet, physiology and ecology of fossil mammals as inferred from stable carbon and nitrogen biogeochemistry: implications for Pleistocene bears. *Palaeogeogr. Palaeoclimatol. Palaeoecol.* 107, 213–225. doi: 10.1016/0031-0182(94)90095-7

Böhme, M., Aiglstorfer, M., Antoine, P.-O., Appel, E., Havlik, P., Métais, G., et al. (2013). Na Duong (northern Vietnam)—an exceptional window into Eocene ecosystems from Southeast Asia. *Zitteliana A* 53, 121–167. doi: 10.5282/UBM/EPUB.19019

Bonafini, M., Pellegrini, M., Ditchfield, P., and Pollard, A. M. (2013). Investigation of the 'canopy effect' in the isotope ecology of temperate woodlands. *J. Archaeol. Sci.* 40, 3926–3935. doi: 10.1016/j.jas.2013.03.028

Bonal, D., Barigah, T. S., Granier, A., and Guehl, J. M. (2000). Late-stage canopy tree species with extremely low δ13 C and high stomatal sensitivity to seasonal soil drought in the tropical rainforest of French Guiana. *Plant Cell Environ.* 23, 445–459. doi: 10.1046/j.1365-3040.2000.00556.x

Bond, A. L., and Hobson, K. A. (2012). Reporting stable-isotope ratios in ecology: recommended terminology, guidelines and best practices. *Waterbirds* 35, 324–331. doi: 10.1675/063.035.0213

Bonferroni, C. (1936). Teoria statistica delle classi e calcolo delle probabilità. *Pubblicazioni del R Instituto Superiore di Scienze Economiche e Commericiali di Firenze* 8, 3–62.

Burke, K. D., Williams, J. W., Chandler, M. A., Haywood, A. M., Lunt, D. J., and Otto-Bliesner, B. L. (2018). Pliocene and Eocene provide best analogs for near-future climates. *Proc. Natl. Acad. Sci. U. S. A.* 115, 13288–13293. doi: 10.1073/pnas.1809600115

Cerling, T. E., and Harris, J. M. (1999). Carbon isotope fractionation between diet and bioapatite in ungulate mammals and implications for ecological anc paleoecological studies. *Oecologia* 120, 347–363. doi: 10.1007/s004420050868

Cerling, T. E., Harris, J. M., Leakey, M. G., Passey, B. H., and Levin, N. E. (2010). "Stable carbon and oxygen isotopes in east African mammals: modern and fossil" in *Cenozoic Mammals of Africa*. ed. L. Werdelin (Berkeley, Los Angeles: University of California Press), 941–952.

Cerling, T. E., Harris, J. M., MacFadden, B. J., Leakey, M. G., Quade, J., Eisenmann, V., et al. (1997). Global vegetation change through the Miocene/Pliocene boundary. *Nature* 389, 153–158. doi: 10.1038/38229

Cerling, T. E., Wang, Y., and Quade, J. (1993). Expansion of C4 ecosystems as an indicator of global ecological change in the late Miocene. *Nature* 361, 344–345. doi: 10.1038/361344a0

Chaimanee, Y., Chavasseau, O., Beard, K. C., Kyaw, A. A., Soe, A. N., Sein, C., et al. (2012). Late middle Eocene primate from Myanmar and the initial anthropoid colonization of Africa. *Proc. Natl. Acad. Sci. U. S. A.* 109, 10293–10297. doi: 10.1073/pnas.1200644109

Clementz, M. T., Holroyd, P. A., and Koch, P. L. (2008). Identifying aquatic habits of herbivorous mammals through stable isotope analysis. *PALAIOS* 23, 574–585. doi: 10.2110/palo.2007.p07-054r

Clementz, M. T., and Koch, P. L. (2001). Differentiating aquatic mammal habitat and foraging ecology with stable isotopes in tooth enamel. *Oecologia* 129, 461–472. doi: 10.1007/s004420100745

Cooper, L. N., Clementz, M. T., Usip, S., Bajpai, S., Hussain, S. T., and Hieronymus, T. L. (2016). Aquatic habits of cetacean ancestors: integrating bone microanatomy and stable isotopes. *Integr. Comp. Biol.* 56, 1370–1384. doi: 10.1093/icb/icw119

Coplen, T. B. (1988). Normalization of oxygen and hydrogen isotope data. *Chem. Geol. (Isotope Geosci. Sect.)* 72, 293–297. doi: 10.1016/0168-9622(88)90042-5

Coplen, T. B. (2011). Guidelines and recommended terms for expression of stable-isotope-ratio and gas-ratio measurment results. *Rapid Commun. Mass Spectrom.* 25, 2538–2560. doi: 10.1002/rcm.5129

Coster, P. M., Soe, A. N., Beard, K. C., Chaimanee, Y., Sein, C., Lazzari, V., et al. (2018). Astragalus of Pondaungimys (Rodentia, Anomaluroidea) from the late middle Eocene Pondaung formation, Central Myanmar. *J. Vertebr. Paleontol.* 38:e1552156. doi: 10.1080/02724634.2018.1552156

Dansgaard, W. (1964). Stable isotopes in precipitation. *Tellus* 16, 436–468. doi: 10.1111/j.2153-3490.1964.tb00181.x

de Bonis, L., Solé, F., Chaimanee, Y., Naing Soe, A., Sein, C., Lazzari, V., et al. (2018). New hyaenodonta (Mammalia) from the middle Eocene of Myanmar. *Comptes Rendus Palevol* 17, 357–365. doi: 10.1016/j.crpv.2017.12.003

Ducrocq, S. (1999). The late Eocene Anthracotheriidae (Mammalia, Artiodactyla) from Thailand. *Palaeontogr. Abt. A* 252, 93–140. doi: 10.1127/pala/252/1999/93

Ducrocq, S., Chaimanee, Y., Soe, A. N., Sein, C., Jaeger, J.-J., and Chavasseau, O. (2021). First report of the lower dentition of *Siamotherium pondaungensis* (Cetartiodactyla, Hippopotamoidea) from the late middle Eocene of the Pondaung formation Myanmar. *Neues Jb. Geol. Paläontol. Abh.* 301, 217–228. doi: 10.1127/njgpa/2021/1010

Ducrocq, S., Soe, A. N., Aung, A. K., Benammi, M., Bo, B., Chaimanee, Y., et al. (2001). A new anthracotheriid artiodactyl from Myanmar, and the relative ages of the Eocene anthropoid primate-bearing localities of Thailand (Krabi) and Myanmar (Pondaung). *J. Vertebr. Paleontol.* 20, 755–760. doi: 10.1671/0272-4634(2000)020[0755:ANAAFM]2.0.CO;2

Ducrocq, S., Soe, A. N., Chavasseau, O., Sein, C., Chaimanee, Y., Lazzari, V., et al. (2019). New basal ruminants from the Eocene of the Pondaung formation, Myanmar. *J. Vertebrate Paleontol.* 39:e1722682. doi: 10.1080/02724634.2019.1722682

Egi, N., and Tsubamoto, T. (2000). A preliminary report on carnivorous mammals from Pondaung fauna. *Asian Paleoprimatol.* 1, 103–114.

Fleagle, J. G. (2013). *Primate Adaptation and Evolution*. Amsterdam, Elsevier.

Gentis, N., Licht, A., Boura, A., Franceschi, D.de, Win, Z., Wa Aung, D., et al. (2021). Fossil woods from the lower Miocene of Myanmar (Natma formation): Paleoenvironmental and biogeographic implications. *Geodiversitas* 44, 853–909. doi: 10.5252/geodiversitas2022v44a28

Habinger, S. G., Chavasseau, O., Jaeger, J.-J., Chaimanee, Y., Soe, A. N., Sein, C., et al. (2022). Evolutionary ecology of Miocene hominoid primates in Southeast Asia. *Sci. Rep.* 12:11841. doi: 10.1038/s41598-022-15574-z

Head, J. J., Gunnell, G. F., Holroyd, P. A., Hutchison, J. H., and Ciochon, R. L. (2013). Giant lizards occupied herbivorous mammalian ecospace during the Paleogene greenhouse in Southeast Asia. *Proc. Biol. Sci.* 280:20130665. doi: 10.1098/rspb.2013.0665

Holroyd, P. A., and Ciochon, R. L. (2000). *Bunobrontops savagei* a new genus and species of brontotheriid perissodactyl from the Eocene Pondaung fauna of Myanmar. *J. Vertebr. Paleontol.* 20, 408–410. doi: 10.1671/0272-4634(2000)020[0408:BSANGA]2.0.CO;2

Huang, H., Morley, R. J., Licht, A., Dupont-Nivet, G., Pérez-Pinedo, D., Westerweel, J., et al. (2023). A proto-monsoonal climate in the late Eocene of Southeast Asia: evidence from a sedimentary record in Central Myanmar. *Geosci. Front.* 14:101457. doi: 10.1016/j.gsf.2022.101457

Hutchinson, G. E. (1957). Concluding remarks. *Cold Spring Harb. Symp. Quant. Biol.* 22, 415–427. doi: 10.1101/SQB.1957.022.01.039

Hutchinson, G. E. (1978). *An Introduction to Population Ecology*. New Haven, London: Yale University Press.

Hutchison, J. H., Holroyd, P. A., and Ciochon, R. L. (2004). Preliminary report on Southeast Asia's oldest Cenozoic turtle Fauna from the late middle Eocene Pongaung formation, Myanmar. *Asiatic Herpetol. Res.* 10, 38–52. https://escholarship.org/uc/item/2xf1v8tb

Jackson, A. L., Inger, R., Parnell, A. C., and Bearhop, S. (2011). Comparing isotopic niche widths among and within communities: SIBER—stable isotope Bayesian ellipses in R. *J. Anim. Ecol.* 80, 595–602. doi: 10.1111/j.1365-2656.2011.01806.x

Jackson, P. C., Meinzer, F. C., Goldstein, G., Holbrook, N. M., Cavelier, J., and Rada, F. (1993). "Environmental and physiological influences on carbon isotope composition of gap and understory plants in a lowland tropical Forest" in *Stable Isotopes and Plant Carbon-Water Relations*. eds. J. R. Ehleringer, A. E. Hall and G. D. Farquhar (San Diego: Academic Press), 131–140.

Jaeger, J.-J., Sein, C., Gebo, D. L., Chaimanee, Y., Nyein, M. T., Oo, T. Z., et al. (2020). Amphipithecine primates are stem anthropoids: cranial and postcranial evidence. *Proc. R. Soc. B* 287:20202129. doi: 10.1098/rspb.2020.2129

Kay, R. F., Schmitt, D., Vinyard, C. J., Perry, J. M. G., Shigehara, N., Takai, M., et al. (2004). The paleobiology of Amphipithecidae, south Asian late Eocene primates. *J. Hum. Evol.* 46, 3–25. doi: 10.1016/j.jhevol.2003.09.009

Keeling, C. D., Piper, S. C., Bacastow, R. B., Wahlen, M., Whorf, T. P., Heimann, M., et al. (2005). "Atmospheric CO_2 and $^{13}CO_2$ exchange with the terrestrial biosphere and oceans from 1978 to 2000: observations and carbon cycle implications" in *A History of Atmospheric CO^2 and its Effects on Plants, Animals, and Ecosystems*. eds. J. R. Ehleringer, T. E. Cerling and M. D. Dearing (New York, Great Britain: Springer), 83–113.

Koch, P. L., Tuross, N., and Fogel, M. L. (1997). The effects of sample treatment and diagenesis on the isotopic integrity of carbonate in biogenic Hydroxylapatite. *J. Archaeol. Sci.* 24, 417–429. doi: 10.1006/jasc.1996.0126

Kohn, M. J. (2010). Carbon isotope compositions of terrestrial C3 plants as indicators of (paleo)ecology and (paleo)climate. *Proc. Natl. Acad. Sci.* 107, 19691–19695. doi: 10.1073/pnas.1004933107

Law, R., Marrow, P., and Dieckmann, U. (1997). On evolution under asymmetric competition. *Evol. Ecol.* 11, 485–501. doi: 10.1023/A:1018441108982

Layman, C. A., Arrington, D. A., Montaña, C. G., and Post, D. M. (2007). Can stable isotope ratios provide for community-wide measures of trophic structure? *Ecology* 88, 42–48. doi: 10.1890/0012-9658(2007)88[42:CSIRPF]2.0.CO;2

Leffler, J. A., and Enquist, B. J. (2002). Carbon isotope composition of tree leaves from Guanacaste, Costa Rica: comparison across tropical forests and tree life history. *J. Trop. Ecol.* 18, 151–159. doi: 10.1017/S0266467402002109

Licht, A., and Boura, A., Franceschi, D. de, Ducrocq, S., Soe, A. N., and Jaeger, J.-J. (2014a). Fossil woods from the late middle Eocene Pondaung formation, Myanmar. *Rev. Palaeobot. Palynol.* 202, 29–46. doi: 10.1016/j.revpalbo.2013.12.002

Licht, A., and Boura, A., Franceschi, D. de, Utescher, T., Sein, C., and Jaeger, J.-J. (2015). Late middle Eocene fossil wood of Myanmar: implications for the landscape and the climate of the Eocene Bengal Bay. *Rev. Palaeobot. Palynol.* 216, 44–54. doi: 10.1016/j.revpalbo.2015.01.010

Licht, A., Cojan, I., Caner, L., Soe, A. N., Jaeger, J.-J., and France-Lanord, C. (2014b). Role of permeability barriers in alluvial hydromorphic palaeosols: the Eocene Pondaung formation, Myanmar. *Sedimentology* 61, 362–382. doi: 10.1111/sed.12059

Licht, A., France-Lanord, C., Reisberg, L., Fontaine, C., Soe, A. N., and Jaeger, J.-J. (2013). A palaeo Tibet-Myanmar connection? Reconstructing the late Eocene dranage system of Central Myanmar using a multi-proxy approach. *J. Geol. Soc. Lond.* 170, 929–939. doi: 10.1144/jgs2012-126

Licht, A., van Cappelle, M., Abels, H. A., Ladant, J.-B., Tracucho-Alexandre, J., France-Lanord, C., et al. (2014c). Asian monsoons in a late Eocene greenhouse world. *Nature* 513, 501–506. doi: 10.1038/nature13704

Lihoreau, F., Boisserie, J.-R., Manthi, F. K., and Ducrocq, S. (2015). Hippos stem from the longest sequence of terrestrial cetartiodactyl evolution in Africa. *Nat. Commun.* 6:6264. doi: 10.1038/ncomms7264

Lihoreau, F., and Ducrocq, S. (2007). "Family Anthracotheriidae" in *The Evolution of Atiodactyls*. eds. D. R. Prothero and S. E. Foss (Baltimore: The Johns Hopkin University Press), 89–105.

Mader, B. J. (1998). "Bronthotheriidae," in *Evolution of Tertiary Mammals of North America: Volume 1, Terrestrial Carnivores, Ungulates, and Ungulate Like Mammals*, eds. C. M. Janis, K. M. Scott and L. L. Jacobs (Cambridge: Cambridge University Press), 525–536.

Marivaux, L., Beard, K. C., Chaimanee, Y., Dagosto, M., Gebo, D. L., Guy, F., et al. (2010). Talar morphology, phylogenetic affinities, and locomotor adaptation of a large-bodied amphipithecid primate from the late middle Eocene of Myanmar. *Am. J. Phys. Anthropol.* 143, 208–222. doi: 10.1002/ajpa.21307

Marivaux, L., Beard, K. C., Chaimanee, Y., Jaeger, J.-J., Marandat, B., Soe, A. N., et al. (2008a). Anatomy of the bony pelvis of a relatively large-bodied strepsirrhine primate from the late middle Eocene Pondaung formation (Central Myanmar). *J. Hum. Evol.* 54, 391–404. doi: 10.1016/j.jhevol.2007.09.007

Marivaux, L., Beard, K. C., Chaimanee, Y., Jaeger, J.-J., Marandat, B., Soe, A. N., et al. (2008b). Proximal femoral anatomy of a sivaladapid primate from the late middle Eocene Pondaung formation (Central Myanmar). *Am. J. Phys. Anthropol.* 137, 263–273. doi: 10.1002/ajpa.20866

Marivaux, L., Chaimanee, Y., Ducrocq, S., Marandat, B., Sudre, J., Soe, A. N., et al. (2003). The anthropoid status of a primate from the late middle Eocene Pondaung formation (Central Myanmar): tarsal evidence. *Proc. Natl. Acad. Sci. U. S. A.* 100, 13173–13178. doi: 10.1073/pnas.2332542100

Marivaux, L., Ducrocq, S., Jaeger, J.-J., Marandat, B., Sudre, J., Chaimanee, Y., et al. (2005). New remains of *Pondaungimys anomaluropsis* (Rodentia, Anomaluroidea) from the latest middle Eocene Pondaung formation of Central Myanmar. *J. Vertebr. Paleontol.* 25, 214–227. doi: 10.1671/0272-4634(2005)025[0214:NROPAR]2.0.CO;2

Maung, M., Htike, T., Tsubamoto, T., Suzuki, H., Sein, C., Egi, N., et al. (2005). Stratigraphy of the primate-bearing beds of the Eocene Pondaung formation at Paukkaung area, Myanmar. *Anthropol. Sci.* 113, 11–15. doi: 10.1537/ase.04S002

Métivier, F., Gaudemer, Y., Tapponnier, P., and Klein, M. (1999). Mass accumulation rates in Asia during the Cenozoic. *Geophys. J. Int.* 137, 280–318. doi: 10.1046/j.1365-246X.1999.00802.x

Morley, R. J. (2018). Assembly and division of the south and south-east Asian flora in relation to tectonics and climate change. *J. Trop. Ecol.* 34, 209–234. doi: 10.1017/S0266467418000202

Ogloff, W. R., Yurkowski, D. J., Davoren, G. K., and Ferguson, S. H. (2019). Diet and isotopic niche overlap elucidate competition potential between seasonally sympatric phocids in the Canadian Arctic. *Mar. Biol.* 166, 1–12. doi: 10.1007/s00227-019-3549-6

Oo, K. L., Zaw, K., Meffre, S., Myitta, Aung D. W., and Lai, C.-K. (2015). Provenance of the Eocene sandstones in the southern Chindwin Basin, Myanmar: Implications for the unroofing history of the Cretaceous–Eocene magmatic arc. *J. Asian Earth Sci.* 107, 172–194. doi: 10.1016/j.jseaes.2015.04.029

Orliac, M. J., Antoine, P.-O., Charruault, A.-L., Hervet, S., Prodeo, F., and Duranthon, F. (2013). Specialization for amphibiosis in *Brachyodus onoideus* (Artiodactyla, Hippopotamoidea) from the early Miocene of France. *Swiss J. Geosci.* 106, 265–278. doi: 10.1007/s00015-013-0121-0

Pagani, M., Zachos, J., Freeman, K., Tipple, B., and Bohaty, S. (2005). Marked decline in atmospheric carbon dioxide concentrations during the Paleogene. *Science* 309, 600–603. doi: 10.1126/science.1110063

Passey, B. H., Robinson, T. F., Ayliffe, L. K., Cerling, T. E., Sponheimer, M., Dearing, M. D., et al. (2005). Carbon isotope fractionation between diet, breath CO2, and bioapatite in different mammals. *J. Archaeol. Sci.* 32, 1459–1470. doi: 10.1016/j.jas.2005.03.015

Persson, L. (1985). Asymmetrical competition: are larger animals competitively superior? *Am. Nat.* 126, 261–266. doi: 10.1086/284413

Ramdarshan, A., Merceron, G., Tafforeau, P., and Marivaux, L. (2010). Dietary reconstruction of the Amphipithecidae (primates, Anthropoidea) from the Paleogene of South Asia and paleoecological implications. *J. Hum. Evol.* 59, 96–108. doi: 10.1016/j.jhevol.2010.04.007

Schoener, T. W. (1983). Field experiments on interspecific competition. *Am. Nat.* 122, 240–285. doi: 10.1086/284133

Sheppard, C. E., Inger, R., McDonald, R. A., Barker, S., Jackson, A. L., Thompson, F. J., et al. (2018). Intragroup competition predicts individual foraging specialisation in a group-living mammal. *Ecol. Lett.* 21, 665–673. doi: 10.1111/ele.12933

Soe, A. N. (2008). A new study of the anthracotheres (mammalia, artiodactyla) from Pondaung formation, Myanmar: systematics implications. *Palaeovertebrata* 36, 89–157. doi: 10.18563/pv.36.1-4.89-157

Soe, A. N., Chavasseau, O., Chaimanee, Y., Sein, C., Jaeger, J.-J., Valentin, X., et al. (2017). New remains of *Siamotherium pondaungensis* (Cetartiodactyla, Hippopotamoidea) from the Eocene of Pondaung, Myanmar: Paleoecologic and phylogenetic implications. *J. Vertebr. Paleontol.* 37:e1270290. doi: 10.1080/02724634.2017.1270290

Soe, A. N., Myitta, T. S. T., Aung, A. K., Thein, T., Marandat, B., Ducrocq, S., et al. (2002). Sedimentary facies of the late middle Eocene Pondaung formation (Central Myanmar) and the palaeoenvironments of its anthropoid primates. *Comptes Rendus Palevol* 1, 153–160. doi: 10.1016/S1631-0683(02)00020-9

Stamp, L. D. (1922). An outline of the tertiary geology of Burma. *Geol. Mag.* 59, 481–501. doi: 10.1017/S001675680010915X

Sun, F., Wang, Y., Jablonski, N. G., Hou, S., Ji, X., Wolff, B., et al. (2021). Paleoenvironment of the late Miocene Shuitangba hominoids from Yunnan, Southwest China: insights from stable isotopes. *Chem. Geol.* 569:120123. doi: 10.1016/j.chemgeo.2021.120123

Suzuki, H., Maung, M., Win, Z., Tsubamoto, T., Thein, Z. M. M., Egi, N., et al. (2006). Stratigraphic positions of the Eocene vertebrate localities in the Paukkaung area (Pondaung formation, Central Myanmar). *Asian Paleoprimatol.* 4, 67–74. http://hdl.handle.net/2433/199770

Szpak, P., Metcalfe, J. Z., and Macdonald, R. A. (2017). Best practices for calibrating and reporting stable isotope measurments in archaeology. *J. Archaeol. Sci. Rep.* 13, 609–616. doi: 10.1016/j.jasrep.2017.05.007

Tejada-Lara, J. V., MacFadden, B. J., Bermudez, L., Rojas, G., Salas-Gismondi, R., and Flynn, J. J. (2018). Body mass predicts isotope enrichment in herbivorous mammals. *Proc. Biol. Sci.* 285:20181020. doi: 10.1098/rspb.2018.1020

Thein, Z. M. M., Takai, M., Uno, H., Wynn, J. G., Egi, N., Tsubamoto, T., et al. (2011). Stable isotope analysis of the tooth enamel of Chaingzauk mammalian fauna (late Neogene, Myanmar) and its implication to paleoenvironment and paleogeography. *Palaeogeogr. Palaeoclimatol. Palaeoecol.* 300, 11–22. doi: 10.1016/j.palaeo.2010.11.016

Thewissen, J. G. M., Cooper, L. N., Clementz, M. T., Bajpai, S., and Tiwari, B. N. (2007). Whales originated from aquatic artiodactyls in the Eocene epoch of India. *Nature* 450, 1190–1194. doi: 10.1038/nature06343

Tierney, J. E., Poulsen, C. J., Montañez, I. P., Bhattacharya, T., Feng, R., Ford, H. L., et al. (2020). Past climates inform our future. *Science* 370, 1–9. doi: 10.1126/science.aay3701

Tipple, B. J., Meyers, S. R., and Pagani, M. (2010). Carbon isotope ratio of Cenozoic CO_2: a comparative evaluation of available geochemical proxies. *Paleoceanography* 25, 1–11. doi: 10.1029/2009PA001851

Toumoulin, A., Tardif, D., Donnadieu, Y., Licht, A., Ladant, J.-B., Kunzmann, L., et al. (2022). Evolution of continental temperature seasonality from the Eocene greenhouse to the Oligocene icehouse –a model–data comparison. *Clim. Past* 18, 341–362. doi: 10.5194/cp-18-341-2022

Tsubamoto, T., Egi, N., and Takai, M. (2006a). Notes on fish, reptilian, and several fragmentary mammalian dental fossils from the Pondaung formation. *Asian Paleoprimatol.* 4, 98–110. Available at: http://hdl.handle.net/2433/199768

Tsubamoto, T., Egi, N., Takai, M., Sein, C., and Maung, M. (2005). Middle Eocene ungulate mammals from Myanmar: a review with description of new specimens. *Acta Palaeontol. Pol.* 50, 117–138.

Tsubamoto, T., Egi, N., Takai, M., Shigehara, N., Suzuki, H., Nishimura, T., et al. (2006b). A summary of the Pondaung fossil expeditions. *Asian Paleontol.* 4, 1–66. Available at: http://hdl.handle.net/2433/199771

Tsubamoto, T., Takai, M., Egi, N., Shigehara, N., Thura, S., Aung, A. K., et al. (2002). The Anthracotheriidae (Mammalia; Artiodactyla) from the Eocene Pondaung formation (Myanmar) and comments on some other anthracotheres from the Eocene of Asia. *Paleontol. Res.* 6, 363–384. doi: 10.2517/prpsj.6.363

van der Merwe, N. J., and Medina, E. (1989). Photosynthesis and ratios in Amazonian rain forests. *Geochim. Cosmochim. Acta* 53, 1091–1094. doi: 10.1016/0016-7037(89)90213-5

Westerweel, J., Licht, A., Cogné, N., Roperch, P., Dupont-Nivet, G., Kay Thi, M., et al. (2020). Burma terrane collision and northward indentation in the eastern Himalayas recorded in the Eocene-Miocene Chindwin Basin (Myanmar). *Tectonics* 39, 1–30. doi: 10.1029/2020TC006413

Westerweel, J., Roperch, P., Licht, A., Dupont-Nivet, G., Win, Z., Poblete, F., et al. (2019). Burma terrane part of the trans-Tethyan arc during collision with India according to palaeomagnetic data. *Nat. Geosci.* 12, 863–868. doi: 10.1038/s41561-019-0443-2

Wright, L. E., and Schwarcz, H. P. (1999). Correspondence between stable carbon, oxygen and nitrogen isotopes in human tooth enamel and dentine: infant diets at Kaminaljuyú. *J. Archaeol. Sci.* 26, 1159–1170. doi: 10.1006/jasc.1998.0351

Yoshida, N., and Miyazaki, N. (1991). Oxygen isotope correlation of cetacean bone phosphate with environmental water. *J. Geophys. Res.* 96, 815–820. doi: 10.1029/90JC01580

Zachos, J., Pagani, M., Sloan, L., Thomas, E., and Billups, K. (2001). Trends, rhythms, and aberrations in global climate 65 ma to present. *Science* 292, 686–693. doi: 10.1126/science.1059412

Zaw, K., Meffre, S., Takai, M., Suzuki, H., Burrett, C., Thaung-Htike, , et al. (2014). The oldest anthropoid primates in SE Asia: Evidence from LA-ICP-MS U-Pb zircon age in the late middle Eocene Pondaung Formatio, Myanmar. *Gondwana Res.* 26, 122–131. doi: 10.1016/j.gr.2013.04.007

Supplementary Information

Table SI 1 Summary of coordinates used to create the map (Fig. 1) including references. DeziN and DeziE refer to decimal degree of latitude and longitude respectively.

Area	Locality	N			E			DeziN	DeziE	Reference
		°	'	"	°	'	"			
Bahin	BH 4	21	43	34.2	94	38	30.6	**21.73**	**94.64**	(Tsubamoto et al. 2006)
Bahin	Changan	21	44	56	94	39	14	**21.75**	**94.65**	-
Bahin	Ganleh	21	44	3	94	43	26.3	**21.73**	**94.72**	(Licht et al. 2014)
Bahin	Nyaung Pinle	21	44	46	94	37	50	**21.75**	**94.63**	-
Bahin	PK1	21	45	25.9	94	38	27.1	**21.76**	**94.64**	(Licht et al. 2014)
Bahin	PK10	21	45	11.76	94	38	50.64	**21.75**	**94.65**	(Tsubamoto et al. 2006)
Bahin	PK11	21	45	6	94	38	58.8	**21.75**	**94.65**	(Tsubamoto et al. 2006)
Bahin	PK12	21	44	56.4	94	39	13.8	**21.75**	**94.65**	(Tsubamoto et al. 2006)
Bahin	PK13	21	45	9	94	41	10.8	**21.75**	**94.69**	(Tsubamoto et al. 2006)
Bahin	PK2	21	45	15	94	39	12.6	**21.75**	**94.65**	(Tsubamoto et al. 2006)
Bahin	PK4	21	45	7.5	94	38	50.2	**21.75**	**94.65**	(Tsubamoto et al. 2006)
Bahin	PK5	21	45	20.3	94	38	32.8	**21.76**	**94.64**	(Tsubamoto et al. 2006)
Bahin	Tha Duat 2	21	45	57	94	40	5.4	**21.77**	**94.67**	(Tsubamoto et al. 2006)
Bahin	Tha Duat 3	21	46	0.6	94	40	13.8	**21.77**	**94.67**	(Tsubamoto et al. 2006)
Bahin	Yarshe	21	44	12.5	94	38	15.3	**21.74**	**94.64**	(Licht et al. 2014)
Mogaung	Chauk Magyi	21	57	6.4	94	30	20.7	**21.95**	**94.51**	-
Mogaung	Kyawdaw	22	2	8	94	29	11	**22.04**	**94.49**	-
Mogaung	Lema Kyitchaung	21	57	8.1	94	32	19.3	**21.95**	**94.54**	(Licht et al. 2014)
Mogaung	Mogaung	21	54	40	94	32	30	**21.91**	**94.54**	(Licht et al. 2014)
Mogaung	Segyauk	21	56	21	94	32	3	**21.94**	**94.53**	-
Mogaung	Tandon/Thandong	21	57	55.8	94	32	39.2	**21.97**	**94.54**	(Licht et al. 2014)
Mogaung	Wetkya	21	58	7	94	28	8	**21.97**	**94.5**	-
Pangan	Myauk Se	21	44	4	94	50	10.4	**21.73**	**94.84**	(Licht et al. 2014)
Pangan	Pangan 1	21	42	31	94	49	21.6	**21.71**	**94.82**	(Licht et al. 2014)
Pangan	Thaminchauk	21	45	41	94	50	29.4	**21.76**	**94.84**	(Licht et al. 2014)
Pangan	Than U Daw	21	41	7.4	94	48	37.5	**21.69**	**94.81**	(Licht et al. 2014)

Evaluation of diagenesis

To evaluate potential biases due to diagenetic alterations of the biogenic isotopic signal we analyzed dentine and sediment samples in addition to the fossil enamel. All the dentine and sediment results are reported in Table SI 3. The sediments of the Pondaung Fm. are low in carbonates, which reduces the risk of diagenetic alteration in general. Normally we use only 0.1 mg of sediment in the IRMS analysis, in the case of the Pondaung samples, we had to increase sample size to 2.5 – 3 mg to be able to measure the carbonate fraction of the sediments. Still the percentage of $CaCO_3$ content in these samples was lower than both dentine and enamel (Fig. SI 1), with the exception of two outliers (PND-14 sed = 46.3 %, PND-6 sed = 69.8 %). This fact alone increases the confidence in the biogenic origin of the isotopic composition of the fossil enamel. In addition, the dentine has a higher content of $CaCO_3$ than the enamel. Dentine is not as highly mineralized as enamel and the bioapatite crystals have a different structure; both characteristics that make this tissue more prone to diagenetic alterations

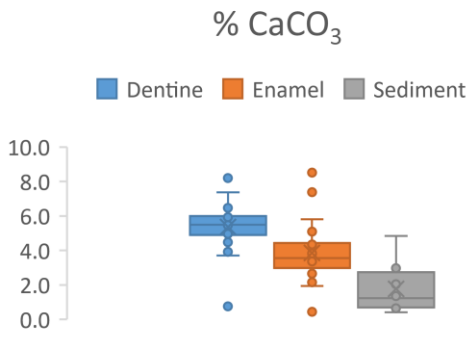

Fig. SI 1Boxplot of the carbonate content (%$CaCO_3$) dentine and sediment samples as well as the associated fossil enamel samples.

(Goldberg et al. 2011; Hillson 2005). Although the Pondaung sediments are low in carbonate content, the dentine % $CaCO_3$ values are consistent with the possibility of a contamination. The fact that % $CaCO_3$ content is not enriched in the enamel samples again increases the confidence that their isotopic composition is biogenic.

When we plot the $\delta^{13}C$ and $\delta^{18}O$ values from all the dentine, enamel, and sediment samples against one another, we see that there is no clear separation between the tissue types. This is especially true for the dentine and enamel samples, but also around half of the sediment samples plot in the cluster of dental tissue samples (PNG-120-121 sed, PNG-122 sed, PNG-123-124 sed, PNG-134 sed, PNG-137 sed, PNG-139 sed). None of these samples were directly associated with fossil mammal specimen though, as are some of the ones plotting apart from the dentine/enamel data points. They were rather collected in association with some gastropods (Table SI 3). Also, the sediment samples have extremely variable isotopic compositions. The sediment samples plotting close to the cluster of dentine and enamel samples originate from different sites across all three areas, one from Mogaung, one from Pangan, and four from Bahin). All of the sediment samples with $\delta^{13}C$ values below -15 ‰ had too low peak heights during the IRMS analysis, indicating a too low carbonate concentration for a measurement even with increased sample sizes. This can result from a too low output of CO2 during the reaction of the sample with the phosphoric acid at during analysis. Such an analytical bias could have resulted in such low $\delta^{13}C$ values. Their measured results therefore are compromised, hence they are not shown in Fig. SI 2, but still reported in Table SI3, where they are marked in red and with a comment. Three more sediment samples also had low peak heights (PNG- 120-121 sed, PNG-134 sed, and PNG-137 sed). Their measurements however are not depleted in C^{13} and plot among the cluster of dentine and enamel samples. Nevertheless these samples are marked in yellow and with a comment in Table SI 3.

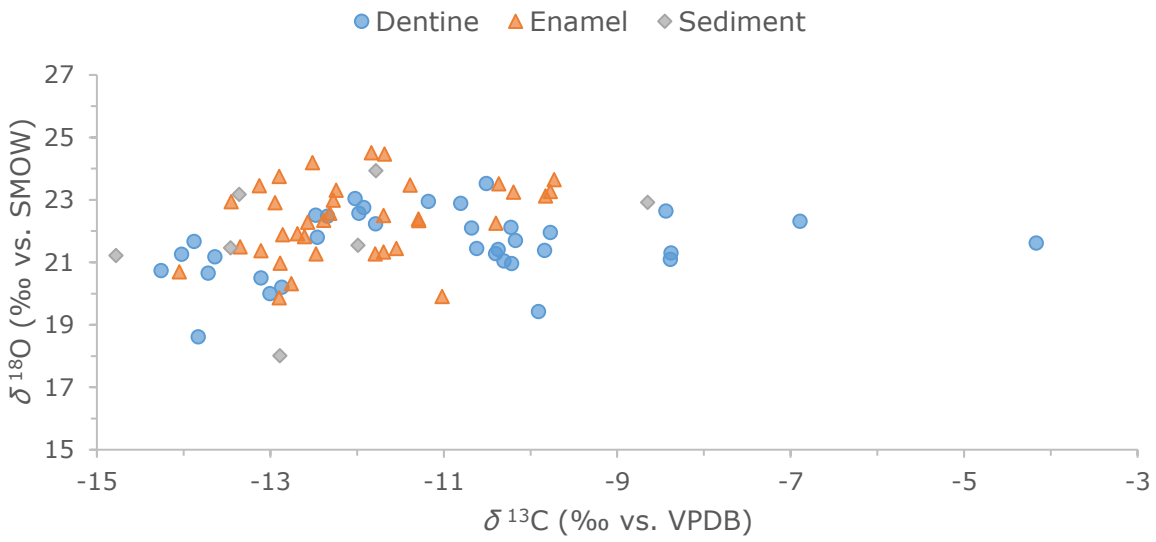

Fig. SI 2 Scatter plot of the $\delta^{13}C$ and $\delta^{18}O$ values dentine and sediment samples as well as the associated fossil enamel samples.

Although these results are not the ideal case in regard to diagenesis, where we like to see all sediment samples plotting separately from dental tissues, we are still confident in the biogenic origin of the isotopic signal in the fossil enamel given the low concentration of $CaCO_3$ in the sediment and the difference in % $CaCO_3$ in dentine and enamel discussed above.

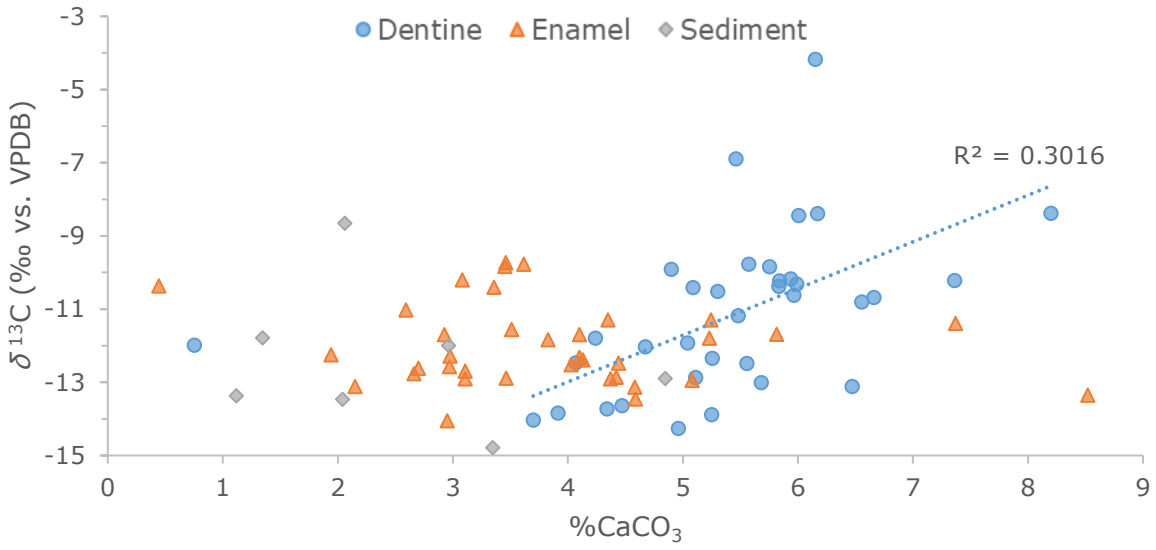

Fig. SI 3 Scatter plot of the $\delta^{13}C$ values and the carbonate concentration (%$CaCO_3$) of the dentine and sediment samples as well as the associated fossil enamel samples. The linear regression (y = 1.2755x – 18.091) of the dentine values (shown here excluding the outlier PNG-35) shows a slight tendency towards increasing $\delta^{13}C$ values with increasing %$CaCO_3$.

We then checked, if the dentine samples with high $\delta^{13}C$ values also have high contents of $CaCO_3$. The linear regression line (y = 1.2755x – 18.091, R^2 = 0.3016) visualized in Fig. SI 3 shows, that there is a weak trend there, which would be consistent with diagenetic alteration of the isotopic composition in the dentine, but not in the enamel. For this regression line the outlier PNG-35 was excluded. If we include it, the regression line (y = 0.8187x – 15.494, R^2 = 0.2135)becomes a bit flatter, but still shows a slight trend towards higher $\delta^{13}C$ values in samples with higher %$CaCO_3$.

In addition, although the dentine and enamel samples plot close together (Fig. SI 2) there are shifts in the $\delta^{13}C$ and $\delta^{18}O$ values when we compare the two tissue types sampled on a single tooth. These shifts are visualized using black arrows in Fig. SI 3. Although there is not one consistent trend regarding the directionality of these shifts across all taxonomic groups they are still detectable in all specimens. However, in two specimens, the Amynodontidae PNG-50 and the Rhinocerotoidea PND-22, they are only minimal.

In Brontotheriidae (Fig. SI 4 A) and Anthracotheriidae (Fig. SI 4 B), enamel values are shifted most prominently towards higher $\delta^{18}O$ values whereas the tendency in Rhinocerotoidea is towards lower $\delta^{13}C$ values in the enamel than in the dentine (Fig. SI 4 D). In the four Amynodontidae specimens, no clear trend is visible (Fig. SI 4 C). The significance of the differing directionality of the shifts from dentine cannot be interpreted due to a lack of studies in this direction, though dentine is a complex tissue and the characteristics and mineralization of the dentine on different areas of a tooth (Goldberg et al. 2011) might provide a possible explanation for differences in the shifts between taxonomic groups.

However, the presence of a shift in the $\delta^{13}C$ and $\delta^{18}O$ values across taxonomic groups together with the results on the percentage of $CaCO_3$ in the different tissue types provide a reasonable basis on which we can establish the biogenic origin of the isotopic composition in the fossil enamel.

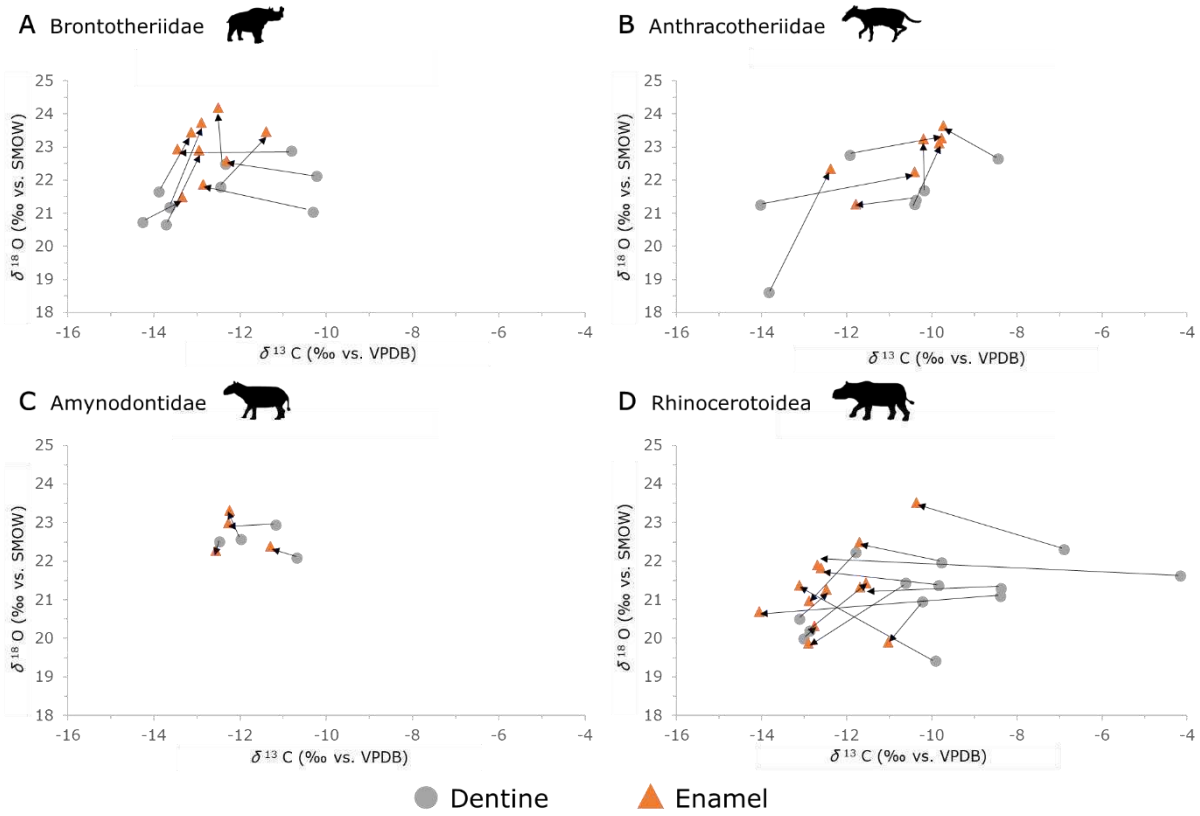

Fig. SI 4 Plots visualizing the shifts in $\delta^{13}C$ and $\delta^{18}O$ values fromt the dentine (grey dots) to the enamel samples (orange triangles). The black arrows connect the dentine with the enamel sample taken from the same tooth.. Silhouettes are from Phylopic under CC 3.0 licence by Zimices.

Table SI 2 Table reporting all the stable isotope data used in this study including the species specific enrichment factor (ε). In cases where intra-individual serial sampling was conducted we report the results from the individual samples as well as the average used for the niche modelling.*

➔ Table as a separate Excel file

Table SI 3 Calibrated data from the dentine and sediment samples from the Pondaung Fm. that we used to assess diagenesis in the fossil enamel samples

Lab Code	Area	Locality	Taxonomy	Tissue	$\delta^{13}C_{VPDB}$	SD C	$\delta^{18}O_{VPDB}$	$\delta^{18}O_{SMOW}$	SD O	CO3 (%)	Comment
PND-1 dent		Wadja jodor	Rhinocerotoidae	dentine	-11.8	0.1	-8.4	22.2	0.1	4.2	
PND-14 sed		PK1	Anthracotheriidae	sediment	-13.2	0.1	-9.8	20.9	0.2	46.3	
PND-19 dent		Lema	Rhinocerotoidae	dentine	-10.6	0.0	-9.2	21.4	0.1	6.0	
PND-22 dent		Than-U-Daw	Rhinocerotoidae	dentine	-13.0	0.1	-10.6	20.0	0.1	5.7	
PND-26 dent		Kyawdaw	Anthracotheriidae	dentine	-13.8	0.0	-11.9	18.6	0.1	3.9	
PND-31 dent		Kyawdaw	Rhinocerotoidae	dentine	-9.8	0.0	-9.2	21.4	0.1	5.8	
PND-34 dent		Kyawdaw	Rhinocerotoidae	dentine	-9.9	0.1	-11.1	19.4	0.1	4.9	
PND-6 sed		Pangan 1	Anthracotheriidae	sediment	-12.3	0.0	-11.1	19.5	0.6	69.8	
PND-8 dent		Pangan 1	Brontotheriidae	dentine	-12.0	0.1	-7.6	23.0	0.1	4.7	
PNG-106 dent		Kyawdaw	Brontotheriidae	dentine	-13.7	0.0	-10.0	20.7	0.1	4.3	
PNG-107 dent		Lema	Rhinocerotoidae	dentine	-8.4	0.0	-9.3	21.3	0.0	8.2	
PNG-108 dent		Thandong	Rhinocerotoidae	dentine	-13.1	0.0	-10.1	20.5	0.0	6.5	
PNG-109 dent		Tha Duat 2	Brontotheriidae	dentine	-10.2	0.0	-8.5	22.1	0.1	5.8	
PNG-110 dent		Kyawdaw	Brontotheriidae	dentine	-14.3	0.1	-9.9	20.7	0.1	5.0	
PNG-111 dent		Thandong	Rhinocerotoidae	dentine	-12.9	0.0	-10.4	20.2	0.1	5.1	
PNG-112 dent		Lema	Brontotheriidae	dentine	-10.3	0.0	-9.6	21.0	0.1	6.0	
PNG-113 dent		Kyawdaw	Rhinocerotoidae	dentine	-8.4	0.0	-9.5	21.1	0.1	6.2	
PNG-114 dent		Lema	Rhinocerotoidae	dentine	-10.2	0.0	-9.7	21.0	0.1	7.4	
PNG-115 dent		Kyawdaw	Anthracotherium	dentine	-10.4	0.0	-9.2	21.4	0.1	5.8	
PNG-116 dent		Kyawdaw	Brontotheriidae	dentine	-13.6	0.0	-9.4	21.2	0.1	4.5	
PNG-118 dent		Segyauk	Brontotheriidae	dentine	-10.8	0.0	-7.8	22.9	0.1	6.6	
PNG-119 dent		Segyauk	Paramynodon	dentine	-10.7	0.0	-8.6	22.1	0.1	6.7	
PNG-120-121 sed		PK5	Gastropoda	sediment	-13.4	0.5	-7.5	23.2	0.2	1.1	too low peak heights
PNG-122 sed		PK1	Gastropoda	sediment	-13.5	0.5	-9.2	21.5	0.2	2.0	
PNG-123-124 sed		Ganle	Gastropoda	sediment	-8.7	0.1	-7.8	22.9	0.4	2.1	
PNG-126 sed		PK2	Gastropoda	sediment	-25.8	1.0	-10.6	20.0	0.8	0.4	too low peak heights
PNG-129 sed		PK2	Crab	sediment	-26.2	1.2	-10.4	20.2	1.4	0.7	too low peak heights
PNG-130 sed		Than-U-Daw	Gastropoda	sediment	-16.2	0.0	-7.9	22.8	0.1	1.1	too low peak heights
PNG-132 sed		Tandon	Gastropoda	sediment	-21.5	1.2	-9.6	21.0	0.9	0.7	too low peak heights
PNG-133 sed		Tandon	Gastropoda	sediment	-12.9	0.1	-12.5	18.0	0.3	4.8	too low peak heights
PNG-134 sed		Lema	Gastropoda	sediment	-11.8	0.1	-6.8	23.9	0.2	1.3	too low peak heights
PNG-136 sed		Kyawdaw	Gastropoda	sediment	-23.4	0.4	-5.7	25.1	0.7	0.7	too low peak heights
PNG-137 sed		BH4	Gastropoda	sediment	-12.0	0.1	-9.1	21.5	0.4	3.0	too low peak heights
PNG-139 sed		Pangan 1	Gastropoda	sediment	-14.8	1.0	-9.4	21.2	2.2	3.3	
PNG-29a dent		Ganle	Rhinocerotoidae	dentine	-4.2	0.0	-9.0	21.6	0.1	6.2	
PNG-29b dent		Ganle	Rhinocerotoidae	dentine	-9.8	0.1	-8.7	22.0	0.2	5.6	
PNG-29c dent		Ganle	Rhinocerotoidae	dentine	-6.9	0.1	-8.3	22.3	0.1	5.5	
PNG-35 dent		PK2	Amynodontidae	dentine	-12.0	0.0	-8.1	22.6	0.2	0.8	
PNG-36 dent		Ganle	Anthracotherium pangan	dentine	-10.4	0.0	-9.3	21.3	0.1	5.1	
PNG-38 dent		Pangan-1	Brontotheriidae	dentine	-12.5	0.1	-8.8	21.8	0.1	4.1	
PNG-39 dent		Pangan-1	Brontotheriidae	dentine	-13.9	0.0	-9.0	21.7	0.1	5.3	
PNG-41 dent		PK2	Brontotheriidae	dentine	-12.3	0.0	-8.2	22.5	0.1	5.3	
PNG-42 dent		Than-U-Daw	Anthracotherium pangan	dentine	-14.0	0.0	-9.4	21.3	0.1	3.7	
PNG-50 dent		Thaminchauk	Amynodontidae	dentine	-12.5	0.1	-8.2	22.5	0.1	5.6	
PNG-53 dent		Pangan-1	Bahinolophos?	dentine	-10.5	0.1	-7.2	23.5	0.1	5.3	
PNG-57 dent		Myauk Se	Anthracotherium crassum	dentine	-11.9	0.1	-7.9	22.8	0.1	5.0	
PNG-61 dent		PK2	Amynodontidae	dentine	-11.2	0.1	-7.7	22.9	0.2	5.5	
PNG-83 dent		Ganle	Anthracotherium	dentine	-8.4	0.1	-8.0	22.6	0.1	6.0	
PNG-85 dent		Ganle	Anthracotherium pangan	dentine	-10.2	0.0	-8.9	21.7	0.0	5.9	

Sympatry and sampling across localities

We tried our best to collect a homogenous sample across all of the three areas. Although all major taxonomic groups (also including *Anthracokeryx* and *Anthracotherium*) were present at all three areas, not all localities are that well represented. Table SI 4 reports and visualizes the distribution of the sampled specimen across localities and also summarizes them per area. Referencing back to the map (Fig. 1) it also has to be kept in mind that many of the localities, such as the PK localities, are located in close geographical proximity. Hence, even though not many sympatric occurrences are visible in Table 4, for some localities with very small sample sizes, a comparison with other localities close by is evidence that indeed most terrestrial mammals from the Pondaung Fm. occurred together and therefore can be discussed as a community of fossil mammals.

Table SI 4 also includes a summary of the occurrences of the different primate taxa for each locality (an x signifies that at least one fossil of this primate has been found at a specific locality). As no samples for isotopic analysis have been taken from them, they are not considered in the number of co-occurring taxa under "Sympatry". Eosimiidae have the most restricted occurrence and have only been found at two localities from the Bahin area, while *Afrasia dijidae* also occurred at at least one locality of the Pangan area. Although the fossil record of Sivaladapidae is also very scarce, specimens from both the Bahin and the Pangan area have been published. The most diverse and numerous fossil record is those of the anthropoid primate family Amphipithecidae. They were present in all three areas. On the genus level however, this is only true for *Pondaungia*. *Aseanpithecus* and *Ganlea* that can be found at two areas each (Bahin and Pangan, and Bahin and Mogaung respectively), while *Myanmarpithecus* has only been recorded from Bahin. The most complete fossil primate record is from the Bahin area and there especially from the PK2 locality, where all taxonomic primate groups were present. This is evidence for sympatry of all the different primate taxa. Differences in their distribution across in the other areas of the Pondaung Fm. could be linked to different ecological tolerances, given the differences in microhabitat that we established in this study. However, due to the relatively small size of the primates a sampling/taphonomic bias cannot be excluded.

Table SI 4 Summary of co-occurrence and sympatry of the different taxonomic groups per area and per locality. All of the four main taxonomic groups are present in all areas and most localities. For Bahin, especially the PK localities are very close geographically (see also Fig. 1). The numbers under "Sympatry" simply indicate how many taxonomic groups are present in our data set for stable isotope analysis at this locality/area. Preservation and the resulting level of taxonomic resolution of course heavily bias this number. Occurrences of the primate taxa are according to (Jaeger et al. 2020;

Area	Locality	Sympatry	Brontotheriidae	*Bunobrontops savagei*	Anthracotheriidae	*Anthracokeryx*	*A. birmanicum*	*A. tenuis*	*Anthracotherium*	*A. crassum*	*A. pangan*	*Siamotherium pondaungensis*	Amynodontidae	*Paramynodon*	*P. birmanicus*	Rhinocerotoidea	*Bahinolophos*	Eomoropidae	*Indolophus*	Ruminantia	Amphipithecidae	*Aseanpithecus*	*Ganlea*	*Myanmarpithecus*	*Pondaungia*	Eosimiidae	*Bahinia pondaungensis*	*Eosimias paukkaungensis*	*Afrasia dijidae* (Eosimiiformes)	Sivaladapidae	*Kytchaungia takaii*
BAHIN	-	**13**	10	1	6	5	3	2	2	2	6		10			7			1	1	x	x	x	x	x	x	x	x	x	x	x
"	Ganle	**7**			1	2			2	1	4		1			3					x		x								
"	PK 2	**5**	2		2		1						3							1	x	x	x	x	x	x		x	x	x	
"	Nyaung Pinle	**3**			1			1								2					x		x							x	
"	PK 13	**3**		1			1				1																				
"	Tha Duat 3	**3**	5										3						1												
"	Changan	**2**			2								2																		
"	PK 1	**2**					1	1													x				x						
"	Tha Duat 2	**2**	1			3																									
"	BH	**1**	2																												
"	PK	**1**														1															
"	PK 10	**1**														1															
"	PK 11	**1**									1																				
"	PK 12	**1**								1																					
"	PK 3	**0**																			x				x						
"	PK 5	**0**																			x				x						
"	Yarshe	**0**																			x	x		x		x	x				
"	PK 4	**1**											1																		
MOGAUNG	-	**7**	8				1		4	1			1	1		15					x	x			x						
"	Kyawdaw	**5**	4				1		3	1						6															
"	Lema	**3**	2										1			3					x				x						
"	Thandong	**3**	1						1							2					x	x			x						
"	Segyauk	**2**	1											1							x				x						
"	Chauk Magyi	**1**														1															
"	Wadja jodor	**1**														3															
PANGAN	-	**14**	5		6	1	2	2	1	3	5	4	3		1	4	2	1			x		x		x				x	x	x
"	Pangan 1	**8**	4		5		1		1			4	1			1	2				x				x						
"	Pangan 2	**0**																			x				x						
"	Myauk Se	**5**								3	3		1			1		1													
"	Than-U-Daw	**5**			1		1	2			1					2					x		x								
"	Thaminchauk	**3**				1					1		1								x		x						x	x	x
"	Pangan	**2**	1												1																

Marivaux et al. 2010; Beard et al. 2009; Ramdarshan et al. 2010; Marivaux et al. 2008; Beard et al. 2007; Marivaux et al. 2003; Ciochon and Gunnell 2002; Gebo et al. 2002; Jaeger et al. 1999; Maung et al. 2005; Chaimanee et al. 2012).

Detail visualization of serially sampled individuals

Here, we report visualizations of all the serially sampled individuals (Fig. SI 5) including the individuals sampled by Licht et al. (2014). Sinusoidal patterns are visible in many of the specimens. Although some tooth crowns were too low to get enough samples for a sinusoidal pattern to show, even in those teeth there is a variation pattern of $\delta^{18}O$ values visible that further corroborates our discussion of paleoseasonality at 40 Ma at the localities of the Pondaung Fm. The parallel plot of $\delta^{13}C$ and $\delta^{18}O$ values per specimen also illustrates the degree and the pattern of co-variation of these two proxies.

Fig. SI 5 Plots of all serially sampled individuals. Although the minima and maxima of displayed values on the two y-axis are different between the plots, all of them encompass an interval of 6 ‰ as to facilitate the visual comparison of the variation patterns from one specimen to the next. The plots are ordered by taxonomic by Lab-Code/Sample ID.

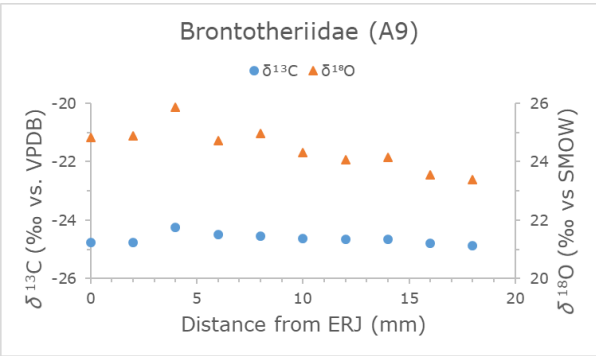
Brontotheriidae (A9)
δ13C δ18O
δ 13C (‰ vs. VPDB)
δ 18O (‰ vs SMOW)
Distance from ERJ (mm)

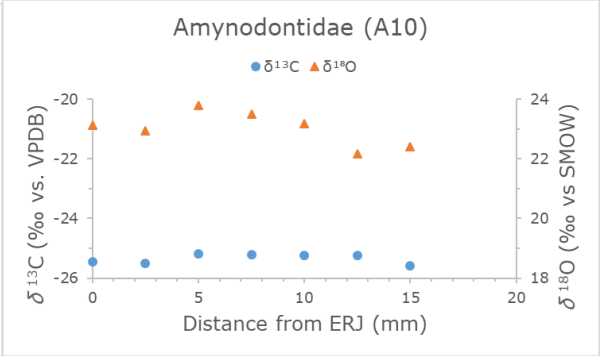
Amynodontidae (A10)
δ13C δ18O
δ 13C (‰ vs. VPDB)
δ 18O (‰ vs SMOW)
Distance from ERJ (mm)

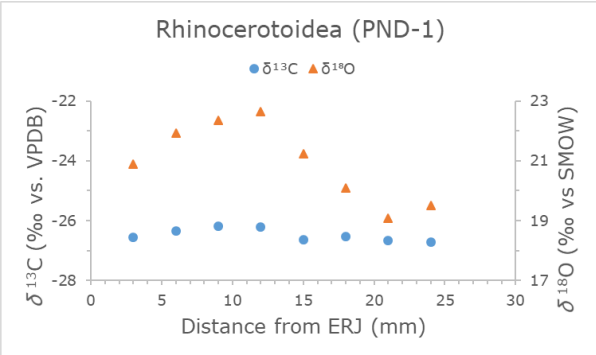
Rhinocerotoidea (PND-1)
δ13C δ18O
δ 13C (‰ vs. VPDB)
δ 18O (‰ vs SMOW)
Distance from ERJ (mm)

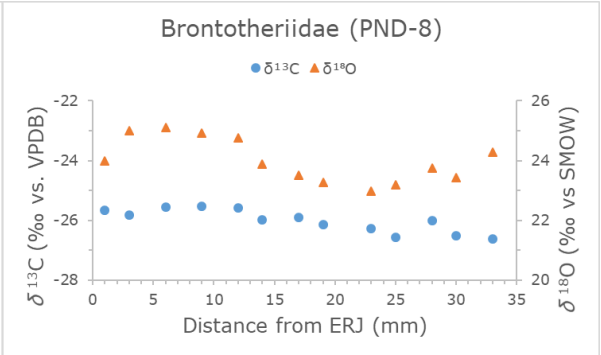
Brontotheriidae (PND-8)
δ13C δ18O
δ 13C (‰ vs. VPDB)
δ 18O (‰ vs SMOW)
Distance from ERJ (mm)

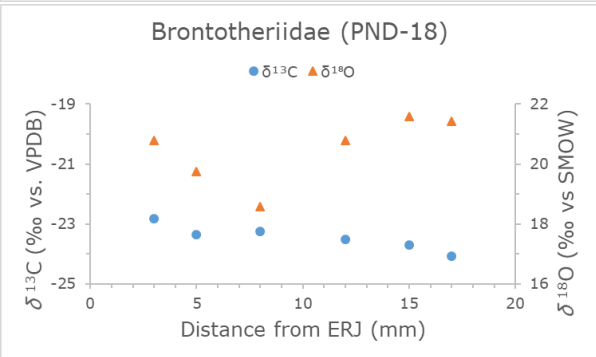
Brontotheriidae (PND-18)
δ13C δ18O
δ 13C (‰ vs. VPDB)
δ 18O (‰ vs SMOW)
Distance from ERJ (mm)

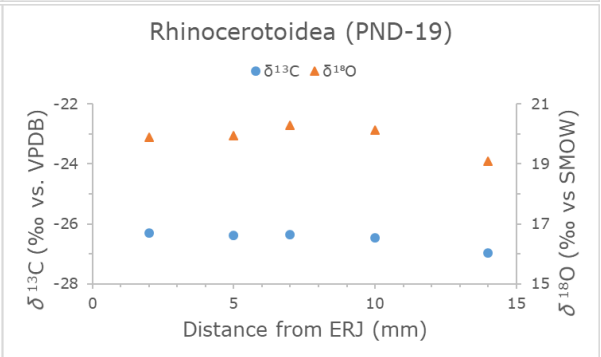
Rhinocerotoidea (PND-19)
δ13C δ18O
δ 13C (‰ vs. VPDB)
δ 18O (‰ vs SMOW)
Distance from ERJ (mm)

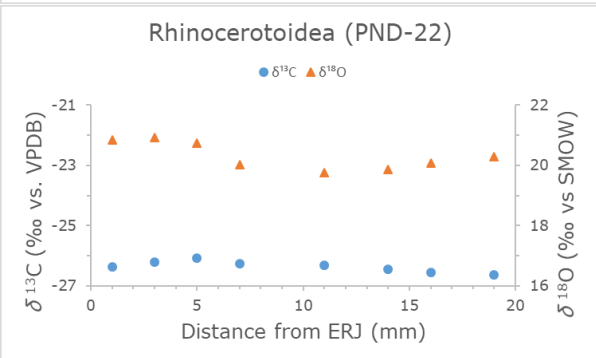
Rhinocerotoidea (PND-22)
δ13C δ18O
δ 13C (‰ vs. VPDB)
δ 18O (‰ vs SMOW)
Distance from ERJ (mm)

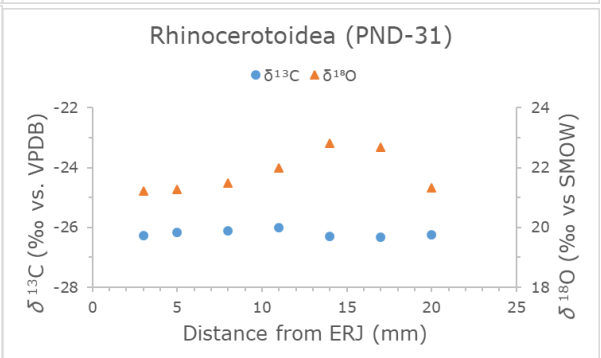
Rhinocerotoidea (PND-31)
δ13C δ18O
δ 13C (‰ vs. VPDB)
δ 18O (‰ vs SMOW)
Distance from ERJ (mm)

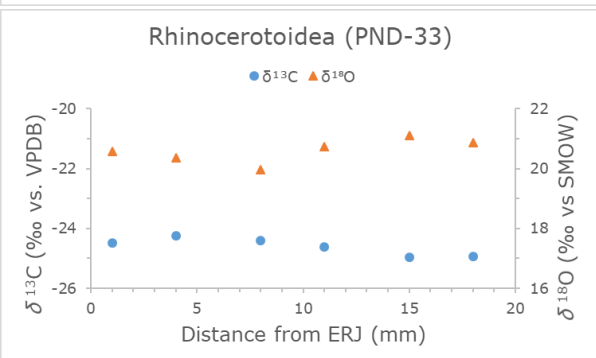
Rhinocerotoidea (PND-33)
δ13C δ18O
δ 13C (‰ vs. VPDB)
δ 18O (‰ vs SMOW)
Distance from ERJ (mm)

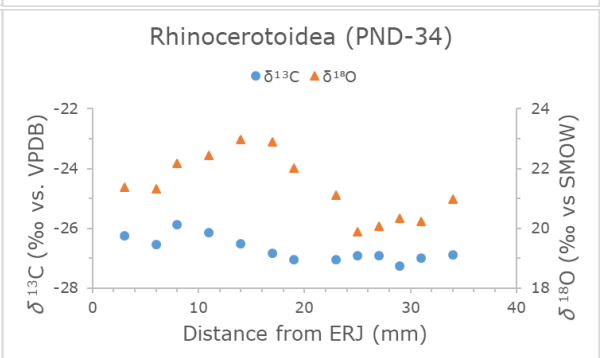
Rhinocerotoidea (PND-34)
δ13C δ18O
δ 13C (‰ vs. VPDB)
δ 18O (‰ vs SMOW)
Distance from ERJ (mm)

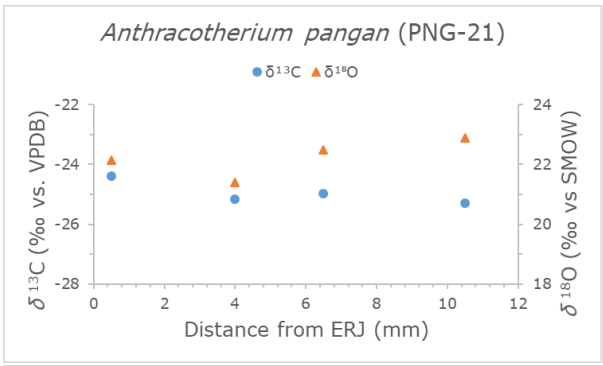
Anthracotherium pangan (PNG-21)
δ13C δ18O
δ 13C (‰ vs. VPDB)
δ 18O (‰ vs SMOW)
Distance from ERJ (mm)

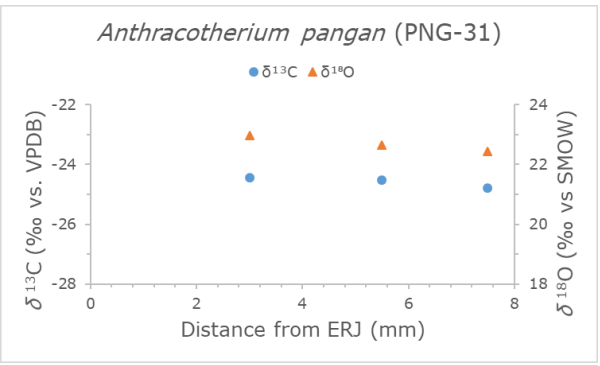
Anthracotherium pangan (PNG-31)
δ13C δ18O
δ 13C (‰ vs. VPDB)
δ 18O (‰ vs SMOW)
Distance from ERJ (mm)

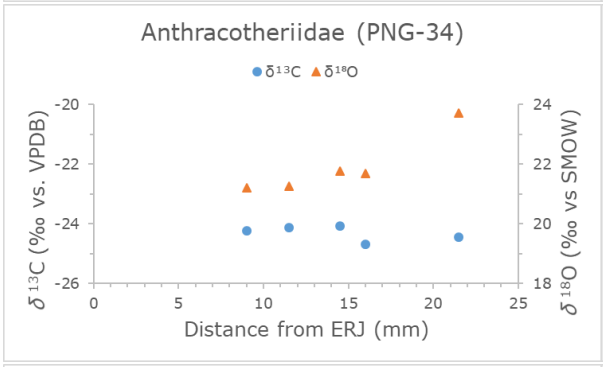
Anthracotheriidae (PNG-34)
δ13C δ18O
δ 13C (‰ vs. VPDB)
δ 18O (‰ vs SMOW)
Distance from ERJ (mm)

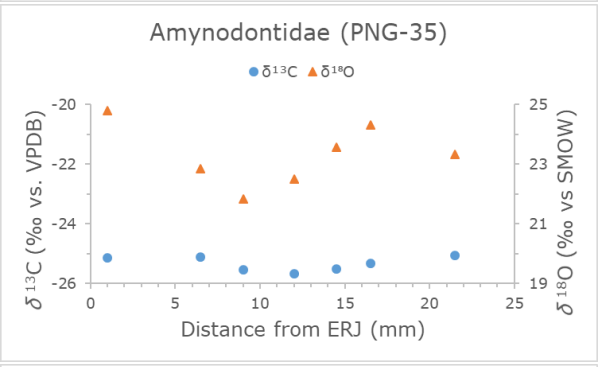
Amynodontidae (PNG-35)
δ13C δ18O
δ 13C (‰ vs. VPDB)
δ 18O (‰ vs SMOW)
Distance from ERJ (mm)

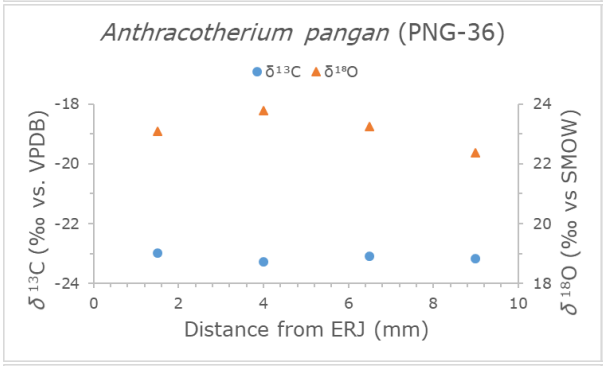
Anthracotherium pangan (PNG-36)
δ13C δ18O
δ 13C (‰ vs. VPDB)
δ 18O (‰ vs SMOW)
Distance from ERJ (mm)

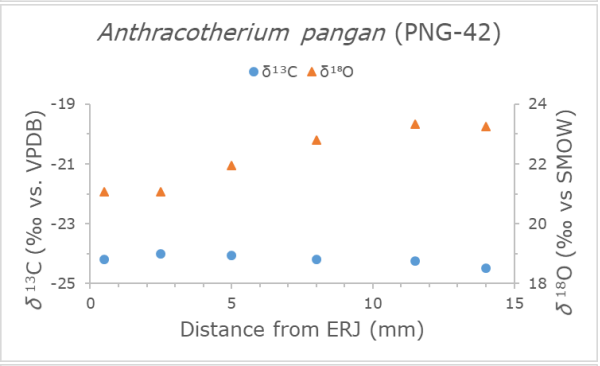
Anthracotherium pangan (PNG-42)
δ13C δ18O
δ 13C (‰ vs. VPDB)
δ 18O (‰ vs SMOW)
Distance from ERJ (mm)

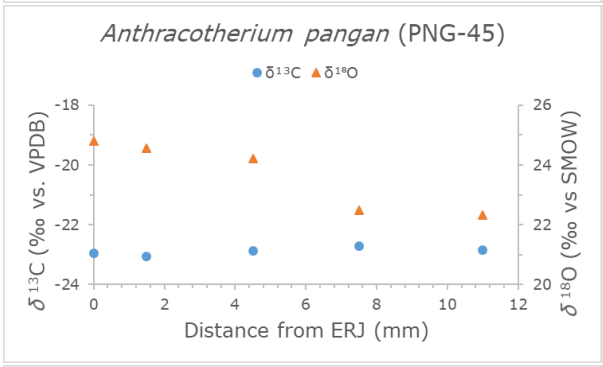
Anthracotherium pangan (PNG-45)
δ13C δ18O
δ 13C (‰ vs. VPDB)
δ 18O (‰ vs SMOW)
Distance from ERJ (mm)

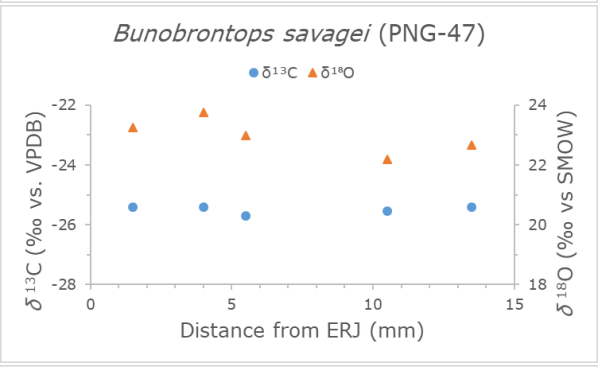
Bunobrontops savagei (PNG-47)
δ13C δ18O
δ 13C (‰ vs. VPDB)
δ 18O (‰ vs SMOW)
Distance from ERJ (mm)

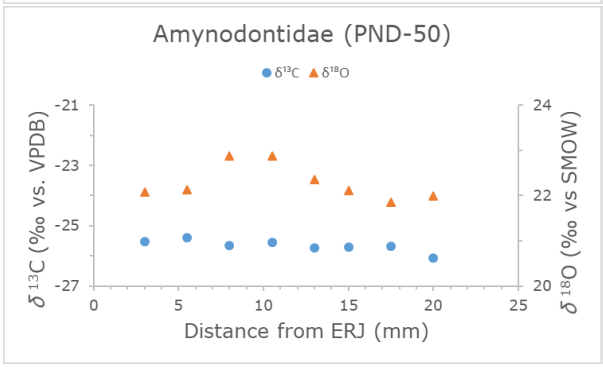
Amynodontidae (PND-50)
δ13C δ18O
δ 13C (‰ vs. VPDB)
δ 18O (‰ vs SMOW)
Distance from ERJ (mm)

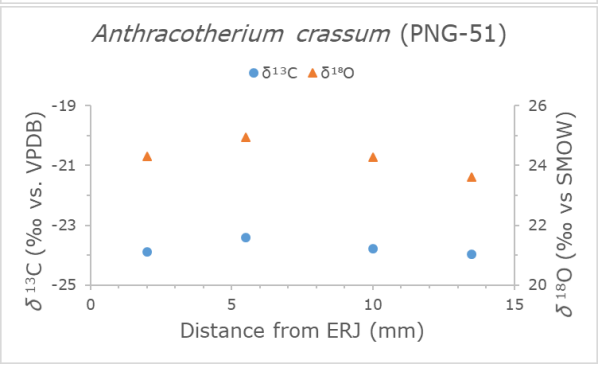
Anthracotherium crassum (PNG-51)
δ13C δ18O
δ 13C (‰ vs. VPDB)
δ 18O (‰ vs SMOW)
Distance from ERJ (mm)

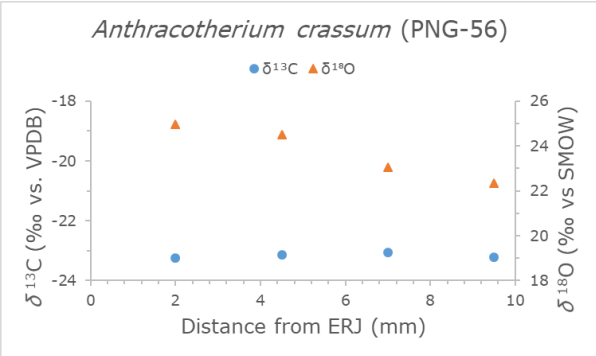
Anthracotherium crassum (PNG-56)
δ13C
δ18O
δ 13C (‰ vs. VPDB)
δ 18O (‰ vs SMOW)
Distance from ERJ (mm)

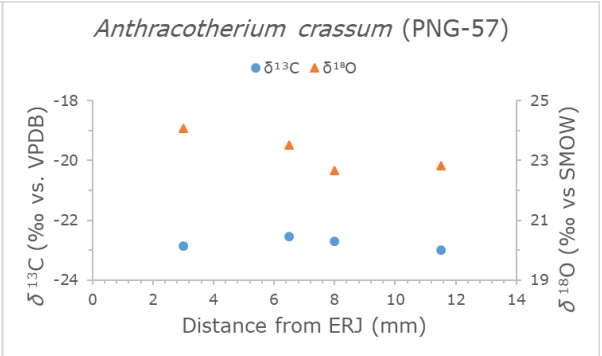
Anthracotherium crassum (PNG-57)
δ13C
δ18O
δ 13C (‰ vs. VPDB)
δ 18O (‰ vs SMOW)
Distance from ERJ (mm)

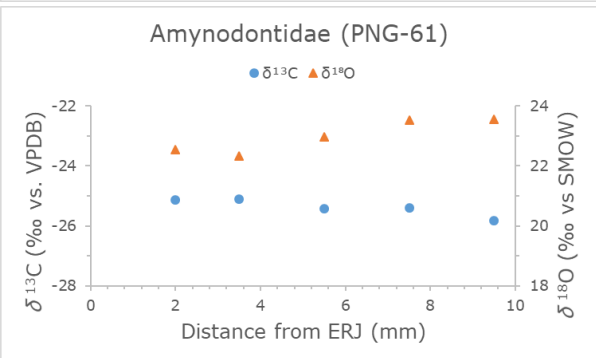
Amynodontidae (PNG-61)
δ13C
δ18O
δ 13C (‰ vs. VPDB)
δ 18O (‰ vs SMOW)
Distance from ERJ (mm)

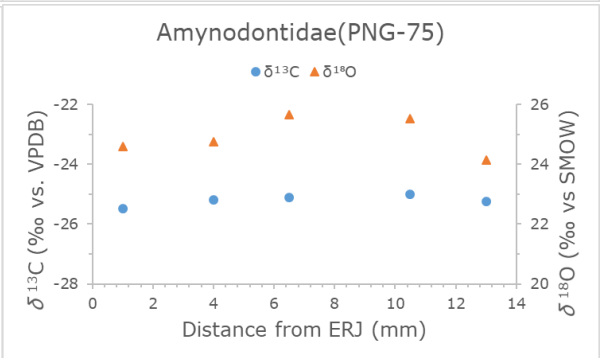
Amynodontidae(PNG-75)
δ13C
δ18O
δ 13C (‰ vs. VPDB)
δ 18O (‰ vs SMOW)
Distance from ERJ (mm)

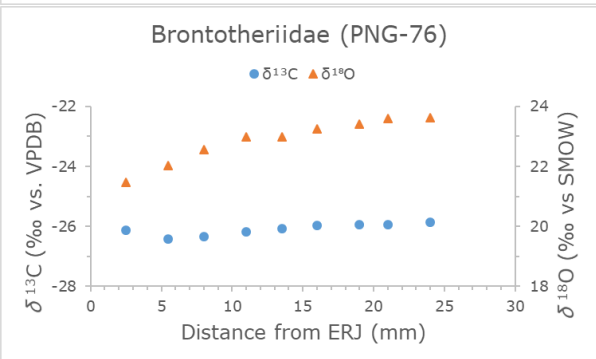
Brontotheriidae (PNG-76)
δ13C
δ18O
δ 13C (‰ vs. VPDB)
δ 18O (‰ vs SMOW)
Distance from ERJ (mm)

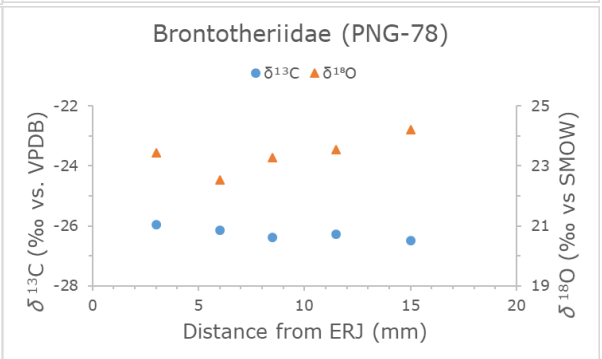
Brontotheriidae (PNG-78)
δ13C
δ18O
δ 13C (‰ vs. VPDB)
δ 18O (‰ vs SMOW)
Distance from ERJ (mm)

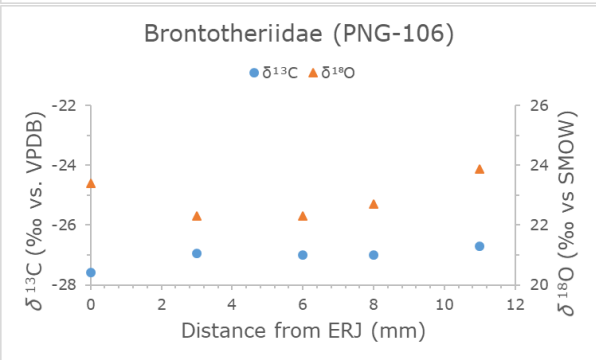
Brontotheriidae (PNG-106)
δ13C
δ18O
δ 13C (‰ vs. VPDB)
δ 18O (‰ vs SMOW)
Distance from ERJ (mm)

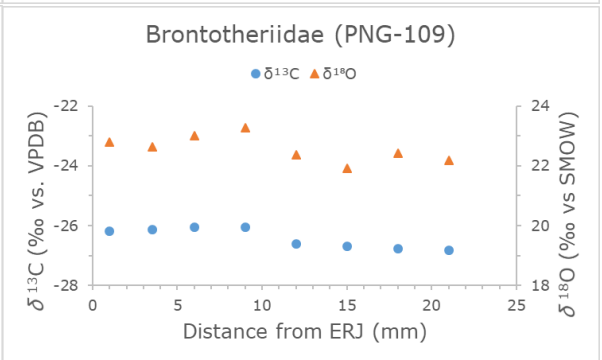
Brontotheriidae (PNG-109)
δ13C
δ18O
δ 13C (‰ vs. VPDB)
δ 18O (‰ vs SMOW)
Distance from ERJ (mm)

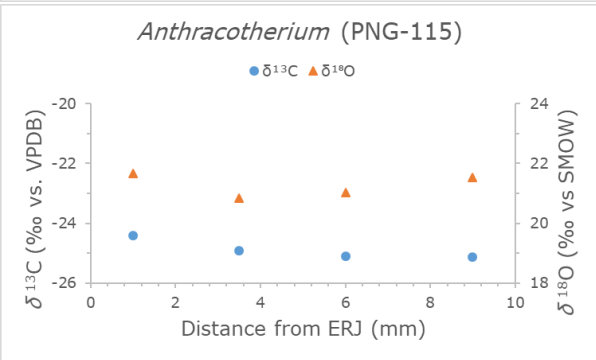
Anthracotherium (PNG-115)
δ13C
δ18O
δ 13C (‰ vs. VPDB)
δ 18O (‰ vs SMOW)
Distance from ERJ (mm)

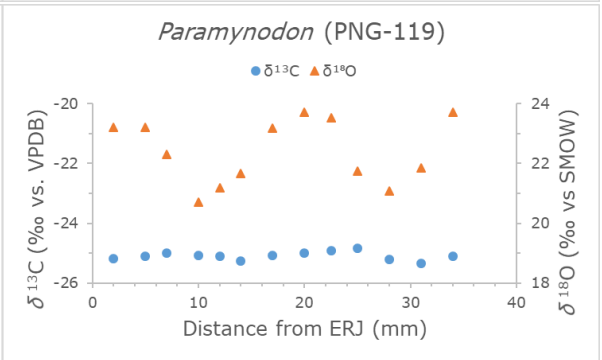
Paramynodon (PNG-119)
δ13C
δ18O
δ 13C (‰ vs. VPDB)
δ 18O (‰ vs SMOW)
Distance from ERJ (mm)

References

Beard, K. Christopher; Marivaux, Laurent; Chaimanee, Yaowalak; Jaeger, Jean-Jacques; Marandat, Bernard; Tafforeau, Paul et al. (2009): A new primate from the Eocene Pondaung Formation of Myanmar and the monophyly of Burmese amphipithecids. In *Proceedings. Biological sciences* 276 (1671), pp. 3285–3294. DOI: 10.1098/rspb.2009.0836.

Beard, K. Christopher; Marivaux, Laurent; Tun, Soe Thura; Soe, Aung Naing; Chaimanee, Yaowalak; Htoon, Wanna et al. (2007): New Sivaladapid Primates from the Eocene Pondaung Formation of Myanmar and the Anthropoid Status of Amphipithecidae. In *Bulletin of Carnegie Museum of Natural History* 39, pp. 67–76. DOI: 10.2992/0145-9058(2007)39[67:NSPFTE]2.0.CO;2.

Chaimanee, Yaowalak; Chavasseau, Olivier; Beard, K. Christopher; Kyaw, Aung Aung; Soe, Aung Naing; Sein, Chit et al. (2012): Late Middle Eocene primate from Myanmar and the initial anthropoid colonization of Africa. In *Proceedings of the National Academy of Sciences of the United States of America* 109 (26), pp. 10293–10297. DOI: 10.1073/pnas.1200644109.

Ciochon, Russell L.; Gunnell, Gregg F. (2002): Chronology of primate discoveries in Myanmar: Influences on the anthropoid origins debate. In *American journal of physical anthropology* 119 (S35), pp. 2–35. Available online at https://www.academia.edu/33511258/Chronology_of_primate_discoveries_in_Myanmar_Influences_on_the_anthropoid_origins_debate?email_work_card=view-paper.

Gebo, Daniel L.; Gunnell, Gregg F.; Ciochon, Russell L.; Takai, Masanaru; Tsubamoto, Takehisa; Egi, Naoko (2002): New eosimiid primate from Myanmar. In *Journal of Human Evolution* 43, pp. 549–553.

Goldberg, Michel; Kulkarni, Askok B.; Young, Marian; Boskey, Adele (2011): Dentin: structure, composition and mineralization. In *Frontiers in Bioscience (Elite Edition)* 3 (2), pp. 711–735. DOI: 10.2741/e281.

Hillson, Simon (2005): Teeth. 2nd ed. Cambridge: Cambridge University Press (Cambridge Manuals in Archaeologw).

Jaeger, J.; Thein, T.; Benammi, M.; Chaimanee, Y.; Soe, A. N.; Lwin, T. et al. (1999): A new primate from the Middle Eocene of Myanmar and the Asian early origin of anthropoids. In *Science (New York, N.Y.)* 286 (5439), pp. 528–530. DOI: 10.1126/science.286.5439.528.

Jaeger, Jean-Jacques; Chit Sein; Gebo, Daniel L.; Chaimanee, Yaowalak; M. T. Nyein; Oo, T. Z. et al. (2020): Amphipithecine primates are stem anthropoids: cranial and postcranial evidence. In *Proceedings of the Royal Society B* 287, p. 20202129. Available online at https://doi.org/10.1098/rspb.2020.2129.

Licht, Alexis; van Cappelle, M.; Abels, H. A.; Ladant, Jean-Baptiste; Tracucho-Alexandre, J.; France-Lanord, Christian et al. (2014): Asian monsoons in a late Eocene greenhouse world. In *Nature* 513 (7519), pp. 501–506.

Marivaux, Laurent; Beard, K. Christopher; Chaimanee, Yaowalak; Dagosto, Marian; Gebo, Daniel L.; Guy, Franck et al. (2010): Talar morphology, phylogenetic affinities, and locomotor adaptation of a large-bodied amphipithecid primate from the late middle Eocene of Myanmar. In *Am. J. Phys. Anthropol.* 143 (2), pp. 208–222. DOI: 10.1002/ajpa.21307.

Marivaux, Laurent; Beard, K. Christopher; Chaimanee, Yaowalak; Jaeger, Jean-Jacques; Marandat, Bernard; Soe, Aung Naing et al. (2008): Proximal femoral anatomy of a sivaladapid primate from the late middle Eocene Pondaung formation (central Myanmar). In *Am. J. Phys. Anthropol.* 137 (3), pp. 263–273. DOI: 10.1002/ajpa.20866.

Marivaux, Laurent; Chaimanee, Yaowalak; Ducrocq, Stéphane; Marandat, Bernard; Sudre, Jean; Soe, Aung Naing et al. (2003): The anthropoid status of a primate from the late middle Eocene Pondaung Formation (Central Myanmar): tarsal evidence. In *Proceedings of the National Academy of Sciences of the United States of America* 100 (23), pp. 13173–13178. DOI: 10.1073/pnas.2332542100.

Maung, Maung; Htike, Thaung; Tsubamoto, Takehisa; Suzuki, Hisashi; Sein, Chit; Egi, Naoko et al. (2005): Stratigraphy of the primate-bearing beds of the Eocene Pondaung Formation at Paukkaung area, Myanmar. In *Anthropological Science* 113 (1), pp. 11–15. DOI: 10.1537/ase.04S002.

Ramdarshan, Anusha; Merceron, Gildas; Tafforeau, Paul; Marivaux, Laurent (2010): Dietary reconstruction of the Amphipithecidae (Primates, Anthropoidea) from the Paleogene of South Asia and paleoecological implications. In *Journal of Human Evolution* 59 (1), pp. 96–108. DOI: 10.1016/j.jhevol.2010.04.007.

Table SI 2 Table reporting all the stable isotope data used in this study including the species specific enrichment factor ε*). In cases where intra-individual serial sampling was conducted we report the results from the individual samples as well as the average used for the niche modelling. Teeth are given by upper or lower case letters, differentiating upper and lower teeth, accompanied by r or l if the side (right or left) is known.

Lab Code	Sample n°	Museum n°	Area	Locality	Taxonomy	Tooth	Tissue	$\delta^{13}C_{VPDB}$	ε^*	$\delta^{13}C_{diet}$	SD C	$\delta^{18}O_{VPDB}$	$\delta^{18}O_{SMOW}$	SD O	CO3 (%)	Distance ERJ (mm)	Reference
A1	1	-	Pangan	Pangan	*Paramynodon birmanicus*	-	enamel	-13.1	-13.6	-26.7	0.09	-6.8	23.9	0.13	-	0.0	(Licht et al. 2014c)
A1	2	-	Pangan	Pangan	*Paramynodon birmanicus*	-	enamel	-12.9	-13.6	-26.5	0.03	-7.2	23.5	0.09	-	2.5	(Licht et al. 2014c)
A1	3	-	Pangan	Pangan	*Paramynodon birmanicus*	-	enamel	-12.2	-13.6	-25.8	0.06	-7.8	22.8	0.14	-	5.0	(Licht et al. 2014c)
A1	4	-	Pangan	Pangan	*Paramynodon birmanicus*	-	enamel	-12.7	-13.6	-26.3	0.02	-7.9	22.8	0.07	-	7.5	(Licht et al. 2014c)
A1	5	-	Pangan	Pangan	*Paramynodon birmanicus*	-	enamel	-12.2	-13.6	-25.8	0.02	-7.6	23.1	0.09	-	10.0	(Licht et al. 2014c)
A1	6	-	Pangan	Pangan	*Paramynodon birmanicus*	-	enamel	-12.5	-13.6	-26.1	0.02	-7.1	23.6	0.07	-	12.5	(Licht et al. 2014c)
A1	7	-	Pangan	Pangan	*Paramynodon birmanicus*	-	enamel	-12.5	-13.6	-26.1	0.04	-7.1	23.6	0.06	-	15.0	(Licht et al. 2014c)
A1	8	-	Pangan	Pangan	*Paramynodon birmanicus*	-	enamel	-12.6	-13.6	-26.2	0.03	-7.2	23.5	0.06	-	17.5	(Licht et al. 2014c)
A1	9	-	Pangan	Pangan	*Paramynodon birmanicus*	-	enamel	-13.5	-13.6	-27.1	0.03	-6.5	24.2	0.06	-	20.0	(Licht et al. 2014c)
A1	average	-	Pangan	Pangan	*Paramynodon birmanicus*	-	enamel	-12.7	-13.6	-26.3	0.04	-7.2	23.5	0.09	-	-	(Licht et al. 2014c)
A10	1	-	Bahin	PK 4	Amynodontidae	-	enamel	-12.3	-13.1	-25.4	0.03	-7.6	23.1	0.09	-	0.0	(Licht et al. 2014c)
A10	2	-	Bahin	PK 4	Amynodontidae	-	enamel	-12.4	-13.1	-25.5	0.03	-7.7	22.9	0.08	-	2.5	(Licht et al. 2014c)
A10	3	-	Bahin	PK 4	Amynodontidae	-	enamel	-12.1	-13.1	-25.2	0.03	-6.9	23.8	0.05	-	5.0	(Licht et al. 2014c)
A10	4	-	Bahin	PK 4	Amynodontidae	-	enamel	-12.1	-13.1	-25.2	0.03	-7.2	23.5	0.09	-	7.5	(Licht et al. 2014c)
A10	5	-	Bahin	PK 4	Amynodontidae	-	enamel	-12.2	-13.1	-25.3	0.01	-7.5	23.2	0.02	-	10.0	(Licht et al. 2014c)
A10	6	-	Bahin	PK 4	Amynodontidae	-	enamel	-12.1	-13.1	-25.2	0.10	-8.5	22.2	0.18	-	12.5	(Licht et al. 2014c)
A10	7	-	Bahin	PK 4	Amynodontidae	-	enamel	-12.5	-13.1	-25.6	0.02	-8.3	22.4	0.08	-	15.0	(Licht et al. 2014c)
A10	average	-	Bahin	PK 4	Amynodontidae	-	enamel	-12.2	-13.1	-25.3	0.04	-7.7	23.0	0.08	-	-	(Licht et al. 2014c)
A2	1	-	Bahin	Ganle	Amynodontidae	-	enamel	-8.8	-13.1	-21.9	0.03	-6.7	24.0	0.07	-	0.0	(Licht et al. 2014c)
A2	2	-	Bahin	Ganle	Amynodontidae	-	enamel	-8.5	-13.1	-21.6	0.03	-9.1	21.5	0.07	-	2.5	(Licht et al. 2014c)
A2	3	-	Bahin	Ganle	Amynodontidae	-	enamel	-8.9	-13.1	-22.0	0.03	-9.6	21.0	0.07	-	5.0	(Licht et al. 2014c)
A2	4	-	Bahin	Ganle	Amynodontidae	-	enamel	-8.1	-13.1	-21.2	0.03	-8.0	22.7	0.08	-	7.5	(Licht et al. 2014c)
A2	5	-	Bahin	Ganle	Amynodontidae	-	enamel	-9.3	-13.1	-22.4	0.03	-9.4	21.2	0.07	-	10.0	(Licht et al. 2014c)
A2	6	-	Bahin	Ganle	Amynodontidae	-	enamel	-9.2	-13.1	-22.3	0.03	-9.9	20.7	0.06	-	12.5	(Licht et al. 2014c)
A2	7	-	Bahin	Ganle	Amynodontidae	-	enamel	-9.0	-13.1	-22.1	0.02	-9.1	21.5	0.07	-	15.0	(Licht et al. 2014c)
A2	8	-	Bahin	Ganle	Amynodontidae	-	enamel	-9.5	-13.1	-22.6	0.02	-9.1	21.5	0.06	-	17.5	(Licht et al. 2014c)
A2	9	-	Bahin	Ganle	Amynodontidae	-	enamel	-9.1	-13.1	-22.2	0.03	-7.0	23.7	0.06	-	20.0	(Licht et al. 2014c)
A2	10	-	Bahin	Ganle	Amynodontidae	-	enamel	-8.7	-13.1	-21.8	0.02	-7.7	23.0	0.07	-	22.5	(Licht et al. 2014c)
A2	11	-	Bahin	Ganle	Amynodontidae	-	enamel	-8.7	-13.1	-21.8	0.03	-9.5	21.1	0.07	-	25.0	(Licht et al. 2014c)
A2	12	-	Bahin	Ganle	Amynodontidae	-	enamel	-8.3	-13.1	-21.4	0.03	-10.0	20.6	0.07	-	27.5	(Licht et al. 2014c)
A2	13	-	Bahin	Ganle	Amynodontidae	-	enamel	-9.9	-13.1	-23.0	0.03	-9.8	20.8	0.08	-	30.0	(Licht et al. 2014c)
A2	14	-	Bahin	Ganle	Amynodontidae	-	enamel	-8.6	-13.1	-21.7	0.03	-9.3	21.3	0.07	-	32.5	(Licht et al. 2014c)
A2	15	-	Bahin	Ganle	Amynodontidae	-	enamel	-10.1	-13.1	-23.2	0.02	-8.2	22.5	0.06	-	35.0	(Licht et al. 2014c)
A2	16	-	Bahin	Ganle	Amynodontidae	-	enamel	-9.2	-13.1	-22.3	0.02	-7.7	22.9	0.06	-	37.5	(Licht et al. 2014c)
A2	17	-	Bahin	Ganle	Amynodontidae	-	enamel	-10.2	-13.1	-23.3	0.04	-9.5	21.1	0.06	-	40.0	(Licht et al. 2014c)
A2	average	-	Bahin	Ganle	Amynodontidae	-	enamel	-9.1	-13.1	-22.2	0.03	-8.8	21.8	0.07	-	-	(Licht et al. 2014c)
A3	1	-	Mogaung	Chauk Magyi	Rhinocerotoidea	-	enamel	-11.3	-13.6	-24.9	0.03	-10.0	20.6	0.09	-	0.0	(Licht et al. 2014c)
A3	2	-	Mogaung	Chauk Magyi	Rhinocerotoidea	-	enamel	-11.1	-13.6	-24.7	0.04	-10.4	20.2	0.08	-	2.5	(Licht et al. 2014c)
A3	3	-	Mogaung	Chauk Magyi	Rhinocerotoidea	-	enamel	-11.3	-13.6	-24.9	0.05	-9.2	21.4	0.09	-	5.0	(Licht et al. 2014c)
A3	4	-	Mogaung	Chauk Magyi	Rhinocerotoidea	-	enamel	-10.1	-13.6	-23.7	0.07	-8.2	22.4	0.10	-	7.5	(Licht et al. 2014c)
A3	average	-	Mogaung	Chauk Magyi	Rhinocerotoidea	-	enamel	-11.0	-13.6	-24.6	0.05	-9.5	21.2	0.09	-	-	(Licht et al. 2014c)
A4	1	-	Bahin	Ganle	Anthracotheriidae	-	enamel	-13.8	-12.5	-26.3	0.05	-9.9	20.7	0.13	-	0.0	(Licht et al. 2014c)
A4	2	-	Bahin	Ganle	Anthracotheriidae	-	enamel	-13.1	-12.5	-25.6	0.04	-8.4	22.2	0.06	-	2.5	(Licht et al. 2014c)
A4	3	-	Bahin	Ganle	Anthracotheriidae	-	enamel	-13.7	-12.5	-26.2	0.03	-8.3	22.3	0.07	-	5.0	(Licht et al. 2014c)
A4	average	-	Bahin	Ganle	Anthracotheriidae	-	enamel	-13.5	-12.5	-26.0	0.04	-8.9	21.8	0.08	-	-	(Licht et al. 2014c)
A5	1	-	Mogaung	Lema	Amynodontidae	-	enamel	-8.1	-13.1	-21.2	0.02	-6.5	24.2	0.06	-	0.0	(Licht et al. 2014c)
A5	2	-	Mogaung	Lema	Amynodontidae	-	enamel	-10.8	-13.1	-23.9	0.03	-7.9	22.8	0.09	-	2.5	(Licht et al. 2014c)
A5	3	-	Mogaung	Lema	Amynodontidae	-	enamel	-10.1	-13.1	-23.2	0.03	-8.4	22.2	0.07	-	5.0	(Licht et al. 2014c)
A5	4	-	Mogaung	Lema	Amynodontidae	-	enamel	-11.2	-13.1	-24.3	0.10	-10.3	20.3	0.12	-	7.5	(Licht et al. 2014c)
A5	5	-	Mogaung	Lema	Amynodontidae	-	enamel	-10.9	-13.1	-24.0	0.04	-9.6	21.0	0.06	-	10.0	(Licht et al. 2014c)
A5	6	-	Mogaung	Lema	Amynodontidae	-	enamel	-11.0	-13.1	-24.1	0.07	-10.1	20.5	0.11	-	12.5	(Licht et al. 2014c)
A5	7	-	Mogaung	Lema	Amynodontidae	-	enamel	-10.8	-13.1	-23.9	0.03	-9.4	21.2	0.06	-	15.0	(Licht et al. 2014c)
A5	8	-	Mogaung	Lema	Amynodontidae	-	enamel	-10.7	-13.1	-23.8	0.04	-8.9	21.7	0.07	-	17.5	(Licht et al. 2014c)
A5	9	-	Mogaung	Lema	Amynodontidae	-	enamel	-11.1	-13.1	-24.2	0.02	-8.4	22.3	0.07	-	20.0	(Licht et al. 2014c)
A5	10	-	Mogaung	Lema	Amynodontidae	-	enamel	-11.1	-13.1	-24.2	0.03	-8.0	22.7	0.07	-	22.5	(Licht et al. 2014c)
A5	11	-	Mogaung	Lema	Amynodontidae	-	enamel	-11.5	-13.1	-24.6	0.05	-9.6	21.0	0.15	-	25.0	(Licht et al. 2014c)
A5	average	-	Mogaung	Lema	Amynodontidae	-	enamel	-10.7	-13.1	-23.8	0.04	-8.8	21.8	0.08	-	-	(Licht et al. 2014c)
A6	1	-	Pangan	Pangan	Brontotheriidae	-	enamel	-12.8	-14.1	-26.9	0.08	-8.5	22.1	0.16	-	0.0	(Licht et al. 2014c)
A6	2	-	Pangan	Pangan	Brontotheriidae	-	enamel	-12.8	-14.1	-26.9	0.05	-7.6	23.1	0.13	-	2.5	(Licht et al. 2014c)

A6	3	-	Pangan	Pangan	Brontotheriidae	-	enamel	-12.5	-14.1	-26.6	0.02	-7.1	23.6	0.07	-	5.0	(Licht et al. 2014c)
A6	average	-	Pangan	Pangan	Brontotheriidae	-	enamel	-12.7	-14.1	-26.8	0.05	-7.7	23.0	0.12	-	-	(Licht et al. 2014c)
A7	1	-	Bahin	Nyaung Pinle	Rhinocerotoidea	-	enamel	-10.8	-13.6	-24.4	0.03	-7.3	23.3	0.06	-	0.0	(Licht et al. 2014c)
A7	2	-	Bahin	Nyaung Pinle	Rhinocerotoidea	-	enamel	-11.6	-13.6	-25.2	0.03	-7.2	23.5	0.06	-	3.0	(Licht et al. 2014c)
A7	3	-	Bahin	Nyaung Pinle	Rhinocerotoidea	-	enamel	-11.4	-13.6	-25.0	0.02	-7.1	23.6	0.05	-	6.0	(Licht et al. 2014c)
A7	4	-	Bahin	Nyaung Pinle	Rhinocerotoidea	-	enamel	-11.5	-13.6	-25.1	0.04	-8.5	22.1	0.12	-	9.0	(Licht et al. 2014c)
A7	average	-	Bahin	Nyaung Pinle	Rhinocerotoidea	-	enamel	-11.3	-13.6	-24.9	0.03	-7.5	23.1	0.07	-	-	(Licht et al. 2014c)
A8	1	-	Mogaung	Tandon	Anthracotherium	-	enamel	-9.4	-13.1	-22.5	0.03	-6.0	24.8	0.05	-	0.0	(Licht et al. 2014c)
A8	2	-	Mogaung	Tandon	Anthracotherium	-	enamel	-9.9	-13.1	-23.0	0.04	-7.3	23.4	0.07	-	2.5	(Licht et al. 2014c)
A8	3	-	Mogaung	Tandon	Anthracotherium	-	enamel	-10.3	-13.1	-23.4	0.03	-8.0	22.7	0.06	-	5.0	(Licht et al. 2014c)
A8	4	-	Mogaung	Tandon	Anthracotherium	-	enamel	-11.1	-13.1	-24.2	0.06	-8.9	21.8	0.17	-	7.5	(Licht et al. 2014c)
A8	average	-	Mogaung	Tandon	Anthracotherium	-	enamel	-10.2	-13.1	-23.3	0.04	-7.5	23.1	0.09	-	-	(Licht et al. 2014c)
A9	1	-	Mogaung	Tandon	Brontotheriidae	-	enamel	-10.7	-14.1	-24.8	0.03	-5.9	24.8	0.07	-	0.0	(Licht et al. 2014c)
A9	2	-	Mogaung	Tandon	Brontotheriidae	-	enamel	-10.7	-14.1	-24.8	0.02	-5.9	24.9	0.06	-	2.0	(Licht et al. 2014c)
A9	3	-	Mogaung	Tandon	Brontotheriidae	-	enamel	-10.2	-14.1	-24.3	0.03	-4.9	25.9	0.05	-	4.0	(Licht et al. 2014c)
A9	4	-	Mogaung	Tandon	Brontotheriidae	-	enamel	-10.4	-14.1	-24.5	0.05	-6.0	24.7	0.08	-	6.0	(Licht et al. 2014c)
A9	5	-	Mogaung	Tandon	Brontotheriidae	-	enamel	-10.5	-14.1	-24.6	0.02	-5.8	25.0	0.06	-	8.0	(Licht et al. 2014c)
A9	6	-	Mogaung	Tandon	Brontotheriidae	-	enamel	-10.5	-14.1	-24.6	0.03	-6.4	24.3	0.06	-	10.0	(Licht et al. 2014c)
A9	7	-	Mogaung	Tandon	Brontotheriidae	-	enamel	-10.6	-14.1	-24.7	0.03	-6.6	24.1	0.06	-	12.0	(Licht et al. 2014c)
A9	8	-	Mogaung	Tandon	Brontotheriidae	-	enamel	-10.6	-14.1	-24.7	0.07	-6.6	24.2	0.08	-	14.0	(Licht et al. 2014c)
A9	9	-	Mogaung	Tandon	Brontotheriidae	-	enamel	-10.7	-14.1	-24.8	0.03	-7.2	23.5	0.07	-	16.0	(Licht et al. 2014c)
A9	10	-	Mogaung	Tandon	Brontotheriidae	-	enamel	-10.8	-14.1	-24.9	0.10	-7.3	23.4	0.18	-	18.0	(Licht et al. 2014c)
A9	average	-	Mogaung	Tandon	Brontotheriidae	-	enamel	-10.5	-14.1	-24.6	0.04	-6.2	24.5	0.08	-	-	(Licht et al. 2014c)
PND-1	a	21/11/99	Mogaung	Wadja jodor	Rhinocerotoidea	M	enamel	-13.0	-13.6	-26.6	0.05	-9.7	20.9	0.08	3.5	3.0	this study
PND-1	b	21/11/99	Mogaung	Wadja jodor	Rhinocerotoidea	M	enamel	-12.8	-13.6	-26.4	0.10	-8.7	21.9	0.11	2.8	6.0	this study
PND-1	c	21/11/99	Mogaung	Wadja jodor	Rhinocerotoidea	M	enamel	-12.6	-13.6	-26.2	0.05	-8.3	22.4	0.06	3.0	9.0	this study
PND-1	d	21/11/99	Mogaung	Wadja jodor	Rhinocerotoidea	M	enamel	-12.6	-13.6	-26.2	0.06	-8.0	22.6	0.09	3.1	12.0	this study
PND-1	e	21/11/99	Mogaung	Wadja jodor	Rhinocerotoidea	M	enamel	-13.1	-13.6	-26.7	0.12	-9.4	21.2	0.05	3.0	15.0	this study
PND-1	f	21/11/99	Mogaung	Wadja jodor	Rhinocerotoidea	M	enamel	-12.9	-13.6	-26.5	0.09	-10.5	20.1	0.09	2.7	18.0	this study
PND-1	g	21/11/99	Mogaung	Wadja jodor	Rhinocerotoidea	M	enamel	-13.1	-13.6	-26.7	0.06	-11.5	19.1	0.11	2.9	21.0	this study
PND-1	h	21/11/99	Mogaung	Wadja jodor	Rhinocerotoidea	M	enamel	-13.1	-13.6	-26.7	0.04	-11.1	19.5	0.15	3.5	24.0	this study
PND-1	average	21/11/99	Mogaung	Wadja jodor	Rhinocerotoidea	M	enamel	-12.9	-13.6	-26.5	0.07	-9.6	21.0	0.09	3.5	-	this study
PND-10	bulk	10/11/99	Pangan	Pangan 1	Anthracotheriidae	P	enamel	-11.6	-12.5	-24.1	0.03	-6.0	24.7	0.17	3.1	-	this study
PND-11	bulk	10/11/99	Pangan	Pangan 1	Anthracotheriidae	P	enamel	-13.9	-12.5	-26.4	0.07	-8.4	22.3	0.19	2.5	-	this study
PND-12	bulk	10/01/12	Pangan	Pangan 1	*Bahinolophos*	m	enamel	-12.0	-12.6	-24.6	0.06	-6.1	24.6	0.17	3.1	-	this study
PND-13	bulk	10/01/12	Pangan	Pangan 1	Rhinocerotoidea	P	enamel	-12.0	-13.6	-25.6	0.07	-7.1	23.6	0.14	2.7	-	this study
PND-14	bulk	19/02/10	Bahin	PK 1	*Anthracokeryx birmanicum*	p_4/m_1	enamel	-11.7	-12.7	-24.4	0.11	-6.3	24.5	0.14	5.8	-	this study
PND-15	bulk	-	Bahin	PK	Rhinocerotoidea	m	enamel	-10.1	-13.6	-23.7	0.06	-8.3	22.4	0.09	2.0	-	this study
PND-16	bulk	06/11/99	Bahin	Yarshe	Perissodactyla	-	enamel	-11.1	-14.0	-25.1	0.06	-7.2	23.5	0.10	2.8	-	this study
PND-17	bulk	13/11/99	Pangan	Thaminchauk	*Anthracokeryx*	M	enamel	-9.6	-12.3	-21.9	0.05	-8.4	22.3	0.11	3.5	-	this study
PND-18	a	-	Mogaung	Lema	Brontotheriidae	M	enamel	-8.7	-14.1	-22.8	0.08	-10.3	20.3	0.14	4.6	3.0	this study
PND-18	b	-	Mogaung	Lema	Brontotheriidae	M	enamel	-9.3	-14.1	-23.4	0.06	-11.3	19.3	0.10	4.4	5.0	this study
PND-18	c	-	Mogaung	Lema	Brontotheriidae	M	enamel	-9.2	-14.1	-23.3	0.07	-12.4	18.1	0.11	4.8	8.0	this study
PND-18	d	-	Mogaung	Lema	Brontotheriidae	M	enamel	-9.4	-14.1	-23.5	0.07	-10.3	20.3	0.09	4.2	12.0	this study
PND-18	e	-	Mogaung	Lema	Brontotheriidae	M	enamel	-9.6	-14.1	-23.7	0.10	-9.5	21.1	0.08	3.8	15.0	this study
PND-18	f	-	Mogaung	Lema	Brontotheriidae	M	enamel	-10.0	-14.1	-24.1	0.08	-9.7	20.9	0.10	4.2	17.0	this study
PND-18	average	-	Mogaung	Lema	Brontotheriidae	M	enamel	-9.4	-14.1	-23.5	0.08	-10.6	20.0	0.10	4.3	-	this study
PND-19	a	15/11/99	Mogaung	Lema	Rhinocerotoidea	m	enamel	-12.7	-13.6	-26.3	0.07	-10.7	19.9	0.16	3.1	2.0	this study
PND-19	b	15/11/99	Mogaung	Lema	Rhinocerotoidea	m	enamel	-12.8	-13.6	-26.4	0.10	-10.6	19.9	0.11	3.0	5.0	this study
PND-19	c	15/11/99	Mogaung	Lema	Rhinocerotoidea	m	enamel	-12.8	-13.6	-26.4	0.08	-10.3	20.3	0.19	3.1	7.0	this study
PND-19	d	15/11/99	Mogaung	Lema	Rhinocerotoidea	m	enamel	-12.9	-13.6	-26.5	0.08	-10.5	20.1	0.14	2.9	10.0	this study
PND-19	e	15/11/99	Mogaung	Lema	Rhinocerotoidea	m	enamel	-13.4	-13.6	-27.0	0.11	-11.5	19.1	0.12	3.4	14.0	this study
PND-19	average	15/11/99	Mogaung	Lema	Rhinocerotoidea	m	enamel	-12.9	-13.6	-26.5	0.09	-10.7	19.9	0.14	3.1	-	this study
PND-2	bulk	21/11/99	Mogaung	Wadja jodor	Rhinocerotoidea	M	enamel	-11.9	-13.6	-25.5	0.08	-8.2	22.5	0.10	2.8	-	this study
PND-20	bulk	-	Pangan	Myauk Se	Rhinocerotoidea	M	enamel	-13.5	-13.6	-27.1	0.08	-9.0	21.6	0.07	3.5	-	this study
PND-21	bulk	-	Pangan	Myauk Se	Eomoropidae	M	enamel	-11.7	-12.2	-23.9	0.07	-10.0	20.6	0.15	2.5	-	this study
PND-22	a	11/11/99	Pangan	Than-U-Daw	Rhinocerotoidea	m	enamel	-12.8	-13.6	-26.4	0.07	-9.8	20.8	0.16	2.5	1.0	this study
PND-22	b	11/11/99	Pangan	Than-U-Daw	Rhinocerotoidea	m	enamel	-12.6	-13.6	-26.2	0.08	-9.7	20.9	0.13	2.7	3.0	this study
PND-22	c	11/11/99	Pangan	Than-U-Daw	Rhinocerotoidea	m	enamel	-12.5	-13.6	-26.1	0.06	-9.9	20.7	0.10	2.6	5.0	this study
PND-22	d	11/11/99	Pangan	Than-U-Daw	Rhinocerotoidea	m	enamel	-12.7	-13.6	-26.3	0.07	-10.6	20.0	0.11	2.7	7.0	this study
PND-22	e	11/11/99	Pangan	Than-U-Daw	Rhinocerotoidea	m	enamel	-12.7	-13.6	-26.3	0.07	-10.8	19.8	0.19	2.5	11.0	this study
PND-22	f	11/11/99	Pangan	Than-U-Daw	Rhinocerotoidea	m	enamel	-12.9	-13.6	-26.5	0.08	-10.7	19.9	0.10	2.6	14.0	this study

PND-22	g	11/11/99	Pangan	Than-U-Daw	Rhinocerotoidea	m	enamel	-12.9	-13.6	-26.5	0.08	-10.5	20.1	0.16	2.9	16.0	this study
PND-22	h	11/11/99	Pangan	Than-U-Daw	Rhinocerotoidea	m	enamel	-13.0	-13.6	-26.6	0.04	-10.3	20.3	0.06	2.9	19.0	this study
PND-22	average	11/11/99	Pangan	Than-U-Daw	Rhinocerotoidea	m	enamel	-12.8	-13.6	-26.4	0.07	-10.3	20.3	0.13	2.7	-	this study
PND-23	bulk	11/11/99	Pangan	Than-U-Daw	Rhinocerotoidea	M	enamel	-12.6	-13.6	-26.2	0.10	-9.8	20.8	0.17	2.3	-	this study
PND-24	bulk	11/11/99	Pangan	Than-U-Daw	Anthracotheriidae	M	enamel	-8.8	-12.5	-21.3	0.12	-8.8	21.8	0.13	2.6	-	this study
PND-25	bulk	25/01/12	Mogaung	Kyawdaw	*Anthracotherium*	M	enamel	-12.5	-13.1	-25.6	0.09	-6.6	24.1	0.16	4.9	-	this study
PND-26	bulk	22/11/99	Mogaung	Kyawdaw	*Anthracotherium crassum*	-	enamel	-12.4	-13.0	-25.4	0.08	-8.3	22.3	0.15	4.1	-	this study
PND-27	bulk	22/11/99	Mogaung	Kyawdaw	*Anthracokeryx birmanicum*	m	enamel	-12.3	-12.7	-25.0	0.06	-6.9	23.8	0.14	4.5	-	this study
PND-28	bulk	21/11/99	Mogaung	Kyawdaw	Brontotheriidae	m	enamel	-10.7	-14.1	-24.8	0.06	-6.1	24.6	0.09	2.6	-	this study
PND-29	bulk	25/01/12	Mogaung	Kyawdaw	Rhinocerotoidea	m/M	enamel	-12.0	-13.6	-25.6	0.09	-8.0	22.7	0.21	3.1	-	this study
PND-3	bulk	21/11/99	Mogaung	Wadja jodor	Rhinocerotoidea	M	enamel	-12.4	-13.6	-26.0	0.07	-9.5	21.1	0.17	2.7	-	this study
PND-30	bulk	25/01/12	Mogaung	Kyawdaw	*Anthracotherium*	m_3	enamel	-12.0	-13.1	-25.1	0.05	-8.4	22.2	0.12	3.1	-	this study
PND-31	a	21/11/99	Mogaung	Kyawdaw	Rhinocerotoidea	m	enamel	-12.7	-13.6	-26.3	0.17	-9.4	21.2	0.12	2.3	3.0	this study
PND-31	b	21/11/99	Mogaung	Kyawdaw	Rhinocerotoidea	m	enamel	-12.6	-13.6	-26.2	0.08	-9.4	21.3	0.12	2.5	5.0	this study
PND-31	c	21/11/99	Mogaung	Kyawdaw	Rhinocerotoidea	m	enamel	-12.5	-13.6	-26.1	0.11	-9.1	21.5	0.12	2.5	8.0	this study
PND-31	d	21/11/99	Mogaung	Kyawdaw	Rhinocerotoidea	m	enamel	-12.4	-13.6	-26.0	0.07	-8.7	22.0	0.14	2.7	11.0	this study
PND-31	e	21/11/99	Mogaung	Kyawdaw	Rhinocerotoidea	m	enamel	-12.7	-13.6	-26.3	0.12	-7.8	22.8	0.17	2.6	14.0	this study
PND-31	f	21/11/99	Mogaung	Kyawdaw	Rhinocerotoidea	m	enamel	-12.7	-13.6	-26.3	0.09	-8.0	22.7	0.21	2.6	17.0	this study
PND-31	g	21/11/99	Mogaung	Kyawdaw	Rhinocerotoidea	m	enamel	-12.6	-13.6	-26.2	0.06	-9.3	21.3	0.10	3.7	20.0	this study
PND-31	average	21/11/99	Mogaung	Kyawdaw	Rhinocerotoidea	m	enamel	-12.6	-13.6	-26.2	0.10	-8.8	21.8	0.14	2.7	-	this study
PND-32	bulk	21/11/99	Mogaung	Kyawdaw	Rhinocerotoidea	M	enamel	-15.6	-13.6	-29.2	0.08	-8.6	22.1	0.18	3.6	-	this study
PND-33	a	22/11/99	Mogaung	Kyawdaw	Rhinocerotoidea	m	enamel	-10.9	-13.6	-24.5	0.04	-10.0	20.6	0.13	3.5	1.0	this study
PND-33	b	22/11/99	Mogaung	Kyawdaw	Rhinocerotoidea	m	enamel	-10.7	-13.6	-24.3	0.11	-10.2	20.3	0.09	2.9	4.0	this study
PND-33	c	22/11/99	Mogaung	Kyawdaw	Rhinocerotoidea	m	enamel	-10.8	-13.6	-24.4	0.15	-10.6	20.0	0.15	2.8	8.0	this study
PND-33	d	22/11/99	Mogaung	Kyawdaw	Rhinocerotoidea	m	enamel	-11.0	-13.6	-24.6	0.04	-9.9	20.7	0.19	2.6	11.0	this study
PND-33	e	22/11/99	Mogaung	Kyawdaw	Rhinocerotoidea	m	enamel	-11.4	-13.6	-25.0	0.08	-9.5	21.1	0.10	2.7	15.0	this study
PND-33	f	22/11/99	Mogaung	Kyawdaw	Rhinocerotoidea	m	enamel	-11.3	-13.6	-24.9	0.07	-9.7	20.9	0.19	3.0	18.0	this study
PND-33	average	22/11/99	Mogaung	Kyawdaw	Rhinocerotoidea	m	enamel	-11.0	-13.6	-24.6	0.08	-10.0	20.6	0.14	2.9	-	this study
PND-34	a	22/11/99	Mogaung	Kyawdaw	Rhinocerotoidea	M	enamel	-12.6	-13.6	-26.2	0.07	-9.3	21.4	0.13	2.0	3.0	this study
PND-34	b	22/11/99	Mogaung	Kyawdaw	Rhinocerotoidea	M	enamel	-12.9	-13.6	-26.5	0.09	-9.3	21.3	0.16	1.9	6.0	this study
PND-34	c	22/11/99	Mogaung	Kyawdaw	Rhinocerotoidea	M	enamel	-12.3	-13.6	-25.9	0.20	-8.5	22.2	0.11	2.1	8.0	this study
PND-34	d	22/11/99	Mogaung	Kyawdaw	Rhinocerotoidea	M	enamel	-12.6	-13.6	-26.2	0.13	-8.2	22.4	0.18	2.0	11.0	this study
PND-34	e	22/11/99	Mogaung	Kyawdaw	Rhinocerotoidea	M	enamel	-12.9	-13.6	-26.5	0.13	-7.7	23.0	0.18	2.2	14.0	this study
PND-34	f	22/11/99	Mogaung	Kyawdaw	Rhinocerotoidea	M	enamel	-13.2	-13.6	-26.8	0.13	-7.8	22.9	0.19	1.9	17.0	this study
PND-34	g	22/11/99	Mogaung	Kyawdaw	Rhinocerotoidea	M	enamel	-13.4	-13.6	-27.0	0.11	-8.6	22.0	0.18	2.2	19.0	this study
PND-34	h	22/11/99	Mogaung	Kyawdaw	Rhinocerotoidea	M	enamel	-13.5	-13.6	-27.1	0.06	-9.5	21.1	0.23	2.2	23.0	this study
PND-34	i	22/11/99	Mogaung	Kyawdaw	Rhinocerotoidea	M	enamel	-13.3	-13.6	-26.9	0.04	-10.7	19.9	0.16	2.0	25.0	this study
PND-34	j	22/11/99	Mogaung	Kyawdaw	Rhinocerotoidea	M	enamel	-13.3	-13.6	-26.9	0.20	-10.5	20.1	0.24	2.4	27.0	this study
PND-34	k	22/11/99	Mogaung	Kyawdaw	Rhinocerotoidea	M	enamel	-13.7	-13.6	-27.3	0.04	-10.3	20.3	0.13	2.7	29.0	this study
PND-34	l	22/11/99	Mogaung	Kyawdaw	Rhinocerotoidea	M	enamel	-13.4	-13.6	-27.0	0.08	-10.3	20.2	0.19	2.2	31.0	this study
PND-34	m	22/11/99	Mogaung	Kyawdaw	Rhinocerotoidea	M	enamel	-13.3	-13.6	-26.9	0.04	-9.6	21.0	0.11	2.0	34.0	this study
PND-34	average	22/11/99	Mogaung	Kyawdaw	Rhinocerotoidea	M	enamel	-13.1	-13.6	-26.7	0.10	-9.3	21.4	0.17	2.1	-	this study
PND-4	bulk	06/03/16	Pangan	Pangan 1	*Anthracotherium*	m_1/m_2	enamel	-9.9	-13.1	-23.0	0.10	-8.4	22.2	0.19	2.9	-	this study
PND-5	bulk	13/01/15	Pangan	Pangan 1	Anthracotheriidae	M	enamel	-11.9	-12.5	-24.4	0.08	-9.2	21.4	0.07	3.1	-	this study
PND-6	bulk	-	Pangan	Pangan 1	Anthracotheriidae	m_3	enamel	-11.3	-12.5	-23.8	0.10	-8.3	22.3	0.16	5.2	-	this study
PND-7	bulk	10/11/99	Pangan	Pangan 1	Perissodactyla	-	enamel	-12.1	-14.0	-26.1	0.07	-7.7	23.0	0.19	3.1	-	this study
PND-8	a	10/11/99	Pangan	Pangan 1	Brontotheriidae	m/M	enamel	-11.6	-14.1	-25.7	0.09	-6.7	24.0	0.10	3.0	1.0	this study
PND-8	b	10/11/99	Pangan	Pangan 1	Brontotheriidae	m/M	enamel	-11.7	-14.1	-25.8	0.10	-5.7	25.0	0.12	3.3	3.0	this study
PND-8	c	10/11/99	Pangan	Pangan 1	Brontotheriidae	m/M	enamel	-11.4	-14.1	-25.5	0.13	-5.6	25.1	0.10	3.1	6.0	this study
PND-8	d	10/11/99	Pangan	Pangan 1	Brontotheriidae	m/M	enamel	-11.4	-14.1	-25.5	0.09	-5.8	24.9	0.16	3.5	9.0	this study
PND-8	e	10/11/99	Pangan	Pangan 1	Brontotheriidae	m/M	enamel	-11.5	-14.1	-25.6	0.07	-6.0	24.8	0.20	3.6	12.0	this study
PND-8	f	10/11/99	Pangan	Pangan 1	Brontotheriidae	m/M	enamel	-11.9	-14.1	-26.0	0.04	-6.8	23.9	0.03	3.2	14.0	this study
PND-8	g	10/11/99	Pangan	Pangan 1	Brontotheriidae	m/M	enamel	-11.8	-14.1	-25.9	0.03	-7.2	23.5	0.15	3.1	17.0	this study
PND-8	h	10/11/99	Pangan	Pangan 1	Brontotheriidae	m/M	enamel	-12.0	-14.1	-26.1	0.10	-7.4	23.3	0.17	3.6	19.0	this study
PND-8	i	10/11/99	Pangan	Pangan 1	Brontotheriidae	m/M	enamel	-12.2	-14.1	-26.3	0.08	-7.7	23.0	0.09	3.6	23.0	this study
PND-8	j	10/11/99	Pangan	Pangan 1	Brontotheriidae	m/M	enamel	-12.5	-14.1	-26.6	0.04	-7.5	23.2	0.11	3.8	25.0	this study
PND-8	k	10/11/99	Pangan	Pangan 1	Brontotheriidae	m/M	enamel	-11.9	-14.1	-26.0	0.08	-6.9	23.8	0.09	3.3	28.0	this study
PND-8	l	10/11/99	Pangan	Pangan 1	Brontotheriidae	m/M	enamel	-12.4	-14.1	-26.5	0.06	-7.2	23.4	0.10	3.8	30.0	this study
PND-8	m	10/11/99	Pangan	Pangan 1	Brontotheriidae	m/M	enamel	-12.5	-14.1	-26.6	0.08	-6.4	24.3	0.10	3.5	33.0	this study
PND-8	average	10/11/99	Pangan	Pangan 1	Brontotheriidae	m/M	enamel	-11.9	-14.1	-26.0	0.08	-6.7	24.0	0.12	3.4	-	this study
PND-9	bulk	10/11/99	Pangan	Pangan 1	Brontotheriidae	m/M	enamel	-11.9	-14.1	-26.0	0.08	-7.0	23.6	0.12	3.1	-	this study
PNG-101	bulk	private collection	Bahin	Tha Duat 3	*Indolophus guptai*	m	enamel	-8.5	-12.2	-20.7	0.06	-7.9	22.8	0.15	3.0	-	this study

PNG-102	bulk	NMMP-2020-ThaDuat2-125a	Bahin	Tha Duat 2	*Anthracokeryx*	r m_2	enamel	-11.1	-12.3	-23.4	0.02	-7.9	22.7	0.08	6.4	-	this study
PNG-103	bulk	NMMP-2020-ThaDuat2-125b	Bahin	Tha Duat 2	*Anthracokeryx*	r m_3	enamel	-10.1	-12.3	-22.4	0.05	-7.4	23.2	0.15	4.6	-	this study
PNG-104	bulk	NMMP-2020-ThaDuat2-125c	Bahin	Tha Duat 2	*Anthracokeryx*	l m_1/m_2	enamel	-11.2	-12.3	-23.5	0.05	-6.7	24.0	0.13	5.1	-	this study
PNG-106	average	NMMP-2020-Lema-144	Mogaung	Kyawdaw	Brontotheriidae	r m	enamel	-12.9	-14.1	-27.0	0.04	-7.8	22.9	0.10	5.1	-	this study
PNG-106	a	NMMP-2020-Kyawdaw-174	Mogaung	Kyawdaw	Brontotheriidae	r m	enamel	-12.6	-14.1	-26.7	0.03	-6.8	23.9	0.09	4.7	11.0	this study
PNG-106	b	NMMP-2020-Kyawdaw-174	Mogaung	Kyawdaw	Brontotheriidae	r m	enamel	-12.9	-14.1	-27.0	0.02	-8.0	22.7	0.09	4.4	8.0	this study
PNG-106	c	NMMP-2020-Kyawdaw-174	Mogaung	Kyawdaw	Brontotheriidae	r m	enamel	-12.9	-14.1	-27.0	0.02	-8.4	22.3	0.12	4.6	6.0	this study
PNG-106	d	NMMP-2020-Kyawdaw-174	Mogaung	Kyawdaw	Brontotheriidae	r m	enamel	-12.8	-14.1	-26.9	0.05	-8.4	22.3	0.10	4.6	3.0	this study
PNG-106	e	NMMP-2020-Kyawdaw-174	Mogaung	Kyawdaw	Brontotheriidae	r m	enamel	-13.5	-14.1	-27.6	0.06	-7.3	23.4	0.08	7.1	0.0	this study
PNG-107	bulk	NMMP-2020-Lema-134	Mogaung	Lema	Rhinocerotoidea	l M	enamel	-11.7	-13.6	-25.3	0.03	-9.3	21.3	0.05	4.1	-	this study
PNG-108	bulk	NMMP-2020-Thandong-160	Mogaung	Thandong	Rhinocerotoidea	r M	enamel	-12.5	-13.6	-26.1	0.03	-9.4	21.3	0.10	4.4	-	this study
PNG-109	average	NMMP-2020-ThaDuat2-123	Bahin	Tha Duat 2	Brontotheriidae	m	enamel	-12.3	-14.1	-26.4	0.03	-8.1	22.6	0.11	4.1	-	this study
PNG-109	a	NMMP-2020-ThaDuat2-123	Bahin	Tha Duat 2	Brontotheriidae	m	enamel	-12.7	-14.1	-26.8	0.03	-8.5	22.2	0.13	4.0	21.0	this study
PNG-109	b	NMMP-2020-ThaDuat2-123	Bahin	Tha Duat 2	Brontotheriidae	m	enamel	-12.7	-14.1	-26.8	0.04	-8.2	22.4	0.10	4.1	18.0	this study
PNG-109	c	NMMP-2020-ThaDuat2-123	Bahin	Tha Duat 2	Brontotheriidae	m	enamel	-12.6	-14.1	-26.7	0.03	-8.7	21.9	0.09	3.6	15.0	this study
PNG-109	d	NMMP-2020-ThaDuat2-123	Bahin	Tha Duat 2	Brontotheriidae	m	enamel	-12.5	-14.1	-26.6	0.02	-8.3	22.4	0.11	3.7	12.0	this study
PNG-109	e	NMMP-2020-ThaDuat2-123	Bahin	Tha Duat 2	Brontotheriidae	m	enamel	-12.0	-14.1	-26.1	0.03	-7.4	23.3	0.08	3.9	9.0	this study
PNG-109	f	NMMP-2020-ThaDuat2-123	Bahin	Tha Duat 2	Brontotheriidae	m	enamel	-11.9	-14.1	-26.0	0.04	-7.7	23.0	0.11	4.3	6.0	this study
PNG-109	g	NMMP-2020-ThaDuat2-123	Bahin	Tha Duat 2	Brontotheriidae	m	enamel	-12.0	-14.1	-26.1	0.03	-8.0	22.6	0.11	4.3	3.5	this study
PNG-109	h	NMMP-2020-ThaDuat2-123	Bahin	Tha Duat 2	Brontotheriidae	m	enamel	-12.1	-14.1	-26.2	0.01	-7.9	22.8	0.12	4.9	1.0	this study
PNG-110	bulk	NMMP-2020-KyawdDaw-174	Mogaung	Kyawdaw	Brontotheriidae	m	enamel	-13.4	-14.1	-27.5	0.02	-9.1	21.5	0.06	8.5	-	this study
PNG-111	bulk	NMMP-2020-ThanDong-163	Mogaung	Thandong	Rhinocerotoidea	l M	enamel	-11.6	-13.6	-25.2	0.02	-9.2	21.4	0.08	3.5	-	this study
PNG-112	bulk	NMMP-2020-Lema-140	Mogaung	Lema	Brontotheriidae	l P	enamel	-12.9	-14.1	-27.0	0.05	-8.8	21.9	0.08	4.4	-	this study
PNG-113	bulk	NMMP-2020-KyawDaw-176	Mogaung	Kyawdaw	Rhinocerotoidea	l m	enamel	-14.1	-13.6	-27.7	0.02	-9.9	20.7	0.08	3.0	-	this study
PNG-114	bulk	NMMP-2020-Lema-137	Mogaung	Lema	Rhinocerotoidea	m/M	enamel	-11.0	-13.6	-24.6	0.04	-10.7	19.9	0.11	2.6	-	this study
PNG-115	average	NMMP-2020-KyawDaw-175	Mogaung	Kyawdaw	*Anthracotherium*	l m_3	enamel	-11.8	-13.1	-24.9	0.05	-9.4	21.3	0.09	5.2	-	this study
PNG-115	a	NMMP-2020-KyawDaw-175	Mogaung	Kyawdaw	*Anthracotherium*	l m_3	enamel	-12.0	-13.1	-25.1	0.06	-9.1	21.5	0.09	4.5	9.0	this study
PNG-115	b	NMMP-2020-KyawDaw-175	Mogaung	Kyawdaw	*Anthracotherium*	l m_3	enamel	-12.0	-13.1	-25.1	0.03	-9.6	21.0	0.08	4.9	6.0	this study
PNG-115	c	NMMP-2020-KyawDaw-175	Mogaung	Kyawdaw	*Anthracotherium*	l m_3	enamel	-11.8	-13.1	-24.9	0.04	-9.8	20.8	0.13	5.5	3.5	this study
PNG-115	d	NMMP-2020-KyawDaw-175	Mogaung	Kyawdaw	*Anthracotherium*	l m_3	enamel	-11.3	-13.1	-24.4	0.07	-9.0	21.7	0.07	5.9	1.0	this study
PNG-116	bulk	NMMP-2020-Kyawdaw-177	Mogaung	Kyawdaw	Brontotheriidae	m	enamel	-12.9	-14.1	-27.0	0.04	-7.0	23.7	0.09	4.4	-	this study
PNG-118	bulk	NMMP-2020-Segyauk-183	Mogaung	Segyauk	Brontotheriidae	M	enamel	-13.5	-14.1	-27.6	0.05	-7.7	22.9	0.09	4.6	-	this study
PNG-119	average	NMMP-2020-Segyauk-182	Mogaung	Segyauk	*Paramynodon*	l C	enamel	-11.3	-13.8	-25.1	0.04	-8.3	22.4	0.10	4.3	-	this study
PNG-119	a	NMMP-2020-Segyauk-182	Mogaung	Segyauk	*Paramynodon*	l C	enamel	-11.3	-13.8	-25.1	0.03	-7.0	23.7	0.09	5.0	34.0	this study
PNG-119	b	NMMP-2020-Segyauk-182	Mogaung	Segyauk	*Paramynodon*	l C	enamel	-11.6	-13.8	-25.4	0.05	-8.8	21.8	0.10	4.9	31.0	this study
PNG-119	c	NMMP-2020-Segyauk-182	Mogaung	Segyauk	*Paramynodon*	l C	enamel	-11.4	-13.8	-25.2	0.04	-9.6	21.1	0.07	4.5	28.0	this study
PNG-119	d	NMMP-2020-Segyauk-182	Mogaung	Segyauk	*Paramynodon*	l C	enamel	-11.0	-13.8	-24.8	0.02	-8.9	21.7	0.10	4.1	25.0	this study
PNG-119	e	NMMP-2020-Segyauk-182	Mogaung	Segyauk	*Paramynodon*	l C	enamel	-11.1	-13.8	-24.9	0.02	-7.2	23.5	0.13	4.1	22.5	this study
PNG-119	f	NMMP-2020-Segyauk-182	Mogaung	Segyauk	*Paramynodon*	l C	enamel	-11.2	-13.8	-25.0	0.02	-7.0	23.7	0.05	4.1	20.0	this study
PNG-119	g	NMMP-2020-Segyauk-182	Mogaung	Segyauk	*Paramynodon*	l C	enamel	-11.3	-13.8	-25.1	0.06	-7.5	23.2	0.13	4.4	17.0	this study
PNG-119	h	NMMP-2020-Segyauk-182	Mogaung	Segyauk	*Paramynodon*	l C	enamel	-11.5	-13.8	-25.3	0.03	-9.0	21.7	0.08	4.1	14.0	this study
PNG-119	i	NMMP-2020-Segyauk-182	Mogaung	Segyauk	*Paramynodon*	l C	enamel	-11.3	-13.8	-25.1	0.04	-9.4	21.2	0.06	4.2	12.0	this study
PNG-119	j	NMMP-2020-Segyauk-182	Mogaung	Segyauk	*Paramynodon*	l C	enamel	-11.3	-13.8	-25.1	0.02	-9.9	20.7	0.07	4.1	10.0	this study
PNG-119	k	NMMP-2020-Segyauk-182	Mogaung	Segyauk	*Paramynodon*	l C	enamel	-11.2	-13.8	-25.0	0.02	-8.4	22.3	0.12	4.2	7.0	this study
PNG-119	l	NMMP-2020-Segyauk-182	Mogaung	Segyauk	*Paramynodon*	l C	enamel	-11.3	-13.8	-25.1	0.03	-7.5	23.2	0.12	4.2	5.0	this study
PNG-119	lm	NMMP-2020-Segyauk-182	Mogaung	Segyauk	*Paramynodon*	l C	enamel	-11.4	-13.8	-25.2	0.09	-7.5	23.2	0.14	4.7	2.0	this study
PNG-140	bulk	23.02.2020	-	-	Rhinocerotoidea	-	enamel	-10.7	-13.6	-24.3	0.04	-9.5	21.2	0.07	35.3	-	this study
PNG-141 M3	bulk	-	Pangan	Pangan 1	*Siamotherium pondaungensis*	l m_3	enamel	-10.7	-11.8	-22.5	0.03	-7.1	23.6	0.02	4.9	-	this study
PNG-141-M2	bulk	-	Pangan	Pangan 1	*Siamotherium pondaungensis*	l m_2	enamel	-10.3	-11.8	-22.1	0.02	-6.7	24.0	0.03	4.7	-	this study
PNG-20 M2	bulk	PGN-293/Box-2	Pangan	Pangan 1	*Siamotherium pondaungensis*	r M^2	enamel	-12.0	-11.8	-23.8	0.07	-7.8	22.9	0.12	0.3	-	this study
PNG-20 M3	bulk	PGN-293/Box-2	Pangan	Pangan 1	*Siamotherium pondaungensis*	r M^3	enamel	-12.1	-11.8	-23.9	0.04	-7.1	23.6	0.05	4.4	-	this study
PNG-21	a	NMMP-2018-PK11-024	Bahin	PK 11	*Anthracotherium pangan*	r M	enamel	-12.0	-13.3	-25.3	0.05	-7.8	22.9	0.07	2.9	10.5	this study
PNG-21	b	NMMP-2018-PK11-024	Bahin	PK 11	*Anthracotherium pangan*	r M	enamel	-11.7	-13.3	-25.0	0.07	-8.2	22.5	0.09	2.9	6.5	this study
PNG-21	c	NMMP-2018-PK11-024	Bahin	PK 11	*Anthracotherium pangan*	r M	enamel	-11.9	-13.3	-25.2	0.08	-9.2	21.4	0.10	3.3	4.0	this study
PNG-21	d	NMMP-2018-PK11-024	Bahin	PK 11	*Anthracotherium pangan*	r M	enamel	-11.1	-13.3	-24.4	0.02	-8.5	22.2	0.02	4.0	0.5	this study
PNG-21	average	NMMP-2018-PK11-024	Bahin	PK 11	*Anthracotherium pangan*	r M	enamel	-11.7	-13.3	-25.0	0.06	-8.4	22.2	0.07	3.3	-	this study
PNG-22 M3	bulk	NMMP-2018-Than-U-Daw-66	Pangan	Than-U-Daw	*Anthracokeryx tenuis*	r M^3	enamel	-11.7	-12.1	-23.8	0.04	-5.7	25.0	0.09	3.4	-	this study
PNG-24	bulk	NMMP-2018-NPL-026	Bahin	Nyaung Pinle	Rhinocerotoidea	P	enamel	-12.4	-13.6	-26.0	0.04	-8.4	22.3	0.07	1.4	-	this study
PNG-25 M3	bulk	NMMP-2018-NPL-027	Bahin	Nyaung Pinle	*Anthracokeryx tenuis*	l m_3	enamel	-10.7	-12.1	-22.8	0.04	-7.2	23.5	0.03	4.9	-	this study
PNG-26	bulk	NMMP-PK2-2013-001	Bahin	PK 2	Amynodontidae	r m	enamel	-12.8	-13.1	-25.9	0.04	-7.6	23.1	0.19	2.9	-	this study

PNG-27	bulk	NMMP-2018-Ganle-035	Bahin	Ganle	*Anthracokeryx*	l m_1/m_2	enamel	-12.3	-12.3	-24.6	0.07	-9.8	20.8	0.13	4.1	-	this study
PNG-28	bulk	NMMP-2018-Ganle-034	Bahin	Ganle	*Anthracokeryx*	l m_1/m_2	enamel	-11.0	-12.3	-23.3	0.04	-8.9	21.7	0.08	4.2	-	this study
PNG-29a	bulk	NMMP-2018-Ganle-036	Bahin	Ganle	Rhinocerotoidea	P	enamel	-12.7	-13.6	-26.3	0.02	-8.7	21.9	0.08	3.1	-	this study
PNG-29b	bulk	NMMP-2018-Ganle-036	Bahin	Ganle	Rhinocerotoidea	P	enamel	-11.7	-13.6	-25.3	0.02	-8.2	22.5	0.09	2.9	-	this study
PNG-29c	bulk	NMMP-2018-Ganle-036	Bahin	Ganle	Rhinocerotoidea	P	enamel	-10.4	-13.6	-24.0	0.05	-7.2	23.5	0.08	0.4	-	this study
PNG-30	bulk	NMMP-2018-Myaukse-56	Pangan	Myauk Se	*Anthracotherium pangan*	r m_3	enamel	-11.2	-13.3	-24.5	0.06	-9.3	21.3	0.08	3.3	-	this study
PNG-31	a	NMMP-2018-Myaukse-55	Pangan	Myauk Se	*Anthracotherium pangan*	r M	enamel	-11.5	-13.3	-24.8	0.08	-8.2	22.4	0.06	3.5	7.5	this study
PNG-31	b	NMMP-2018-Myaukse-55	Pangan	Myauk Se	*Anthracotherium pangan*	r M	enamel	-11.2	-13.3	-24.5	0.04	-8.0	22.6	0.08	2.9	5.5	this study
PNG-31	c	NMMP-2018-Myaukse-55	Pangan	Myauk Se	*Anthracotherium pangan*	r M	enamel	-11.1	-13.3	-24.4	0.05	-7.7	23.0	0.09	3.6	3.0	this study
PNG-31	average	NMMP-2018-Myaukse-55	Pangan	Myauk Se	*Anthracotherium pangan*	r M	enamel	-11.3	-13.3	-24.6	0.06	-8.0	22.7	0.08	3.3	-	this study
PNG-32	bulk	NMMP-2018-Myaukse-57	Pangan	Myauk Se	*Anthracotherium crassum*	r M	enamel	-10.8	-13.0	-23.8	0.04	-6.9	23.8	0.09	4.2	-	this study
PNG-33	bulk	NMMP-2018-Changan-008	Pangan	Myauk Se	Amynodontidae	r m	enamel	-12.6	-13.1	-25.7	0.07	-6.2	24.5	0.12	4.8	-	this study
PNG-34	ab	NMMP-2018-PK2-011	Bahin	PK 2	Anthracotheriidae	l C	enamel	-12.0	-12.5	-24.5	0.00	-7.0	23.7	0.01	0.4	21.5	this study
PNG-34	cd	NMMP-2018-PK2-011	Bahin	PK 2	Anthracotheriidae	l C	enamel	-12.2	-12.5	-24.7	0.29	-9.0	21.7	0.41	0.2	16.0	this study
PNG-34	d	NMMP-2018-PK2-011	Bahin	PK 2	Anthracotheriidae	l C	enamel	-11.6	-12.5	-24.1	-	-8.9	21.8	-	0.3	14.5	this study
PNG-34	ef	NMMP-2018-PK2-011	Bahin	PK 2	Anthracotheriidae	l C	enamel	-11.6	-12.5	-24.1	0.20	-9.4	21.3	0.23	0.3	11.5	this study
PNG-34	f	NMMP-2018-PK2-011	Bahin	PK 2	Anthracotheriidae	l C	enamel	-11.7	-12.5	-24.2	0.02	-9.4	21.2	0.02	0.3	9.0	this study
PNG-34	average	NMMP-2018-PK2-011	Bahin	PK 2	Anthracotheriidae	l C	enamel	-11.8	-12.5	-24.3	0.13	-8.7	21.9	0.17	0.3	-	this study
PNG-35	ab	NMMP-2018-PK2-012	Bahin	PK 2	Amynodontidae	r c	enamel	-12.0	-13.1	-25.1	0.08	-7.4	23.3	0.23	0.3	21.5	this study
PNG-35	cd	NMMP-2018-PK2-012	Bahin	PK 2	Amynodontidae	r c	enamel	-12.2	-13.1	-25.3	0.09	-6.4	24.3	0.13	0.4	16.5	this study
PNG-35	d	NMMP-2018-PK2-012	Bahin	PK 2	Amynodontidae	r c	enamel	-12.4	-13.1	-25.5	0.07	-7.1	23.6	0.03	3.3	14.5	this study
PNG-35	e	NMMP-2018-PK2-012	Bahin	PK 2	Amynodontidae	r c	enamel	-12.6	-13.1	-25.7	0.10	-8.2	22.5	0.08	3.6	12.0	this study
PNG-35	f	NMMP-2018-PK2-012	Bahin	PK 2	Amynodontidae	r c	enamel	-12.4	-13.1	-25.5	0.04	-8.8	21.8	0.09	3.7	9.0	this study
PNG-35	gh	NMMP-2018-PK2-012	Bahin	PK 2	Amynodontidae	r c	enamel	-12.0	-13.1	-25.1	0.11	-7.8	22.8	0.14	1.9	6.5	this study
PNG-35	i	NMMP-2018-PK2-012	Bahin	PK 2	Amynodontidae	r c	enamel	-12.0	-13.1	-25.1	0.23	-5.9	24.8	0.21	0.5	1.0	this study
PNG-35	average	NMMP-2018-PK2-012	Bahin	PK 2	Amynodontidae	r c	enamel	-12.2	-13.1	-25.3	0.10	-7.4	23.3	0.13	1.9	-	this study
PNG-36	average	NMMP-2018-Ganlea-037	Bahin	Ganle	*Anthracotherium pangan*	l m_3	enamel	-9.8	-13.3	-23.1	0.05	-7.6	23.1	0.17	3.5	-	this study
PNG-36	a	NMMP-2018-Ganlea-037	Bahin	Ganle	*Anthracotherium pangan*	l m_3	enamel	-9.9	-13.3	-23.2	0.04	-8.3	22.4	0.16	3.5	9.0	this study
PNG-36	b	NMMP-2018-Ganlea-037	Bahin	Ganle	*Anthracotherium pangan*	l m_3	enamel	-9.8	-13.3	-23.1	0.03	-7.4	23.2	0.19	3.4	6.5	this study
PNG-36	c	NMMP-2018-Ganlea-037	Bahin	Ganle	*Anthracotherium pangan*	l m_3	enamel	-10.0	-13.3	-23.3	0.09	-6.9	23.8	0.14	3.5	4.0	this study
PNG-36	d	NMMP-2018-Ganlea-037	Bahin	Ganle	*Anthracotherium pangan*	l m_3	enamel	-9.7	-13.3	-23.0	0.03	-7.6	23.1	0.18	3.5	1.5	this study
PNG-37	bulk	NMMP-2018-Myaukse-058	Pangan	Myauk Se	*Anthracotherium pangan*	r m_3	enamel	-9.3	-13.3	-22.6	0.01	-7.0	23.7	0.13	0.7	-	this study
PNG-38	bulk	NMMP-2018-PGN1-051a	Pangan	Pangan 1	Brontotheriidae	r m_1/m_2	enamel	-11.4	-14.1	-25.5	0.06	-7.2	23.5	0.11	7.4	-	this study
PNG-39	bulk	NMMP-2018-PGN1-051b	Pangan	Pangan 1	Brontotheriidae	r m_1/m_2	enamel	-13.1	-14.1	-27.2	0.03	-7.2	23.4	0.13	4.6	-	this study
PNG-40	bulk	NMMP-2015-67-PK10	Bahin	PK 10	Rhinocerotoidea	l M^3	enamel	-11.2	-13.6	-24.8	0.03	-8.1	22.6	0.12	3.0	-	this study
PNG-41	bulk	NMMP-2015-65-PK2	Bahin	PK 2	Brontotheriidae	M	enamel	-12.5	-14.1	-26.6	0.03	-6.5	24.2	0.15	4.0	-	this study
PNG-42	average	NMMP-2015-68a-Tanudo	Pangan	Than-U-Daw	*Anthracotherium pangan*	l M^3	enamel	-10.4	-13.3	-23.7	0.06	-8.4	22.2	0.13	3.4	-	this study
PNG-42	a	NMMP-2015-68a-Tanudo	Pangan	Than-U-Daw	*Anthracotherium pangan*	l M^3	enamel	-10.7	-13.3	-24.0	0.06	-7.4	23.3	0.18	3.1	14.0	this study
PNG-42	b	NMMP-2015-68a-Tanudo	Pangan	Than-U-Daw	*Anthracotherium pangan*	l M^3	enamel	-10.4	-13.3	-23.7	0.08	-7.4	23.3	0.10	3.0	11.5	this study
PNG-42	c	NMMP-2015-68a-Tanudo	Pangan	Than-U-Daw	*Anthracotherium pangan*	l M^3	enamel	-10.4	-13.3	-23.7	0.04	-7.9	22.8	0.14	3.0	8.0	this study
PNG-42	d	NMMP-2015-68a-Tanudo	Pangan	Than-U-Daw	*Anthracotherium pangan*	l M^3	enamel	-10.3	-13.3	-23.6	0.05	-8.7	21.9	0.12	3.4	5.0	this study
PNG-42	e	NMMP-2015-68a-Tanudo	Pangan	Than-U-Daw	*Anthracotherium pangan*	l M^3	enamel	-10.2	-13.3	-23.5	0.04	-9.5	21.1	0.07	3.6	2.5	this study
PNG-42	f	NMMP-2015-68a-Tanudo	Pangan	Than-U-Daw	*Anthracotherium pangan*	l M^3	enamel	-10.4	-13.3	-23.7	0.08	-9.5	21.1	0.14	3.8	0.5	this study
PNG-43	bulk	NMMP-2015-68b-Tanudo	Pangan	Than-U-Daw	*Anthracokeryx birmanicum*	r m_3	enamel	-12.3	-12.7	-25.0	0.05	-9.0	21.7	0.11	5.4	-	this study
PNG-44	bulk	NMMP-2015-68c-Tanudo	Pangan	Than-U-Daw	*Anthracokeryx tenuis*	l m_3	enamel	-9.4	-12.1	-21.5	0.04	-7.6	23.0	0.09	4.6	-	this study
PNG-45	average	NMMP-2015-44a-PK13	Bahin	PK 13	*Anthracotherium pangan*	r M^1/M^2	enamel	-9.6	-13.3	-22.9	0.05	-7.0	23.7	0.13	4.5	-	this study
PNG-45	ab	NMMP-2015-44a-PK13	Bahin	PK 13	*Anthracotherium pangan*	r M^1/M^2	enamel	-9.5	-13.3	-22.8	0.08	-8.3	22.3	0.17	3.9	11.0	this study
PNG-45	b	NMMP-2015-44a-PK13	Bahin	PK 13	*Anthracotherium pangan*	r M^1/M^2	enamel	-9.4	-13.3	-22.7	0.05	-8.2	22.5	0.14	3.9	7.5	this study
PNG-45	c	NMMP-2015-44a-PK13	Bahin	PK 13	*Anthracotherium pangan*	r M^1/M^2	enamel	-9.6	-13.3	-22.9	0.05	-6.5	24.2	0.12	3.6	4.5	this study
PNG-45	d	NMMP-2015-44a-PK13	Bahin	PK 13	*Anthracotherium pangan*	r M^1/M^2	enamel	-9.8	-13.3	-23.1	0.04	-6.1	24.6	0.11	4.6	1.5	this study
PNG-45	e	NMMP-2015-44a-PK13	Bahin	PK 13	*Anthracotherium pangan*	r M^1/M^2	enamel	-9.7	-13.3	-23.0	0.01	-5.9	24.8	0.10	6.2	0.0	this study
PNG-46	bulk	NMMP-2015-44b-PK13	Bahin	PK 13	*Anthracokeryx birmanicum*	r M^1/M^2	enamel	-10.5	-12.7	-23.2	0.10	-6.4	24.3	0.20	5.2	-	this study
PNG-47	average	NMMP-2015-43-PK13	Bahin	PK 13	*Bunobrontops savagei*	r M^1/M^2	enamel	-11.6	-13.9	-25.5	0.05	-7.7	23.0	0.15	3.1	-	this study
PNG-47	a	NMMP-2015-43-PK13	Bahin	PK 13	*Bunobrontops savagei*	r M^1/M^2	enamel	-11.5	-13.9	-25.4	0.07	-8.0	22.7	0.22	3.4	13.5	this study
PNG-47	bc	NMMP-2015-43-PK13	Bahin	PK 13	*Bunobrontops savagei*	r M^1/M^2	enamel	-11.7	-13.9	-25.6	0.04	-8.5	22.2	0.13	2.9	10.5	this study
PNG-47	d	NMMP-2015-43-PK13	Bahin	PK 13	*Bunobrontops savagei*	r M^1/M^2	enamel	-11.8	-13.9	-25.7	0.02	-7.7	23.0	0.09	2.9	5.5	this study
PNG-47	e	NMMP-2015-43-PK13	Bahin	PK 13	*Bunobrontops savagei*	r M^1/M^2	enamel	-11.5	-13.9	-25.4	0.04	-7.0	23.7	0.19	3.0	4.0	this study

PNG-47	f	NMMP-2015-43-PK13	Bahin	PK 13	*Bunobrontops savagei*	r M^1/M^2	enamel	-11.5	-13.9	-25.4	0.08	-7.4	23.2	0.14	3.5	1.5	this study
PNG-49	bulk	NMMP-2015-48-TMC	Pangan	Thaminchauk	*Anthracotherium pangan*	l M^1/M^2	enamel	-8.9	-13.3	-22.2	0.02	-8.5	22.1	0.12	3.4	-	this study
PNG-50	average	NMMP-TMC-2013-005	Pangan	Thaminchauk	Amynodontidae	l M^1/M^2	enamel	-12.6	-13.1	-25.7	0.05	-8.4	22.3	0.12	3.0	-	this study
PNG-50	a	NMMP-TMC-2013-005	Pangan	Thaminchauk	Amynodontidae	l M^1/M^2	enamel	-13.0	-13.1	-26.1	0.02	-8.7	22.0	0.09	3.4	20.0	this study
PNG-50	b	NMMP-TMC-2013-005	Pangan	Thaminchauk	Amynodontidae	l M^1/M^2	enamel	-12.6	-13.1	-25.7	0.03	-8.8	21.8	0.17	2.9	17.5	this study
PNG-50	c	NMMP-TMC-2013-005	Pangan	Thaminchauk	Amynodontidae	l M^1/M^2	enamel	-12.6	-13.1	-25.7	0.03	-8.5	22.1	0.15	2.9	15.0	this study
PNG-50	d	NMMP-TMC-2013-005	Pangan	Thaminchauk	Amynodontidae	l M^1/M^2	enamel	-12.6	-13.1	-25.7	0.04	-8.3	22.4	0.02	2.7	13.0	this study
PNG-50	e	NMMP-TMC-2013-005	Pangan	Thaminchauk	Amynodontidae	l M^1/M^2	enamel	-12.5	-13.1	-25.6	0.06	-7.8	22.9	0.14	2.7	10.5	this study
PNG-50	f	NMMP-TMC-2013-005	Pangan	Thaminchauk	Amynodontidae	l M^1/M^2	enamel	-12.6	-13.1	-25.7	0.08	-7.8	22.9	0.13	3.0	8.0	this study
PNG-50	g	NMMP-TMC-2013-005	Pangan	Thaminchauk	Amynodontidae	l M^1/M^2	enamel	-12.3	-13.1	-25.4	0.08	-8.5	22.1	0.18	3.0	5.5	this study
PNG-50	h	NMMP-TMC-2013-005	Pangan	Thaminchauk	Amynodontidae	l M^1/M^2	enamel	-12.4	-13.1	-25.5	0.03	-8.6	22.1	0.07	3.0	3.0	this study
PNG-51	average	NMMP-PK12-2014-044	Bahin	PK 12	*Anthracotherium crassum*	m_3	enamel	-10.8	-13.0	-23.8	0.04	-6.4	24.3	0.11	3.4	-	this study
PNG-51	a	NMMP-PK12-2014-044	Bahin	PK 12	*Anthracotherium crassum*	m_3	enamel	-11.0	-13.0	-24.0	0.08	-7.1	23.6	0.06	3.2	13.5	this study
PNG-51	b	NMMP-PK12-2014-044	Bahin	PK 12	*Anthracotherium crassum*	m_3	enamel	-10.8	-13.0	-23.8	0.01	-6.4	24.3	0.15	2.9	10.0	this study
PNG-51	c	NMMP-PK12-2014-044	Bahin	PK 12	*Anthracotherium crassum*	m_3	enamel	-10.4	-13.0	-23.4	0.05	-5.8	24.9	0.14	2.9	5.5	this study
PNG-51	d	NMMP-PK12-2014-044	Bahin	PK 12	*Anthracotherium crassum*	m_3	enamel	-10.9	-13.0	-23.9	0.02	-6.4	24.3	0.07	4.7	2.0	this study
PNG-52	bulk	NMMP-PNG1-2014-029a	Pangan	Pangan 1	*Anthracokeryx birmanicum*	l m_1/m_2	enamel	-11.3	-12.7	-24.0	0.05	-6.4	24.3	0.18	4.7	-	this study
PNG-53	bulk	NMMP-PNG1-2014-029b	Pangan	Pangan 1	*Bahinolophos*	r m	enamel	-11.8	-12.6	-24.4	0.03	-6.2	24.5	0.15	3.8	-	this study
PNG-55	bulk	NMMP-PK2-2014-008	Bahin	PK 2	*Anthracokeryx birmanicum*	r P/M	enamel	-11.0	-12.7	-23.7	0.02	-6.8	23.9	0.13	4.5	-	this study
PNG-56	a	NMMP-MS-2014-016a	Pangan	Myauk Se	*Anthracotherium crassum*	l M^2/M^3	enamel	-10.2	-13.0	-23.2	0.10	-8.3	22.4	0.15	4.0	9.5	this study
PNG-56	b	NMMP-MS-2014-016a	Pangan	Myauk Se	*Anthracotherium crassum*	l M^2/M^3	enamel	-10.1	-13.0	-23.1	0.01	-7.6	23.1	0.12	3.9	7.0	this study
PNG-56	c	NMMP-MS-2014-016a	Pangan	Myauk Se	*Anthracotherium crassum*	l M^2/M^3	enamel	-10.1	-13.0	-23.1	0.07	-6.2	24.5	0.15	4.1	4.5	this study
PNG-56	cd	NMMP-MS-2014-016a	Pangan	Myauk Se	*Anthracotherium crassum*	l M^2/M^3	enamel	-10.2	-13.0	-23.2	0.05	-5.8	25.0	0.15	3.9	2.0	this study
PNG-56	average	NMMP-MS-2014-016a	Pangan	Myauk Se	*Anthracotherium crassum*	l M^2/M^3	enamel	-10.2	-13.0	-23.2	0.06	-7.0	23.7	0.14	4.0	-	this study
PNG-57	a	NMMP-MS-2014-016b	Pangan	Myauk Se	*Anthracotherium crassum*	M^3	enamel	-10.0	-13.0	-23.0	0.09	-7.8	22.8	0.11	4.0	11.5	this study
PNG-57	b	NMMP-MS-2014-016b	Pangan	Myauk Se	*Anthracotherium crassum*	M^3	enamel	-9.7	-13.0	-22.7	0.02	-8.0	22.7	0.15	3.4	8.0	this study
PNG-57	c	NMMP-MS-2014-016b	Pangan	Myauk Se	*Anthracotherium crassum*	M^3	enamel	-9.6	-13.0	-22.6	0.09	-7.2	23.5	0.05	3.5	6.5	this study
PNG-57	de	NMMP-MS-2014-016b	Pangan	Myauk Se	*Anthracotherium crassum*	M^3	enamel	-9.9	-13.0	-22.9	0.06	-6.6	24.1	0.10	3.6	3.0	this study
PNG-57	average	NMMP-MS-2014-016b	Pangan	Myauk Se	*Anthracotherium crassum*	M^3	enamel	-9.8	-13.0	-22.8	0.07	-7.4	23.3	0.10	3.6	-	this study
PNG-61	a	NMMP-2012-21-PK2	Bahin	PK 2	Amynodontidae	l m	enamel	-12.7	-13.1	-25.8	0.04	-7.1	23.6	0.11	3.9	9.5	this study
PNG-61	b	NMMP-2012-21-PK2	Bahin	PK 2	Amynodontidae	l m	enamel	-12.3	-13.1	-25.4	0.06	-7.2	23.5	0.18	2.7	7.5	this study
PNG-61	c	NMMP-2012-21-PK2	Bahin	PK 2	Amynodontidae	l m	enamel	-12.3	-13.1	-25.4	0.07	-7.7	23.0	0.17	2.9	5.5	this study
PNG-61	d	NMMP-2012-21-PK2	Bahin	PK 2	Amynodontidae	l m	enamel	-12.0	-13.1	-25.1	0.03	-8.3	22.3	0.13	2.7	3.5	this study
PNG-61	e	NMMP-2012-21-PK2	Bahin	PK 2	Amynodontidae	l m	enamel	-12.0	-13.1	-25.1	0.04	-8.1	22.5	0.19	2.7	2.0	this study
PNG-61	average	NMMP-2012-21-PK2	Bahin	PK 2	Amynodontidae	l m	enamel	-12.3	-13.1	-25.4	0.05	-7.7	23.0	0.16	3.0	-	this study
PNG-70	bulk	NMMP-2020-PK2-011	Bahin	PK 2	Anthracotheriidae	l	enamel	-13.1	-12.5	-25.6	0.03	-6.7	24.0	0.14	3.8	-	this study
PNG-71	bulk	NMMP-2020-PK2-013	Bahin	PK 2	Ruminantia	i	enamel	-11.1	-12.2	-23.3	0.04	-5.4	25.4	0.12	3.5	-	this study
PNG-72	bulk	NMMP-2020-PK2-016	Bahin	PK 2	Brontotheriidae	M	enamel	-12.2	-14.1	-26.3	0.04	-8.3	22.4	0.11	4.6	-	this study
PNG-73	bulk	NMMP-2020-Changan-023	Bahin	Changan	Anthracotheriidae	l p_4	enamel	-11.4	-12.5	-23.9	0.04	-4.9	25.9	0.09	5.9	-	this study
PNG-74	bulk	NMMP-2020-Changan-024	Bahin	Changan	Anthracotheriidae	l p_3	enamel	-11.2	-12.5	-23.7	0.03	-6.5	24.2	0.12	5.7	-	this study
PNG-75	a	NMMP-2020-Changan-025	Bahin	Changan	Amynodontidae	c	enamel	-12.1	-13.1	-25.2	0.03	-6.6	24.2	0.17	3.5	13.0	this study
PNG-75	b	NMMP-2020-Changan-025	Bahin	Changan	Amynodontidae	c	enamel	-11.9	-13.1	-25.0	0.05	-5.2	25.5	0.15	3.6	10.5	this study
PNG-75	c	NMMP-2020-Changan-025	Bahin	Changan	Amynodontidae	c	enamel	-12.0	-13.1	-25.1	0.01	-5.1	25.7	0.11	3.7	6.5	this study
PNG-75	d	NMMP-2020-Changan-025	Bahin	Changan	Amynodontidae	c	enamel	-12.1	-13.1	-25.2	0.06	-6.0	24.7	0.17	3.5	4.0	this study
PNG-75	e	NMMP-2020-Changan-025	Bahin	Changan	Amynodontidae	c	enamel	-12.4	-13.1	-25.5	0.04	-6.1	24.6	0.20	3.2	1.0	this study
PNG-75	average	NMMP-2020-Changan-025	Bahin	Changan	Amynodontidae	c	enamel	-12.1	-13.1	-25.2	0.04	-5.8	24.9	0.16	3.5	-	this study
PNG-76	a	NMMP-2020-BH4-031	Bahin	BH 4	Brontotheriidae	M	enamel	-11.7	-14.1	-25.8	0.01	-7.1	23.6	0.11	4.4	24.0	this study
PNG-76	b	NMMP-2020-BH4-031	Bahin	BH 4	Brontotheriidae	M	enamel	-11.8	-14.1	-25.9	0.04	-7.1	23.6	0.12	4.4	21.0	this study
PNG-76	c	NMMP-2020-BH4-031	Bahin	BH 4	Brontotheriidae	M	enamel	-11.9	-14.1	-26.0	0.04	-7.3	23.4	0.08	4.7	19.0	this study
PNG-76	d	NMMP-2020-BH4-031	Bahin	BH 4	Brontotheriidae	M	enamel	-11.9	-14.1	-26.0	0.05	-7.4	23.3	0.10	4.9	16.0	this study
PNG-76	e	NMMP-2020-BH4-031	Bahin	BH 4	Brontotheriidae	M	enamel	-12.0	-14.1	-26.1	0.04	-7.7	23.0	0.04	4.9	13.5	this study
PNG-76	f	NMMP-2020-BH4-031	Bahin	BH 4	Brontotheriidae	M	enamel	-12.1	-14.1	-26.2	0.05	-7.7	23.0	0.14	4.7	11.0	this study
PNG-76	g	NMMP-2020-BH4-031	Bahin	BH 4	Brontotheriidae	M	enamel	-12.3	-14.1	-26.4	0.06	-8.1	22.6	0.07	4.9	8.0	this study
PNG-76	h	NMMP-2020-BH4-031	Bahin	BH 4	Brontotheriidae	M	enamel	-12.3	-14.1	-26.4	0.03	-8.6	22.0	0.13	4.7	5.5	this study
PNG-76	i	NMMP-2020-BH4-031	Bahin	BH 4	Brontotheriidae	M	enamel	-12.0	-14.1	-26.1	0.05	-9.1	21.5	0.09	4.7	2.5	this study
PNG-76	average	NMMP-2020-BH4-031	Bahin	BH 4	Brontotheriidae	M	enamel	-12.0	-14.1	-26.1	0.04	-7.8	22.9	0.10	4.7	-	this study
PNG-77	bulk	NMMP-2020-BH-033	Bahin	BH	Brontotheriidae	M	enamel	-10.0	-14.1	-24.1	0.06	-8.18	22.5	0.15	3.7	-	this study
PNG-78	a	NMMP-2020-BH-034	Bahin	BH	Brontotheriidae	M	enamel	-12.4	-14.1	-26.5	0.05	-6.5	24.2	0.04	3.4	15.0	this study

PNG-78	b	NMMP-2020-BH-034	Bahin	BH	Brontotheriidae	M	enamel	-12.2	-14.1	-26.3	0.02	-7.1	23.6	0.13	3.6	11.5	this study
PNG-78	c	NMMP-2020-BH-034	Bahin	BH	Brontotheriidae	M	enamel	-12.3	-14.1	-26.4	0.07	-7.4	23.3	0.13	4.0	8.5	this study
PNG-78	d	NMMP-2020-BH-034	Bahin	BH	Brontotheriidae	M	enamel	-12.1	-14.1	-26.2	0.03	-8.1	22.5	0.09	3.9	6.0	this study
PNG-78	e	NMMP-2020-BH-034	Bahin	BH	Brontotheriidae	M	enamel	-11.9	-14.1	-26.0	0.06	-7.2	23.4	0.04	4.1	3.0	this study
PNG-78	average	NMMP-2020-BH-034	Bahin	BH	Brontotheriidae	M	enamel	-12.2	-14.1	-26.3	0.05	-7.3	23.4	0.09	3.8	-	this study
PNG-80	bulk	NMMP-2020-PGN1-048	Bahin	Pangan 1	Anthracotheriidae	M	enamel	-11.7	-12.5	-24.2	0.02	-4.6	26.2	0.11	4.7	-	this study
PNG-81	bulk	NMMP-2020-PGN1-051	Bahin	Pangan 1	Amynodontidae	l m	enamel	-11.8	-13.1	-24.9	0.01	-6.0	24.7	0.22	3.9	-	this study
PNG-83	bulk	NMMP-2020-Ganle-065	Bahin	Ganle	*Anthracotherium*	r M^1/M^2	enamel	-9.7	-13.1	-22.8	0.05	-7.0	23.6	0.15	3.5	-	this study
PNG-84	bulk	NMMP-2020-Ganle-066	Bahin	Ganle	*Anthracotherium*	l M^1/M^2	enamel	-10.1	-13.1	-23.2	0.03	-6.9	23.8	0.04	5.7	-	this study
PNG-85	bulk	NMMP-2020-Ganle-064	Bahin	Ganle	*Anthracotherium pangan*	l M3	enamel	-10.2	-13.3	-23.5	0.02	-7.4	23.2	0.08	3.1	-	this study
PNG-86	bulk	NMMP-2020-PK1-056	Bahin	PK 1	*Anthracokeryx tenuis*	l c	enamel	-12.5	-12.1	-24.6	0.10	-7.7	22.9	0.06	6.9	-	this study
PNG-87	bulk	NMMP-2020-Ganle-072	Bahin	Ganle	*Anthracotherium crassum*	l m_3	enamel	-9.8	-13.0	-22.8	0.05	-7.9	22.8	0.15	3.7	-	this study
PNG-88	bulk	NMMP-2020-Ganle-073	Bahin	Ganle	*Anthracotherium pangan*	l M^3	enamel	-9.5	-13.3	-22.8	0.02	-8.0	22.7	0.05	3.7	-	this study
PNG-89	bulk	NMMP-2020-Ganle-069	Bahin	Ganle	*Anthracotherium pangan*	l M^3	enamel	-11.4	-13.3	-24.7	0.04	-10.0	20.6	0.09	3.7	-	this study
PNG-90	bulk	NMMP-2020-Changan-022	Bahin	Changan	Amynodontidae	l M^3	enamel	-12.4	-13.1	-25.5	0.02	-6.8	23.9	0.08	4.1	-	this study
PNG-91	bulk	NMMP-2020-NPLWest-085	Bahin	Nyaung Pinle	Anthracotheriidae	l m	enamel	-10.8	-12.5	-23.3	0.04	-5.4	25.4	0.07	6.8	-	this study
PNG-92	bulk	private collection	Bahin	Tha Duat 3	Amynodontidae	m_3	enamel	-11.2	-13.1	-24.3	0.06	-9.8	20.8	0.15	3.0	-	this study
PNG-93	bulk	private collection	Bahin	Tha Duat 3	Amynodontidae	l m_2	enamel	-10.8	-13.1	-23.9	0.03	-10.0	20.6	0.14	2.9	-	this study
PNG-94	bulk	private collection	Bahin	Tha Duat 3	Brontotheriidae	r m_1/m_2	enamel	-11.3	-14.1	-25.4	0.01	-8.4	22.3	0.12	3.2	-	this study
PNG-95	bulk	private collection	Bahin	Tha Duat 3	Brontotheriidae	r M	enamel	-11.1	-14.1	-25.2	0.06	-8.3	22.4	0.11	2.9	-	this study
PNG-96	bulk	private collection	Bahin	Tha Duat 3	Brontotheriidae	r p_4	enamel	-11.6	-14.1	-25.7	0.04	-9.3	21.3	0.10	3.4	-	this study
PNG-97	bulk	private collection	Bahin	Tha Duat 3	Brontotheriidae	l p	enamel	-11.5	-14.1	-25.6	0.06	-8.2	22.5	0.12	3.3	-	this study
PNG-98	bulk	private collection	Bahin	Tha Duat 3	Brontotheriidae	r M^1/M^2	enamel	-11.4	-14.1	-25.5	0.12	-8.0	22.7	0.12	3.3	-	this study
PNG-99	bulk	private collection	Bahin	Tha Duat 3	Amynodontidae	l M^1	enamel	-13.3	-13.1	-26.4	0.03	-9.9	20.7	0.07	3.8	-	this study
PND-M1	a	-	-	-	*Bos*	m/M	enamel	-1.3	-14	-15.3	0.07	-3.0	27.8	0.12	4.9	3.0	(Habinger et al. 2022)
PND-M1	b	-	-	-	*Bos*	m/M	enamel	-1.2	-14	-15.2	0.07	-1.3	29.5	0.16	4.0	6.0	(Habinger et al. 2022)
PND-M1	c	-	-	-	*Bos*	m/M	enamel	-2.0	-14	-16.0	0.08	-0.8	30.1	0.14	4.5	9.0	(Habinger et al. 2022)
PND-M1	d	-	-	-	*Bos*	m/M	enamel	-2.6	-14	-16.6	0.11	-0.4	30.5	0.10	3.4	11.0	(Habinger et al. 2022)
PND-M1	e	-	-	-	*Bos*	m/M	enamel	-2.9	-14	-16.9	0.07	-0.7	30.1	0.14	3.7	13.0	(Habinger et al. 2022)
PND-M1	f	-	-	-	*Bos*	m/M	enamel	-2.5	-14	-16.5	0.05	-1.0	29.9	0.05	4.3	16.0	(Habinger et al. 2022)
PND-M1	g	-	-	-	*Bos*	m/M	enamel	-2.5	-14	-16.5	0.09	-1.3	29.5	0.12	3.8	18.0	(Habinger et al. 2022)
PND-M1	h	-	-	-	*Bos*	m/M	enamel	-2.4	-14	-16.4	0.05	-1.9	29.0	0.12	3.5	21.0	(Habinger et al. 2022)
PND-M1	i	-	-	-	*Bos*	m/M	enamel	-2.2	-14	-16.2	0.06	-2.4	28.4	0.15	3.4	24.0	(Habinger et al. 2022)
PND-M1	j	-	-	-	*Bos*	m/M	enamel	-2.7	-14	-16.7	0.05	-2.6	28.2	0.17	4.1	26.0	(Habinger et al. 2022)
PND-M1	k	-	-	-	*Bos*	m/M	enamel	-2.1	-14	-16.1	0.02	-2.9	27.9	0.09	3.2	28.0	(Habinger et al. 2022)
PND-M1	l	-	-	-	*Bos*	m/M	enamel	-2.1	-14	-16.1	0.06	-3.7	27.1	0.08	3.7	31.0	(Habinger et al. 2022)
PND-M1	m	-	-	-	*Bos*	m/M	enamel	-1.6	-14	-15.6	0.10	-3.7	27.1	0.04	3.4	34.0	(Habinger et al. 2022)
PND-M1	n	-	-	-	*Bos*	m/M	enamel	-1.5	-14	-15.5	0.08	-5.7	25.0	0.13	3.0	36.0	(Habinger et al. 2022)
PND-M1	o	-	-	-	*Bos*	m/M	enamel	-1.5	-14	-15.5	0.05	-3.9	26.9	0.12	3.4	39.0	(Habinger et al. 2022)
PND-M1	p	-	-	-	*Bos*	m/M	enamel	-1.5	-14	-15.5	0.05	-1.4	29.5	0.08	3.0	41.0	(Habinger et al. 2022)
PND-M1	q	-	-	-	*Bos*	m/M	enamel	-1.5	-14	-15.5	0.06	-2.0	28.8	0.08	3.3	44.0	(Habinger et al. 2022)
PND-M1	r	-	-	-	*Bos*	m/M	enamel	-1.4	-14	-15.4	0.05	-1.7	29.2	0.03	3.8	48.0	(Habinger et al. 2022)
PND-M1	s	-	-	-	*Bos*	m/M	enamel	-2.2	-14	-16.2	0.06	-2.1	28.8	0.06	3.0	52.0	(Habinger et al. 2022)

Publication 3

Characterisation of a circa 1890 orangutan population's diet using dental microwear texture analysis: A reference database for intra- and interspecific variation of dental microwear of extant hominids

Authors: Sophie G. Habinger, Gildas Merceron, Anneke van Heteren, Valeria Rojas Cuyutupa, Hervé Bocherens, Olivier Chavasseau

Journal: submission planned to International Journal of Primatology

Initial submission: 12.05.2023

Accepted: no

DOI: -

Publication date: -

Journal volume: -

Article number: -

Characterisation of a circa 1890 orangutan population's diet using dental microwear texture analysis

A reference database for intra- and interspecific variation of dental microwear of extant hominids

Sophie G. Habinger[1, 2*], Gildas Merceron[1], Anneke H. van Heteren[3, 4, 5], Valeria Rojas Cuyutupa[3], Hervé Bocherens[2, 6], Olivier Chavasseau[1]

[1]Laboratoire PALEVOPRIM, UMR CNRS 7262, Université de Poitiers, Poitiers, France

[2]Department of Geosciences, Eberhard Karls Universität Tübingen, Tübingen, Germany

[3]Zoologische Staatssammlung München, Staatliche Naturkundliche Sammlungen Bayerns München, Germany

[4]GeoBio-Center, Ludwig-Maximilians-Universität München, München, Germany

[5]Department Biologie II, Ludwig-Maximilians-Universität München, Planegg-Martinsried, Germany

[6]Senckenberg Centre for Human Evolution and Palaeoenvironment at the University of Tübingen, Tübingen, Germany

Abstract

Orangutans (*Pongo*) are the extant apes with the most extensive fossil record. This makes them an important taxonomic group for enhancing our understanding of hominid evolution and the environment and ecology of Southeast Asia from the Miocene to today. In the last decades, several studies using stable isotope analysis, dental topography or dental microwear analysis have been conducted to reconstruct palaeoecology and -diet of some of the fossil pongines known from this region. However, palaeodietary reconstructions based on the dental microwear of fossil pongines lacked a well-defined and extensive reference data set of extant *Pongo*. Here, we present the results of the dental microwear texture analysis, a 3D quantitative approach to assess the food properties and thus diet of a given individual, on the orangutans originated from the island of Borneo, collected by Emil Selenka, and curated at the Zoologische Staatssammlung München, Germany. Our study will provide insights into dietary variation in extant *Pongo* and will be an important reference dataset in future palaeodietary reconstruction. We examine intraspecific variation in diet in a late 19th century orangutan population (from 1892 to 1894) regarding sex, age, and localities and found no significant differences. This indicates a homogenous diet across all individuals of the population regarding

physical properties of the dietary resources consumed. Our data is not consistent with the hypothesis that different dietary ecologies caused the higher incidence of dental pathologies in female orangutans. We propose non-dietary reasons, such as the increased susceptibility for periodontal infections during pregnancies as possible explanations.

Introduction

Forest habitats all over the world are impacted by human activities. Deforestation has led to fragmentation or complete destruction of many habitats such as tropical rain forests. As these habitats have high species diversity, they are of great importance for conservation efforts (Lindenmayer, Franklin, & Fischer, 2006; Perfecto & Vandermeer, 2008, and references therein). The islands of the Sunda Shelf in Southeast Asia with and their dipterocarp rainforest are no exception to this continued process of habitat transformation (Cannon, Morley, & Bush, 2009; Kettle, Maycock, & Burslem, 2012; Turner, 1996). This endangers the subsistence of many animals living there, for example the orangutans (*Pongo* spp.). Their population sizes have been reduced by more than 50 % during the last 50 years (Meijaard et al., 2011). Due to their large home ranges and high caloric needs, apes such as orangutans are more threatened by habitat destruction than other primates (Campbell-Smith, Campbell-Smith, Singleton, & Linkie, 2011).

Orangutans are the largest arboreal mammals in the world. They are also a keystone species (Paine, 1995) in the rainforests of Southeast Asia, i.e. they have, given their abundance, a disproportionally high impact on the associated fauna and the ecology of their habitat. Orangutans also act as important fruit dispersers that influence the regeneration and distribution of plants, and they are therefore essential for maintaining natural forest dynamics (McConkey, 2018; Tarszisz, Tomlinson, Harrison, Morrogh-Bernard, & Munn, 2018). A recent study suggests that Ponginae were important fruit dispersers since the Late Miocene (around 9 Ma) (Spengler et al., 2023). Today, the orangutan range is restricted to the tropical forests of Sumatra and Borneo (Spehar et al., 2018), but in the Miocene various pongine taxa (*Gigantopithecus*, *Khoratpithecus*, *Sivapithecus, Indopithecus* and *Ankarapithecus*) inhabited large areas from Turkey to the Siwaliks of India and Pakistan to southern China. The first record of the genus *Pongo* from the islands of the Sunda Shelf dates to the Middle Pleistocene (Hooijer, 1948).

The fossil record of orangutans is the most extensive of all extant apes, as no chimps or gorillas have been found in sediments older than Holocene times. Tracking the ecology of the species of *Pongo* through time is therefore a good model to track human impact on ape populations and more generally on tropical forested habitats from the very first contact between orangutans and modern humans at least 50,000 years ago (Piper & Rabett, 2009) until present time. One possibility to characterize human

pressure on ape habitats and populations is to use diet as a proxy. Dietary proxies useable on both extinct and extant species includes bone and dental stable isotope geochemistry (e.g. Habinger et al., 2022; Schoeninger, Moore, & Sept, 1999; Sponheimer et al., 2006), dental topographic analysis (Berthaume, Lazzari, & Guy, 2020; Merceron, Blondel, Bonis, Koufos, & Viriot, 2005 and citations therein), and dental microwear analysis (Merceron, Taylor, Scott, Chaimanee, & Jaeger, 2006; Scott, Teaford, & Ungar, 2012).

Orangutans are described as very opportunistic feeders that use a large variety of food sources (e.g. Galdikas, 1978; MacKinnon, 1974), but fruits represent more than 50 % of the diet (Galdikas, 1988). However, the composition of their diet varies markedly from month to month. Fruit represent up to 90 % in July and August but about 20 % from February to May (MacKinnon, 1974). Most of these fruits are figs, which are multi-seeded but soft. Leaves and insects (and about 30 % of lianas and barks when fruits are not available anymore) complete the diet (Galdikas, 1988; Kanamori, Kuze, Bernard, Malim, & Kohshima, 2010; MacKinnon, 1974; Rodman, 1977, 1988; Ungar, 1995; Vogel et al., 2015; Vogel et al., 2017). This affects the way in which we can interpret our results, as dental microwear provides direct evidence of an animal's diet during the last days to weeks of an animal's life. This is known as the last supper effect (Grine, 1986). The turnover rate of dental microwear signal depends on food mechanical properties with harder/stiffer foods leading to a more rapid turnover than softer/ductile food items (Teaford & Oyen, 1989; Teaford, Ross, Ungar, Vinyard, & Laird, 2021; Teaford, Ungar, Taylor, Ross, & Vinyard, 2017; Winkler et al., 2020). Dental microwear texture analysis allows to track seasonal variations in diet (Berlioz, Azorit, Blondel, Tellado Ruiz, & Merceron, 2017; Merceron, Escarguel, Angibault, & Verheyden-Tixier, 2010; Percher et al., 2018; Teaford & Robinson, 1989).

Part of the dental microwear variation we could observe in the Selenka *Pongo* collection might be caused by such kind of seasonal differences in diet or by variations in local resources availability. Unfortunately, we do not have precise information about the time of the year when the individuals were killed to control for the effect of season of death on the DMTA patterns. Some historical records however suggest that Selenka and his team were not actively hunting when the rainy season reached its acme. During that time period it would have been difficult, if not impossible to move in such flooded habitats. A more detailed discussion of our reconstruction of the timing of Selenka's expedition can be found in the Materials and Methods chapter.

Another factor that could influence the dental microwear variation in the Selenka *Pongo* is sex. Galdikas (1978) found ecological differences between male and female orangutans that also impact the composition of their respective diets. Adult males travel farther per day, resulting in a larger home range covered in the course of their lives in conjunction with an increased time spent on the ground.

This behaviour results in a heightened incorporation of termites and other terrestrial food sources instead of bark or young leaves found higher up in the canopy.

Grinding and shearing are two different phases of the mastication process that result in wear facets on different areas of each tooth (Krueger, Scott, Kay, & Ungar, 2008; Maier & Schneck, 1981). Thus, a comparison of these two facet types allows for a more comprehensive reconstruction of an animal's diet. It is worth noting that Merceron et al. (2005) did not find significant differences in dental microwear pattern on both shearing and crushing facets between male and female *Pongo*, neither among females depending on gross tooth wear. In the following section, we want to give a brief overview over studies using either 2D dental microwear or 3D dental microwear texture analysis (DMTA) on orangutans and their fossil relatives.

Earliest work on dental microwear analysis on extant orangutans and one of its fossil relatives (*Sivapithecus*) was performed as part of a comparative study on different primate taxa by Teaford and Walker (1984). This work, as well as most other studies on dental microwear, focused on molars or sometimes also including premolars. Ungar (1994) on the other hand showed that incisor microwear of Sumatran anthropoid primates (including *P. abelii*) also has the potential to allow inferences on diet and tooth use. Using a semi-automatic method to quantify microwear features Merceron et al. (2005) worked on the paleodietary reconstruction of *Ouranopithecus macedoniensis*. As part of their reference database they also analysed *P. pygmaeus* (n = 56), and briefly discussed intrapopulation dietary variation on 42 specimen from the Skalau population of the Selenka collection, which is also part of the sample of this study.

The first set of dental microwear textures for orangutans (*P. pygmaeus*, n = 7) was published by Merceron et al. (2006) as part of the reference data set used to reconstruct the paleodiet of *Khoratpithecus*, the sister-group of extant *Pongo* (Chaimanee et al., 2022; Chaimanee, Lazzari, Chaivanich, & Jaeger, 2019; Pugh, 2022). With the dental microwear texture and dental topography data, they showed that *Khoratpithecus* was predominantly frugivorous without the addition of hard or tough food items (Merceron et al., 2006). More orangutan individuals were analysed as part of a study attempting to establish a comparative baseline for DMTA across 21 anthropoid primate species (*P. pygmaeus*, n = 15)(Scott et al., 2012). These data were then used recently in an investigation of the diet of Pleistocene *Pongo* from Sumatra (Louys et al., 2021). For the reference data set 12 additional modern *P. pygmaeus* specimen were analysed. They found that Pleistocene *Pongo* from Sumatra consumed less tough food (e.g. lianas, bark, and mature leaves) than the modern individuals from Borneo. This difference corresponds to observations on dietary differences between *P. abelii* and *P. pygmaeus* today (Louys et al., 2021).

All of these DMTA studies on orangutans and their fossil relatives had relatively small sample sizes in the modern reference samples they used. They also solely focused on the facets associated with grinding or phase II of the masticatory process (f9, located on the inner side of the hypoconid on lower molars) and did not include data on the shearing facets resulting from phase I (e.g. f3, f6, located on the mesiobuccal side of the hypoconid and on the inner side of the entoconid/hypoconulid, respectively) (Kay & Hiiemae, 1974; Maier & Schneck, 1981). Therefore, given the importance of *Pongo* and its fossil record, there is a need for an extensive reference data set for both ecological studies and paleodietary reconstructions.

Research Questions

In our study, we want to characterize the diet of a wild orangutan population (*Pongo pygmaeus*) hunted in Borneo from 1892 to 1894 and assess the dietary variation within this population. The majority of the sampled data set of 94 individuals is part of the Selenka collection (*P. pygmaeus*, n = 89). Five *P. abelii* specimen from different collections of the Zoologischen Staatssammlung München (ZSM) were also analysed. Although there were definite human-orangutan interactions as early as around 50 ka documented at Niah Cave, Borneo (Piper & Rabett, 2009), and possibly even earlier due to their co-occurrence at Lida Ajer on Sumatra (Westaway et al., 2017), humans did not have a significant impact on orangutan distribution before 10 ka (Spehar et al., 2018). Nevertheless, the end of the 19th century is a time period when anthropogenic destruction and fragmentation of orangutan habitat was less prevalent than it is now. Understanding changes in orangutan diet and its variability at different time periods and the different stages of anthropogenic impact on their habitat is essential. It can inform both conservation efforts for modern orangutans and palaeoecological reconstructions of fossil pongines and early hominids. Based on this general objective we formulated several specific research questions that we will discuss with our data.

Firstly, we want to establish if the dental microwear of some of our specimens could have been influenced by a mast fruiting event. All the localities in Borneo are in West Kalimantan, north of the Kapuas River. In addition, we have a small set of individuals from the Sumatra Island. For the interpretation of the dietary ecology in the Selenka orangutans and the use of the data as reference data set, it is vital to assess the possibility of the dietary variation being influenced by a mast fruiting period, as the proportion of fruit in their diet is heavily influenced by these circumstances. Should the Selenka *Pongo* be sampled from a mast fruiting period, we expect their dental microwear textures to differ drastically from those of the five *P. abelii* specimens, as the effects of mast fruiting are less pronounced in the Sumatran forests (Delgado & van Schaik, 2000). As our sample from Sumatra is very small, we will also use historical precipitation records and indices modelling the ENSO cycle (El Niño Southern Oscillation), which is heavily linked to mast fruiting (Williamson & Ickes, 2002), to assess if

mast fruiting events have occurred in the years the Selenka *Pongo* were collected. Based on these findings we will discuss intraspecific dietary variability and test if there are any significant dietary differences between sexes, age groups or the different localities.

Only few studies discuss the possible impact of dietary factors on the abundance of dental pathologies and the connection between them in nonhuman primates (Crovella & Ardito, 1994; Guatelli-Steinberg, Ferrell, & Spence, 2012; Lovell, 1991; Phillips-Conroy, Hildebolt, Altmann, Jolly, & Muruthi, 1993; Stoner, 1995; Strum, 2001). However, there is a general trend towards an increase in pathologies with individual age, which is not surprising. In general, a lot of variation of the abundance of dental pathologies is observed on both the inter- and intrapopulation level. To some extent, the intrapopulation variation of dental pathologies has been associated with the sex of the individuals. However, this pattern is not universal across different primate taxa. For instance, in baboons, old males often display severe alveolar destruction linked to decayed or damaged teeth, while this is rare in females (Bramblett, 1967), while in contrast, in gorillas (*Gorilla gorilla gorilla*), there is no significant difference in the occurrence of dental pathologies between the sexes (Kakehashi, Baer, & White, 1963).

In the case of *Pongo*, a previous study on dental pathologies showed that old adult females have more dental pathologies than males of the same age category (Stoner, 1995). This difference is statistically significant for local infections and horizontal bone loss. However, the sample size for both sexes was not well balanced with 62 old adult females but only 32 old adult males. Based on these results, Stoner formulated the hypothesis that different dietary choices and strategies between the sexes were the cause for the different dental pathology patterns, as diet is an important cause for these types of pathologies. For this study, she also worked with the orangutans from the Selenka collection (Stoner, 1995). Here, we want to test this hypothesis with dental microwear patterns, which are a direct indicator for an animal's diet. As dental microwear reflects the diet in the weeks before an animal's death while dental pathologies develop during much longer time period, an absence of differentiation in microwear pattern in adult individuals would not negate Stoners hypothesis. Therefore, we have also considered different age categories. If a dietary sex difference is already present in the younger age categories, this would be evidence for Stoner's hypothesis, even more so when females show indications for a less varied and more frugivorous diet. However, should it be impossible to separate juvenile and subadult orangutans into male and female based on the dental microwear, this would indicate that dietary differences between the sexes in the older individuals are rather caused by the different distribution of dental pathologies and not vice-versa, given that there is a difference in adult dental microwear textures. Merceron et al. (2010) showed that it is possible with DMTA to detect inter-individual and intra-population differences in diet. This possibility has again been demonstrated by

197 Percher et al. (2018) for primates and Louail et al. (2021) for pigs. However, we need to acknowledge
198 the difference in time period represented by the dental microwear texture data and the time it takes
199 to develop certain dental pathologies discussed by Stoner (1995)

200 Materials and Methods

201 The Selenka *Pongo* collection and the origin of the specimens

202 Before we introduce the data set used for the dietary characterisation of the Bornean orangutan
203 populations, we want to give a brief summary of the expedition of Emil Selenka during which they were
204 collected. Emil Selenka (27 February 1842 – 21 January 1902) was a German zoologist who started his
205 scientific career with the study of marine invertebrates before switching his focus to embryology.
206 During his time as professor at the University of Erlangen, he conducted two expeditions to South and
207 Southeast Asia together with his wife Margarethe Lenore Selenka, who also studied Paleontology,
208 Zoology and Anthropology. The first one in 1889 led them to Java and Borneo, where he collected
209 material on anthropoid primates. The orangutans that are today part of the Selenka collection at the
210 ZSM were collected during the second expedition. After his arrival in Singapore mid-November 1892,
211 he started an eight months long hunting expedition to Borneo and Sumatra during which he collected
212 orangutan, gibbon and siamang specimens (PAW(1812-1945/II-VII-113[1]); Selenka & Selenka, 1905; The
213 Singapore Free Press and Mercantile Advertiser, 19.11.1892). In late 1893, most of the material was
214 lost in shipwreck during transportation on the Kapuas River in West Kalimantan (Borneo) (Selenka,
215 1896). In February 1894, Selenka and his wife organized a second ten month hunting expedition that
216 was carried out in his absence, as health problems and the nearing end of his leave from university
217 forced him to return to Europe (UBH NL 238 : Aa 6,1[2]; Selenka, 1896). Margarete Lenore Selenka led
218 this second hunting expedition (Hubrecht, 1902-1903; Selenka & Selenka, 1905). Hence, although
219 Selenkas expedition took place from 1892 to 1894, most orangutan skulls in the collection of the
220 Zoologischen Staatssammlung München were likely collected in a ten-month period in 1894. His
221 hunters were active in the area on the right bank of the Kapuas River. Here they also traded and
222 purchased orangutan skulls from the local Dajak and Malay. The Selenka collection then counted
223 around 300 orangutan skulls across all age groups from the West Kalimantan province, on Borneo
224 (Selenka, 1896, 1898). On the map (Fig. 1), the areas where the individuals were hunted are marked.

[1] Documents and correspondence concerning research funding of his expedition by the Königlich Preußischen Akademie der Wissenschaften housed in the Archive of the Berlin-Brandenburgischen Akademie der Wissenschaften.

[2] Letter from Emil Selenka to his parents written in Medan, Sumatra on February 1st 1894 housed at the University library in Basel.

The habitat north of the Kapuas River is a mixed dipterocarp forest, with peat swamp forests only present in the most southwest parts of the Landak region close to the coast (Phillips, 1998). During another expedition around the same time, a Dutch team around Büttikofer and Jentink only observed the orangutan at altitudes of 700 m (Büttikofer, 1896). Unfortunately, no similar observations are reported from Selenka himself. The range of altitudes of the collection area in (Fig. 2), however, are all very low, usually below 300 m, with the exceptions of Mount Genepai ("Berg Genepai" on the map, which probably corresponds to Gunung Kenepai, 1112 m, 0° 42' 36'' N, 111° 43' 3'' E), Mount Dadap ("Berg Dadap on the map, which probably corresponds to Gunung Tutoop, 805 m, 0° 55' 00'' N, 111° 37' 53'' E), Mount Gedang ("Berg Gedang" in the map, which corresponds to an unnamed peak of 835 m, 0° 54' 87'' N, 111° 27' 13'' E), and Mount Rabor ("Berg Rabor" on the map, which probably corresponds to Gunung Kehuma, 1210 m, 0° 56' 6'' N, 111° 20' 18'' E) (mountains listed here from east to west).

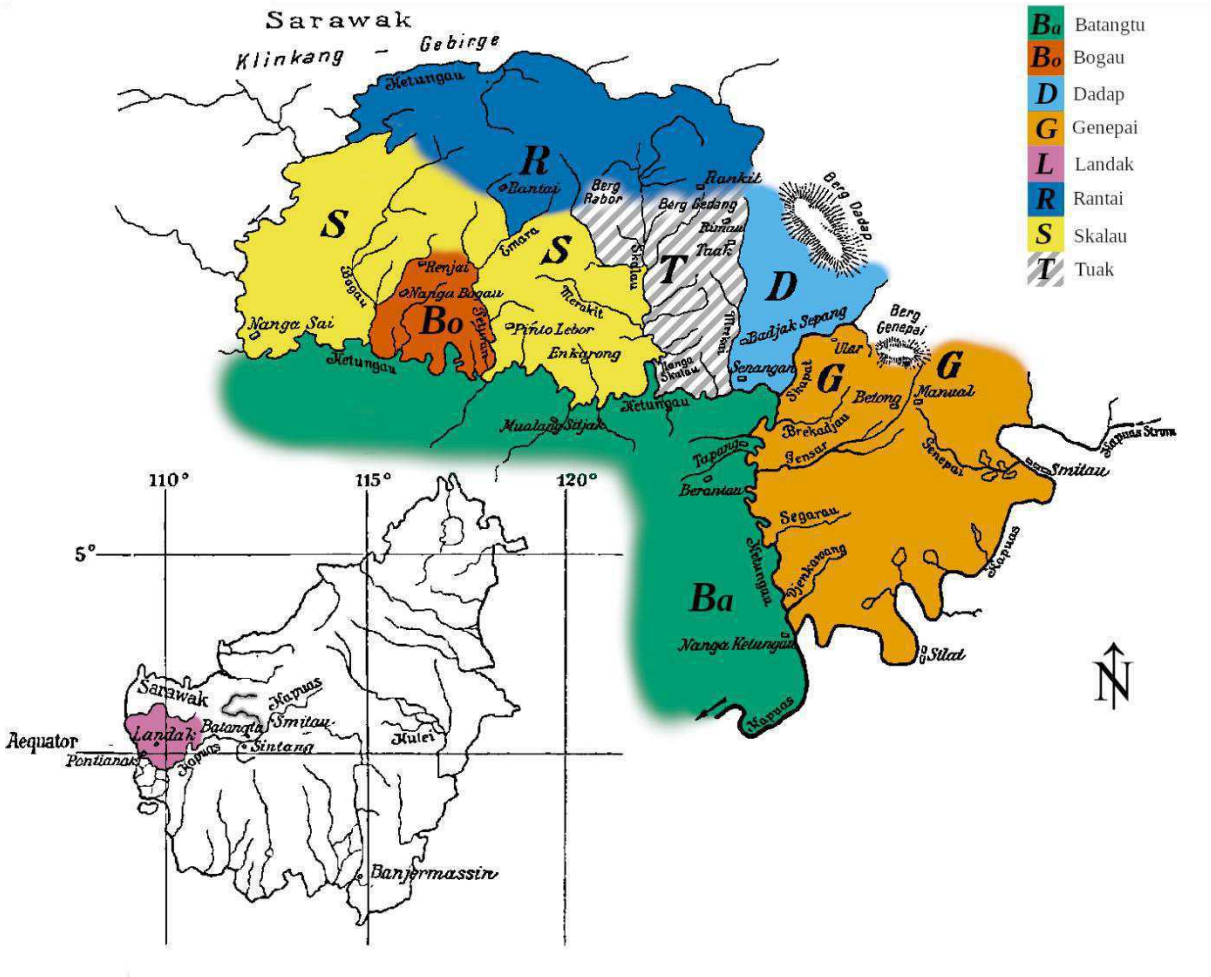

Fig. 1 These two maps were modified from Selenka's first extensive publication on the orangutan material that he obtained during his expedition 1892 – 1894 (Selenka, 1898). The area of the more detailed map (right) can be correlated with the overview showing Landak (left) with the location of the Ketungau river (highlighted in grey) and the city of Smitau, which are

visible in both. He marked the areas from which he collected specimen with letters that he originally correlated with local morphotypes. We use these attributions only for estimates of areas of origin for each specimen. We displayed each area by shading in different colours, the extent of each area being based on the description of distribution of the local morphotypes in Selenka's publication and natural barriers such as mountains and major rivers. The Bogau area is not correlated with a morphotype described by Selenka and therefore was not marked in the original map. Nevertheless, it is used in the original labelling of some of the specimen. We estimated its location based on the location of the village Nanga Bogau. The Klingklang-Gebirge refers to the mountain ranges south of the border to Sarawak (Malaysian Borneo).

We studied dental microwear texture of 89 wild *Pongo pygmaeus* individuals from the Selenka collection. From each specimen we analysed one grinding (f9) and one shearing facet (f6) (Maier & Schneck, 1981). All of the locations in Fig. 1 except for Tuak are represented in this data set. We completed this sample with five adult *Pongo abelii* individuals collected by Schmidt, Schmidt and Adam in 1913 (Table 1). All specimens are housed in the Zoologische Staatssammlung München, Germany (SNSB-ZSM). Both sexes are represented equally in the *P. abelii* sample. In the case of the Selenka sample females are far more numerous than males. The representation of different age groups is also finer grained in the Selenka *Pongo*.

Table 1 Summary of the number of individuals for each age and sex group from which f9 and f6 were analysed.

	female				**male**			**indet**
	juvenile	subadult	adult	senil	juvenile	subadult	adult	adult
Pongo abelii	-	-	2	-	-	-	2	1
Pongo pygmaeus	5	4	45	1	1	6	27	-

Preparation and scanning of moulds

Dental microwear texture analysis is a 3D-approach to characterize the texture created on wear facets of the occlusal surface of teeth during mastication. The method has been proven to reduce inter- and intra-observer errors compared to former approaches based on visual counting, measurements and classifications through stereomicroscopes or computer screen (DeSantis et al., 2013; Galbany et al., 2005; Grine, Ungar, & Teaford, 2002; Mihlbachler, Beatty, Caldera-Siu, Chan, & Lee, 2012). DMTA is therefore more objective and produces more repeatable results(Scott et al., 2006).

To remove any dirt or coatings used for preservation, we cleaned the teeth respectively with ethanol or acetone using cotton swabs before sampling. We took silicone moulds (President Regular Body, ref. 6015 - ISO 4823, medium consistency, polyvinylsiloxane addition-type, Coltène-Whaledent) of the second molars. These teeth are preferred for microwear analysis, as they are usually not too worn, but worn enough to display the wear facets that are necessary for this type of analysis. Although there is no statistically significant difference between the microwear texture of upper and lower second molars

(Merceron et al., 2006; Teaford & Walker, 1984), we chose to sample the lower second molar whenever possible to maximize sample homogeneity.

Specific wear facets were scanned with "TRIDENT", a Leica DCM 8 white-light scanning confocal microscope (Leica Microsystems) with a 100x objective (Numerical aperture = 0.90, Working distance = 0.9 mm) located in the facilities of the PALEVOPRIM laboratory, CNRS and Université de Poitiers, France. We chose facets that represented both phase I shearing facets (f6) and phase II grinding facets (f9) (Maier & Schneck, 1981). Each scan generates a point cloud of 350 x 264 µm. These surfaces were then imported in the LeicaMap v. 8.0 software (Mountain technology, Leica microsystems), and treated following Merceron et al. (2016, see supplementary material). After mirroring the surface along the z-axis, the non-measured points (which do not exceed 2 % of the total number of pixels) were filled with a shape calculated from adjacent points (Laplacian filter). Furthermore, aberrant peaks were removed following an automated workflow including a morphological filter described by Merceron et al. (2006). After this step, the exact 200 x 200 µm grid (1550 × 1550 pixels) that was later used to calculate the textural parameters, was automatically generated in the centre of the levelled surface. In cases where there were dirt particles, resin residue from preservation efforts or other disturbances present, we shifted the grid to remove these artefacts from the frame. When this was impossible, these spots were smoothened (Laplacian filter) along a manually set border (For the use of Laplacian filter and possible alternatives, see Francisco et al. (2020).) Photosimulations and false colour maps of all scans used in this study are attached as Supplementary Material.

Textural parameters

Once the surfaces are saved in .sur file format, a second workflow is applied as a template on each of the surfaces. It includes a subtraction of a second-order least square polynomial surface (PS2) to remove convexity of the dental facets as it allows for a better visualisation of the relief formed by dental microwear (Francisco, Blondel, Brunetière, Ramdarshan, & Merceron, 2018; Francisco, Brunetière, & Merceron, 2018). Then, a combination of spatial filtering (denoising median 5 × 5 filter size and Gaussian 3 × 3 filter size) and levelling (least square plane by subtraction) is run before extracting surface texture parameters.

The Scale Sensitive Fractal Analysis (SSFA) parameters (Scott et al., 2006) were calculated. This analysis is based on a principle from fractal geometry that states that a surface that appears to be smooth on a large scale, can have a rougher more textured profile on a sufficiently fine scale (Scott et al., 2005). Additionally, we also computed Surface Texture Analysis (STA) parameters following well-established procedures (Kaiser, Clauss, & Schulz-Kornas, 2016; Schulz, Calandra, & Kaiser, 2013), as the

combination of both SSFA and ISO 25178-2 textural parameters allow for a comprehensive representation of the surface textural information (Calandra, Schulz, Pinnow, Krohn, & Kaiser, 2012).

Complexity (Area-scale fractal complexity – Asfc) is associated with the hardness of food items, with harder items or a larger proportion of harder items in an organism's diet leading to higher Asfc values. Overlapping pits and scratches of varying sizes and depths characterize these types of highly complex surfaces. Anisotropy (exact proportion Length-scale anisotropy of relief – epLsar) is an indication of food toughness and increasing values with structures on the relief that share a similar orientation such as parallel striations (Merceron et al., 2006). The heterogeneity of the complexity (Heterogeneity of the Area scale fractal complexity) describes variations of the complexity across a surface. The parameter is calculated on the surface subdivided into a matrix of 3 x3 (HAsfc9) or 9 x 9 (HAsfc81) sub-surfaces.

For STA we focused on height (Sq, Ssk, Sku, Sp, Sv, Sz, Sa), surface (Sal2_0.5, Str2_0.5), and volume (metf, medf) parameters. All parameters are presented in Table 2. A detailed description of STA parameters is available in Calandra et al. (2012); but see also Kaiser et al. (2016), and Schulz et al. (2013).

Table 2 Description of the SSFA and STA parameters used in this study. STA parameters are indicated based on ISO/FDIS 25178 analysis.

Abbreviation	Parameter type	Description	Unit
Asfc	SSFA	Complexity, area-scale fractal complexity	-
epLSar	SSFA	Anisotropy, exact proportion Length-scale anisotropy of relief	-
HAsfc9	SSFA	Heterogeneity of complexity, surface subdivided into 9 x 9 sub-surfaces	-
HAsfc81	SSFA	Heterogeneity of complexity, surface subdivided into 3 x 3 sub-surfaces	-
Sq	STA	Standard deviation of the height distribution, or root mean square values (RMS) surface roughness	µm
Ssk	STA	Skewness of the height distribution	-
Sku	STA	Kurtosis of the height distribution	-
Sp	STA	Maximum peak height, height between the highest peak and the mean plane	µm
Sv	STA	Maximum pit height, height between the mean plane and the deepest valley	µm
Sz	STA	Maximum height, height between the highest peak and the deepest valley	µm
Sa	STA	Arithmetic mean height or mean surface roughness	µm
Sal2_0.5	STA	Auto-correlation length (s=0.5)	µm
Str2_0.5	STA	Texture aspect ration (s=0.5)	-
metf	STA	Mean depth of furrows	µm
medf	STA	Mean density of furrows	cm/cm^2

Statistical analysis

As the analysis is run on two types of dental facets per individual, the number of variables is high and quite difficult to deal with. To reduce dimensionality of the data and to identify the most contributing parameters, we ran two principal component analysis (PCA). In the first one we included all the *P. pygmaeus* individuals and all parameters described in Table 2. For the second run, only parameters that significantly contributed to PC1 and PC2 were included (Fig. SI 1). This workflow allows to maximize variations along a lower number of components. To check, if the five specimen of *P. abelii* would have an impact on the results of the PCAs, we repeated the workflow with the extended data

set of 94 individuals. The results are reported in the Supplementary Information. We used the FactoMinR package (version 1.34) for the PCA and stats package (version 4.1.3) for other statistical analysis such ANOVAs in R.

For the SSFA parameters we also visualized the variation per sex, sex-age, and locality group for both facets including the five Sumatran specimen. We also report boxplots for SSFA parameters on sexes, sex-age groups and localities on both facets in the Supplementary Information (Fig. SI 7 – SI 9). Data visualisations were created with the ggplot2 package (version 3.3.6) and further edited with GIMP (version 2.10.18).

Results

Here we will report the results of the second PCA, whereas results of the first PCA can be found in the Supplementary Information (Fig. SI 1 and SI 2). PC1 accounts for 39.1 % of the total variance, the second PC for 31.1 % (Fig. 2). There is significant drop with PC3 and PC4 accounting for less than 10 % of the total variance each (Fig SI 3). As all the parameters of crushing (f9) and shearing (f6) facets were combined in the analysis the most contributing variables along PC1 are from the shearing facet and represent height, volume and heterogeneity of complexity. PC2 reflects variability in parameters on the crushing facet representing similar height and volume as well as general surface complexity. To sum up, PC1 and PC2 are positively correlated with roughness on shearing and crushing molar facets, respectively.

Looking at individual distribution, there is no visible differences in DMTA pattern between males and females (Fig. SI 4). Looking at age and sex-age groups, adults had higher variability than the subadults and juveniles (Fig. 2 B and Fig. SI 5). All the localities have very similar DMTA patterns (Fig. 2 C and Fig. SI 6). We confirmed the absence of differences in DMTA pattern based on the PCA results with ANOVAs run on all the texture parameters (after rank-transformation) (Conover & Iman, 1981).

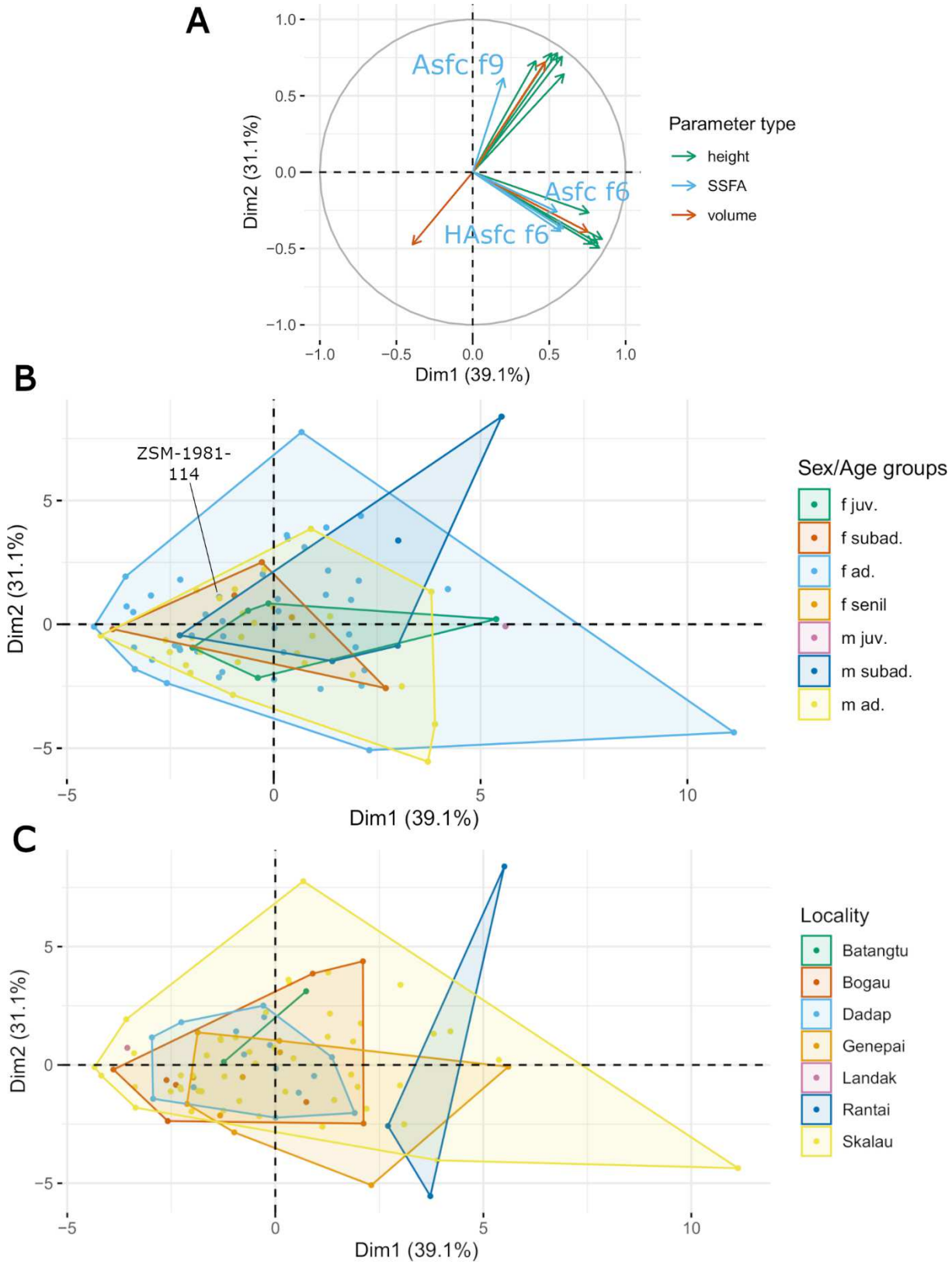

Fig. 2 Correlation circle (A) and distributions of individuals along PC1 and PC2 of the different sex-age groups (B) and localities (C). Specimen ZSM-1981-114 is highlighted as the antagonist of the tooth moulded has a big occlusal carious lesion. This however did not lead to the individual being an outlier. Different colours in the correlation circle correspond to different parameter types, SSFA parameters are labelled to make the distributions more easily interpretable.

There are some interesting patterns if we only focus on the SSFA parameters. We looked at complexity (Asfc), anisotropy (epLsar), and heterogeneity (HAsfc) for each of the three facets. There was no difference in any of these parameters between males and females across all age groups. However, when looking at sex-age and location groups, some tendencies were visible. As there are many sources of variation for which we cannot control such as seasonality or social rank; we will not discuss these in detail. When we looked at the different locations, it appears that the individuals from Sumatra show no different microwear textures than the patterns observed at the localities from Borneo (Fig. 3). The only exception from the otherwise quite homogeneous distributions of Asfc values is in the crushing facet f9 of the Batangtu individuals, which are higher than in all other localities.

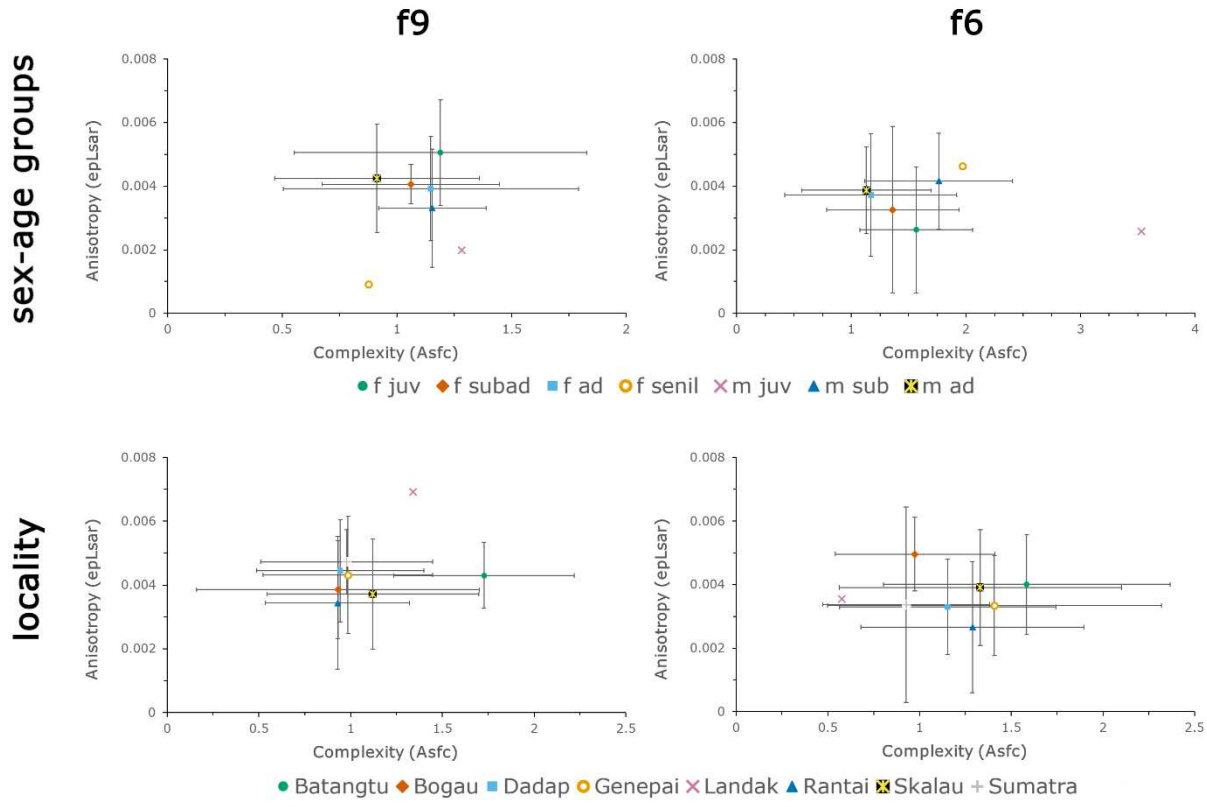

Fig. 3 Plots of mean complexity and anisotropy values ± 1 SD of the individuals separated per facet (f9 = left, f6 = right) and two different grouping factors (sex-age = top, locality = bottom).

It is worth noting that some tendencies are found when looking at complexity through age, particularly when focusing on females. Complexity (Asfc) decreases with age on the shearing facet, whereas it remains relatively stable on the grinding facet (Fig. 4). The same trend was also visible in males. However, it was generally less pronounced except between adult and subadult males in the shearing facet f6. Boxplots on all three SSFA parameters (Asfc, epLsar, and HAsfc81) can be found in the SI (Fig. SI 7 – 9).

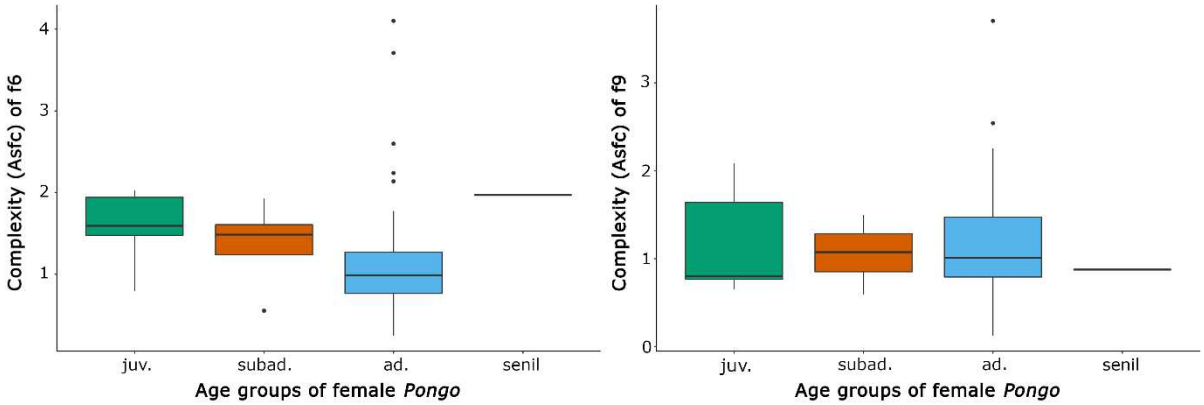

Fig. 4 Boxplots of complexity (Asfc) on the shearing facet (left) and grinding facet (right) the female individuals by age groups.

Discussion

Dietary variation in *Pongo*

Mast fruiting events, which occur supra-annually, have an enormous impact on orangutan dietary ecology. This effect is more pronounced in Borneo than in Sumatra and also affects mixed dipterocarp forests, such as the study area north of the Kapuas River more than peat swamp forests (Delgado & van Schaik, 2000; T. Harrison, 2010). In these years, observational studies have shown that the percentage of fruit in these apes' diet may reach 100 % (Kanamori et al., 2010). But even in periods of fruit scarcity fruit still accounts for at least 12-20 % of the orangutan diet (Kanamori et al., 2010; MacKinnon, 1974). For our data set, it is important to assess the probability that the specimens were collected in a mast fruiting year as this would drastically impact their dental microwear textures. Unfortunately, there are no field notes from the Selenka expedition available where such information could be found. Other reports from zoological expeditions to the area around the same time, also make no mention of mast fruiting (Büttikofer, 1896, 1897; Jentink, 1897). However, historical precipitation records from several meteorological stations have been recently published covering the years from 1879 to 1900 (Fig. 5) (Kajita, 2019). One of the three stations from Borneo is located in Pontianak northeast of the Kapuas River delta. It is the closest one to our study area. Mast fruiting events have been shown to be linked to the ENSO cycle in a way that the fruiting occurs right at the end of an ENSO low (precipitation) El Niño event (Ashton, Givnish, & Appanah, 1988; Williamson & Ickes, 2002; Yasuda et al., 1999). Therefore, the drastic drop in annual amount of precipitation in 1891 is a good indication for a mast fruiting event. No such drop in precipitation is visible for any of the years of the Selenka expedition (1892 – 1894). Another indication comes from the extended MEI (Multivariate ENSO index) established by Wolter and Timlin (2011) based on reconstructed SST (sea surface temperature) (Kaplan et al., 1998; Rayner, 2003; Smith & Reynolds, 2003) and SLP (sea level pressure) (Allan & Ansell, 2006) grids. From 1888 to 1898 this index documents three El Niño events, two strong ones in 1888/1889 and 1896/1897,

and a weak one corresponding to the drop in precipitation in 1891 visible in the precipitation records (Fig. 5) (Wolter & Timlin, 2011). A comparison of dental microwear texture of the Bornean Selenka orangutans with five specimens from Sumatra, where masting events have a significantly less severe effect on orangutan diet (Delgado & van Schaik, 2000; Knott, 1998; Wich, Utami-Atmoko, Mitra Setia, Djoyosudharmo, & Geurts, 2006), in our data set showed no significant differences. This is consistent with the historical precipitation data (Kajita 2019) and further strengthens the interpretation that the no mast fruiting occurred during the time of Selenka's expedition.

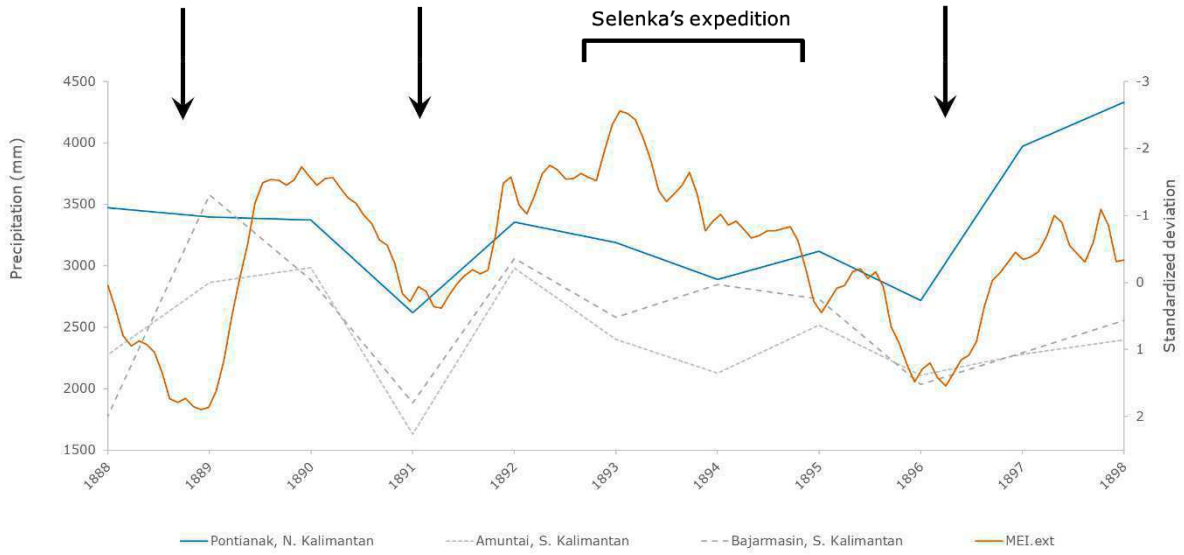

Fig. 5 Annual precipitation data recorded at Pontianak and originally published in the Regenwaarnemingen in the Nederlandsch-Indie by the Batavia Landsdrukkerij (Kajita, 2019). The red line indicates the ENSO index MEI.ext represented by standardized departure. Arrows mark El Niño events (values >|2| strong ENSO events (ENSO high precipitation/La Niña = negative values, ENSO low precipitation/El Niño = positive values) (Wolter & Timlin, 2011). MEI.ext data from https://psl.noaa.gov/enso/mei.ext/ (9.3.2023).

Unlike Percher et al. (2018) who found variation of Asfc, epLsar, and HAsfc reflecting seasonal differences in mandrill diets as well as separation of the sexes in Asfc, no significant differences could be detected in the Selenka orangutans. The absence of significant differences between sexes and age groups indicates a homogenous diet for the whole population, at least in regard to the physical properties of the food items consumed. The same is true, when we group the individuals by the localities they were found at. Most localities are from a relatively confined area north of the Kapuas River along both sides of the Ketungau River, except for Landak (n = 1), which is farther to the west and much closer to the coast. The fact that Bornean orangutans in particular consume a wide variety of plant taxa might be one factor responsible for this pattern (Russon et al., 2009). If a species focuses its diet on a limited amount of taxa thus representing a limited amount of physical properties, switches or to other resources or deviations from this resource pool should be more visible than when many items with different textures and consistencies are consumed as a baseline.

Does subsistence strategy correlate with pathologies?

Unfortunately, it was not possible to directly correlate all of the individuals with identified pathologies in Stoner's study with the specimen we sampled as her publication only includes summary statistics. Nevertheless, some of the individuals could be identified from mentions in the text and the figures in Stoner's study (Table 3). Only one young adult female could be identified in our data set that had a dental pathology studied by Stoner (1995). We moulded the right lower M_2, which is antagonistic to the tooth displaying a large occlusal cavity. Although an influence of this pathology on the dental microwear texture of this individual could be expected, the specimen did plot centrally in the distribution of individuals in the adult female sex-age group (Fig. 2 B)

Table 3 List of identifiable specimens (mentioned in the text or shown in the figures with their ID) and the dental lesions recorded by Stoner (1995). Only one of them ZSM-1981-114 is part of the data set with the tooth antagonistic to the tooth with an occlusal cavity. Sex and Age estimations are from Stoner.

Museum ID	tooth for DMTA	Sex	Age	pathologies (teeth affected) pathology 1	pathology 2
ZSM-1981-84	-	f	old ad.	bone resorption due to premortem loss of buccal roots (left M^1)	interproximal cavity left P^4
ZSM-1981-92	-	f	old ad.	premortem tooth loss (right I^1, P^3-M^2, left P^4-M^3)	-
ZSM-1981-101	-	f	old ad.	interproximal cavity (right and left I^1)	interproximal cavity (left P^2)
ZSM-1981-114	right M_2	f	young ad.	large occlusal cavity, right (M^2)	-
ZSM-1981-176	-	f	old ad.	occlusal cavity (left M^1)	-
ZSM-1981-181	-	f	old ad.	infa-alveolar osseous defect (right M_1-M_2)	horizontal bone loss on the entire mandible
ZSM-1981-185	-	f	old ad.	lingual periapical osseous defect (left M^1)	-
ZSM-1981-201	-	f	old ad.	horizontal bone loss on entire mandible and maxilla	-
ZSM-1981-223	-	f	old ad.	premortem tooth loss (left lower C)	-
ZSM-1981-238	-	m	old ad.	periapical osseous defects (left upper C, P^3, M^1)	horizontal bone loss on the left maxilla
ZSM-1981-242	-	m	old ad.	interproximal cavity (right and left I^1)	-
ZSM-1981-243	-	f	old ad.	cemental root caries (right P^3-P^4)	cemental root caries (right M_1-M_2)
ZSM-1981-251	-	f	young ad.	periapical abcess (left P^3)	horizontal bone loss on left maxilla and periapical osseous defects (P^4, M^2)
ZSM-1981-999	-	f	old ad.	cavity (right M^2) that continues in lingual roots (right M^1-M^2)	-

As we have discussed in the previous section, the diet of the 19th century Selenka orangutans is very homogenous. There are no statistically significant differences between any of the sexes, sex age groups or localities. This is the case when we are considering the SSFA parameters on their own as well as when we add in the STA parameters like we have done with the PCA.

When only considering some SSFA parameters (complexity, anisotropy, and heterogeneity) there seems to be some differences in DMTA signal between juveniles, subadults, and adults. These trends are more consistently visible and pronounced in females across the different wear facets (Fig. 4). One exception seems to be the shearing facet f6 where the trends are more pronounced in the males in

some instances. These patterns could correspond to differences in dietary ecology across ontology, however they are not significantly different.

Furthermore, these patterns do not correspond to the expectations based on the hypothesis proposed by Stoner (1995) that the higher percentage of sugar rich and soft fruits in female orangutans lead to the higher incidence rates of dental pathologies in them. Such differences in dietary ecology have been also proposed by Galdikas (1978, 1988) and Rodman (1977, 1988). Based on their observations and Stoner's hypothesis, we would expect more complex wear facets in males as they spend more time foraging on resources closer to the ground, whereas females could have facets with higher anisotropy as they incorporate more young leaves and bark into their diet. Additionally, there should be a higher dispersion of complexity scores as well as higher HAsfc values in males, as they tend to incorporate a bigger variety of food sources into their diet, given the larger distances they travel. As there are no such differences in either the adults or the younger individuals, we cannot substantiate the hypothesis that diet caused differences in pathology patterns between sexes.

Pregnancy is an explanation for the higher incidence rate on all types of dental pathologies and especially those that are related to infectious diseases of the periodontal tissue in females than in males that is not related to dietary ecology. During a pregnancy immunological and physiological changes occur in the mother, to prevent rejection of the foetus, leading to a dramatic increase of inflammations of the periodontal tissue (Armitage, 2013). Local infections and horizontal bone loss, the two lesion types in which differences between sexes were significant (Stoner, 1995), with higher incidence rates in females than in males are associated with them (Lovell, 1991).

Another possible explanation is survivorship bias, which favours the survival of female orangutans with dental pathologies in comparison to males suffering from the same conditions as given the lower energetic needs due to lower body mass. Although the difference in energetic needs is less pronounced between adult females and unflanged males and the former might have even higher caloric requirements when the additional costs of reproduction are considered (M. E. Harrison, Morrogh-Bernard, & Chivers, 2010).

Aggressive behaviour would also be a possible cause for more dental lesions, as cracked or broken teeth are more susceptible for caries formation and thus successive infectious lesions. When using teeth in conflicts the canines and incisors would be more heavily impacted (Lovell, 1991). This does not fit the prevalence of dental pathologies in the posterior teeth of the Selenka orangutan females (Stoner, 1995). General trends toward female apes showing less aggressive conflicts and the mostly solitary ranging behaviour that reduces the change of encounters are additional reasons why trauma is an unlikely cause for the higher incidence of dental lesions in female orangutans (Knott et al., 2008).

Conclusion

We assessed dietary variation in orangutans from 19th century Borneo. Using historical precipitation data, an ENSO index and the small outgroup sample of five *P. abelii* from Sumatra we demonstrated that the Selenka orangutans were not collected during a mast fruiting event. Thus, the dietary variation of this orangutan population represents time periods of neutral fruit abundances. Neither sex, nor age or locality from which an individual was collected had a significant influence on their diet or more precisely the overall physical properties of the food items consumed in the weeks before its death. Although differences dietary ecology between sexes were expected due to results of some observational studies (Galdikas, 1978, 1988; Rodman, 1977, 1988), none were detected in the dental microwear textures of our sample. Our data thus does not confirm the hypothesis that differences in dietary ecologies were the reason for higher incidence rates of dental pathologies, especially local infections and horizontal bone loss (Stoner, 1995), in the Selenka orangutans. We propose the hypothesis that non-dietary differences between the sexes, such as pregnancies and the increased susceptibility to periodontal infections probably are more likely to have caused the increase in dental pathologies in females. In this study we did not only address these hypothesis, but are also providing an extensive and important reference data set for future paleodietary reconstructions of extant hominids and studies focusing on conservational ecology of primates and orangutans especially.

Acknowledgments

This research was funded by the ANR (grant ANR-18-CE92-0029) and DFG (grant BO 3478/7-1). The moulds were taken at the Zoologischen Staatssammlung in München, Germany. Scanning was done at the PALEVOPRIM laboratory at the Université de Poitiers.

References

Allan, R., & Ansell, T. (2006). A New Globally Complete Monthly Historical Gridded Mean Sea Level Pressure Dataset (HadSLP2): 1850–2004. *Journal of Climate*, *19*(22), 5816–5842. https://doi.org/10.1175/JCLI3937.1

Armitage, G. C. (2013). Bi-directional relationship between pregnancy and periodontal disease. *Periodontology 2000*, *61*(1), 160–176. https://doi.org/10.1111/j.1600-0757.2011.00396.x

Ashton, P. S., Givnish, T. J., & Appanah, S. (1988). Staggered Flowering in the Dipterocarpaceae: New Insights Into Floral Induction and the Evolution of Mast Fruiting in the Aseasonal Tropics. *The American Naturalist*, *132*(1), 44–66. https://doi.org/10.1086/284837

Berlioz, E., Azorit, C., Blondel, C., Tellado Ruiz, M. S., & Merceron, G. (2017). Deer in an arid habitat: Dental microwear textures track feeding adaptability. *Hystrix, the Italian Journal of Mammalogy*, *28*(2), 222–230. https://doi.org/10.4404/hystrix-28.2-12048

Berthaume, M. A., Lazzari, V., & Guy, F. (2020). The landscape of tooth shape: Over 20 years of dental topography in primates. *Evolutionary Anthropology: Issues, News, and Reviews*, *29*(5), 245–262. https://doi.org/10.1002/evan.21856

Bramblett, C. A. (1967). Pathology in the Darajani baboon. *American Journal of Physical Anthropology*, *26*(3), 331–340. https://doi.org/10.1002/ajpa.1330260308

Büttikofer, M. J. (1896). Zoologische Skizzen aus der niederländischen Expedition nach Central-Borneo. In P. P. C. Hoek (Ed.), *Compte-rendu des séances du Troisième congrès international de zoologie: Leyden - 16-21 Septembre - 1895* (pp. 212–227). Leyden: E.J. Brill.

Büttikofer, M. J. (1897). Zoological results of the Dutch scientific expedition to Central Borneo: Introduction. *Notes from the Leyden Museum*, *19*, 1–25.

Calandra, I., Schulz, E., Pinnow, M., Krohn, S., & Kaiser, T. M. (2012). Teasing apart the contributions of hard dietary items on 3D dental microtextures in primates. *Journal of Human Evolution*, *63*(1), 85–98. https://doi.org/10.1016/j.jhevol.2012.05.001

Campbell-Smith, G., Campbell-Smith, M., Singleton, I., & Linkie, M. (2011). Raiders of the lost bark: Orangutan foraging strategies in a degraded landscape. *Plos ONE*, *6*(6), e20962. https://doi.org/10.1371/journal.pone.0020962

Cannon, C. H., Morley, R. J., & Bush, A. B. G. (2009). The current refugial rainforests of Sundaland are unrepresentative of their biogeographic past and highly vulnerable to disturbance. *Proceedings of the National Academy of Sciences of the United States of America*, *106*(27), 11188–11193. https://doi.org/10.1073/pnas.0809865106

Chaimanee, Y., Lazzari, V., Chaivanich, K., & Jaeger, J.-J. (2019). First maxilla of a late Miocene hominid from Thailand and the evolution of pongine derived characters. *Journal of Human Evolution*, *134*, 102636. https://doi.org/10.1016/j.jhevol.2019.06.007

Chaimanee, Y., Lazzari, V., Yamee, C., Suraprasit, K., Rugbumrung, M., Chaivanich, K., & Jaeger, J.-J. (2022). New materials of *Khoratpithecus*, a late Miocene hominoid from Nakhon Ratchasima Province, Northeaster Thailand, confirm its pongine affinities. *Palaeontographica Abteilung a*, *323*(4-6), 147–186. https://doi.org/10.1127/pala/2022/0129

Conover, W. J., & Iman, R. L. (1981). Rank Transformations as a Bridge between Parametric and Nonparametric Statistics. *The American Statistician*, *35*(3), 124–129.

Crovella, S., & Ardito, G. (1994). Frequencies of oral pathologies in a sample of 767 non-human primates. *Primates*, *35*(2), 225–230. https://doi.org/10.1007/BF02382058

Delgado, R. A., & van Schaik, C. P. (2000). The behavioral ecology and conservation of the orangutan (*Pongo pygmaeus*): A tale of two islands. *Evolutionary Anthropology: Issues, News, and Reviews*, *9*(5), 201–218.

DeSantis, L. R. G., Scott, J. R., Schubert, B. W., Donohue, S. L., McCray, B. M., van Stolk, C. A., . . . O'Hara, M. C. (2013). Direct comparisons of 2D and 3D dental microwear proxies in extant herbivorous and carnivorous mammals. *Plos ONE*, *8*(8), e71428. https://doi.org/10.1371/journal.pone.0071428

Francisco, A., Blondel, C., Brunetière, N., Ramdarshan, A., & Merceron, G. (2018). Enamel surface topography analysis for diet discrimination. A methodology to enhance and select discriminative parameters. *Surface Topography: Metrology and Properties*, *6*(1), 15002. https://doi.org/10.1088/2051-672X/aa9dd3

Francisco, A., Brunetière, N., & Merceron, G. (2018). Gathering and Analyzing Surface Parameters for Diet Identification Purposes. *Technologies*, *6*(3), 75. https://doi.org/10.3390/technologies6030075

559 Francisco, A., Brunetière, N., & Merceron, G. (2020). Damaged digital surfaces also deserve realistic
560 healing. *Surface Topography: Metrology and Properties*, *8*(3), 35008.
561 https://doi.org/10.1088/2051-672X/aba7a3
562 Galbany, J. [J.], Martínez, L. M., López-Amor, H. M., Espurz, V., Hiraldo, O., Romero, A. [A.], . . . Pérez-
563 Pérez, A. (2005). Error rates in buccal-dental microwear quantification using scanning electron
564 microscopy. *Scanning*, *27*(1), 23–29. https://doi.org/10.1002/sca.4950270105
565 Galdikas, B. M. F. (1978). *Orangutan Adaptation at Tanjung Puting Reserve, Central Borneo* (PhD
566 thesis). University of California, Los Angeles.
567 Galdikas, B. M. F. (1988). Orangutan diet, range, and activity at Tanjung Puting, Central Borneo.
568 *International Journal of Primatology*, *9*(1), 1–35. https://doi.org/10.1007/BF02740195
569 Grine, F. E. (1986). Dental evidence for dietary differences in *Australopithecus* and *Paranthropus*: a
570 quantitative analysis of permanent molar microwear. *Journal of Human Evolution*, *15*(8), 783–822.
571 https://doi.org/10.1016/S0047-2484(86)80010-0
572 Grine, F. E., Ungar, P. S., & Teaford, M. F. (2002). Error rates in dental microwear quantification using
573 scanning electron microscopy. *Scanning*, *24*(3), 144–153. https://doi.org/10.1002/sca.4950240307
574 Guatelli-Steinberg, D., Ferrell, R. J., & Spence, J. (2012). Linear enamel hypoplasia as an indicator of
575 physiological stress in great apes: Reviewing the evidence in light of enamel growth variation.
576 *American Journal of Physical Anthropology*, *148*(2), 191–204. https://doi.org/10.1002/ajpa.21619
577 Habinger, S. G., Chavasseau, O., Jaeger, J.-J., Chaimanee, Y., Soe, A. N., Sein, C., & Bocherens, H.
578 (2022). Evolutionary ecology of Miocene hominoid primates in Southeast Asia. *Scientific Reports*,
579 *12*(1), 11841. https://doi.org/10.1038/s41598-022-15574-z
580 Harrison, M. E., Morrogh-Bernard, H. C., & Chivers, D. J. (2010). Orangutan Energetics and the
581 Influence of Fruit Availability in the Nonmasting Peat-swamp Forest of Sabangau, Indonesian
582 Borneo. *International Journal of Primatology*, *31*(4), 585–607. https://doi.org/10.1007/s10764-
583 010-9415-5
584 Harrison, T. (2010). Apes among the tangled branches of human origins. *Science*, *327*(5965), 532–534.
585 https://doi.org/10.1126/science.1184703
586 Hooijer, D. A. (1948). Prehistoric teeth of man and of the orang-utan from central Sumatra, with notes
587 on the fossil orang-utan from Java and southern China. *Zoologische Mededeelingen*, *29*, 175–301.
588 Hubrecht, A. A. W. (1902-1903). Emil Selenka. In E. Selenka (Ed.), *Menschenaffen (Anthropomorphae):*
589 *Studien über Entwicklung und Schädelbau* (pp. 1–14). Wiesbaden: C.W. Kreidel.
590 Jentink, F. A. (1897). Zoological results of the Dutch scientific expedition to Central Borneo: The
591 mammals. *Notes from the Leyden Museum*, *19*, 26–66.
592 Kaiser, T. M., Clauss, M., & Schulz-Kornas, E. (2016). A set of hypotheses on tribology of mammalian
593 herbivore teeth. *Surface Topography: Metrology and Properties*, *4*(1), 14003.
594 https://doi.org/10.1088/2051-672X/4/1/014003
595 Kajita, R. (2019). Historical precipitation data in Sumatra and Kalimantan from 1879 to 1900, by using
596 Dutch colonial materials. *IOP Conference Series: Earth and Environmental Science*, *361*(1), 12003.
597 https://doi.org/10.1088/1755-1315/361/1/012003
598 Kakehashi, S., Baer, P. N., & White, C. L. (1963). Comparative pathology of periodontal disease.: I.
599 Gorilla. *Oral Surgery, Oral Medicine, Oral Pathology*, *16*(4), 397–406. https://doi.org/10.1016/0030-
600 4220(63)90166-X
601 Kanamori, T., Kuze, N., Bernard, H., Malim, T. P., & Kohshima, S. (2010). Feeding ecology of Bornean
602 orangutans (*Pongo pygmaeus morio*) in Danum Valley, Sabah, Malaysia: A 3-year record including

two mast fruitings. *American Journal of Primatology*, *72*(9), 820–840. https://doi.org/10.1002/ajp.20848

Kaplan, A., Cane, M. A., Kushnir, Y., Clement, A. C., Blumenthal, M. B., & Rajagopalan, B. (1998). Analyses of global sea surface temperature 1856-1991. *Journal of Geophysical Research: Oceans*, *103*(C9), 18567–18589. https://doi.org/10.1029/97JC01736

Kay, R. F., & Hiiemae, K. M. (1974). Jaw movement and tooth use in recent and fossil primates. *American Journal of Physical Anthropology*, *40*(2), 227–256. https://doi.org/10.1002/ajpa.1330400210

Kettle, C. J., Maycock, C. R., & Burslem, D. (2012). New Directions in Dipterocarp Biology and Conservation: A Synthesis. *Biotropica*, *44*(5), 658–660. https://doi.org/10.1111/j.1744-7429.2012.00912.x

Knott, C. D. (1998). Changes in Orangutan Caloric Intake, Energy Balance, and Ketones in Response to Fluctuating Fruit Availability. *International Journal of Primatology*, *19*(6), 1061–1079. https://doi.org/10.1023/A:1020330404983

Knott, C. D., Beaudrot, L., Snaith, T., White, S., Tschauner, H., & Planansky, G. (2008). Female-Female Competition in Bornean Orangutans. *International Journal of Primatology*, *29*, 975–997.

Krueger, K. L., Scott, J. R., Kay, R. F., & Ungar, P. S. (2008). Technical note: Dental microwear textures of "Phase I" and "Phase II" facets. *American Journal of Physical Anthropology*, *137*(4), 485–490. https://doi.org/10.1002/ajpa.20928

Lindenmayer, D. B., Franklin, J. F., & Fischer, J. (2006). General management principles and a checklist of strategies to guide forest biodiversity conservation. *Biological Conservation*, *131*(3), 433–445. https://doi.org/10.1016/j.biocon.2006.02.019

Louail, M., Ferchaud, S., Souron, A., Walker, A. E. C., & Merceron, G. (2021). Dental microwear textures differ in pigs with overall similar diets but fed with different seeds. *Palaeogeography, Palaeoclimatology, Palaeoecology*, *572*, 110415. https://doi.org/10.1016/j.palaeo.2021.110415

Louys, J. [Julien], Zaim, Y., Rizal, Y. [Yan], Aswan, Puspaningrum, M. R., Trihascaryo, A. [Agus], . . . DeSantis, L. R. G. (2021). Sumatran orangutan diets in the Late Pleistocene as inferred from dental microwear texture analysis. *Quaternary International*, *603*, 74–81. https://doi.org/10.1016/j.quaint.2020.08.040

Lovell, N. C. (1991). An evolutionary framework for assessing illness and injury in nonhuman primates. *American Journal of Physical Anthropology*, *34*(S13), 117–155. https://doi.org/10.1002/ajpa.1330340608

MacKinnon, J. (1974). The behaviour and ecology of wild orang-utans (*Pongo pygmaeus*). *Animal Behaviour*, *22*(1), 3–12.

Maier, W., & Schneck, G. (1981). Konstruktionsmorphologische Untersuchungen am Gebiß der hominoiden Primaten. *Zeitschrift Für Morphologie Und Anthropologie*, *72*(2), 127–169. Retrieved from www.jstor.org/stable/25756541

McConkey, K. R. (2018). Seed Dispersal by Primates in Asian Habitats: From Species, to Communities, to Conservation. *International Journal of Primatology*, *39*(3), 466–492. https://doi.org/10.1007/s10764-017-0013-7

Meijaard, E., Buchori, D., Hadiprakarsa, Y., Utami-Atmoko, S. S., Nurcahyo, A., Tjiu, A., . . . Mengersen, K. (2011). Quantifying killing of orangutans and human-orangutan conflict in Kalimantan, Indonesia. *Plos ONE*, *6*(11), e27491. https://doi.org/10.1371/journal.pone.0027491

Merceron, G., Blondel, C., Bonis, L. de, Koufos, G. D., & Viriot, L. (2005). A New Method of Dental Microwear Analysis: Application to Extant Primates and *Ouranopithecus macedoniensis* (Late Miocene of Greece). *Palaios*, *20*, 551–561.

Merceron, G., Escarguel, G., Angibault, J.-M., & Verheyden-Tixier, H. (2010). Can dental microwear textures record inter-individual dietary variations? *Plos ONE*, *5*(3), e9542. https://doi.org/10.1371/journal.pone.0009542

Merceron, G., Novello, A., & Scott, R. S. (2016). Paleoenvironments inferred from phytoliths and Dental Microwear Texture Analyses of meso-herbivores. *Geobios*, *49*(1-2), 135–146. https://doi.org/10.1016/j.geobios.2016.01.004

Merceron, G., Taylor, S., Scott, R., Chaimanee, Y., & Jaeger, J.-J. (2006). Dietary characterization of the hominoid *Khoratpithecus* (Miocene of Thailand): Evidence from dental topographic and microwear texture analyses. *Naturwissenschaften*, *93*(7), 329–333. https://doi.org/10.1007/s00114-006-0107-0

Mihlbachler, M. C., Beatty, B. L., Caldera-Siu, A., Chan, D., & Lee, R. (2012). Error rates and observer bias in dental microwear analysis using light microscopy. *Palaeontologia Electronica*, *15*(1), 1–22. https://doi.org/10.26879/298

Paine, R. T. (1995). A Conversation on Refining the Concept of Keystone Species. *Conservation Biology*, *9*(4), 962–964. Retrieved from http://www.jstor.org/stable/2387008

Percher, A. M., Merceron, G., Nsi Akoue, G., Galbany, J. [Jordi], Romero, A. [Alejandro], & Charpentier, M. J. (2018). Dental microwear textural analysis as an analytical tool to depict individual traits and reconstruct the diet of a primate. *American Journal of Physical Anthropology*, *165*(1), 123–138. https://doi.org/10.1002/ajpa.23337

Perfecto, I., & Vandermeer, J. (2008). Biodiversity conservation in tropical agroecosystems: A new conservation paradigm. *Annals of the New York Academy of Sciences*, *1134*(1), 173–200. https://doi.org/10.1196/annals.1439.011

Phillips, V. D. (1998). Peatswamp ecology and sustainable development in Borneo. *Biodiversity and Conservation*, *7*(5), 651–671. https://doi.org/10.1023/A:1008808519096

Phillips-Conroy, J. E., Hildebolt, C. F., Altmann, J., Jolly, C. J., & Muruthi, P. (1993). Periodontal health in free-ranging baboons of Ethiopia and Kenya. *American Journal of Physical Anthropology*, *90*(3), 359–371. https://doi.org/10.1002/ajpa.1330900310

Piper, P. J., & Rabett, R. J. (2009). Hunting in a tropical rainforest: evidence from the Terminal Pleistocene at Lobang Hangus, Niah Caves, Sarawak. *International Journal of Osteoarchaeology*, *19*(4), 551–565. https://doi.org/10.1002/oa.1046

Pugh, K. D. (2022). Phylogenetic analysis of Middle-Late Miocene apes. *Journal of Human Evolution*, *165*, 1–33. Retrieved from https://doi.org/10.1016/j.jhevol.2021.103140

Rayner, N. A. (2003). Global analyses of sea surface temperature, sea ice, and night marine air temperature since the late nineteenth century. *Journal of Geophysical Research: Oceans*, *108*(D14). https://doi.org/10.1029/2002JD002670

Rodman, P. S. (1977). Feeding behavior of orang-utans of the Kutai Nature Reserve, East Kalimantan. In T. H. Clutton-Brock (Ed.), *Primate Ecology: Studies of feeding and ranging behaviour in lemurs, monkeys and apes* (pp. 383–413). London: Academic Press.

Rodman, P. S. (1988). Diversity and Consistency in Ecology and Behavior. In J. H. Schwartz (Ed.), *Orang-Utan biology* (pp. 31–51). Oxford: Oxford University Press.

Russon, A. E., Wich, S. A., Ancrenaz, M., Kanamori, T., Knott, C. D., Kuze, N., . . . van Schaik, C. P. (2009). Geographic variation in orangutan diets. In S. A. Wich, S. S. Utami-Atmoko, T. Mitra Setia, &

C. P. van Schaik (Eds.), *Orangutans: Geographic variation in behavioral ecology and conservation* (pp. 135–156). Oxford University Press.

Schoeninger, M. J., Moore, J., & Sept, J. M. (1999). Subsistence strategies of two "savanna" chimpanzee populations: The stable isotope evidence. *American Journal of Primatology*, *49*(4), 297–314. https://doi.org/10.1002/(SICI)1098-2345(199912)49:4<297::AID-AJP2>3.0.CO;2-N

Schulz, E., Calandra, I., & Kaiser, T. M. (2013). Feeding ecology and chewing mechanics in hoofed mammals: 3D tribology of enamel wear. *Wear*, *300*(1-2), 169–179. https://doi.org/10.1016/j.wear.2013.01.115

Scott, R. S., Teaford, M. F., & Ungar, P. S. (2012). Dental microwear texture and anthropoid diets. *American Journal of Physical Anthropology*, *147*(4), 551–579. https://doi.org/10.1002/ajpa.22007

Scott, R. S., Ungar, P. S., Bergstrom, T. S., Brown, C. A., Childs, B. E., Teaford, M. F., & Walker, A. [Alan] (2006). Dental microwear texture analysis: technical considerations. *Journal of Human Evolution*, *51*, 339–349.

Scott, R. S., Ungar, P. S., Bergstrom, T. S., Brown, C. A., Grine, F. E., Teaford, M. F., & Walker, A. [Alan] (2005). Dental microwear texture analysis shows within-species diet variability in fossil hominins. *Nature*, *436*(7051), 693–695. https://doi.org/10.1038/nature03822

Selenka, E. (1896). Die Rassen und der Zahnwechsel des Orang-Utan: vorgelegt von Hrn. Schulze am 5. März. *Sitzungsberichte Der Königlich Preussischen Akademie Der Wissenschaften Zu Berlin*. (16), 381–392.

Selenka, E. (1898). *Menschenaffen (Anthropomorphae) : Studien über Entwickelung und Schädelbau: Erste Lieferung: Rassen, Schädel und Bezahnung des Orangutan*. Wiesbaden: C.W. Kreidel. https://doi.org/10.5962/bhl.title.118615

Selenka, E., & Selenka, L. (1905). *Sonnige Welten: Ostasiatische Reiseskizzen* (2nd ed.). Wiesbaden: C.W. Kreidel.

Smith, T. M. [Thomas M.], & Reynolds, R. W. (2003). Extended Reconstruction of Global Sea Surface Temperatures Based on COADS Data (1854-1997). *Journal of Climate*, *16*(10), 1495–1510. https://doi.org/10.1175/1520-0442(2003)016<1495:EROGSS>2.0.CO;2

Spehar, S. N., Sheil, D., Harrison, T., Louys, J. [Julien], Ancrenaz, M., Marshall, A. J., . . . Meijaard, E. (2018). Orangutans venture out of the rainforest and into the Anthropocene. *Science Advances*, *4*(6), e1701422. https://doi.org/10.1126/sciadv.1701422

Spengler, R. N., Kienast, F., Roberts, P., Boivin, N., Begun, D. R., Ashastina, K., & Petraglia, M. (2023). Bearing Fruit: Miocene Apes and Rosaceous Fruit Evolution. *Biological Theory*, 1–18. https://doi.org/10.1007/s13752-022-00413-1

Sponheimer, M., Loudon, J. E., Codron, D. [D.], Howells, M. E., Pruetz, J. D., Codron, J., . . . Lee-Thorp, J. A. (2006). Do "savanna" chimpanzees consume C_4 resources? *Journal of Human Evolution*, *51*(2), 128–133. https://doi.org/10.1016/j.jhevol.2006.02.002

Stoner, K. E. (1995). Dental pathology in Pongo satyrus borneensis. *American Journal of Physical Anthropology*, *98*(3), 307–321. https://doi.org/10.1002/ajpa.1330980305

Strum, S. C. (2001). *Almost Human: A Journey into the World of Baboons* (2nd ed.). Chicago, London: University of Chicago Press.

Tarszisz, E., Tomlinson, S., Harrison, M. E., Morrogh-Bernard, H. C., & Munn, A. J. (2018). Gardeners of the forest: effects of seed handling and ingestion by orangutans on germination success of peat forest plants. *Biological Journal of the Linnean Society*, *123*(1), 125–134. https://doi.org/10.1093/biolinnean/blx133

Teaford, M. F., & Oyen, O. J. (1989). In vivo and in vitro turnover in dental microwear. *American Journal of Physical Anthropology*, *80*(4), 447–460. https://doi.org/10.1002/ajpa.1330800405

Teaford, M. F., & Robinson, J. G. (1989). Seasonal or ecological differences in diet and molar microwear in Cebus nigrivittatus. *American Journal of Physical Anthropology*, *80*(3), 391–401. https://doi.org/10.1002/ajpa.1330800312

Teaford, M. F., Ross, C. F., Ungar, P. S., Vinyard, C. J., & Laird, M. F. (2021). Grit your teeth and chew your food: Implications of food material properties and abrasives for rates of dental microwear formation in laboratory Sapajus apella (Primates). *Palaeogeography, Palaeoclimatology, Palaeoecology*, *583.* https://doi.org/10.1016/j.palaeo.2021.110644

Teaford, M. F., Ungar, P. S., Taylor, A. B., Ross, C. F., & Vinyard, C. J. (2017). In vivo rates of dental microwear formation in laboratory primates fed different food items. *Biosurface and Biotribology*, *3*(4), 166–173. https://doi.org/10.1016/j.bsbt.2017.11.005

Teaford, M. F., & Walker, A. [A.] (1984). Quantitative differences in dental microwear between primate species with different diets and a comment on the presumed diet of Sivapithecus. *American Journal of Physical Anthropology*, *64*(2), 191–200. https://doi.org/10.1002/ajpa.1330640213

Turner, I. M. (1996). Species Loss in Fragments of Tropical Rain Forest: A Review of the Evidence. *The Journal of Applied Ecology*, *33*(2), 200. https://doi.org/10.2307/2404743

Ungar, P. S. (1994). Incisor microwear of Sumatran anthropoid primates. *American Journal of Physical Anthropology*, *94*(3), 339–363. https://doi.org/10.1002/ajpa.1330940305

Ungar, P. S. (1995). Fruit preferences of four sympatric primate species at Ketambe, northern Sumatra, Indonesia. *International Journal of Primatology*, *16*(2), 221–245. https://doi.org/10.1007/BF02735479

Vogel, E. R., Alavi, S. E., Utami-Atmoko, S. S., van Noordwijk, M. A., Bransford, T. D., Erb, W. M., . . . Rothman, J. M. (2017). Nutritional ecology of wild Bornean orangutans (*Pongo pygmaeus wurmbii*) in a peat swamp habitat: Effects of age, sex, and season. *American Journal of Primatology*, *79*(4), 1–20. https://doi.org/10.1002/ajp.22618

Vogel, E. R., Harrison, M. E., Zulfa, A., Bransford, T. D., Alavi, S. E., Husson, S., . . . Farida, W. R. (2015). Nutritional Differences between Two Orangutan Habitats: Implications for Population Density. *Plos ONE*, *10*(10), e0138612. https://doi.org/10.1371/journal.pone.0138612

Westaway, K. E., Louys, J. [J.], Awe, R. D., Morwood, M. J., Price, G. J. [G. J.], Zhao, J.-X., . . . Sulistyanto, B. (2017). An early modern human presence in Sumatra 73,000-63,000 years ago. *Nature*, *548*(7667), 322–325. https://doi.org/10.1038/nature23452

Wich, S. A., Utami-Atmoko, S. S., Mitra Setia, T., Djoyosudharmo, S., & Geurts, M. L. (2006). Dietary and Energetic Responses of Pongo abelii to Fruit Availability Fluctuations. *International Journal of Primatology*, *27*(6), 1535–1550. https://doi.org/10.1007/s10764-006-9093-5

Williamson, G. B., & Ickes, K. (2002). Mast fruiting and ENSO cycles - does the cue betray a cause? *Oikos*, *97*(3), 459–461. https://doi.org/10.1034/j.1600-0706.2002.970317.x

Winkler, D. E., Schulz-Kornas, E., Kaiser, T. M., Codron, D. [Daryl], Leichliter, J., Hummel, J., . . . Tütken, T. (2020). The turnover of dental microwear texture: Testing the" last supper" effect in small mammals in a controlled feeding experiment. *Palaeogeography, Palaeoclimatology, Palaeoecology*, *557*, 109930. https://doi.org/10.1016/j.palaeo.2020.109930

Wolter, K., & Timlin, M. S. (2011). El Niño/Southern Oscillation behaviour since 1871 as diagnosed in an extended multivariate ENSO index (MEI.Ext). *International Journal of Climatology*, *31*(7), 1074–1087. https://doi.org/10.1002/joc.2336

779 Yasuda, M., Matsumoto, J., Osada, N., Ichikawa, S., Kachi, N., Tani, M., . . . Manokaran, N. (1999). The
780 mechanism of general flowering in Dipterocarpaceae in the Malay Peninsula. *Journal of Tropical*
781 *Ecology*, *15*(4), 437–449. https://doi.org/10.1017/S0266467499000930
782

Table SI 1 Table reporting all the parameters measured for each individual in the data set including metadata such as about the individuals and the teeth sampled in each case. One phase I (f6, below) and one phase II (f9, top) on the same tooth of each individual was analyzed

Specimen ID	Taxonomy	sex	Age	Year of death	locality	upper/ lower	right/ left	crushing facet (f9)													
								Sq.f9	Ssk.f9	Sku.f9	Sp.f9	Sv.f9	Sz.f9	Sa.f9	Sal2_0.5.f9	Str2_0.5.f9	metf.f9	medf.f9	Asfc.f9	HAsfc9.f9	HAsfc81.f9	epLsar.f9
ZSM-1913-1452	*P. abelii*	f	adult	1913	Sumatra, west coast	lower	right	0.442809	-0.766984	6.7462	1.523806	2.888541	4.412347	0.319429	13.908733	0.523825	0.237612	3925.012481	0.519216	0.327388	0.384684	0.004498
ZSM-1913-1465	*P. abelii*	m	adult	1913	Sumatra, Deli	lower	right	0.38019	-3.335903	20.57047	0.814207	3.335156	4.149363	0.243986	8.300124	0.470784	0.291215	4045.405429	0.64977	0.191558	0.521944	0.00624
ZSM-1913-1466	*P. abelii*	m	adult	1913	Sumatra, Deli	lower	right	0.635051	-2.801688	13.748074	1.310808	4.164899	5.475707	0.373283	16.264749	0.825735	0.339075	4183.538244	1.387841	1.072675	1.289445	0.003458
ZSM-1913-1469	*P. abelii*	f	adult	1913	Sumatra, Deli	lower	right	0.977999	-0.604811	3.78399	3.665624	3.884334	7.549958	0.756254	16.108277	0.823981	0.576893	3617.940738	1.566031	0.297712	0.484966	0.004459
ZSM-1913-1471	*P. abelii*	indet	adult	1913	Sumatra, Deli	lower	right	0.304827	-3.074876	16.385562	0.693835	2.367647	3.061482	0.179669	9.463773	0.513331	0.196852	4653.06361	0.769015	0.275494	0.634619	0.00498
ZSM-1981-102	*P. pygmaeus*	f	adult	1892-1894	Skalau	lower	right	1.194413	-0.929212	4.475898	4.493897	4.711047	9.204944	0.883368	13.538415	0.678097	0.729266	4198.328432	3.705707	0.152827	0.344962	0.001192
ZSM-1981-103	*P. pygmaeus*	m	subadult	1892-1894	Skalau	lower	right	0.39189	-0.166387	3.297127	1.166208	2.026611	3.192819	0.311631	18.677965	0.760648	0.211682	4797.560968	0.944297	0.25714	0.41892	0.001085
ZSM-1981-105	*P. pygmaeus*	f	adult	1892-1894	Skalau	lower	right	0.402262	-3.512464	21.212672	0.868292	3.265827	4.134119	0.242329	9.762519	0.492825	0.273372	4802.104517	1.477138	0.277697	0.646464	0.002741
ZSM-1981-106	*P. pygmaeus*	f	adult	1892-1894	Skalau	lower	right	0.410221	-1.596029	10.177577	1.370271	2.956345	4.326616	0.291196	5.049351	0.559127	0.365774	4036.571464	2.542249	0.300492	0.602459	0.003403
ZSM-1981-107	*P. pygmaeus*	f	adult	1892-1894	Skalau	lower	right	0.798731	-1.804024	7.136769	1.240274	4.152108	5.392382	0.577146	12.113684	0.748814	0.615505	3678.702629	1.658445	0.404339	0.806612	0.002193
ZSM-1981-108	*P. pygmaeus*	f	adult	1892-1894	Skalau	lower	left	0.362798	-2.629161	13.510312	1.036427	2.907396	3.943823	0.229493	10.624023	0.454046	0.167116	5051.535674	0.435617	0.620117	1.00197	0.004634
ZSM-1981-111	*P. pygmaeus*	f	adult	1892-1894	Skalau	lower	right	0.172002	-1.615944	7.499647	0.6534	1.142894	1.796294	0.123569	7.84461	0.623239	0.153346	4927.411281	0.776364	0.330686	0.700619	0.004113
ZSM-1981-112	*P. pygmaeus*	f	adult	1892-1894	Skalau	lower	right	0.253529	-1.585598	7.235845	0.541809	1.769522	2.311331	0.18734	6.419493	0.563197	0.268951	4117.137881	0.836457	0.239312	0.408176	0.005091
ZSM-1981-113	*P. pygmaeus*	f	adult	1892-1894	Skalau	lower	right	0.693422	-0.923663	3.457329	1.052283	2.649955	3.702238	0.560003	20.282412	0.47486	0.167742	5045.736056	0.126525	0.567897	0.858822	0.004995
ZSM-1981-114	*P. pygmaeus*	f	adult	1892-1894	Skalau	lower	left	0.422179	0.837994	7.941886	3.538082	1.387166	4.925248	0.330489	10.835534	0.649652	0.337514	4308.130152	0.959282	0.452793	0.837541	0.002685
ZSM-1981-116	*P. pygmaeus*	f	adult	1892-1894	Dadap	lower	right	0.60047	-1.582832	6.718923	1.109257	3.651893	4.76115	0.446047	8.980102	0.635495	0.547811	3970.014797	2.119993	0.477349	0.873044	0.00389
ZSM-1981-117	*P. pygmaeus*	m	adult	1892-1894	Dadap	lower	right	0.60158	-1.096472	5.321455	1.628771	3.323913	4.952684	0.443256	12.852894	0.740848	0.434187	3924.053361	0.916836	0.310688	0.653684	0.003994
ZSM-1981-119	*P. pygmaeus*	m	adult	1892-1894	Dadap	lower	right	0.473964	-0.99004	4.939775	1.463723	2.698348	4.162071	0.355462	9.29712	0.610856	0.408711	4140.191364	0.819237	0.508229	0.911739	0.006087
ZSM-1981-122	*P. pygmaeus*	f	adult	1892-1894	Dadap	lower	right	0.437506	-1.693972	8.019948	1.154553	3.230607	4.38516	0.32553	8.328992	0.642736	0.351109	3726.609597	0.717377	0.216663	0.600875	0.004222
ZSM-1981-124	*P. pygmaeus*	f	adult	1892-1894	Dadap	lower	right	0.290717	-1.065682	5.361633	0.842994	1.638326	2.48132	0.217323	15.414538	0.596052	0.143327	4737.92678	0.341345	0.543488	0.781247	0.000749
ZSM-1981-125	*P. pygmaeus*	f	adult	1892-1894	Dadap	lower	right	0.504894	-0.963677	4.306926	1.130573	2.191252	3.321825	0.395892	11.446504	0.527063	0.349085	3911.15392	0.542425	0.319633	0.616846	0.006054
ZSM-1981-129	*P. pygmaeus*	m	adult	1892-1894	Dadap	lower	right	0.446924	-2.169117	10.942502	1.307635	3.989585	5.29722	0.309051	10.598053	0.760944	0.299061	4398.434655	0.84362	0.547484	0.811832	0.003566
ZSM-1981-130	*P. pygmaeus*	f	subadult	1892-1894	Dadap	lower	right	0.669254	-1.844119	10.303095	1.352331	4.872396	6.224727	0.487275	10.579596	0.571289	0.475564	3874.886663	1.213507	0.457006	0.908458	0.004664
ZSM-1981-133	*P. pygmaeus*	f	juvenile	1892-1894	Dadap	lower	right	0.550295	-1.690569	8.06739	1.592094	3.187221	4.779315	0.370967	8.264284	0.354784	0.416263	4403.421734	1.640933	0.230381	0.59944	0.007297
ZSM-1981-134	*P. pygmaeus*	f	juvenile	1892-1894	Dadap	lower	right	0.258862	-3.029239	23.117301	0.904707	2.917968	3.822675	0.170505	7.076246	0.480076	0.200137	4650.459387	0.765924	0.457928	0.99029	0.005216
ZSM-1981-135-B	*P. pygmaeus*	f	adult	1892-1894	Dadap	lower	right	0.60027	-0.674445	3.161503	2.079685	2.171132	4.250817	0.487588	14.31161	0.542476	0.368541	4428.72952	1.022308	0.225839	0.410568	0.005657
ZSM-1981-136	*P. pygmaeus*	f	adult	1892-1894	Dadap	lower	right	0.287844	-1.143527	7.555053	1.050912	2.201787	3.252699	0.201773	8.580131	0.543892	0.216412	4559.006656	0.586944	0.375845	0.748529	0.002835
ZSM-1981-141	*P. pygmaeus*	m	adult	1892-1894	Bogau	lower	left	0.315342	-0.532037	4.386346	0.939659	1.578717	2.518376	0.238131	10.436057	0.60195	0.251583	3906.54946	0.279695	0.871068	1.639465	0.004454
ZSM-1981-142	*P. pygmaeus*	m	juvenile	1892-1894	Genepai	lower	right	0.787811	-0.526014	4.487893	2.238754	4.376008	6.614762	0.614538	11.63928	0.397243	0.460593	3787.265121	1.281783	0.198812	0.391319	0.001979
ZSM-1981-143	*P. pygmaeus*	m	adult	1892-1894	Bogau	lower	right	0.480011	-0.985718	4.508424	0.818521	2.566672	3.385193	0.37914	12.591409	0.603609	0.322672	4159.262002	0.453274	0.451175	0.985179	0.005012
ZSM-1981-144	*P. pygmaeus*	m	adult	1892-1894	Bogau	lower	right	0.804956	-2.596216	12.63033	1.199038	5.761209	6.960247	0.541461	11.623369	0.803494	0.687391	3344.561218	2.044289	0.457412	1.38338	0.001426
ZSM-1981-149	*P. pygmaeus*	m	adult	1892-1894	Genepai	lower	right	0.312303	-0.582481	3.420791	1.029218	1.801607	2.830825	0.252018	11.810819	0.793245	0.27295	4173.921654	0.982718	0.220654	0.409584	0.003067
ZSM-1981-150	*P. pygmaeus*	m	adult	1892-1894	Genepai	lower	right	0.460516	-1.733216	10.337215	0.939794	3.627991	4.567785	0.336731	15.156713	0.800474	0.226134	4562.505046	0.53457	0.706234	1.187095	0.004361
ZSM-1981-151	*P. pygmaeus*	m	adult	1892-1894	Genepai	lower	right	0.497102	-0.682796	3.985907	1.528683	2.209196	3.737879	0.380922	13.534908	0.616937	0.401138	4347.05508	1.885921	0.242253	0.418997	0.003927
ZSM-1981-153	*P. pygmaeus*	m	adult	1892-1894	Genepai	lower	right	0.246406	-0.301008	3.843246	0.868971	1.183738	2.052709	0.189825	7.91138	0.446377	0.182099	4289.128116	0.464451	0.624929	0.745813	0.007499
ZSM-1981-154	*P. pygmaeus*	m	adult	1892-1894	Genepai	lower	right	0.189597	-3.239941	20.752299	0.427386	2.034332	2.461718	0.117166	6.117786	0.804665	0.174502	5150.902546	1.046146	0.363758	0.7254	0.003305
ZSM-1981-155	*P. pygmaeus*	f	adult	1892-1894	Genepai	lower	right	0.505903	-1.776522	7.718007	0.904528	3.196043	4.100571	0.36844	7.728384	0.753539	0.574375	3510.230264	1.448086	0.325661	0.604242	0.00343
ZSM-1981-156	*P. pygmaeus*	f	adult	1892-1894	Bogau	lower	right	0.446798	-1.325945	5.789209	1.083363	2.26094	3.344303	0.336415	12.916357	0.672144	0.262872	4002.683789	0.470029	0.193452	0.36352	0.004428
ZSM-1981-159	*P. pygmaeus*	f	adult	1892-1894	Bogau	lower	right	0.14473	-0.844212	4.671094	0.558217	0.836799	1.395016	0.111003	4.732231	0.415604	0.139556	4642.157058	0.80912	0.237139	0.428923	0.00612
ZSM-1981-162	*P. pygmaeus*	f	subadult	1892-1894	Bogau	lower	right	0.327051	-0.040511	3.67292	1.238435	1.651196	2.889631	0.255011	11.093278	0.195229	0.165274	4815.880875	0.594968	0.218349	0.364558	0.00417
ZSM-1981-163	*P. pygmaeus*	f	adult	1892-1894	Bogau	lower	right	0.900703	-1.352502	5.842627	2.486947	5.066606	7.553553	0.683138	10.101415	0.764698	0.753476	3428.68461	2.257801	0.584779	1.120503	0.002323
ZSM-1981-165	*P. pygmaeus*	f	adult	1892-1894	Genepai	lower	right	0.428573	-2.181035	12.847257	0.927238	3.748028	4.675266	0.29905	6.911042	0.568478	0.429952	3296.464957	1.046333	0.304316	0.505683	0.007041
ZSM-1981-166	*P. pygmaeus*	f	adult	1892-1894	Bogau	lower	right	0.359609	-0.646139	3.060523	0.773821	1.564729	2.33855	0.290021	16.054857	0.655105	0.209977	4208.501218	0.540723	0.561026	0.86232	0.002879
ZSM-1981-167	*P. pygmaeus*	f	adult	1892-1894	Genepai	lower	right	0.192116	-2.227624	11.894457	0.494543	1.495009	1.989552	0.128006	4.670498	0.228508	0.158523	4713.660371	0.605108	0.246468	0.550468	0.005679
ZSM-1981-168	*P. pygmaeus*	f	adult	1892-1894	Genepai	lower	right	0.268962	-1.388199	6.876001	0.977603	1.571219	2.548822	0.194777	13.188759	0.839675	0.182156	4845.715662	0.562083	0.157517	0.341839	0.002868
ZSM-1981-179	*P. pygmaeus*	f	adult	1892-1894	Landak	lower	right	0.405863	-0.009646	3.096562	1.305991	1.758812	3.064803	0.317901	13.254943	0.410993	0.255666	4701.20832	1.341083	0.213762	0.359814	0.006918
ZSM-1981-182	*P. pygmaeus*	f	adult	1892-1894	Batangtu	lower	right	0.435536	-1.467982	6.818041	1.217865	2.564281	3.782146	0.309297	9.503296	0.470373	0.321298	4480.297772	1.378727	0.358207	0.456153	0.003565
ZSM-1981-188	*P. pygmaeus*	f	adult	1892-1894	Batangtu	lower	right	0.738797	-1.070348	6.101654	2.321546	4.080695	6.402241	0.554095	7.422183	0.363825	0.616403	4081.418309	2.075088	0.444643	0.848298	0.00503
ZSM-1981-196	*P. pygmaeus*	m	adult	1892-1894	Dadap	lower	right	0.575593	-0.794929	3.708818	1.507355	2.882567	4.389922	0.457285	11.293628	0.61729	0.43373	3975.690992	1.083108	0.332564	0.583153	0.00335
ZSM-1981-198	*P. pygmaeus*	m	adult	1892-1894	Dadap	lower	right	0.571174	-0.353568	2.910418	1.557562	2.085874	3.643435	0.459886	17.47997	0.650106	0.227723	4506.990919	0.539946	0.239401	0.375025	0.003697
ZSM-1981-199	*P. pygmaeus*	m	adult	1892-1894	Dadap	lower	right	0.42589	-1.539067	6.251283	0.933434	2.280615	3.214049	0.316645	8.427738	0.561117	0.340434	3941.052777	1.006012	0.311002	0.609898	0.005517
ZSM-1981-203	*P. pygmaeus*	m	adult	1892-1894	Rantai	lower	right	0.243028	-1.652519	9.875863	0.638385	2.096819	2.735204	0.165552	10.236967	0.543139	0.138629	4700.984824	0.533502	0.246648	0.584658	0.005015
ZSM-1981-204	*P. pygmaeus*	m	subadult	1892-1894	Rantai	lower	right	1.790031	-0.640568	4.02666	5.826866	7.434655	13.261521	1.380385	20.219015	0.801831	0.602184	3453.330549	1.316268	0.407105	0.867153	0.001084
ZSM-1981-209	*P. pygmaeus*	f	subadult	1892-1894	Rantai	lower	right	0.457665	-0.584549	3.493872	1.635666	1.914948	3.550614	0.358645	15.079359	0.684885	0.241098	4492.887094	0.935758	0.19254	0.236198	0.004219
ZSM-1981-21	*P. pygmaeus*	f	juvenile	1892-1894	Skalau	lower	right	0.591235	-0.651823	3.36226	1.260576	2.78093	4.041506	0.468404	13.115469	0.561584	0.351966	4081.395946	0.802018	0.717832	1.157853	0.00359
ZSM-1981-216	*P. pygmaeus*	m	subadult	1892-1894	Ketungau	lower	right	0.58895	-1.141015	4.771891	1.081513	3.069521	4.151034	0.460123	11.800431	0.444357	0.469962	4656.026318	1.556057	0.340072	0.934795	0.003995
ZSM-1981-22	*P. pygmaeus*	f	juvenile	1892-1894	Skalau	lower	right	0.289888	-0.783211	5.426212	0.788046	1.913125	2.701171	0.216824	11.165701	0.826773	0.233509	4474.257568	0.65268	0.354014	0.698084	0.003283
ZSM-1981-23	*P. pygmaeus*	f	juvenile	1892-1894	Skalau	lower	right	0.759554	-0.581584	3.211519	2.252328	2.614368	4.866696	0.6014	11.082062	0.535475	0.736139	3779.195681	2.086351	0.217534	0.431493	0.005878
ZSM-1981-234	*P. pygmaeus*	m	adult	1892-1894	Skalau	lower	right	0.841478	-2.122007	8.605908	2.253813	4.1441	6.397913	0.548644	10.428885	0.546128	0.640153	3555.083633	1.417168	0.632606	7.552987	0.004693
ZSM-1981-25	*P. pygmaeus*	m	adult	1892-1894	Skalau	lower	right	0.503489	-1.586649	6.188015	1.188893	3.201577	4.39047	0.379489	9.912425	0.63246	0.347333	4322.27531	1.504772	0.221196	0.354889	0.003617
ZSM-1981-26	*P. pygmaeus*	m	subadult	1892-1894	Skalau	lower	right	1.271745	-0.528163	3.215281	3.51169	5.424669	8.936359	0.996228	17.759632	0.516403	0.257456	4779.883713	1.011405	0.198028	0.437588	0.003709
ZSM-1981-27	*P. pygmaeus*	m	adult	1892-1894	Skalau	lower	right	0.727208	-1.03807	3.569968	1.31572	2.701965	4.017685	0.567856	16.420036	0.439586	0.358483	4382.581579	1.23954	0.401109	0.659358	0.007532
ZSM-1981-28	*P. pygmaeus*	f	adult	1892-1894	Skalau	lower	right	0.733458	-2.095388	11.249641	2.0957	4.403101	6.498801	0.457976	15.799184	0.762916	0.361743	4455.958279	1.194456	0.471712	0.536008	0.004595
ZSM-1981-32	*P. pygmaeus*	m	subadult	1892-1894	Skalau	lower	right	0.528656	-3.630661	22.929467	1.067923	4.970865	6.038788	0.312489	12.49607	0.961782	0.362637	4080.014061	1.035488	1.14996	1.498325	0.005739
ZSM-1981-33	*P. pygmaeus*	f	adult	1892-1894	Skalau	lower	right	0.603918	-1.216561	4.377729	1.216556	2.700975	3.917531	0.469078	12.031584	0.620982	0.425192	4270.432687	1.007535	0.163367	0.310162	0.004821
ZSM-1981-45	*P. pygmaeus*	m	adult	1892-1894	Skalau	lower	right	0.35143	-2.038398	11.494241	0.843049	2.859238	3.702287	0.250236	8.069988	0.702004	0.378974	3976.167851	1.046065	0.206574	0.439806	0.003746
ZSM-1981-50	*P. pygmaeus*	f	adult	1892-1894	Skalau	lower	right	0.736352	-2.260345	10.575947	1.239125	5.292451	6.531576	0.494873	12.186343	0.640505	0.536499	3776.013851	0.927552	1.005106	2.432534	0.003427
ZSM-1981-53	*P. pygmaeus*	m	adult	1892-1894	Skalau	lower	right	0.45641	-1.009091	5.481492	1.363006	3.059256	4.422262	0.341428	10.047231	0.551417	0.312886	4249.865144	1.182682	0.159275	0.462282	0.00577
ZSM-1981-60	*P. pygmaeus*	f	adult	1892-1894	Skalau	lower	right	0.89439	-0.73748	4.660013	2.249334	5.167261	7.416595	0.675676	14.928473	0.707518	0.496678	3664.410499	0.834483	0.391825	2.121726	0.002968
ZSM-1981-62	*P. pygmaeus*	f	adult	1892-1894	Skalau	lower	right	0.330027	-0.592829	3.50894	0.896232	1.555876	2.452108	0.259649	9.933042	0.645566	0.325138	3843.44115	0.949465	0.133553	0.389861	0.003893
ZSM-1981-63	*P. pygmaeus*	m	subadult	1892-1894	Skalau	lower	right	0.380026	-1.506807	7.067179	1.371363	2.276279	3.647642	0.270412	7.94014	0.566017	0.328627	3842.208061	1.062461	0.253038	0.606735	0.004232
ZSM-1981-64	*P. pygmaeus*	m	adult	1892-1894	Skalau	lower	right	0.663562	-2.680197	13.85646	1.291913	5.232576	6.524489	0.435738	12.384219	0.813823	0.452889	4079.753816	1.153115	0.787294	1.089052	0.001078
ZSM-1981-67	*P. pygmaeus*	f	subadult	1892-1894	Skalau	lower	right	0.433351	-2.467005	10.934257	0.902808	4.093832	4.99664	0.288179	8.067606	0.710746	0.445328	4109.450519	1.49793	0.401664	0.908568	0.003198
ZSM-1981-68	*P. pygmaeus*	m	adult	1892-1894	Skalau	lower	right	0.267048	-0.888138	4.769431	1.03379	1.721684	2.755474	0.203263	8.131856	0.518999	0.260697	4215.251555	0.579709	0.108692	0.348757	0.006578
ZSM-1981-69	*P. pygmaeus*	m	adult	1892-1894	Skalau	lower	right	0.312469	-3.199193	18.31541	0.545287	2.873766	3.419053	0.19162	7.321527	0.604135	0.237559	4695.148009	0.92189	0.364143	1.001356	0.002632

ZSM-1981-70	*P. pygmaeus*	m	adult	1892-1894	Skalau	lower	right	0.342053	0.132817	4.297825	1.298464	1.925576	3.22404	0.261302	15.771609	0.60596	0.177709	5117.397039	0.36599	0.276743	0.520759	0.004269
ZSM-1981-71	*P. pygmaeus*	m	adult	1892-1894	Skalau	lower	right	0.394983	-1.191823	7.795549	1.320912	2.692625	4.013537	0.292847	17.945844	0.641984	0.168362	4430.243586	0.403109	0.154411	0.344566	0.002424
ZSM-1981-74	*P. pygmaeus*	f	adult	1892-1894	Skalau	lower	right	0.87627	-1.451973	5.209546	1.300679	4.147101	5.44778	0.663799	10.425661	0.434035	0.754823	3361.556914	1.500966	0.231234	1.081098	0.006279
ZSM-1981-75	*P. pygmaeus*	f	adult	1892-1894	Skalau	lower	right	0.898954	-0.488573	3.691424	2.677498	3.453102	6.1306	0.696555	13.818339	0.632998	0.465088	4124.693473	1.064983	0.33247	0.622311	0.003586
ZSM-1981-76	*P. pygmaeus*	f	adult	1892-1894	Skalau	lower	right	0.697731	-1.243752	6.326269	1.521179	3.884922	5.406101	0.497195	10.943519	0.743706	0.531004	3375.686512	0.897087	1.34482	2.941626	0.002745
ZSM-1981-78	*P. pygmaeus*	f	adult	1892-1894	Skalau	lower	right	0.3589	-2.726297	13.237737	0.596793	2.777806	3.374599	0.237773	9.714971	0.675805	0.240928	4677.830756	0.790377	0.359385	0.542483	0.002858
ZSM-1981-79	*P. pygmaeus*	f	adult	1892-1894	Skalau	lower	right	0.925824	-1.155361	5.455362	1.973089	4.851404	6.824493	0.70863	17.183858	0.771582	0.518026	4205.500437	1.494524	0.827259	1.386325	0.002741
ZSM-1981-83	*P. pygmaeus*	f	adult	1892-1894	Skalau	lower	right	0.260683	-0.495729	2.938304	0.80718	1.089937	1.897117	0.212011	10.31317	0.591568	0.224334	4118.651605	0.828225	0.326163	0.586524	0.00456
ZSM-1981-86	*P. pygmaeus*	f	adult	1892-1894	Skalau	lower	right	0.214768	-1.742357	8.422268	0.785361	1.622822	2.408183	0.155627	5.156584	0.372289	0.214137	4278.660891	0.848154	0.450378	0.650338	0.004757
ZSM-1981-88	*P. pygmaeus*	f	adult	1892-1894	Skalau	lower	right	0.241396	-1.35125	5.723511	0.758906	1.412987	2.171892	0.183368	4.560531	0.409728	0.236863	3936.73693	1.048827	0.262104	0.389068	0.006885
ZSM-1981-89	*P. pygmaeus*	f	adult	1892-1894	Skalau	lower	right	0.387465	-2.168678	11.979343	1.313737	2.80727	4.121007	0.237655	7.956016	0.781442	0.335478	4648.444114	1.692473	0.607201	1.248673	0.001511
ZSM-1981-90	*P. pygmaeus*	f	adult	1892-1894	Skalau	lower	right	0.317013	-2.355349	14.345635	0.820485	3.283633	4.104118	0.213393	9.323356	0.745185	0.250006	5214.792001	1.125423	0.279157	0.631186	0.002273
ZSM-1981-91	*P. pygmaeus*	f	adult	1892-1894	Skalau	lower	right	0.233692	-0.705524	4.512198	0.775703	1.449884	2.225587	0.177645	9.441226	0.770296	0.207062	5274.761462	1.474002	0.24756	0.462754	0.000146
ZSM-1981-92	*P. pygmaeus*	f	senil	1892-1894	Skalau	lower	right	0.603368	-1.089382	5.785115	1.422741	3.621571	5.044312	0.452634	17.978059	0.750486	0.316533	4334.401979	0.875722	0.303136	0.634797	0.000919
ZSM-1981-94	*P. pygmaeus*	m	adult	1892-1894	Skalau	lower	right	0.240438	-0.898606	6.141644	0.607013	1.59011	2.197123	0.183917	10.322718	0.649452	0.174302	4551.435533	0.533976	0.17183	0.41271	0.000972
ZSM-1981-95	*P. pygmaeus*	f	adult	1892-1894	Skalau	lower	right	0.386994	-0.406126	3.527405	1.136493	2.18471	3.321203	0.310632	7.519631	0.387736	0.451236	3975.240944	1.577609	0.174481	0.394801	0.005846
ZSM-1981-96	*P. pygmaeus*	f	adult	1892-1894	Skalau	lower	right	0.881883	-0.693023	4.404905	3.137678	4.192879	7.330557	0.68804	14.7729	0.837319	0.589215	3298.439951	1.203628	0.62516	1.09638	0.004709
ZSM-1981-97	*P. pygmaeus*	f	adult	1892-1894	Skalau	lower	right	0.474917	-2.887576	15.306114	1.164139	3.345489	4.509627	0.29503	13.616007	0.587216	0.265872	4519.950008	1.001417	0.200303	0.496991	0.001642
ZSM-1981-99	*P. pygmaeus*	m	adult	1892-1894	Skalau	lower	right	0.229872	-1.503446	6.713424	0.615923	1.566361	2.182284	0.164988	6.979738	0.497029	0.195202	4288.380744	0.64403	0.212339	0.655374	0.005786
Specimen ID	**Taxonomy**	**sex**	**Age**	**Year of death**	**locality**	**upper/ lower**	**right/ left**	**shearing facet (f6)**												
								Sq.f6	**Ssk.f6**	**Sku.f6**	**Sp.f6**	**Sv.f6**	**Sz.f6**	**Sa.f6**	**Sal2_0.5.f6**	**Str2_0.5.f6**	**metf.f6**	**medf.f6**	**Asfc.f6**	**HAsfc9.f6**	**HAsfc81.f6**	**epLsar.f6**
ZSM-1913-1452	*P. abelii*	f	adult	1913	Sumatra, west coast	lower	right	0.631285	-0.431931	4.85643	2.937023	2.758578	5.695601	0.465788	15.277288	0.744569	0.299041	3489.0517	0.482555	0.263226	0.61164	0.000621
ZSM-1913-1465	*P. abelii*	m	adult	1913	Sumatra, Deli	lower	right	0.379009	-0.624626	4.497908	1.600082	2.054384	3.654466	0.28863	11.110424	0.473364	0.255519	3898.783746	0.524859	0.192638	0.497886	0.005726
ZSM-1913-1466	*P. abelii*	m	adult	1913	Sumatra, Deli	lower	right	0.444495	-1.34321	5.718063	1.135183	2.489631	3.624814	0.329667	11.078999	0.751866	0.334827	3833.750065	0.906534	0.390774	0.87522	0.00222
ZSM-1913-1469	*P. abelii*	f	adult	1913	Sumatra, Deli	lower	right	0.226163	-1.299762	6.166338	0.717138	1.829245	2.546383	0.16846	5.905923	0.770306	0.231279	4222.260413	1.147764	0.224178	0.42675	0.000817
ZSM-1913-1471	*P. abelii*	indet	adult	1913	Sumatra, Deli	lower	right	1.164819	-2.100342	12.116912	4.847709	7.451136	12.298845	0.669478	13.167654	0.792772	0.549656	4113.813013	1.57255	3.033443	3.555587	0.007479
ZSM-1981-102	*P. pygmaeus*	f	adult	1892-1894	Skalau	lower	right	0.250506	-0.664488	3.964761	0.694066	1.358376	2.052442	0.193881	5.206193	0.304693	0.269409	4358.234751	1.035155	0.235264	0.312126	0.006233
ZSM-1981-103	*P. pygmaeus*	m	subadult	1892-1894	Skalau	lower	right	0.34891	-2.310994	11.983546	0.726518	2.949063	3.675581	0.241842	6.9868	0.651778	0.33964	4122.57586	1.624252	0.317917	0.560204	0.006119
ZSM-1981-105	*P. pygmaeus*	f	adult	1892-1894	Skalau	lower	right	0.629327	-1.460726	7.907029	1.449008	4.497209	5.946217	0.451523	10.474908	0.822811	0.550548	4035.789558	1.772982	0.31176	0.879958	0.001295
ZSM-1981-106	*P. pygmaeus*	f	adult	1892-1894	Skalau	lower	right	0.952137	-1.73969	6.92501	2.257645	4.906461	7.164106	0.675513	14.920591	0.669972	0.54992	4139.415836	1.270655	0.393827	0.549962	0.004313
ZSM-1981-107	*P. pygmaeus*	f	adult	1892-1894	Skalau	lower	right	0.570605	-1.914835	8.414034	1.061232	4.012068	5.0733	0.407357	8.488214	0.844627	0.592982	3829.8602	1.607253	0.205206	0.5859	0.002122
ZSM-1981-108	*P. pygmaeus*	f	adult	1892-1894	Skalau	lower	left	0.465539	-1.318458	6.524362	1.062117	3.04739	4.109507	0.341543	11.316636	0.588566	0.367238	4380.905447	1.121354	0.332521	0.736142	0.003276
ZSM-1981-111	*P. pygmaeus*	f	adult	1892-1894	Skalau	lower	right	0.336545	-1.551943	9.160671	0.973313	2.757011	3.730324	0.245866	8.640487	0.377409	0.249491	4637.430897	0.958491	0.360703	0.707018	0.000735
ZSM-1981-112	*P. pygmaeus*	f	adult	1892-1894	Skalau	lower	right	0.305526	-0.912265	5.279258	1.079235	1.983381	3.062616	0.227565	4.272314	0.233183	0.463058	4431.257973	1.377242	0.545318	0.840894	0.008095
ZSM-1981-113	*P. pygmaeus*	f	adult	1892-1894	Skalau	lower	right	0.508952	-1.300494	6.050985	1.338754	2.756295	4.095049	0.363221	11.664302	0.536487	0.385778	4115.326151	0.554204	0.587493	0.753368	0.005561
ZSM-1981-114	*P. pygmaeus*	f	adult	1892-1894	Skalau	lower	left	0.425956	-1.09912	5.480781	1.211713	2.550232	3.761945	0.328161	12.167202	0.593667	0.288276	4679.899412	0.835286	0.354381	0.614175	0.001597
ZSM-1981-116	*P. pygmaeus*	f	adult	1892-1894	Dadap	lower	right	0.548626	-0.193419	2.953903	1.573013	2.170071	3.743084	0.442006	14.936624	0.565257	0.286679	4158.810599	0.919669	0.282987	0.624053	0.004093
ZSM-1981-117	*P. pygmaeus*	m	adult	1892-1894	Dadap	lower	right	0.871806	-0.662854	3.474758	2.395428	3.464342	5.85977	0.673654	16.138547	0.622335	0.480939	3479.3584	1.135791	0.211809	0.476745	0.004102
ZSM-1981-119	*P. pygmaeus*	m	adult	1892-1894	Dadap	lower	right	0.568897	-0.608812	6.320998	2.9175	3.202102	6.119602	0.40537	9.374877	0.683334	0.540359	3800.37984	2.620774	0.32828	0.515013	0.00235
ZSM-1981-122	*P. pygmaeus*	f	adult	1892-1894	Dadap	lower	right	0.680227	-0.874014	3.865281	1.36129	3.107864	4.469154	0.531535	10.856108	0.320614	0.410221	4080.542049	0.658328	0.434404	1.068378	0.006444
ZSM-1981-124	*P. pygmaeus*	f	adult	1892-1894	Dadap	lower	right	0.376593	-1.014599	3.912467	0.962229	1.713999	2.676228	0.294947	11.687467	0.704077	0.237561	4350.988354	0.569859	0.591236	1.184384	0.002482
ZSM-1981-125	*P. pygmaeus*	f	adult	1892-1894	Dadap	lower	right	0.306792	-0.395355	3.058822	0.785607	1.301204	2.086811	0.246278	13.614173	0.573831	0.226412	4289.88338	0.731943	0.169065	0.296645	0.00357
ZSM-1981-129	*P. pygmaeus*	m	adult	1892-1894	Dadap	lower	right	0.508537	-0.740535	4.194283	1.589736	2.485167	4.074903	0.388783	10.437126	0.538649	0.412414	3746.749814	1.116984	0.224286	0.592053	0.003478
ZSM-1981-130	*P. pygmaeus*	f	subadult	1892-1894	Dadap	lower	right	0.396705	-1.294236	5.310352	1.099589	2.261104	3.360693	0.297284	8.187784	0.816836	0.375701	4121.225365	1.92506	0.185422	0.357225	0.00184
ZSM-1981-133	*P. pygmaeus*	f	juvenile	1892-1894	Dadap	lower	right	0.554754	-1.335622	5.101111	0.991491	3.119183	4.110674	0.416483	11.864267	0.690672	0.447919	4315.211863	2.029061	0.351007	0.581473	0.001234
ZSM-1981-134	*P. pygmaeus*	f	juvenile	1892-1894	Dadap	lower	right	0.388275	-3.924278	27.693929	1.076098	3.321344	4.397442	0.225	12.406366	0.698062	0.232422	4784.832622	0.79238	0.601114	0.994969	0.000989
ZSM-1981-135-B	*P. pygmaeus*	f	adult	1892-1894	Dadap	lower	right	0.297975	-0.249105	3.224627	1.197072	1.349609	2.546681	0.233027	12.167017	0.729147	0.233812	4345.962538	0.765995	0.264124	0.366872	0.001921
ZSM-1981-136	*P. pygmaeus*	f	adult	1892-1894	Dadap	lower	right	0.85005	-0.952094	4.308838	1.997144	4.075538	6.072682	0.647797	17.654836	0.649517	0.538426	3718.595153	1.108096	0.318282	0.568852	0.004402
ZSM-1981-141	*P. pygmaeus*	m	adult	1892-1894	Bogau	lower	left	0.469908	0.136004	2.863967	1.461178	1.399379	2.860557	0.382544	13.434133	0.31198	0.241086	4222.358419	0.299225	0.470344	0.598029	0.005205
ZSM-1981-142	*P. pygmaeus*	m	juvenile	1892-1894	Genepai	lower	right	1.011659	-1.194864	5.868065	3.292185	5.792257	9.084442	0.737666	11.140302	0.586601	0.782769	4099.943956	3.532164	0.617762	0.913722	0.00258
ZSM-1981-143	*P. pygmaeus*	m	adult	1892-1894	Bogau	lower	right	0.738957	-1.970725	10.106464	1.413097	4.94957	6.362667	0.513582	14.872925	0.610872	0.469677	3823.352504	1.056398	0.950405	0.910219	0.002697
ZSM-1981-144	*P. pygmaeus*	m	adult	1892-1894	Bogau	lower	right	0.442233	-0.90728	5.223299	1.255186	2.585746	3.840932	0.335852	12.302877	0.668044	0.331538	4328.667322	0.889954	0.369855	0.739655	0.004593
ZSM-1981-149	*P. pygmaeus*	m	adult	1892-1894	Genepai	lower	right	0.430021	-1.211154	4.860083	0.94398	2.093535	3.037515	0.322844	7.560934	0.785741	0.446426	3593.758773	1.489834	0.36243	0.658079	0.002248
ZSM-1981-150	*P. pygmaeus*	m	adult	1892-1894	Genepai	lower	right	0.457819	-1.72083	6.695811	1.057389	2.703686	3.761075	0.327584	8.23185	0.832841	0.428802	3781.177044	1.173598	0.604079	1.262293	0.003443
ZSM-1981-151	*P. pygmaeus*	m	adult	1892-1894	Genepai	lower	right	0.328089	-1.917105	8.500788	0.876972	2.139611	3.016583	0.22655	8.416743	0.76485	0.310935	4363.34388	1.54788	0.256268	0.47658	0.001095
ZSM-1981-153	*P. pygmaeus*	m	adult	1892-1894	Genepai	lower	right	0.516688	-0.129754	5.264705	2.596462	1.963729	4.560191	0.378577	9.846183	0.207503	0.334377	3939.747319	0.490442	0.256363	0.539589	0.005953
ZSM-1981-154	*P. pygmaeus*	m	adult	1892-1894	Genepai	lower	right	0.719655	-1.680896	7.688074	1.827611	3.975006	5.802617	0.491988	14.473461	0.408306	0.359944	4190.590614	0.503686	0.664926	1.140553	0.004591
ZSM-1981-155	*P. pygmaeus*	f	adult	1892-1894	Genepai	lower	right	0.649558	-0.903147	4.552345	1.442676	3.252237	4.694913	0.487341	10.195034	0.32725	0.425561	3948.340165	0.859468	0.309415	0.47287	0.005477
ZSM-1981-156	*P. pygmaeus*	f	adult	1892-1894	Bogau	lower	right	1.242479	-0.712769	2.980501	2.226474	4.166973	6.393447	1.006883	17.895387	0.574356	0.790174	3252.038093	1.207198	0.239828	0.727386	0.006453
ZSM-1981-159	*P. pygmaeus*	f	adult	1892-1894	Bogau	lower	right	0.46445	-1.34999	5.807769	1.261357	2.536861	3.798218	0.346079	7.153694	0.616533	0.484126	3426.836582	1.732644	0.199436	0.632594	0.004293
ZSM-1981-162	*P. pygmaeus*	f	subadult	1892-1894	Bogau	lower	right	0.266475	-0.878199	4.296221	0.780366	1.442062	2.222428	0.205506	12.470782	0.454556	0.167381	4793.283949	0.554008	0.274845	0.503318	0.004885
ZSM-1981-163	*P. pygmaeus*	f	adult	1892-1894	Bogau	lower	right	0.543597	-1.855802	7.938063	1.16877	3.655665	4.824435	0.396167	10.054872	0.350303	0.413103	4089.987248	1.169438	0.299743	0.779054	0.00596
ZSM-1981-165	*P. pygmaeus*	f	adult	1892-1894	Genepai	lower	right	0.671609	-2.11421	9.000964	1.134587	3.747236	4.881823	0.451185	14.141969	0.773422	0.415293	3287.639654	0.942782	0.401401	0.60649	0.002983
ZSM-1981-166	*P. pygmaeus*	f	adult	1892-1894	Bogau	lower	right	0.469467	-0.807139	4.37707	1.335665	2.403849	3.739514	0.354043	11.457402	0.351392	0.295992	4070.627897	0.886756	0.203606	0.529561	0.00559
ZSM-1981-167	*P. pygmaeus*	f	adult	1892-1894	Genepai	lower	right	1.242146	-2.056662	8.086271	1.935829	6.35648	8.292309	0.864333	12.957664	0.931456	0.923671	3630.887327	2.239004	0.589808	1.024549	0.001831
ZSM-1981-168	*P. pygmaeus*	f	adult	1892-1894	Genepai	lower	right	0.688888	-0.57374	4.000626	2.02329	3.336838	5.360128	0.534442	14.974622	0.454461	0.355599	4065.599474	1.306573	0.268416	0.414304	0.003206
ZSM-1981-179	*P. pygmaeus*	f	adult	1892-1894	Landak	lower	right	0.237158	-2.191579	11.993338	0.569216	2.007964	2.57718	0.165621	10.156917	0.786556	0.178976	4842.287223	0.575501	0.211493	0.389047	0.003548
ZSM-1981-182	*P. pygmaeus*	f	adult	1892-1894	Batangtu	lower	right	0.554399	-0.950759	6.127702	1.444761	3.260137	4.704898	0.414248	15.853567	0.599591	0.28335	4473.700952	1.031788	0.203636	0.393592	0.0029
ZSM-1981-188	*P. pygmaeus*	f	adult	1892-1894	Batangtu	lower	right	0.460661	-1.904434	8.306852	0.89686	3.391522	4.288382	0.335663	6.585154	0.386068	0.473478	3936.087768	2.136841	0.145323	0.383781	0.005114
ZSM-1981-196	*P. pygmaeus*	m	adult	1892-1894	Dadap	lower	right	0.457005	-0.21742	3.577617	1.703695	1.88625	3.589945	0.354128	8.141411	0.380832	0.410601	3344.792731	0.790691	0.17882	0.412235	0.005101
ZSM-1981-198	*P. pygmaeus*	m	adult	1892-1894	Dadap	lower	right	0.905096	-2.623021	15.403237	2.415672	6.918882	9.334554	0.588085	15.638152	0.665822	0.347739	4638.103647	0.839458	0.63298	1.026924	0.003351
ZSM-1981-199	*P. pygmaeus*	m	adult	1892-1894	Dadap	lower	right	0.709713	-2.275102	10.056022	1.946163	4.624576	6.570739	0.450995	12.008608	0.830164	0.437899	4384.523558	1.290925	0.493746	0.931733	0.004112
ZSM-1981-203	*P. pygmaeus*	m	adult	1892-1894	Rantai	lower	right	1.294055	-1.216423	5.37851	2.422659	6.116731	8.53939	0.967953	16.231394	0.806878	0.715167	3248.243648	1.786469	1.848204	1.792096	0.004265
ZSM-1981-204	*P. pygmaeus*	m	subadult	1892-1894	Rantai	lower	right	0.63692	0.064156	3.556256	2.852149	2.761056	5.613205	0.49925	13.326106	0.520393	0.34292	3729.661987	0.611472	0.382757	0.737764	0.003384
ZSM-1981-209	*P. pygmaeus*	f	subadult	1892-1894	Rantai	lower	right	1.273223	-0.394437	3.357557	3.231158	4.580767	7.811925	0.983587	16.003467	0.726515	0.73828	3834.964028	1.467205	0.351739	0.495021	0.000333
ZSM-1981-21	*P. pygmaeus*	f	juvenile	1892-1894	Skalau	lower	right	0.490681	-1.03399	4.872272	1.357351	2.602688	3.960039	0.366838	7.843037	0.40637	0.441252	3553.649775	1.474887	0.284152	0.628001	0.004343
ZSM-1981-216	*P. pygmaeus*	m	subadult	1892-1894	Ketungau	lower	right	0.81892	-0.927728	5.027595	2.40129	3.590647	5.991937	0.586166	11.843393	0.727055	0.710866	3920.364896	2.119437	0.434456	0.579794	0.002382
ZSM-1981-22	*P. pygmaeus*	f	juvenile	1892-1894	Skalau	lower	right	0.760897	-1.060346	4.098212	1.738675	3.503851	5.242526	0.599166	8.764206	0.562893	0.602845	3513.625798	1.592693	0.191102	0.631178	0.005182
ZSM-1981-23	*P. pygmaeus*	f	juvenile	1892-1894	Skalau	lower	right	1.030904	-0.650435	6.322647	4.131463	6.696355	10.827818	0.72731	11.812175	0.64141	0.578566	4021.958808	1.943269	0.364472	1.062107	0.001377

ZSM-1981-234	*P. pygmaeus*	m	adult	1892-1894	Skalau	lower	right	0.921274	-0.65523	3.194034	1.961218	4.309594	6.270812	0.744829	16.662456	0.754799	0.5679	3208.161323	0.884568	0.919508	1.39641	0.002154
ZSM-1981-25	*P. pygmaeus*	m	adult	1892-1894	Skalau	lower	right	0.399318	-0.768348	4.611814	1.133412	2.281166	3.414578	0.311798	7.708523	0.548782	0.347967	4598.987812	1.817488	0.256904	0.364163	0.006042
ZSM-1981-26	*P. pygmaeus*	m	subadult	1892-1894	Skalau	lower	right	0.647768	-0.489347	3.420075	2.017586	3.313488	5.331074	0.514052	7.22762	0.363176	0.695933	3785.677991	2.377237	0.137239	0.296148	0.005892
ZSM-1981-27	*P. pygmaeus*	m	adult	1892-1894	Skalau	lower	right	0.599576	-1.208746	4.673391	1.475033	2.961636	4.436669	0.456322	9.99637	0.716356	0.457591	3939.398296	1.507291	0.230784	0.610397	0.003193
ZSM-1981-28	*P. pygmaeus*	f	adult	1892-1894	Skalau	lower	right	0.769874	-0.359521	2.806672	2.09693	2.470977	4.567907	0.610136	13.646296	0.327996	0.538042	4509.944273	0.857142	0.409006	0.66186	0.005526
ZSM-1981-32	*P. pygmaeus*	m	subadult	1892-1894	Skalau	lower	right	1.06642	-1.027698	4.251999	1.832172	5.397078	7.22925	0.850414	15.821262	0.757454	0.722998	3525.146076	1.621752	0.337202	0.705004	0.003295
ZSM-1981-33	*P. pygmaeus*	f	adult	1892-1894	Skalau	lower	right	0.845928	-0.78202	5.026086	2.29107	4.890371	7.181441	0.629574	13.736855	0.608548	0.568418	3430.446354	0.98849	0.672895	0.921009	0.006075
ZSM-1981-45	*P. pygmaeus*	m	adult	1892-1894	Skalau	lower	right	1.12228	-0.649389	4.925934	3.554137	5.549889	9.104026	0.851292	15.614555	0.388099	0.563425	4063.92071	1.818855	0.553816	0.657086	0.003724
ZSM-1981-50	*P. pygmaeus*	f	adult	1892-1894	Skalau	lower	right	1.770626	-1.541692	5.693875	3.572859	8.186342	11.759201	1.30029	20.483678	0.856125	0.889848	4059.579287	4.101354	2.962676	2.932379	0.002346
ZSM-1981-53	*P. pygmaeus*	m	adult	1892-1894	Skalau	lower	right	0.528245	-2.353443	11.496213	0.798121	3.916292	4.714413	0.364527	8.826304	0.546133	0.390381	4362.108925	0.900755	0.440203	1.079878	0.005967
ZSM-1981-60	*P. pygmaeus*	f	adult	1892-1894	Skalau	lower	right	0.891636	-1.053818	4.327479	3.490235	4.138667	7.628902	0.679485	17.938863	0.80677	0.462444	3591.721896	0.917049	0.638655	1.241041	0.00205
ZSM-1981-62	*P. pygmaeus*	f	adult	1892-1894	Skalau	lower	right	0.307497	-0.601632	3.218346	0.852141	1.22131	2.073451	0.243697	10.028531	0.583649	0.273695	3804.073462	0.547227	0.142272	0.360983	0.004578
ZSM-1981-63	*P. pygmaeus*	m	subadult	1892-1894	Skalau	lower	right	0.8473	-1.540928	6.707056	1.536295	4.889775	6.42607	0.628453	11.219759	0.595365	0.740328	3798.047149	2.220574	0.355438	0.601293	0.003866
ZSM-1981-64	*P. pygmaeus*	m	adult	1892-1894	Skalau	lower	right	0.466104	-1.324753	4.888921	1.206586	2.392583	3.599169	0.357467	11.381633	0.709624	0.344577	3828.077986	0.765255	0.376074	0.587431	0.003259
ZSM-1981-67	*P. pygmaeus*	f	subadult	1892-1894	Skalau	lower	right	0.421813	-1.38475	5.353273	0.965812	2.257924	3.223736	0.316884	6.666852	0.366292	0.419702	4113.815823	1.501523	0.236627	0.685124	0.005968
ZSM-1981-68	*P. pygmaeus*	m	adult	1892-1894	Skalau	lower	right	0.52908	-0.77997	4.396998	1.737792	2.783388	4.52118	0.405168	15.077684	0.725641	0.336042	3932.300604	0.886387	0.253495	0.520715	0.005097
ZSM-1981-69	*P. pygmaeus*	m	adult	1892-1894	Skalau	lower	right	0.664312	-1.582608	5.765393	1.049434	3.151329	4.200763	0.500601	10.993092	0.719516	0.555813	3340.111093	2.108902	0.190738	0.658002	0.003466
ZSM-1981-70	*P. pygmaeus*	m	adult	1892-1894	Skalau	lower	right	0.462856	-1.6068	7.500552	0.882124	3.310453	4.192577	0.333645	13.600141	0.624756	0.250142	4345.472035	0.413387	0.365163	0.67372	0.001634
ZSM-1981-71	*P. pygmaeus*	m	adult	1892-1894	Skalau	lower	right	1.120262	-2.497124	12.696559	2.196953	8.602355	10.799308	0.743989	12.655254	0.639825	0.563944	3759.253053	1.769324	1.089165	1.666117	0.003699
ZSM-1981-74	*P. pygmaeus*	f	adult	1892-1894	Skalau	lower	right	0.430557	-2.101009	11.645744	1.082435	3.242039	4.324474	0.297154	12.102233	0.684122	0.254409	3938.549663	0.467888	0.322305	0.602951	0.002015
ZSM-1981-75	*P. pygmaeus*	f	adult	1892-1894	Skalau	lower	right	0.691	-1.186951	5.555528	1.38046	4.443513	5.823973	0.536695	10.544115	0.758529	0.57828	3676.192029	1.197408	0.339429	0.809979	0.002248
ZSM-1981-76	*P. pygmaeus*	f	adult	1892-1894	Skalau	lower	right	0.661546	-2.640621	12.647754	1.274745	4.711547	5.986292	0.428529	10.566224	0.866046	0.488913	3673.263954	1.069163	0.416025	1.444811	0.001128
ZSM-1981-78	*P. pygmaeus*	f	adult	1892-1894	Skalau	lower	right	1.027526	-0.985974	4.973287	2.216234	4.706841	6.923075	0.766756	14.215196	0.42805	0.676591	3870.827301	1.029633	0.308119	0.678009	0.007039
ZSM-1981-79	*P. pygmaeus*	f	adult	1892-1894	Skalau	lower	right	0.35043	-2.045907	13.186677	0.933041	2.855805	3.788846	0.246072	10.124588	0.751806	0.254535	4764.81784	0.745788	0.423705	1.114812	0.000568
ZSM-1981-83	*P. pygmaeus*	f	adult	1892-1894	Skalau	lower	right	0.579395	-1.559609	8.099129	1.318196	4.107876	5.426072	0.413053	11.859676	0.796709	0.377639	4197.67619	1.254163	0.484406	0.738077	0.00349
ZSM-1981-86	*P. pygmaeus*	f	adult	1892-1894	Skalau	lower	right	0.196443	-1.091793	5.767978	0.611985	1.113525	1.72551	0.147334	11.30829	0.427372	0.13135	5067.582364	0.250891	0.329142	0.661819	0.006435
ZSM-1981-88	*P. pygmaeus*	f	adult	1892-1894	Skalau	lower	right	0.497495	-0.860189	4.392611	1.143616	2.516451	3.660067	0.375885	13.829723	0.564258	0.335126	4314.310593	0.869536	0.296439	0.603106	0.005844
ZSM-1981-89	*P. pygmaeus*	f	adult	1892-1894	Skalau	lower	right	0.833263	-1.561029	6.314334	1.711186	5.287674	6.99886	0.610118	11.651281	0.798887	0.78284	4339.381534	3.709229	0.281764	0.871761	0.002754
ZSM-1981-90	*P. pygmaeus*	f	adult	1892-1894	Skalau	lower	right	0.333188	-0.235182	4.449524	1.585064	2.114161	3.699225	0.255689	10.485342	0.493138	0.243631	5357.101827	2.598188	0.306903	0.463525	0.003328
ZSM-1981-91	*P. pygmaeus*	f	adult	1892-1894	Skalau	lower	right	0.385924	-1.191181	5.407746	1.178072	2.134131	3.312203	0.289218	14.12775	0.615013	0.245435	4804.734194	0.982816	0.210979	0.361064	0.003532
ZSM-1981-92	*P. pygmaeus*	f	senil	1892-1894	Skalau	lower	right	0.54442	-1.707002	7.972157	1.412672	4.298848	5.71152	0.403247	7.032854	0.572147	0.469909	4203.851395	1.970858	0.187785	0.628301	0.004627
ZSM-1981-94	*P. pygmaeus*	m	adult	1892-1894	Skalau	lower	right	0.470034	-1.761574	8.580229	1.356649	3.473874	4.830523	0.325607	10.089458	0.80547	0.404085	4106.56235	1.081993	0.361749	0.665783	0.003879
ZSM-1981-95	*P. pygmaeus*	f	adult	1892-1894	Skalau	lower	right	0.139333	-0.530474	3.494047	0.552511	0.842553	1.395064	0.110176	6.897711	0.4162	0.146719	4665.384999	0.406181	0.24291	0.582796	0.00463
ZSM-1981-96	*P. pygmaeus*	f	adult	1892-1894	Skalau	lower	right	0.404648	-0.59499	3.78424	1.681557	2.377463	4.05902	0.319142	10.491294	0.572099	0.343153	4364.262488	0.662258	0.646888	0.814742	0.003421
ZSM-1981-97	*P. pygmaeus*	f	adult	1892-1894	Skalau	lower	right	0.421378	-1.151974	4.165942	1.012288	1.944591	2.956879	0.319977	12.302125	0.560001	0.329754	4904.08977	1.359025	0.440622	0.627877	0.002939
ZSM-1981-99	*P. pygmaeus*	m	adult	1892-1894	Skalau	lower	right	0.213639	-0.269926	3.603087	0.803235	1.151888	1.955123	0.1702	8.296071	0.621879	0.159028	4557.072629	0.395412	0.301049	0.698863	0.005534

t.

Supplementary Information

Results of the first principal component analysis

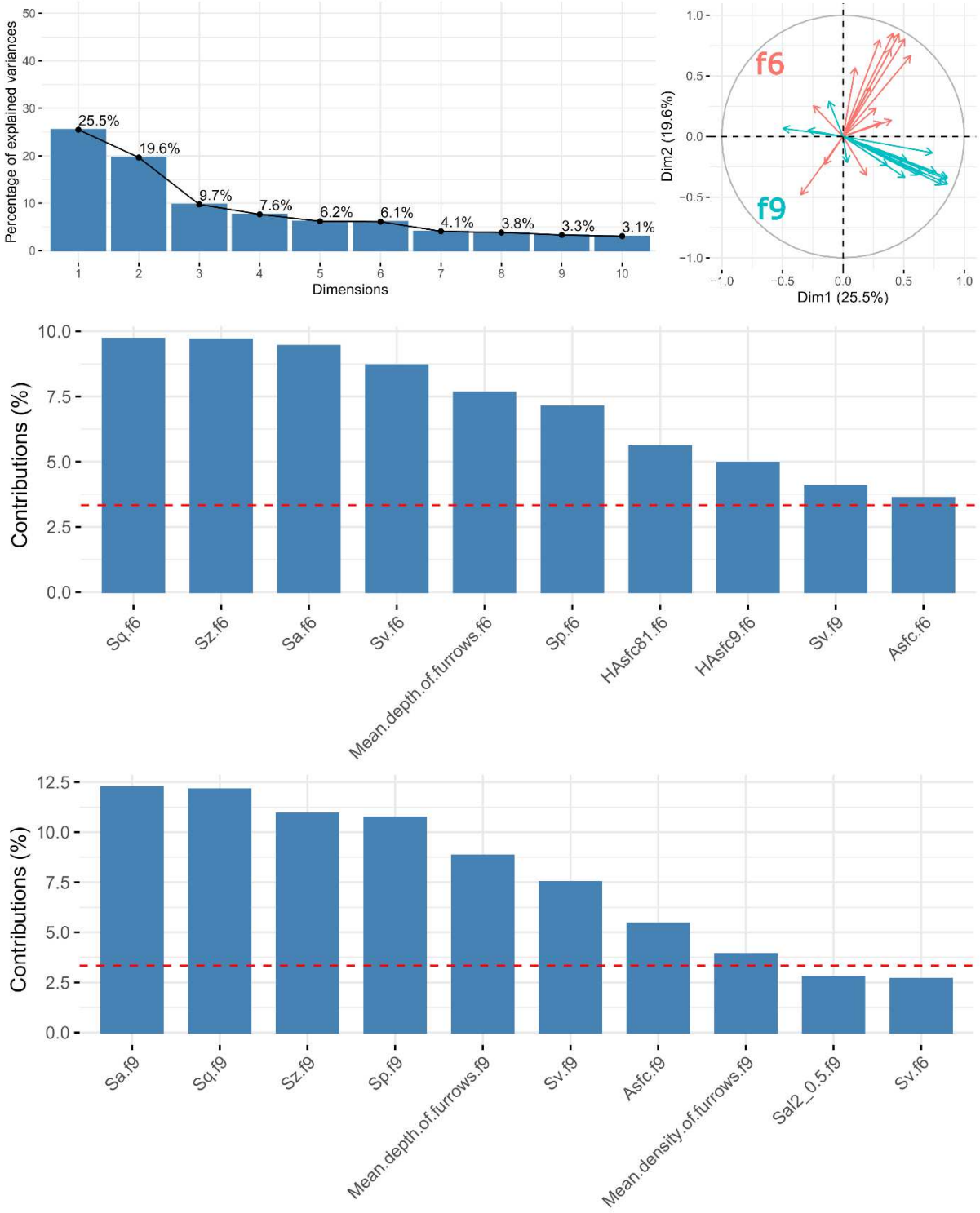

Fig. SI 1 Plots from the first PCA round. Scree plot (top left), correlation circle (top right), most contributing variables PC 1 (middle) and PC 2 (bottom). The colours in the correlation circle differentiate between parameters from the two different facets (f6 = red, f9 = blue). The red dashed line indicates the expected contribution per variable, if all of them contributed equally. Thus, variables whose contributions are above this threshold have an important contribution to the PC and were included in the second PCA round.

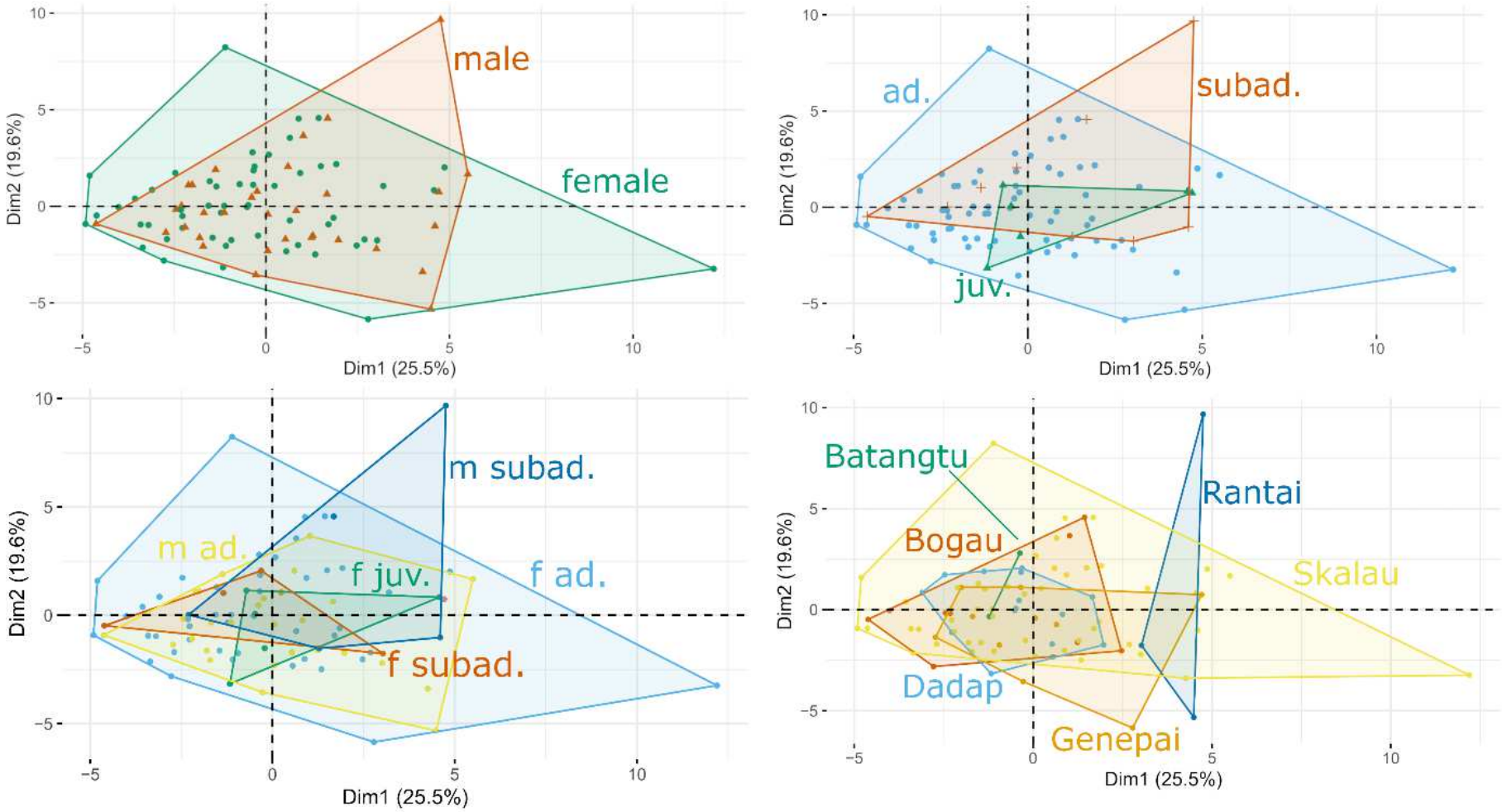

Fig. SI 2 Distribution of the individuals along PC 1 and PC 2 of the first PCA round grouped by sexes (top left), age groups (top right), sex-age groups (bottom left), and localities (bottom right).s

Extended figures PCA round 2

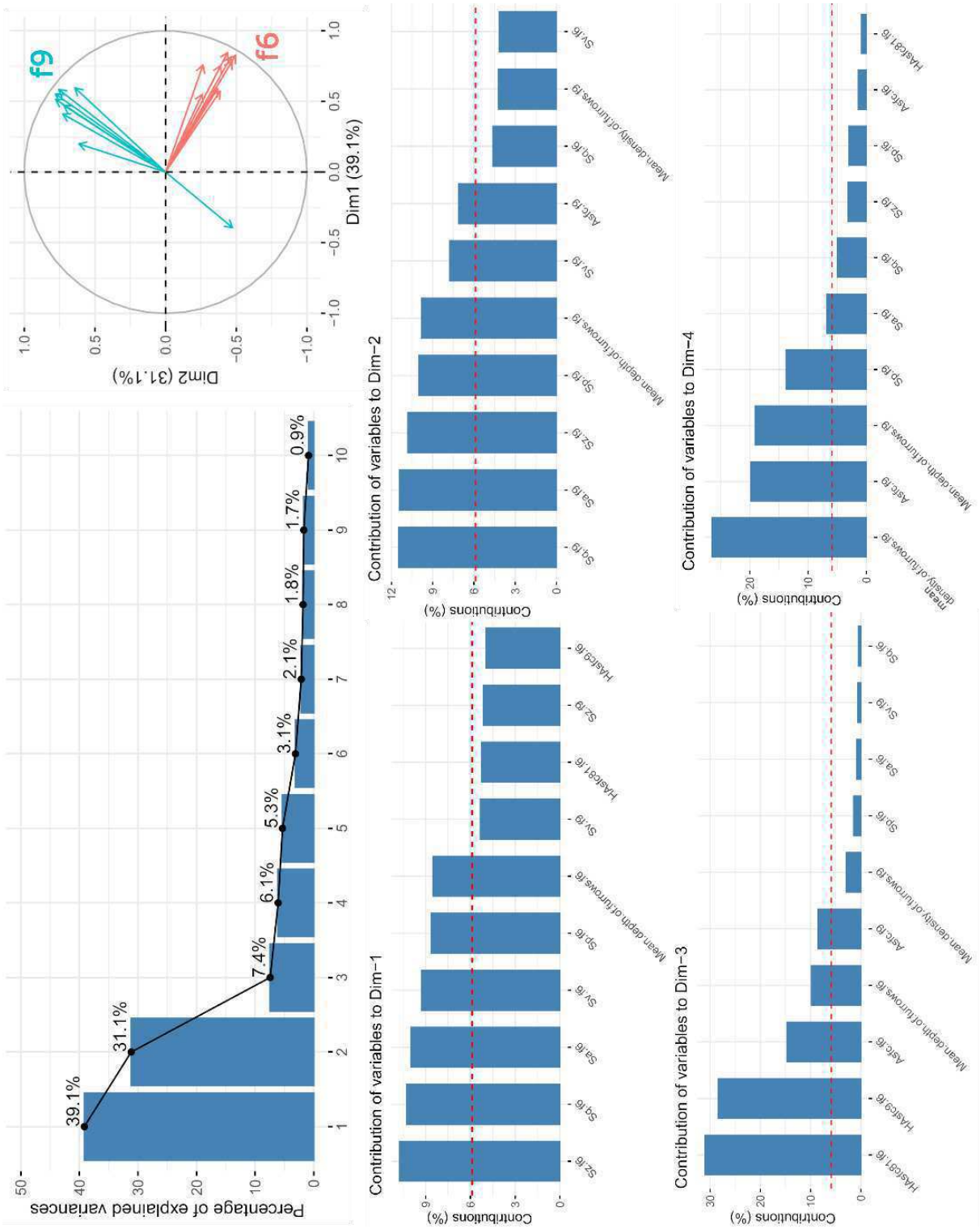

Fig. SI 3 Plots from the second PCA round. Scree plot (top left), correlation circle (top right), most contributing variables PC 1 (middle left), PC 2 (middle right), PC 3 (bottom left), and PC 4 (bottom right). The colours in the correlation circle differentiate between parameters from the two different facets (height = red, volume = blue, SSFA = green).

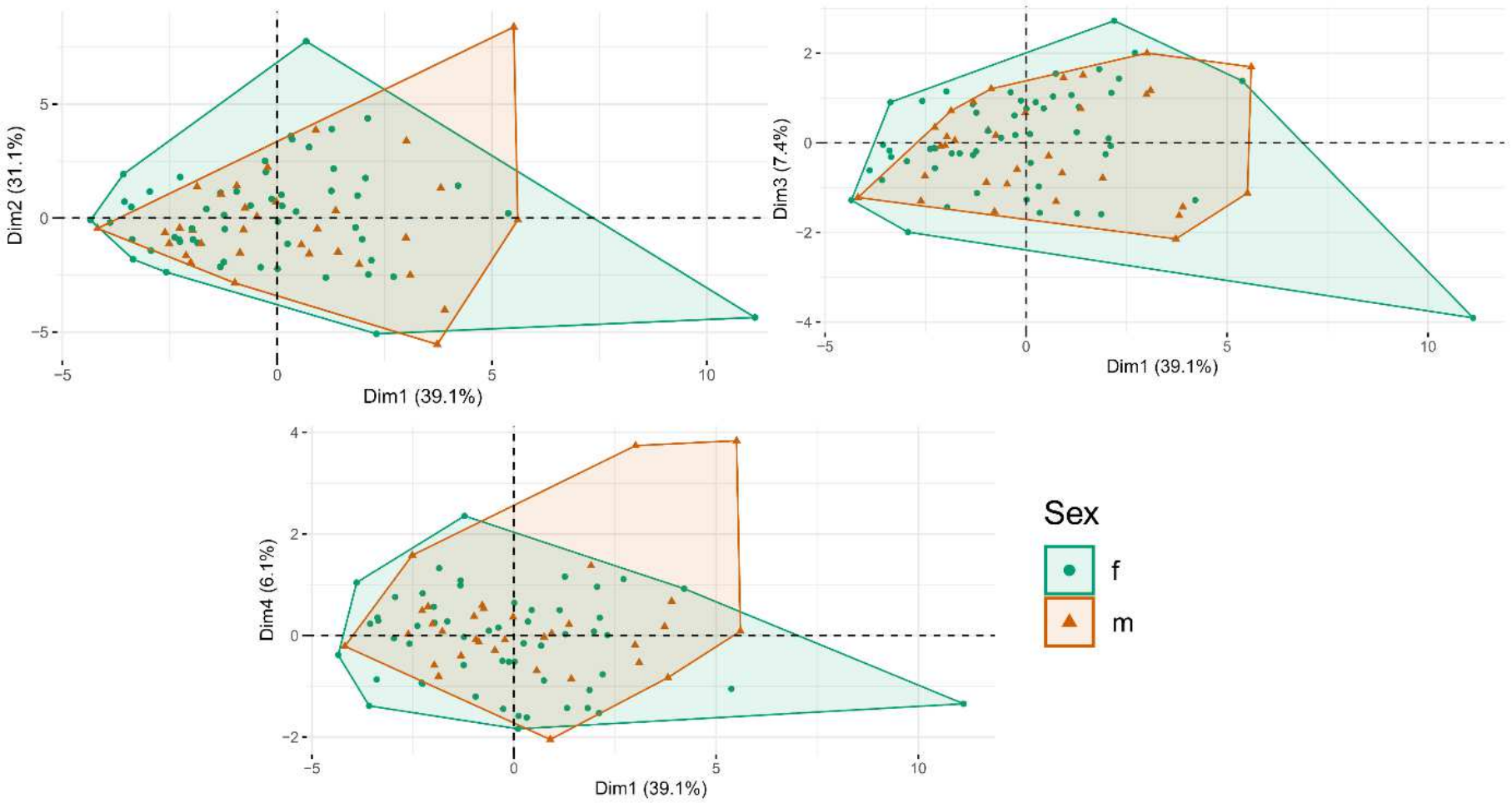

Fig. SI 4 Distribution of the individuals along PC 1 and PC 2 (top left), PC 3 (top right), or PC 4 (bottom) grouped per sex

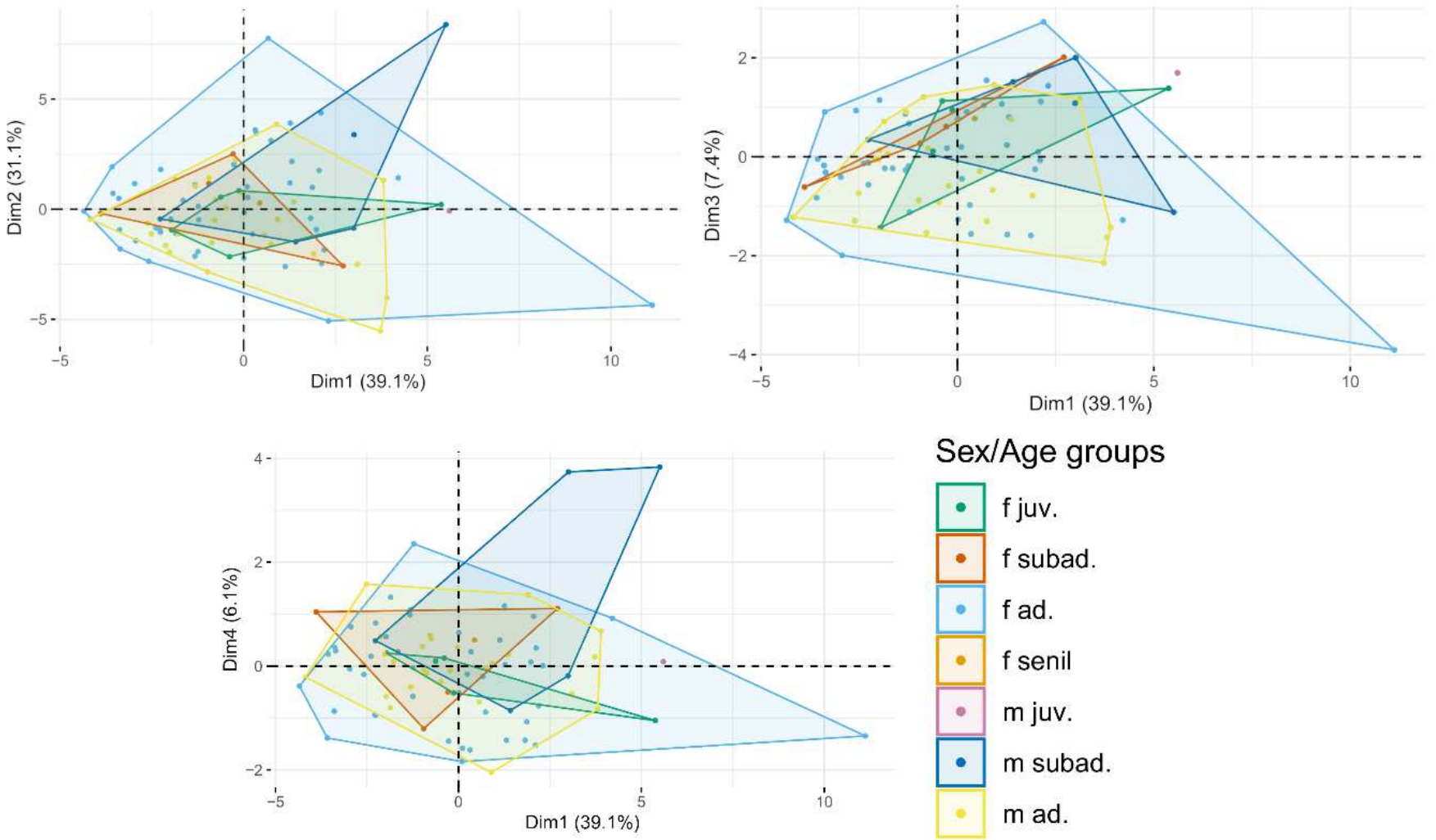

Fig. SI 5 Distribution of the individuals along PC 1 and PC 2 (top left), PC 3 (top right), or PC 4 (bottom) grouped per sex-age group.

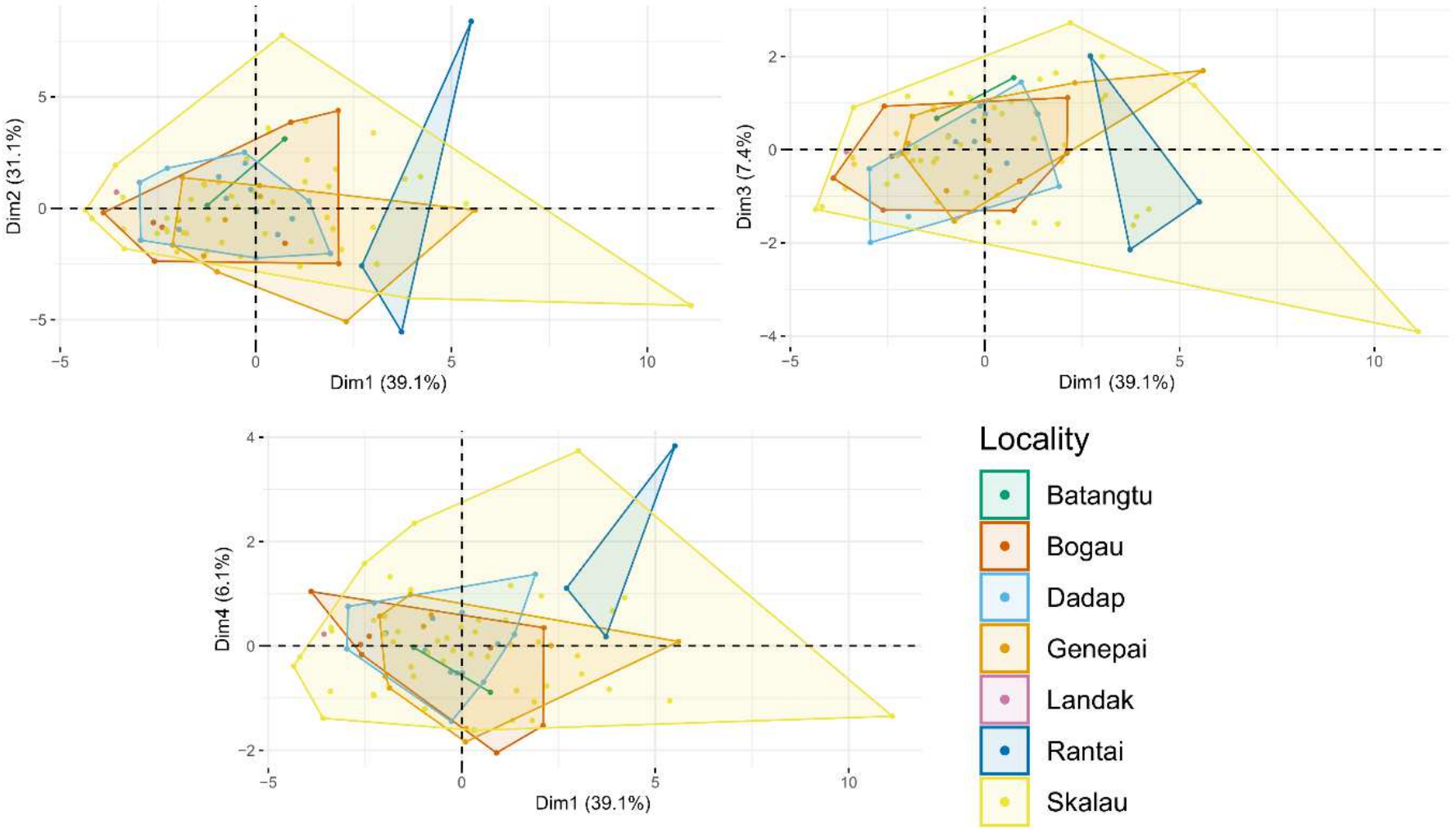

Fig. SI 6 Distribution of the individuals along PC 1 and PC 2 (top left), PC 3 (top right), or PC 4 (bottom) grouped per locality.

Boxplots for SSFA parameters on all groupings and each facet

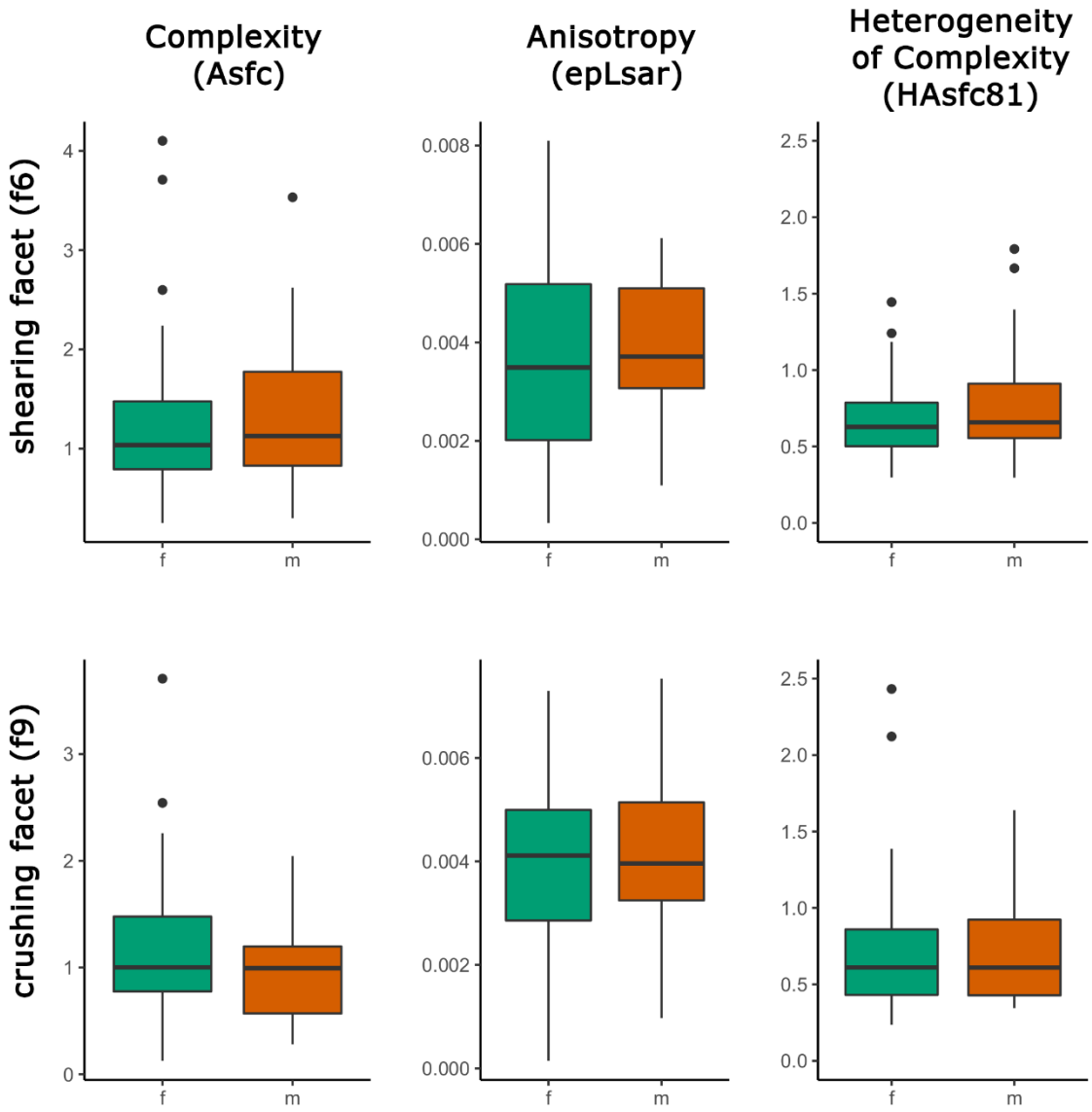

Fig. SI 7 Boxplots of three SSFA parameters for female (f) and male (m) individuals of the complete data set (including Sumatran specimens) for crushing and shearing facets.

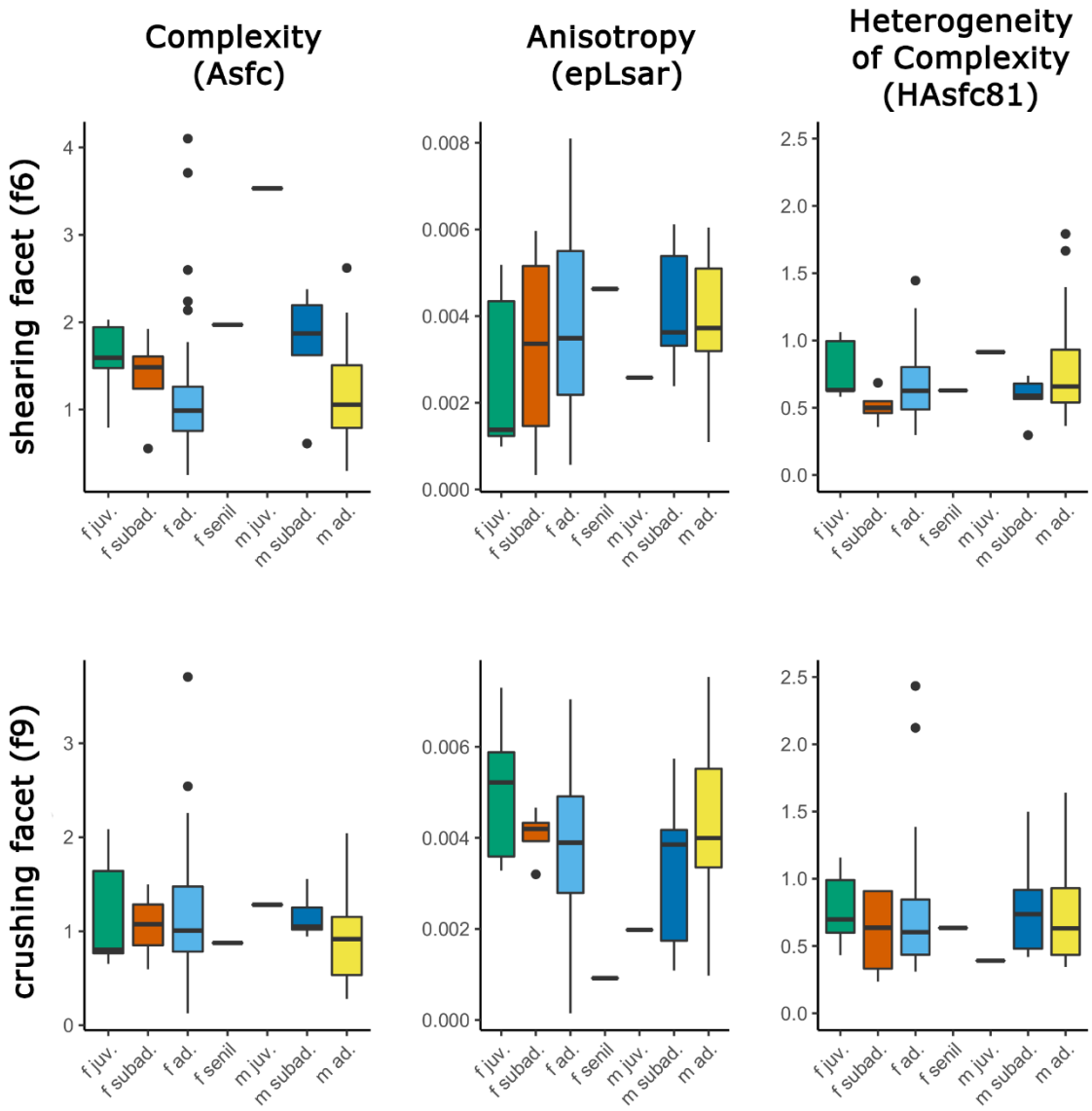

Fig. SI 8 Boxplots of three SSFA parameters for sex-age groups of all in the data set (including Sumatran specimens) for crushing and shearing facets. Female (f), male (m), juvenile (juv.), subadult (subad.), adult (ad.).

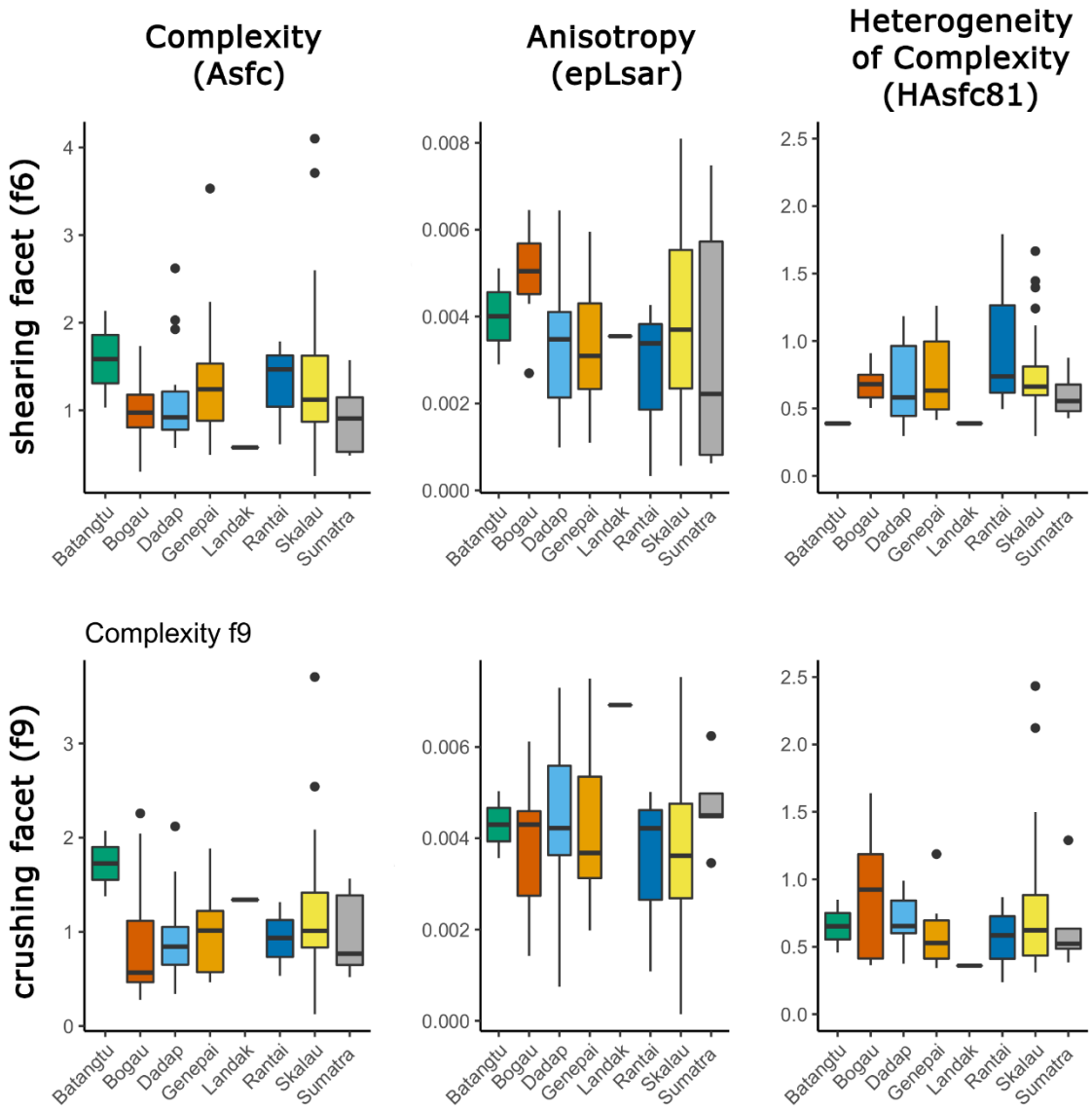

Fig. SI 9 Boxplots of all individuals in the data set per locality groups from the Borneo Islands. Sumatran specimens are included as a separate group.

Photosimulations and false colour maps of all scans

Photosimulations and false colour elevation maps of scanned molar phase I and phase II facets of *P. pygmaeus* and *P. abelii* from Borneo (1892-1894) and Sumatra (1913).

Moulds by Valeria Rojas Cuyutupa (2021/2022) Zoologische Staatssammlung München. Scanned at the PALEVOPRIM lab by Sophie Gabriele Habinger, Université de Poitiers, France and Eberhard Karls Universität Tübingen, Germany with “TRIDENT”, white light confocal microscope Leica DCM8 (2021/2022). Quality controled by Gildas Merceron 2022. The research was part of the EVEPRIMASIA project (ANR 18-CE92-0029 and DFG BO 3478/7-1), PIs Olivier Chavasseau and Hervé Bocherens.

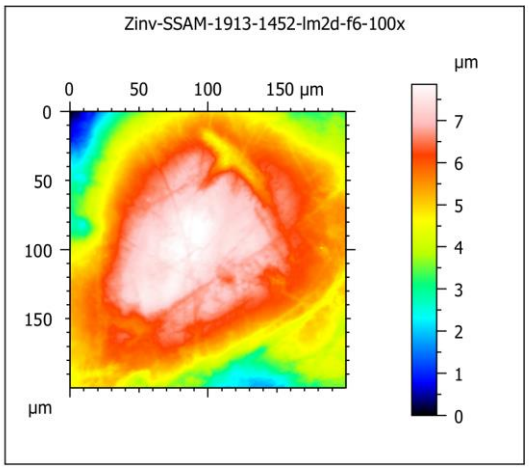

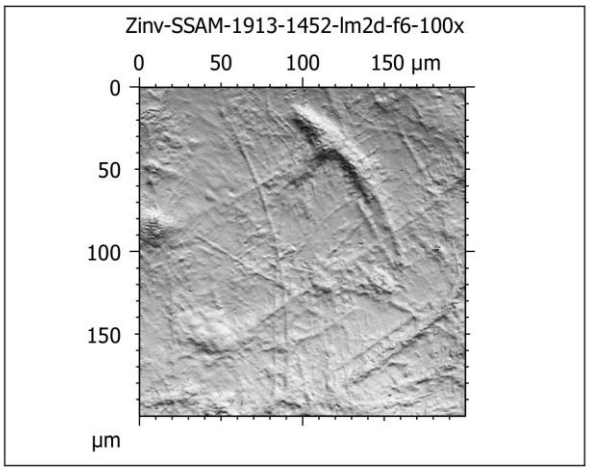

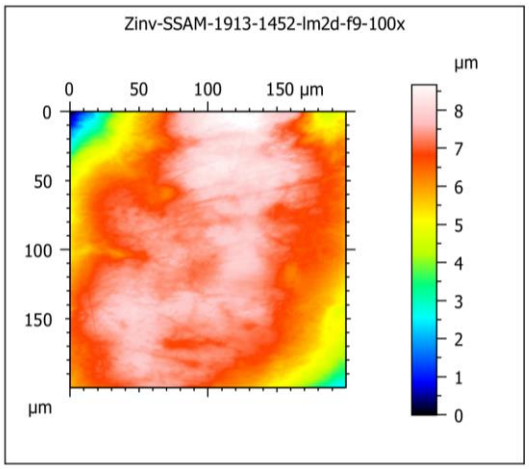

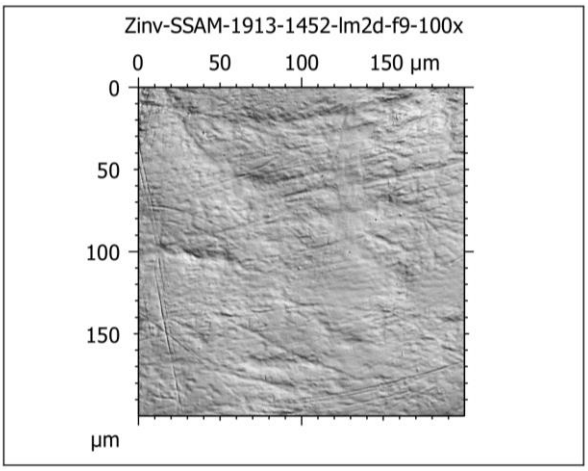

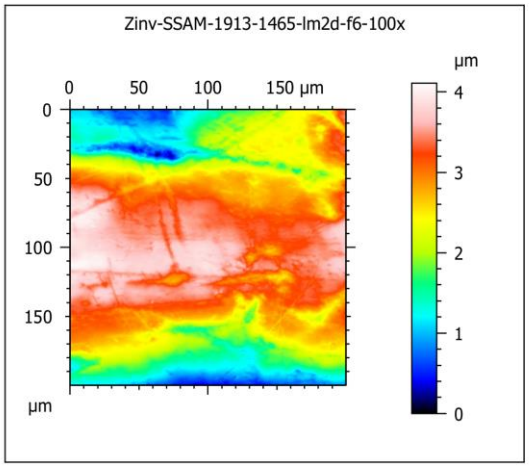

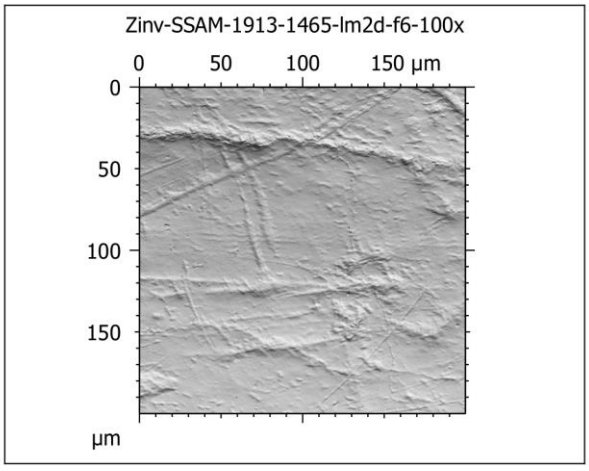

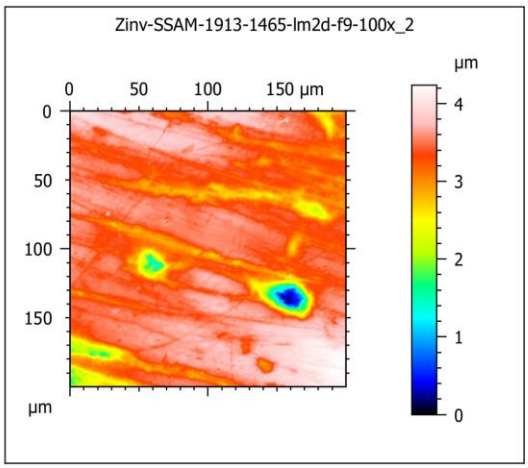
Zinv-SSAM-1913-1465-lm2d-f9-100x_2
0
50
100
150 µm
µm
0
50
100
150
µm
4
3
2
1
0

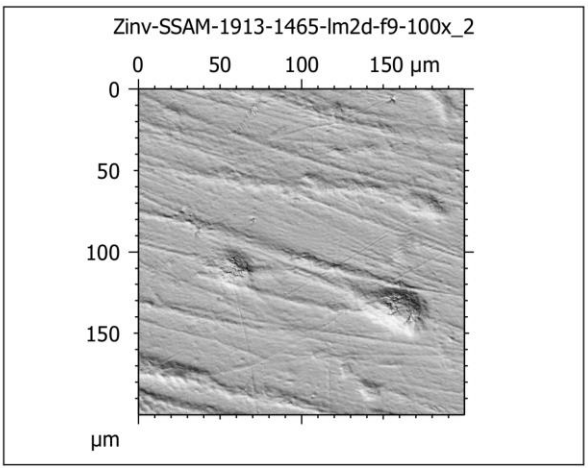
Zinv-SSAM-1913-1465-lm2d-f9-100x_2
0
50
100
150 µm
0
50
100
150
µm

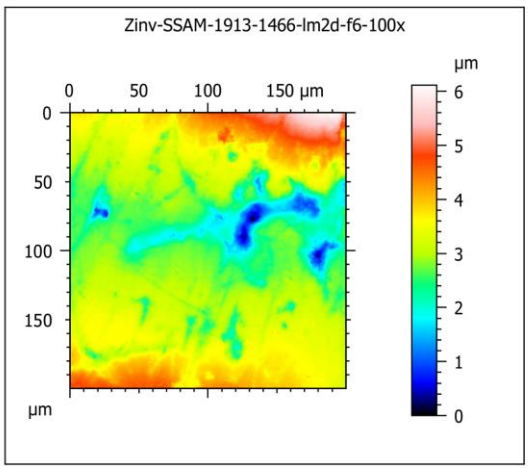
Zinv-SSAM-1913-1466-lm2d-f6-100x
0
50
100
150 µm
µm
0
50
100
150
µm
6
5
4
3
2
1
0

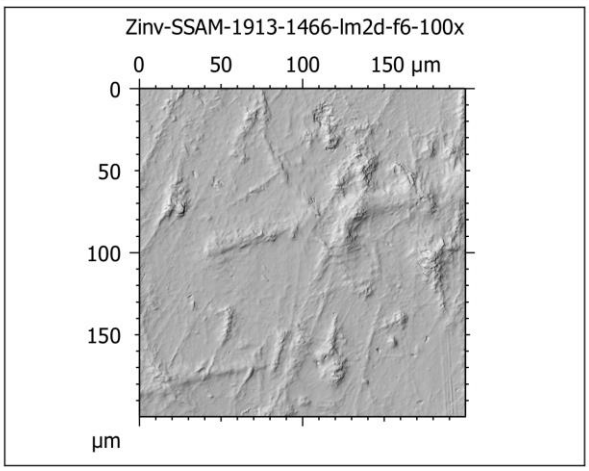
Zinv-SSAM-1913-1466-lm2d-f6-100x
0
50
100
150 µm
0
50
100
150
µm

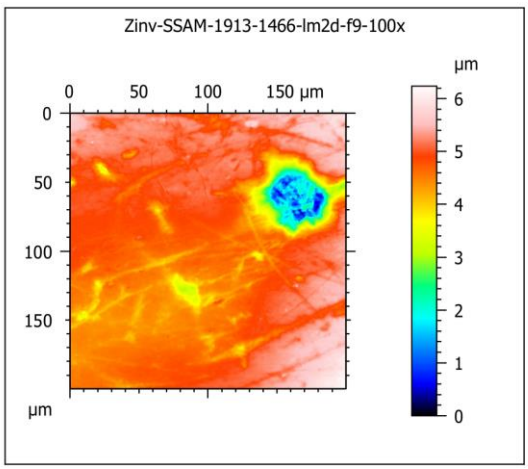
Zinv-SSAM-1913-1466-lm2d-f9-100x
0
50
100
150 µm
µm
0
50
100
150
µm
6
5
4
3
2
1
0

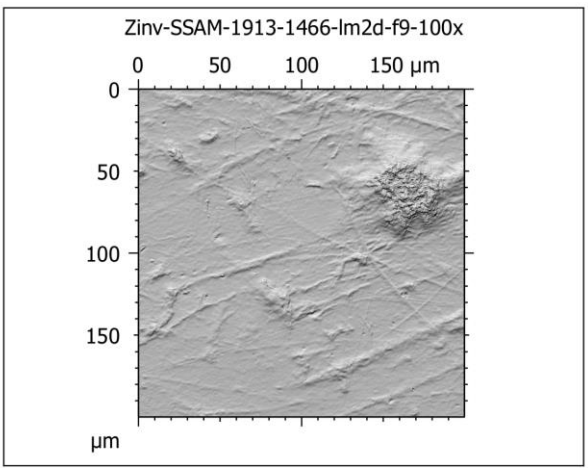
Zinv-SSAM-1913-1466-lm2d-f9-100x
0
50
100
150 µm
0
50
100
150
µm

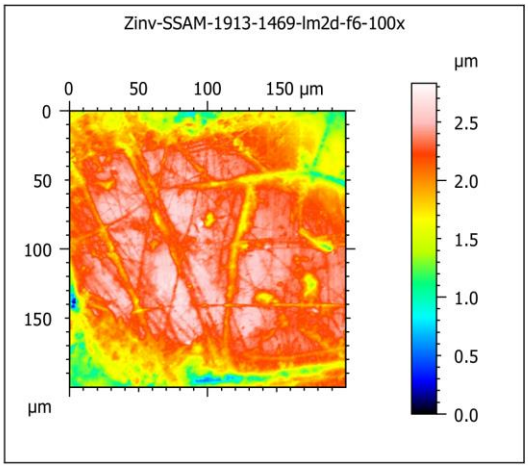
Zinv-SSAM-1913-1469-lm2d-f6-100x
0
50
100
150 µm
µm
2.5
2.0
1.5
1.0
0.5
0.0

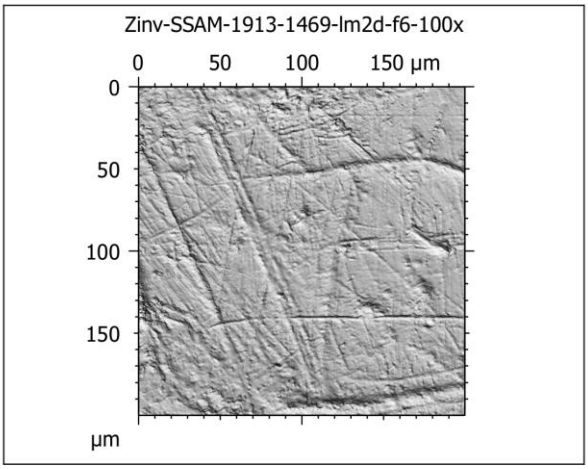
Zinv-SSAM-1913-1469-lm2d-f6-100x
0
50
100
150 µm
µm

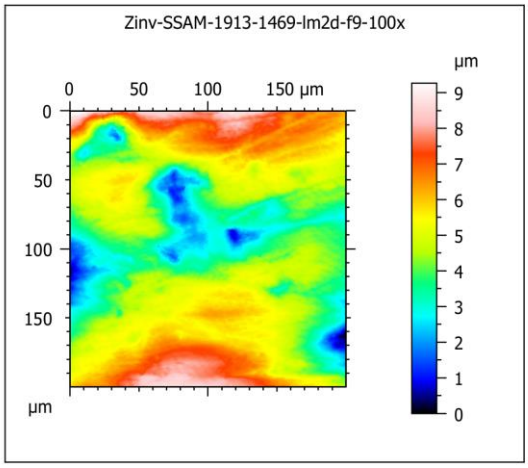
Zinv-SSAM-1913-1469-lm2d-f9-100x
0
50
100
150 µm
µm
9
8
7
6
5
4
3
2
1
0

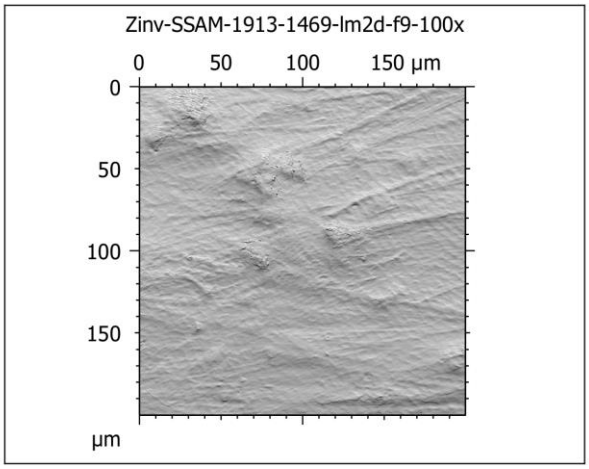
Zinv-SSAM-1913-1469-lm2d-f9-100x
0
50
100
150 µm
µm

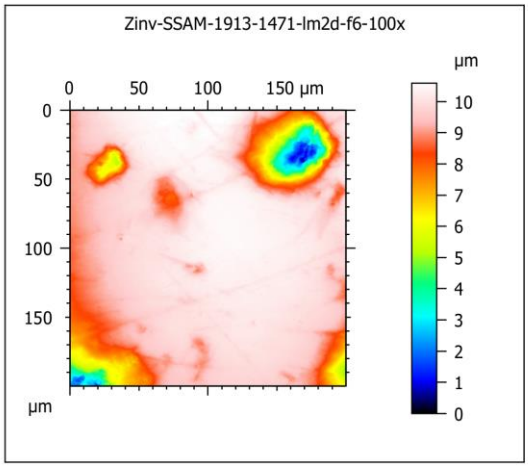
Zinv-SSAM-1913-1471-lm2d-f6-100x
0
50
100
150 µm
µm
10
9
8
7
6
5
4
3
2
1
0

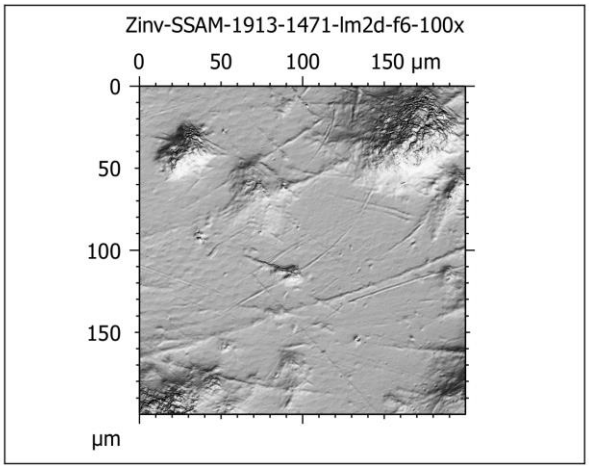
Zinv-SSAM-1913-1471-lm2d-f6-100x
0
50
100
150 µm
µm

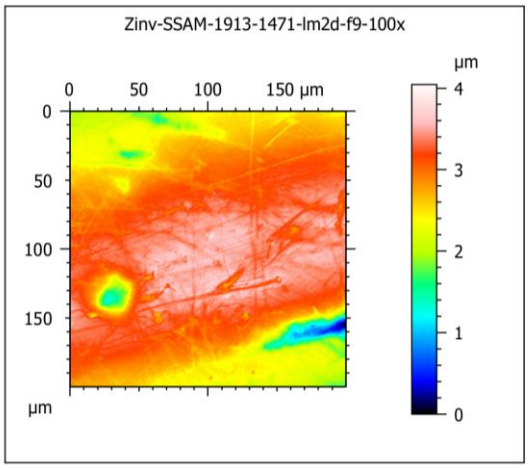
Zinv-SSAM-1913-1471-lm2d-f9-100x
0
50
100
150 µm
µm
4
3
2
1
0

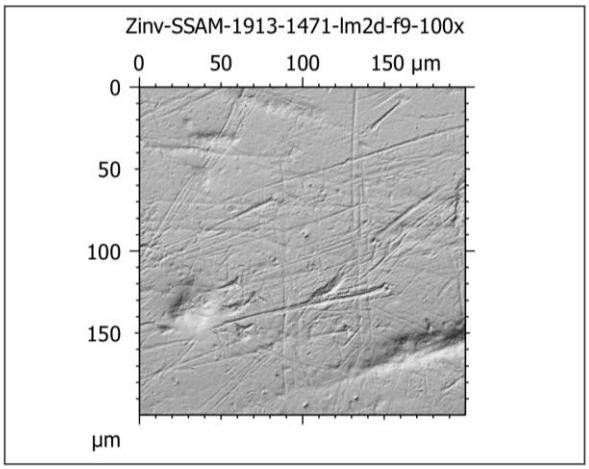
Zinv-SSAM-1913-1471-lm2d-f9-100x
0
50
100
150 µm
µm

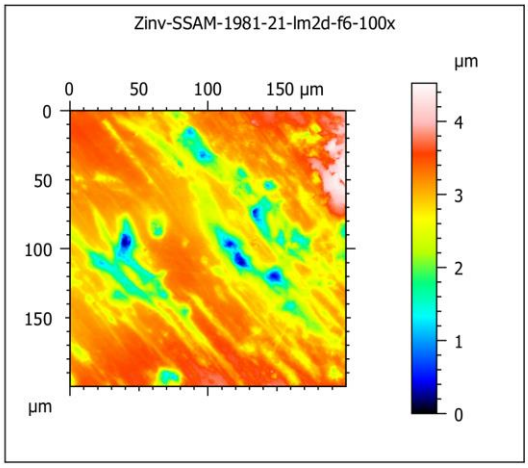
Zinv-SSAM-1981-21-lm2d-f6-100x
0
50
100
150 µm
µm
4
3
2
1
0

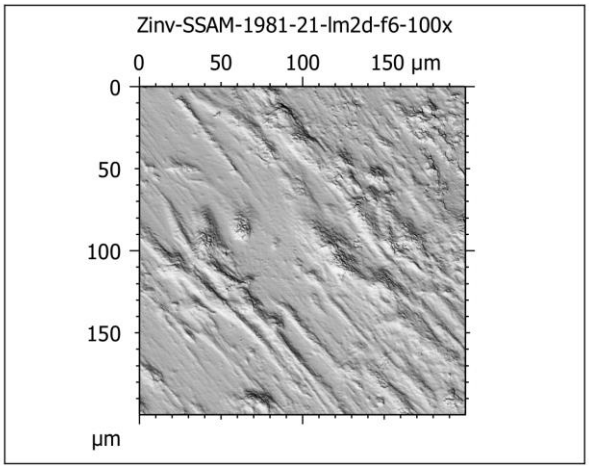
Zinv-SSAM-1981-21-lm2d-f6-100x
0
50
100
150 µm
µm

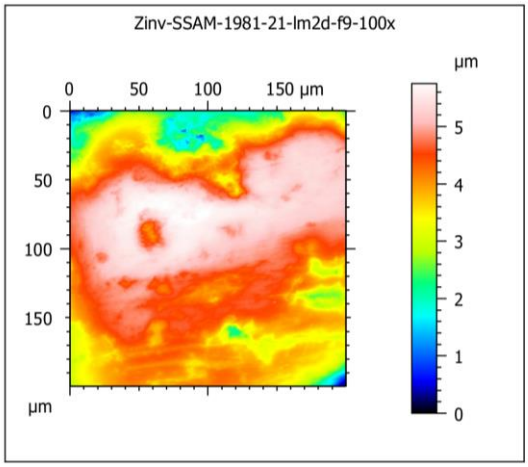
Zinv-SSAM-1981-21-lm2d-f9-100x
0
50
100
150 µm
µm
5
4
3
2
1
0

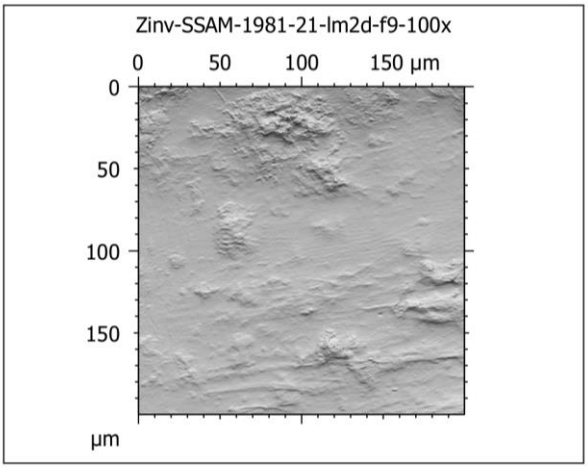
Zinv-SSAM-1981-21-lm2d-f9-100x
0
50
100
150 µm
µm

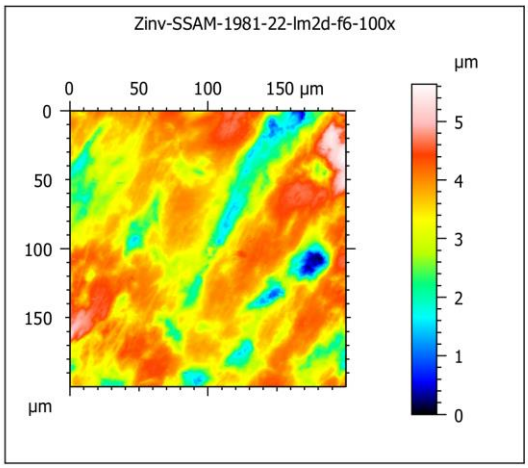
Zinv-SSAM-1981-22-lm2d-f6-100x
0
50
100
150 µm
µm
5
4
3
2
1
0

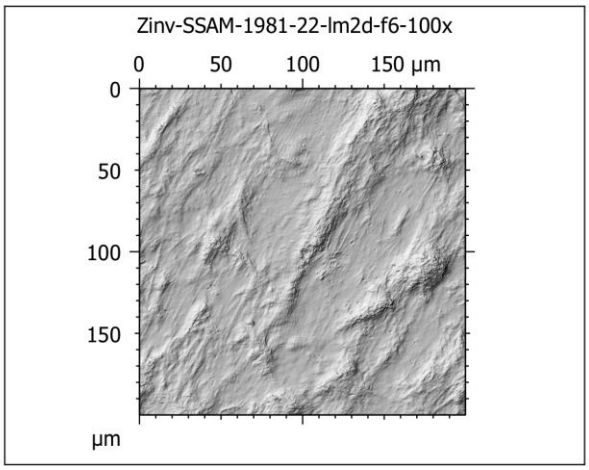
Zinv-SSAM-1981-22-lm2d-f6-100x
0
50
100
150 µm
µm

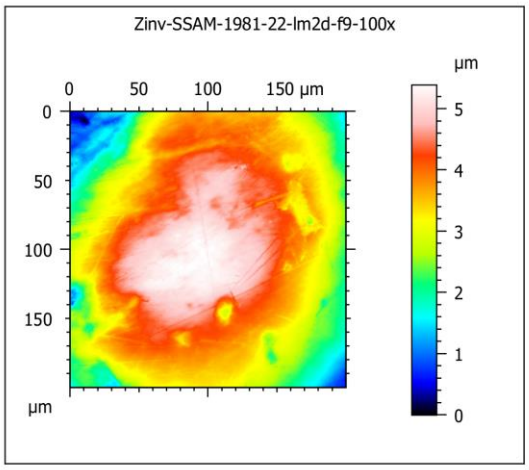
Zinv-SSAM-1981-22-lm2d-f9-100x
0
50
100
150 µm
µm
5
4
3
2
1
0

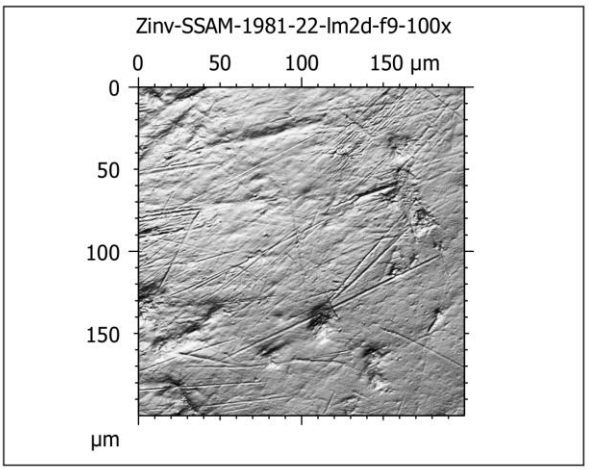
Zinv-SSAM-1981-22-lm2d-f9-100x
0
50
100
150 µm
µm

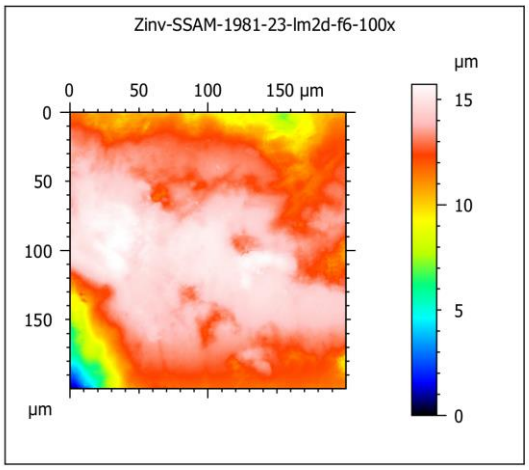
Zinv-SSAM-1981-23-lm2d-f6-100x
0
50
100
150 µm
µm
15
10
5
0

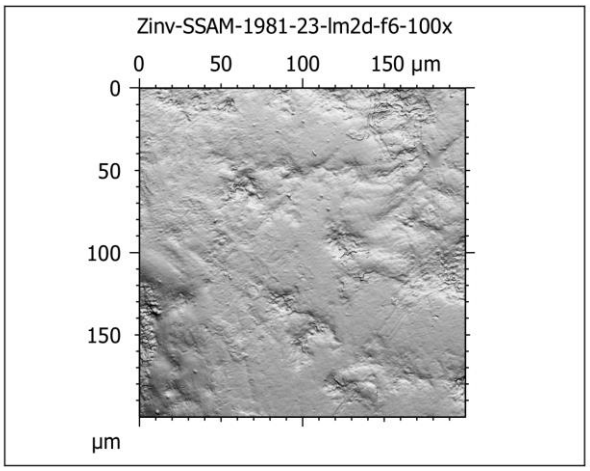
Zinv-SSAM-1981-23-lm2d-f6-100x
0
50
100
150 µm
µm

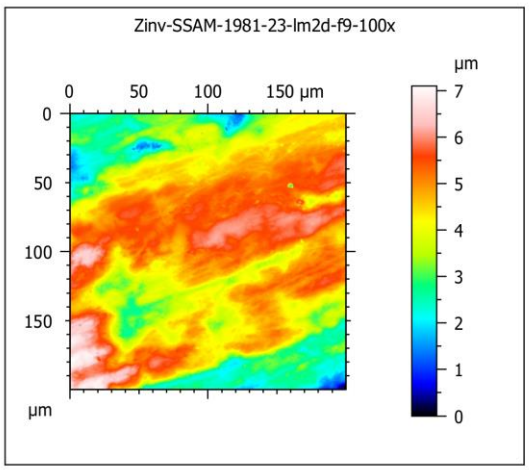
Zinv-SSAM-1981-23-lm2d-f9-100x
0
50
100
150 µm
µm
7
6
5
4
3
2
1
0

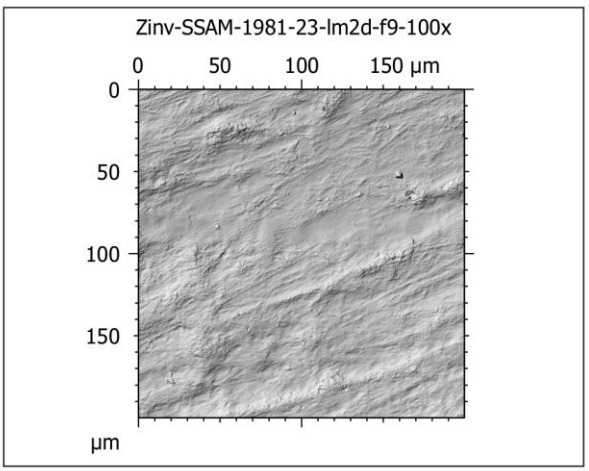
Zinv-SSAM-1981-23-lm2d-f9-100x
0
50
100
150 µm
µm

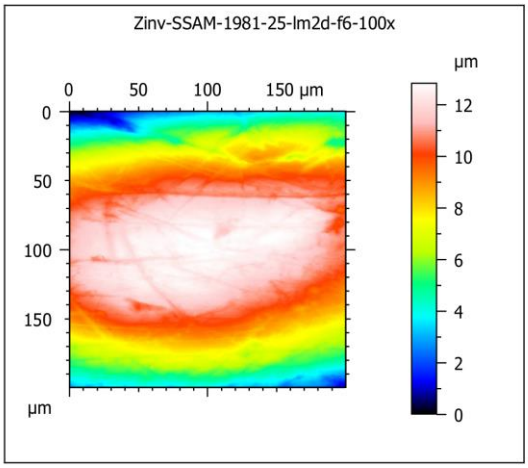
Zinv-SSAM-1981-25-lm2d-f6-100x
0
50
100
150 µm
µm
12
10
8
6
4
2
0

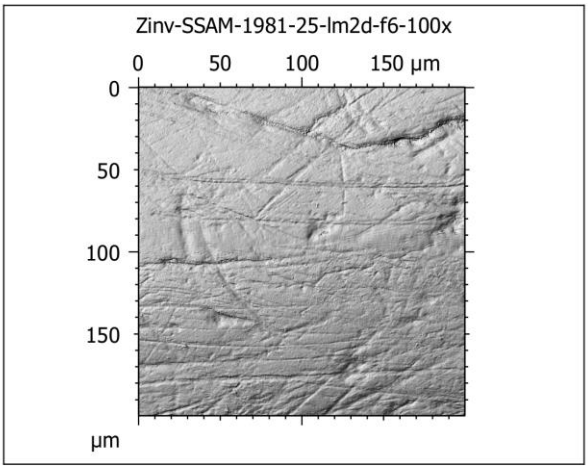
Zinv-SSAM-1981-25-lm2d-f6-100x
0
50
100
150 µm
µm

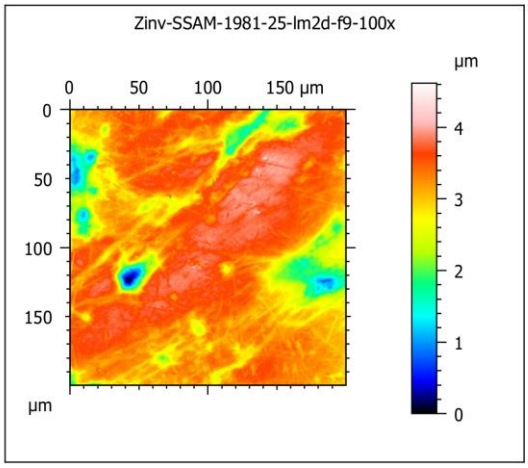
Zinv-SSAM-1981-25-lm2d-f9-100x
0
50
100
150 µm
µm
4
3
2
1
0

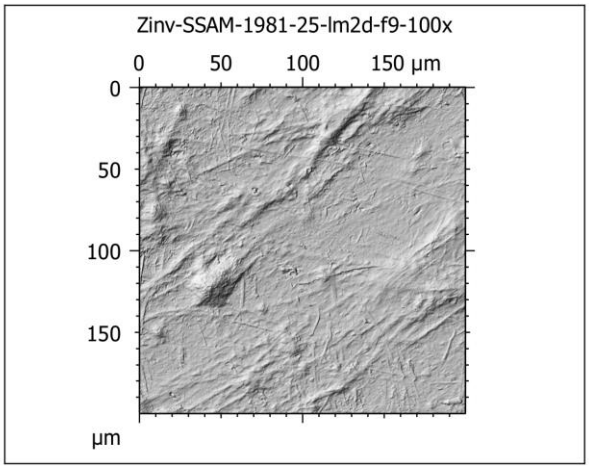
Zinv-SSAM-1981-25-lm2d-f9-100x
0
50
100
150 µm
µm

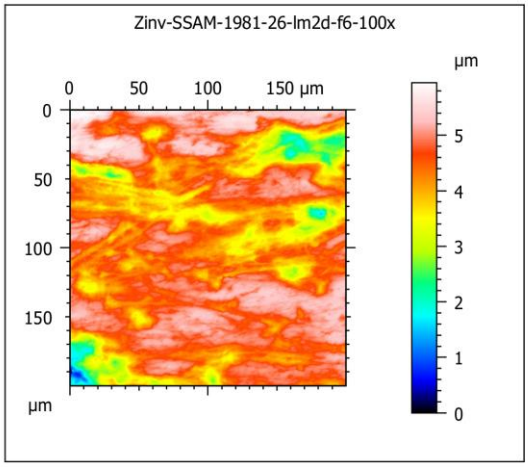
Zinv-SSAM-1981-26-lm2d-f6-100x
0
50
100
150 µm
µm
5
4
3
2
1
0

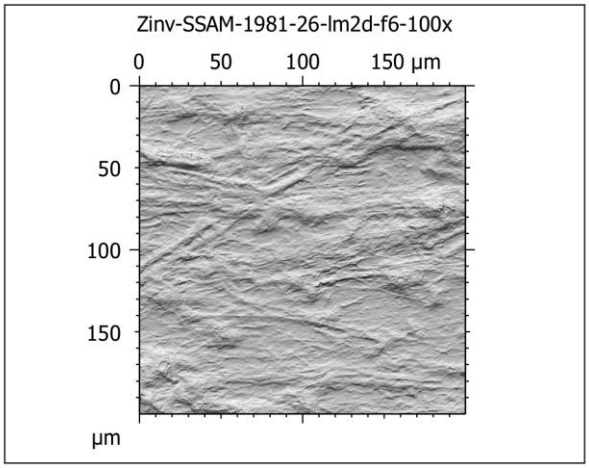
Zinv-SSAM-1981-26-lm2d-f6-100x
0
50
100
150 µm
µm

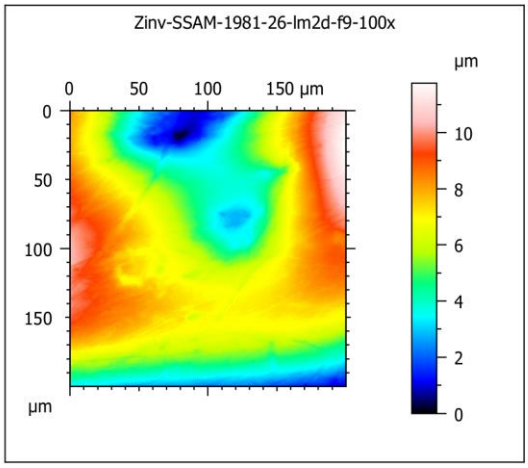
Zinv-SSAM-1981-26-lm2d-f9-100x
0
50
100
150 µm
µm
0
50
100
150
µm
10
8
6
4
2
0

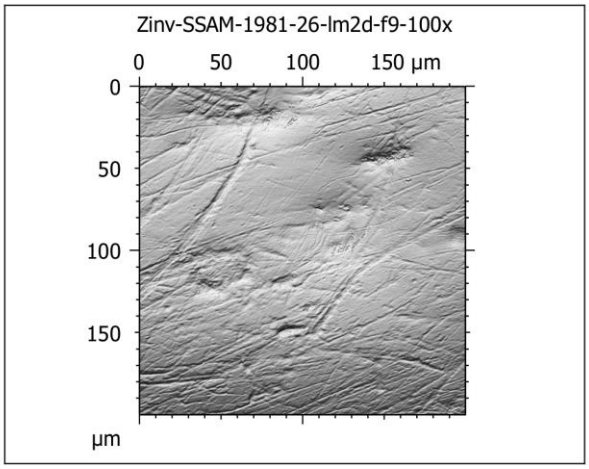
Zinv-SSAM-1981-26-lm2d-f9-100x
0
50
100
150 µm
0
50
100
150
µm

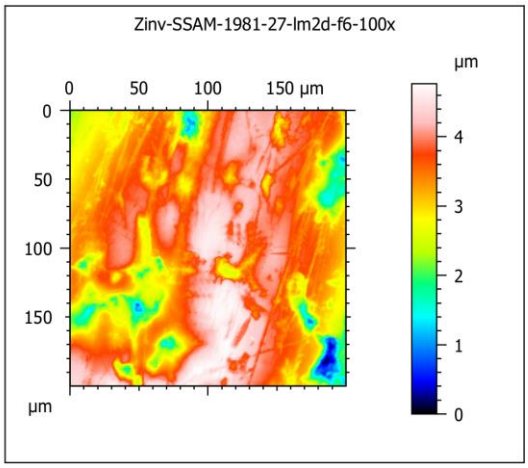
Zinv-SSAM-1981-27-lm2d-f6-100x
0
50
100
150 µm
µm
0
50
100
150
µm
4
3
2
1
0

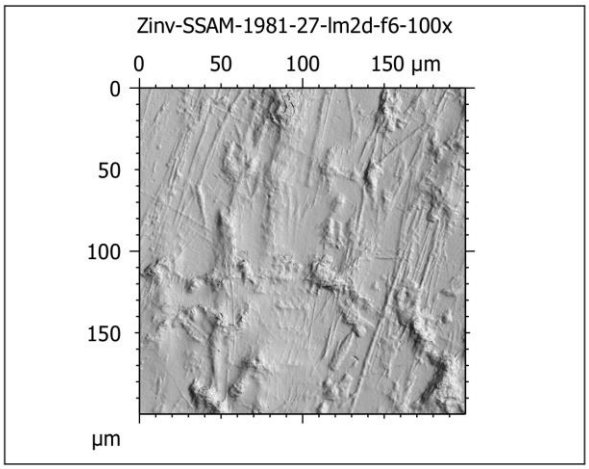
Zinv-SSAM-1981-27-lm2d-f6-100x
0
50
100
150 µm
0
50
100
150
µm

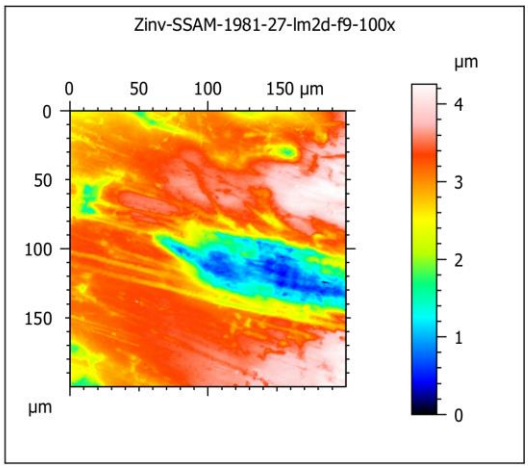
Zinv-SSAM-1981-27-lm2d-f9-100x
0
50
100
150 µm
µm
0
50
100
150
µm
4
3
2
1
0

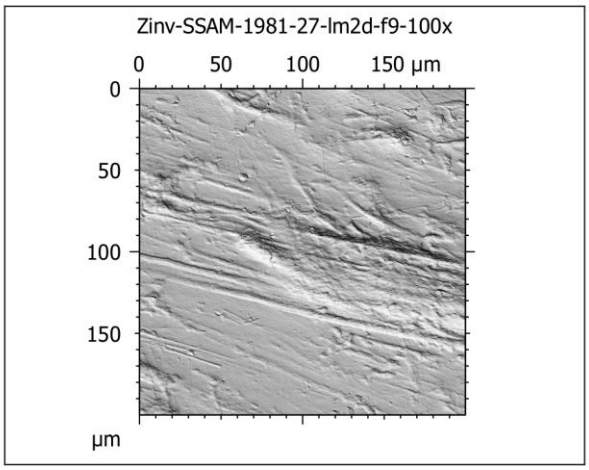
Zinv-SSAM-1981-27-lm2d-f9-100x
0
50
100
150 µm
0
50
100
150
µm

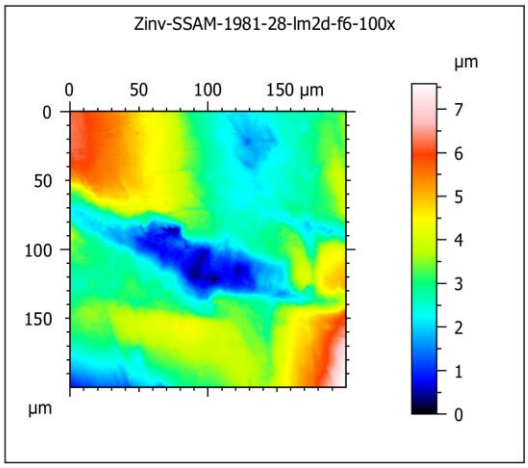
Zinv-SSAM-1981-28-lm2d-f6-100x
0
50
100
150 µm
µm
7
6
5
4
3
2
1
0

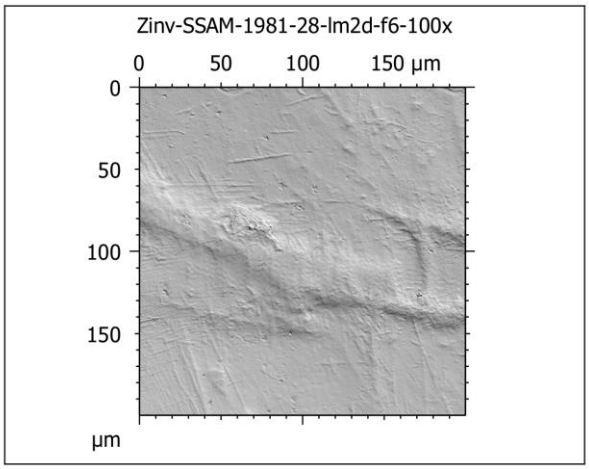
Zinv-SSAM-1981-28-lm2d-f6-100x
0
50
100
150 µm
µm

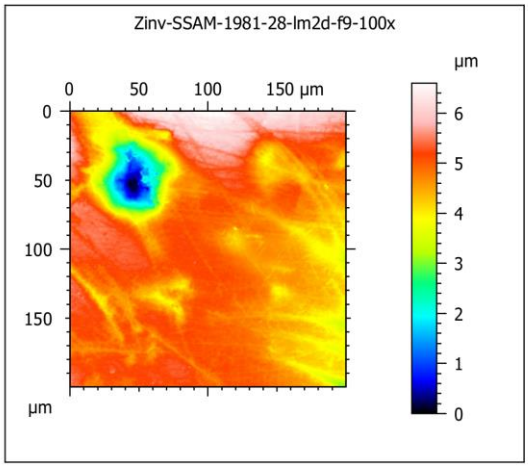
Zinv-SSAM-1981-28-lm2d-f9-100x
0
50
100
150 µm
µm
6
5
4
3
2
1
0

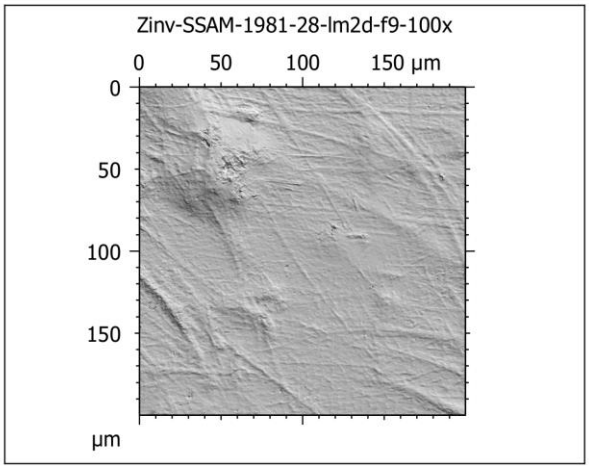
Zinv-SSAM-1981-28-lm2d-f9-100x
0
50
100
150 µm
µm

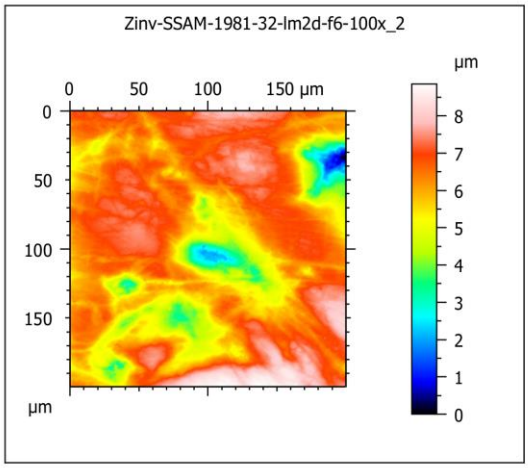
Zinv-SSAM-1981-32-lm2d-f6-100x_2
0
50
100
150 µm
µm
8
7
6
5
4
3
2
1
0

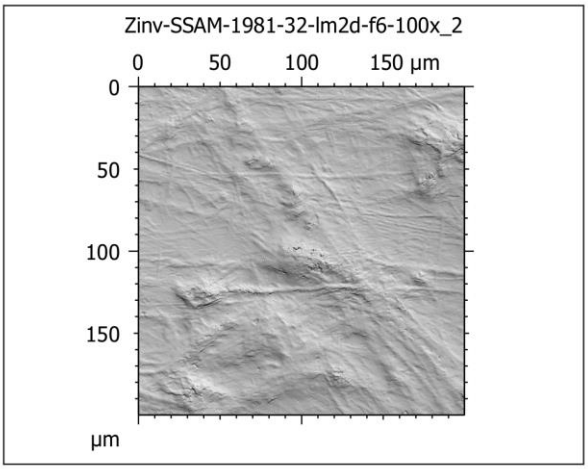
Zinv-SSAM-1981-32-lm2d-f6-100x_2
0
50
100
150 µm
µm

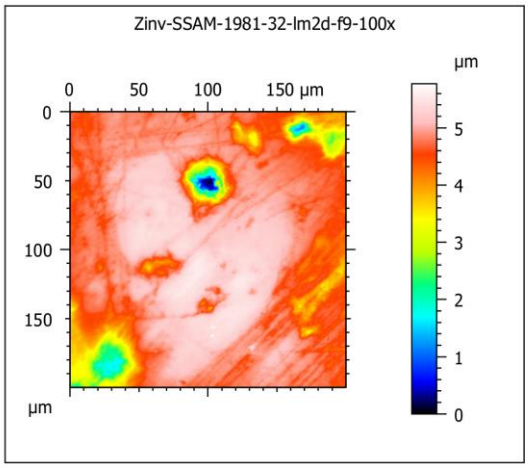
Zinv-SSAM-1981-32-lm2d-f9-100x
0
50
100
150 µm
µm
0
50
100
150
µm
5
4
3
2
1
0

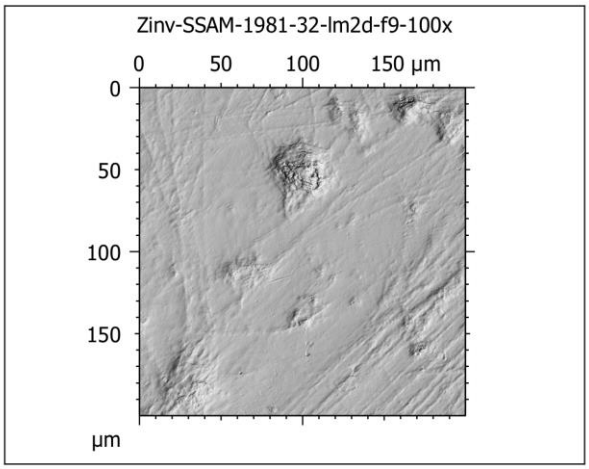
Zinv-SSAM-1981-32-lm2d-f9-100x
0
50
100
150 µm
0
50
100
150
µm

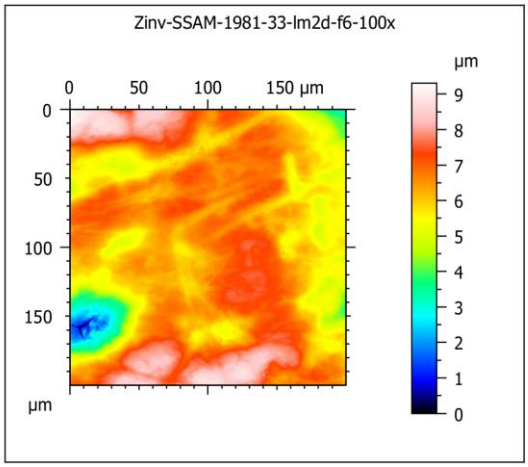
Zinv-SSAM-1981-33-lm2d-f6-100x
0
50
100
150 µm
µm
0
50
100
150
µm
9
8
7
6
5
4
3
2
1
0

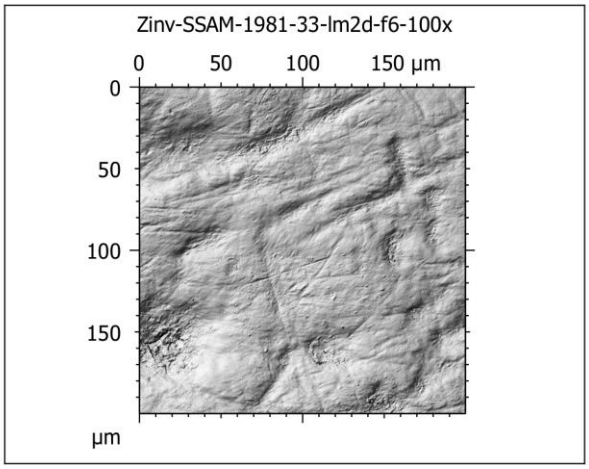
Zinv-SSAM-1981-33-lm2d-f6-100x
0
50
100
150 µm
0
50
100
150
µm

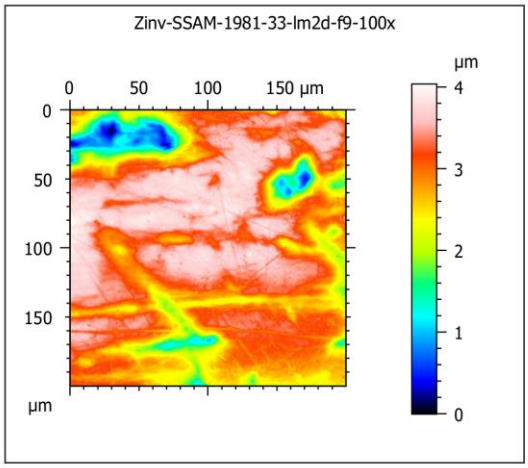
Zinv-SSAM-1981-33-lm2d-f9-100x
0
50
100
150 µm
µm
0
50
100
150
µm
4
3
2
1
0

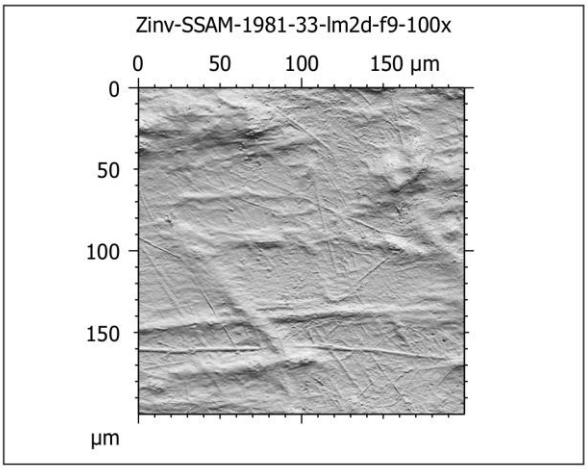
Zinv-SSAM-1981-33-lm2d-f9-100x
0
50
100
150 µm
0
50
100
150
µm

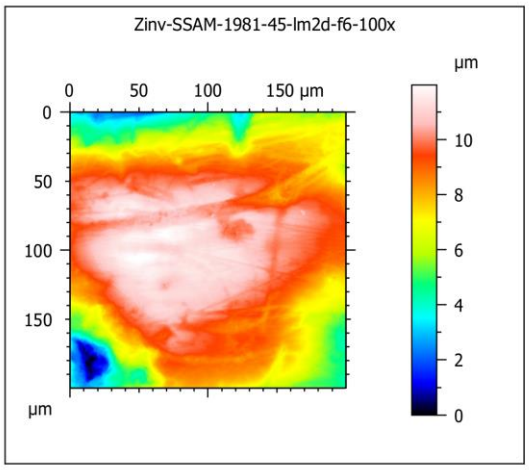
Zinv-SSAM-1981-45-lm2d-f6-100x
µm
0 50 100 150 µm
0
50
100
150
µm
10
8
6
4
2
0

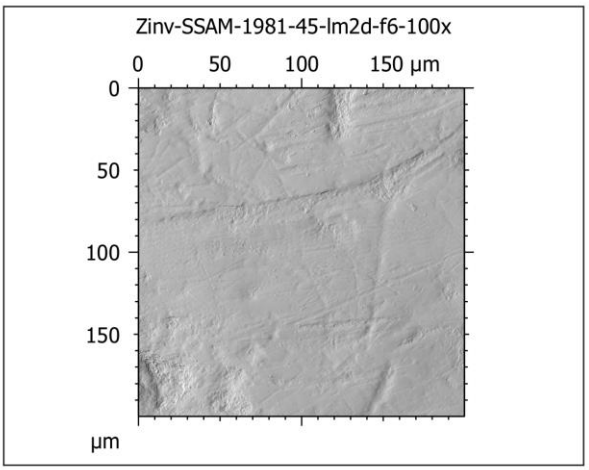
Zinv-SSAM-1981-45-lm2d-f6-100x
0 50 100 150 µm
0
50
100
150
µm

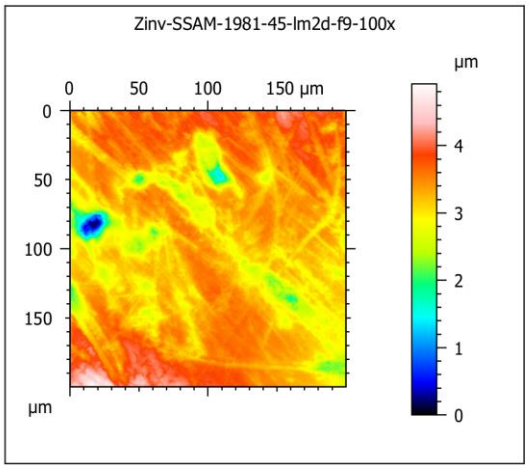
Zinv-SSAM-1981-45-lm2d-f9-100x
µm
0 50 100 150 µm
0
50
100
150
µm
4
3
2
1
0

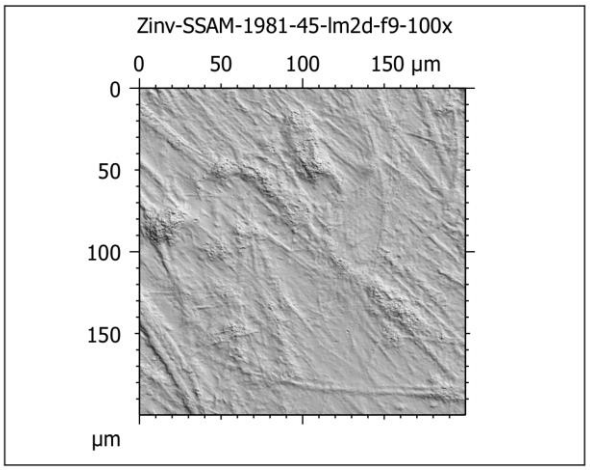
Zinv-SSAM-1981-45-lm2d-f9-100x
0 50 100 150 µm
0
50
100
150
µm

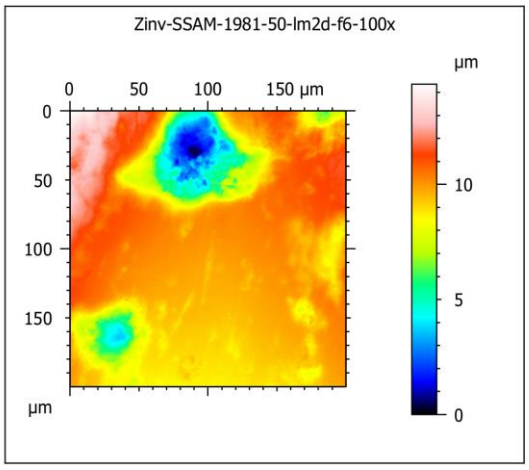
Zinv-SSAM-1981-50-lm2d-f6-100x
µm
0 50 100 150 µm
0
50
100
150
µm
10
5
0

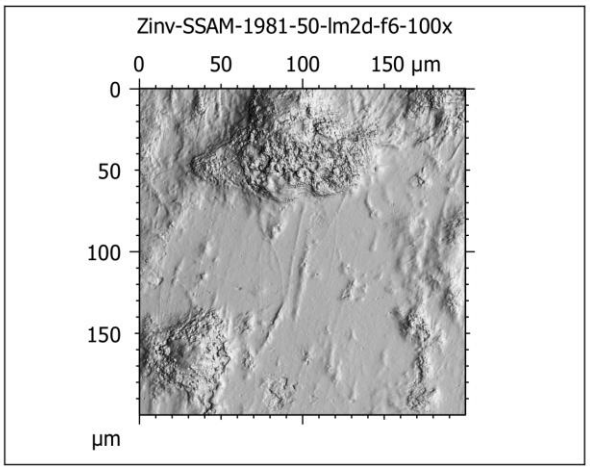
Zinv-SSAM-1981-50-lm2d-f6-100x
0 50 100 150 µm
0
50
100
150
µm

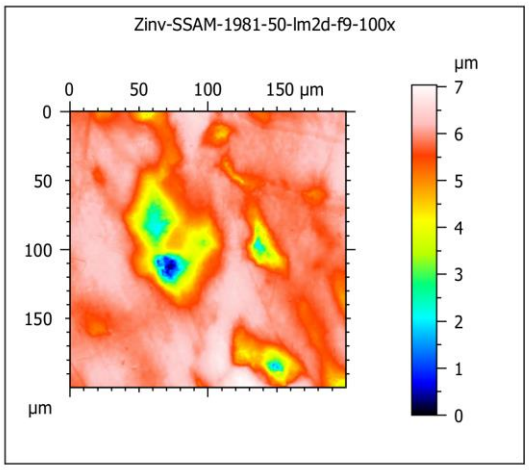
Zinv-SSAM-1981-50-lm2d-f9-100x
0
50
100
150 µm
µm
7
6
5
4
3
2
1
0

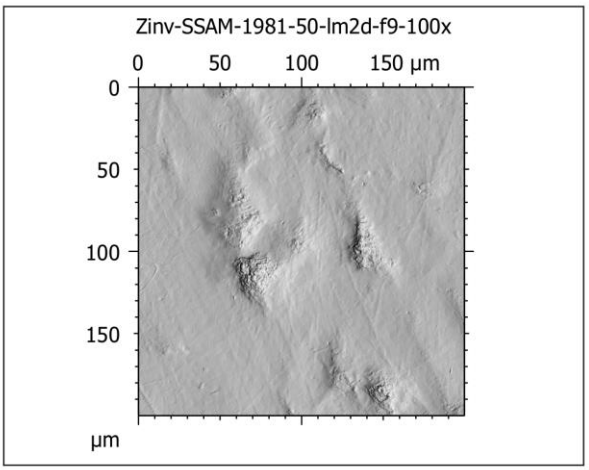
Zinv-SSAM-1981-50-lm2d-f9-100x
0
50
100
150 µm
µm

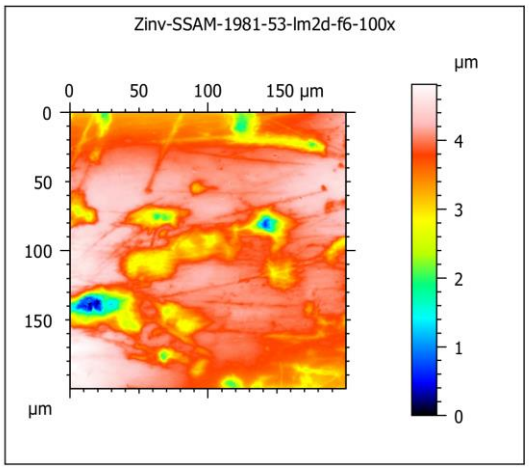
Zinv-SSAM-1981-53-lm2d-f6-100x
0
50
100
150 µm
µm
4
3
2
1
0

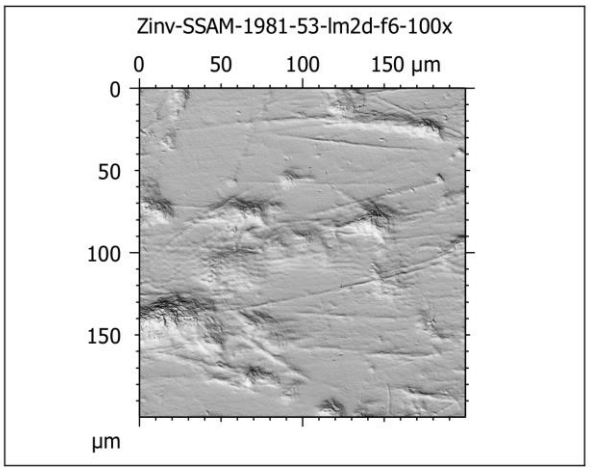
Zinv-SSAM-1981-53-lm2d-f6-100x
0
50
100
150 µm
µm

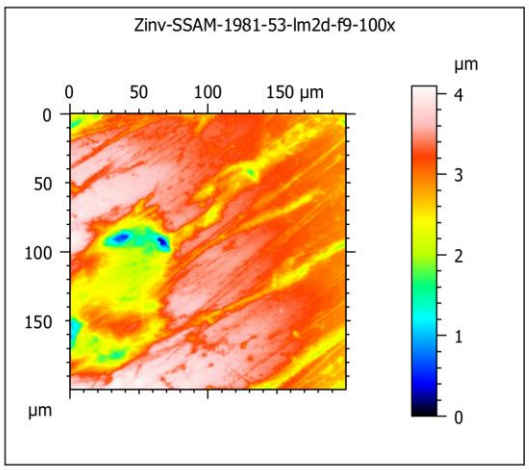
Zinv-SSAM-1981-53-lm2d-f9-100x
0
50
100
150 µm
µm
4
3
2
1
0

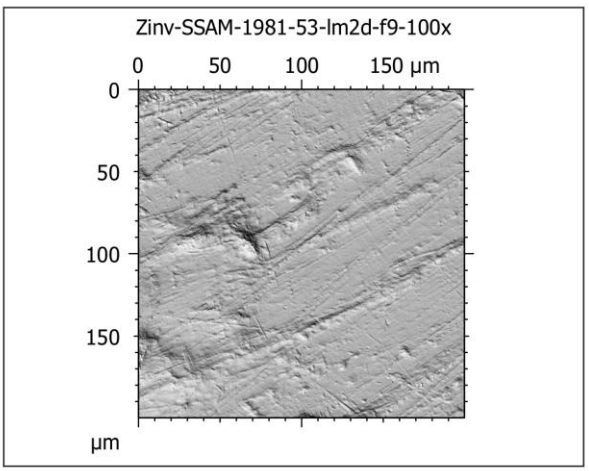
Zinv-SSAM-1981-53-lm2d-f9-100x
0
50
100
150 µm
µm

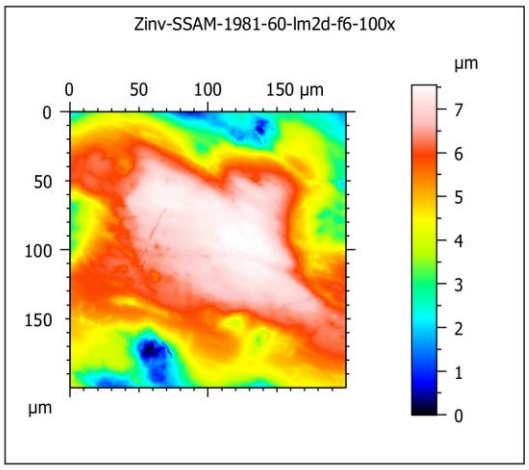
Zinv-SSAM-1981-60-lm2d-f6-100x
0
50
100
150 µm
µm
7
6
5
4
3
2
1
0

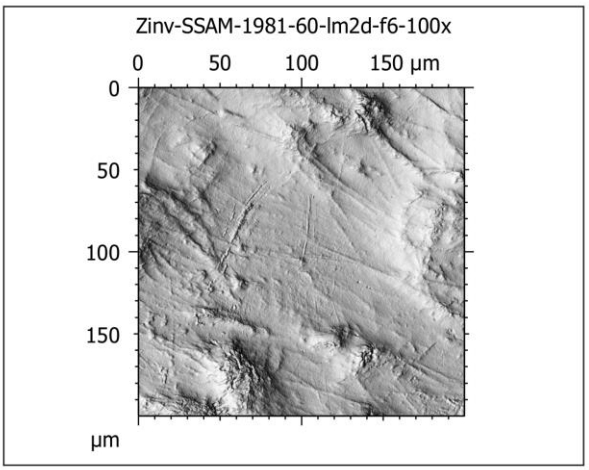
Zinv-SSAM-1981-60-lm2d-f6-100x
0
50
100
150 µm
µm

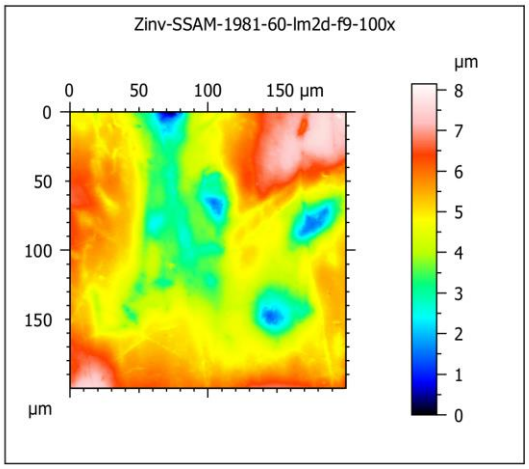
Zinv-SSAM-1981-60-lm2d-f9-100x
0
50
100
150 µm
µm
8
7
6
5
4
3
2
1
0

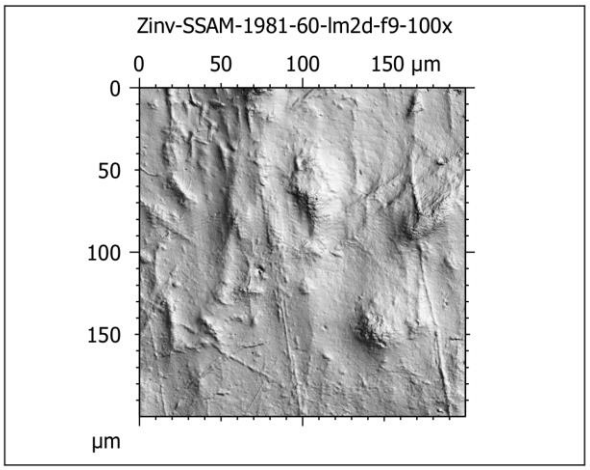
Zinv-SSAM-1981-60-lm2d-f9-100x
0
50
100
150 µm
µm

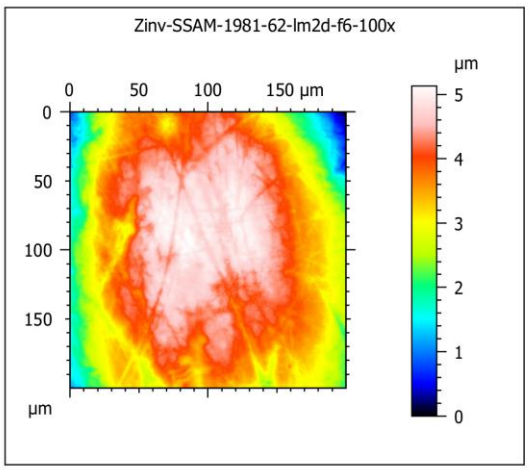
Zinv-SSAM-1981-62-lm2d-f6-100x
0
50
100
150 µm
µm
5
4
3
2
1
0

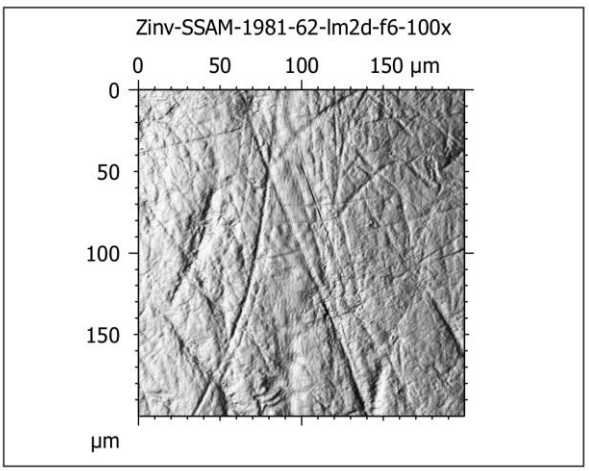
Zinv-SSAM-1981-62-lm2d-f6-100x
0
50
100
150 µm
µm

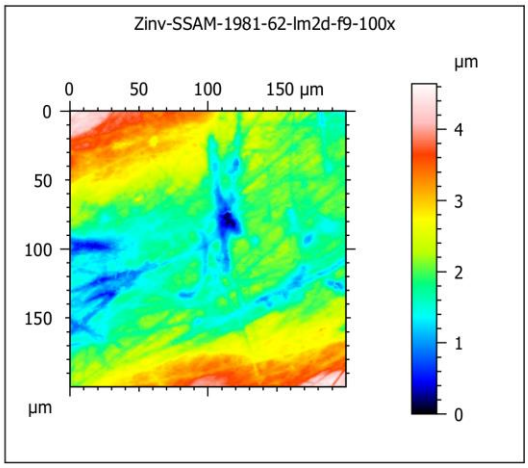
Zinv-SSAM-1981-62-lm2d-f9-100x
0
50
100
150 µm
µm
4
3
2
1
0

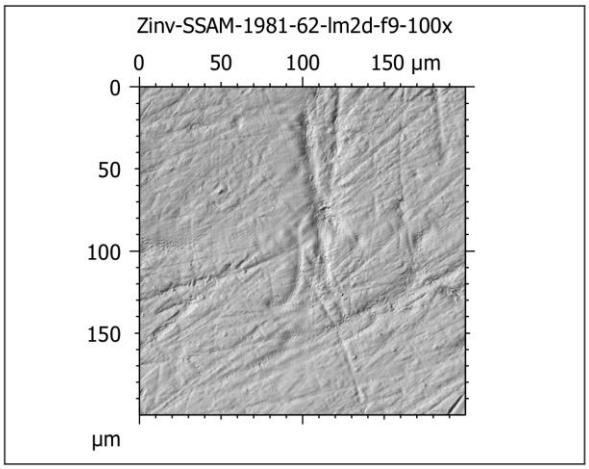
Zinv-SSAM-1981-62-lm2d-f9-100x
0
50
100
150 µm
µm

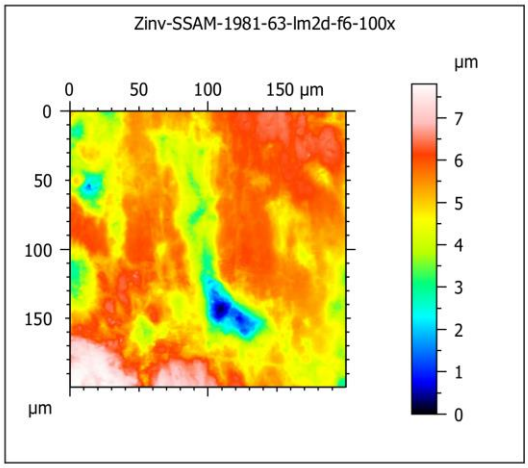
Zinv-SSAM-1981-63-lm2d-f6-100x
0
50
100
150 µm
µm
7
6
5
4
3
2
1
0

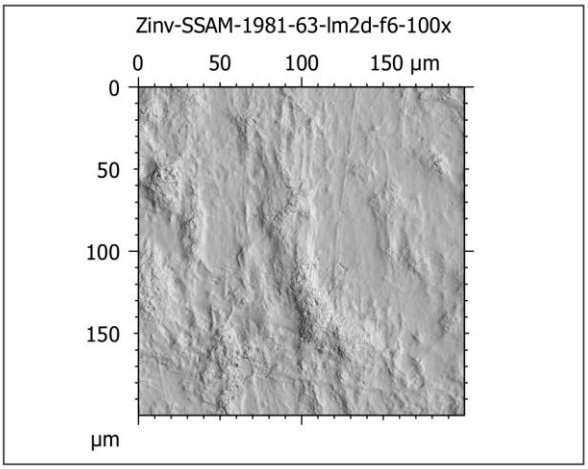
Zinv-SSAM-1981-63-lm2d-f6-100x
0
50
100
150 µm
µm

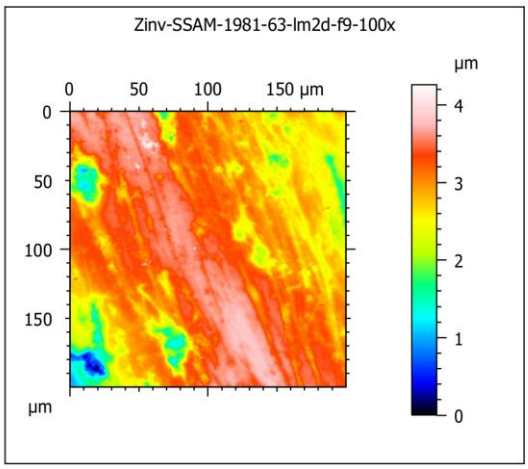
Zinv-SSAM-1981-63-lm2d-f9-100x
0
50
100
150 µm
µm
4
3
2
1
0

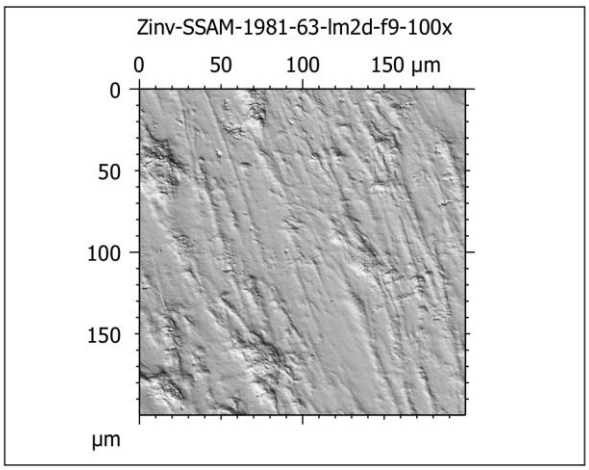
Zinv-SSAM-1981-63-lm2d-f9-100x
0
50
100
150 µm
µm

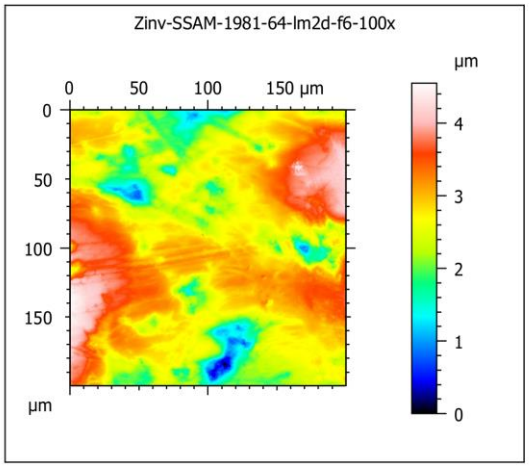
Zinv-SSAM-1981-64-lm2d-f6-100x
0
50
100
150 µm
µm
0
50
100
150
µm
4
3
2
1
0

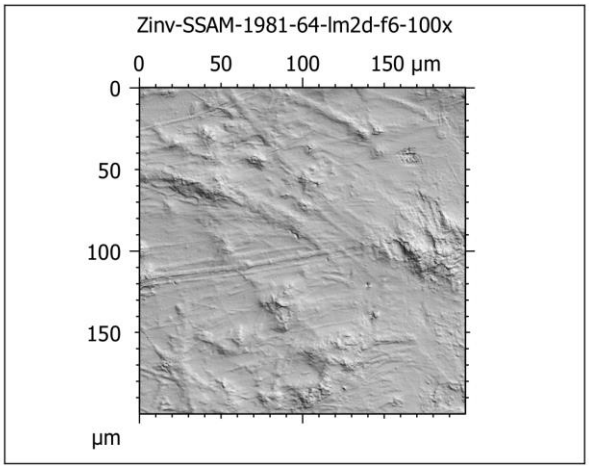
Zinv-SSAM-1981-64-lm2d-f6-100x
0
50
100
150 µm
0
50
100
150
µm

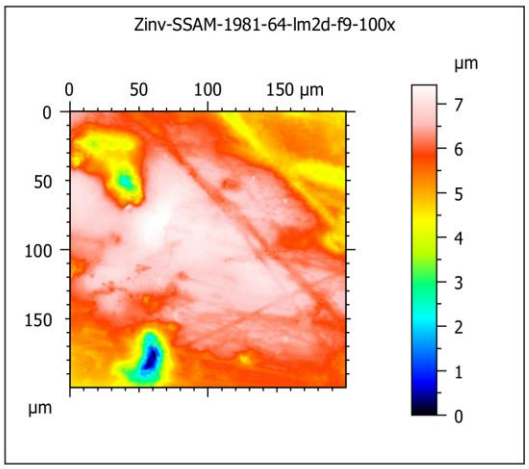
Zinv-SSAM-1981-64-lm2d-f9-100x
0
50
100
150 µm
µm
0
50
100
150
µm
7
6
5
4
3
2
1
0

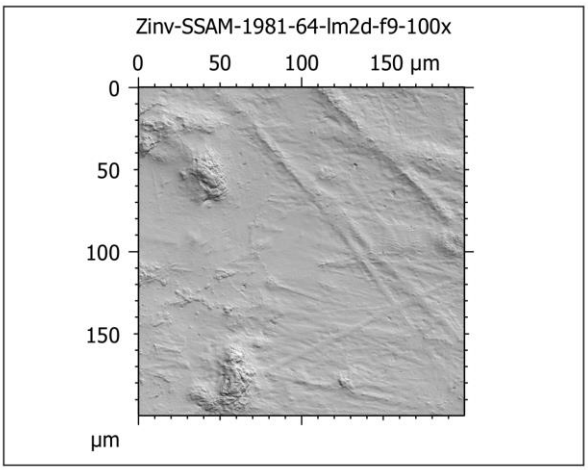
Zinv-SSAM-1981-64-lm2d-f9-100x
0
50
100
150 µm
0
50
100
150
µm

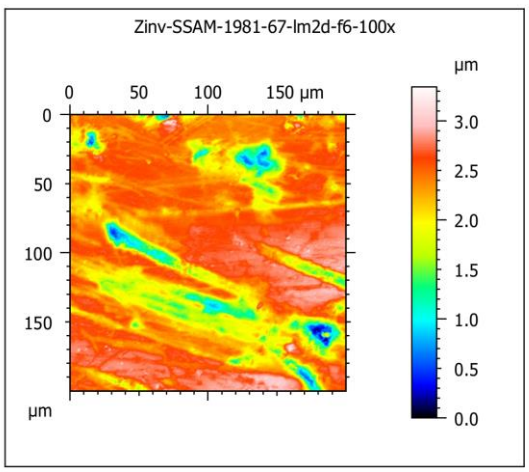
Zinv-SSAM-1981-67-lm2d-f6-100x
0
50
100
150 µm
µm
0
50
100
150
µm
3.0
2.5
2.0
1.5
1.0
0.5
0.0

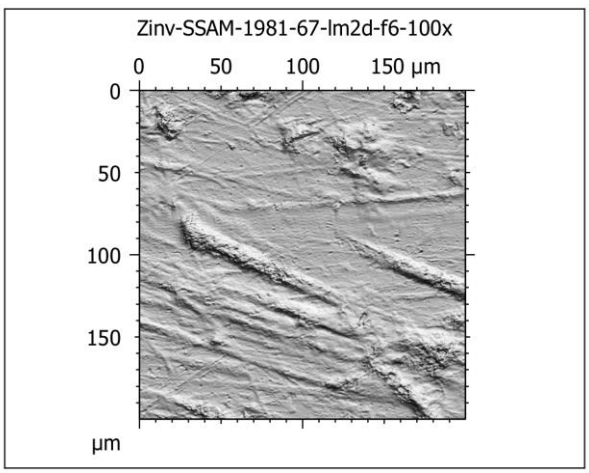
Zinv-SSAM-1981-67-lm2d-f6-100x
0
50
100
150 µm
0
50
100
150
µm

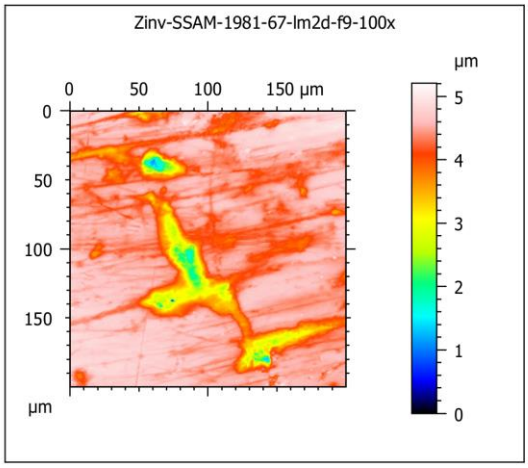
Zinv-SSAM-1981-67-lm2d-f9-100x
µm
0 50 100 150 µm
0
50
100
150
µm
5
4
3
2
1
0

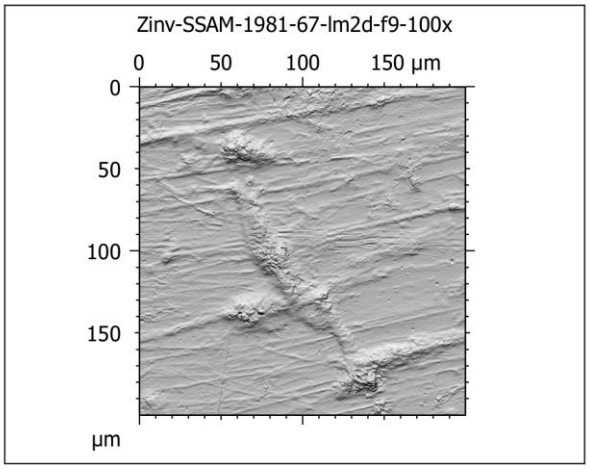
Zinv-SSAM-1981-67-lm2d-f9-100x
0 50 100 150 µm
0
50
100
150
µm

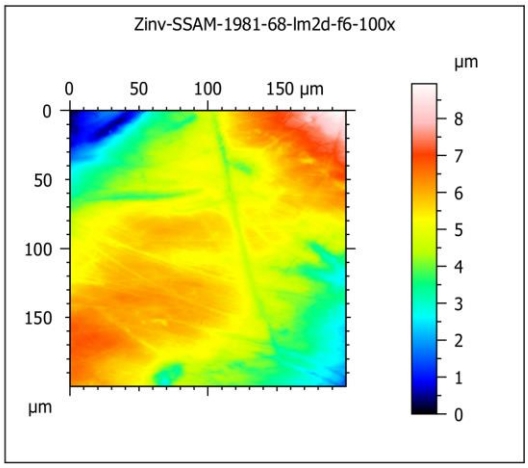
Zinv-SSAM-1981-68-lm2d-f6-100x
µm
0 50 100 150 µm
0
50
100
150
µm
8
7
6
5
4
3
2
1
0

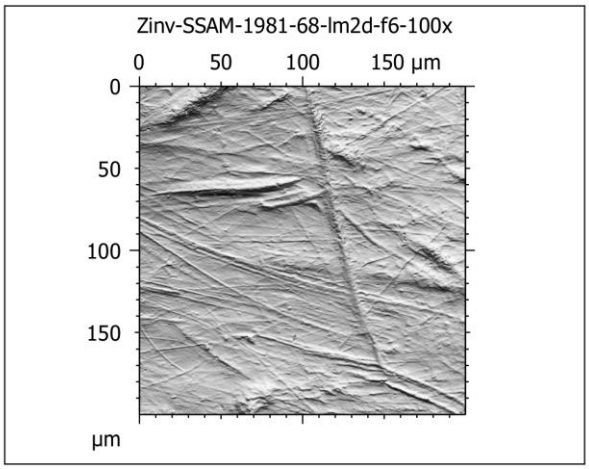
Zinv-SSAM-1981-68-lm2d-f6-100x
0 50 100 150 µm
0
50
100
150
µm

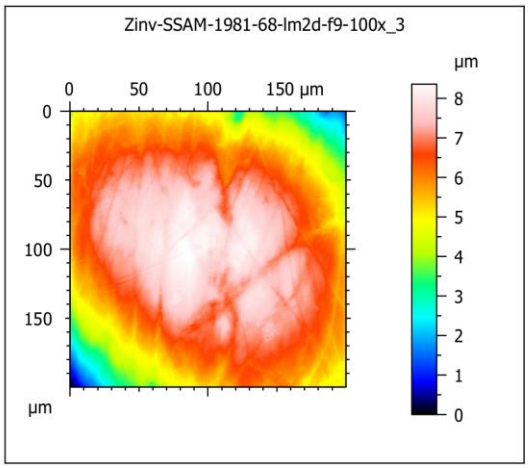
Zinv-SSAM-1981-68-lm2d-f9-100x_3
µm
0 50 100 150 µm
0
50
100
150
µm
8
7
6
5
4
3
2
1
0

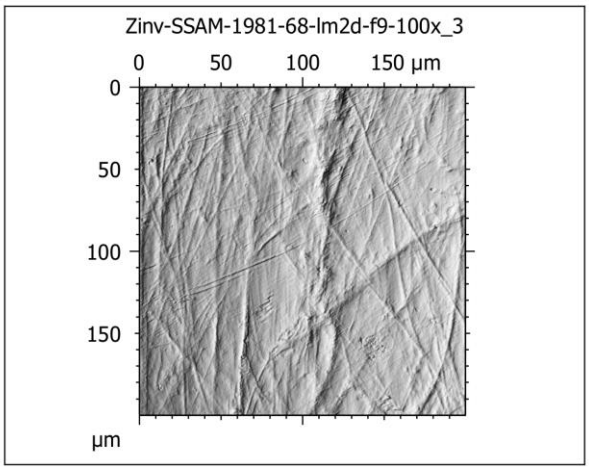
Zinv-SSAM-1981-68-lm2d-f9-100x_3
0 50 100 150 µm
0
50
100
150
µm

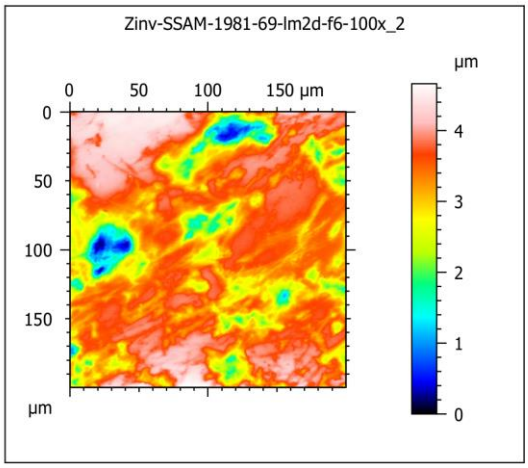
Zinv-SSAM-1981-69-lm2d-f6-100x_2
0
50
100
150 µm
µm
4
3
2
1
0

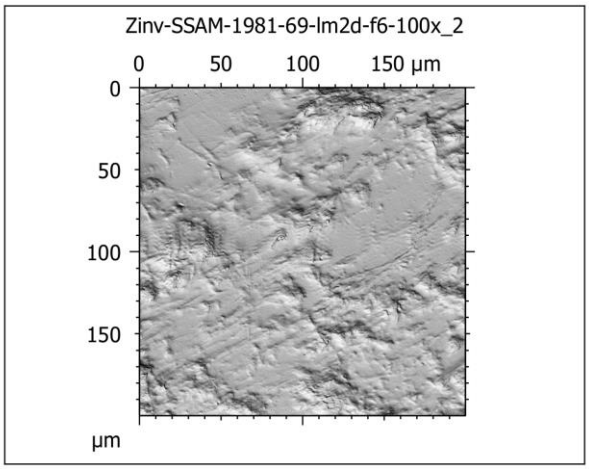
Zinv-SSAM-1981-69-lm2d-f6-100x_2
0
50
100
150 µm
µm

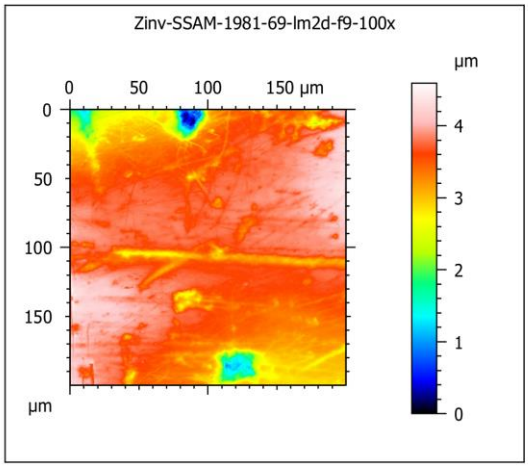
Zinv-SSAM-1981-69-lm2d-f9-100x
0
50
100
150 µm
µm
4
3
2
1
0

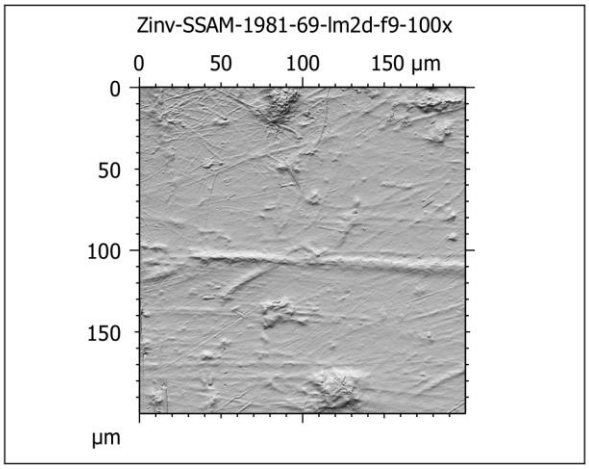
Zinv-SSAM-1981-69-lm2d-f9-100x
0
50
100
150 µm
µm

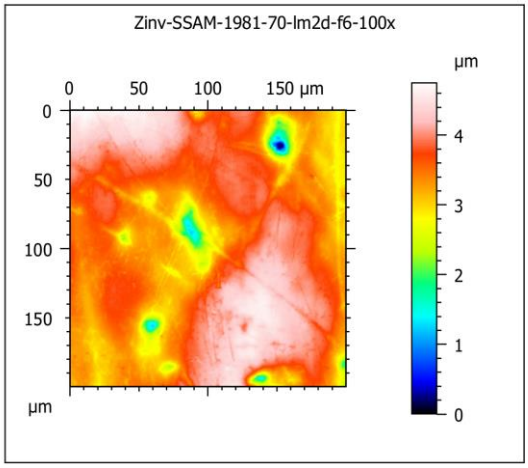
Zinv-SSAM-1981-70-lm2d-f6-100x
0
50
100
150 µm
µm
4
3
2
1
0

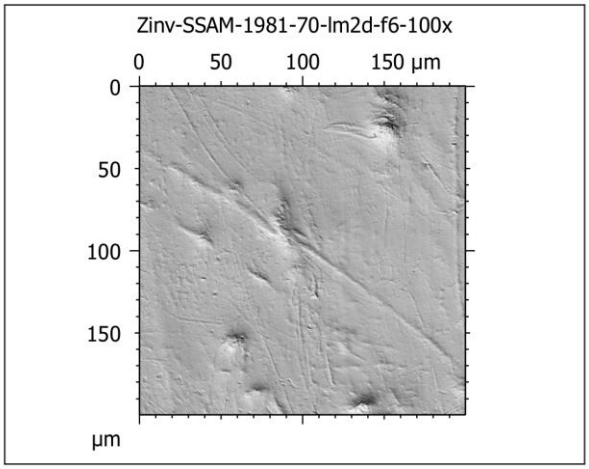
Zinv-SSAM-1981-70-lm2d-f6-100x
0
50
100
150 µm
µm

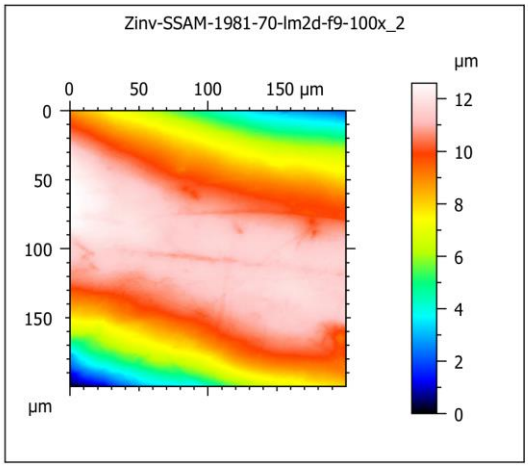
Zinv-SSAM-1981-70-lm2d-f9-100x_2
0
50
100
150 µm
µm
12
10
8
6
4
2
0

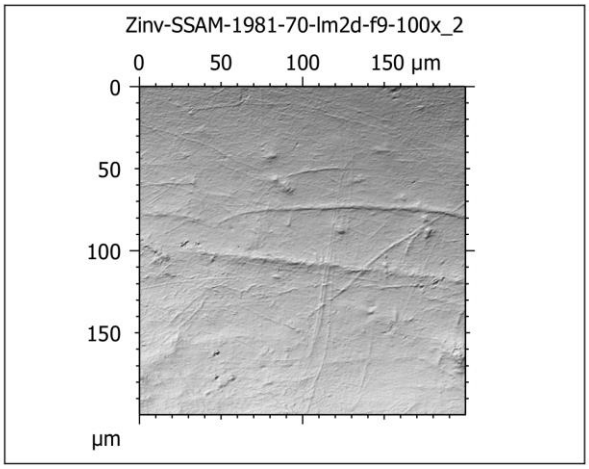
Zinv-SSAM-1981-70-lm2d-f9-100x_2
0
50
100
150 µm
µm

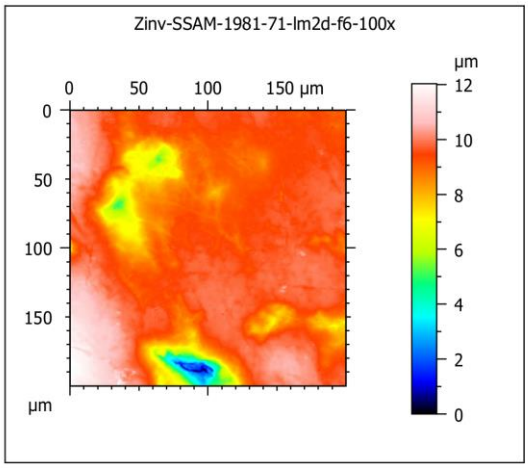
Zinv-SSAM-1981-71-lm2d-f6-100x
0
50
100
150 µm
µm
12
10
8
6
4
2
0

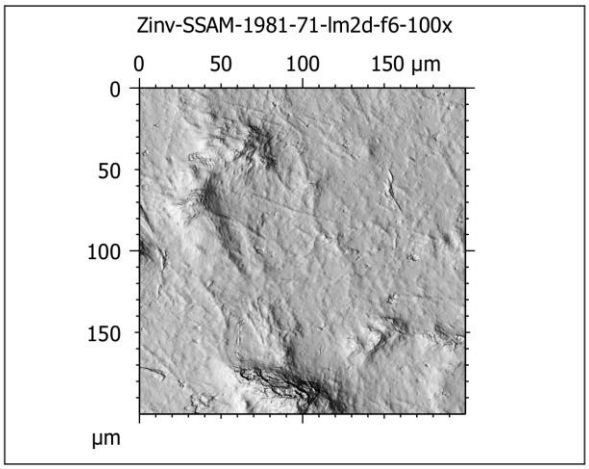
Zinv-SSAM-1981-71-lm2d-f6-100x
0
50
100
150 µm
µm

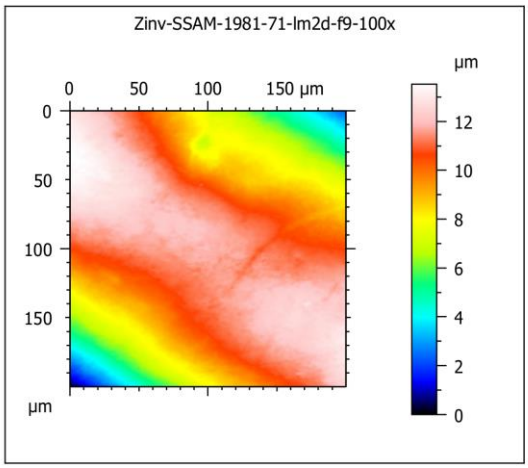
Zinv-SSAM-1981-71-lm2d-f9-100x
0
50
100
150 µm
µm
12
10
8
6
4
2
0

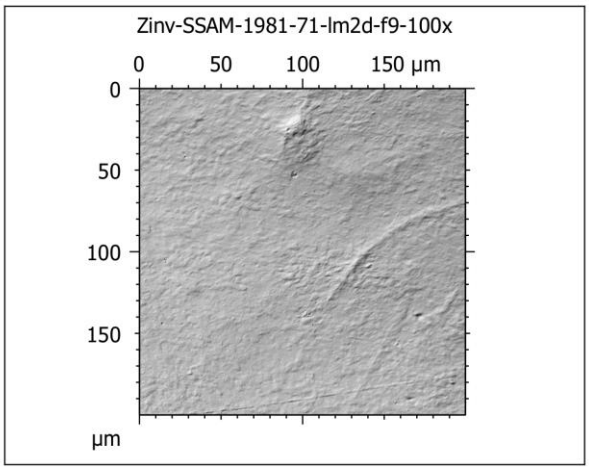
Zinv-SSAM-1981-71-lm2d-f9-100x
0
50
100
150 µm
µm

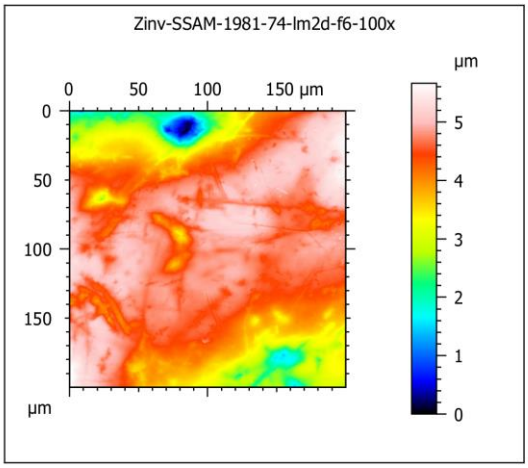
Zinv-SSAM-1981-74-lm2d-f6-100x
0
50
100
150 µm
µm
0
50
100
150
µm
0
1
2
3
4
5

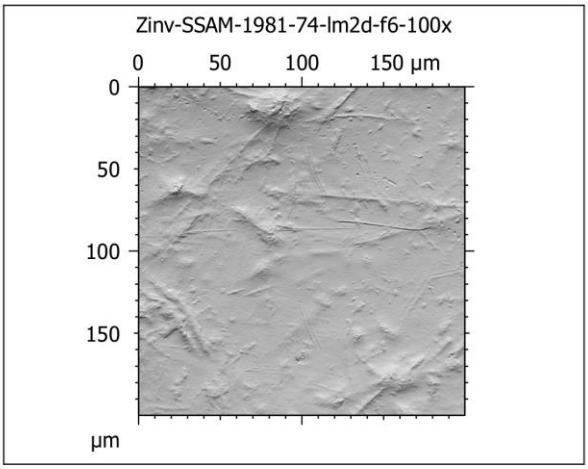
Zinv-SSAM-1981-74-lm2d-f6-100x
0
50
100
150 µm
0
50
100
150
µm

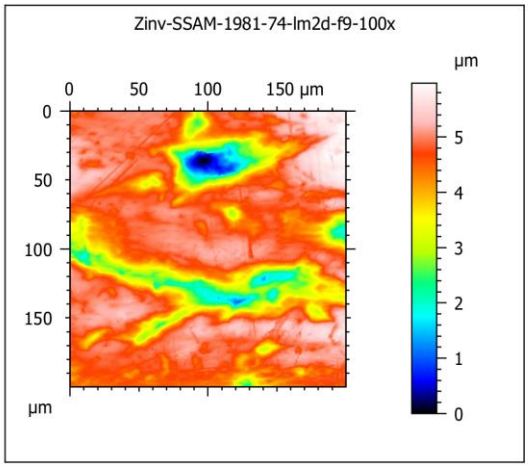
Zinv-SSAM-1981-74-lm2d-f9-100x
0
50
100
150 µm
µm
0
50
100
150
µm
0
1
2
3
4
5

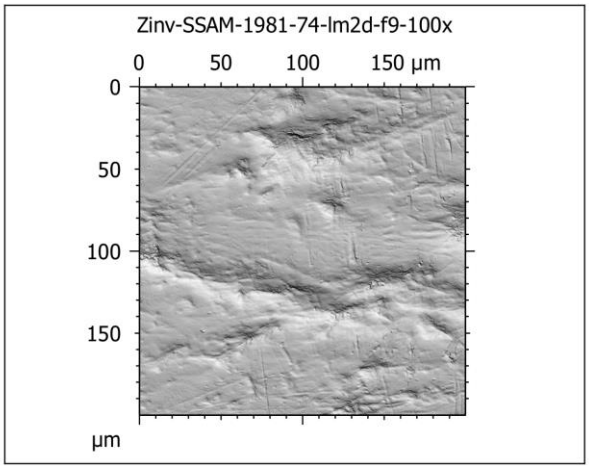
Zinv-SSAM-1981-74-lm2d-f9-100x
0
50
100
150 µm
0
50
100
150
µm

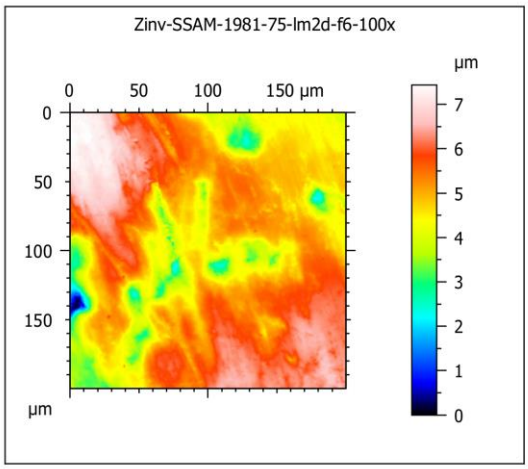
Zinv-SSAM-1981-75-lm2d-f6-100x
0
50
100
150 µm
µm
0
50
100
150
µm
0
1
2
3
4
5
6
7

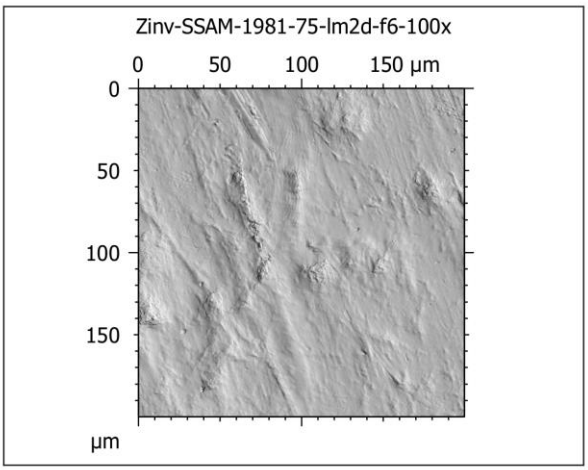
Zinv-SSAM-1981-75-lm2d-f6-100x
0
50
100
150 µm
0
50
100
150
µm

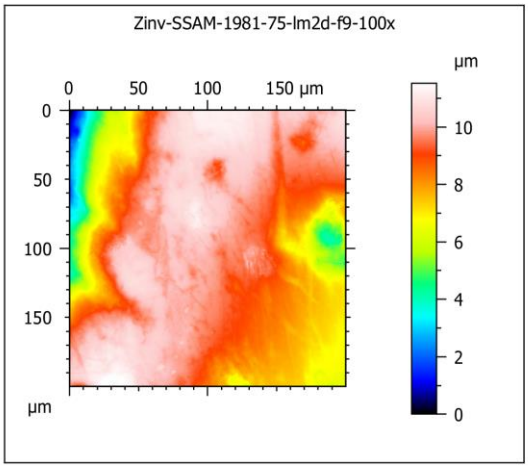
Zinv-SSAM-1981-75-lm2d-f9-100x
0
50
100
150 µm
µm
10
8
6
4
2
0

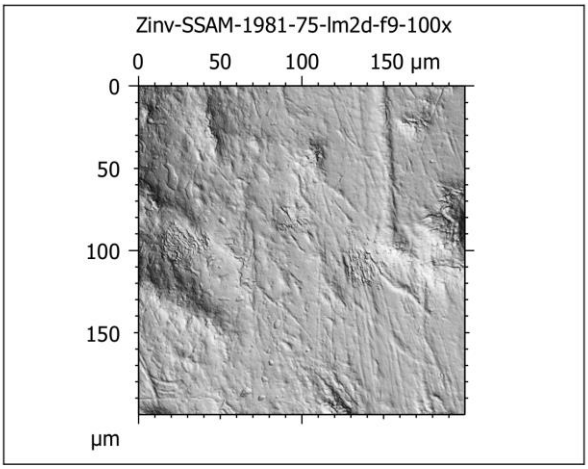
Zinv-SSAM-1981-75-lm2d-f9-100x
0
50
100
150 µm
µm

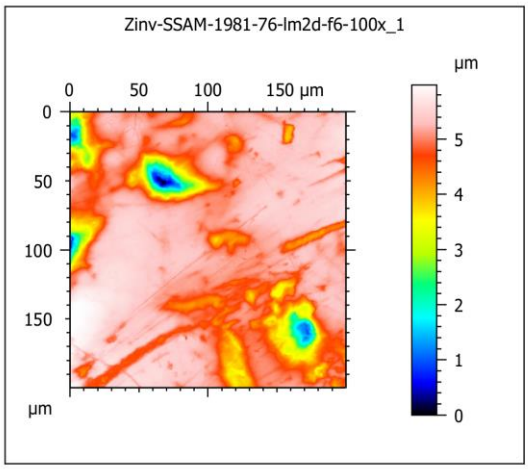
Zinv-SSAM-1981-76-lm2d-f6-100x_1
0
50
100
150 µm
µm
5
4
3
2
1
0

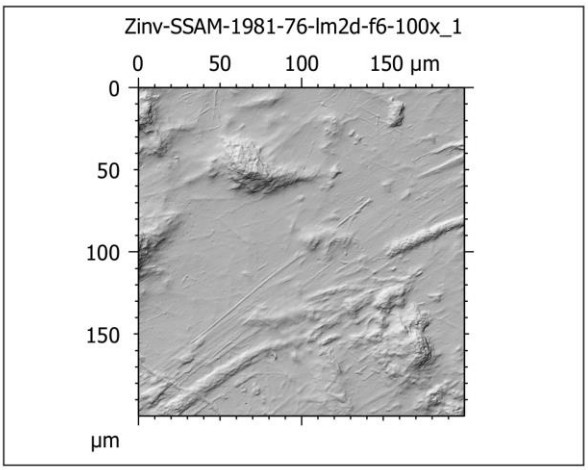
Zinv-SSAM-1981-76-lm2d-f6-100x_1
0
50
100
150 µm
µm

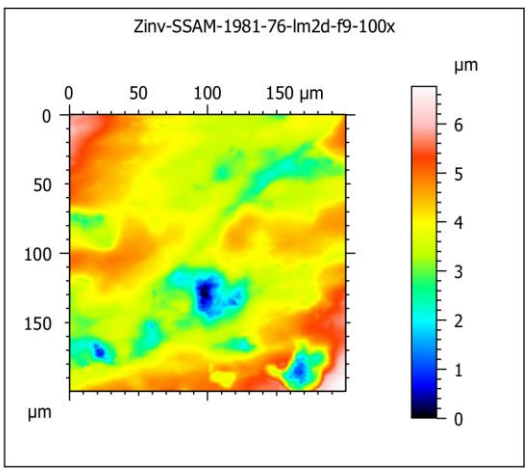
Zinv-SSAM-1981-76-lm2d-f9-100x
0
50
100
150 µm
µm
6
5
4
3
2
1
0

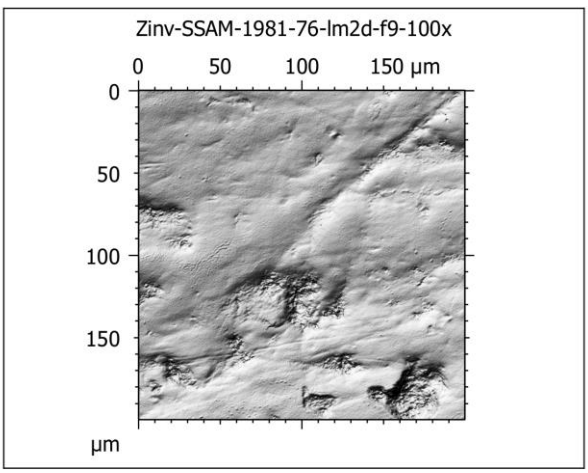
Zinv-SSAM-1981-76-lm2d-f9-100x
0
50
100
150 µm
µm

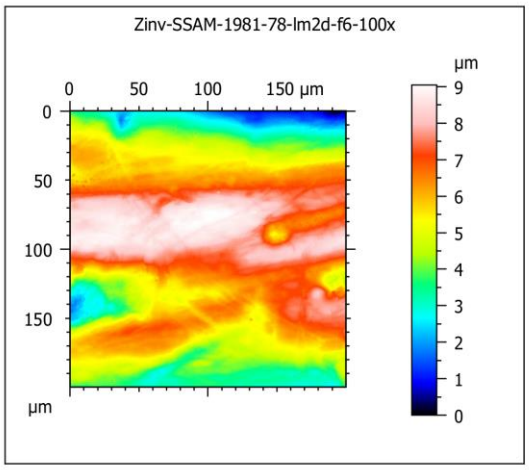
Zinv-SSAM-1981-78-lm2d-f6-100x
0
50
100
150 µm
µm
9
8
7
6
5
4
3
2
1
0

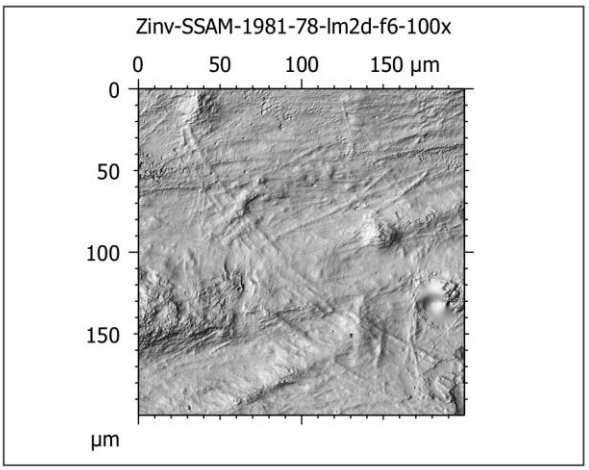
Zinv-SSAM-1981-78-lm2d-f6-100x
0
50
100
150 µm
µm

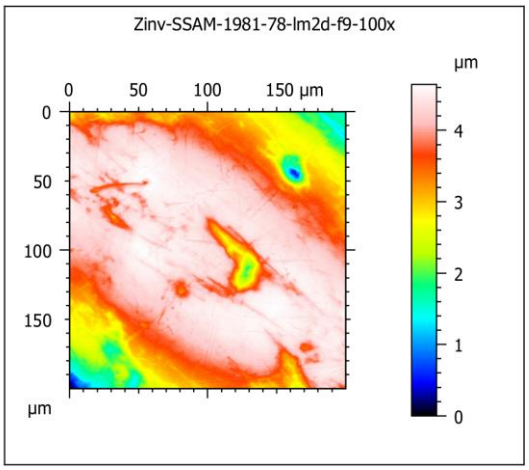
Zinv-SSAM-1981-78-lm2d-f9-100x
0
50
100
150 µm
µm
4
3
2
1
0

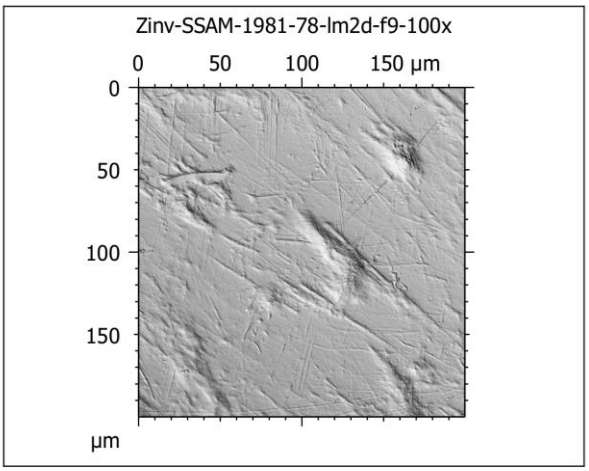
Zinv-SSAM-1981-78-lm2d-f9-100x
0
50
100
150 µm
µm

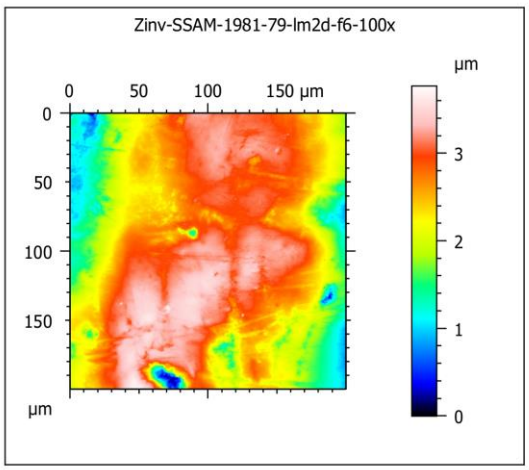
Zinv-SSAM-1981-79-lm2d-f6-100x
0
50
100
150 µm
µm
3
2
1
0

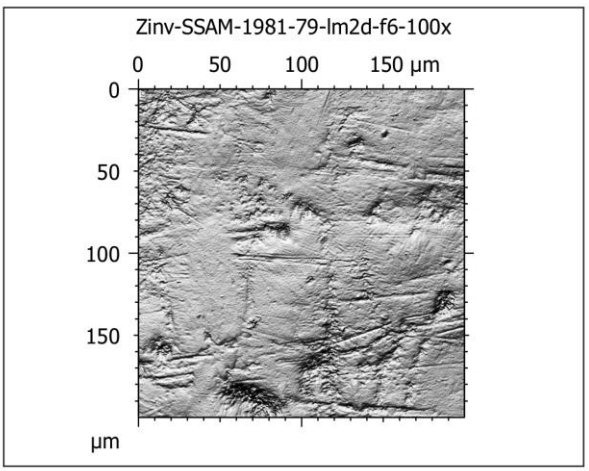
Zinv-SSAM-1981-79-lm2d-f6-100x
0
50
100
150 µm
µm

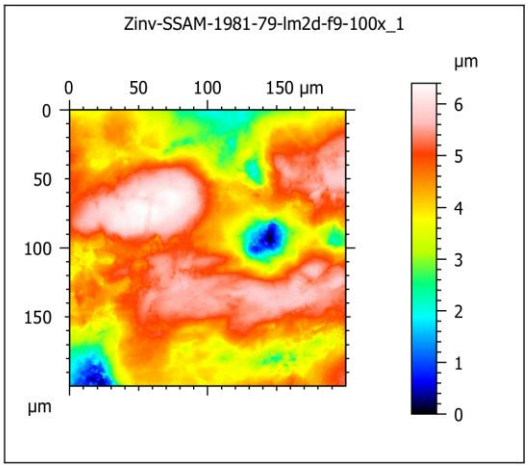
Zinv-SSAM-1981-79-lm2d-f9-100x_1
0
50
100
150 µm
µm
6
5
4
3
2
1
0

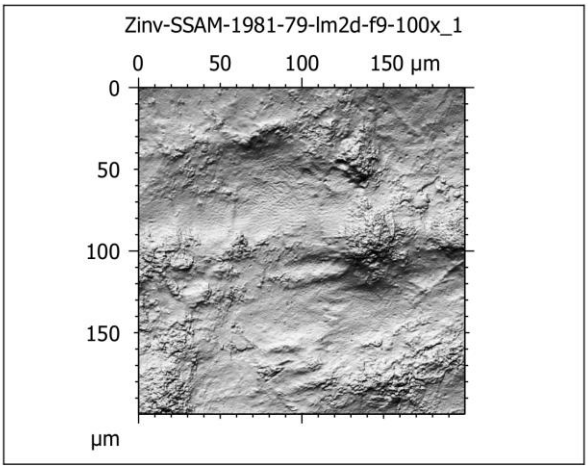
Zinv-SSAM-1981-79-lm2d-f9-100x_1
0
50
100
150 µm
µm

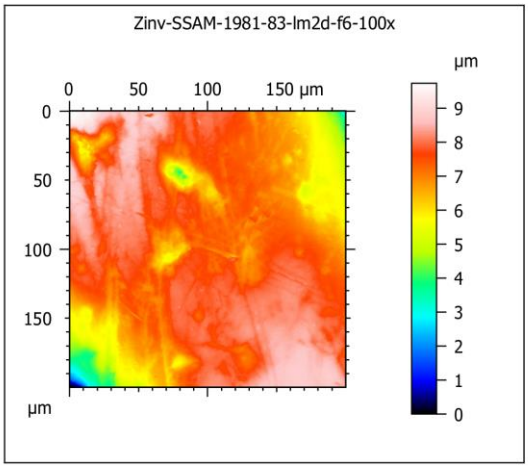
Zinv-SSAM-1981-83-lm2d-f6-100x
0
50
100
150 µm
µm
9
8
7
6
5
4
3
2
1
0

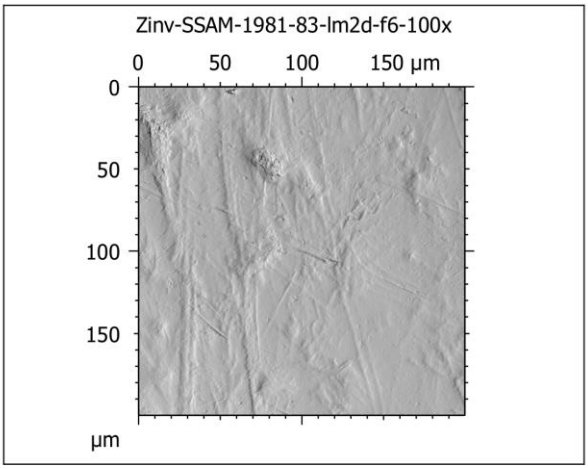
Zinv-SSAM-1981-83-lm2d-f6-100x
0
50
100
150 µm
µm

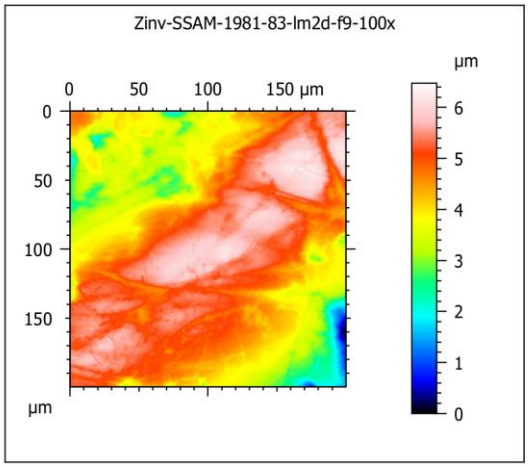
Zinv-SSAM-1981-83-lm2d-f9-100x
0
50
100
150 µm
µm
6
5
4
3
2
1
0

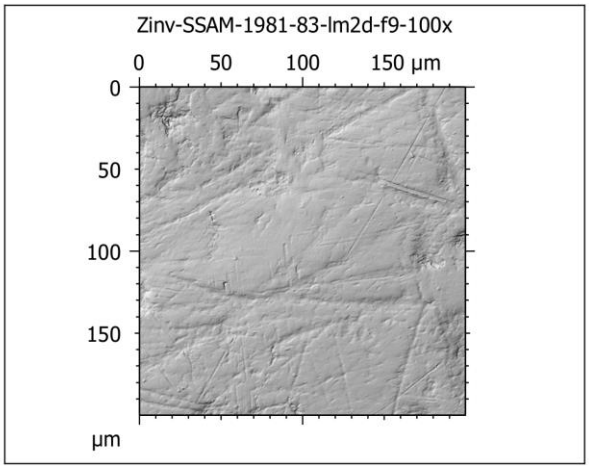
Zinv-SSAM-1981-83-lm2d-f9-100x
0
50
100
150 µm
µm

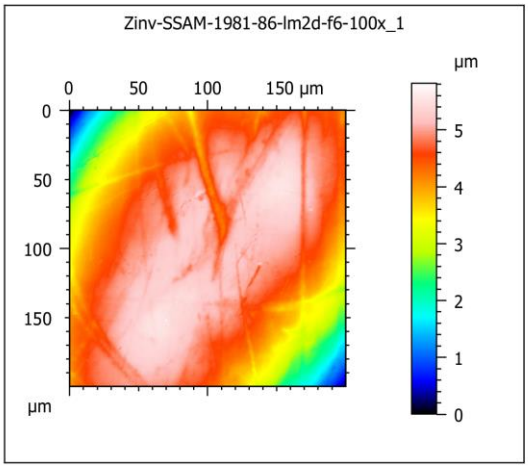
Zinv-SSAM-1981-86-lm2d-f6-100x_1
0
50
100
150 µm
µm
5
4
3
2
1
0

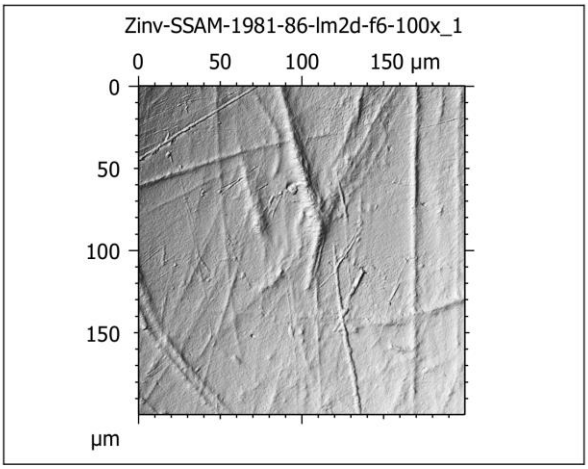
Zinv-SSAM-1981-86-lm2d-f6-100x_1
0
50
100
150 µm
µm

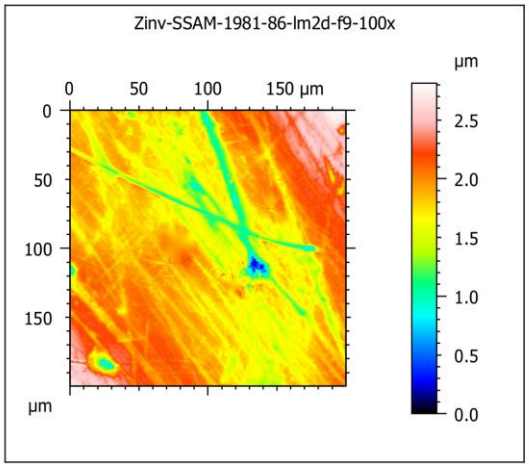
Zinv-SSAM-1981-86-lm2d-f9-100x
0
50
100
150 µm
µm
2.5
2.0
1.5
1.0
0.5
0.0

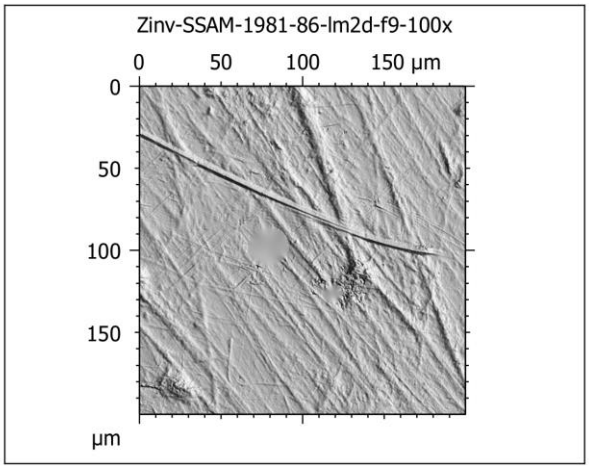
Zinv-SSAM-1981-86-lm2d-f9-100x
0
50
100
150 µm
µm

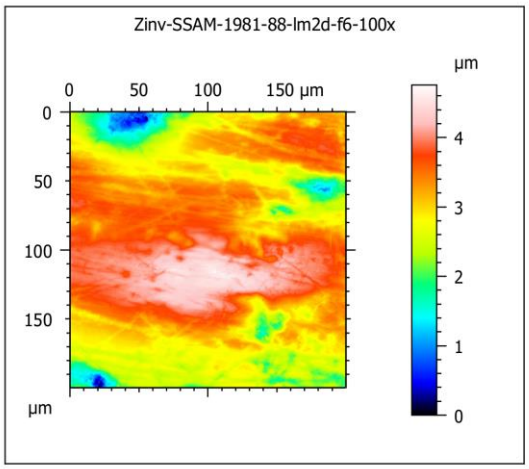
Zinv-SSAM-1981-88-lm2d-f6-100x
0
50
100
150 µm
µm
4
3
2
1
0

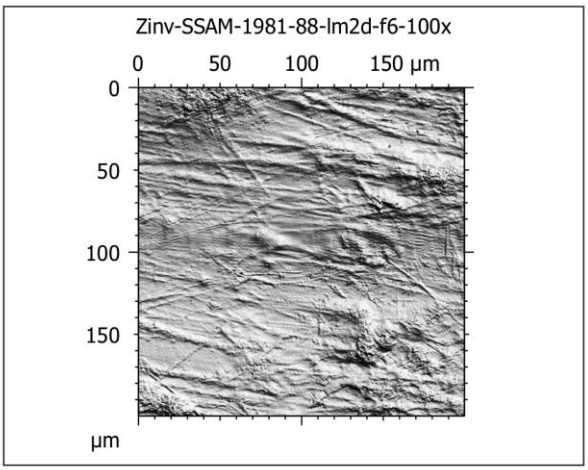
Zinv-SSAM-1981-88-lm2d-f6-100x
0
50
100
150 µm
µm

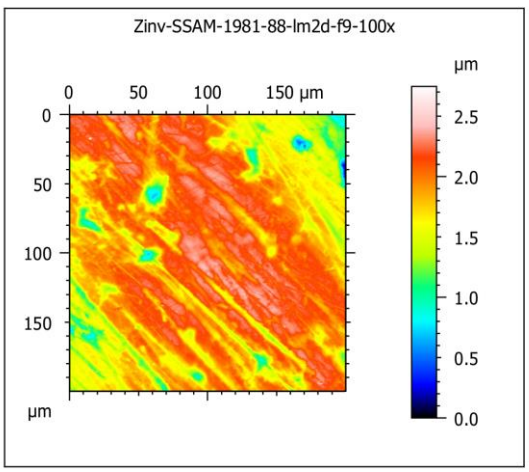
Zinv-SSAM-1981-88-lm2d-f9-100x
0
50
100
150 µm
µm
2.5
2.0
1.5
1.0
0.5
0.0

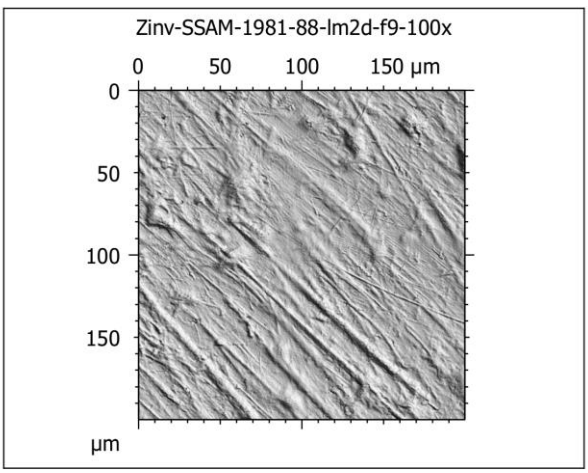
Zinv-SSAM-1981-88-lm2d-f9-100x
0
50
100
150 µm
µm

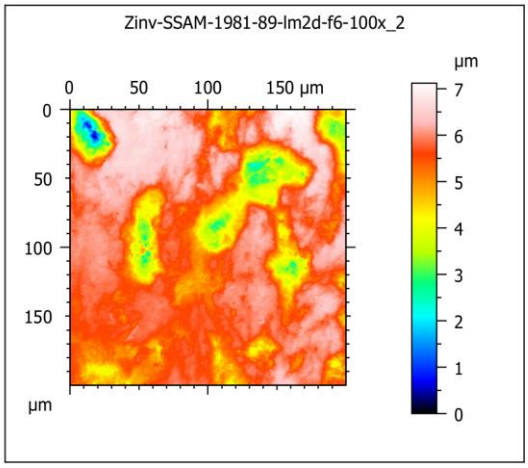
Zinv-SSAM-1981-89-lm2d-f6-100x_2
µm
0 50 100 150 µm
0
50
100
150
µm
7
6
5
4
3
2
1
0

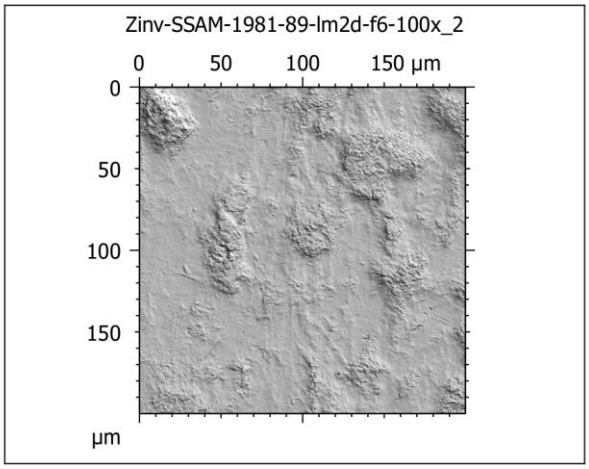
Zinv-SSAM-1981-89-lm2d-f6-100x_2
0 50 100 150 µm
0
50
100
150
µm

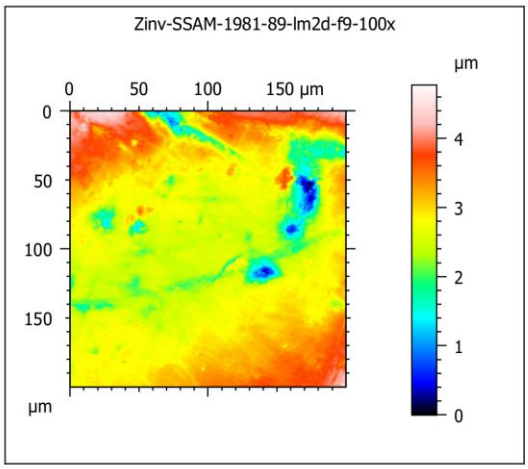
Zinv-SSAM-1981-89-lm2d-f9-100x
µm
0 50 100 150 µm
0
50
100
150
µm
4
3
2
1
0

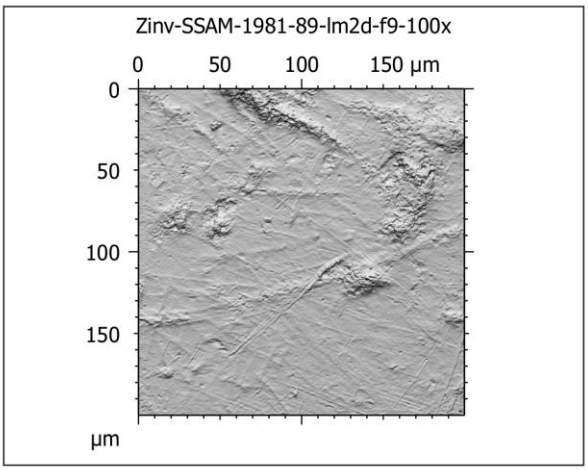
Zinv-SSAM-1981-89-lm2d-f9-100x
0 50 100 150 µm
0
50
100
150
µm

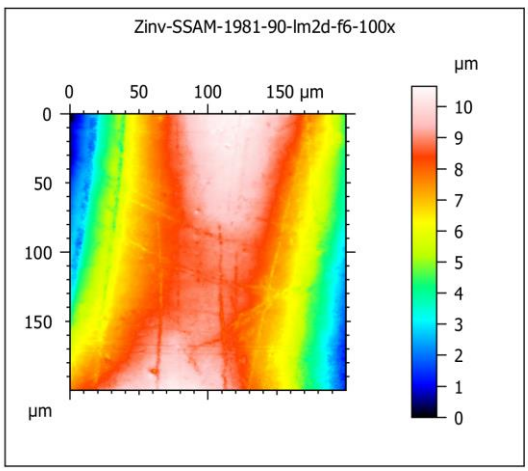
Zinv-SSAM-1981-90-lm2d-f6-100x
µm
0 50 100 150 µm
0
50
100
150
µm
10
9
8
7
6
5
4
3
2
1
0

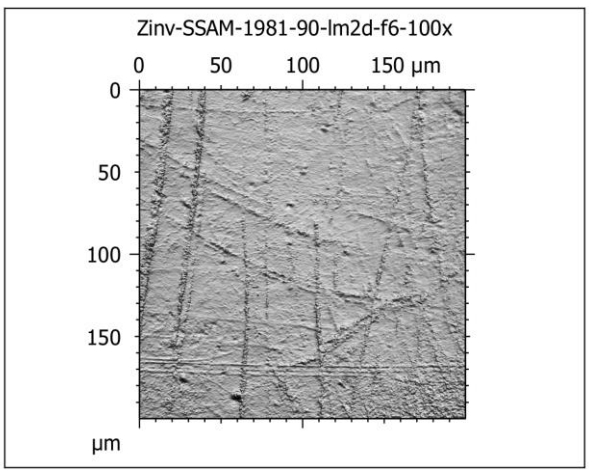
Zinv-SSAM-1981-90-lm2d-f6-100x
0 50 100 150 µm
0
50
100
150
µm

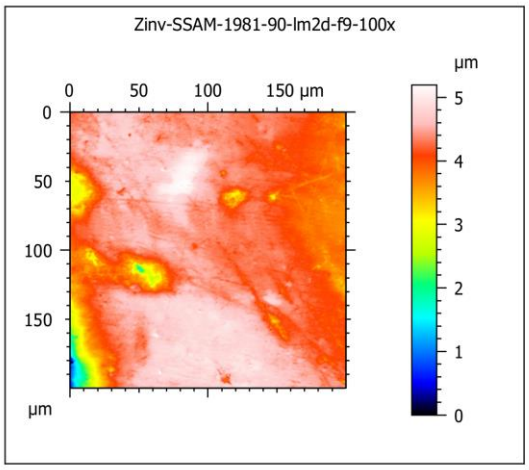
Zinv-SSAM-1981-90-lm2d-f9-100x
0
50
100
150 µm
µm
5
4
3
2
1
0

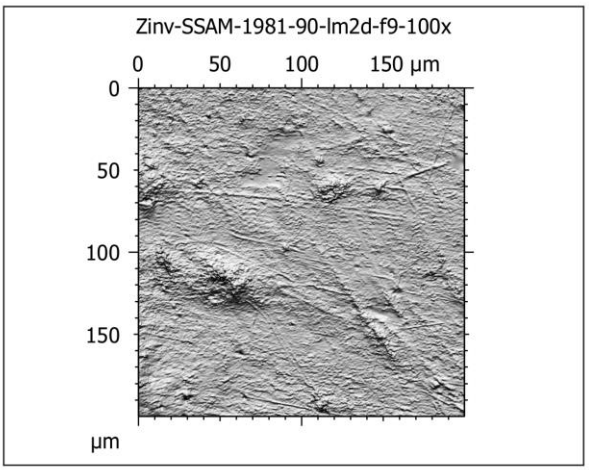
Zinv-SSAM-1981-90-lm2d-f9-100x
0
50
100
150 µm
µm

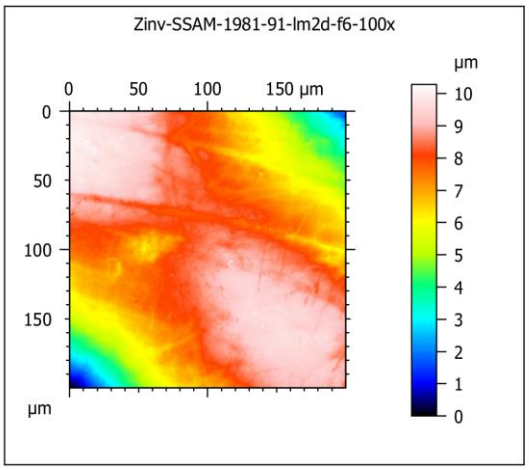
Zinv-SSAM-1981-91-lm2d-f6-100x
0
50
100
150 µm
µm
10
9
8
7
6
5
4
3
2
1
0

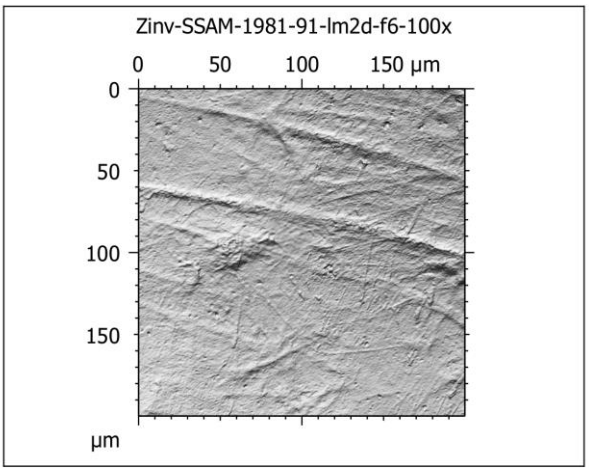
Zinv-SSAM-1981-91-lm2d-f6-100x
0
50
100
150 µm
µm

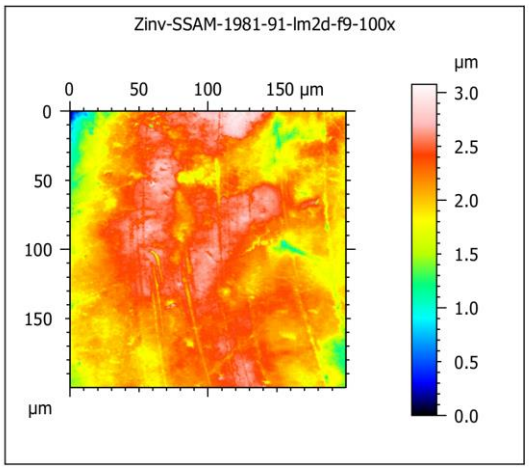
Zinv-SSAM-1981-91-lm2d-f9-100x
0
50
100
150 µm
µm
3.0
2.5
2.0
1.5
1.0
0.5
0.0

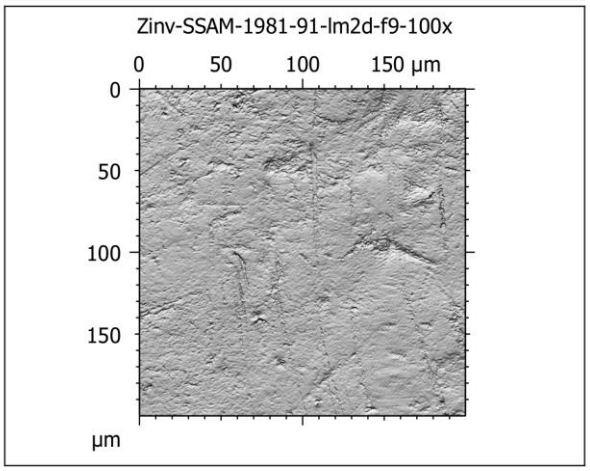
Zinv-SSAM-1981-91-lm2d-f9-100x
0
50
100
150 µm
µm

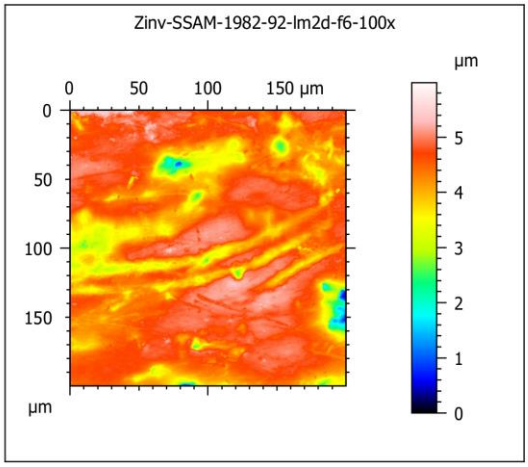
Zinv-SSAM-1982-92-lm2d-f6-100x
µm
0 50 100 150 µm
0
50
100
150
µm
5
4
3
2
1
0

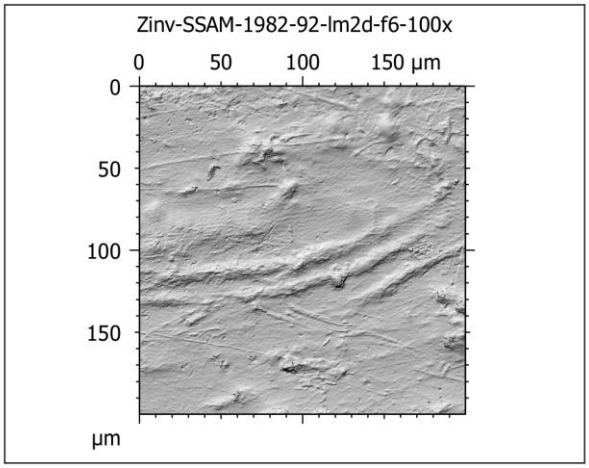
Zinv-SSAM-1982-92-lm2d-f6-100x
0 50 100 150 µm
0
50
100
150
µm

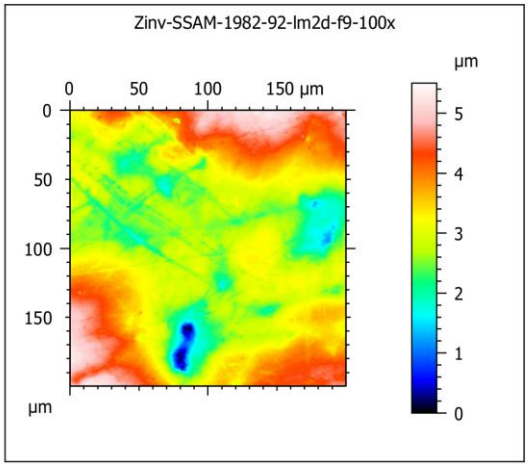
Zinv-SSAM-1982-92-lm2d-f9-100x
µm
0 50 100 150 µm
0
50
100
150
µm
5
4
3
2
1
0

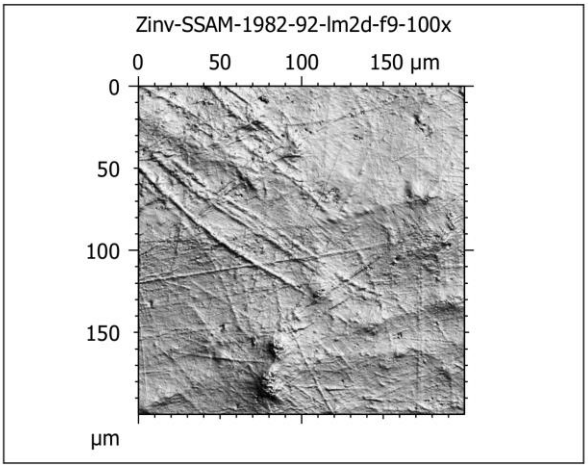
Zinv-SSAM-1982-92-lm2d-f9-100x
0 50 100 150 µm
0
50
100
150
µm

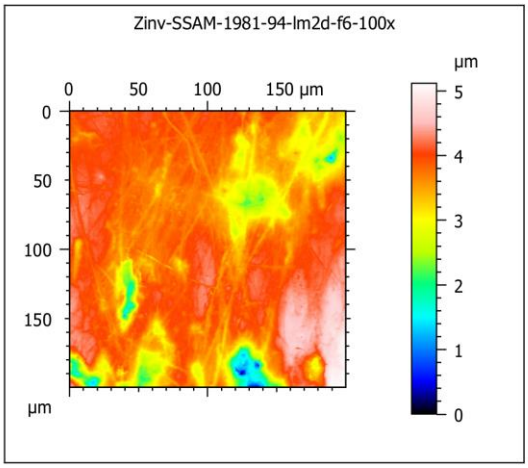
Zinv-SSAM-1981-94-lm2d-f6-100x
µm
0 50 100 150 µm
0
50
100
150
µm
5
4
3
2
1
0

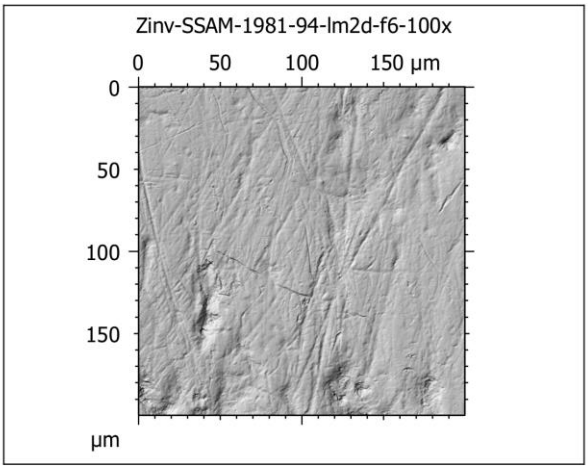
Zinv-SSAM-1981-94-lm2d-f6-100x
0 50 100 150 µm
0
50
100
150
µm

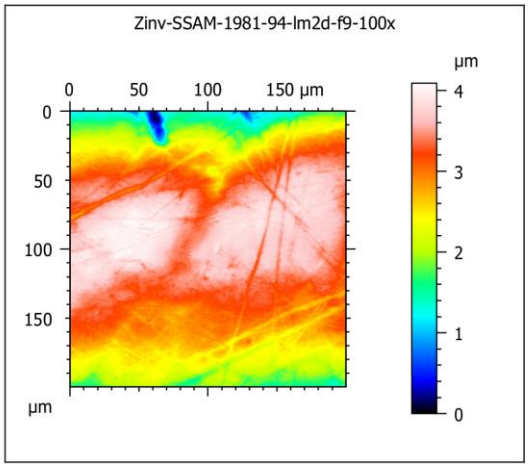
Zinv-SSAM-1981-94-lm2d-f9-100x
µm
0 50 100 150 µm
0
50
100
150
µm
4
3
2
1
0

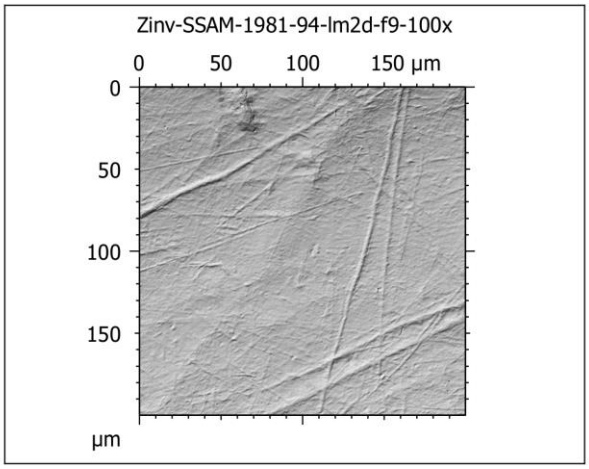
Zinv-SSAM-1981-94-lm2d-f9-100x
0 50 100 150 µm
0
50
100
150
µm

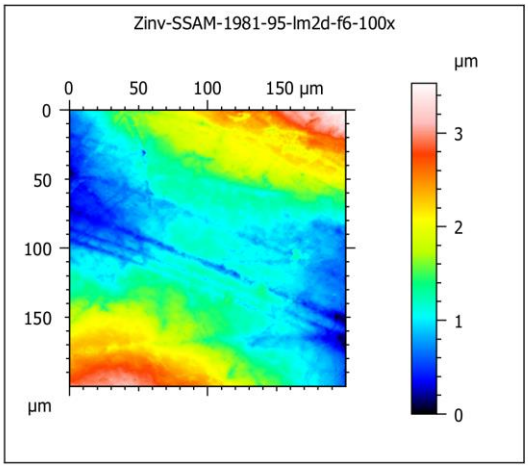
Zinv-SSAM-1981-95-lm2d-f6-100x
µm
0 50 100 150 µm
0
50
100
150
µm
3
2
1
0

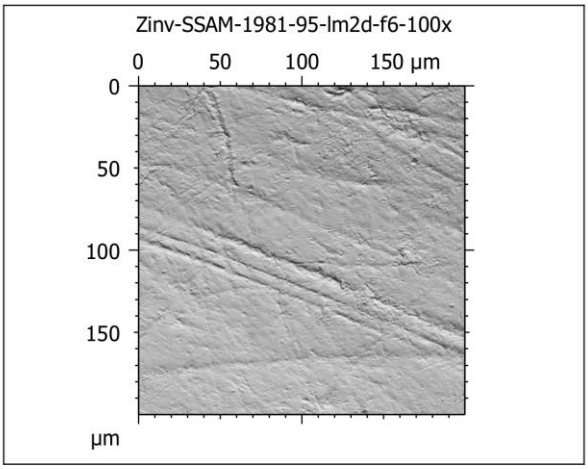
Zinv-SSAM-1981-95-lm2d-f6-100x
0 50 100 150 µm
0
50
100
150
µm

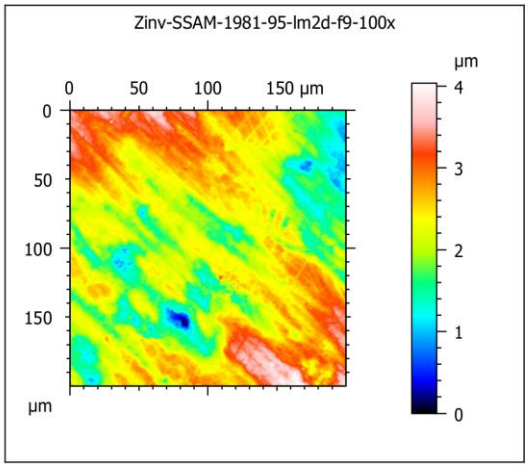
Zinv-SSAM-1981-95-lm2d-f9-100x
µm
0 50 100 150 µm
0
50
100
150
µm
4
3
2
1
0

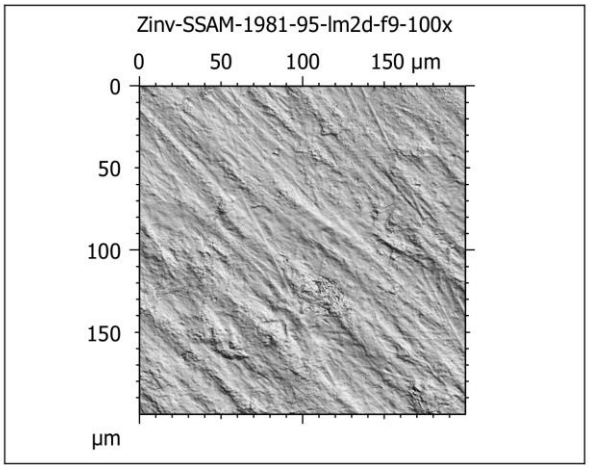
Zinv-SSAM-1981-95-lm2d-f9-100x
0 50 100 150 µm
0
50
100
150
µm

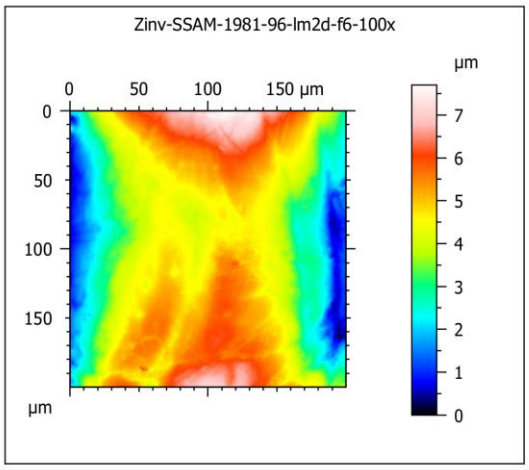
Zinv-SSAM-1981-96-lm2d-f6-100x
µm
0 50 100 150 µm
0
50
100
150
µm
7
6
5
4
3
2
1
0

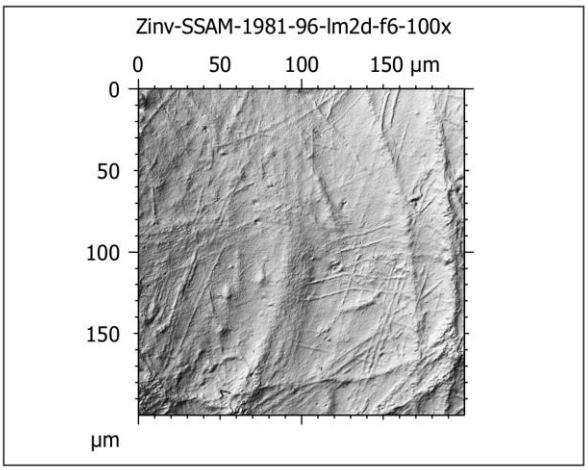
Zinv-SSAM-1981-96-lm2d-f6-100x
0 50 100 150 µm
0
50
100
150
µm

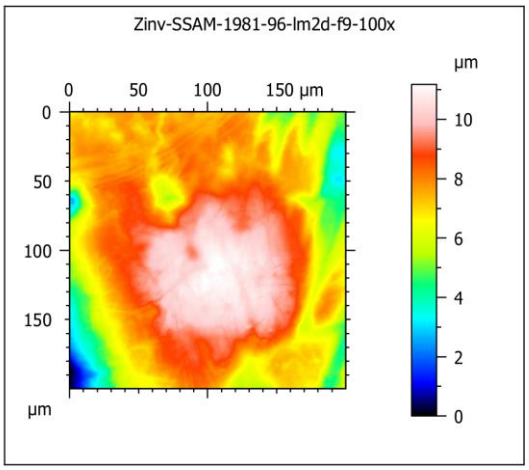
Zinv-SSAM-1981-96-lm2d-f9-100x
µm
0 50 100 150 µm
0
50
100
150
µm
10
8
6
4
2
0

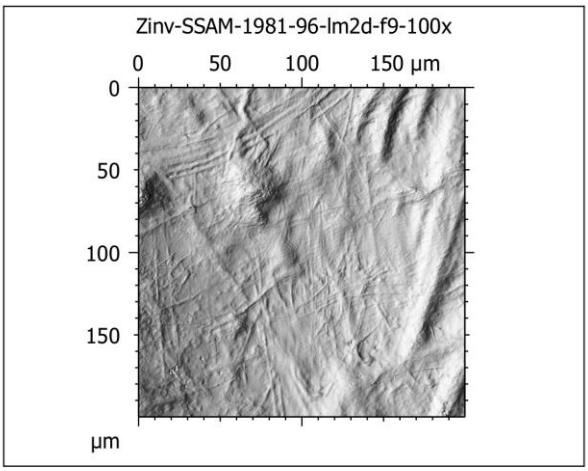
Zinv-SSAM-1981-96-lm2d-f9-100x
0 50 100 150 µm
0
50
100
150
µm

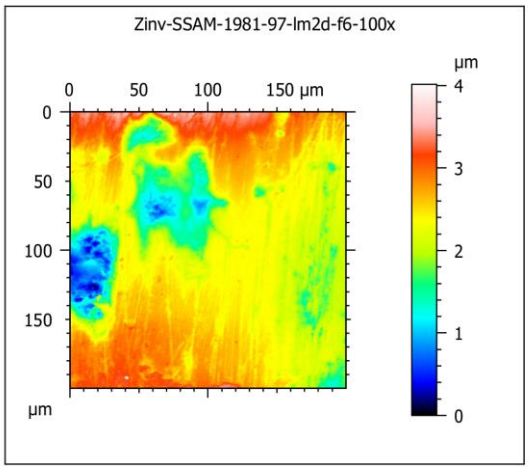
Zinv-SSAM-1981-97-lm2d-f6-100x
µm
0 50 100 150 µm
0
50
100
150
µm
4
3
2
1
0

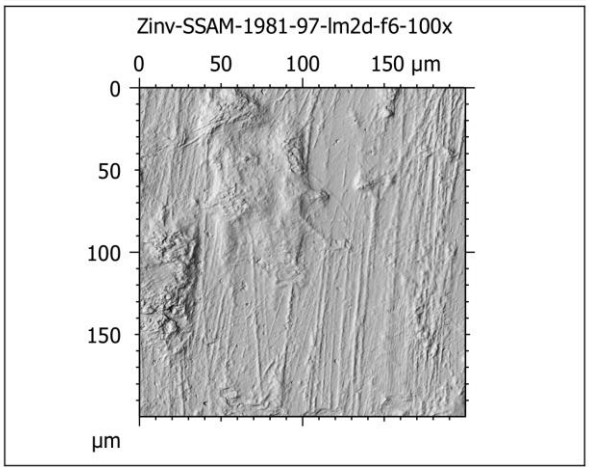
Zinv-SSAM-1981-97-lm2d-f6-100x
0 50 100 150 µm
0
50
100
150
µm

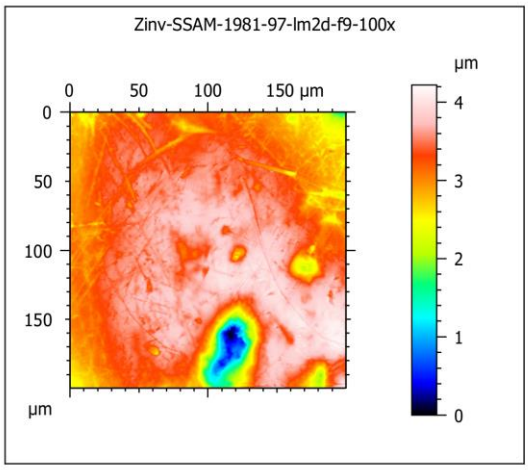
Zinv-SSAM-1981-97-lm2d-f9-100x
µm
0 50 100 150 µm
0
50
100
150
µm
4
3
2
1
0

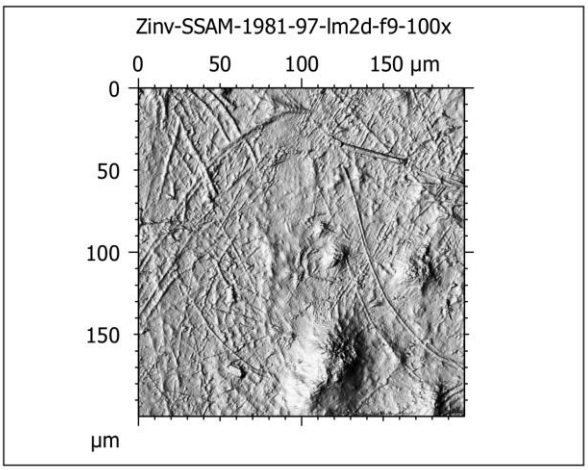
Zinv-SSAM-1981-97-lm2d-f9-100x
0 50 100 150 µm
0
50
100
150
µm

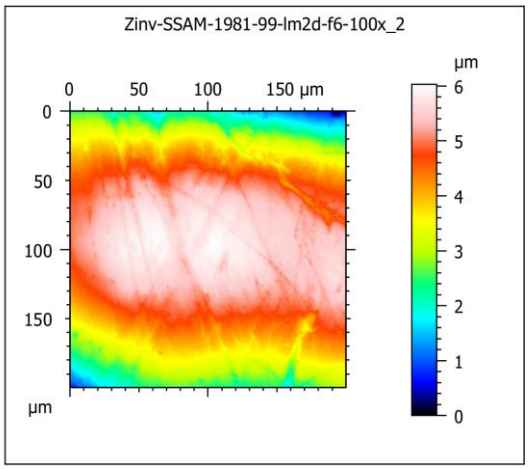
Zinv-SSAM-1981-99-lm2d-f6-100x_2
µm
0 50 100 150 µm
0
50
100
150
µm
6
5
4
3
2
1
0

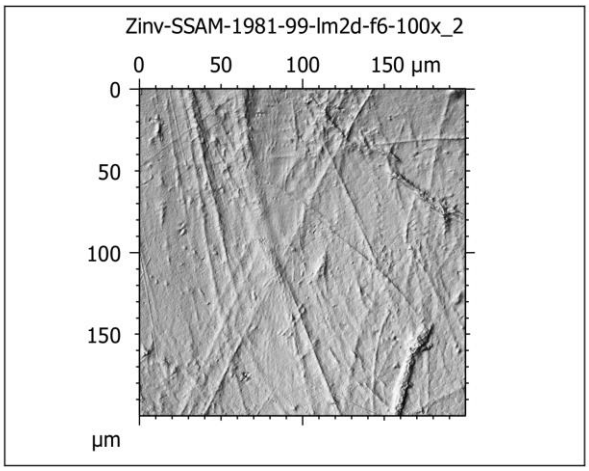
Zinv-SSAM-1981-99-lm2d-f6-100x_2
0 50 100 150 µm
0
50
100
150
µm

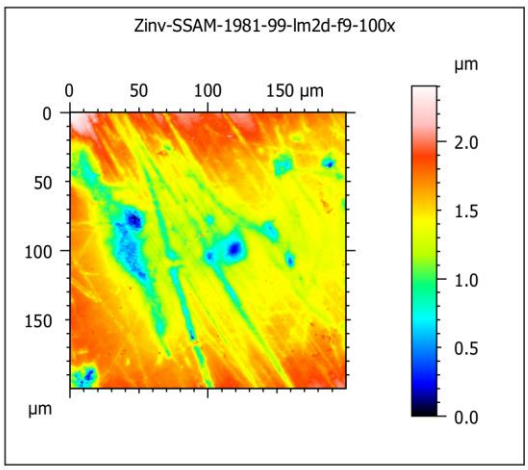
Zinv-SSAM-1981-99-lm2d-f9-100x
µm
0 50 100 150 µm
0
50
100
150
µm
2.0
1.5
1.0
0.5
0.0

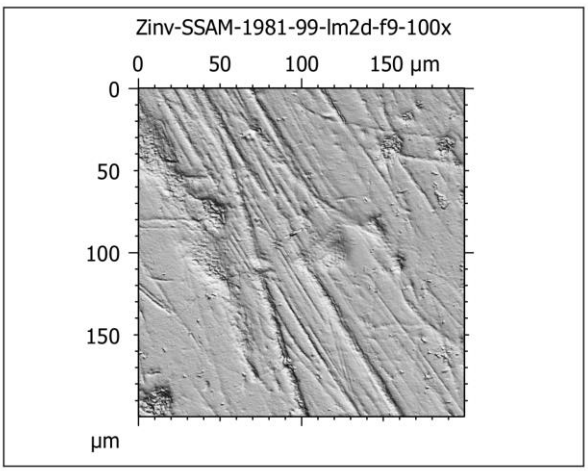
Zinv-SSAM-1981-99-lm2d-f9-100x
0 50 100 150 µm
0
50
100
150
µm

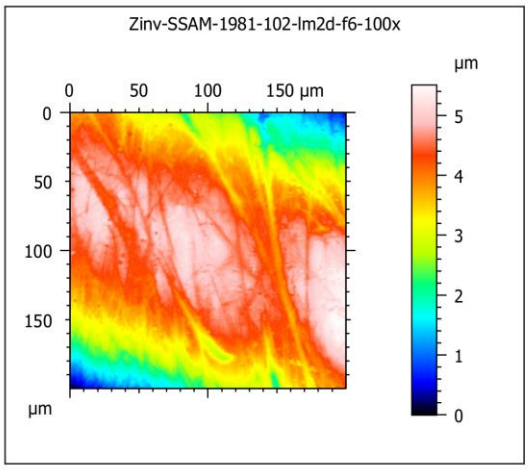
Zinv-SSAM-1981-102-lm2d-f6-100x
0
50
100
150 µm
µm
5
4
3
2
1
0

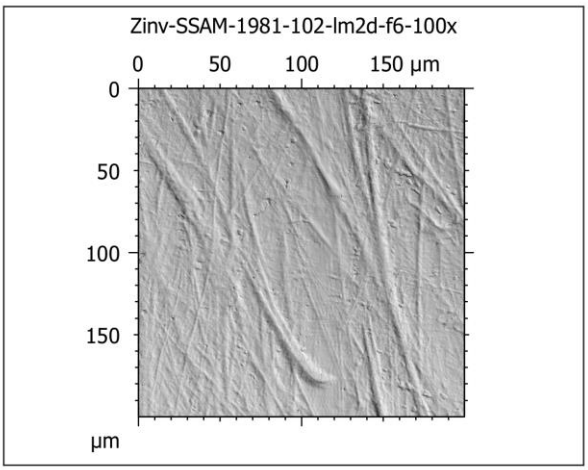
Zinv-SSAM-1981-102-lm2d-f6-100x
0
50
100
150 µm
µm

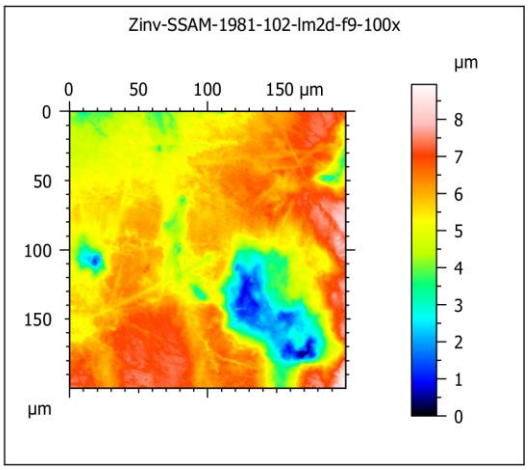
Zinv-SSAM-1981-102-lm2d-f9-100x
0
50
100
150 µm
µm
8
7
6
5
4
3
2
1
0

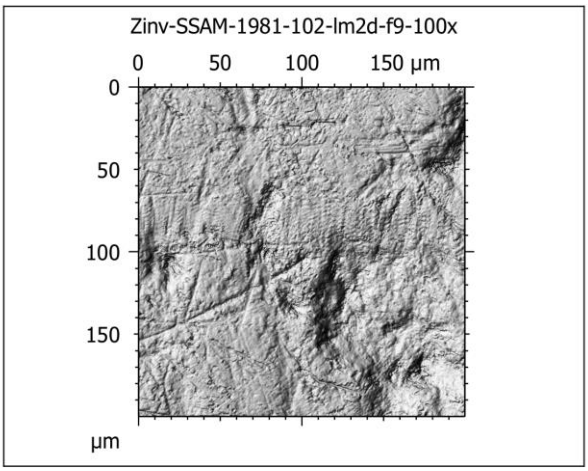
Zinv-SSAM-1981-102-lm2d-f9-100x
0
50
100
150 µm
µm

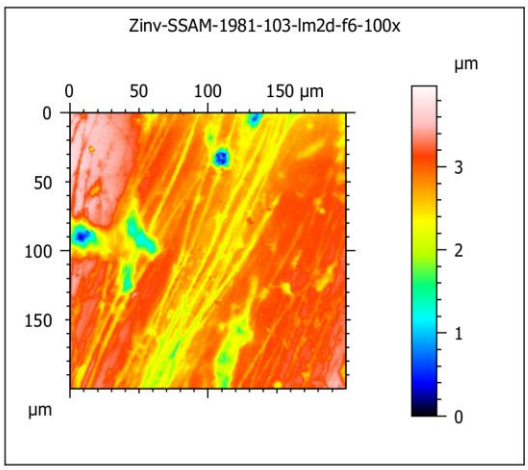
Zinv-SSAM-1981-103-lm2d-f6-100x
0
50
100
150 µm
µm
3
2
1
0

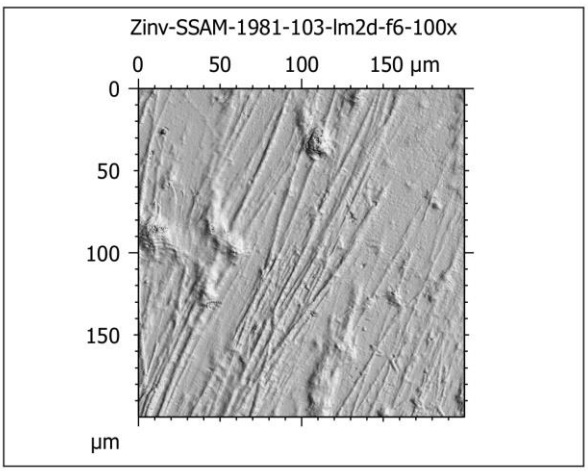
Zinv-SSAM-1981-103-lm2d-f6-100x
0
50
100
150 µm
µm

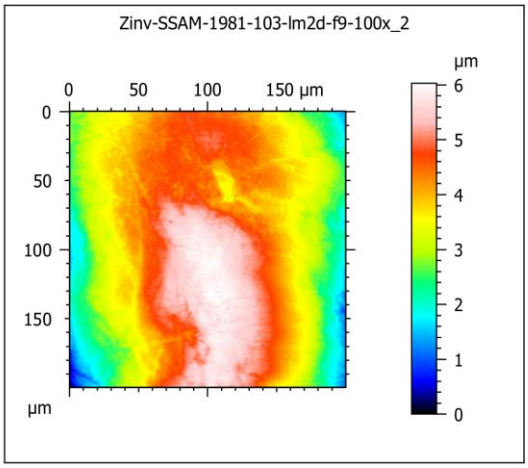
Zinv-SSAM-1981-103-lm2d-f9-100x_2
0
50
100
150 µm
µm
6
5
4
3
2
1
0

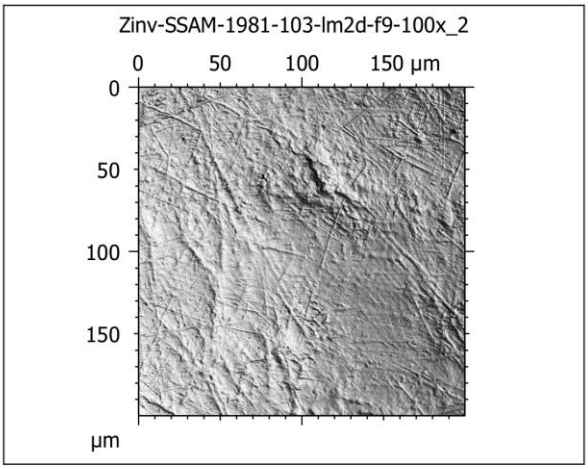
Zinv-SSAM-1981-103-lm2d-f9-100x_2
0
50
100
150 µm
µm

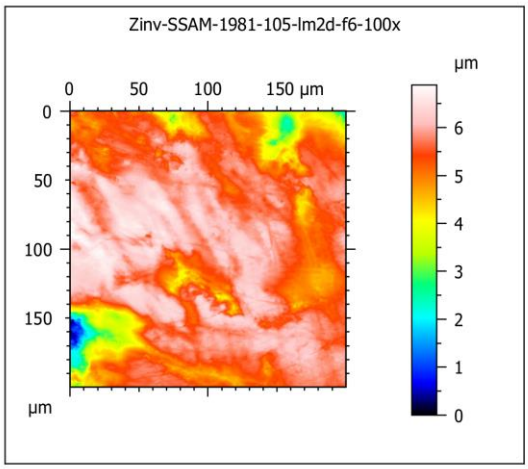
Zinv-SSAM-1981-105-lm2d-f6-100x
0
50
100
150 µm
µm
6
5
4
3
2
1
0

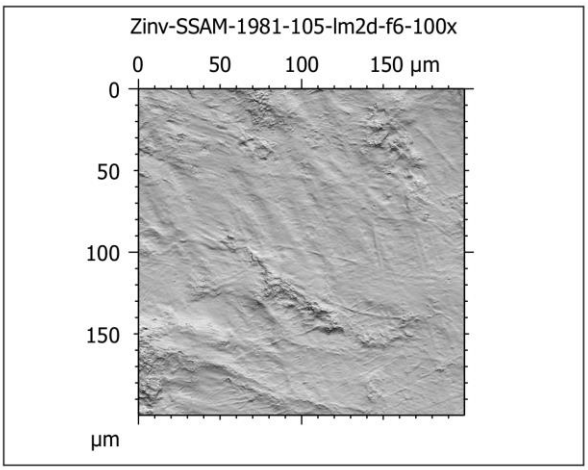
Zinv-SSAM-1981-105-lm2d-f6-100x
0
50
100
150 µm
µm

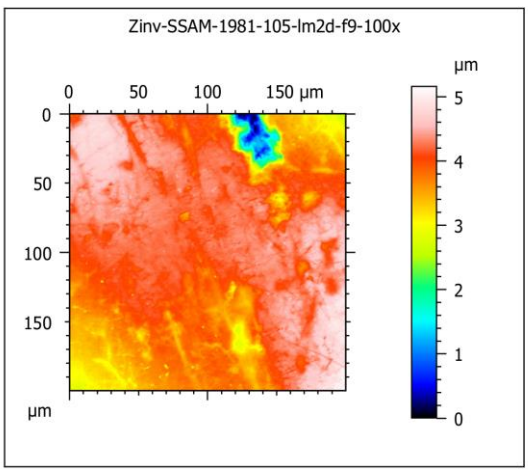
Zinv-SSAM-1981-105-lm2d-f9-100x
0
50
100
150 µm
µm
5
4
3
2
1
0

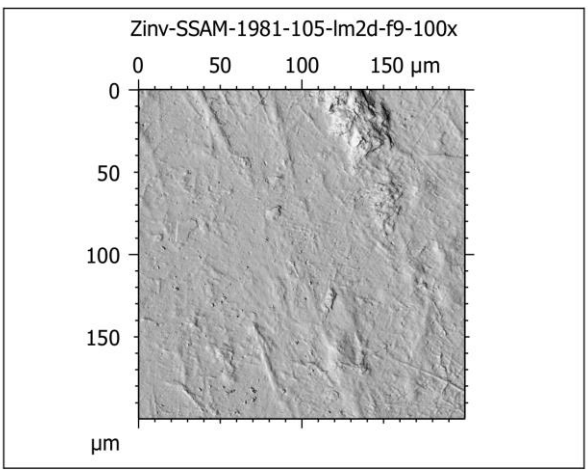
Zinv-SSAM-1981-105-lm2d-f9-100x
0
50
100
150 µm
µm

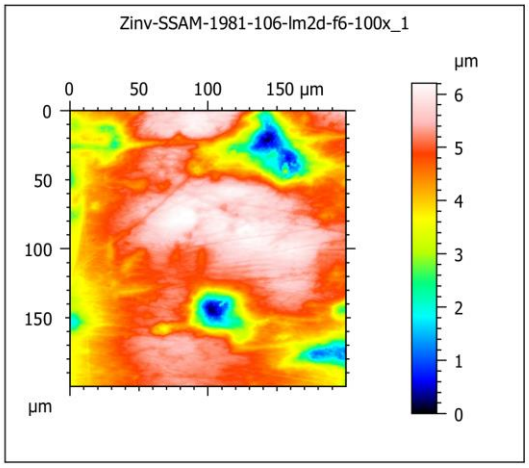
Zinv-SSAM-1981-106-lm2d-f6-100x_1
µm
0 50 100 150 µm
0
50
100
150
µm
6
5
4
3
2
1
0

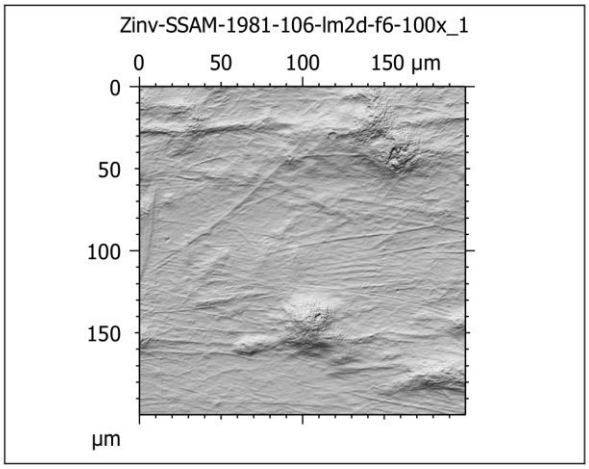
Zinv-SSAM-1981-106-lm2d-f6-100x_1
0 50 100 150 µm
0
50
100
150
µm

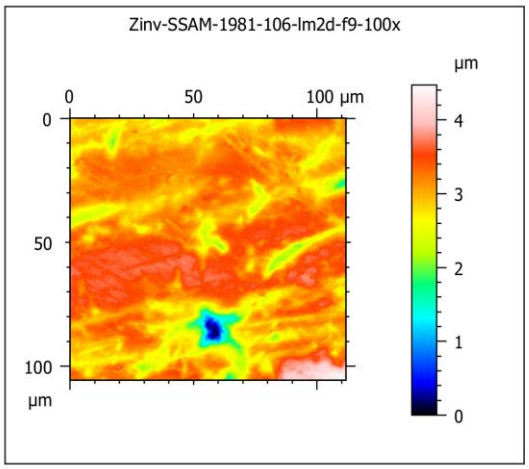
Zinv-SSAM-1981-106-lm2d-f9-100x
µm
0 50 100 µm
0
50
100
µm
4
3
2
1
0

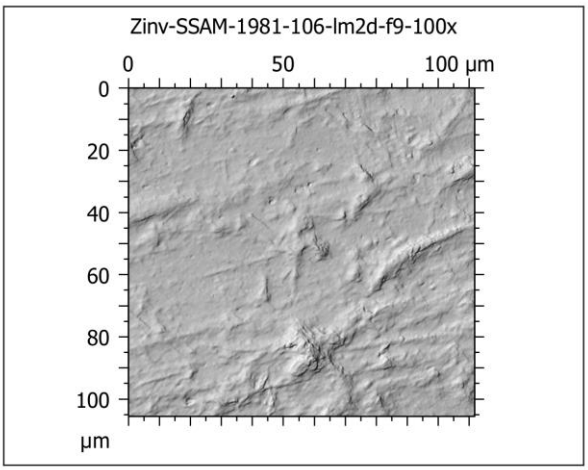
Zinv-SSAM-1981-106-lm2d-f9-100x
0 50 100 µm
0
20
40
60
80
100
µm

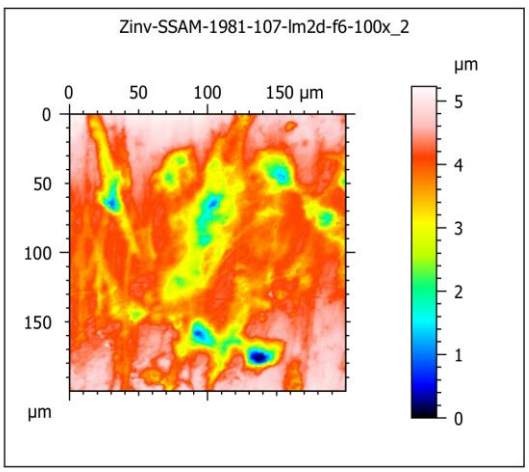
Zinv-SSAM-1981-107-lm2d-f6-100x_2
µm
0 50 100 150 µm
0
50
100
150
µm
5
4
3
2
1
0

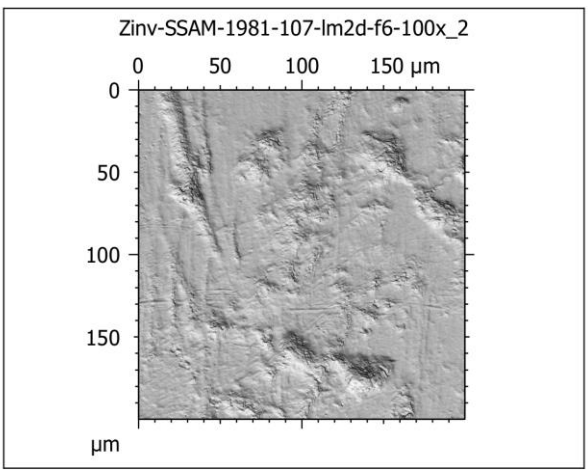
Zinv-SSAM-1981-107-lm2d-f6-100x_2
0 50 100 150 µm
0
50
100
150
µm

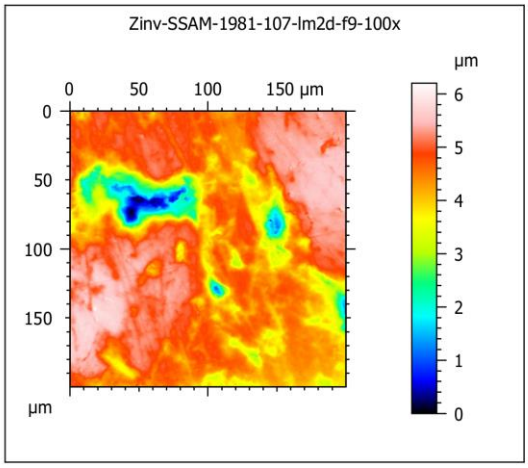
Zinv-SSAM-1981-107-lm2d-f9-100x
µm
0 50 100 150 µm
0
50
100
150
µm
6
5
4
3
2
1
0

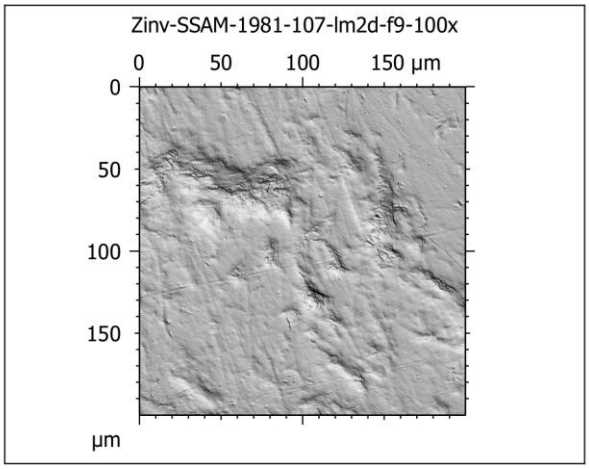
Zinv-SSAM-1981-107-lm2d-f9-100x
0 50 100 150 µm
0
50
100
150
µm

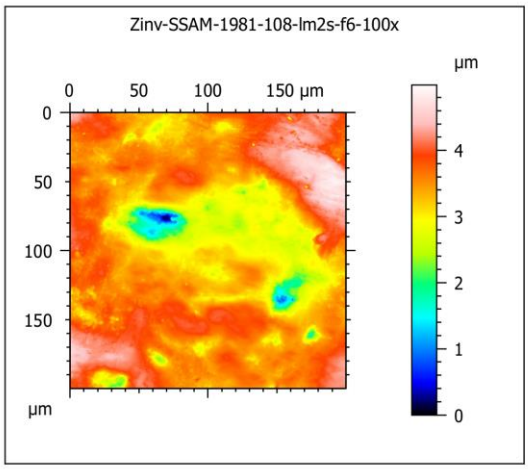
Zinv-SSAM-1981-108-lm2s-f6-100x
µm
0 50 100 150 µm
0
50
100
150
µm
4
3
2
1
0

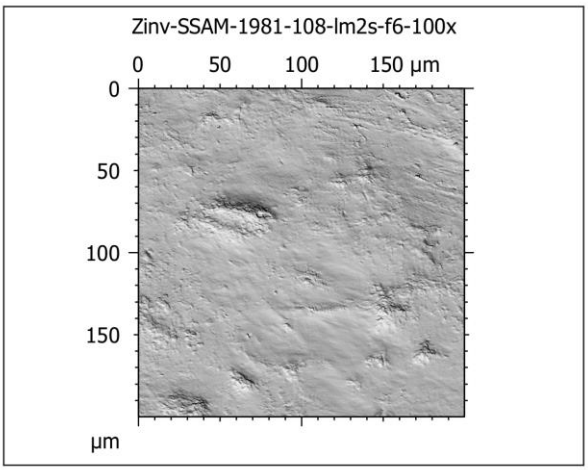
Zinv-SSAM-1981-108-lm2s-f6-100x
0 50 100 150 µm
0
50
100
150
µm

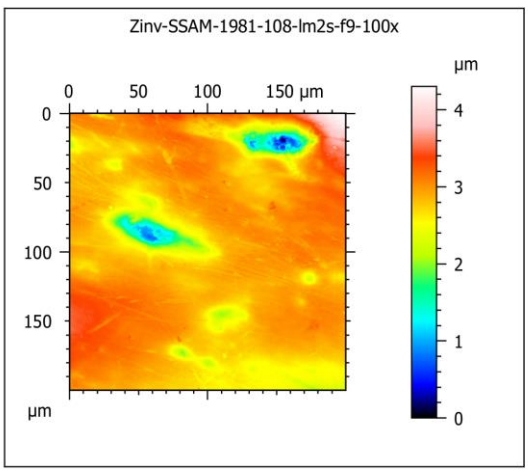
Zinv-SSAM-1981-108-lm2s-f9-100x
µm
0 50 100 150 µm
0
50
100
150
µm
4
3
2
1
0

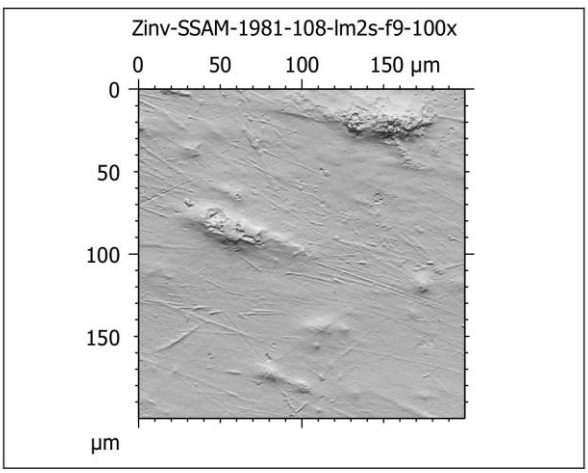
Zinv-SSAM-1981-108-lm2s-f9-100x
0 50 100 150 µm
0
50
100
150
µm

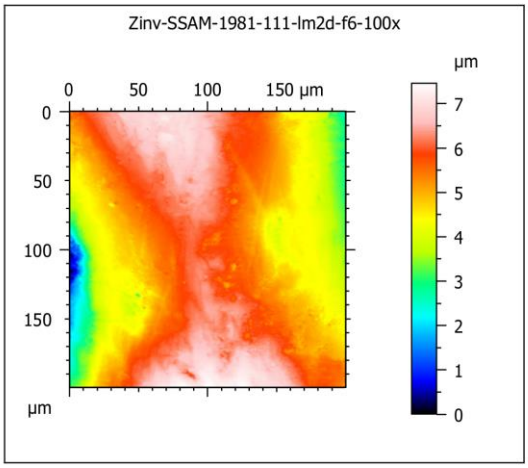
Zinv-SSAM-1981-111-lm2d-f6-100x
0
50
100
150 µm
µm
7
6
5
4
3
2
1
0

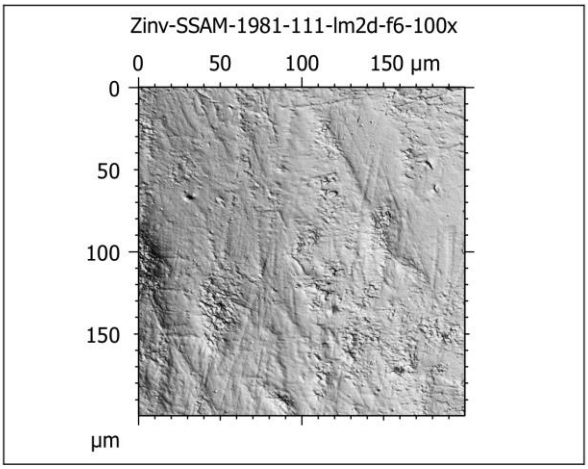
Zinv-SSAM-1981-111-lm2d-f6-100x
0
50
100
150 µm
µm

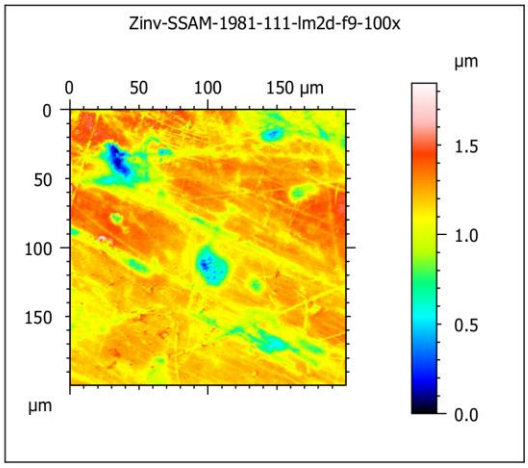
Zinv-SSAM-1981-111-lm2d-f9-100x
0
50
100
150 µm
µm
1.5
1.0
0.5
0.0

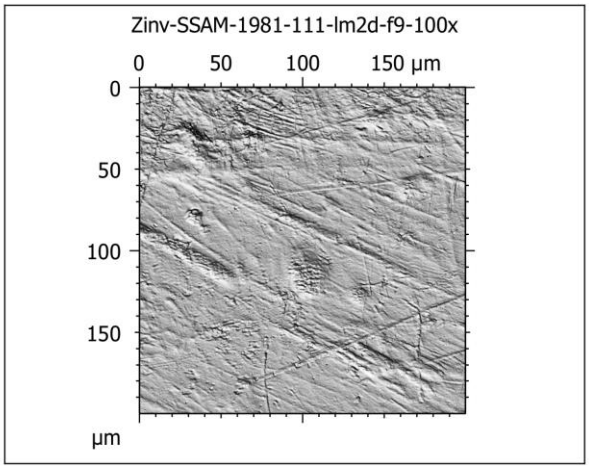
Zinv-SSAM-1981-111-lm2d-f9-100x
0
50
100
150 µm
µm

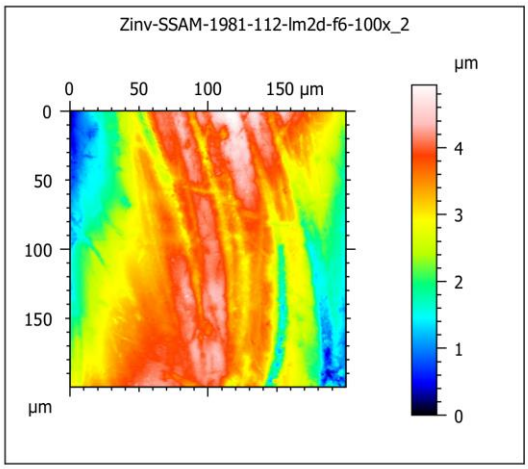
Zinv-SSAM-1981-112-lm2d-f6-100x_2
0
50
100
150 µm
µm
4
3
2
1
0

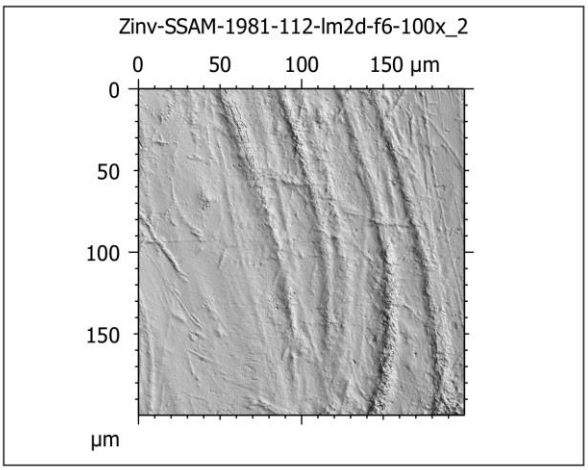
Zinv-SSAM-1981-112-lm2d-f6-100x_2
0
50
100
150 µm
µm

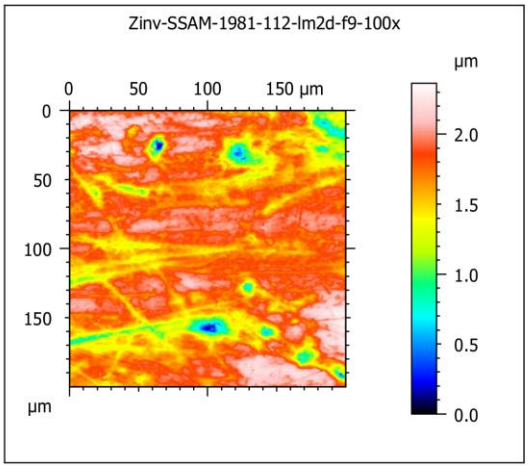
Zinv-SSAM-1981-112-lm2d-f9-100x
0
50
100
150 µm
µm
2.0
1.5
1.0
0.5
0.0

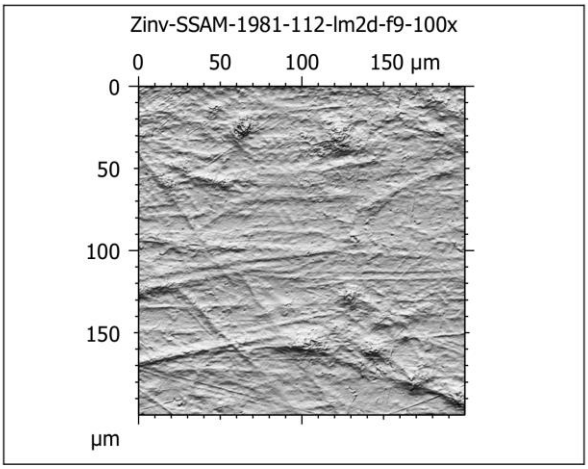
Zinv-SSAM-1981-112-lm2d-f9-100x
0
50
100
150 µm
µm

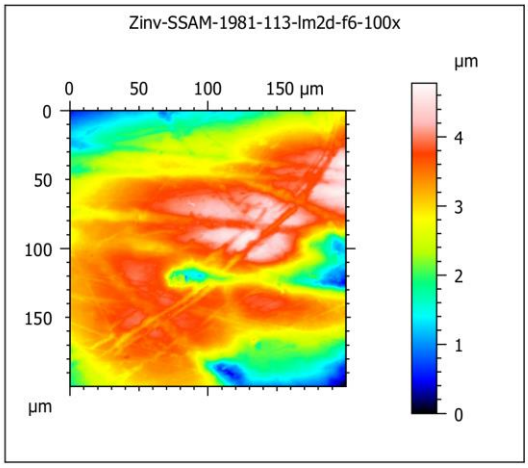
Zinv-SSAM-1981-113-lm2d-f6-100x
0
50
100
150 µm
µm
4
3
2
1
0

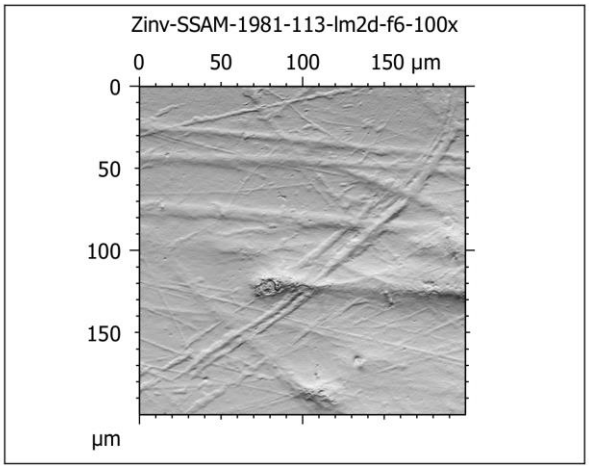
Zinv-SSAM-1981-113-lm2d-f6-100x
0
50
100
150 µm
µm

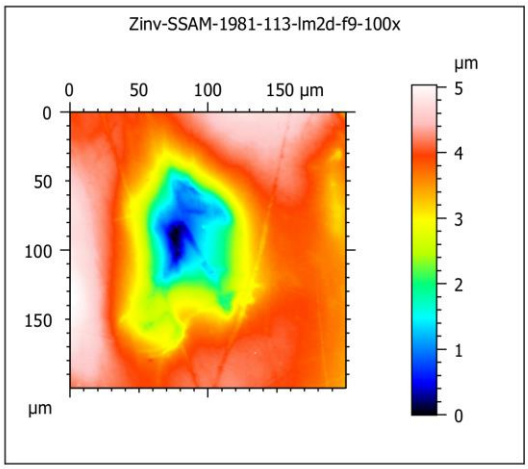
Zinv-SSAM-1981-113-lm2d-f9-100x
0
50
100
150 µm
µm
5
4
3
2
1
0

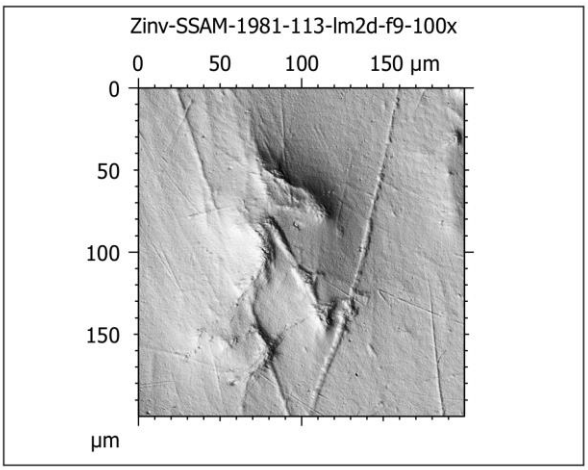
Zinv-SSAM-1981-113-lm2d-f9-100x
0
50
100
150 µm
µm

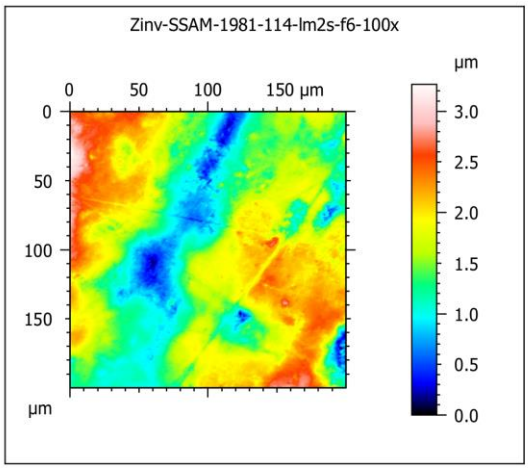
Zinv-SSAM-1981-114-lm2s-f6-100x
0
50
100
150 µm
µm
3.0
2.5
2.0
1.5
1.0
0.5
0.0

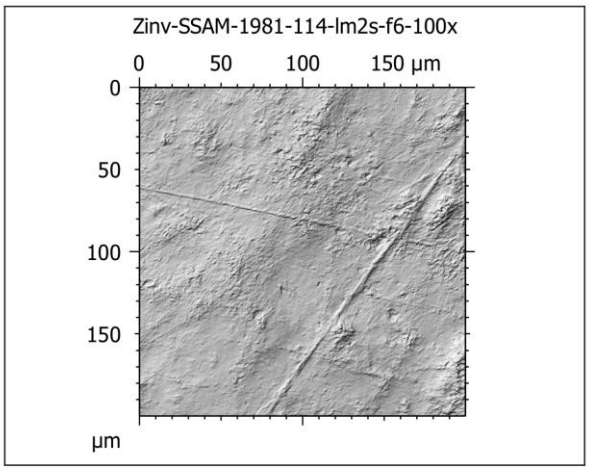
Zinv-SSAM-1981-114-lm2s-f6-100x
0
50
100
150 µm
µm

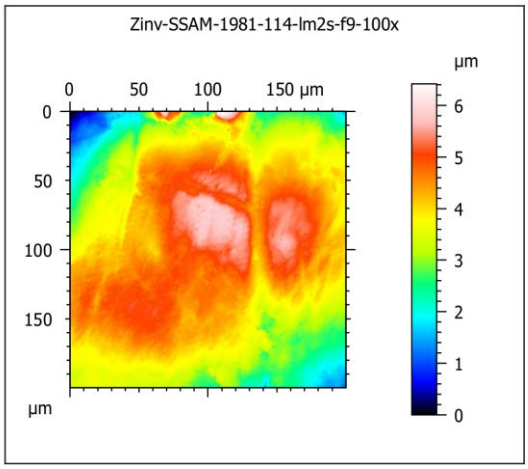
Zinv-SSAM-1981-114-lm2s-f9-100x
0
50
100
150 µm
µm
6
5
4
3
2
1
0

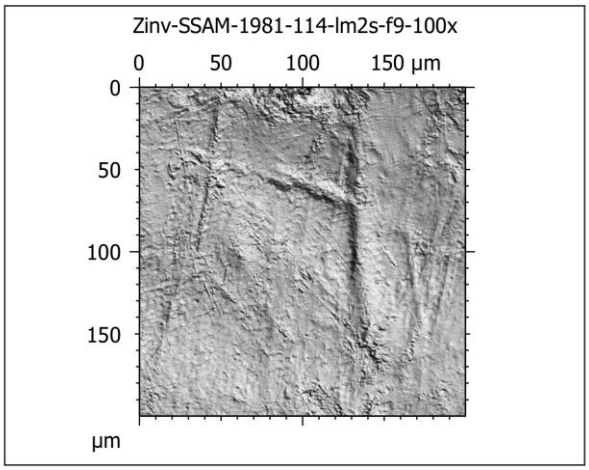
Zinv-SSAM-1981-114-lm2s-f9-100x
0
50
100
150 µm
µm

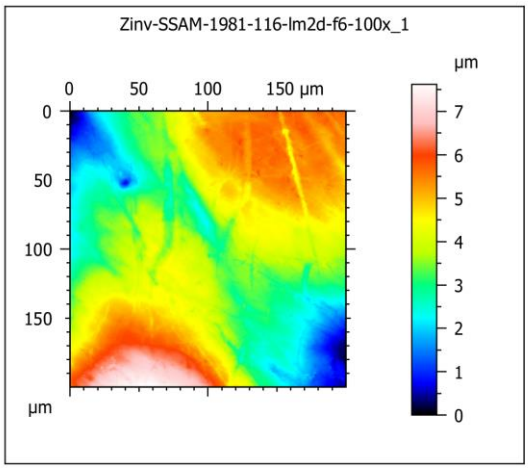
Zinv-SSAM-1981-116-lm2d-f6-100x_1
0
50
100
150 µm
µm
7
6
5
4
3
2
1
0

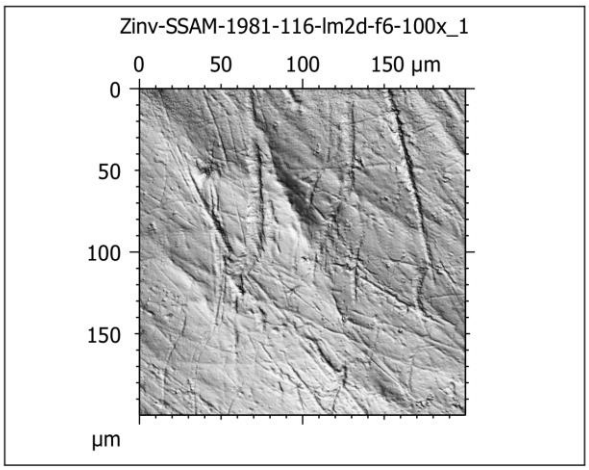
Zinv-SSAM-1981-116-lm2d-f6-100x_1
0
50
100
150 µm
µm

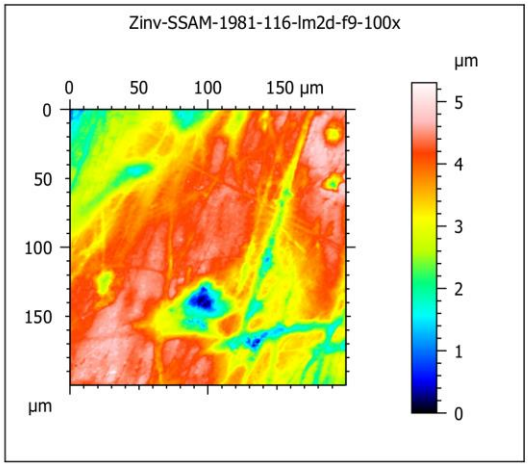
Zinv-SSAM-1981-116-lm2d-f9-100x
0
50
100
150 µm
µm
0
50
100
150
µm
5
4
3
2
1
0

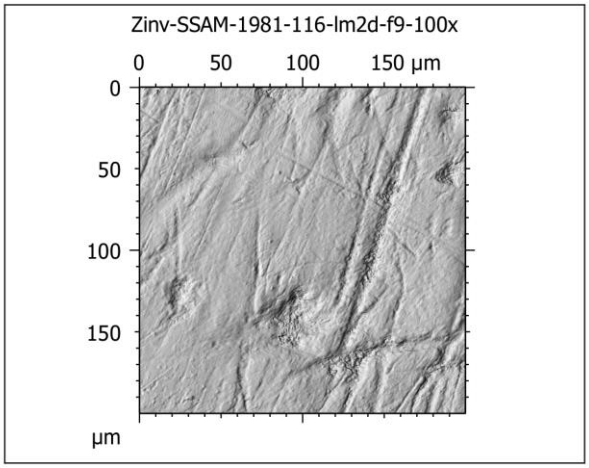
Zinv-SSAM-1981-116-lm2d-f9-100x
0
50
100
150 µm
0
50
100
150
µm

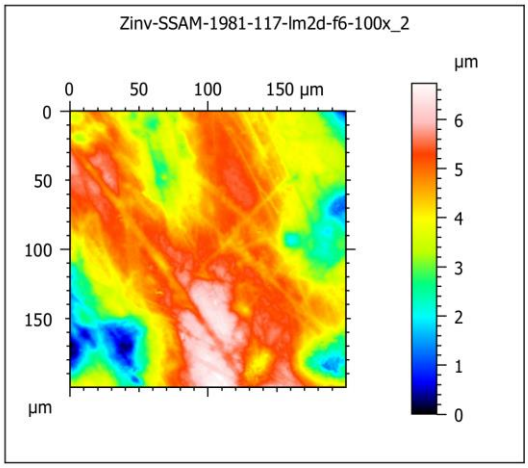
Zinv-SSAM-1981-117-lm2d-f6-100x_2
0
50
100
150 µm
µm
0
50
100
150
µm
6
5
4
3
2
1
0

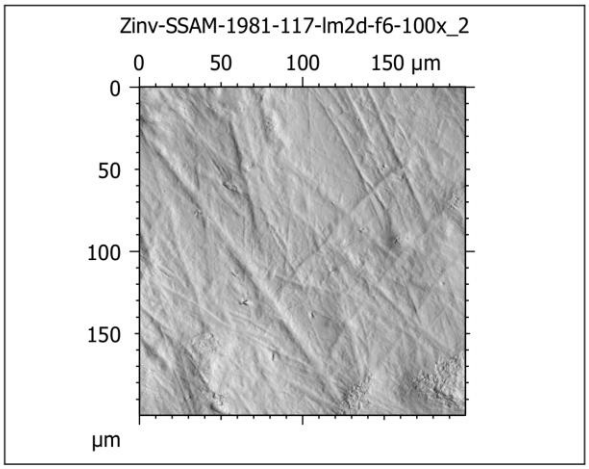
Zinv-SSAM-1981-117-lm2d-f6-100x_2
0
50
100
150 µm
0
50
100
150
µm

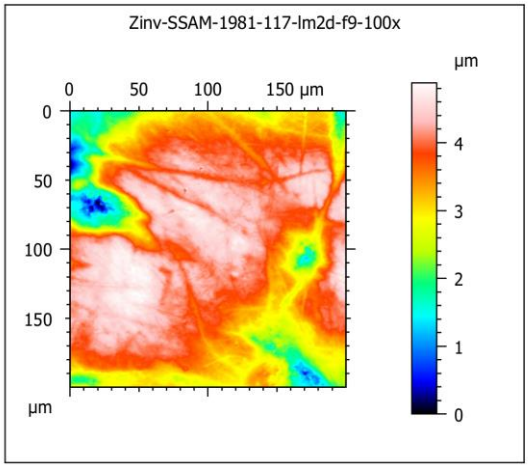
Zinv-SSAM-1981-117-lm2d-f9-100x
0
50
100
150 µm
µm
0
50
100
150
µm
4
3
2
1
0

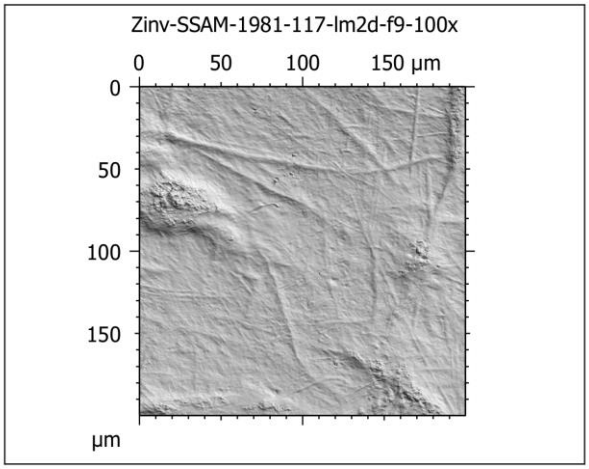
Zinv-SSAM-1981-117-lm2d-f9-100x
0
50
100
150 µm
0
50
100
150
µm

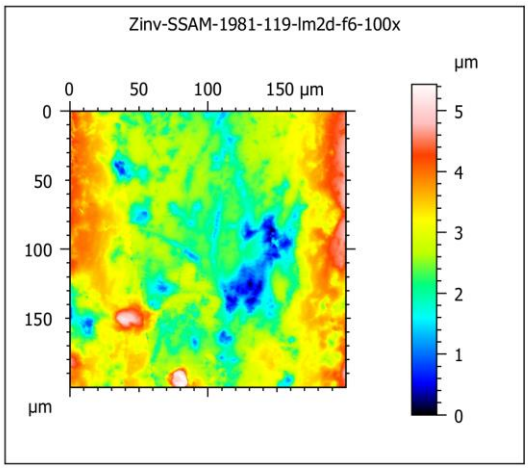
Zinv-SSAM-1981-119-lm2d-f6-100x
0
50
100
150 µm
µm
5
4
3
2
1
0

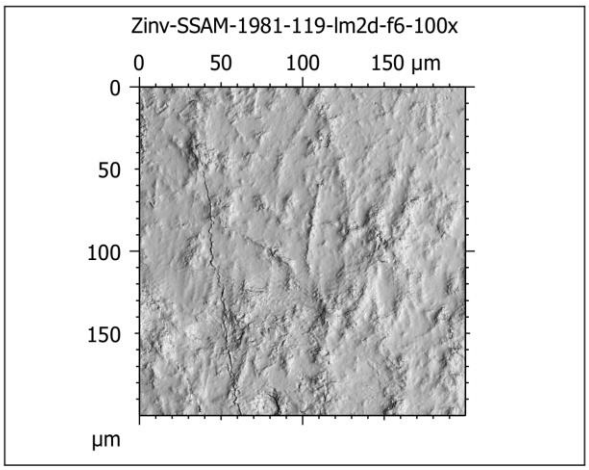
Zinv-SSAM-1981-119-lm2d-f6-100x
0
50
100
150 µm
µm

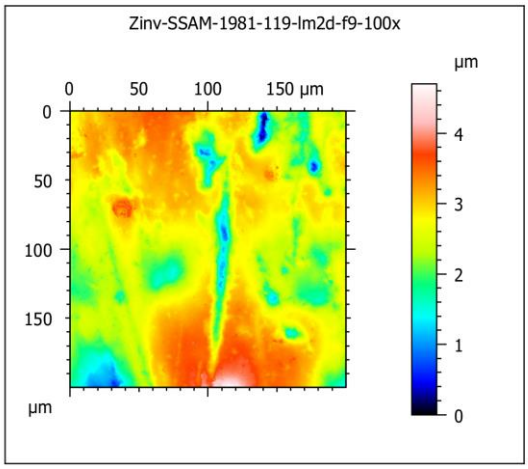
Zinv-SSAM-1981-119-lm2d-f9-100x
0
50
100
150 µm
µm
4
3
2
1
0

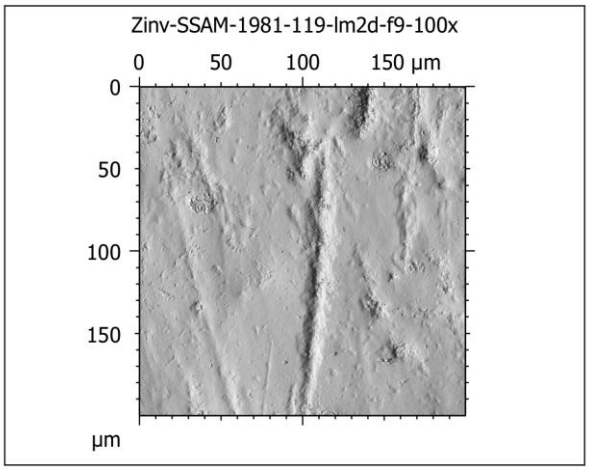
Zinv-SSAM-1981-119-lm2d-f9-100x
0
50
100
150 µm
µm

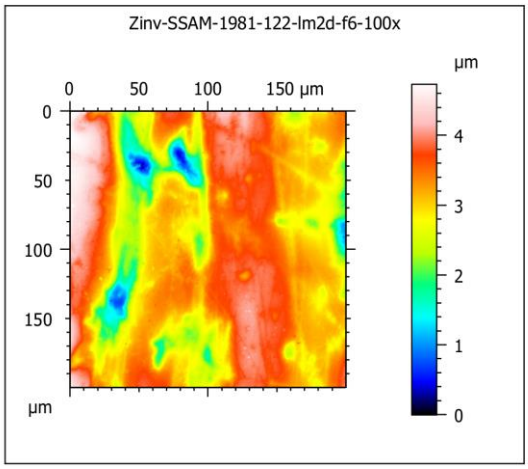
Zinv-SSAM-1981-122-lm2d-f6-100x
0
50
100
150 µm
µm
4
3
2
1
0

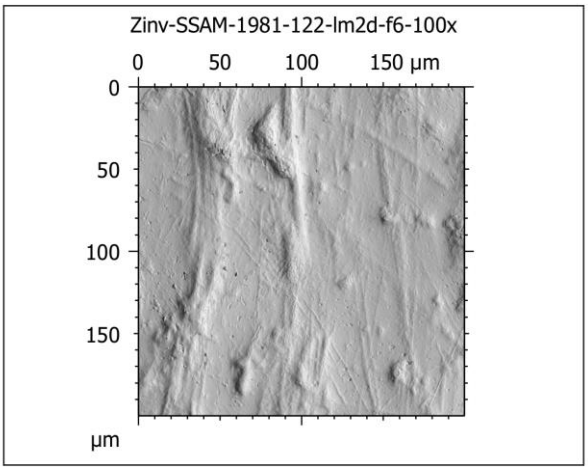
Zinv-SSAM-1981-122-lm2d-f6-100x
0
50
100
150 µm
µm

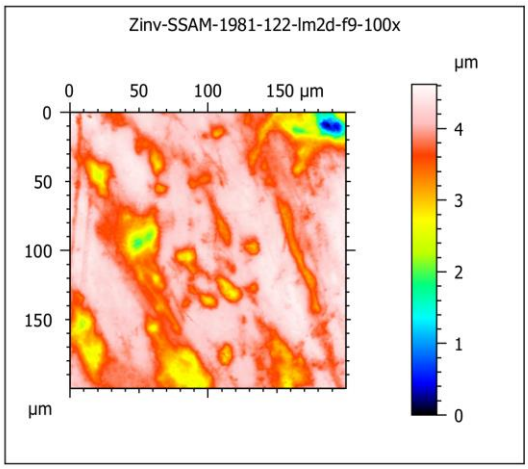
Zinv-SSAM-1981-122-lm2d-f9-100x
µm
0 50 100 150 µm
0
50
100
150
µm
4
3
2
1
0

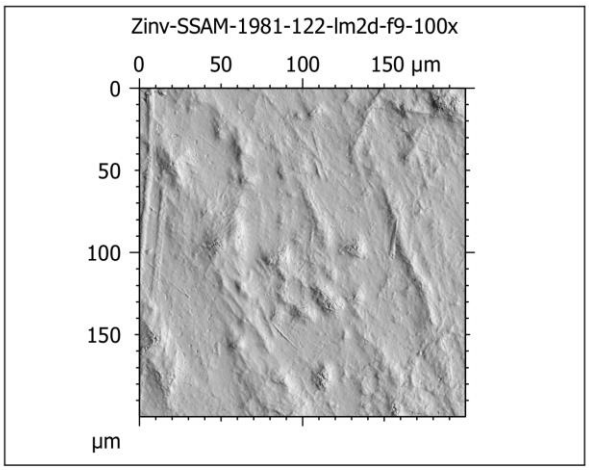
Zinv-SSAM-1981-122-lm2d-f9-100x
0 50 100 150 µm
0
50
100
150
µm

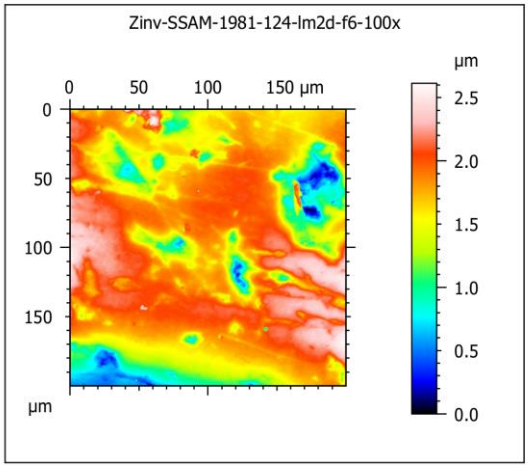
Zinv-SSAM-1981-124-lm2d-f6-100x
µm
0 50 100 150 µm
0
50
100
150
µm
2.5
2.0
1.5
1.0
0.5
0.0

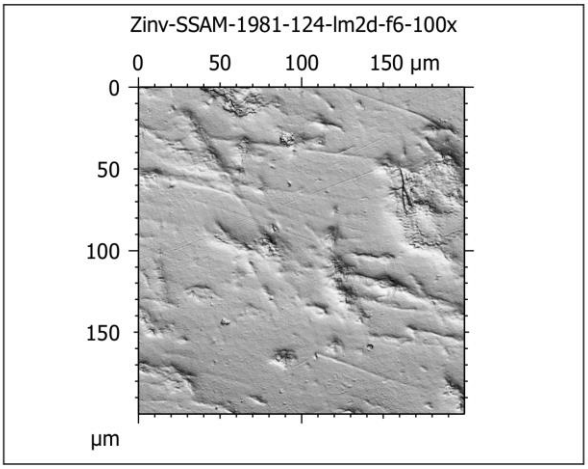
Zinv-SSAM-1981-124-lm2d-f6-100x
0 50 100 150 µm
0
50
100
150
µm

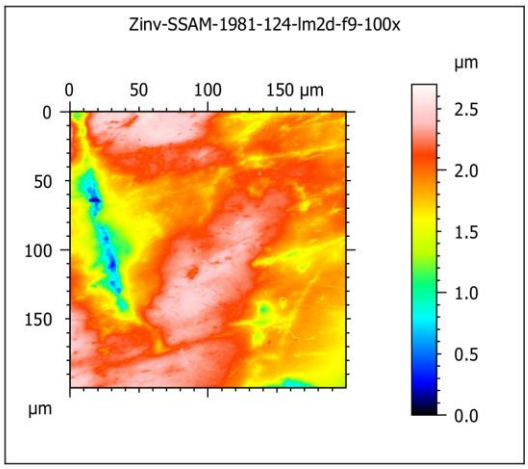
Zinv-SSAM-1981-124-lm2d-f9-100x
µm
0 50 100 150 µm
0
50
100
150
µm
2.5
2.0
1.5
1.0
0.5
0.0

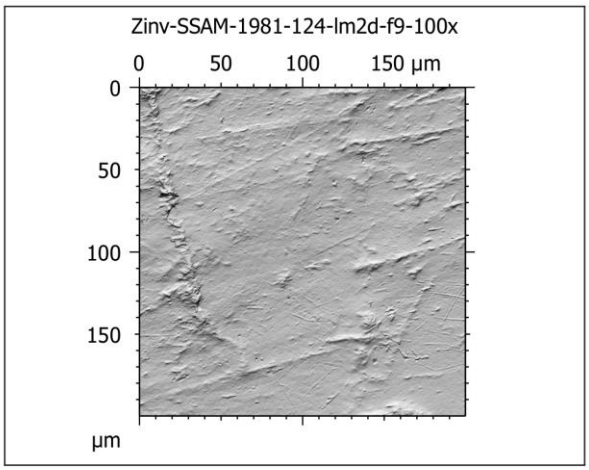
Zinv-SSAM-1981-124-lm2d-f9-100x
0 50 100 150 µm
0
50
100
150
µm

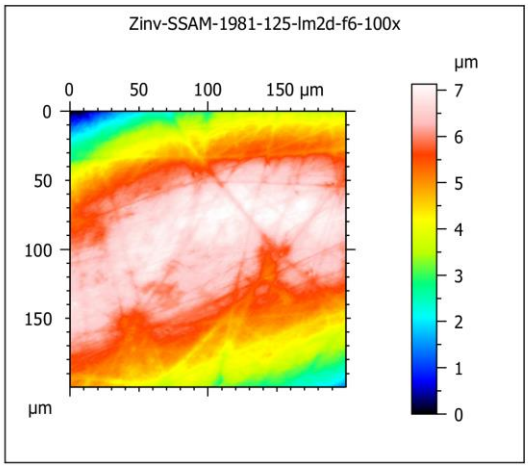
Zinv-SSAM-1981-125-lm2d-f6-100x
0
50
100
150 µm
µm
7
6
5
4
3
2
1
0

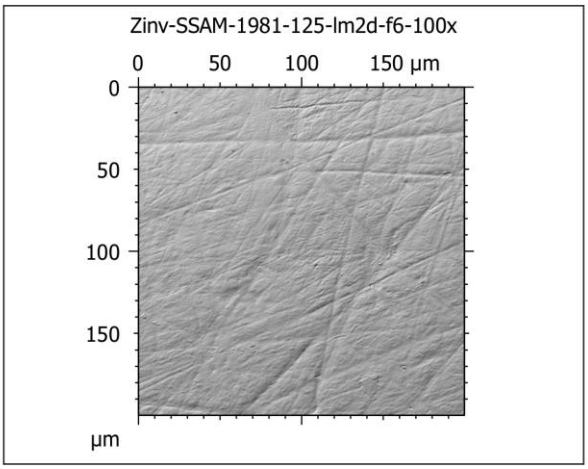
Zinv-SSAM-1981-125-lm2d-f6-100x
0
50
100
150 µm
µm

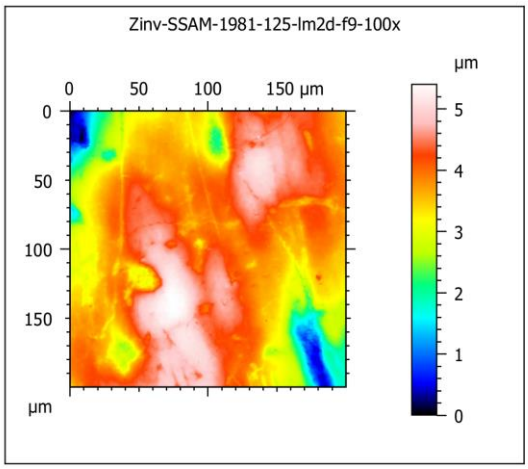
Zinv-SSAM-1981-125-lm2d-f9-100x
0
50
100
150 µm
µm
5
4
3
2
1
0

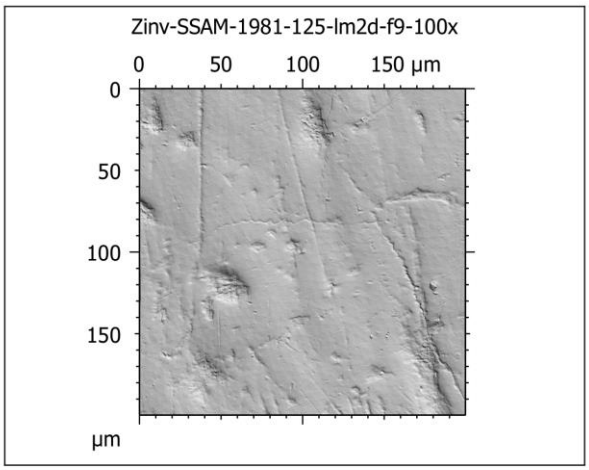
Zinv-SSAM-1981-125-lm2d-f9-100x
0
50
100
150 µm
µm

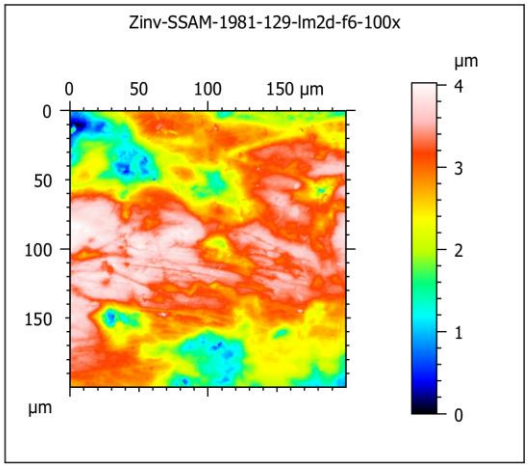
Zinv-SSAM-1981-129-lm2d-f6-100x
0
50
100
150 µm
µm
4
3
2
1
0

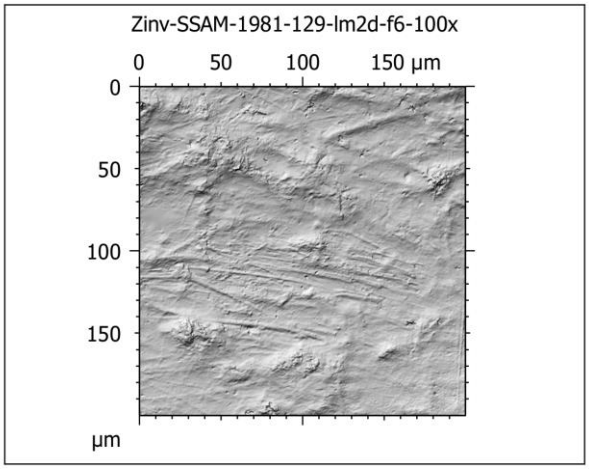
Zinv-SSAM-1981-129-lm2d-f6-100x
0
50
100
150 µm
µm

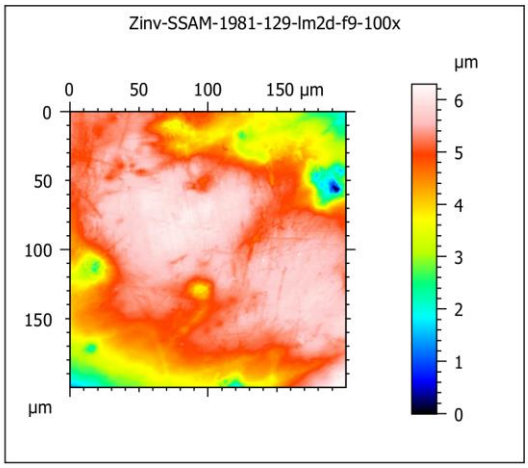
Zinv-SSAM-1981-129-lm2d-f9-100x
0
50
100
150 µm
µm
0
50
100
150
µm
6
5
4
3
2
1
0

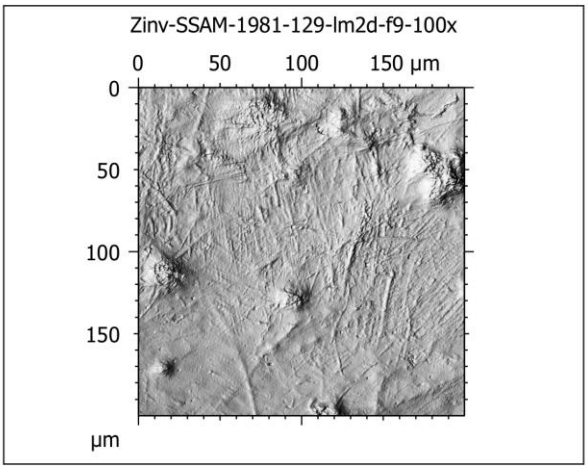
Zinv-SSAM-1981-129-lm2d-f9-100x
0
50
100
150 µm
0
50
100
150
µm

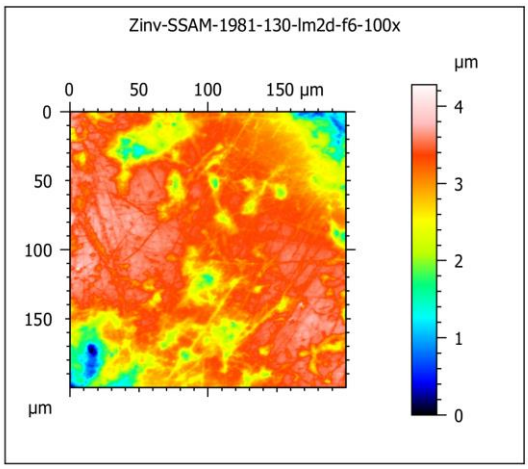
Zinv-SSAM-1981-130-lm2d-f6-100x
0
50
100
150 µm
µm
0
50
100
150
µm
4
3
2
1
0

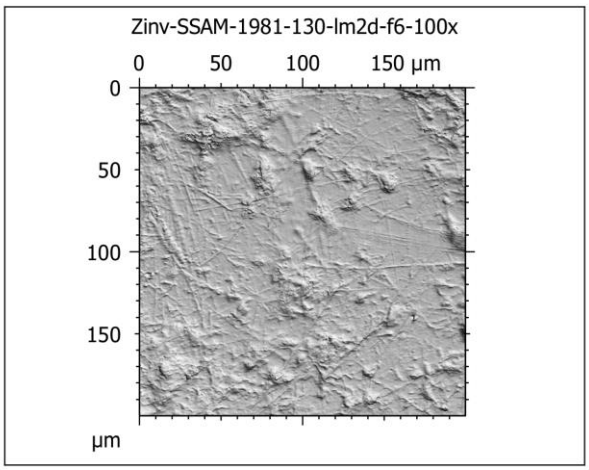
Zinv-SSAM-1981-130-lm2d-f6-100x
0
50
100
150 µm
0
50
100
150
µm

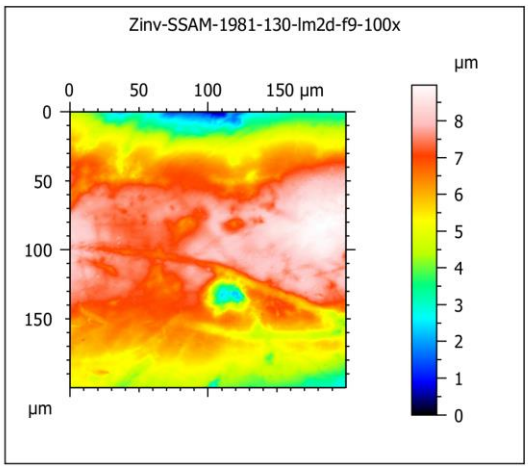
Zinv-SSAM-1981-130-lm2d-f9-100x
0
50
100
150 µm
µm
0
50
100
150
µm
8
7
6
5
4
3
2
1
0

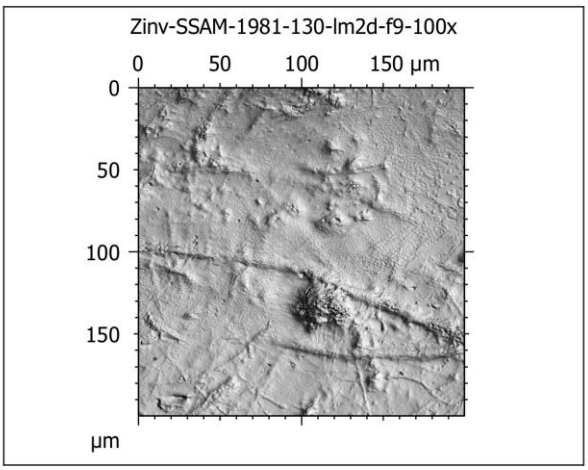
Zinv-SSAM-1981-130-lm2d-f9-100x
0
50
100
150 µm
0
50
100
150
µm

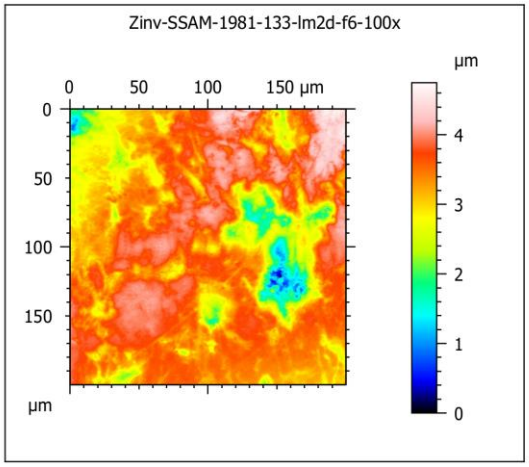
Zinv-SSAM-1981-133-lm2d-f6-100x
0
50
100
150 µm
µm
0
50
100
150
µm
4
3
2
1
0

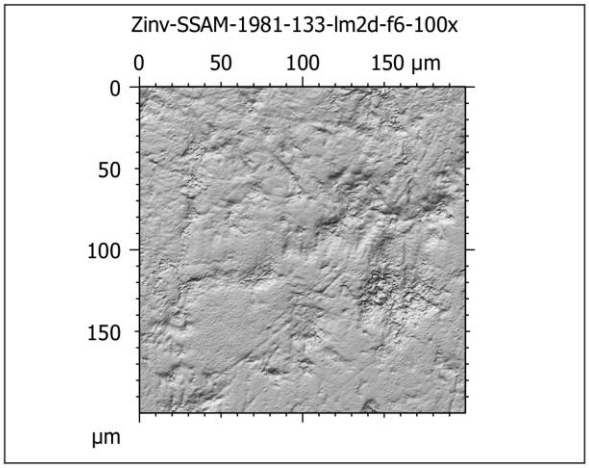
Zinv-SSAM-1981-133-lm2d-f6-100x
0
50
100
150 µm
0
50
100
150
µm

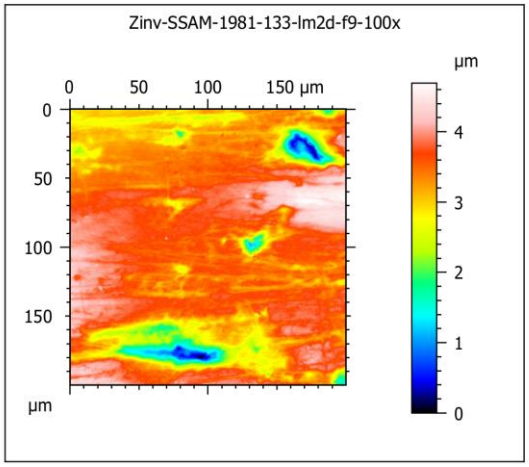
Zinv-SSAM-1981-133-lm2d-f9-100x
0
50
100
150 µm
µm
0
50
100
150
µm
4
3
2
1
0

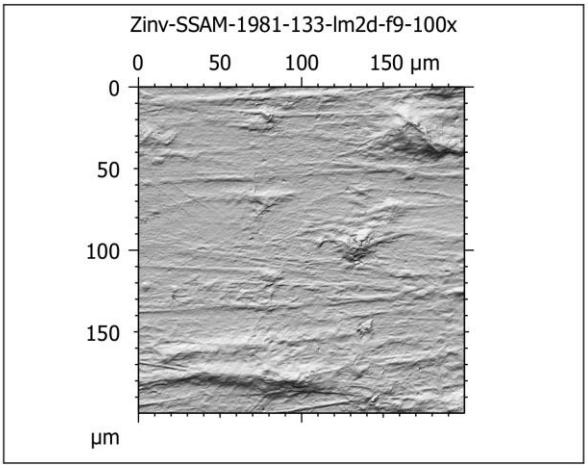
Zinv-SSAM-1981-133-lm2d-f9-100x
0
50
100
150 µm
0
50
100
150
µm

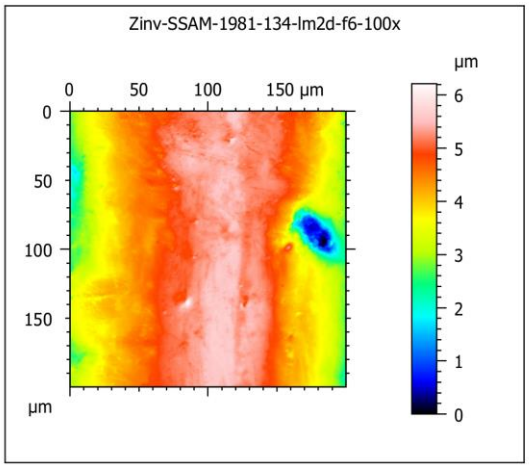
Zinv-SSAM-1981-134-lm2d-f6-100x
0
50
100
150 µm
µm
0
50
100
150
µm
6
5
4
3
2
1
0

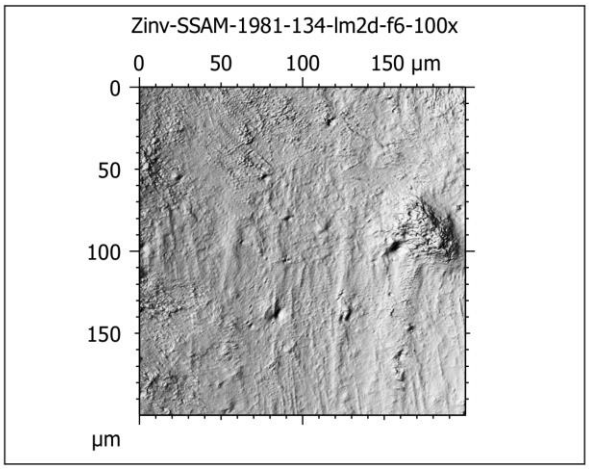
Zinv-SSAM-1981-134-lm2d-f6-100x
0
50
100
150 µm
0
50
100
150
µm

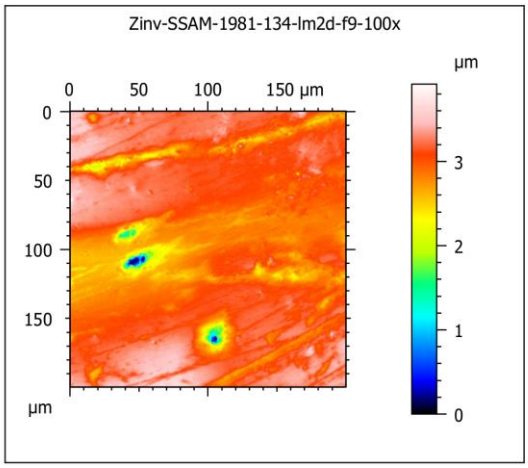
Zinv-SSAM-1981-134-lm2d-f9-100x
0
50
100
150 µm
µm
3
2
1
0

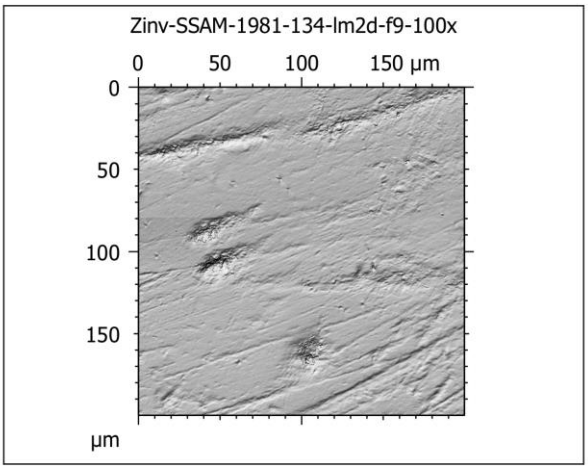
Zinv-SSAM-1981-134-lm2d-f9-100x
0
50
100
150 µm
µm

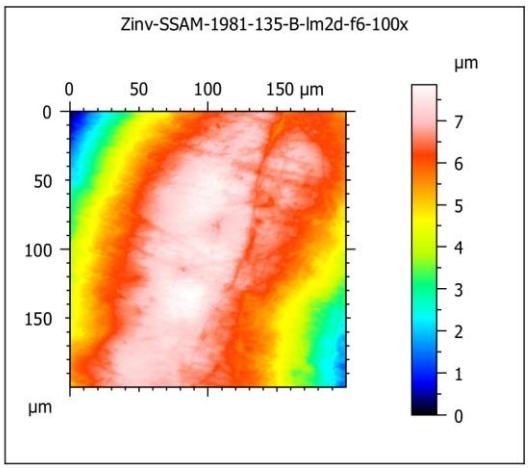
Zinv-SSAM-1981-135-B-lm2d-f6-100x
0
50
100
150 µm
µm
7
6
5
4
3
2
1
0

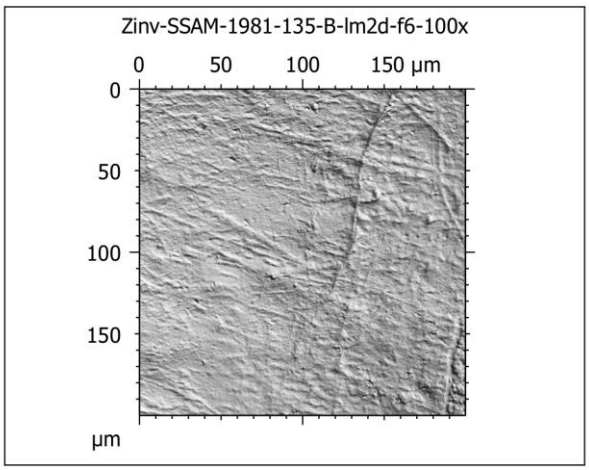
Zinv-SSAM-1981-135-B-lm2d-f6-100x
0
50
100
150 µm
µm

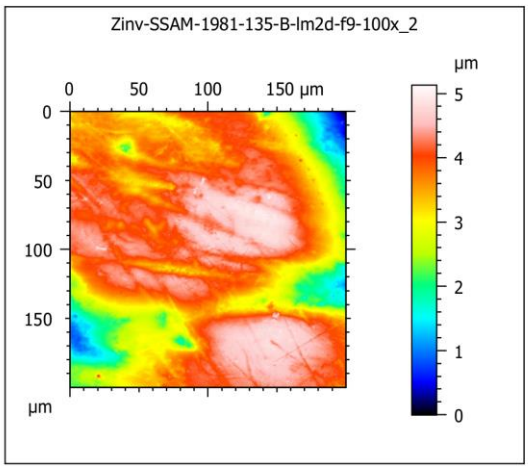
Zinv-SSAM-1981-135-B-lm2d-f9-100x_2
0
50
100
150 µm
µm
5
4
3
2
1
0

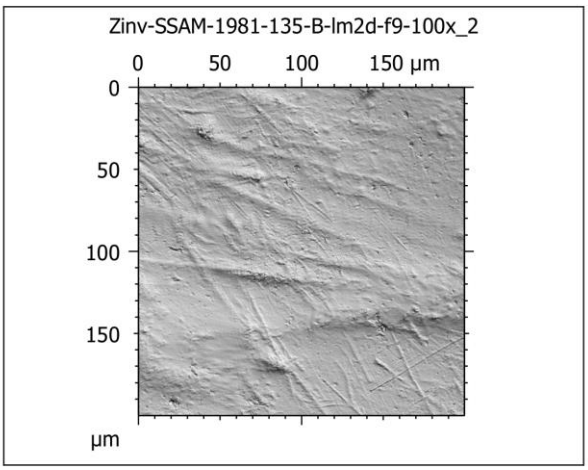
Zinv-SSAM-1981-135-B-lm2d-f9-100x_2
0
50
100
150 µm
µm

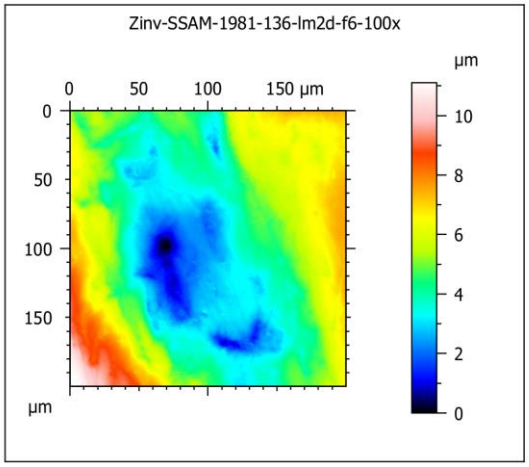
Zinv-SSAM-1981-136-lm2d-f6-100x
0
50
100
150 µm
µm
10
8
6
4
2
0

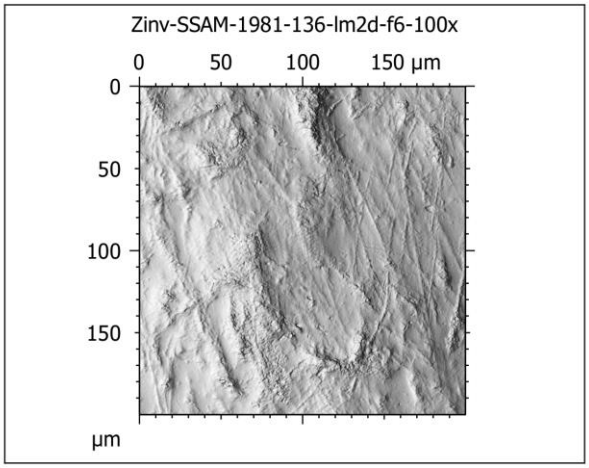
Zinv-SSAM-1981-136-lm2d-f6-100x
0
50
100
150 µm
µm

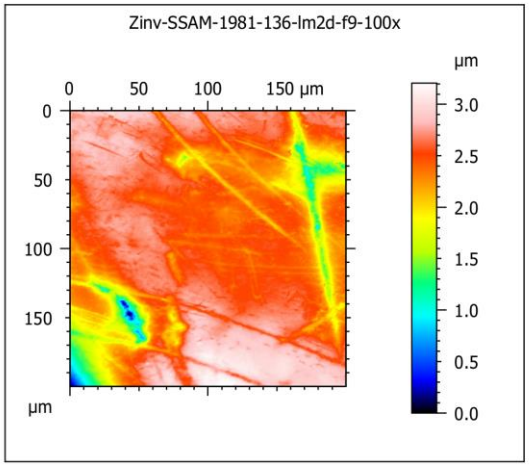
Zinv-SSAM-1981-136-lm2d-f9-100x
0
50
100
150 µm
µm
3.0
2.5
2.0
1.5
1.0
0.5
0.0

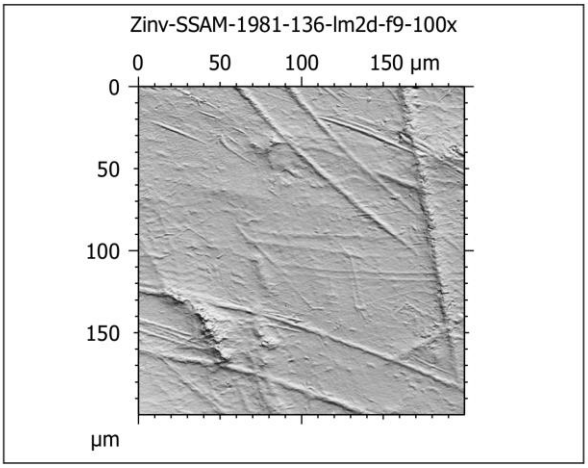
Zinv-SSAM-1981-136-lm2d-f9-100x
0
50
100
150 µm
µm

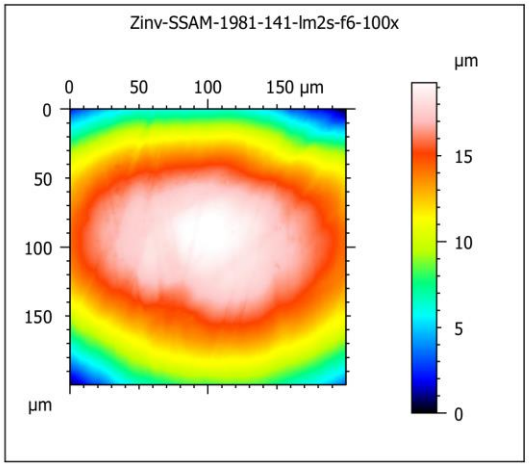
Zinv-SSAM-1981-141-lm2s-f6-100x
0
50
100
150 µm
µm
15
10
5
0

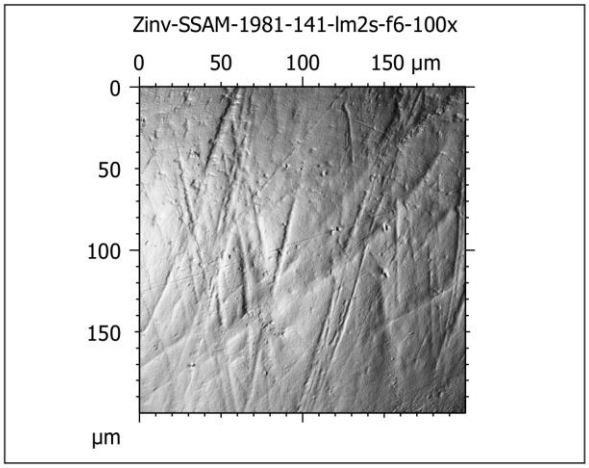
Zinv-SSAM-1981-141-lm2s-f6-100x
0
50
100
150 µm
µm

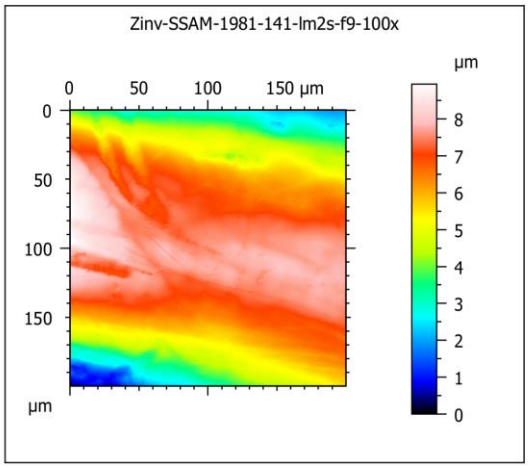
Zinv-SSAM-1981-141-lm2s-f9-100x
µm
0 50 100 150 µm
0
50
100
150
µm
8
7
6
5
4
3
2
1
0

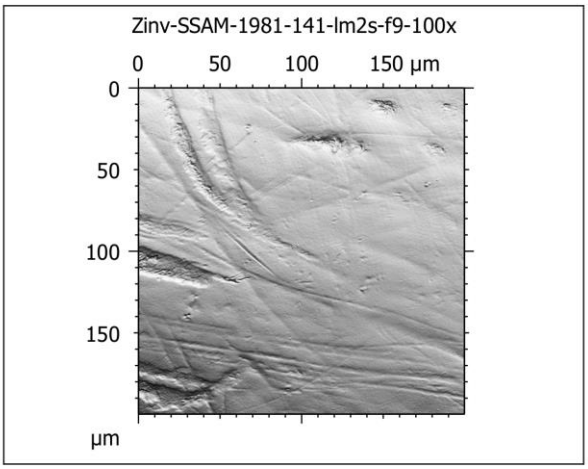
Zinv-SSAM-1981-141-lm2s-f9-100x
0 50 100 150 µm
0
50
100
150
µm

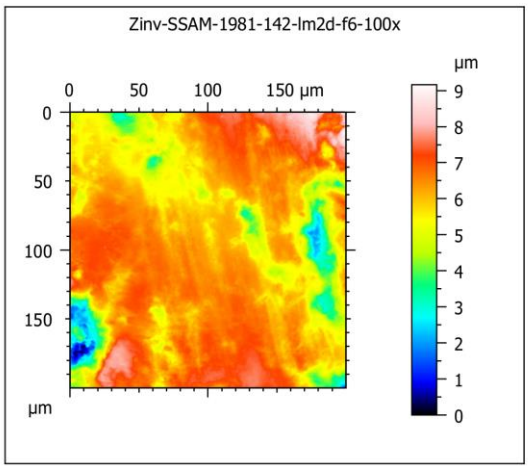
Zinv-SSAM-1981-142-lm2d-f6-100x
µm
0 50 100 150 µm
0
50
100
150
µm
9
8
7
6
5
4
3
2
1
0

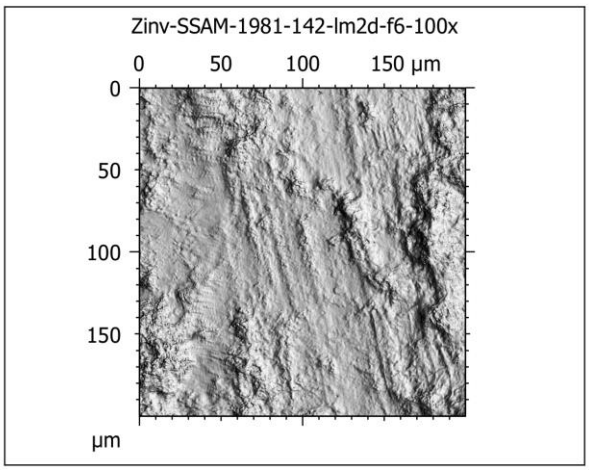
Zinv-SSAM-1981-142-lm2d-f6-100x
0 50 100 150 µm
0
50
100
150
µm

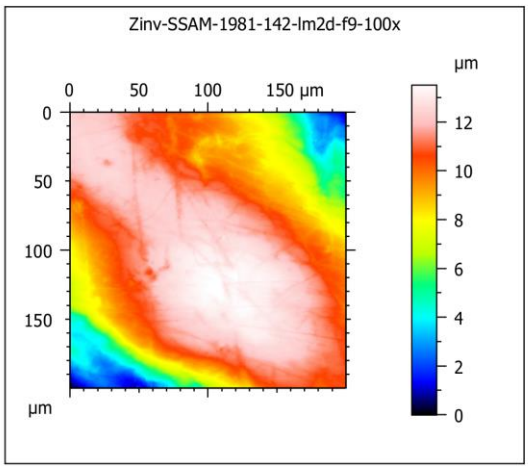
Zinv-SSAM-1981-142-lm2d-f9-100x
µm
0 50 100 150 µm
0
50
100
150
µm
12
10
8
6
4
2
0

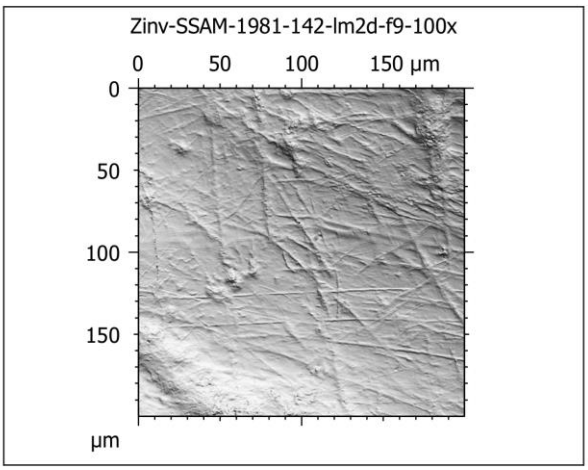
Zinv-SSAM-1981-142-lm2d-f9-100x
0 50 100 150 µm
0
50
100
150
µm

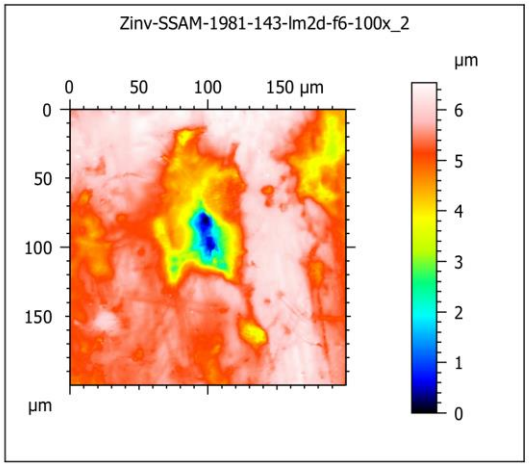
Zinv-SSAM-1981-143-lm2d-f6-100x_2
0
50
100
150 µm
µm
6
5
4
3
2
1
0

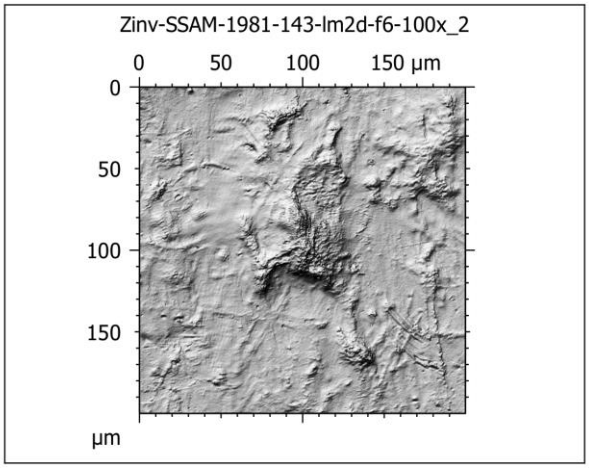
Zinv-SSAM-1981-143-lm2d-f6-100x_2
0
50
100
150 µm
µm

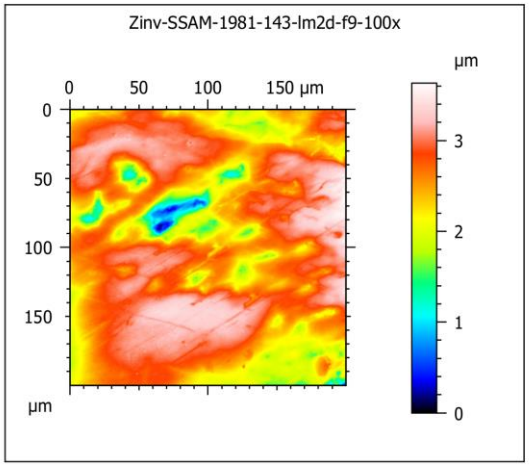
Zinv-SSAM-1981-143-lm2d-f9-100x
0
50
100
150 µm
µm
3
2
1
0

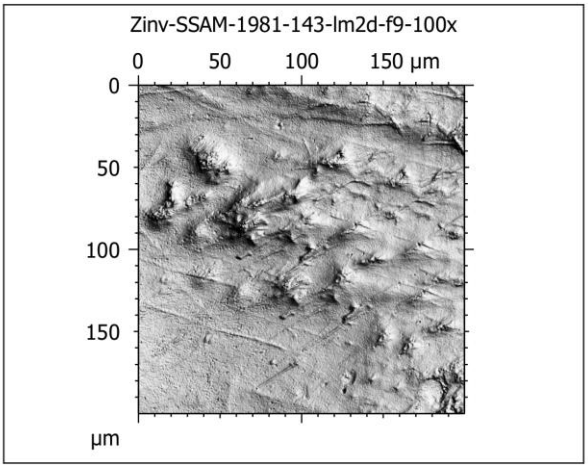
Zinv-SSAM-1981-143-lm2d-f9-100x
0
50
100
150 µm
µm

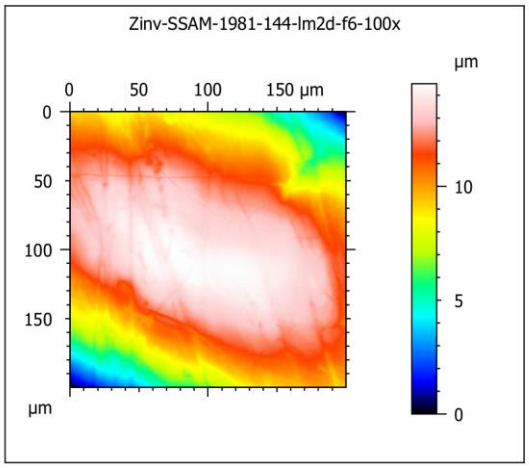
Zinv-SSAM-1981-144-lm2d-f6-100x
0
50
100
150 µm
µm
10
5
0

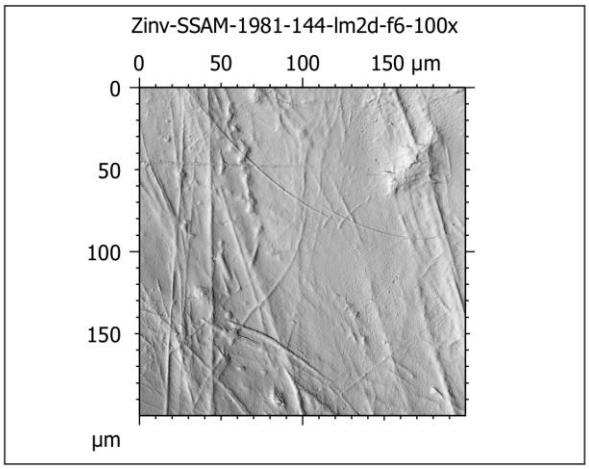
Zinv-SSAM-1981-144-lm2d-f6-100x
0
50
100
150 µm
µm

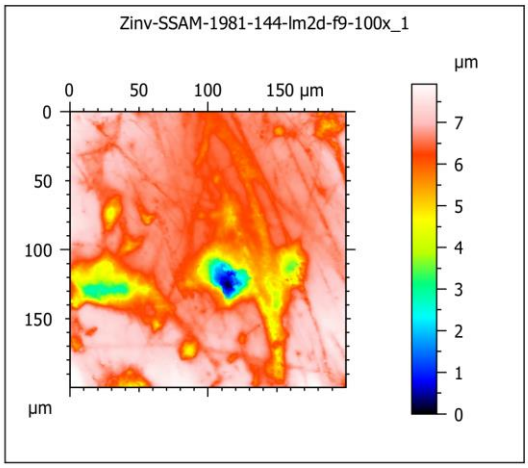
Zinv-SSAM-1981-144-lm2d-f9-100x_1
µm
0 50 100 150 µm
0
50
100
150
µm
7
6
5
4
3
2
1
0

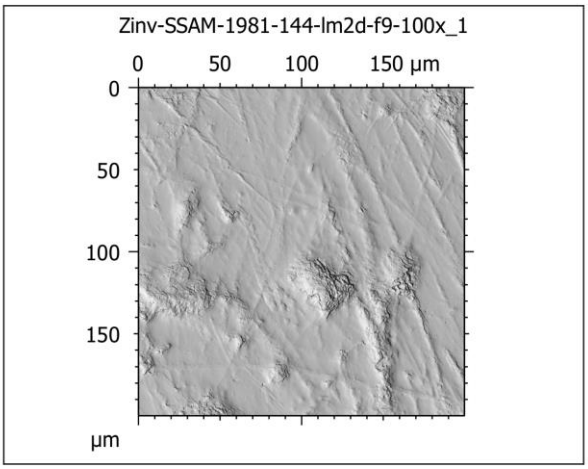
Zinv-SSAM-1981-144-lm2d-f9-100x_1
0 50 100 150 µm
0
50
100
150
µm

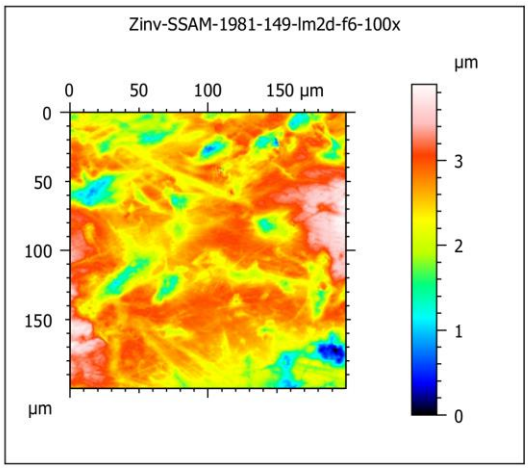
Zinv-SSAM-1981-149-lm2d-f6-100x
µm
0 50 100 150 µm
0
50
100
150
µm
3
2
1
0

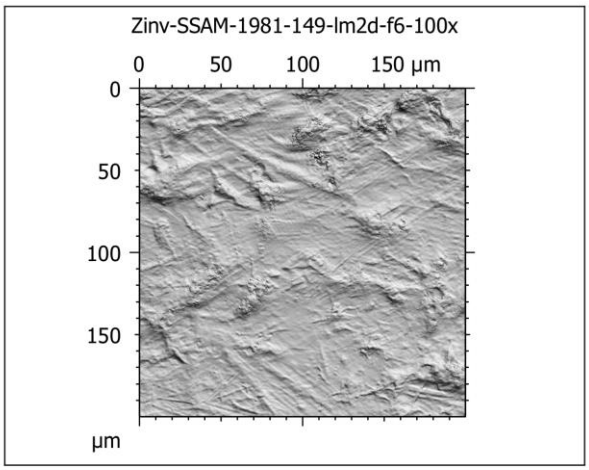
Zinv-SSAM-1981-149-lm2d-f6-100x
0 50 100 150 µm
0
50
100
150
µm

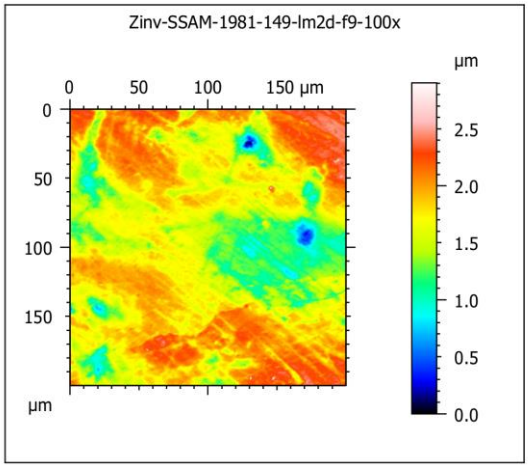
Zinv-SSAM-1981-149-lm2d-f9-100x
µm
0 50 100 150 µm
0
50
100
150
µm
2.5
2.0
1.5
1.0
0.5
0.0

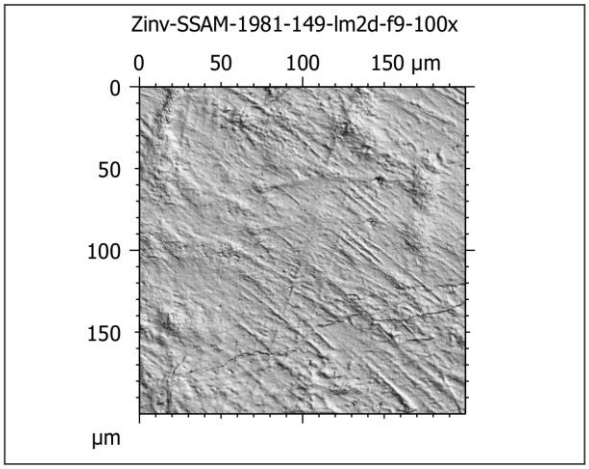
Zinv-SSAM-1981-149-lm2d-f9-100x
0 50 100 150 µm
0
50
100
150
µm

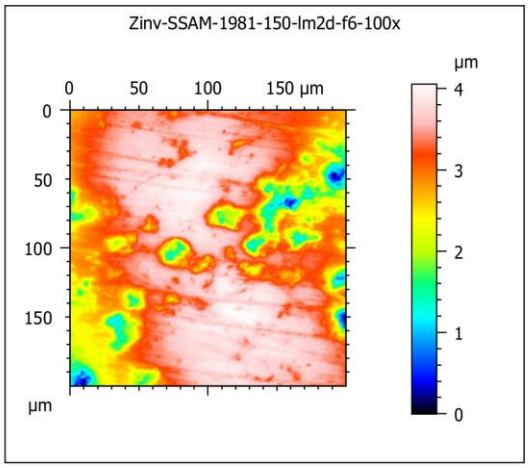
Zinv-SSAM-1981-150-lm2d-f6-100x
µm
0 50 100 150 µm
0
50
100
150
µm
4
3
2
1
0

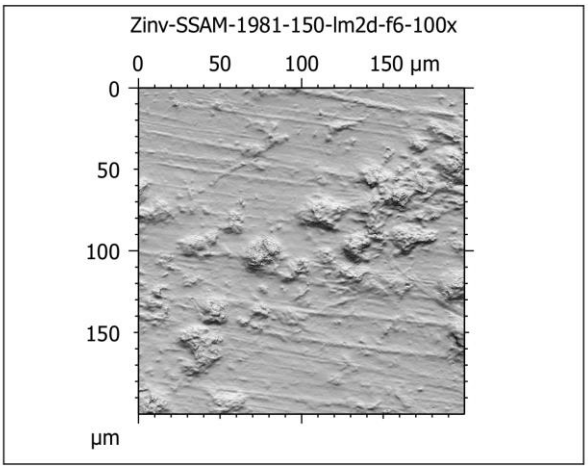
Zinv-SSAM-1981-150-lm2d-f6-100x
0 50 100 150 µm
0
50
100
150
µm

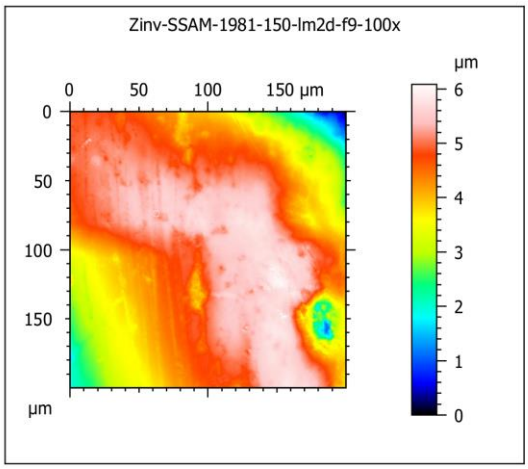
Zinv-SSAM-1981-150-lm2d-f9-100x
µm
0 50 100 150 µm
0
50
100
150
µm
6
5
4
3
2
1
0

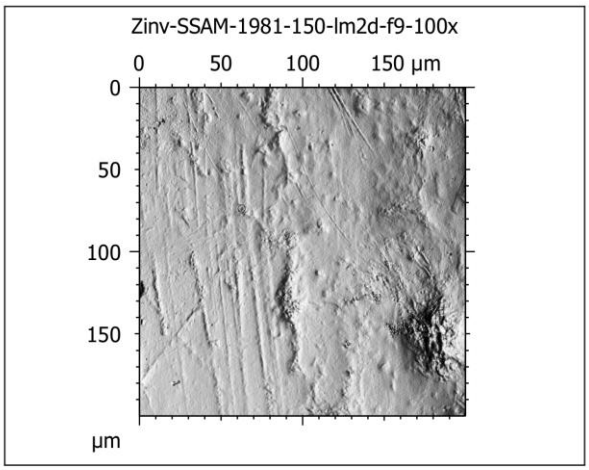
Zinv-SSAM-1981-150-lm2d-f9-100x
0 50 100 150 µm
0
50
100
150
µm

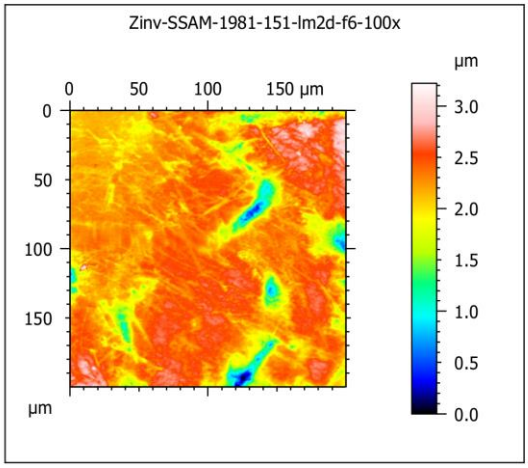
Zinv-SSAM-1981-151-lm2d-f6-100x
µm
0 50 100 150 µm
0
50
100
150
µm
3.0
2.5
2.0
1.5
1.0
0.5
0.0

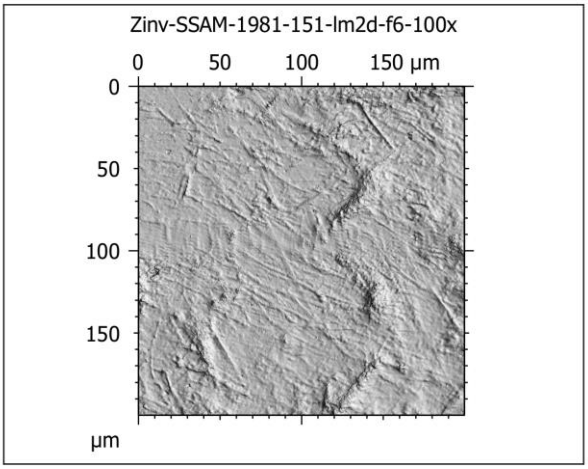
Zinv-SSAM-1981-151-lm2d-f6-100x
0 50 100 150 µm
0
50
100
150
µm

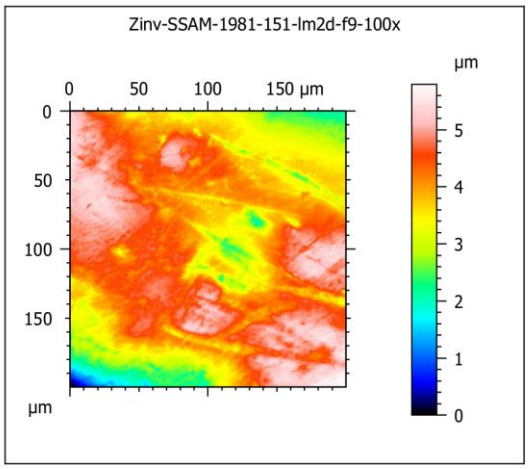
Zinv-SSAM-1981-151-lm2d-f9-100x
0
50
100
150 µm
µm
0
50
100
150
µm
µm
5
4
3
2
1
0

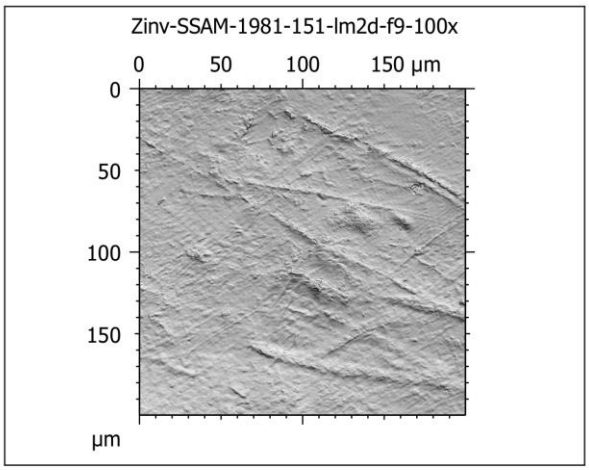
Zinv-SSAM-1981-151-lm2d-f9-100x
0
50
100
150 µm
0
50
100
150
µm

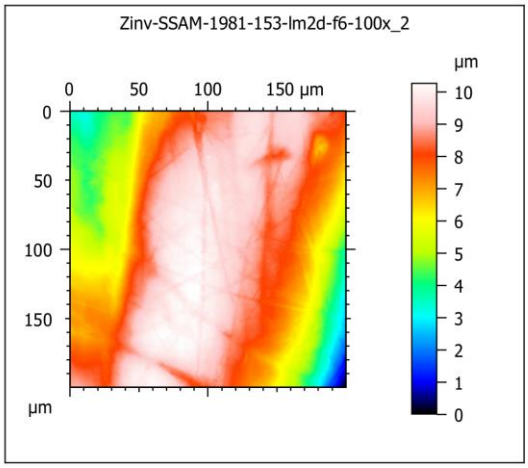
Zinv-SSAM-1981-153-lm2d-f6-100x_2
0
50
100
150 µm
µm
0
50
100
150
µm
µm
10
9
8
7
6
5
4
3
2
1
0

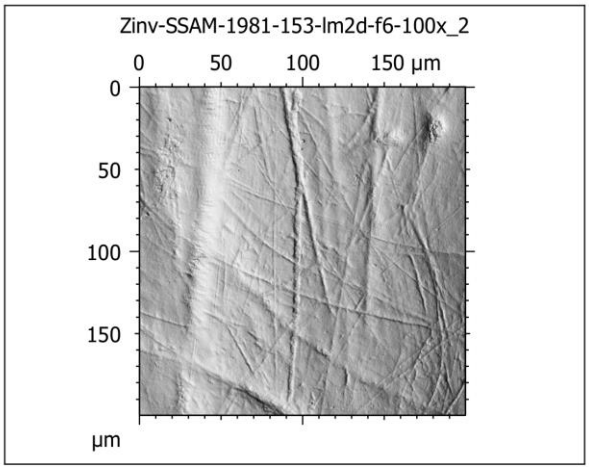
Zinv-SSAM-1981-153-lm2d-f6-100x_2
0
50
100
150 µm
0
50
100
150
µm

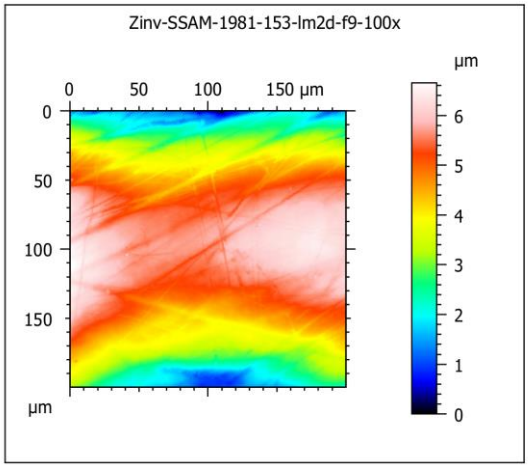
Zinv-SSAM-1981-153-lm2d-f9-100x
0
50
100
150 µm
µm
0
50
100
150
µm
µm
6
5
4
3
2
1
0

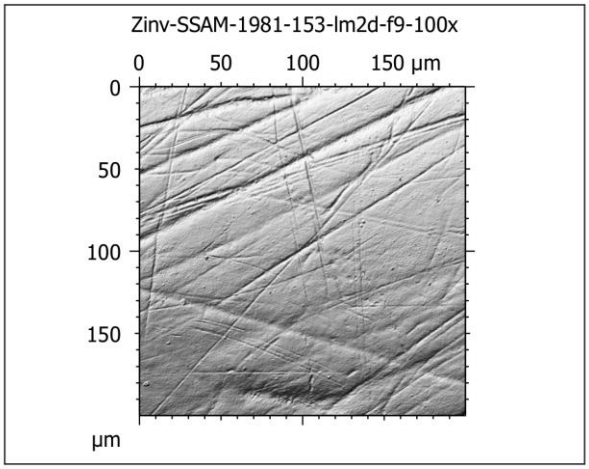
Zinv-SSAM-1981-153-lm2d-f9-100x
0
50
100
150 µm
0
50
100
150
µm

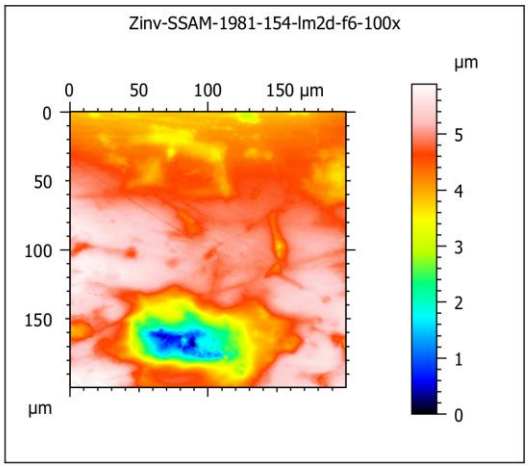
Zinv-SSAM-1981-154-lm2d-f6-100x
0
50
100
150 µm
µm
5
4
3
2
1
0

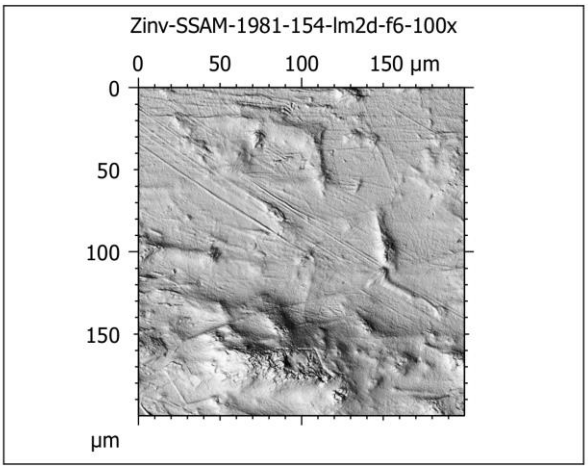
Zinv-SSAM-1981-154-lm2d-f6-100x
0
50
100
150 µm
µm

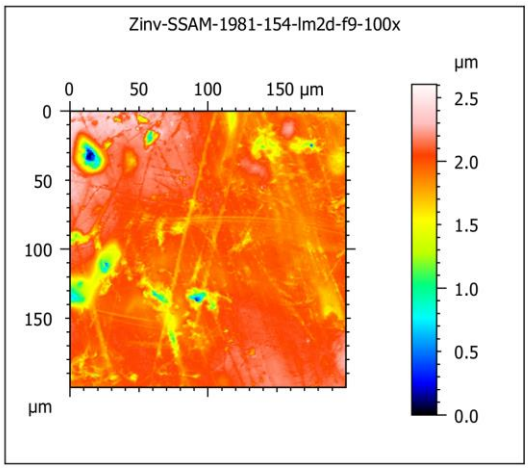
Zinv-SSAM-1981-154-lm2d-f9-100x
0
50
100
150 µm
µm
2.5
2.0
1.5
1.0
0.5
0.0

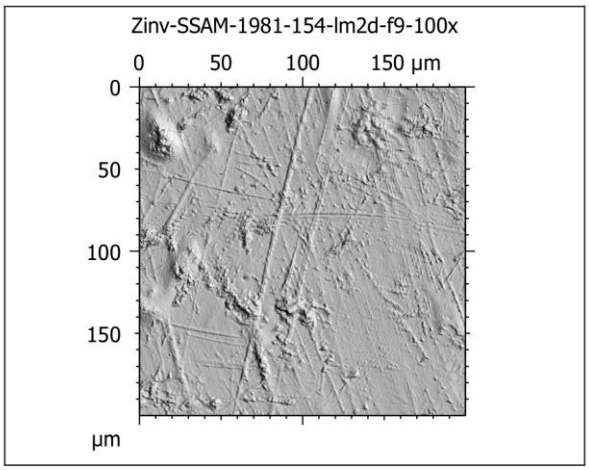
Zinv-SSAM-1981-154-lm2d-f9-100x
0
50
100
150 µm
µm

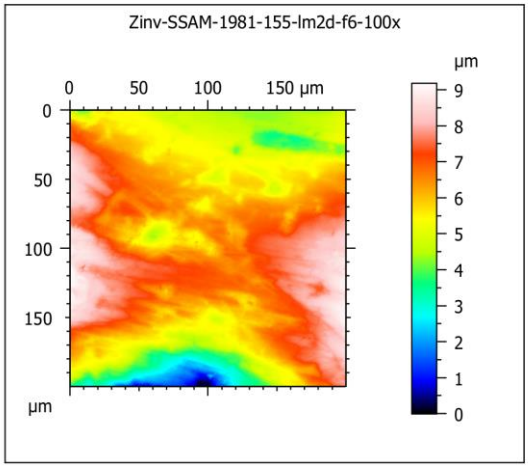
Zinv-SSAM-1981-155-lm2d-f6-100x
0
50
100
150 µm
µm
9
8
7
6
5
4
3
2
1
0

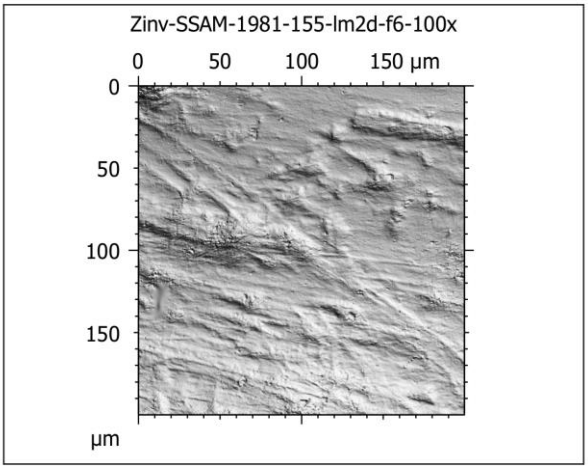
Zinv-SSAM-1981-155-lm2d-f6-100x
0
50
100
150 µm
µm

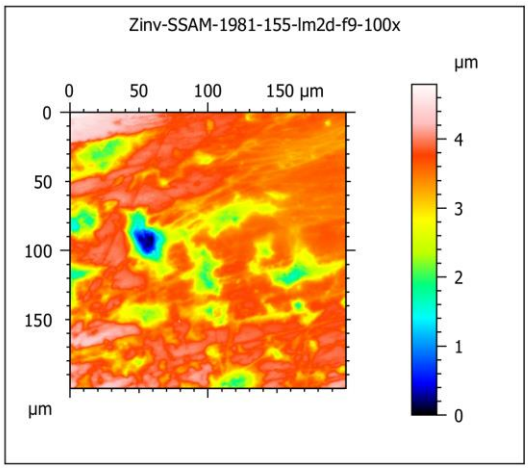
Zinv-SSAM-1981-155-lm2d-f9-100x
µm
0 50 100 150 µm
0
50
100
150
µm
4
3
2
1
0

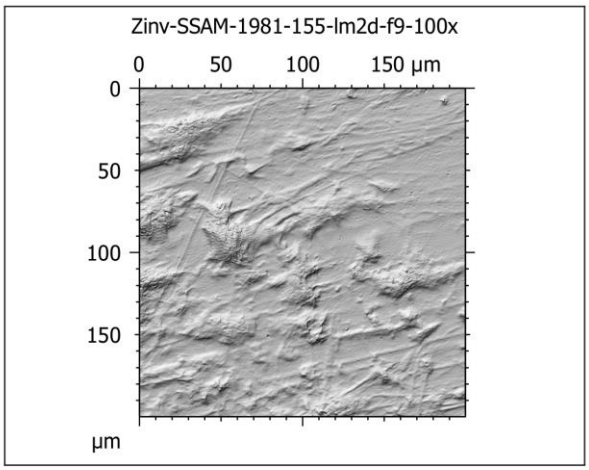
Zinv-SSAM-1981-155-lm2d-f9-100x
0 50 100 150 µm
0
50
100
150
µm

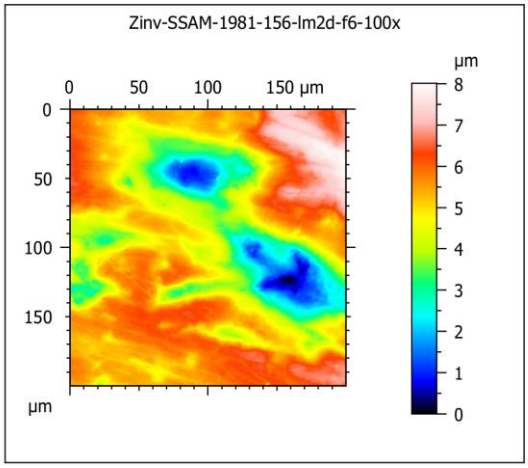
Zinv-SSAM-1981-156-lm2d-f6-100x
µm
0 50 100 150 µm
0
50
100
150
µm
8
7
6
5
4
3
2
1
0

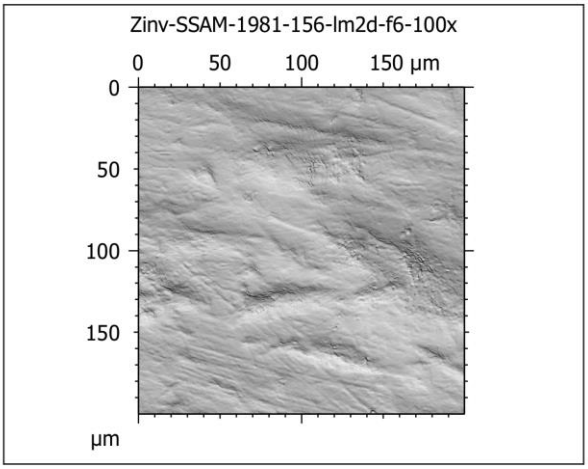
Zinv-SSAM-1981-156-lm2d-f6-100x
0 50 100 150 µm
0
50
100
150
µm

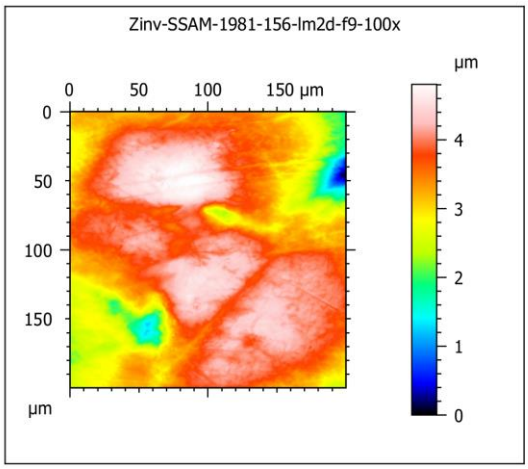
Zinv-SSAM-1981-156-lm2d-f9-100x
µm
0 50 100 150 µm
0
50
100
150
µm
4
3
2
1
0

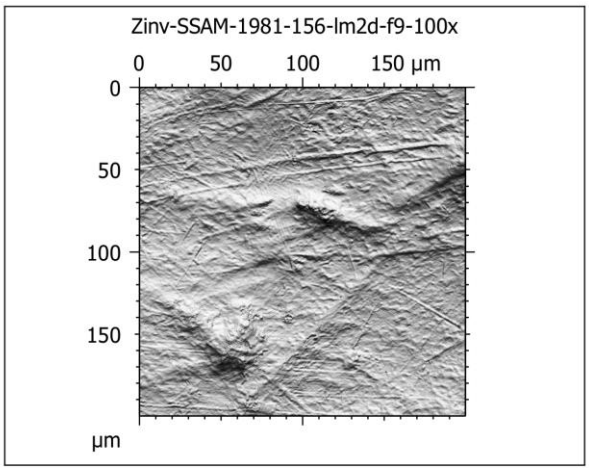
Zinv-SSAM-1981-156-lm2d-f9-100x
0 50 100 150 µm
0
50
100
150
µm

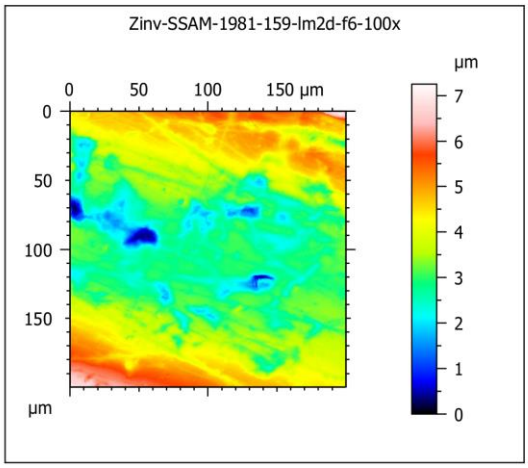
Zinv-SSAM-1981-159-lm2d-f6-100x
0
50
100
150 µm
µm
7
6
5
4
3
2
1
0

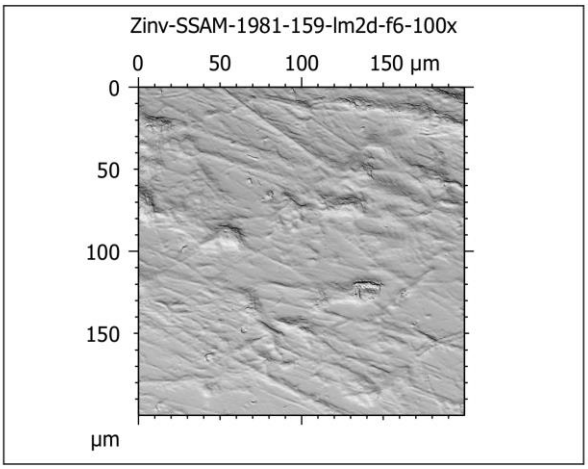
Zinv-SSAM-1981-159-lm2d-f6-100x
0
50
100
150 µm
µm

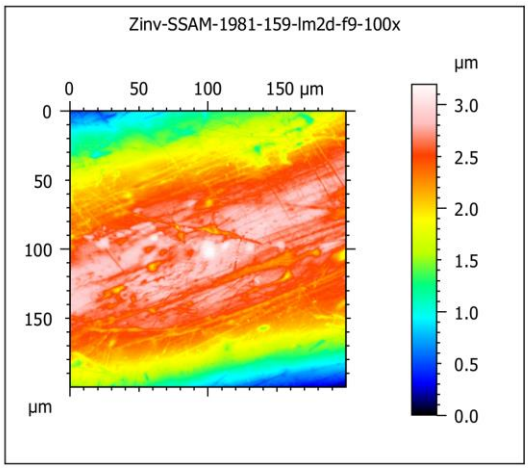
Zinv-SSAM-1981-159-lm2d-f9-100x
0
50
100
150 µm
µm
3.0
2.5
2.0
1.5
1.0
0.5
0.0

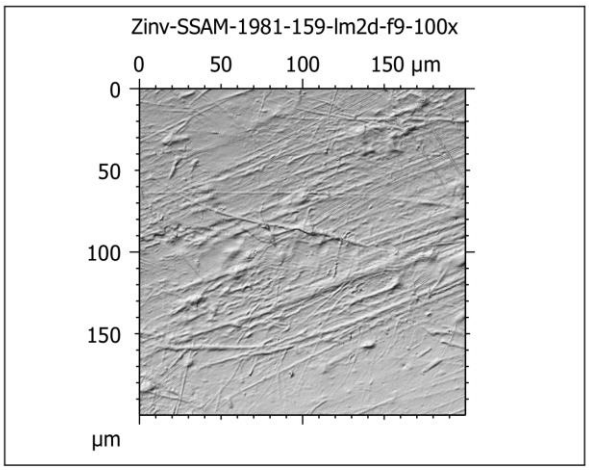
Zinv-SSAM-1981-159-lm2d-f9-100x
0
50
100
150 µm
µm

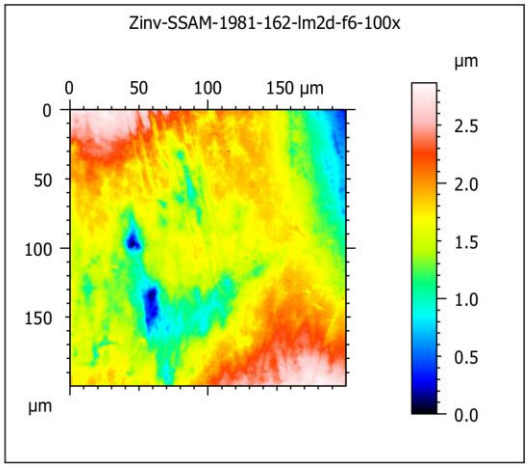
Zinv-SSAM-1981-162-lm2d-f6-100x
0
50
100
150 µm
µm
2.5
2.0
1.5
1.0
0.5
0.0

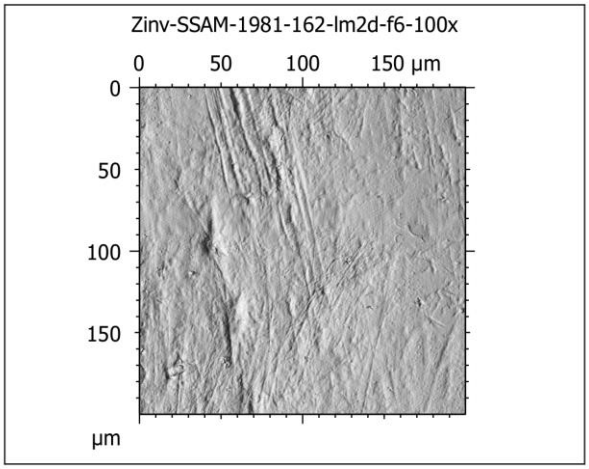
Zinv-SSAM-1981-162-lm2d-f6-100x
0
50
100
150 µm
µm

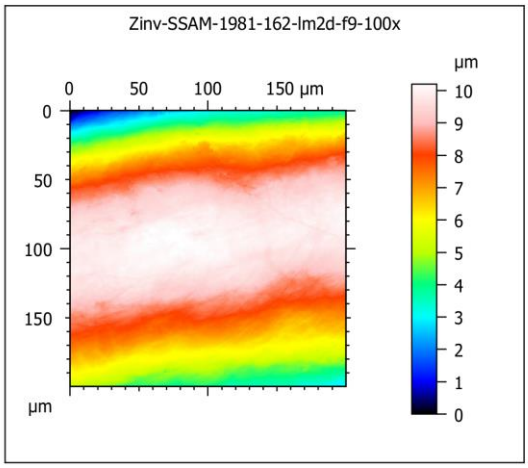
Zinv-SSAM-1981-162-lm2d-f9-100x
0
50
100
150 µm
µm
10
9
8
7
6
5
4
3
2
1
0

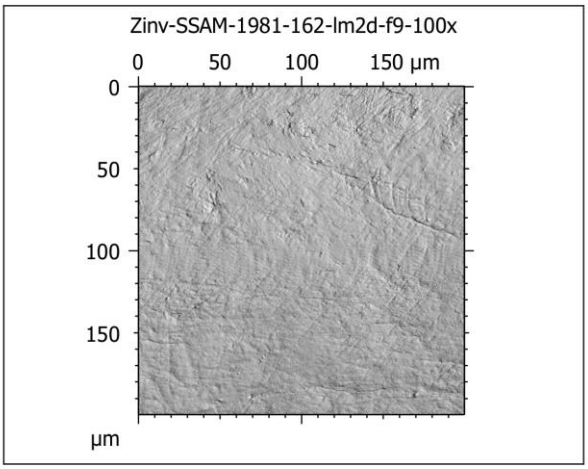
Zinv-SSAM-1981-162-lm2d-f9-100x
0
50
100
150 µm
µm

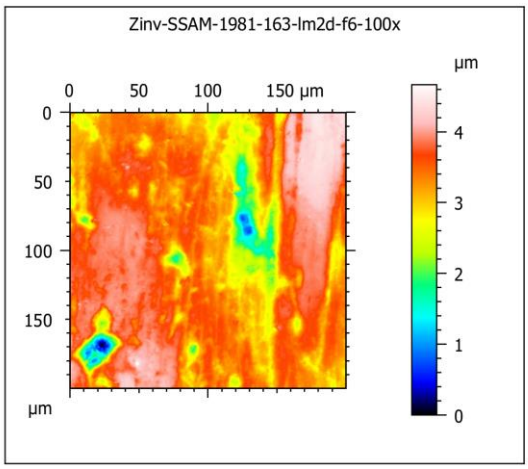
Zinv-SSAM-1981-163-lm2d-f6-100x
0
50
100
150 µm
µm
4
3
2
1
0

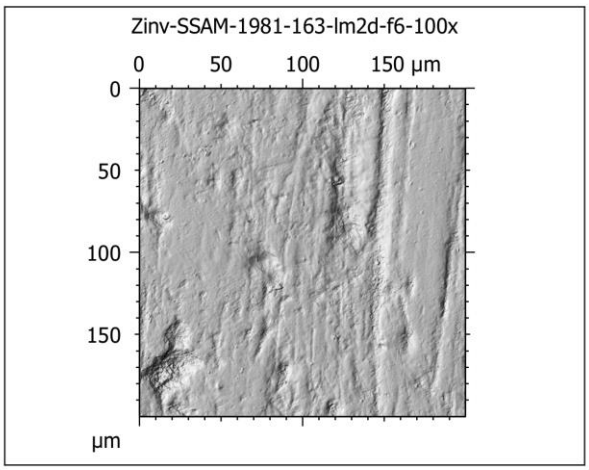
Zinv-SSAM-1981-163-lm2d-f6-100x
0
50
100
150 µm
µm

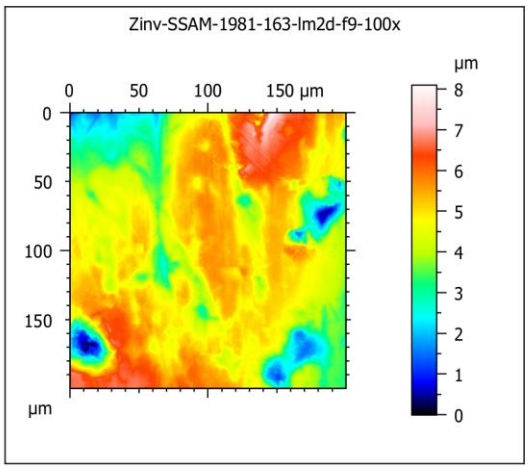
Zinv-SSAM-1981-163-lm2d-f9-100x
0
50
100
150 µm
µm
8
7
6
5
4
3
2
1
0

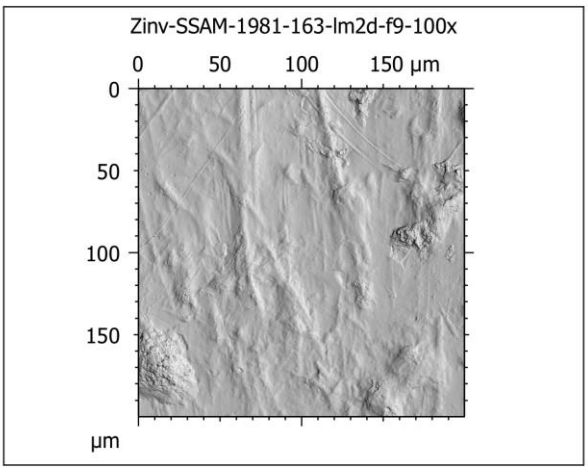
Zinv-SSAM-1981-163-lm2d-f9-100x
0
50
100
150 µm
µm

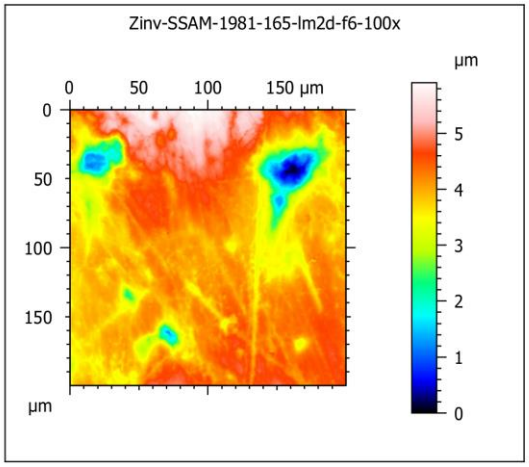
Zinv-SSAM-1981-165-lm2d-f6-100x
µm
0 50 100 150 µm
0
50
100
150
µm
5
4
3
2
1
0

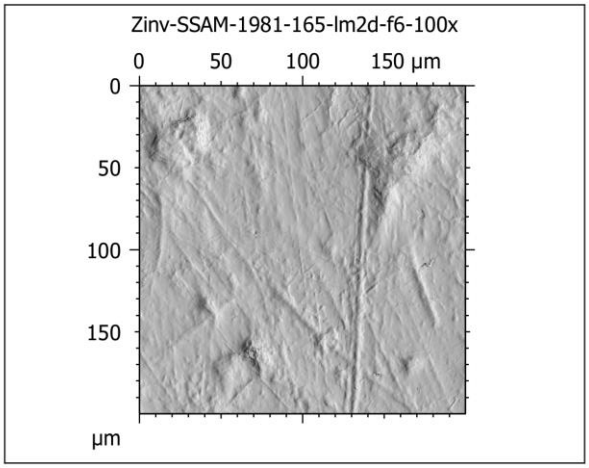
Zinv-SSAM-1981-165-lm2d-f6-100x
0 50 100 150 µm
0
50
100
150
µm

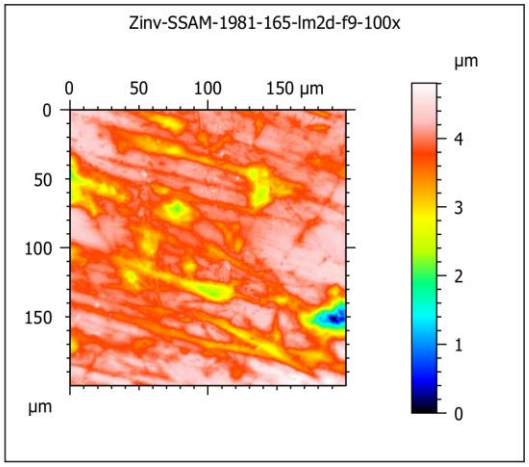
Zinv-SSAM-1981-165-lm2d-f9-100x
µm
0 50 100 150 µm
0
50
100
150
µm
4
3
2
1
0

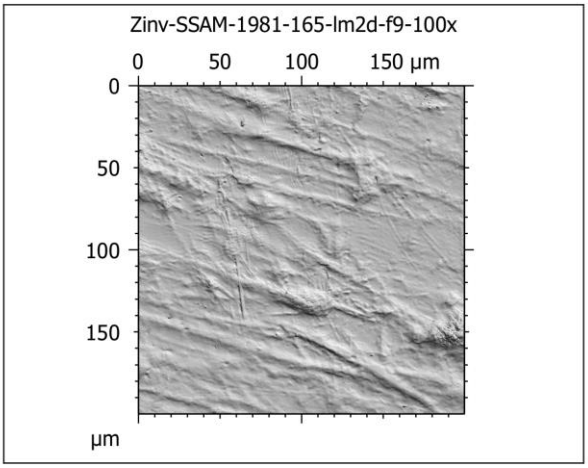
Zinv-SSAM-1981-165-lm2d-f9-100x
0 50 100 150 µm
0
50
100
150
µm

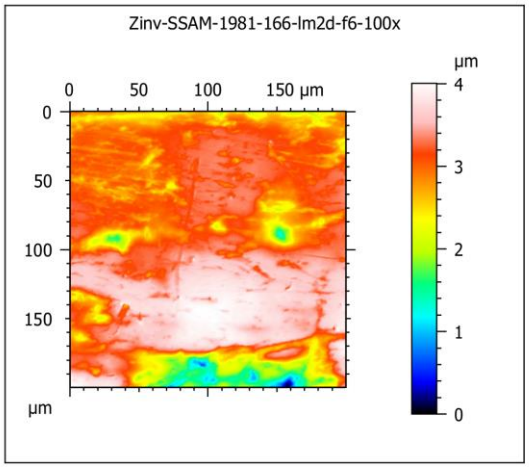
Zinv-SSAM-1981-166-lm2d-f6-100x
µm
0 50 100 150 µm
0
50
100
150
µm
4
3
2
1
0

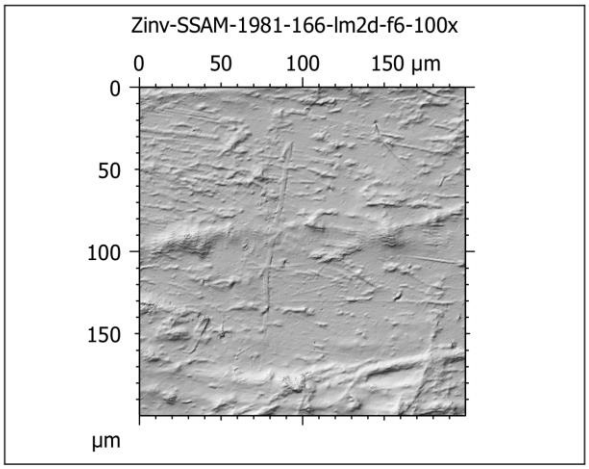
Zinv-SSAM-1981-166-lm2d-f6-100x
0 50 100 150 µm
0
50
100
150
µm

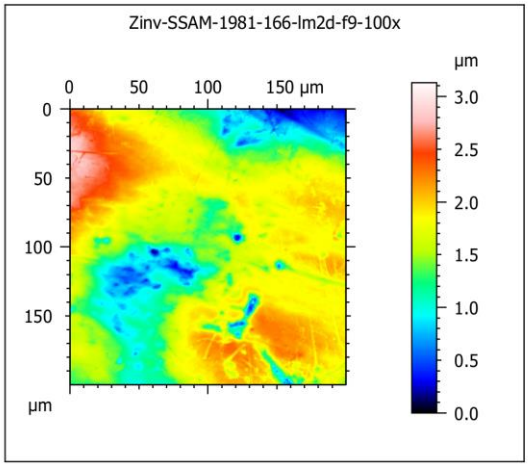
Zinv-SSAM-1981-166-lm2d-f9-100x
0
50
100
150 µm
µm
3.0
2.5
2.0
1.5
1.0
0.5
0.0

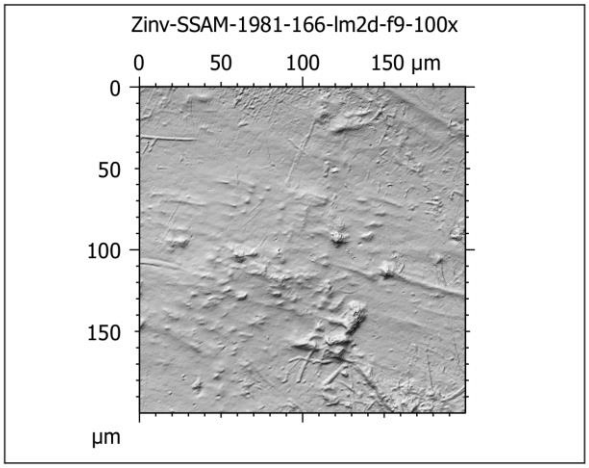
Zinv-SSAM-1981-166-lm2d-f9-100x
0
50
100
150 µm

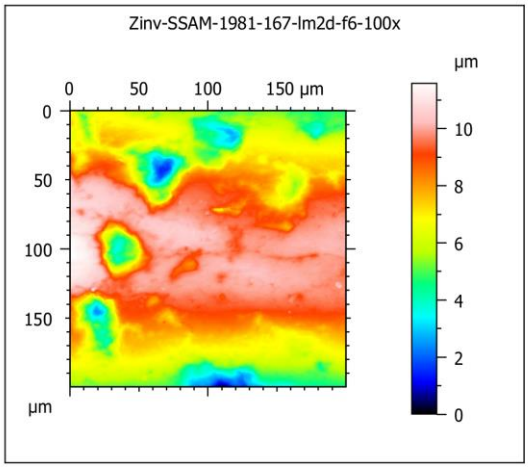
Zinv-SSAM-1981-167-lm2d-f6-100x
0
50
100
150 µm
µm
10
8
6
4
2
0

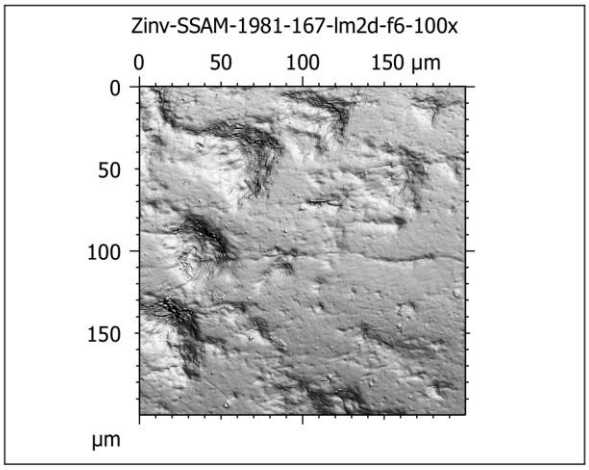
Zinv-SSAM-1981-167-lm2d-f6-100x
0
50
100
150 µm

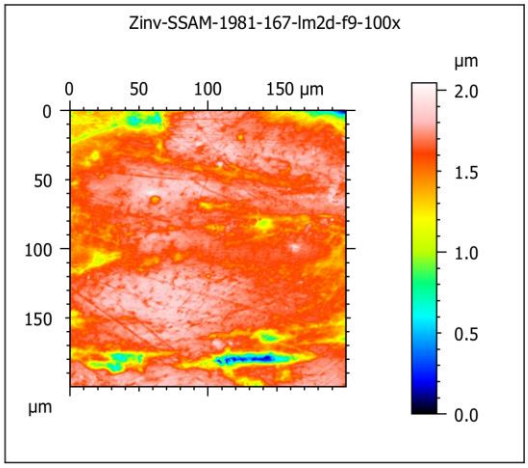
Zinv-SSAM-1981-167-lm2d-f9-100x
0
50
100
150 µm
µm
2.0
1.5
1.0
0.5
0.0

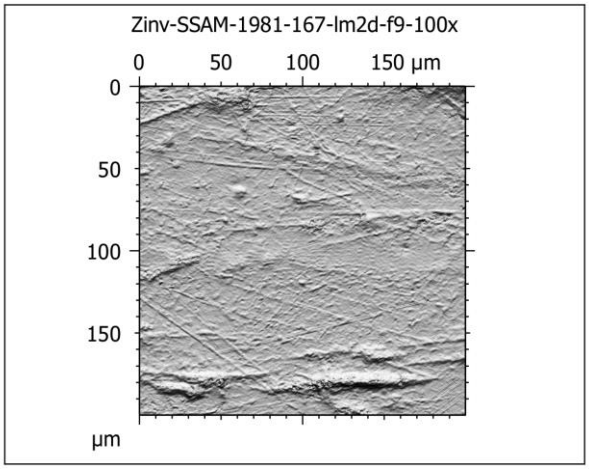
Zinv-SSAM-1981-167-lm2d-f9-100x
0
50
100
150 µm

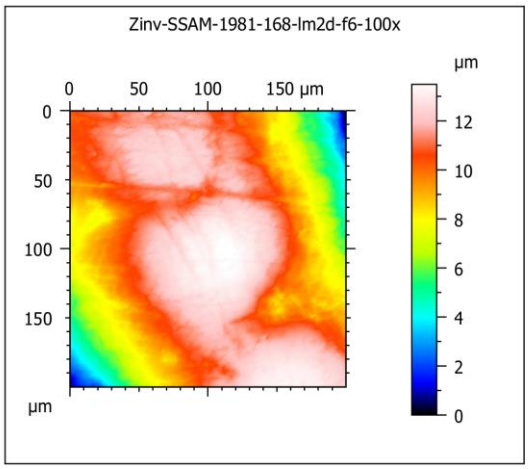
Zinv-SSAM-1981-168-lm2d-f6-100x
0
50
100
150 µm
µm
12
10
8
6
4
2
0

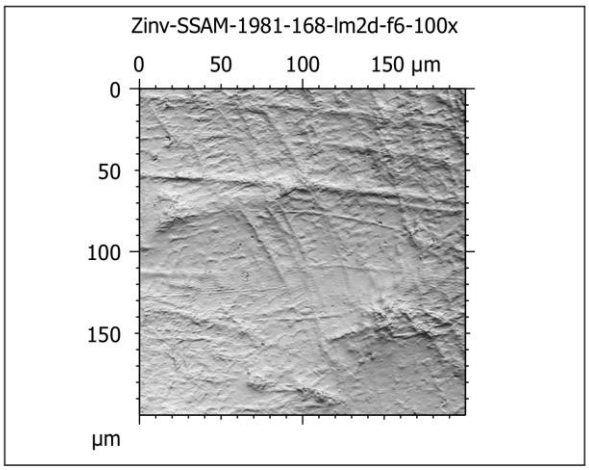
Zinv-SSAM-1981-168-lm2d-f6-100x
0
50
100
150 µm
µm

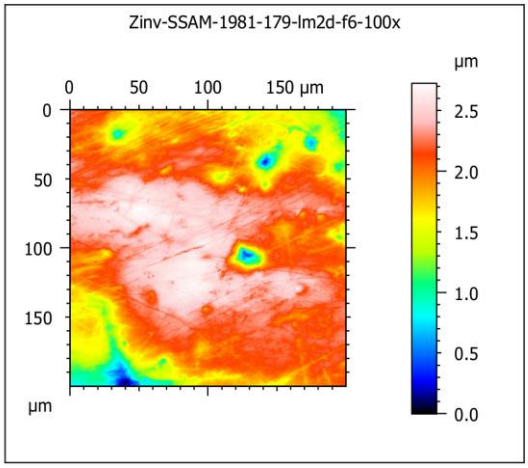
Zinv-SSAM-1981-179-lm2d-f6-100x
0
50
100
150 µm
µm
2.5
2.0
1.5
1.0
0.5
0.0

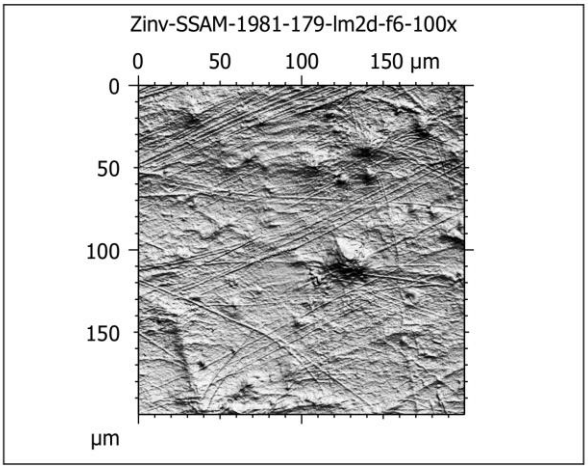
Zinv-SSAM-1981-179-lm2d-f6-100x
0
50
100
150 µm
µm

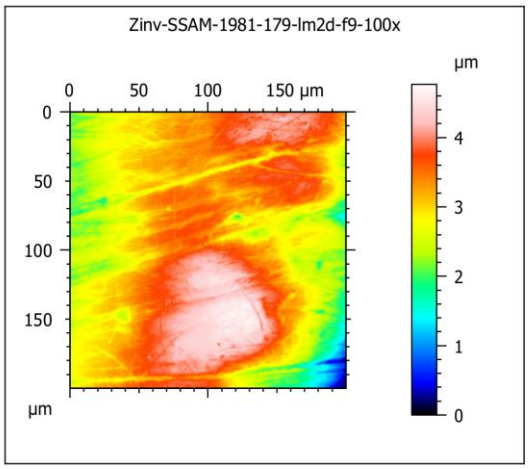
Zinv-SSAM-1981-179-lm2d-f9-100x
0
50
100
150 µm
µm
4
3
2
1
0

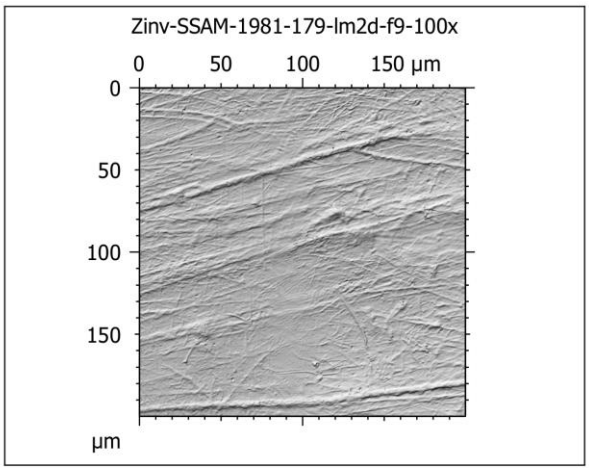
Zinv-SSAM-1981-179-lm2d-f9-100x
0
50
100
150 µm
µm

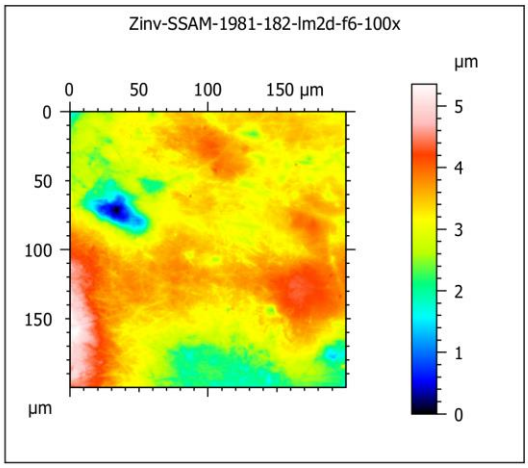
Zinv-SSAM-1981-182-lm2d-f6-100x
0
50
100
150 µm
µm
5
4
3
2
1
0

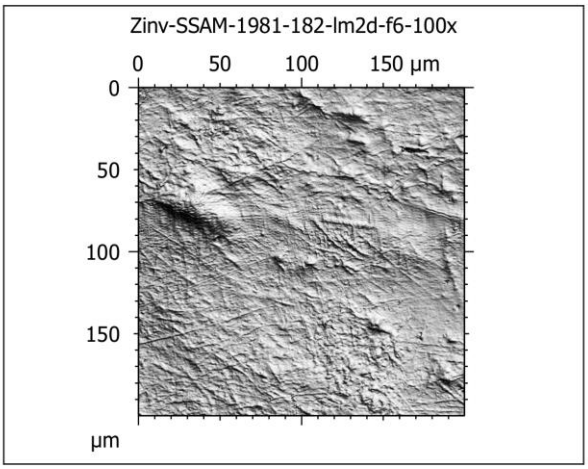
Zinv-SSAM-1981-182-lm2d-f6-100x
0
50
100
150 µm
µm

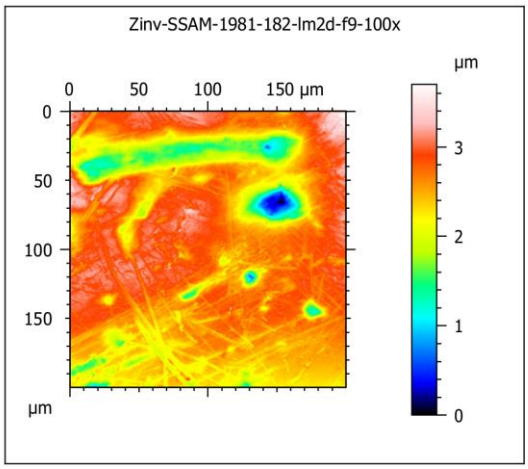
Zinv-SSAM-1981-182-lm2d-f9-100x
0
50
100
150 µm
µm
3
2
1
0

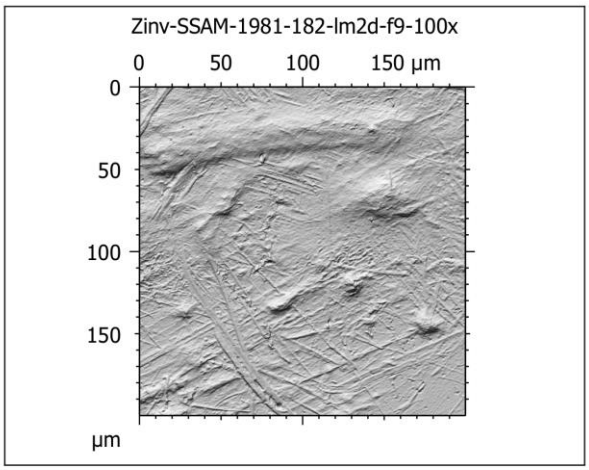
Zinv-SSAM-1981-182-lm2d-f9-100x
0
50
100
150 µm
µm

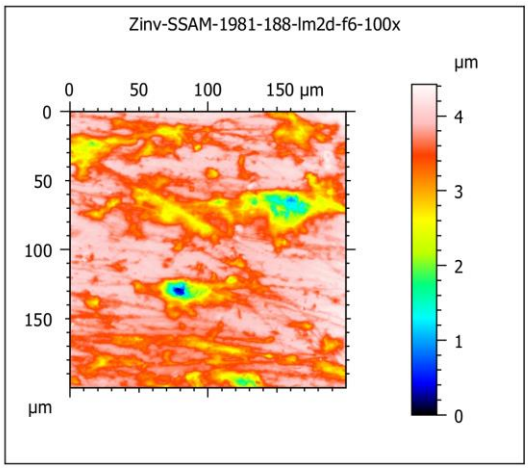
Zinv-SSAM-1981-188-lm2d-f6-100x
0
50
100
150 µm
µm
4
3
2
1
0

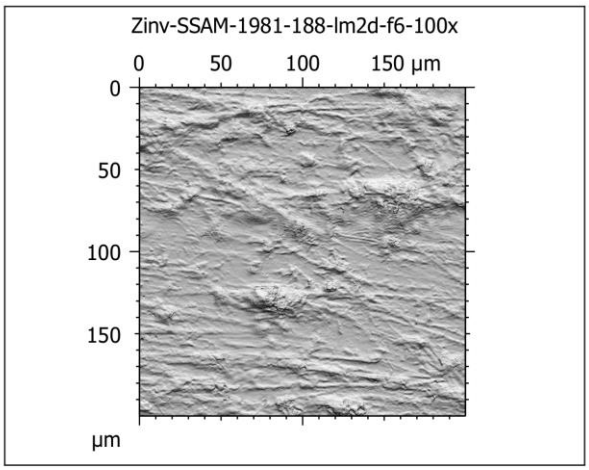
Zinv-SSAM-1981-188-lm2d-f6-100x
0
50
100
150 µm
µm

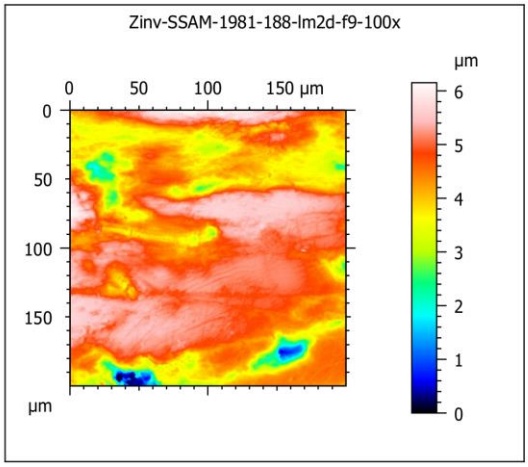
Zinv-SSAM-1981-188-lm2d-f9-100x
0
50
100
150 µm
µm
6
5
4
3
2
1
0

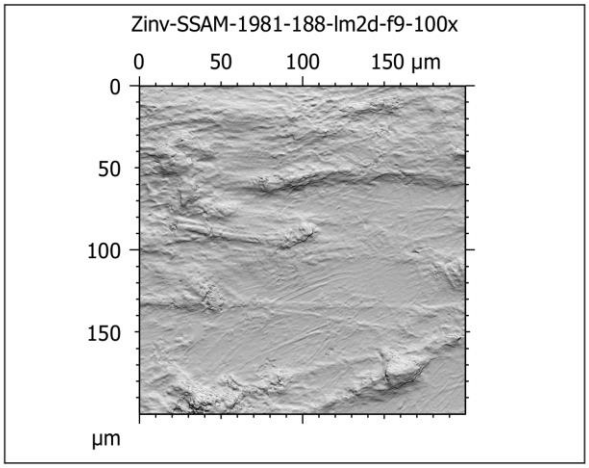
Zinv-SSAM-1981-188-lm2d-f9-100x
0
50
100
150 µm
µm

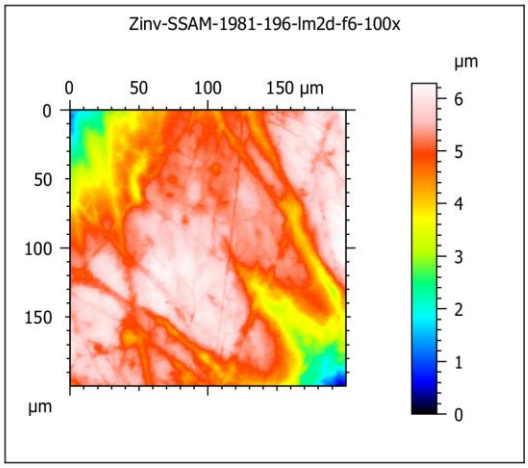
Zinv-SSAM-1981-196-lm2d-f6-100x
0
50
100
150 µm
µm
6
5
4
3
2
1
0

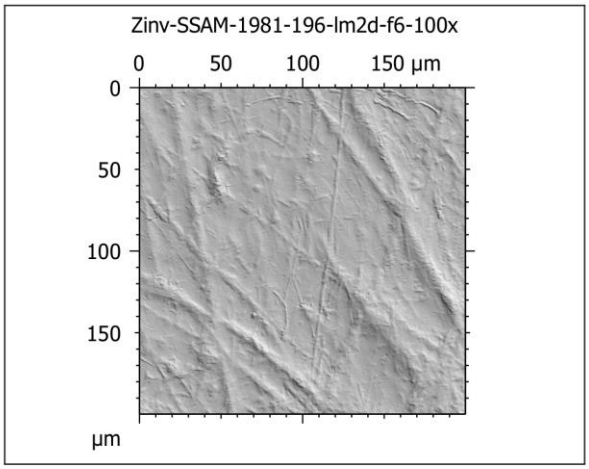
Zinv-SSAM-1981-196-lm2d-f6-100x
0
50
100
150 µm
µm

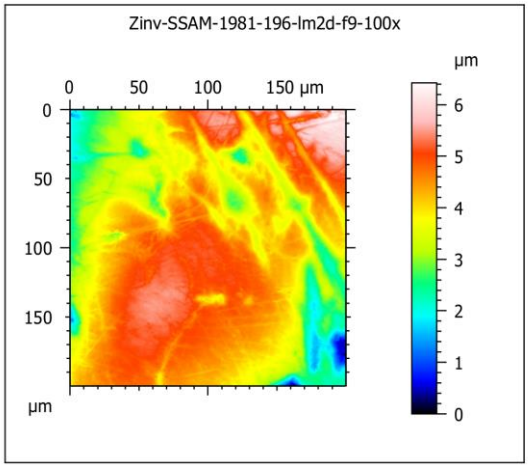
Zinv-SSAM-1981-196-lm2d-f9-100x
0
50
100
150 µm
µm
6
5
4
3
2
1
0

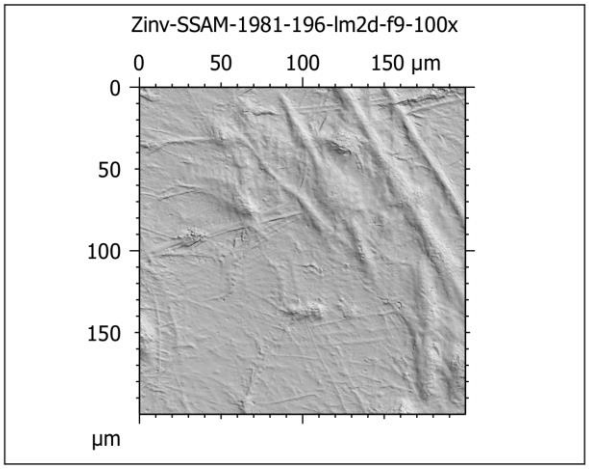
Zinv-SSAM-1981-196-lm2d-f9-100x
0
50
100
150 µm
µm

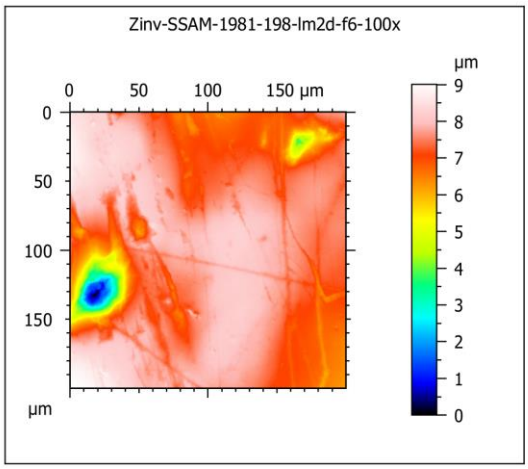
Zinv-SSAM-1981-198-lm2d-f6-100x
0
50
100
150 µm
µm
9
8
7
6
5
4
3
2
1
0

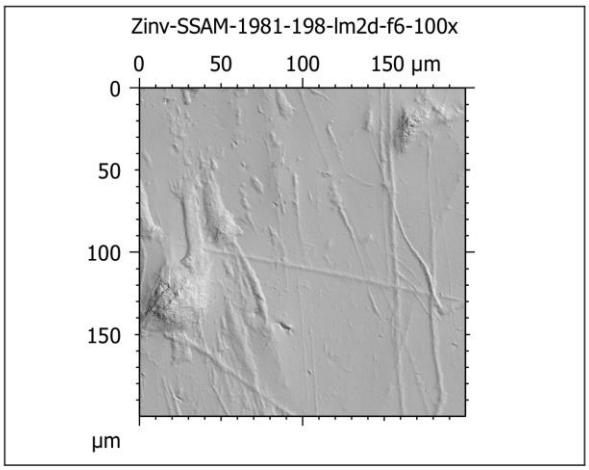
Zinv-SSAM-1981-198-lm2d-f6-100x
0
50
100
150 µm
µm

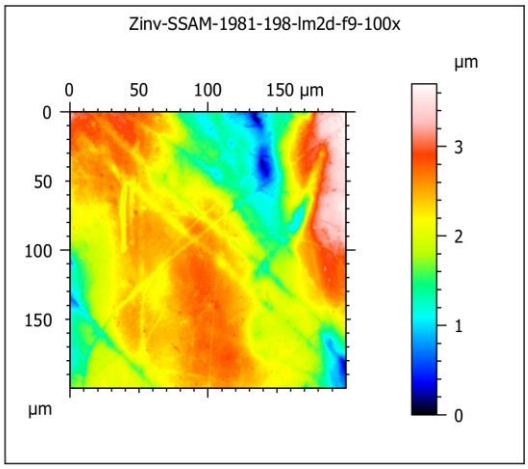
Zinv-SSAM-1981-198-lm2d-f9-100x
0
50
100
150 µm
µm
3
2
1
0

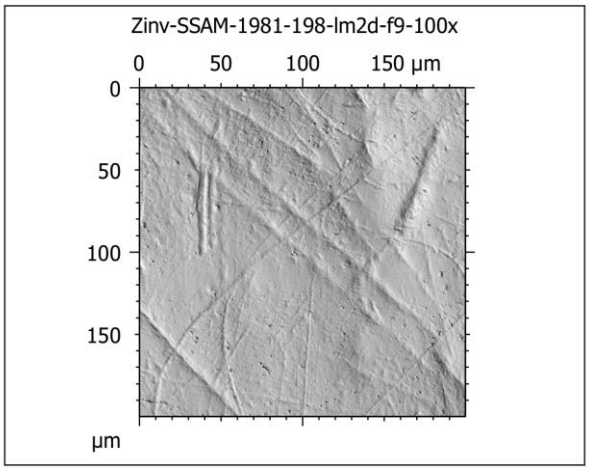
Zinv-SSAM-1981-198-lm2d-f9-100x
0
50
100
150 µm
µm

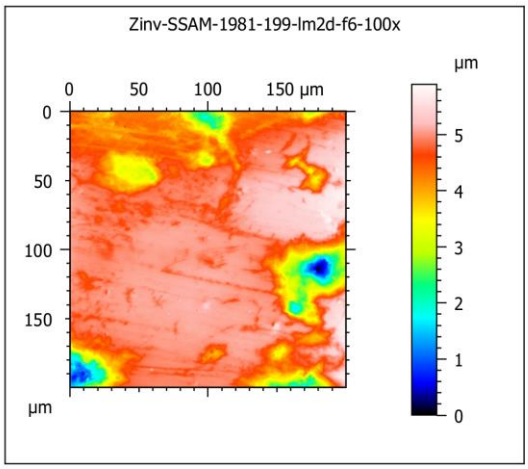
Zinv-SSAM-1981-199-lm2d-f6-100x
0
50
100
150 µm
µm
5
4
3
2
1
0

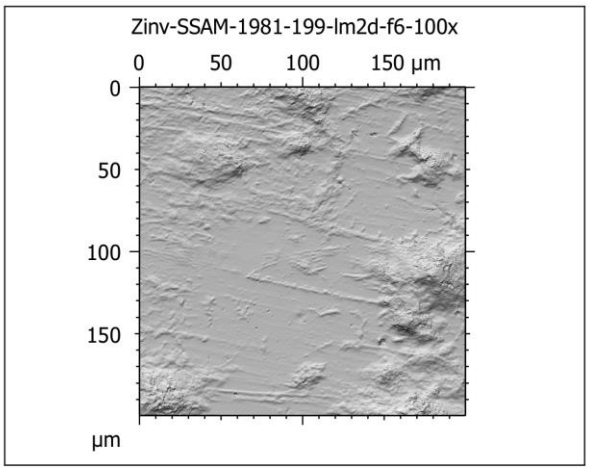
Zinv-SSAM-1981-199-lm2d-f6-100x
0
50
100
150 µm
µm

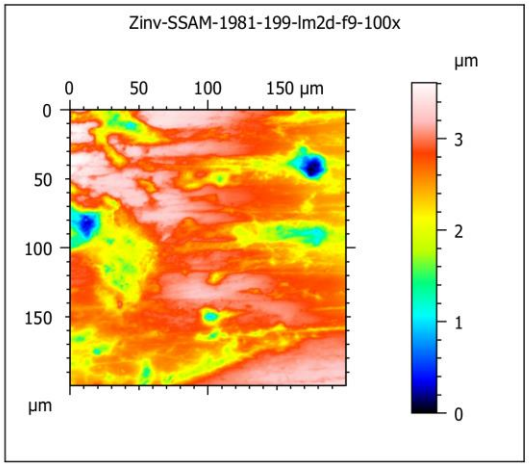
Zinv-SSAM-1981-199-lm2d-f9-100x
0
50
100
150 µm
µm
3
2
1
0

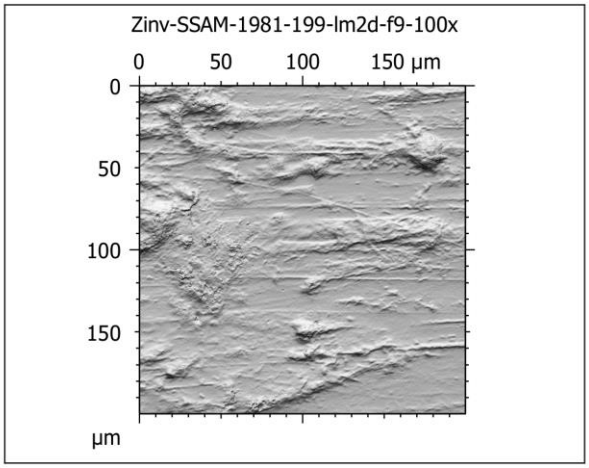
Zinv-SSAM-1981-199-lm2d-f9-100x
0
50
100
150 µm
µm

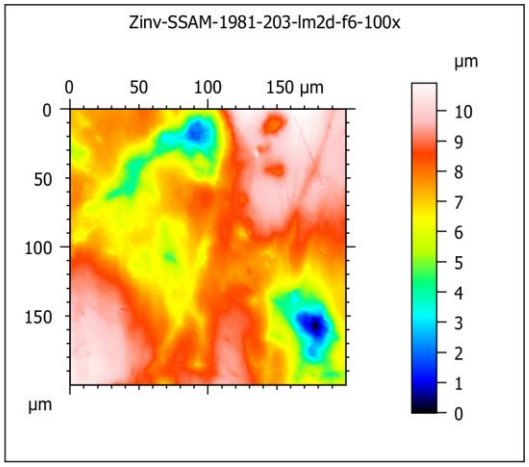
Zinv-SSAM-1981-203-lm2d-f6-100x
0
50
100
150 µm
µm
10
9
8
7
6
5
4
3
2
1
0

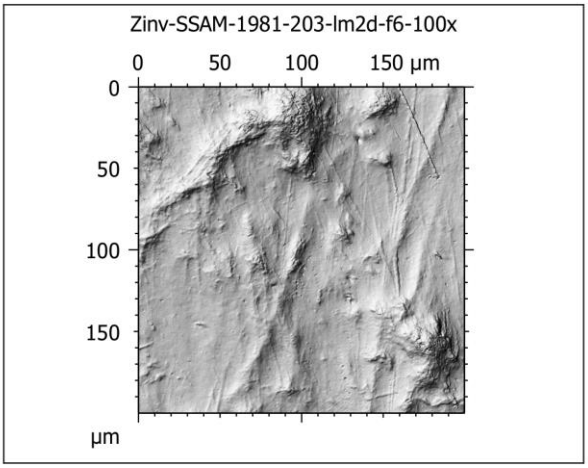
Zinv-SSAM-1981-203-lm2d-f6-100x
0
50
100
150 µm
µm

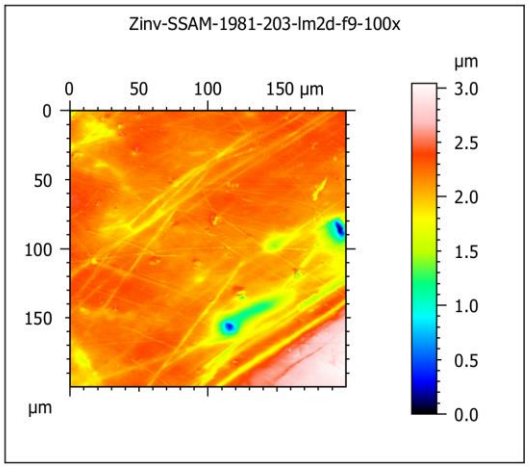
Zinv-SSAM-1981-203-lm2d-f9-100x
0
50
100
150 µm
µm
3.0
2.5
2.0
1.5
1.0
0.5
0.0

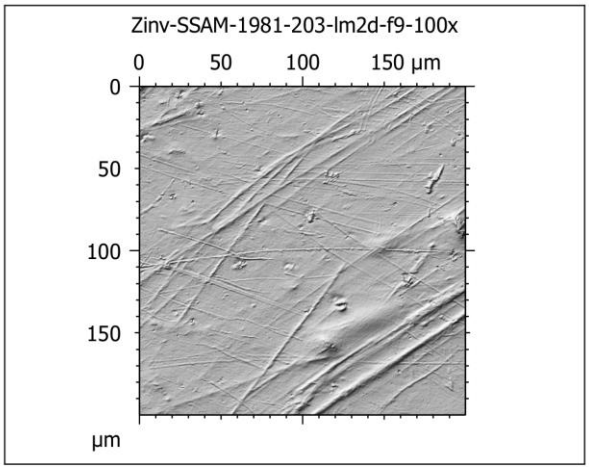
Zinv-SSAM-1981-203-lm2d-f9-100x
0
50
100
150 µm
µm

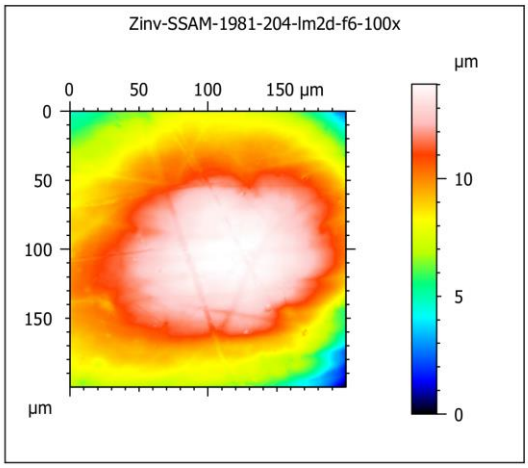
Zinv-SSAM-1981-204-lm2d-f6-100x
0
50
100
150 µm
µm
10
5
0

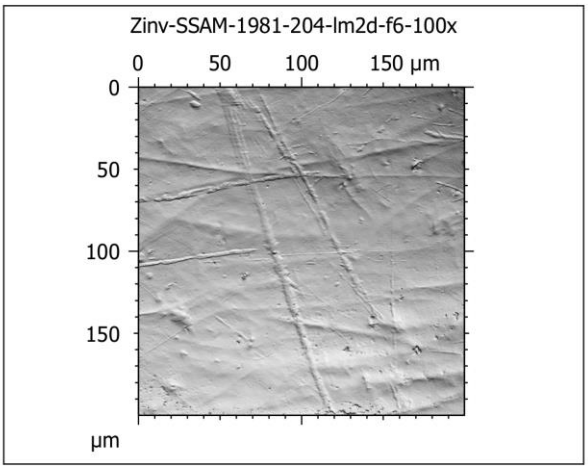
Zinv-SSAM-1981-204-lm2d-f6-100x
0
50
100
150 µm
µm

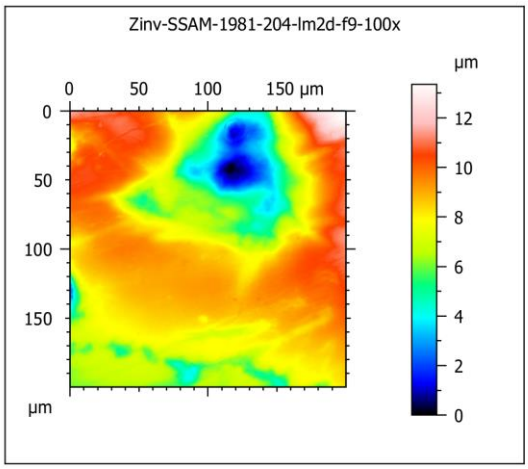
Zinv-SSAM-1981-204-lm2d-f9-100x
0
50
100
150 µm
µm
12
10
8
6
4
2
0

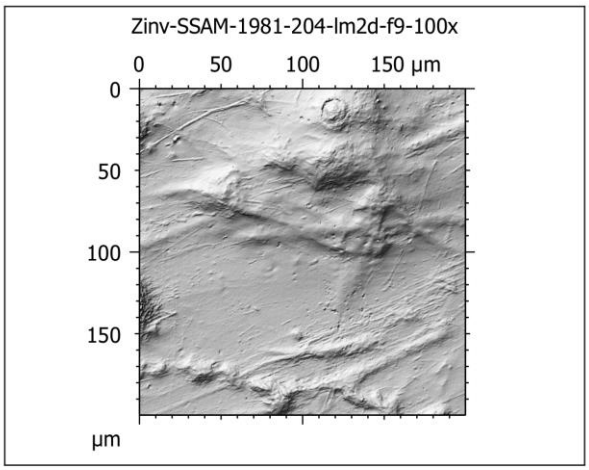
Zinv-SSAM-1981-204-lm2d-f9-100x
0
50
100
150 µm
µm

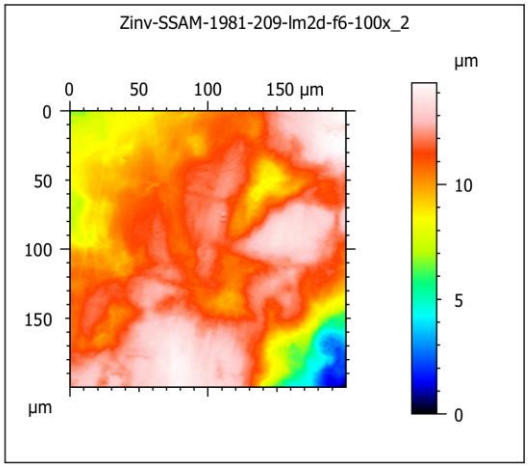
Zinv-SSAM-1981-209-lm2d-f6-100x_2
0
50
100
150 µm
µm
10
5
0

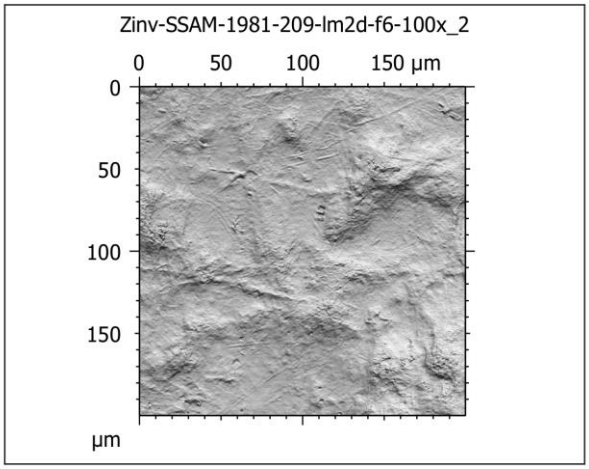
Zinv-SSAM-1981-209-lm2d-f6-100x_2
0
50
100
150 µm
µm

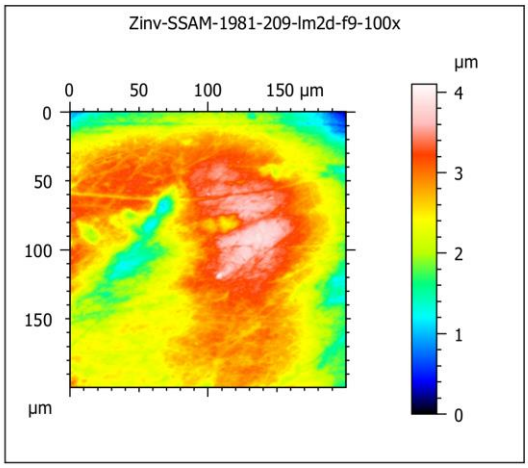
Zinv-SSAM-1981-209-lm2d-f9-100x
0
50
100
150 µm
µm
4
3
2
1
0

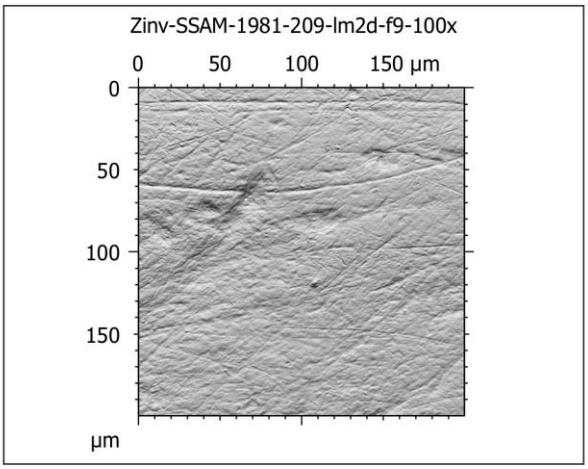
Zinv-SSAM-1981-209-lm2d-f9-100x
0
50
100
150 µm
µm

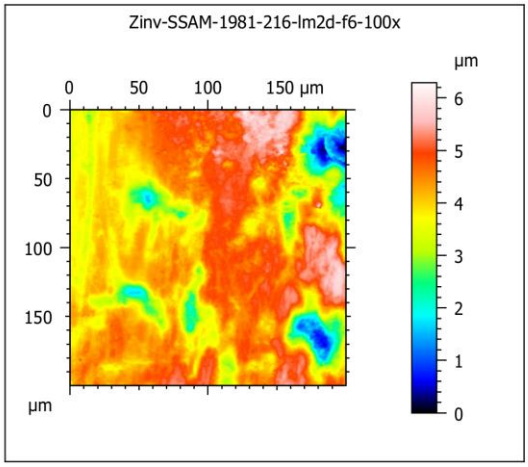
Zinv-SSAM-1981-216-lm2d-f6-100x
0
50
100
150 µm
µm
6
5
4
3
2
1
0

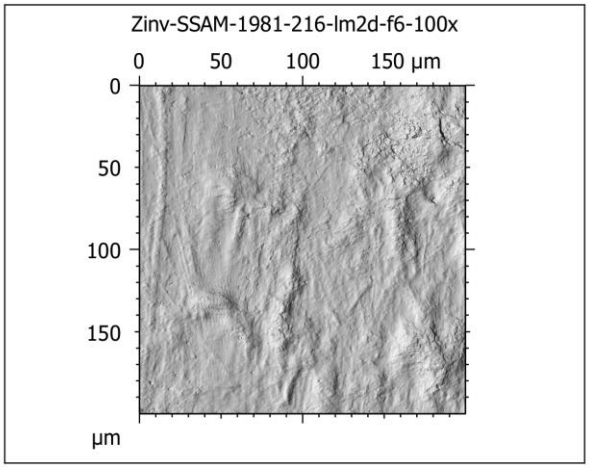
Zinv-SSAM-1981-216-lm2d-f6-100x
0
50
100
150 µm
µm

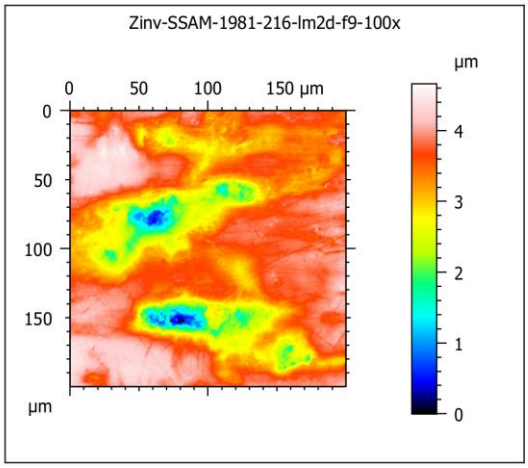
Zinv-SSAM-1981-216-lm2d-f9-100x
0
50
100
150 µm
µm
4
3
2
1
0

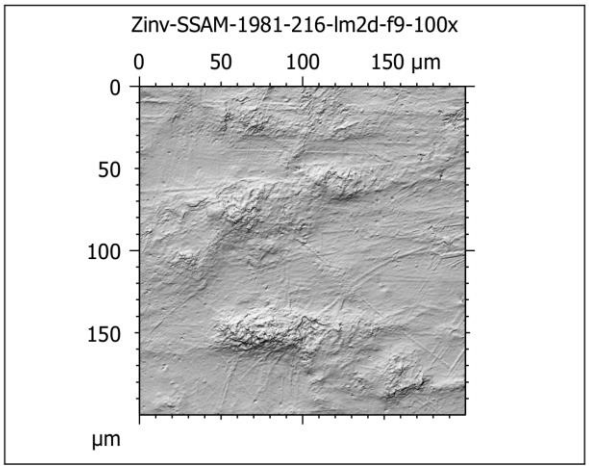
Zinv-SSAM-1981-216-lm2d-f9-100x
0
50
100
150 µm
µm

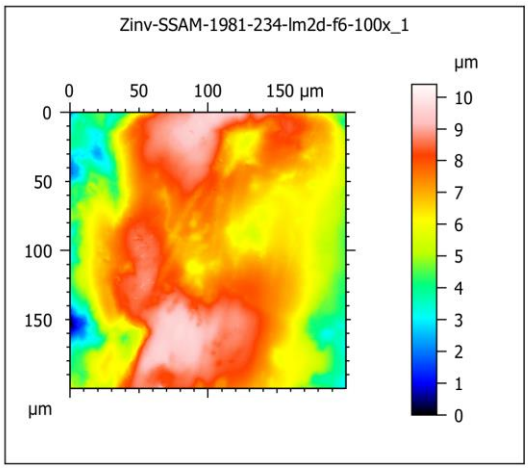
Zinv-SSAM-1981-234-lm2d-f6-100x_1
µm
0 50 100 150 µm
0
50
100
150
µm
10
9
8
7
6
5
4
3
2
1
0

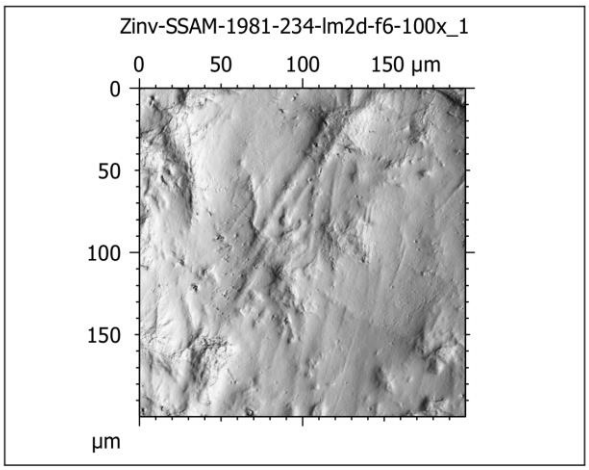
Zinv-SSAM-1981-234-lm2d-f6-100x_1
0 50 100 150 µm
0
50
100
150
µm

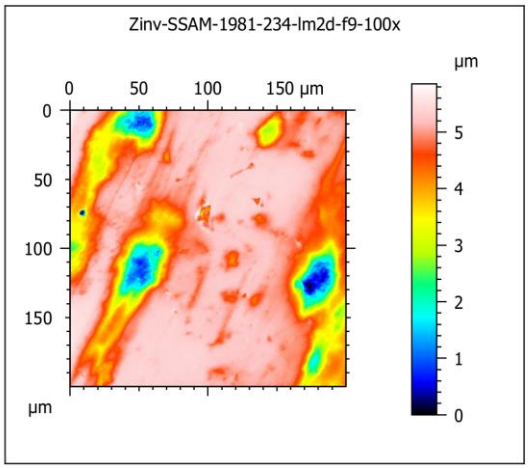
Zinv-SSAM-1981-234-lm2d-f9-100x
µm
0 50 100 150 µm
0
50
100
150
µm
5
4
3
2
1
0

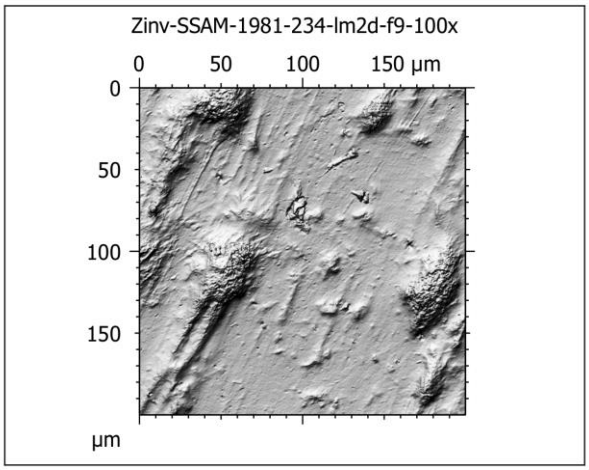
Zinv-SSAM-1981-234-lm2d-f9-100x
0 50 100 150 µm
0
50
100
150
µm

Appendix II

Extended figures and tables

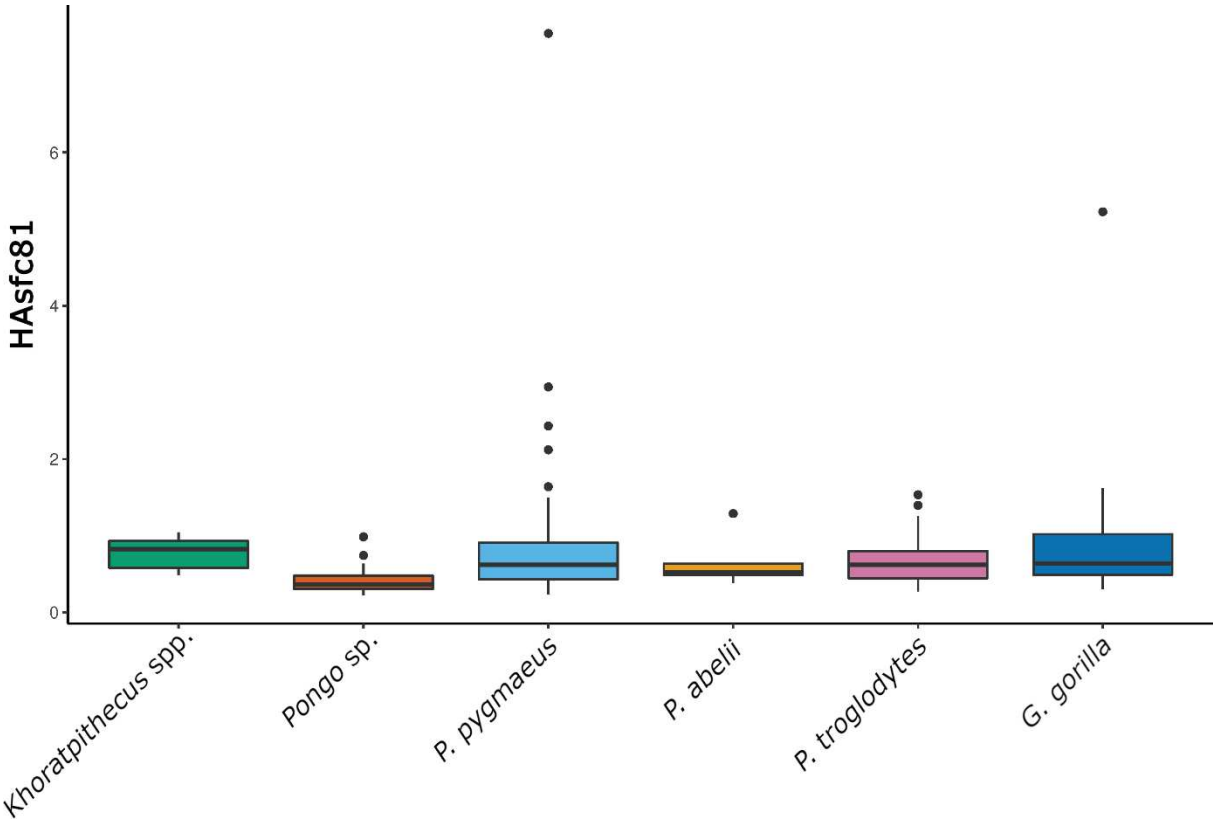

Fig. SI 1 Boxplot of Heterogeneity of Complexity (HAsfc81) per taxonomic group. Khoratpithecus spp. Includes K. piriyai and K. magnus from Thailand and Khoratpithecus sp. and K. ayeyarwadyensis from Myanmar. Even when looking at genus level distribution of HAsfc81 values for Khoratpithecus heterogeneity of complexity and thus dietary variability in regard to physical and mechanical properties of the food items are higher than in the other taxonomic groups.

Table SI 1 Compiled table of published specimens of primate fossils from the late Middle Eocene Pondaung Fm. Some specimens inspected during the fieldwork in February 2020 in the National Museum of Myanmar, Nay Pyi Taw are also listed.

Specimen	Genus/species	Description	Area	Locality	Comment	Reference
GSI D201	*Pondaungia cotteri*	L dent. M_{2-3} (holotype)	Pangan	Pangan 1		Pilgrim 1927
GSI D202	*Pondaungia cotteri*	R dent. M_3 (holotype)	Pangan	Pangan 1		Pilgrim 1927
GSI D203	*Pondaungia cotteri*	L max. M^{1-2} (holotype)	Pangan	Pangan 1		Pilgrim 1927
AMNH 32520	*Amphipithecus mogaungensis*	L dent. P_3 - M_1 (holotype)	Mogaung	Thandaung		Colbert 1937
NMMP 1	*Pondaungia savagei*	R dent. M_{2-3} (holotype)	Mogaung	Lema		Pilgrim 1927
NMMP 2	*Amphipithecus mogaungensis*	L dent. M_{1-2}	Mogaung	Thandaung		Colbert 1937
NMMP 3	*Pondaungia savagei*	L dent. M_{2-3} (part of holotype?)	Mogaung	Lema		Pilgrim 1927
NMMP 4	*Pondaungia cotteri*	R dent. M_{1-3}	Mogaung	Lema		Ciochon et al. 1985, Ciochon & Gunnell 2002
NMMP 5	*Pondaungia savagei*	R dent. M_{2-3}	Mogaung	Lema		Pilgrim 1927
NMMP 6	*Amphipithecus mogaungensis*	L dent. M_{1-2}	Mogaung	Thandaung		Colbert 1937
NMMP 7	*Amphipithecus mogaungensis*	L and R dents.	Bahin	Yarshe		Colbert 1937
NMMP 8	*Myanmarpithecus yarshensis*	R max. P^4 - M^3 (holotype)	Bahin	Yarshe		Takai et al. 2001, Ciochon & Gunnell 2002
NMMP 9	*Myanmarpithecus yarshensis*	L dent. C_1-P_3 (holotype)	Bahin	Yarshe		Ciochon & Gunnell 2002
NMMP 10	*Myanmarpithecus yarshensis*	L dent. M_{2-3} (holotype)	Bahin	Yarshe		Takai et al. 2001
NMMP 11	*Myanmarpithecus yarshensis*	L dent. M_3	Bahin	Yarshe		Ciochon & Gunnell 2002
NMMP 12	*Pondaungia savagei*	L max. I^1, C^1, P^3, M^2, frags. of P^4, M^1, M^3	Pangan	PGN2 (Taungnigyin)	= NMMP-KU 0003	Ciochon & Gunnell 2002
NMMP 13	*Bahinia pondaungensis*	L dent. P_2 - M_1	Bahin	Yarshe	= NMMP-KU 0129, same individual as NMMP 16	Ciochon & Gunnell 2002
NMMP 14	*Bahinia pondaungensis*	L max. P^2 - M^2	Bahin	Yarshe		Jaeger et al. 1999
NMMP 15	*Bahinia pondaungensis*	R max. P^2 - M^2	Bahin	Yarshe		Jaeger et al. 1999
NMMP 16	*Bahinia pondaungensis*	R dent. P_2 - M_1	Bahin	Yarshe		Jaeger et al. 1999
NMMP 17	*Pondaungia cotteri*	R dent. P2 - M3	Mogaung	Thandaung		Chaimanee et al. 2000
NMMP 18	*Amphipithecus mogaungensis*	R max. P^4 - M^3	Bahin	PK2	= NMMP-KU 0228, same individual as NMMP 13	Ciochon & Gunnell 2002, Maung et al. 2005
NMMP 19	Sivaladapidae	frontal	Bahin	PK2		Ciochon & Gunnell 2002

NMMP 20	Sivaladapidae	nearly complete right humerus, proximal right humerus fragment, right proximal ulna, left proximal ulna, distal half of a left calcaneum, two long bone shaft fragments, fragmentary vertebral centrum; pelvis fragment	Bahin	PK1 (Sabapondaung kyitchang)		Ciochon et al. 2001; Marivaux et al. 2008a
NMMP 21	*Myanmarpithecus yarshensis*	L M_3	Bahin	PK2		Ciochon & Gunnell 2002
NMMP 22	*Pondaungia cotteri*	R P^4	Mogaung	Lema		Ciochon & Gunnell 2002
NMMP 23	Eosimiidae	R calcaneum	Bahin	PK2		Gebo et al. 2002
NMMP 24	*Pondaungia savagei*	R dent. C_1 - M_3	Bahin	PK2		Jaeger et al. 2004
NMMP 25	*Pondaungia savagei*	L dent. M_1	Mogaung	Lema		Pilgrim 1927
NMMP 27	Sivaladapidae	frontal	Bahin	Payama (PA1), near Sinzwe		Ciochon & Gunnell 2002
NMMP 28	*Kyitchaungia takaii*	R lower M, interpreded as M_2 (holotype)	Bahin	PK2	= NMMP-KU 0626	Beard et al. 2007
NMMP 30	*Amphipithecus* (=*Pondaungia*)	mandible	Bahin	PK3	= NMMP-KU 1125	Pilgrim 1927
NMMP 31	*Bahinia pondaungensis*	L mand. alveoli of P_2-M_3, R mand. M_3	Bahin	PK2	= NMMP-KU 1203	Takai et al. 2005
NMMP 37	*Myanmarpithecus yarshensis*					
NMMP 38	*Pondaungia cotteri*					Pilgrim 1927
NMMP 39	*Pondaungia sp.*	L talus	Mogaung	Segyauk		Marivaux et al. 2003, Marivaux et al. 2010
NMMP 54	*Paukkaungia parva*	L P_3	Bahin	PK2		Beard et al. 2007
NMMP 55	*Paukkaungia parva*	R M_1 (holotype)	Bahin	Nyaung Pinle		Beard et al. 2007
NMMP 56	*Paukkaungia parva*	L P_4	Bahin	Nyaung Pinle		Beard et al. 2007
NMMP 57	*Paukkaungia parva*	R M_2	Bahin	PK2		Beard et al. 2007
NMMP 58	*Kytchaungia takaii*	calcaneum	Pangan	Thamingyauk		Beard et al. 2007
NMMP 59	*Kytchaungia takaii*	right talus, frag. right calcaneus; femur proximal	Pangan	Thamingyauk		Beard et al. 2007; Marivaux et al. 2008b
NMMP 61	*Pondaungia cotteri*					Pilgrim 1927
NMMP 63	*Pondaungia cotteri*					
NMMP 66	*Pondaungia cotteri*					Pilgrim 1927
NMMP 69	*Ganlea megacanina*	L M_1	Bahin	Nyaungpinle		Beard et al. 2009
NMMP 70	*Ganlea megacanina*	R mand. C, M_2, and roots of P_2-M_1 (holotype)	Bahin	Ganle		Beard et al. 2009
NMMP 71	*Ganlea megacanina*	L I_2	Bahin	Nyaungpinle		Beard et al. 2009
NMMP 72	*Ganlea megacanina*	R M_2	Bahin	Nyaungpinle		Beard et al. 2009

NMMP 73	*Ganlea megacanina*	LM_1	Pangan	Thamingyauk		Beard et al. 2009
NMMP 74	*Ganlea megacanina*	R mand. P_3-P_4	Pangan	Thamingyauk		Beard et al. 2009
NMMP 75	*Ganlea megacanina*	L M^1 or M^2	Bahin	PK2		Beard et al. 2009
NMMP 76	*Ganlea megacanina*	L P^4	Bahin	PK2		Beard et al. 2009
NMMP 77	*Afrasia dijidae*	R M_3	Bahin	Nyaungpinle		Chaimanee et al. 2012
NMMP 79	*Afrasia dijidae*	R M_2	Bahin	PK 2		Chaimanee et al. 2012
NMMP 81	*Afrasia dijidae*	R M^2 (holotype)	Bahin	Nyaungpinle		Chaimanee et al. 2012
NMMP 82	*Pondaungia*	talus	Mogaung	Thandaung		Marivaux et al. 2010
NMMP 84	*Ganlea megacanina*	R M_2	Bahin	Nyaungpinle		seen during fieldwork at Nay Pyi Taw
NMMP 85	*Afrasia dijidae*	R M^1	Pangan	Thamingyauk		Chaimanee et al. 2012
NMMP 86	*Pondaungia cotteri*	L M^2	Bahin	PK2		seen during fieldwork at Nay Pyi Taw
NMMP 90	*Myanmarpithecus yarshensis*	R P^2-P^3	Pangan	Pangan 1		seen during fieldwork at Nay Pyi Taw
NMMP 92	*Pondaungia cotteri*	R M^2	Bahin	PK2		seen during fieldwork at Nay Pyi Taw
NMMP 93	*Aseanpithecus myanmarensis*	L M^2-M^3	Bahin	PK2		Jaeger et al. 2019
NMMP 94	*Pondaungia cotteri*	R P_3-M_3	Pangan	Pangan 1		seen during fieldwork at Nay Pyi Taw
NMMP 95	*Aseanpithecus myanmarensis*	R P_2-P_3	Bahin	PK2		Jaeger et al. 2019
NMMP 96	*Aseanpithecus myanmarensis*	R M_3	Bahin	PK2		Jaeger et al. 2019
NMMP 97	*Pondaungia cotteri*	L M_1-M_2	Bahin	Changan		seen during fieldwork at Nay Pyi Taw
NMMP 98	*Pondaungia cotteri*	R M_1	Bahin	Yarshe		seen during fieldwork at Nay Pyi Taw
NMMP 99	*Pondaungia cotteri*	L M_3	Bahin	Yarshe		seen during fieldwork at Nay Pyi Taw
NMMP 101	*Ganlea megacanina*	L mand. P_2-M_3, and root frac of C	Bahin	Than U Daw		Jaeger et al. 2020
NMMP 102	*Ganlea megacanina*	R max. M^1-M^3	Bahin	Than U Daw		Jaeger et al. 2020
NMMP 103	*Ganlea megacanina*	left skull frag. with I^1-I^2, roots of C^1-P^4, lingual frag. of P^3 and M^1, and M^2-M^3	Bahin	Than U Daw		Jaeger et al. 2020
NMMP 104	*Ganlea megacanina*	frontoparietal	Bahin	Than U Daw		Jaeger et al. 2020
NMMP 105	*Ganlea megacanina*	R M^1-M^3	Bahin	PK2		seen during fieldwork at Nay Pyi Taw
NMMP 106	*Ganlea megacanina*	R prox. ulna	Bahin	Than U Daw		Jaeger et al. 2020

Table SI 2 Compiled table of Khoratpithecus specimens from Myanmar and Thailand with additional information on which specimens and which teeth were moulded for DMTA.

Specimen ID	Country	Locality	Taxonomy	Description	scanned for DMTA		Comments	Reference
					tooth	n° teeth		
MFI K-171	Myanmar	Irrawaddy Fm.	*K. ayeyarwadyensis*	left mandible fragment with P_3 - M_2, root of C and M_3 as well as alveoli fragments of I_1 and I_2 present	-	-	holotype specimen, M_3 sampled for SIA, preservation did not allow for DMTA	Jaeger et al. 2011
MFI K-172	Myanmar	Irrawaddy Fm.	*Khoratpithecus sp.*	right M_3	right M_3	1	could be *K. magnus* but assigning it to this new species known from Thailand based solely on an isolated tooth is an uncertain attribution at best	unpublished
MFI K-173	Myanmar	Irrawaddy Fm.	*K. ayeyarwadyensis*	left M_2	left M_2	1		unpublished
MFI 89	Myanmar	Irrawaddy Fm.	*Khoratpithecus* sp.	left M^2	-	-		Jaeger et al. 2011
MZKB-K-001	Myanmar	Irrawaddy Fm., Tebingan area	*Ponginae* indet.	left mandible fragment with M_2 - M_3 roots of P_4 - M_1 and alveoli of C and P_3 present	-	-		Takai et al 2021
MFT-K176	Thailand	Khorat sand pit	*K. piriyai*	maxilla fragment with left I^2 - M^3 and right P^3 - M^3, alveoli of left and right I^1 and right C and root of right I^2 present	right M^2 - M^3	2		Chaimanee et al. 2019
MFT-K177	Thailand	Khorat sand pit	*K. piriyai*	mandible fragment with left P_4 - M_3 and right P_3 - M_3, algeolar fragments of I_1, I_2, and C as well as root of left P_3 present	-	-		Chaimanee et al. 2022
MFT-K178	Thailand	Khorat sand pit	*K. magnus*	mandible fragment with left P_4 - M_2, alveolar fragments of left C and P_3 as well as root of right P_4 present	left M_2	1	holotype	Chaimanee et al. 2022
MFT-K179	Thailand	Khorat sand pit	*Khoratpithecus sp.*	mandible fragment with roots of left C - M_1 and right C - M_2, alveolar fragments of both I_1s and I_2s present	-	-		Chaimanee et al. 2022
MFT-K180	Thailand	Khorat sand pit	*K. piriyai*	left maxillary fragments with P^3 - M^3 and alveoli fragments of I^2 and C present	left M^2	1		Chaimanee et al. 2022
MFT-K181	Thailand	Khorat sand pit	*K. piriyai*	left mandible fragment with P_3 - M_3, alveoli of I_1, I_2, and C present	left M_2	1		Chaimanee et al. 2022
TF 6168	Thailand	Chiang Muan Basin, Ban Sa locality	*K. chiangmuanensis*	right I^1	-	-		Chaimanee et al. 2003
TF 6169	Thailand	Chiang Muan Basin, Ban Sa locality	*K. chiangmuanensis*	right M^2	-	-		Chaimanee et al. 2003
TF 6170	Thailand	Chiang Muan Basin, Ban Sa locality	*K. chiangmuanensis*	left deciduous P_4	-	-		Chaimanee et al. 2003
TF 6171-1	Thailand	Chiang Muan Basin, Ban Sa locality	*K. chiangmuanensis*	right lower C fragment	-	-	holotype specimen	Chaimanee et al. 2003
TF 6171-2	Thailand	Chiang Muan Basin, Ban Sa locality	*K. chiangmuanensis*	left P_3 fragment	-	-	holotype specimen	Chaimanee et al. 2003

TF 6171-3	Thailand	Chiang Muan Basin, Ban Sa locality	*K. chiangmuanensis*	right P_4	-	-	holotype specimen	Chaimanee et al. 2003
TF 6171-4	Thailand	Chiang Muan Basin, Ban Sa locality	*K. chiangmuanensis*	right M_2	-	-	holotype specimen	Chaimanee et al. 2003
TF 6171-5	Thailand	Chiang Muan Basin, Ban Sa locality	*K. chiangmuanensis*	left M_2	-	-	holotype specimen	Chaimanee et al. 2003
TF 6171-6	Thailand	Chiang Muan Basin, Ban Sa locality	*K. chiangmuanensis*	left M_3	-	-	holotype specimen	Chaimanee et al. 2003
TF 6171-7	Thailand	Chiang Muan Basin, Ban Sa locality	*K. chiangmuanensis*	right P_3 fragment	-	-	holotype specimen	Chaimanee et al. 2003
TF 6172	Thailand	Chiang Muan Basin, Ban Sa locality	*K. chiangmuanensis*	right M_3 fragment	-	-		Chaimanee et al. 2003
TF 6173	Thailand	Chiang Muan Basin, Ban Sa locality	*K. chiangmuanensis*	right I^2	-	-		Chaimanee et al. 2003
TF 6174	Thailand	Chiang Muan Basin, Ban Sa locality	*K. chiangmuanensis*	left upper C	-	-		Chaimanee et al. 2003
TF 6175	Thailand	Chiang Muan Basin, Ban Sa locality	*K. chiangmuanensis*	right P^3	-	-		Chaimanee et al. 2003
TF 6176	Thailand	Chiang Muan Basin, Ban Sa locality	*K. chiangmuanensis*	left M^2	-	-	same individual as TF 6177	Chaimanee et al. 2003
TF 6177	Thailand	Chiang Muan Basin, Ban Sa locality	*K. chiangmuanensis*	left M^3	-	-	same individual as TF 6176	Chaimanee et al. 2003
TF 6178	Thailand	Chiang Muan Basin, Ban Sa locality	*K. chiangmuanensis*	left I_1	-	-		Chaimanee et al. 2003
TF 6179	Thailand	Chiang Muan Basin, Ban Sa locality	*K. chiangmuanensis*	left P_4	-	-		Chaimanee et al. 2003
TF 6180	Thailand	Chiang Muan Basin, Ban Sa locality	*K. chiangmuanensis*	right M_2	-	-		Chaimanee et al. 2003
TF 6223	Thailand	Khorat sand pit	*K. piriyai*	mandible fragment with left P_3 - M_3 and right C - M_3, root alveoli of both I_1s and root fragments of both I_2s and left C	-	-	holotype specimen, old specimen ID RIN 765	Chaimanee et al. 2004

Table SI 3 Data from observational studies orangutan diets that was used for Fig. 8.

Study area	Latitude	Longitude	Year	Habitat type main/secondary	Species	Feeding time (percentages of overall feeding time)					Reference	Comments
						Fruit	Leaves	Bark	Insects	Other		
Batang Serangan	3.7331	98.1950	2007-2009	mosaic agroforest	*P. abelii*	46.0	13.0	33.0	0.0	8.0	Campbell et al. 2011	"Fruit" includes both wild and cultivated fruit
Ketambe	3.6833	97.6500	1976-2002	mixed dipterocarp	*P. abelii*	67.5	16.4	2.7	8.8	4.8	Morrogh-Bernard et al. 2008	
Ketambe	3.6833	97.6500	1971-1975	mixed dipterocarp	*P. abelii*	58.0	25.0	3.0	14.0	0.0	Rijksen 1978	
Ranun	3.0284	98.0289	1971	mixed dipterocarp	*P. abelii*	84.7	10.2	4.5	0.6	0.0	MacKinnon 1974	percentages of feeding observations
Suaq Balimbing	3.0667	97.6500	1994-1999	peat swamp	*P. abelii*	66.2	15.5	1.1	13.4	3.8	Morrogh-Bernard et al. 2008	
Suaq Balimbing	3.0667	97.6500	1995-1998	peat swamp	*P. abelii*	68.0	18.0	1.0	12.0	1.0	Fox et al. 2004	
Danum Valley	5.0167	117.8000	2005-2007	mixed dipterocarp	*P. pygmaeus*	60.9	22.2	12.3	0.6	2.5	Kanamori et al. 2010	
Gunung Palung	-1.2167	110.1167	1994-1996	mixed dipterocarp/ peat swamp	*P. pygmaeus*	70.0	13.4	4.9	3.7	8.0	Morrogh-Bernard et al. 2008	
Kinabatangan	5.5333	118.2833	1998-2006	mixed dipterocarp/ freshwater swamp	*P. pygmaeus*	68.0	22.9	6.7	1.2	1.3	Morrogh-Bernard et al. 2008	
Mentoko	0.3667	117.2667	1970-1971	mixed dipterocarp	*P. pygmaeus*	53.8	29.0	14.2	0.8	2.2	Rodman 1977	
Sabangau	-2.3167	114.0000	2003-2005	peat swamp	*P. pygmaeus*	73.8	5.1	1.5	8.6	11.0	Morrogh-Bernard et al. 2008	
Tanjung Puting	-2.7500	111.9500	1971-1975	peat swamp/ mixed dipterocarp	*P. pygmaeus*	60.9	14.7	11.4	4.3	3.9	Galdikas 1978, Galdikas 1988	
Tuanan	-2.1500	114.4333	2003-2005	peat swamp	*P. pygmaeus*	68.6	17.2	1.0	6.3	6.5	Morrogh-Bernard et al. 2008	
Tuanan	-2.1500	114.4333	2003-2012	peat swamp	*P. pygmaeus*	61.6	16.1	3.9	5.3	11.2	Vogel et al. 2017	
Ulu Segama	5.1832	117.8454	1969-1979	mixed dipterocarp	*P. pygmaeus*	62.0	23.5	10.5	1.0	3.0	MacKinnon 1974	percentages of feeding observations

Table S1 4 Compiled SSFA and STA parameters on Khoratpithecus as well as Gorilla, Pan, and Pleistocene and modern Pongo used for the dietary reconstructions of Khoratpithecus from Myanmar and Thailand.

Specimen ID	Taxonomy	Sex	Age	Site	Country	Date of death	tooth	facet	upper/ lower	right/ left	SSFA parameteres				Height parameters							Surface parameters			Volume parameters			References
											Asfc	HAsfc9	HAsfc81	epLsar	Ssk	Sku	Sq	Sp	Sv	Sz	Sa	Sal2_s0.5	Str2_s0.5	Maximum_depth_furrows	Mean_depth_furrows	Mean_density_furrows	
MRAC-15355	*Gorilla gorilla*	f	ad.	Ibatsero, Lubero, KV	DR Congo	20.12.1938	M^2	f9	upper	-	0.3728	0.4899	0.7915	0.0063	-1.9534	9.1996	0.2254	0.6999	1.3622	2.0621	0.1535	6.7119	0.3907	1.2335	0.1901	4222.6558	this study
MRAC-15356	*Gorilla gorilla*	f	ad.	Ibatsero, Lubero, KV	DR Congo	20.12.1938	M_2	f9	lower	-	0.9584	0.3307	0.5516	0.0056	-2.1348	12.6632	0.3040	0.9095	2.8157	3.7252	0.2139	8.0435	0.5476	2.5671	0.2608	3997.3998	this study
MRAC-27755	*Gorilla gorilla*		ad.				M_2	f9	lower	-	2.5071	0.1425	0.3673	0.0051	-1.0255	4.2268	0.6174	1.5353	3.1198	4.6551	0.4759	8.9972	0.3876	3.3002	0.6119	3748.1775	this study
MRAC-27755	*Gorilla gorilla*		ad.				M^2	f9	upper	-	1.0485	0.2958	0.5817	0.0029	-0.6936	3.7402	0.2935	0.8889	1.5400	2.4290	0.2313	10.1140	0.7060	1.7124	0.2993	4152.0410	this study
MRAC-73018-8	*Gorilla gorilla*	indet	ad.	Meyo N'Koulou	Cameroon	1973	M_2	f13	lower	-	1.2159	0.4082	1.6131	0.0033	-2.5547	11.8627	0.5021	0.9310	3.1269	4.0579	0.3126	11.6187	0.8272	3.0582	0.3301	4667.0926	this study
MRAC-73018-3	*Gorilla gorilla*	indet	ad.	Akoabas	Cameroon	1973	M_2	f9	lower	-	0.2246	0.3283	0.6579	0.0052	-0.4918	3.4087	1.0166	3.2413	3.2618	6.5031	0.8012	18.9770	0.4117	2.0413	0.3449	3807.1250	this study
MRAC-75056-12	*Gorilla gorilla*	indet	ad.	Essengbot	Cameroon	1975	M^2	f9	upper	-	1.7233	0.3196	0.7911	0.0041	-0.8613	3.6444	1.0763	2.1404	5.3994	7.5399	0.8575	13.6222	0.7153	4.1751	0.8556	3296.6601	this study
MRAC-75056-2	*Gorilla gorilla*	indet	ad.	Djaposten	Cameroon	7.2.1975	M^2	f9	upper	-	0.8263	0.1875	0.3067	0.0034	-0.8520	5.8685	0.4731	1.4337	3.7876	5.2213	0.3497	11.7877	0.7146	2.3110	0.3583	3888.9894	this study
MRAC-75056-9	*Gorilla gorilla*	indet	ad.	Mang	Cameroon	1975	M_2	f9	lower	-	0.8849	0.1705	0.4869	0.0041	-1.5705	6.9840	0.4906	1.2899	2.9766	4.2664	0.3455	11.2110	0.7569	2.6382	0.4153	4128.0823	this study
MRAC-77032-1	*Gorilla gorilla*	indet	ad.	Dja region, KV	DR Congo	3.5.1977	M^2	f9	upper	-	1.3827	0.5491	1.1647	0.0019	-1.1361	4.8693	0.8892	3.0275	4.2862	7.3137	0.6326	12.7962	0.7532	3.8180	0.5895	3474.8766	this study
MRAC-77032-13	*Gorilla gorilla*	indet	ad.	river Dja, KV	DR Congo	3.5.1977	M^2	f9	upper	-	1.2516	0.4287	1.0606	0.0048	-2.8963	16.6009	0.6555	1.7503	4.8812	6.6316	0.3924	10.1204	0.5518	3.0996	0.3608	3991.1781	this study
MRAC-77032-15	*Gorilla gorilla*	indet	ad.	Moboe, Dja region, KV	DR Congo	25.3.1977	M^2	f9	upper	-	1.5933	0.2167	0.4515	0.0052	-1.1191	7.6582	0.7029	2.3170	4.1324	6.4495	0.4961	13.0080	0.7007	2.6494	0.5296	3639.5640	this study
MRAC-77032-2	*Gorilla gorilla*	indet	ad.	Mimbo Mimbo	DR Congo	25.3.1977	M^2	f9	upper	-	0.6135	0.1355	0.3236	0.0078	-0.7381	4.1530	0.1862	0.6153	1.2101	1.8254	0.1445	4.3483	0.1768	1.1117	0.2368	4025.7911	this study
MRAC-77032-3	*Gorilla gorilla*	indet	ad.	Masins	Cameroon	8.3.1977	M^2	f9	upper	-	1.1775	0.3761	0.6211	0.0047	-1.5366	6.5634	0.5671	1.3335	3.3442	4.6777	0.4186	10.3662	0.6227	2.7911	0.4543	3072.2746	this study
MRAC-77032-5	*Gorilla gorilla*	indet	ad.	Dja region, KV	DR Congo	25.3.1977	M_2	f9	lower	-	0.6742	0.4496	0.9125	0.0045	-1.7312	10.0495	0.1569	1.0303	1.2486	2.2789	0.1061	4.0320	0.3066	1.2797	0.1861	4604.8183	this study
MRAC-77032-7	*Gorilla gorilla*	indet	ad.	Dja region, KV	DR Congo	25.3.1977	M^2	f9	upper	-	1.4090	0.4244	0.9986	0.0033	-1.4658	5.7244	0.6580	1.3818	4.1289	5.5106	0.4941	8.5299	0.5205	3.9161	0.5716	3586.4466	this study
MRAC-77032-M16	*Gorilla gorilla*		ad.				M_2	f9	lower	-	1.2492	0.3149	0.6876	0.0060	-2.7736	17.2244	0.2050	0.5612	2.3792	2.9404	0.1382	4.3325	0.4293	2.2347	0.2051	4453.6553	this study
MRAC-77032-M16	*Gorilla gorilla*		ad.				M_2	f9	lower	-	0.4372	0.2260	0.6271	0.0047	-1.4912	7.1269	0.2100	0.8441	1.1405	1.9846	0.1481	9.3264	0.5840	1.0829	0.1858	4518.4463	this study
MRAC-77032-M18	*Gorilla gorilla*	indet	ad.	Moboe, Dja region, KV	DR Congo	25.3.1977	M_2	crushing	lower	-	0.9569	0.2842	0.8680	0.0049	-3.6838	28.2558	0.1355	0.4982	1.7757	2.2739	0.0854	3.3852	0.5626	1.8440	0.1250	4878.1217	this study
MRAC-77032-M18	*Gorilla gorilla*	indet	ad.	Moboe, Dja region, KV	DR Congo	25.3.1977	M^2	f9	upper	-	0.4364	0.1814	0.3450	0.0018	-0.0344	2.6638	0.1270	0.5462	0.4736	1.0198	0.1039	9.6206	0.8511	0.4882	0.1462	4875.4835	this study
MRAC-9406	*Gorilla gorilla*		ad.				M_2	crushing	lower	-	1.8284	1.2744	1.5543	0.0061	-1.1472	11.4170	0.6265	3.1169	6.6063	9.7231	0.4339	10.5237	0.7699	6.4261	0.4599	4195.4271	this study
MRAC-9424	*Gorilla gorilla*		ad.				M_2	f9	lower	-	0.7228	0.6699	1.0292	0.0071	-2.1058	10.8709	0.2657	0.7010	2.0278	2.7288	0.1854	7.4127	0.5513	1.7324	0.2242	4078.8210	this study
SNG-1133	*Gorilla gorilla*	m	ad.	East Africa		-	M_2	f9	lower	-	0.5731	0.4396	0.6527	0.0028	-0.8181	4.5767	0.5066	1.4030	2.5949	3.9979	0.3859	13.2750	0.6421	2.2951	0.3356	4103.4234	this study
SNG-1135	*Gorilla gorilla*	m	ad.	Delta of Rembo N'Komi, south of Vernan Vaz		2.6.1907	M^2	f9	upper	-	1.0313	0.2349	0.5030	0.0052	-1.6752	6.9226	0.4155	1.3924	2.4334	3.8258	0.2984	8.9665	0.4812	2.1900	0.3549	4085.7032	this study
SNG-1136	*Gorilla gorilla*	f	ad.	Delta of Rembo N'Komi, south of Vernan Vaz		2.6.1907	M^2	f9	upper	-	0.2213	0.1374	0.3011	0.0025	-0.4162	3.3215	0.2098	0.5670	1.0407	1.6077	0.1670	11.6424	0.6647	1.0628	0.1646	4298.5831	this study
SNG-4108	*Gorilla gorilla*	m	ad.	Kumilla, Molundu	Cameroon	-	M^2	f9	upper	-	1.2206	0.1807	0.3615	0.0023	-2.2137	11.0186	0.3457	0.9509	2.4597	3.4106	0.2319	9.2321	0.6823	2.1592	0.3012	4041.0877	this study
SNG-4109	*Gorilla gorilla*	m	ad.	Molundu	Cameroon	31.5.1911	M^2	f9	upper	-	1.1060	0.4636	0.5754	0.0049	-1.5356	7.0120	0.3131	1.0499	2.1072	3.1571	0.2207	6.0662	0.4025	1.8329	0.3009	4294.3765	this study
SNG-45713	*Gorilla gorilla*	m	ad.	Belabo	Cameroon	2.1972	M_2	f9	lower	-	0.7876	1.0074	1.3655	0.0033	-2.2696	12.7771	0.4593	1.3804	3.2711	4.6515	0.2769	11.9445	0.7715	2.2367	0.2950	4019.9242	this study
SNG-45713	*Gorilla gorilla*	m	ad.	Belabo	Cameroon	2.1972	M^2	f9	upper	-	0.8063	1.6310	5.2262	0.0031	-2.1080	10.6111	0.5707	1.5233	4.1520	5.6753	0.3696	11.5589	0.6080	3.6951	0.4151	4006.2016	this study
SNG-73976	*Gorilla gorilla*		ad.				M_2	f13	lower	-	1.2316	0.3306	0.4739	0.0073	-1.8622	9.1862	0.3516	0.8039	2.9599	3.7638	0.2538	8.0392	0.5927	1.8112	0.3359	3896.6581	this study
ZSM-1950-90	*Gorilla gorilla*	m	ad.	SW Cameroon	Cameroon	before 1914	M_2	f9	lower	-	1.4690	0.5889	1.6236	0.0043	-1.9009	8.1770	0.5614	1.4852	3.5106	4.9958	0.3944	9.6047	0.3698	2.9391	0.5429	3998.7192	this study
ZSM-1963-111	*Gorilla gorilla*	m	ad.	SW Cameroon	Cameroon	1938	M^2	f9	upper	-	0.3253	0.6692	1.3854	0.0027	-1.5296	8.7883	0.3080	0.9214	1.9123	2.8337	0.2228	14.8328	0.7421	1.3898	0.1806	3979.7145	this study
ZSM-1974-58	*Gorilla gorilla*	m	ad.	SW Cameroon, Lomié	Cameroon	5.1972	M^2	f13	upper	-	3.4666	0.3034	0.5406	0.0043	-1.4995	6.0958	1.0287	2.6528	7.5403	10.1931	0.7429	12.2777	0.5610	7.5272	0.6476	4076.0811	this study
ZSM-1981-475	*Gorilla gorilla*	f	ad.	SW Cameroon	Cameroon		M_2	f9	lower	-	0.2452	0.2641	0.5387	0.0054	-0.1437	2.3016	0.3893	1.1463	1.0130	2.1593	0.3208	15.3908	0.5292	0.7191	0.1750	4716.7143	this study
MRAC-10481	*Pan troglodytes*	m	ad.	Buta	DR Congo	1930	M^2	f9	upper	-	0.2851	0.3434	0.7594	0.0018	-1.4488	6.8171	0.3233	0.7422	1.8719	2.6141	0.2318	12.6608	0.8375	1.7318	0.2032	4223.0517	this study
MRAC-12089	*Pan troglodytes*	indet	ad.	Moba (Zougne, altitude 1000m)	DR Congo	-	M^2	f9	upper	-	1.2851	0.9681	1.3971	0.0042	-2.1500	10.2801	0.6570	1.8435	3.6668	5.5103	0.4147	7.9047	0.2891	2.8484	0.5483	4090.6649	this study
MRAC-14219	*Pan troglodytes*	indet	ad.	Budjala	DR Congo	-	M_2	f9	lower	-	3.4686	0.5103	0.9343	0.0042	-0.9881	4.8445	0.6019	1.6698	2.9221	4.5919	0.4393	6.8207	0.3658	2.8559	0.5640	3802.7687	this study
MRAC-15238	*Pan troglodytes*	indet	ad.	Bukavu region	DR Congo	-	M_2	f9	lower	-	0.7875	0.2442	0.3744	0.0029	-1.2255	5.8451	0.3702	1.0318	2.2961	3.3279	0.2811	13.4341	0.8340	1.6909	0.3084	3752.3425	this study
MRAC-15581	*Pan troglodytes*	indet	ad.	-	DR Congo	-	M^2	f9	upper	-	1.0352	0.4396	0.6723	0.0065	-2.7526	18.2014	0.3586	1.2618	3.1109	4.3726	0.2352	7.3168	0.4984	2.2262	0.2519	3934.6356	this study
MRAC-20480	*Pan troglodytes*	f	ad.	Ibembo	DR Congo	1951	M^2	f9	upper	-	1.6434	0.2974	0.6510	0.0065	-0.8052	3.5697	0.6992	1.4668	2.8988	4.3656	0.5412	12.8312	0.4361	2.1766	0.5119	3965.0532	this study
MRAC-28131	*Pan troglodytes*	indet	ad.	Kayuyu	DR Congo	-	M^2	f9	upper	-	0.5273	0.1361	0.2729	0.0015	0.3383	3.4748	0.2314	1.0465	0.9036	1.9501	0.1837	11.0770	0.6379	0.7584	0.1951	4339.4384	this study
MRAC-28137	*Pan troglodytes*	m	ad.	Kayuyu	DR Congo	-	M^2	f9	upper	-	2.3649	0.3891	0.6165	0.0058	-1.3107	6.7688	0.6171	1.4808	4.3736	5.8545	0.4574	7.8959	0.7033	2.9983	0.6700	3617.3546	this study
MRAC-29075	*Pan troglodytes*		ad.				M_2	f9	lower	-	1.9542	0.6564	1.2254	0.0023	-1.7117	8.7340	0.3526	0.8294	2.4780	3.3073	0.2462	7.6531	0.8350	2.4948	0.2796	4699.2492	this study
MRAC-2917	*Pan troglodytes*		ad.				M^2	f9	upper	-	1.8188	0.2434	0.6282	0.0052	-1.3387	5.8005	0.6609	1.8239	3.5327	5.3566	0.4870	8.2417	0.4299	2.9477	0.4803	3960.0908	this study
MRAC-73-18-14	*Pan troglodytes*	indet	ad.	Meyo N'Koulou	Cameroon	1973	M_2	f9	lower	-	1.4121	0.4303	1.0453	0.0026	-2.4619	11.4857	0.5810	1.1448	3.8312	4.9761	0.3701	9.7665	0.7699	3.8087	0.4147	3901.8102	this study
MRAC-73-18-24	*Pan troglodytes*	indet	ad.	Alen	Cameroon	1973	M^2	f9	upper	-	2.2458	0.2719	0.4405	0.0054	-1.4572	6.2710	0.4919	1.1946	2.9795	4.1741	0.3615	6.1931	0.4784	2.7608	0.4830	3990.8216	this study
MRAC-73-18-5	*Pan troglodytes*	indet	ad.	Muilimengale	Cameroon	1973	M^2	f9	upper	-	0.9175	0.3077	0.5265	0.0042	-2.8530	15.3014	0.3815	0.7989	3.3185	4.1174	0.2422	7.3397	0.5830	3.2725	0.3511	4210.9631	this study
MRAC-75-56-24	*Pan troglodytes*	indet	ad.	Mang	Cameroon	1975	M^2	f9	upper	-	0.9118	0.1706	0.3719	0.0039	-2.6451	13.8701	0.2970	0.7255	2.2424	2.9678	0.1947	6.6796	0.5658	1.9586	0.2829	4181.8824	this study
MRAC-77032-31	*Pan troglodytes*	indet	ad.	Dja region	Cameroon	1977	M_2	f9	lower	-	1.5252	0.2691	1.2566	0.0020	-2.2435	10.5425	0.3669	0.6512	3.5282	4.1794	0.2517	8.7188	0.8079	3.4636	0.2717	4572.0581	this study
MRAC-77-32-24	*Pan troglodytes*	indet	ad.	Dja region	Cameroon	1977	M^2	f9	upper	-	1.5003	0.2280	0.7421	0.0039	-2.2197	9.9433	0.4967	1.1722	3.2153	4.3875	0.3292	9.0013	0.7679	3.0390	0.4401	4331.9052	this study
MRAC-77-32-25	*Pan troglodytes*	indet	ad.	Dja region	Cameroon	1977	M^2	f9	upper	-	2.3943	0.5088	0.7808	0.0016	-1.8070	7.9097	0.7376	1.3303	4.3638	5.6941	0.5285	13.0666	0.6854	3.4345	0.6077	4054.7412	this study
MRAC-77-32-26	*Pan troglodytes*	indet	ad.	Dja region	Cameroon	1977	M_2	f9	lower	-	1.6490	0.4188	0.8069	0.0020	-0.8149	4.4336	0.4546	1.0225	2.7610	3.7836	0.3516	9.6011	0.6575	2.4953	0.4194	3741.5351	this study
MRAC-77-32-31	*Pan troglodytes*	indet	ad.	Dja region	Cameroon	1977	M_2	f9	lower	-	3.4170	0.2415	0.4375	0.0026	-1.1227	6.1653	0.9383	2.4384	5.5733	8.0117	0.6950	12.1904	0.5623	4.2655	0.8555	3670.4001	this study
MRAC-77-32-32	*Pan troglodytes*	indet	ad.	Dja region	Cameroon	1977	M^2	f9	upper	-	1.4459	0.0832	0.2927	0.0012	-0.5225	3.4637	0.3407	1.1372	1.7302	2.8673	0.2685	8.0427	0.6655	1.7554	0.3695	3980.4672	this study
MRAC-77-32-36	*Pan troglodytes*	indet	ad.	Dja region	Cameroon	1977	M^2	f9	upper	-	2.4256	0.3119	0.4312	0.0003	-1.2717	7.2781	0.6893	1.6216	4.8695	6.4912	0.5115	8.9444	0.7827	2.8745	0.6311	3521.0035	this study
MRAC-9250	*Pan troglodytes*		ad.				M_2	f9	lower	-	1.1331	0.3458	0.5733	0.0024	-0.0379	2.9630	0.3969	1.4095	1.7542	3.1637	0.3209	9.4746	0.8259	1.9547	0.3891	3795.1544	this study
MRAC-9289	*Pan troglodytes*	indet	ad.	Lukolela	DR Congo	1927	M^2	f13	upper	-	1.4119	0.3147	0.4684	0.0021	-1.3792	5.6947	0.3444	0.9391	2.1921	3.1311	0.2587	8.3011	0.7633	2.1202	0.3691	3724.3725	this study
MRAC-9576	*Pan troglodytes*	m	ad.	Bafwaboli	DR Congo	1926	M^2	f9	upper	-	0.8273	0.1821	0.3691	0.0044	-1.1818	6.4703	0.2130	0.6377	1.3853	2.0229	0.1554	6.0029	0.4698	1.3061	0.2388	4509.0600	this study
MRAC-9921	*Pan troglodytes*	indet	ad.	Bafwaboli	DR Congo	1929	M_2	f9	lower	-	2.3054	0.3913	0.5717	0.0015	-1.2717	6.9011	0.3772	1.5016	3.2660	4.7677	0.2835	7.6531	0.6401	3.2407	0.3978	4261.3469	this study
MRAC-9931	*Pan troglodytes*	f	ad.	Ubangi	DR Congo	1929	M^2	f9	upper	-	1.9793	0.2493	0.5648	0.0028	-1.2956	5.0397	1.0076	1.8848	4.7341	6.6189	0.7602	12.9441	0.5548	3.5415	0.7421	3545.2802	this study
SMNS-1797	*Pan troglodytes*		ad.				M^2	f9	upper	-	1.3315	1.4813	1.5349	0.0082	-2.1025	10.9298	1.5004	2.9197	9.6813	12.6010	1.0071	15.2034	0.7194	5.5742	0.6386	3755.2876	this study
SMNS-2738	*Pan troglodytes*	m	ad.	Njem-Gebiet (13°E;3°N)	Cameroon	1907	M^2	f9	upper	-	1.8750	0.2367	0.5905	0.0020	-0.3513	4.1243	1.1828	5.1230	4.8307	9.9537	0.8931	13.4106	0.8229	3.2476	0.8398	3654.5385	this study
SMNS-2739	*Pan troglodytes*	m	ad.	Njem-Gebiet (13°E;3°N)	Cameroon	1907	M^2	f9	upper	-	1.0135	0.2718	0.6317	0.0034	-2.0893	11.0917	0.2601	1.3196	2.5877	3.9073	0.1785	6.9087	0.6575	2.3459	0.2491	4331.3063	this study
SNG-21368	*Pan troglodytes*	f	ad.	-	-	-	M^2	f9	upper	-	0.5097	0.3838	0.6942	0.0025	-1.9344	8.7054	0.2445	0.5719	1.6880	2.2599	0.1728	11.5525	0.9401	1.4536	0.1883	4266.8808	this study
SNG-4103	*Pan troglodytes*	m	ad.	Mokbu, Oubangui	Central African Republic	30.6.1911	M^2	f9	upper	-	1.6053	0.4623	0.5610	0.0027	-1.8717	7.3370	0.5196	1.3110	3.0162	4.3271	0.3725	9.8643	0.7638	2.7923	0.4704	4281.6979	this study
SNG-4105	*Pan troglodytes*	m	ad.	Yukaduma	Cameroon	-	M^2	f9	upper	-	2.9211	0.4283	0.9334	0.0017	0.2127	4.5718	0.6996	2.9844	5.4639	8.4483	0.5368	13.6994	0.5664	4.8975	0.5215	3964.0748	this study
ZSM-1962-3303	*Pan troglodytes*		ad.				M^2	f13	upper	-	2.3124	0.2513	0.3592	0.0068	-2.3052	10.2458	0.4432	0.9656	2.9067	3.8723	0.2961	7.1971	0.4611	2.3513	0.4269	4321.2663	this study
ZSM-1968-626	*Pan troglodytes*	m	ad.	NW Gabon	Gabon	before 1940	M^2	f9	upper	-	0.4299	0.4676	1.2294	0.0039	-0.6411	4.5762	0.6145	2.2476	3.9472	6.1949	0.4738	14.1999	0.6453	1.9098	0.3171	4392.9850	this study
LA15-5	*Pongo* sp.			Lida Ajer	Indonesia	62 - 72 ka	M^1	crushing	upper	left	1.2330	0.2172	0.3889	0.0020	-0.3540	2.7834	0.3059	1.1437	1.1474	2.2911	0.2492	14.8555	0.4361	1.0647	0.2131	4089.1770	Louys et al. 2021, this study
LA15-8	*Pongo* sp.			Lida Ajer	Indonesia	62 - 72 ka	M^1	crushing	upper	right	0.7542	0.1769	0.2454	0.0011	-1.3041	10.7881	0.2261	0.7022	2.4299	3.1321	0.1594	7.0258	0.6701	1.3165	0.2015	3844.0821	Louys et al. 2021, this study
LA30	*Pongo* sp.			Lida Ajer	Indonesia	62 - 72 ka	M_1	crushing	lower	left	0.9723	0.1849	0.3664	0.0058	-0.3928	3.2680	0.2315	0.7771	1.3544	2.1315	0.1854	11.4627	0.4091	1.2883	0.1778	4153.2071	Louys et al. 2021, this study
LA31	*Pongo* sp.			Lida Ajer	Indonesia	62 - 72 ka	P_1	crushing	lower	right	2.3236	0.4943	0.5965	0.0042	-1.4848	5.2399	0.5366	1.0670	3.0174	4.0843	0.4091	7.6255	0.5376	3.1943	0.5488	3641.7591	Louys et al. 2021, this study
LA32	*Pongo* sp.			Lida Ajer	Indonesia	62 - 72 ka	M_1	crushing	lower	right	1.5507	0.1392	0.2560	0.0032	-0.1390	3.2157	0.5198	2.1514	2.0357	4.1871	0.4146	12.1298	0.5678	1.8632	0.3926	3627.8863	Louys et al. 2021, this study
LA33	*Pongo* sp.			Lida Ajer	Indonesia	62 - 72 ka	M_1	crushing	lower	left	1.7830	0.1678	0.3383	0.0017	-0.9679	5.2865	0.2485	0.7041	1.3373	2.0414	0.1868	5.9197	0.2974	1.4956	0.2609	4157.0294	Louys et al. 2021, this study
NG11.10	*Pongo* sp.			Ngalau Gupin	Indonesia	~130 ka	M_1	crushing	lower	left	1.5455	0.1758	0.2229	0.0008	-0.2212	3.7184	0.2577	1.0569	1.1276	2.1845	0.1982	10.0229	0.7245	1.0162	0.2430	3995.1427	Louys et al. 2021, this study
NG11.11	*Pongo* sp.			Ngalau Gupin	Indonesia	~130 ka	M^1	crushing	upper	right	1.4178	0.3325	0.4808	0.0031	0.2018	3.7215	0.7762	3.1239	2.3822	5.5061	0.5922	17.7838	0.6087	1.6277	0.3190	3716.8016	Louys et al. 2021, this study
NG11.12	*Pongo* sp.			Ngalau Gupin	Indonesia	~130 ka	M_2	crushing	lower	right	0.8202	0.3187	0.6337	0.0068	-1.3940	6.0886	0.1628	0.3857	1.1099	1.4956	0.1207	4.7655	0.3788	1.0794	0.1671	4076.6080	Louys et al. 2021, this study
NG11.14	*Pongo* sp.			Ngalau Gupin	Indonesia	~130 ka	M_3	crushing	lower	left	1.3810	0.2256	0.4271	0.0043	-0.9346	4.5751	0.7719	2.1624	3.4798	5.6422	0.5849	13.0174	0.6059	2.8070	0.5433	3336.5591	Louys et al. 2021, this study
NG11.17	*Pongo* sp.			Ngalau Gupin	Indonesia	~130 ka	M^2	crushing	upper	right	1.4469	0.1781	0.3318	0.0034	0.0679	3.1414	0.5035	2.1145	1.8628	3.9773	0.3959	11.5200	0.6305	1.8414	0.4244	3677.3479	Louys et al. 2021, this study
NG11.18	*Pongo* sp.			Ngalau Gupin	Indonesia	~130 ka	P_2	crushing	lower	right	0.8191	0.2435	0.4914	0.0058	-1.2330	4.8446	0.3693	0.9436	1.8487	2.7923	0.2822	9.5372	0.5696	1.6012	0.2733	3479.5915	Louys et al. 2021, this study
NG11.21	*Pongo* sp.			Ngalau Gupin	Indonesia	~130 ka	M^3	crushing	upper	right	1.7714	0.6647	0.9863	0.0054	-0.4255	2.6268	1.1956	2.3575	3.8710	6.2285	0.9681	14.0515	0.3821	2.9808	1.0387	3021.5118	Louys et al. 2021, this study

NG11.22	*Pongo* sp.			Ngalau Gupin	Indonesia	~130 ka	P^1	crushing	upper	-	2.1189	0.3417	0.5482	0.0053	-0.7473	4.6028	0.4972	1.6258	2.6166	4.2425	0.3732	7.3949	0.4071	2.3133	0.4645	3536.4674	Louys et al. 2021, this study
NG11.23	*Pongo* sp.			Ngalau Gupin	Indonesia	~130 ka	P_1	crushing	lower	right	1.8916	0.2889	0.4491	0.0043	0.0398	3.6999	0.4651	1.8728	2.0091	3.8819	0.3608	19.6579	0.7866	1.3071	0.2560	3992.1402	Louys et al. 2021, this study
NG11.24	*Pongo* sp.			Ngalau Gupin	Indonesia	~130 ka	M_2	crushing	lower	left	1.7715	0.2175	0.4240	0.0025	-1.9017	7.7626	1.1181	2.2352	6.7366	8.9718	0.7969	18.3099	0.6177	3.5985	0.5522	3649.8852	Louys et al. 2021, this study
NG11.25	*Pongo* sp.			Ngalau Gupin	Indonesia	~130 ka	P_1	crushing	lower	right	4.1417	0.3833	0.7437	0.0041	-1.4202	6.6500	1.3605	3.1463	7.4552	10.6015	0.9831	10.0317	0.4441	7.0478	1.1260	3496.4958	Louys et al. 2021, this study
NG11.26	*Pongo* sp.			Ngalau Gupin	Indonesia	~130 ka	M_2	crushing	lower	left	3.1164	0.2338	0.3541	0.0020	-1.0377	6.7554	0.6963	2.2974	4.6559	6.9534	0.5094	13.2550	0.7893	3.1356	0.4577	3811.6131	Louys et al. 2021, this study
NG11.27	*Pongo* sp.			Ngalau Gupin	Indonesia	~130 ka	P_1	crushing	lower	left	0.7489	0.2091	0.3502	0.0025	-0.4067	2.9798	0.4854	1.7803	1.7204	3.5007	0.3919	17.3633	0.3323	1.2897	0.1880	4207.0961	Louys et al. 2021, this study
NG11.34	*Pongo* sp.			Ngalau Gupin	Indonesia	~130 ka	M^2	crushing	upper	right	0.9396	0.1282	0.2940	0.0021	-0.2925	2.9541	0.2580	0.8037	1.0399	1.8436	0.2056	11.6581	0.8015	1.1729	0.2539	3732.5945	Louys et al. 2021, this study
NG11.36	*Pongo* sp.			Ngalau Gupin	Indonesia	~130 ka	P^1	crushing	upper	right	1.3805	0.0848	0.3039	0.0024	-2.5672	17.0704	0.4878	1.5430	4.1631	5.7061	0.3117	13.2777	0.7228	2.9981	0.2955	4014.5992	Louys et al. 2021, this study
NG11.42	*Pongo* sp.			Ngalau Gupin	Indonesia	~130 ka	P_2	crushing	lower	-	1.1125	0.1522	0.3060	0.0021	0.2008	7.0294	0.2188	1.3832	1.2950	2.6783	0.1577	8.6878	0.8829	1.2165	0.2250	3887.7741	Louys et al. 2021, this study
NG11.44	*Pongo* sp.			Ngalau Gupin	Indonesia	~130 ka	M^1	crushing	upper	right	2.0819	0.1319	0.2670	0.0005	-0.3963	3.0796	0.4435	1.1858	2.0811	3.2669	0.3596	16.7791	0.2031	1.8099	0.3023	4084.8078	Louys et al. 2021, this study
NG11.45	*Pongo* sp.			Ngalau Gupin	Indonesia	~130 ka	P_2	crushing	lower	left	0.5117	0.0618	0.2250	0.0035	-0.5897	4.1264	0.2006	0.6605	1.1016	1.7622	0.1548	11.1874	0.7686	0.8395	0.1925	3854.1957	Louys et al. 2021, this study
NG11.46	*Pongo* sp.			Ngalau Gupin	Indonesia	~130 ka	P_2	crushing	lower	right	1.4045	0.2276	0.4377	0.0035	-1.5396	6.6645	0.5962	1.4863	3.4283	4.9146	0.4285	9.1619	0.5918	3.0918	0.5025	3379.4586	Louys et al. 2021, this study
NG11.47	*Pongo* sp.			Ngalau Gupin	Indonesia	~130 ka	P_1	crushing	lower	right	2.5962	0.1743	0.3646	0.0041	-0.9451	6.1286	0.3439	1.1453	2.4902	3.6356	0.2501	7.1766	0.6034	1.9650	0.2747	4191.7010	Louys et al. 2021, this study
NG11.48	*Pongo* sp.			Ngalau Gupin	Indonesia	~130 ka	P_1	crushing	lower	right	1.7504	0.1566	0.3199	0.0023	-0.7270	4.0635	0.2859	0.8253	1.8013	2.6266	0.2229	11.9958	0.7041	1.6423	0.2262	4169.4365	Louys et al. 2021, this study
NG15-13	*Pongo* sp.			Ngalau Gupin	Indonesia	~130 ka	M^2	crushing	upper	left	1.0383	0.1655	0.3177	0.0013	-1.1845	5.8883	0.3386	0.9951	2.3126	3.3078	0.2596	10.3209	0.5008	1.3950	0.2496	3780.4535	Louys et al. 2021, this study
NS15-1V3mold2	*Pongo* sp.			Ngalau Sampit	Indonesia	~90 ka	M_3	crushing	lower	-	2.7009	0.3059	0.5362	0.0008	-0.7647	3.6850	1.4276	4.2836	6.5095	10.7932	1.1128	13.0299	0.7781	5.1973	0.9749	3294.8947	Louys et al. 2021, this study
MFI-K172	*Khoratpithecus* sp.	-	ad.	Irrawaddy Fm.	Myanmar	9.5 Ma	M_3	f9	lower	right	1.1307	0.3368	0.6458	0.0025	-2.6039	14.9317	0.6331	1.0588	5.2926	6.3514	0.4354	10.8816	0.6226	4.2272	0.4742	3679.5141	this study
MFI-K173	*K. ayeyarwadyensis*	-	ad.	Irrawaddy Fm.	Myanmar	9.5 Ma	M_2	f9	lower	left	3.1532	0.6756	0.8247	0.0021	-1.1071	8.4626	0.5443	2.2779	3.5896	5.8675	0.3717	8.8370	0.6683	2.9124	0.4268	4735.4002	this study
MFT-K176	*K. piriyai*	-	ad.	Khorat sand pits	Thailand	9 - 6 Ma	M^2	f9	upper	right	1.1577	0.8029	1.0444	0.0038	-0.5101	4.2728	0.6773	2.0450	2.9587	5.0037	0.4919	14.3612	0.7218	2.3250	0.3262	4398.2378	this study
MFT-K176	*K. piriyai*	-	ad.	Khorat sand pits	Thailand	9 - 6 Ma	M^3	f9	upper	right	1.6781	0.4315	0.8574	0.0041	-0.7312	4.8226	0.8558	2.1477	4.4624	6.6101	0.6401	12.1121	0.6913	4.3312	0.6160	4234.6103	this study
MFT-K178	*K. magnus*	-	ad.	Khorat sand pits	Thailand	9 - 6 Ma	M_2	f9	lower	left	0.3801	0.2188	0.4887	0.0040	-0.9708	5.8774	0.4683	1.4211	3.0585	4.4795	0.3569	13.7494	0.6774	2.5973	0.3002	3993.1448	this study
MFT-K180	*K. piriyai*	-	ad.	Khorat sand pits	Thailand	9 - 6 Ma	M^2	f9	upper	left	1.9065	0.2931	0.5145	0.0019	-0.7246	3.8851	0.4707	1.2611	2.7732	4.0344	0.3690	8.8141	0.6512	2.8792	0.4547	3996.2621	this study
MFT-K181	*K. piriyai*	-	ad.	Khorat sand pits	Thailand	9 - 6 Ma	M_2	f9	lower	left	1.9151	0.5922	1.0074	0.0018	-3.9430	32.1753	0.4785	1.0301	5.8052	6.8353	0.2989	9.3556	0.6141	5.0385	0.3368	4374.0114	this study
SSAM-1907-252	*Pongo pygmaeus*	f	ad.	Borneo, Landak	Indonesia	1907	M_2	f9	lower	right	0.5028	0.2975	0.7595	0.0065	-2.3573	10.8192	0.2430	0.6840	1.7962	2.4802	0.1595	6.5521	0.6503	1.7022	0.2166	3974.1525	Habinger et al. in prep
SSAM-1907-483	*Pongo pygmaeus*	f	ad.	Borneo, Landak	Indonesia	1907	M_2	f9	lower	right	0.8259	0.4080	0.5842	0.0058	-1.2913	6.3533	0.1812	0.5787	1.4540	2.0327	0.1324	5.8973	0.4722	1.4962	0.1780	4357.4713	Habinger et al. in prep
SSAM-1913-1452	*Pongo abelii*	f	ad.	Sumatra, west coast	Indonesia	1913	M_2	f9	lower	right	0.5192	0.3274	0.3847	0.0045	-0.7670	6.7462	0.4428	1.5238	2.8885	4.4123	0.3194	13.9087	0.5238	1.1485	0.2376	3925.0125	Habinger et al. in prep
SSAM-1913-1465	*Pongo abelii*	m	ad.	Sumatra, Deli	Indonesia	1913	M_2	f9	lower	right	0.6498	0.1916	0.5219	0.0062	-3.3359	20.5705	0.3802	0.8142	3.3352	4.1494	0.2440	8.3001	0.4708	2.6535	0.2912	4045.4054	Habinger et al. in prep
SSAM-1913-1466	*Pongo abelii*	m	ad.	Sumatra, Deli	Indonesia	1913	M_2	f9	lower	right	1.3878	1.0727	1.2894	0.0035	-2.8017	13.7481	0.6351	1.3108	4.1649	5.4757	0.3733	16.2647	0.8257	2.7934	0.3391	4183.5382	Habinger et al. in prep
SSAM-1913-1467	*Pongo abelii*	f	ad.	Sumatra, Deli	Indonesia	1913	M_2	f9	lower	right	0.5895	0.6470	1.6258	0.0059	-1.0612	4.8684	0.4706	1.1832	2.4323	3.6155	0.3578	15.1588	0.6226	1.6656	0.3140	4170.0867	Habinger et al. in prep
SSAM-1913-1469	*Pongo abelii*	f	ad.	Sumatra, Deli	Indonesia	1913	M_2	f9	lower	right	1.5660	0.2977	0.4850	0.0045	-0.6048	3.7840	0.9780	3.6656	3.8843	7.5500	0.7563	16.1083	0.8240	3.5775	0.5769	3617.9407	Habinger et al. in prep
SSAM-1913-1470	*Pongo abelii*	indet	subad.	Sumatra, Deli	Indonesia	1913	M_2	f9	lower	right	3.5729	0.8608	1.7586	0.0041	-3.1380	16.1770	0.6976	2.9117	4.9156	7.8273	0.4030	8.6716	0.8393	4.1973	0.6959	4118.1964	Habinger et al. in prep
SSAM-1913-1471	*Pongo abelii*	indet	ad.	Sumatra, Deli	Indonesia	1913	M_2	f9	lower	right	0.7690	0.2755	0.6346	0.0050	-3.0749	16.3856	0.3048	0.6938	2.3676	3.0615	0.1797	9.4638	0.5133	1.7642	0.1969	4653.0636	Habinger et al. in prep
SSAM-1955-228	*Pongo pygmaeus*	f	ad.	Borneo Skalau	Indonesia	1892-1894	M_2	f9	lower	right	0.7115	0.2684	0.4079	0.0056	-1.5501	8.4780	0.3068	0.9160	2.4084	3.3243	0.2240	12.6887	0.4629	1.9342	0.2364	4355.7148	Habinger et al. in prep
SSAM-1981-101	*Pongo pygmaeus*	f	ad.	Borneo Skalau	Indonesia	1892-1894	M_2	f9	lower	right	1.2510	0.9661	1.1034	0.0025	-1.8261	10.0513	0.3774	1.2567	3.4665	4.7232	0.2606	7.7328	0.5302	3.4187	0.3748	4115.8042	Habinger et al. in prep
SSAM-1981-102	*Pongo pygmaeus*	m	subad.	Borneo Skalau	Indonesia	1892-1894	M_2	f9	lower	right	3.7057	0.1528	0.3450	0.0012	-0.9292	4.4759	1.1944	4.4939	4.7110	9.2049	0.8834	13.5384	0.6781	4.3031	0.7293	4198.3284	Habinger et al. in prep
SSAM-1981-103	*Pongo pygmaeus*	f	ad.	Borneo Skalau	Indonesia	1892-1894	M_2	f9	lower	right	0.9443	0.2571	0.4189	0.0011	-0.1664	3.2971	0.3919	1.1662	2.0266	3.1928	0.3116	18.6780	0.7606	1.5121	0.2117	4797.5610	Habinger et al. in prep
SSAM-1981-105	*Pongo pygmaeus*	f	ad.	Borneo Skalau	Indonesia	1892-1894	M_2	f9	lower	right	1.4771	0.2777	0.6465	0.0027	-3.5125	21.2127	0.4023	0.8683	3.2658	4.1341	0.2423	9.7625	0.4928	2.6706	0.2734	4802.1045	Habinger et al. in prep
SSAM-1981-106	*Pongo pygmaeus*	f	ad.	Borneo Skalau	Indonesia	1892-1894	M_2	f9	lower	right	2.5422	0.3005	0.6025	0.0034	-1.5960	10.1776	0.4102	1.3703	2.9563	4.3266	0.2912	5.0494	0.5591	2.2802	0.3658	4036.5715	Habinger et al. in prep
SSAM-1981-106	*Pongo pygmaeus*	f	ad.	Borneo Skalau	Indonesia	1892-1894	M_2	f9	lower	left	2.2029	0.3873	0.6463	0.0009	-2.5189	10.7750	0.9606	1.4752	6.5645	8.0397	0.6028	14.6320	0.8193	3.9037	0.5054	4993.3883	Habinger et al. in prep
SSAM-1981-107	*Pongo pygmaeus*	f	ad.	Borneo Skalau	Indonesia	1892-1894	M_2	f9	lower	right	1.6584	0.4043	0.8066	0.0022	-1.8040	7.1368	0.7987	1.2403	4.1521	5.3924	0.5771	12.1137	0.7488	3.6603	0.6155	3678.7026	Habinger et al. in prep
SSAM-1981-108	*Pongo pygmaeus*	f	ad.	Borneo Skalau	Indonesia	1892-1894	M_2	f9	lower	left	0.4356	0.6201	1.0020	0.0046	-2.6292	13.5103	0.3628	1.0364	2.9074	3.9438	0.2295	10.6240	0.4540	2.3362	0.1671	5051.5357	Habinger et al. in prep
SSAM-1981-111	*Pongo pygmaeus*	f	ad.	Borneo Skalau	Indonesia	1892-1894	M_2	f9	lower	right	0.7764	0.3307	0.7006	0.0041	-1.6159	7.4996	0.1720	0.6534	1.1429	1.7963	0.1236	7.8446	0.6232	1.0947	0.1533	4927.4113	Habinger et al. in prep
SSAM-1981-112	*Pongo pygmaeus*	f	ad.	Borneo Skalau	Indonesia	1892-1894	M_2	f9	lower	right	0.8365	0.2393	0.4082	0.0051	-1.5856	7.2358	0.2535	0.5418	1.7695	2.3113	0.1873	6.4195	0.5632	1.9247	0.2690	4117.1379	Habinger et al. in prep
SSAM-1981-113	*Pongo pygmaeus*	f	ad.	Borneo Skalau	Indonesia	1892-1894	M_2	f9	lower	right	0.1265	0.5679	0.8588	0.0050	-0.9237	3.4573	0.6934	1.0523	2.6500	3.7022	0.5600	20.2824	0.4749	1.2683	0.1677	5045.7361	Habinger et al. in prep
SSAM-1981-114	*Pongo pygmaeus*	f	ad.	Borneo, Dadap	Indonesia	1892-1894	M_2	f9	lower	left	0.9593	0.4528	0.8375	0.0027	0.8380	7.9419	0.4222	3.5381	1.3872	4.9252	0.3305	10.8355	0.6497	2.0441	0.3375	4308.1302	Habinger et al. in prep
SSAM-1981-116	*Pongo pygmaeus*	m	ad.	Borneo, Dadap	Indonesia	1892-1894	M_2	f9	lower	right	2.1200	0.4773	0.8730	0.0039	-1.5828	6.7189	0.6005	1.1093	3.6519	4.7611	0.4460	8.9801	0.6355	2.9360	0.5478	3970.0148	Habinger et al. in prep
SSAM-1981-117	*Pongo pygmaeus*	m	ad.	Borneo, Dadap	Indonesia	1892-1894	M_2	f9	lower	right	0.9168	0.3107	0.6537	0.0040	-1.0965	5.3215	0.6016	1.6288	3.3239	4.9527	0.4433	12.8529	0.7408	2.4145	0.4342	3924.0534	Habinger et al. in prep
SSAM-1981-119	*Pongo pygmaeus*	f	ad.	Borneo, Dadap	Indonesia	1892-1894	M_2	f9	lower	right	0.8192	0.5082	0.9117	0.0061	-0.9900	4.9398	0.4740	1.4637	2.6983	4.1621	0.3555	9.2971	0.6109	2.6719	0.4087	4140.1914	Habinger et al. in prep
SSAM-1981-122	*Pongo pygmaeus*	f	ad.	Borneo, Dadap	Indonesia	1892-1894	M_2	f9	lower	right	0.7174	0.2167	0.6009	0.0042	-1.6940	8.0199	0.4375	1.1546	3.2306	4.3852	0.3255	8.3290	0.6427	1.9221	0.3511	3726.6096	Habinger et al. in prep
SSAM-1981-124	*Pongo pygmaeus*	f	ad.	Borneo, Dadap	Indonesia	1892-1894	M_2	f9	lower	right	0.3413	0.5435	0.7812	0.0007	-1.0657	5.3616	0.2907	0.8430	1.6383	2.4813	0.2173	15.4145	0.5961	1.3772	0.1433	4737.9268	Habinger et al. in prep
SSAM-1981-125	*Pongo pygmaeus*	f	subad.	Borneo, Dadap	Indonesia	1892-1894	M_2	f9	lower	right	0.5424	0.3196	0.6168	0.0061	-0.9637	4.3069	0.5049	1.1306	2.1913	3.3218	0.3959	11.4465	0.5271	1.7837	0.3491	3911.1539	Habinger et al. in prep
SSAM-1981-127	*Pongo pygmaeus*	m	ad.	Borneo, Dadap	Indonesia	1892-1894	M_2	f9	lower	right	0.6984	0.4732	0.6471	0.0076	0.1347	4.1172	0.9853	5.6565	3.5041	9.1606	0.7751	10.8867	*****	1.6952	0.3864	4084.3380	Habinger et al. in prep
SSAM-1981-129	*Pongo pygmaeus*	f	subad.	Borneo, Dadap	Indonesia	1892-1894	M_2	f9	lower	right	0.8436	0.5475	0.8118	0.0036	-2.1691	10.9425	0.4469	1.3076	3.9896	5.2972	0.3091	10.5981	0.7609	2.9981	0.2991	4398.4347	Habinger et al. in prep
SSAM-1981-130	*Pongo pygmaeus*	f	juv.	Borneo, Dadap	Indonesia	1892-1894	M_2	f9	lower	right	1.2135	0.4570	0.9085	0.0047	-1.8441	10.3031	0.6693	1.3523	4.8724	6.2247	0.4873	10.5796	0.5713	3.8944	0.4756	3874.8867	Habinger et al. in prep
SSAM-1981-133	*Pongo pygmaeus*	f	juv.	Borneo, Dadap	Indonesia	1892-1894	M_2	f9	lower	right	1.6409	0.2304	0.5994	0.0073	-1.6906	8.0674	0.5503	1.5921	3.1872	4.7793	0.3710	8.2643	0.3548	2.8106	0.4163	4403.4217	Habinger et al. in prep
SSAM-1981-134	*Pongo pygmaeus*	f	ad.	Borneo, Dadap	Indonesia	1892-1894	M_2	f9	lower	right	0.7659	0.4579	0.9903	0.0052	-3.0292	23.1173	0.2589	0.9047	2.9180	3.8227	0.1705	7.0762	0.4801	2.8162	0.2001	4650.4594	Habinger et al. in prep
SSAM-1981-135-B	*Pongo pygmaeus*	f	ad.	Borneo, Dadap	Indonesia	1892-1894	M_2	f9	lower	right	1.0223	0.2258	0.4106	0.0057	-0.6744	3.1615	0.6003	2.0797	2.1711	4.2508	0.4876	14.3116	0.5425	1.7989	0.3685	4428.7295	Habinger et al. in prep
SSAM-1981-136	*Pongo pygmaeus*	m	ad.	Borneo, Bogau	Indonesia	1892-1894	M_2	f9	lower	right	0.5869	0.3758	0.7485	0.0028	-1.1435	7.5551	0.2878	1.0509	2.2018	3.2527	0.2018	8.5801	0.5439	1.9274	0.2164	4559.0067	Habinger et al. in prep
SSAM-1981-141	*Pongo pygmaeus*	m	juv.	Borneo, Genepai	Indonesia	1892-1894	M_2	f9	lower	left	0.2797	0.8711	1.6395	0.0045	-0.5320	4.3863	0.3153	0.9397	1.5787	2.5184	0.2381	10.4361	0.6019	1.4397	0.2516	3906.5495	Habinger et al. in prep
SSAM-1981-142	*Pongo pygmaeus*	m	ad.	Borneo, Bogau	Indonesia	1892-1894	M_2	f9	lower	right	1.2818	0.1988	0.3913	0.0020	-0.5260	4.4879	0.7878	2.2388	4.3760	6.6148	0.6145	11.6393	0.3972	2.2302	0.4606	3787.2651	Habinger et al. in prep
SSAM-1981-143	*Pongo pygmaeus*	m	ad.	Borneo, Bogau	Indonesia	1892-1894	M_2	f9	lower	right	0.4533	0.4512	0.9852	0.0050	-0.9857	4.5084	0.4800	0.8185	2.5667	3.3852	0.3791	12.5914	0.6036	2.1049	0.3227	4159.2620	Habinger et al. in prep
SSAM-1981-144	*Pongo pygmaeus*	m	subad.	Borneo, Genepai	Indonesia	1892-1894	M_2	f9	lower	right	2.0443	0.4574	1.3834	0.0014	-2.5962	12.6303	0.8050	1.1990	5.7612	6.9602	0.5415	11.6234	0.8035	4.6574	0.6874	3344.5612	Habinger et al. in prep
SSAM-1981-147	*Pongo pygmaeus*	m	ad.	Borneo, Genepai	Indonesia	1892-1894	M_2	f9	lower	right	0.8277	0.2696	0.4836	0.0041	-0.8625	4.6605	0.3200	1.1127	2.0497	3.1625	0.2430	6.5986	0.3934	1.1308	0.2822	4206.1596	Habinger et al. in prep
SSAM-1981-149	*Pongo pygmaeus*	m	ad.	Borneo, Genepai	Indonesia	1892-1894	M_2	f9	lower	right	0.9827	0.2207	0.4096	0.0031	-0.5825	3.4208	0.3123	1.0292	1.8016	2.8308	0.2520	11.8108	0.7932	1.6679	0.2730	4173.9217	Habinger et al. in prep
SSAM-1981-150	*Pongo pygmaeus*	m	ad.	Borneo, Genepai	Indonesia	1892-1894	M_2	f9	lower	right	0.5346	0.7062	1.1871	0.0044	-1.7332	10.3372	0.4605	0.9398	3.6280	4.5678	0.3367	15.1567	0.8005	2.3761	0.2261	4562.5050	Habinger et al. in prep
SSAM-1981-151	*Pongo pygmaeus*	m	ad.	Borneo, Genepai	Indonesia	1892-1894	M_2	f9	lower	right	1.8859	0.2423	0.4190	0.0039	-0.6828	3.9859	0.4971	1.5287	2.2092	3.7379	0.3809	13.5349	0.6169	1.9515	0.4011	4347.0551	Habinger et al. in prep
SSAM-1981-152	*Pongo pygmaeus*	m	ad.	Borneo, Genepai	Indonesia	1892-1894	M_2	f9	lower	right	0.5550	0.2397	0.4984	0.0041	-0.4652	3.0515	0.3203	1.4130	1.6117	3.0248	0.2594	13.7089	0.4577	1.2492	0.1824	4403.9414	Habinger et al. in prep
SSAM-1981-153	*Pongo pygmaeus*	m	ad.	Borneo, Genepai	Indonesia	1892-1894	M_2	f9	lower	right	0.4645	0.6249	0.7458	0.0075	-0.3010	3.8432	0.2464	0.8690	1.1837	2.0527	0.1898	7.9114	0.4464	0.7718	0.1821	4289.1281	Habinger et al. in prep
SSAM-1981-154	*Pongo pygmaeus*	f	ad.	Borneo, Genepai	Indonesia	1892-1894	M_2	f9	lower	right	1.0461	0.3638	0.7254	0.0033	-3.2399	20.7523	0.1896	0.4274	2.0343	2.4617	0.1172	6.1178	0.8047	1.9358	0.1745	5150.9025	Habinger et al. in prep
SSAM-1981-155	*Pongo pygmaeus*	f	ad.	Borneo, Bogau	Indonesia	1892-1894	M_2	f9	lower	right	1.4481	0.3257	0.6042	0.0034	-1.7765	7.7180	0.5059	0.9045	3.1960	4.1006	0.3684	7.7284	0.7535	2.9234	0.5744	3510.2303	Habinger et al. in prep
SSAM-1981-156	*Pongo pygmaeus*	f	ad.	Borneo, Bogau	Indonesia	1892-1894	M_2	f9	lower	right	0.4700	0.1935	0.3635	0.0044	-1.3259	5.7892	0.4468	1.0834	2.2609	3.3443	0.3364	12.9164	0.6721	1.7004	0.2629	4002.6838	Habinger et al. in prep
SSAM-1981-159	*Pongo pygmaeus*	f	subad.	Borneo, Bogau	Indonesia	1892-1894	M_2	f9	lower	right	0.8091	0.2371	0.4289	0.0061	-0.8442	4.6711	0.1447	0.5582	0.8368	1.3950	0.1110	4.7322	0.4156	0.8651	0.1396	4642.1571	Habinger et al. in prep
SSAM-1981-162	*Pongo pygmaeus*	f	ad.	Borneo, Bogau	Indonesia	1892-1894	M_2	f9	lower	right	0.5950	0.2183	0.3646	0.0042	-0.0405	3.6729	0.3271	1.2384	1.6512	2.8896	0.2550	11.0933	0.1952	0.6908	0.1653	4815.8809	Habinger et al. in prep
SSAM-1981-163	*Pongo pygmaeus*	f	ad.	Borneo, Genepai	Indonesia	1892-1894	M_2	f9	lower	right	2.2578	0.5848	1.1205	0.0023	-1.3525	5.8426	0.9007	2.4869	5.0666	7.5536	0.6831	10.1014	0.7647	4.1185	0.7535	3428.6846	Habinger et al. in prep
SSAM-1981-165	*Pongo pygmaeus*	f	ad.	Borneo, Bogau	Indonesia	1892-1894	M_2	f9	lower	right	1.0463	0.3043	0.5057	0.0070	-2.1810	12.8473	0.4286	0.9272	3.7480	4.6753	0.2991	6.9110	0.5685	2.8726	0.4300	3296.4650	Habinger et al. in prep
SSAM-1981-166	*Pongo pygmaeus*	f	ad.	Borneo, Genepai	Indonesia	1892-1894	M_2	f9	lower	right	0.5407	0.5610	0.8623	0.0029	-0.6461	3.0605	0.3596	0.7738	1.5647	2.3385	0.2900	16.0549	0.6551	1.5507	0.2100	4208.5012	Habinger et al. in prep
SSAM-1981-167	*Pongo pygmaeus*	f	ad.	Borneo, Genepai	Indonesia	1892-1894	M_2	f9	lower	right	0.6051	0.2465	0.5505	0.0057	-2.2276	11.8945	0.1921	0.4945	1.4950	1.9896	0.1280	4.6705	0.2285	1.4457	0.1585	4713.6604	Habinger et al. in prep
SSAM-1981-168	*Pongo pygmaeus*	f	ad.	Borneo, Landak	Indonesia	1892-1894	M_2	f9	lower	right	0.5621	0.1575	0.3418	0.0029	-1.3882	6.8760	0.2690	0.9776	1.5712	2.5488	0.1948	13.1888	0.8397	1.4863	0.1822	4845.7157	Habinger et al. in prep
SSAM-1981-179	*Pongo pygmaeus*	f	ad.	Borneo, Batangtu	Indonesia	1892-1894	M_2	f9	lower	right	1.3411	0.2138	0.3598	0.0069	-0.0096	3.0966	0.4059	1.3060	1.7588	3.0648	0.3179	13.2549	0.4110	1.4142	0.2557	4701.2083	Habinger et al. in prep
SSAM-1981-182	*Pongo pygmaeus*	m	ad.	Borneo, Batangtu	Indonesia	1892-1894	M_2	f9	lower	right	1.3787	0.3582	0.4562	0.0036	-1.4680	6.8180	0.4355	1.2179	2.5643	3.7821	0.3093	9.5033	0.4704	2.1697	0.3213	4480.2978	Habinger et al. in prep
SSAM-1981-186	*Pongo pygmaeus*	m	ad.	Borneo, Batangtu	Indonesia	1892-1894	M_2	f9	lower	right	1.1999	0.2108	0.4005	0.0017	-0.8382	4.0455	0.6268	2.1192	2.8706	4.9898	0.4858	12.3716	0.7463	2.2137	0.3855	4156.3956	Habinger et al. in prep
SSAM-1981-187	*Pongo pygmaeus*	f	ad.	Borneo, Batangtu	Indonesia	1892-1894	M_2	f9	lower	right	0.8715	0.2318	0.4917	0.0032	-1.2710	5.9098	0.4401	1.0589	2.3300	3.3889	0.3099	12.0058	0.4758	1.8852	0.2633	4514.1756	Habinger et al. in prep
SSAM-1981-188	*Pongo pygmaeus*	m	ad.	Borneo, Dadap	Indonesia	1892-1894	M_2	f9	lower	right	2.0751	0.4446	0.8483	0.0050	-1.0703	6.1017	0.7388	2.3215	4.0807	6.4022	0.5541	7.4222	0.3638	3.4514	0.6164	4081.4183	Habinger et al. in prep
SSAM-1981-196	*Pongo pygmaeus*	m	ad.	Borneo, Dadap	Indonesia	1892-1894	M_2	f9	lower	right	1.0831	0.3326	0.5832	0.0034	-0.7949	3.7088	0.5756	1.5074	2.8826	4.3899	0.4573	11.2936	0.6173	2.1073	0.4337	3975.6910	Habinger et al. in prep
SSAM-1981-198	*Pongo pygmaeus*	m	ad.	Borneo, Dadap	Indonesia	1892-1894	M_2	f9	lower	right	0.5399	0.2394	0.3750	0.0037	-0.3536	2.9104	0.5712	1.5576	2.0859	3.6434	0.4599	17.4800	0.6501	1.3018	0.2277	4506.9909	Habinger et al. in prep
SSAM-1981-199	*Pongo pygmaeus*	m	ad.	Borneo, Rantei	Indonesia	1892-1894	M_2	f9	lower	right	1.0060	0.3110	0.6099	0.0055	-1.5391	6.2513	0.4259	0.9334	2.2806	3.2140	0.3166	8.4277	0.5611	2.2297	0.3404	3941.0528	Habinger et al. in prep
SSAM-1981-202	*Pongo pygmaeus*	m	ad.	Borneo, Rantei	Indonesia	1892-1894	M_2	f9	lower	right	1.0746	0.2039	0.4402	0.0035	-1.6439	9.9509	0.2276	1.0229	2.1438	3.1667	0.1592	6.2503	0.6677	1.8532	0.2183	4684.2123	Habinger et al. in prep
SSAM-1981-203	*Pongo pygmaeus*	m	subad.	Borneo, Rantei	Indonesia	1892-1894	M_2	f9	lower	right	0.5335	0.2466	0.5847	0.0050	-1.6525	9.8759	0.2430	0.6384	2.0968	2.7352	0.1656	10.2370	0.5431	1.5594	0.1386	4700.9848	Habinger et al. in prep
SSAM-1981-204	*Pongo pygmaeus*	f	subad.	Borneo, Rantei	Indonesia	1892-1894	M_2	f9	lower	right	1.3163	0.4071	0.8672	0.0011	-0.6406	4.0267	1.7900	5.8269	7.4347	13.2615	1.3804	20.2190	0.8018	3.3064	0.6022	3453.3305	Habinger et al. in prep
SSAM-1981-207	*Pongo pygmaeus*	f	subad.	Borneo, Rantei	Indonesia	1892-1894	M_2	f9	lower	right	2.2965	0.1722	0.5153	0.0027	-1.3310	4.9958	0.7538	1.6774	4.0360	5.7134	0.5760	11.0723	0.8167	3.2167	0.6574	3634.2547	Habinger et al. in prep

SSAM-1981-209	*Pongo pygmaeus*	f	juv.	Borneo, Skalau	Indonesia	1892-1894	M_2	f9	lower	right	0.9358	0.1925	0.2362	0.0042	-0.5845	3.4939	0.4577	1.6357	1.9149	3.5506	0.3586	15.0794	0.6849	1.6739	0.2411	4492.8871	Habinger et al. in prep
SSAM-1981-21	*Pongo pygmaeus*	m	subad.	Borneo, Ketungau	Indonesia	1892-1894	M_2	f9	lower	right	0.8020	0.7178	1.1579	0.0036	-0.6518	3.3623	0.5912	1.2606	2.7809	4.0415	0.4684	13.1155	0.5616	2.1416	0.3520	4081.3959	Habinger et al. in prep
SSAM-1981-216	*Pongo pygmaeus*	f	juv.	Borneo, Skalau	Indonesia	1892-1894	M_2	f9	lower	right	1.5561	0.3401	0.9348	0.0040	-1.1410	4.7719	0.5889	1.0815	3.0695	4.1510	0.4601	11.8004	0.4444	2.7083	0.4700	4656.0263	Habinger et al. in prep
SSAM-1981-22	*Pongo pygmaeus*	f	juv.	Borneo, Skalau	Indonesia	1892-1894	M_2	f9	lower	right	0.6527	0.3540	0.6981	0.0033	-0.7832	5.4262	0.2899	0.7880	1.9131	2.7012	0.2168	11.1657	0.8268	1.8613	0.2335	4474.2576	Habinger et al. in prep
SSAM-1981-23	*Pongo pygmaeus*	m	ad.	Borneo, Skalau	Indonesia	1892-1894	M_2	f9	lower	right	2.0864	0.2175	0.4315	0.0059	-0.5816	3.2115	0.7596	2.2523	2.6144	4.8667	0.6014	11.0821	0.5355	3.3022	0.7361	3779.1957	Habinger et al. in prep
SSAM-1981-234	*Pongo pygmaeus*	f	juv.	Borneo, Skalau	Indonesia	1892-1894	M_2	f9	lower	right	1.4172	0.6326	7.5530	0.0047	-2.1220	8.6059	0.8415	2.2538	4.1441	6.3979	0.5486	10.4289	0.5461	4.0928	0.6402	3555.0836	Habinger et al. in prep
SSAM-1981-24	*Pongo pygmaeus*	m	ad.	Borneo, Skalau	Indonesia	1892-1894	M_2	f9	lower	right	1.7650	0.5063	0.7620	0.0030	-0.0348	2.9687	0.9185	2.4573	3.8504	6.3077	0.7399	17.5152	0.7180	3.3000	0.5931	3972.4896	Habinger et al. in prep
SSAM-1981-25	*Pongo pygmaeus*	m	subad.	Borneo, Skalau	Indonesia	1892-1894	M_2	f9	lower	right	1.5048	0.2212	0.3549	0.0036	-1.5866	6.1880	0.5035	1.1889	3.2016	4.3905	0.3795	9.9124	0.6325	3.1283	0.3473	4322.2753	Habinger et al. in prep
SSAM-1981-26	*Pongo pygmaeus*	m	ad.	Borneo, Skalau	Indonesia	1892-1894	M_2	f9	lower	right	1.0114	0.1980	0.4376	0.0037	-0.5282	3.2153	1.2717	3.5117	5.4247	8.9364	0.9962	17.7596	0.5164	2.1052	0.2575	4779.8837	Habinger et al. in prep
SSAM-1981-27	*Pongo pygmaeus*	f	ad.	Borneo, Skalau	Indonesia	1892-1894	M_2	f9	lower	right	1.2395	0.4011	0.6594	0.0075	-1.0381	3.5700	0.7272	1.3157	2.7020	4.0177	0.5679	16.4200	0.4396	2.0531	0.3585	4382.5816	Habinger et al. in prep
SSAM-1981-28	*Pongo pygmaeus*	m	subad.	Borneo, Skalau	Indonesia	1892-1894	M_2	f9	lower	right	1.1945	0.4717	0.5360	0.0046	-2.0954	11.2496	0.7335	2.0957	4.4031	6.4988	0.4580	15.7992	0.7629	2.2973	0.3617	4455.9583	Habinger et al. in prep
SSAM-1981-32	*Pongo pygmaeus*	f	ad.	Borneo, Skalau	Indonesia	1892-1894	M_2	f9	lower	right	1.0355	1.1500	1.4983	0.0057	-3.6307	22.9295	0.5287	1.0679	4.9709	6.0388	0.3125	12.4961	0.9618	3.9395	0.3626	4080.0141	Habinger et al. in prep
SSAM-1981-33	*Pongo pygmaeus*	f	juv.	Borneo, Skalau	Indonesia	1892-1894	M_2	f9	lower	right	1.0075	0.1634	0.3102	0.0048	-1.2166	4.3777	0.6039	1.2166	2.7010	3.9175	0.4691	12.0316	0.6210	2.2766	0.4252	4270.4327	Habinger et al. in prep
SSAM-1981-34	*Pongo pygmaeus*	m	ad.	Borneo, Skalau	Indonesia	1892-1894	M_2	f9	lower	right	1.9058	0.2883	0.4869	0.0039	-0.6604	3.6449	0.9018	2.8074	3.9143	6.7217	0.7086	11.7308	0.5995	3.3720	0.6282	3879.1890	Habinger et al. in prep
SSAM-1981-45	*Pongo pygmaeus*	f	ad.	Borneo, Skalau	Indonesia	1892-1894	M_2	f9	lower	right	1.0461	0.2066	0.4398	0.0037	-2.0384	11.4942	0.3514	0.8430	2.8592	3.7023	0.2502	8.0700	0.7020	2.6402	0.3790	3976.1679	Habinger et al. in prep
SSAM-1981-50	*Pongo pygmaeus*	m	ad.	Borneo, Skalau	Indonesia	1892-1894	M_2	f9	lower	right	0.9276	1.0051	2.4325	0.0034	-2.2603	10.5759	0.7364	1.2391	5.2925	6.5316	0.4949	12.1863	0.6405	4.1172	0.5365	3776.0139	Habinger et al. in prep
SSAM-1981-53	*Pongo pygmaeus*	f	ad.	Borneo, Skalau	Indonesia	1892-1894	M_2	f9	lower	right	1.1827	0.1593	0.4623	0.0058	-1.0091	5.4815	0.4564	1.3630	3.0593	4.4223	0.3414	10.0472	0.5514	2.6076	0.3129	4249.8651	Habinger et al. in prep
SSAM-1981-59	*Pongo pygmaeus*	f	ad.	Borneo, Skalau	Indonesia	1892-1894	M_2	f9	lower	right	1.3550	0.2619	0.7457	0.0024	-1.2500	7.3746	0.3157	1.2811	2.5189	3.8001	0.2355	7.0704	0.5717	2.6122	0.3380	4189.9884	Habinger et al. in prep
SSAM-1981-60	*Pongo pygmaeus*	f	ad.	Borneo, Skalau	Indonesia	1892-1894	M_2	f9	lower	right	0.8345	0.3918	2.1217	0.0030	-0.7375	4.6600	0.8944	2.2493	5.1673	7.4166	0.6757	14.9285	0.7075	2.4947	0.4967	3664.4105	Habinger et al. in prep
SSAM-1981-62	*Pongo pygmaeus*	m	subad.	Borneo, Skalau	Indonesia	1892-1894	M_2	f9	lower	right	0.9495	0.1336	0.3899	0.0039	-0.5928	3.5089	0.3300	0.8962	1.5559	2.4521	0.2596	9.9330	0.6456	1.6219	0.3251	3843.4412	Habinger et al. in prep
SSAM-1981-63	*Pongo pygmaeus*	m	ad.	Borneo, Skalau	Indonesia	1892-1894	M_2	f9	lower	right	1.0625	0.2530	0.6067	0.0042	-1.5068	7.0672	0.3800	1.3714	2.2763	3.6476	0.2704	7.9401	0.5660	1.9133	0.3286	3842.2081	Habinger et al. in prep
SSAM-1981-64	*Pongo pygmaeus*	f	subad.	Borneo, Skalau	Indonesia	1892-1894	M_2	f9	lower	right	1.1531	0.7873	1.0891	0.0011	-2.6802	13.8565	0.6636	1.2919	5.2326	6.5245	0.4357	12.3842	0.8138	4.1055	0.4529	4079.7538	Habinger et al. in prep
SSAM-1981-67	*Pongo pygmaeus*	m	ad.	Borneo, Skalau	Indonesia	1892-1894	M_2	f9	lower	right	1.4979	0.4017	0.9086	0.0032	-2.4670	10.9343	0.4334	0.9028	4.0938	4.9966	0.2882	8.0676	0.7107	3.5770	0.4453	4109.4505	Habinger et al. in prep
SSAM-1981-68	*Pongo pygmaeus*	m	ad.	Borneo, Skalau	Indonesia	1892-1894	M_2	f9	lower	right	0.5797	0.1087	0.3488	0.0066	-0.8881	4.7694	0.2670	1.0338	1.7217	2.7555	0.2033	8.1319	0.5190	1.4728	0.2607	4215.2516	Habinger et al. in prep
SSAM-1981-69	*Pongo pygmaeus*	m	ad.	Borneo, Skalau	Indonesia	1892-1894	M_2	f9	lower	right	0.9219	0.3641	1.0014	0.0026	-3.1992	18.3154	0.3125	0.5453	2.8738	3.4191	0.1916	7.3215	0.6041	2.2878	0.2376	4695.1480	Habinger et al. in prep
SSAM-1981-70	*Pongo pygmaeus*	m	ad.	Borneo, Skalau	Indonesia	1892-1894	M_2	f9	lower	right	0.3660	0.2767	0.5208	0.0043	0.1328	4.2978	0.3421	1.2985	1.9256	3.2240	0.2613	15.7716	0.6060	1.1815	0.1777	5117.3970	Habinger et al. in prep
SSAM-1981-71	*Pongo pygmaeus*	f	ad.	Borneo, Skalau	Indonesia	1892-1894	M_2	f9	lower	right	0.4031	0.1544	0.3446	0.0024	-1.1918	7.7955	0.3950	1.3209	2.6926	4.0135	0.2928	17.9458	0.6420	1.8009	0.1684	4430.2436	Habinger et al. in prep
SSAM-1981-74	*Pongo pygmaeus*	f	ad.	Borneo, Skalau	Indonesia	1892-1894	M_2	f9	lower	right	1.5010	0.2312	1.0811	0.0063	-1.4520	5.2095	0.8763	1.3007	4.1471	5.4478	0.6638	10.4257	0.4340	3.0945	0.7548	3361.5569	Habinger et al. in prep
SSAM-1981-75	*Pongo pygmaeus*	f	ad.	Borneo, Skalau	Indonesia	1892-1894	M_2	f9	lower	right	1.0650	0.3325	0.6223	0.0036	-0.4886	3.6914	0.8990	2.6775	3.4531	6.1306	0.6966	13.8183	0.6330	2.1601	0.4651	4124.6935	Habinger et al. in prep
SSAM-1981-76	*Pongo pygmaeus*	f	ad.	Borneo, Skalau	Indonesia	1892-1894	M_2	f9	lower	right	0.8971	1.3448	2.9416	0.0027	-1.2438	6.3263	0.6977	1.5212	3.8849	5.4061	0.4972	10.9435	0.7437	3.0833	0.5310	3375.6865	Habinger et al. in prep
SSAM-1981-77	*Pongo pygmaeus*	f	ad.	Borneo, Skalau	Indonesia	1892-1894	M_2	f9	upper	left	1.5705	0.7352	3.0121	0.0004	-1.3948	5.6810	0.8425	1.6606	4.5360	6.1967	0.6244	13.2741	0.8857	3.5708	0.6004	3772.4526	Habinger et al. in prep
SSAM-1981-78	*Pongo pygmaeus*	f	ad.	Borneo, Skalau	Indonesia	1892-1894	M_2	f9	lower	right	0.7904	0.3594	0.5425	0.0029	-2.7263	13.2377	0.3589	0.5968	2.7778	3.3746	0.2378	9.7150	0.6758	2.6205	0.2409	4677.8308	Habinger et al. in prep
SSAM-1981-79	*Pongo pygmaeus*	f	ad.	Borneo, Skalau	Indonesia	1892-1894	M_2	f9	lower	right	1.4945	0.8273	1.3863	0.0027	-1.1554	5.4554	0.9258	1.9731	4.8514	6.8245	0.7086	17.1839	0.7716	2.9899	0.5180	4205.5004	Habinger et al. in prep
SSAM-1981-82	*Pongo pygmaeus*	f	ad.	Borneo, Skalau	Indonesia	1892-1894	M_2	f9	lower	right	0.8282	0.3262	0.5865	0.0046	-0.4957	2.9383	0.2607	0.8072	1.0899	1.8971	0.2120	10.3132	0.5916	1.0473	0.2243	4118.6516	Habinger et al. in prep
SSAM-1981-83	*Pongo pygmaeus*	f	ad.	Borneo, Skalau	Indonesia	1892-1894	M_2	f9	lower	right	0.9878	0.2226	0.5239	0.0033	0.2816	6.7494	0.5915	3.5795	2.5557	6.1352	0.4337	14.0200	0.6615	2.2586	0.3454	3838.6905	Habinger et al. in prep
SSAM-1981-83	*Pongo pygmaeus*	f	ad.	Borneo, Skalau	Indonesia	1892-1894	M^2	f9	upper	right	0.8071	0.3377	0.4830	0.0067	-0.4762	4.6501	0.2832	1.1717	1.6852	2.8570	0.2088	7.8583	0.2220	1.5971	0.2423	5020.4628	Habinger et al. in prep
SSAM-1981-86	*Pongo pygmaeus*	f	ad.	Borneo, Skalau	Indonesia	1892-1894	M_2	f9	lower	right	0.8482	0.4504	0.6503	0.0048	-1.7424	8.4223	0.2148	0.7854	1.6228	2.4082	0.1556	5.1566	0.3723	1.5890	0.2141	4278.6609	Habinger et al. in prep
SSAM-1981-88	*Pongo pygmaeus*	f	ad.	Borneo, Skalau	Indonesia	1892-1894	M_2	f9	lower	right	1.0488	0.2621	0.3891	0.0069	-1.3513	5.7235	0.2414	0.7589	1.4130	2.1719	0.1834	4.5605	0.4097	1.4046	0.2369	3936.7369	Habinger et al. in prep
SSAM-1981-89	*Pongo pygmaeus*	f	ad.	Borneo, Skalau	Indonesia	1892-1894	M_2	f9	lower	right	1.6925	0.6072	1.2487	0.0015	-2.1687	11.9793	0.3875	1.3137	2.8073	4.1210	0.2377	7.9560	0.7814	2.3295	0.3355	4648.4441	Habinger et al. in prep
SSAM-1981-90	*Pongo pygmaeus*	f	ad.	Borneo, Skalau	Indonesia	1892-1894	M_2	f9	lower	right	1.1254	0.2792	0.6312	0.0023	-2.3553	14.3456	0.3170	0.8205	3.2836	4.1041	0.2134	9.3234	0.7452	2.4391	0.2500	5214.7920	Habinger et al. in prep
SSAM-1981-91	*Pongo pygmaeus*	f	senil	Borneo, Skalau	Indonesia	1892-1894	M_2	f9	lower	right	1.4740	0.2476	0.4628	0.0001	-0.7055	4.5122	0.2337	0.7757	1.4499	2.2256	0.1776	9.4412	0.7703	1.2717	0.2071	5274.7615	Habinger et al. in prep
SSAM-1981-92	*Pongo pygmaeus*	f	senil	f9	Indonesia	1892-1894	M_2	f9	lower	right	0.8757	0.3031	0.6348	0.0009	-1.0894	5.7851	0.6034	1.4227	3.6216	5.0443	0.4526	17.9781	0.7505	2.4296	0.3165	4334.4020	Habinger et al. in prep
SSAM-1981-94	*Pongo pygmaeus*	m	ad.	f9	Indonesia	1892-1894	M_2	f9	lower	right	0.5340	0.1718	0.4127	0.0010	-0.8986	6.1416	0.2404	0.6070	1.5901	2.1971	0.1839	10.3227	0.6495	1.4278	0.1743	4551.4355	Habinger et al. in prep
SSAM-1981-95	*Pongo pygmaeus*	f	ad.	f9	Indonesia	1892-1894	M_2	f9	lower	right	1.5776	0.1745	0.3948	0.0058	-0.4061	3.5274	0.3870	1.1365	2.1847	3.3212	0.3106	7.5196	0.3877	1.9382	0.4512	3975.2409	Habinger et al. in prep
SSAM-1981-95	*Pongo pygmaeus*	f	ad.	f9	Indonesia	1892-1894	M_2	f9	lower	left	1.6526	0.4685	0.6417	0.0032	-1.4076	6.0537	0.4229	1.4595	2.3209	3.7803	0.3066	6.3943	0.4938	2.3577	0.5000	4302.5765	Habinger et al. in prep
SSAM-1981-96	*Pongo pygmaeus*	f	ad.	f9	Indonesia	1892-1894	M_2	f9	lower	right	1.2036	0.6252	1.0964	0.0047	-0.6930	4.4049	0.8819	3.1377	4.1929	7.3306	0.6880	14.7729	0.8373	2.9232	0.5892	3298.4400	Habinger et al. in prep
SSAM-1981-97	*Pongo pygmaeus*	f	ad.	f9	Indonesia	1892-1894	M_2	f9	lower	right	1.0014	0.2003	0.4970	0.0016	-2.8876	15.3061	0.4749	1.1641	3.3455	4.5096	0.2950	13.6160	0.5872	2.3270	0.2659	4519.9500	Habinger et al. in prep
SSAM-1981-99	*Pongo pygmaeus*	m	ad.	f9	Indonesia	1892-1894	M_2	f9	lower	right	0.6440	0.2123	0.6554	0.0058	-1.5034	6.7134	0.2299	0.6159	1.5664	2.1823	0.1650	6.9797	0.4970	1.3746	0.1952	4288.3807	Habinger et al. in prep